

Université de Montréal

**Implication of EphA4 in circadian and sleep physiology  
studied using transcriptional and pharmacological approaches**

*By*

Maria Neus Ballester Roig

Université   
de Montréal



Département de neurosciences, Faculté de médecine

Thesis presented for obtaining the degree Philosophiae Doctor (Ph. D.)

in Neurosciences

August 2022

© Maria Neus Ballester Roig, 2022



Université de Montréal

Département de neurosciences, Faculté de médecine

---

**Implication of EphA4 in circadian and sleep physiology  
studied using transcriptional and pharmacological approaches**

*Presented by*

**Maria Neus Ballester Roig**

*Evaluated by a jury composed of*

**Bénédicte Amilhon**

Jury president

**Valérie Mongrain**

Research supervisor

**Adriana Di Polo**

Jury member

**Kai-Florian Storch**

External jury member

**Sébastien Talbot**

Dean representative



Le sommeil est un comportement qui occupe un tiers de notre vie. L'horaire, la durée, et la qualité du sommeil sont contrôlés par deux processus principaux : la régulation homéostatique du sommeil et l'horloge qui synchronise les rythmes circadiens internes. EPHA4 est une molécule d'adhésion cellulaire qui régule la neurotransmission et qui est exprimée dans des régions cérébrales impliquées dans la régulation circadienne et du sommeil. De manière intéressante, le gène *EphA4* contient des éléments régulateurs des facteurs de transcription circadiens et les souris *Clock* mutantes voient leur expression d'*EphA4* modifiée. De plus, les souris *EphA4* knockout (KO) ont des rythmes circadiens d'activité locomotrice anormaux, moins de sommeil paradoxal dans la période de lumière, et une distribution des oscillations cérébrales du sommeil modifiée sur un cycle de 24 heures. Par conséquent, et étant donné que EPHA4 est crucial pour le neurodéveloppement, il convient d'explorer si les phénotypes du sommeil/circadiens observés chez les souris *EphA4* KO proviennent d'effets sur le développement ou des rôles d'EPHA4 dans la fonction neuronale adulte. Par ailleurs, les mécanismes de régulation transcriptionnelle d'*EphA4* sont encore méconnus. Dans cette thèse, nous avons émis les hypothèses que i) l'expression du gène *EphA4* ou de leurs ligands Éphrines (*Efns*) est régulée de manière circadienne ; et ii) que le modulateur de l'activité d'EPHA4 rhynchophylline (RHY) modifie le sommeil chez les souris adultes d'une manière qui ressemble au phénotype *EphA4* KO. L'étude I montre que les facteurs de transcription de l'horloge (CLOCK/NPAS2 et BMAL1) activent la transcription via les éléments de réponse à l'ADN «boîtes E» trouvées dans les promoteurs putatifs d'*EphA4*, *EfnB2* et *EfnA3 in vitro*. Cependant, les protéines EPHA4 et EFNB2 n'ont pas montré une oscillation circadienne dans le cortex préfrontal et les noyaux suprachiasmatiques (horloge principale) de souris. Dans le projet II, l'effet de RHY sur le sommeil a été étudié chez des souris mâles et femelles avec des enregistrements électroencéphalographiques. Nos données ont démontré que RHY prolonge le sommeil à onde lente, mais les effets sur le sommeil paradoxal dépendent de l'heure d'injection. RHY modifie aussi les oscillations cérébrales pendant l'éveil et le sommeil. Tous ces effets sont notablement plus marqués chez les femelles, ce qui souligne l'importance d'étudier les deux sexes lors des essais pharmacologiques. La transcriptomique spatiale cérébrale révèle que RHY modifie des transcrits liés à des réponses d'inflammation dans tout le cerveau, mais qu'elle affecte

l'expression génique des neuropeptides associés à la régulation du sommeil et hypophysaires particulièrement dans l'hypothalamus. En outre, RHY affecte l'expression des gènes de la transcription/traduction de manière différent selon l'heure d'injection. La première publication met en évidence que la régulation transcriptionnelle d'*EphA4* et des *Efns* pourraient expliquer quelques-uns des phénotypes observés chez les souris KO. La deuxième publication démontre que RHY induit le sommeil chez la souris et souligne l'importance de caractériser des mécanismes inexplorés sous-jacents aux composés naturels. Décrire la régulation moléculaire du sommeil peut apporter des éclairages utiles pour la chronopharmacologie.

**Mots-clés :** Rythme circadien, sommeil à onde lente, sommeil paradoxal, Éphrines, médecine traditionnelle, rhynchophylline, transcriptomique spatiale, facteurs de transcription de l'horloge, transcription

Sleep is a behavior which occupies a third of our lifetime. The schedule, the duration and the quality of sleep are controlled by two main processes: the homeostatic sleep regulation and the clock that synchronizes the internal circadian rhythm. EPHA4 is a cell adhesion molecule regulating neurotransmission and is expressed in brain centers regulating sleep and circadian rhythms. Interestingly, the *EphA4* gene contains regulatory elements for circadian transcription factors, and *Clock* mutant mice have altered *EphA4* expression. Moreover, *EphA4* knockout mice (KO) have abnormal circadian rhythms of locomotor activity, less paradoxical sleep in the light period and altered sleep brain oscillations across the 24 hours. Given that EPHA4 is crucial for development, it should be investigated whether the sleep/circadian phenotypes observed in *EphA4* KO originate from developmental effects or from roles of EPHA4 in adult neuronal function. Moreover, very little is known about the transcriptional regulation of EPHA4. Thus, the hypotheses of this thesis were that i) the gene expression of *EphA4* or that of its ligands Ephrins (*Efns*) is regulated in a circadian manner; and ii) that the modulator of EPHA4 activity rhynchophylline (RHY) modifies sleep in adult mice in manners that resemble the *EphA4* KO phenotype. Project I demonstrates that the clock transcription factors (CLOCK/NPAS2 et BMAL1) activate transcription via the DNA regulatory elements “E-boxes” found in the putative promoters of *EphA4*, *EfnB2* and *EfnA3* *in vitro*. Nevertheless, EPHA4 and EFNB2 proteins did not show a circadian oscillation in the mouse prefrontal cortex and suprachiasmatic nuclei (master clock). In project II, the effect of RHY on sleep was studied in male and female mice with electroencephalographic recordings. RHY extends slow wave sleep and effects on paradoxical sleep depended on the time-of-injection. RHY also modified the brain oscillations during wakefulness and sleep. Importantly, all these effects were larger in females, which highlights the need to consider both sexes in pharmacological studies. Brain spatial transcriptomics reveals that RHY modifies transcripts linked to inflammatory responses throughout the brain, while it affects transcripts linked to sleep regulation and pituitary responses particularly in the hypothalamus. Moreover, RHY affected the expression of genes for transcription/translation differently depending on the time of injection. The first publication underscores that the transcriptional regulation of *EphA4* and *Efns* may underly some of the phenotypes observed in the KO mice. The second

publication demonstrates that RHY induces sleep in mice, that it modifies brain activity associated to cognitive processes and highlights the importance of characterizing unexplored mechanisms of natural compounds. Describing the molecular regulation of sleep may provide useful insights for chronopharmacology.

**Keywords:** Circadian rhythm, slow wave sleep, paradoxical sleep, Ephrins, traditional medicine, rhynchophylline, spatial transcriptomics, clock transcription factors, transcription



# Table of content

---

Résumé .....	5
Abstract .....	7
Table of content.....	9
List of Tables.....	14
List of Figures .....	15
List of abbreviations.....	17
Acknowledgments.....	20
<b>Chapter 1 Introduction.....</b>	<b>22</b>
1.1 Sleep .....	25
1.1.1 The sleep states.....	25
1.1.2 Some sleep variables are influenced by sex .....	27
1.2 Brain systems controlling sleep.....	29
1.2.1. Brain circuits .....	29
1.2.2 Molecular systems within circuits.....	31
1.2.2.1 Channels, receptors and adhesion molecules .....	31
1.2.2.2 Intracellular pathways .....	34
1.3 The two-process model of sleep regulation.....	35
1.3.1 Circadian regulation (process C).....	36
1.3.1.1 The circadian TTFL and clock-controlled genes .....	37
1.3.1.2 SCN outputs .....	39
1.3.1.3 Some circadian variables are influenced by sex.....	40
1.3.1.4 Circadian control at the synapse.....	40
1.3.1.4.1 Circadian regulation of the transcriptome .....	40
1.3.1.4.2 Phosphorylation as accumulative (and time) sensors.....	41
1.3.2 Homeostatic regulation (process S).....	42
1.3.2.1 Potential mechanisms underlying sleep homeostasis .....	43

1.3.2.1.1 Sleep regulatory substances .....	44
1.3.2.1.2 Gene expression reflects sleep-wake history .....	45
1.3.2.1.3 The phosphorylation hypothesis of sleep .....	47
1.3.2.2 Sleep for the brain and the synaptic homeostasis hypothesis (SHY) .....	47
1.3.2.2.1 Potential mechanisms underlying sleep-dependent plasticity .....	49
1.3.3 Integrations of processes C and S .....	50
1.3.3.1 Molecular integration of C and S .....	50
1.4 Ephrins and Eph receptors.....	52
1.4.1 EphA4.....	53
1.4.1.1 EPHA4 activation and signaling .....	54
1.4.1.2 Functions of EPHA4 .....	55
1.4.1.2.1 CNS development .....	55
1.4.1.2.2 Adult neurotransmission .....	56
1.4.1.2.3 Vascular system.....	57
1.4.1.2.4 Immune system and cancer .....	57
1.4.1.3 EphA4 implications in diseases.....	58
1.4.1.4 EphA4 gene and transcriptional regulation.....	58
1.4.2 EphA4 and Ephrins in sleep and circadian physiology.....	60
1.5 Rhynchophylline may uncover EphA4 roles in sleep regulation.....	63
1.5.1 Rhynchophylline reduces EphA4 phosphorylation.....	63
<b>Chapter 2 Cellular effects of Rhynchophylline and relevance to sleep regulation .....</b>	<b>64</b>
Abstract .....	66
1. Introduction .....	67
1.1. Rhynchophylline pharmacology .....	67
1.2 Sleep and its regulation .....	68
1.3 Rhynchophylline and sleep .....	69
2. RHY targets and links to sleep regulation.....	70
2.1 Ion channels.....	70

2.2 NMDA receptors .....	75
2.3 EphA4 and downstream pathways .....	80
2.4 BDNF/TRKB signaling.....	81
2.5 ERK/MAPK pathway.....	82
2.6 PI3K/AKT signaling network .....	83
2.7 NF- $\kappa$ B and neuroinflammation .....	86
2.8 Neurotransmitters signaling .....	87
3. Conclusions .....	89
Acknowledgements .....	91
References .....	91
<b>Chapter 3 Hypotheses and Objectives.....</b>	<b>114</b>
3.1 Overall rationale and general hypotheses.....	115
3.2 Specific aims .....	116
3.2.1 Determine if EphA4 and its ephrin ligands EfnB2 and EfnA3 are under circadian regulation.....	116
3.2.2 Define the effects of Rhynchophylline on sleep and the molecular mechanisms underlying its effects .....	117
3.3 Specific contributions of the candidate .....	119
3.3.1 In determining if EphA4 and its Ephrin ligands EfnB2 and EfnA3 are under circadian regulation.....	119
3.3.2 In defining the effects of Rhynchophylline on sleep and the molecular mechanisms underlying its effects .....	119
<b>Chapter 4 Transcriptional regulation of EphA4, Ephrin-B2 and Ephrin-A3 by the circadian clock machinery.....</b>	<b>120</b>
Abstract .....	122
Introduction .....	123
Methods.....	125
Promoter analysis .....	125
Cloning.....	129
Design of <i>EphA4<sub>D</sub></i> with mutated E-boxes .....	130
Cell culture and transfection .....	131
Luciferase assays.....	132

Brain tissue punches and protein extraction.....	133
Immunoblotting and protein quantification.....	134
Spatial gene expression quantification.....	135
Statistical analysis .....	135
Results.....	136
Discussion .....	141
References .....	146
<b>Chapter 5 Probing pathways by which Rhynchophylline modifies sleep using spatial transcriptomics .....</b>	<b>156</b>
Graphical abstract.....	158
Highlights .....	158
eTOC blurb.....	158
Summary .....	159
Introduction.....	160
Results.....	162
RHY increases SWS and state fragmentation.....	162
RHY impacts the ECoG in a state-dependent manner .....	164
Specific RHY targets correlate with sleep variables.....	166
RHY shapes the brain transcriptome in injection-time- and sex-dependent ways.....	168
Gene ontology analysis of RHY time- and sex-dependent effects.....	171
Core RHY-controlled genes are downstream of inflammation/immune pathways .....	172
Brain region-specific effects of RHY on the transcriptome.....	173
RHY regulates sleep-related genes .....	175
Discussion .....	177
Author contributions .....	181
Acknowledgements .....	181
Star★Methods.....	182
KEY RESOURCES TABLE.....	182
RESOURCE AVAILABILITY.....	183
EXPERIMENTAL MODEL AND SUBJECT DETAILS.....	183
METHOD DETAILS .....	184

QUANTIFICATIONS AND STATISTICAL ANALYSES.....	188
ADDITIONAL RESOURCES.....	191
References.....	191
Supplemental information.....	199
<b>Chapter 6 Discussion.....</b>	<b>210</b>
6.1 EphA4 in sleep and circadian regulation.....	213
6.1.1 The molecular circadian clock regulates <i>EphA4</i> , <i>EfnB2</i> and <i>EfnA3</i> .....	213
6.1.1.1 Regulation by clock transcription factors may be restricted in time and space ...	214
6.1.1.2 Transcriptional modulation by GSK3 .....	215
6.1.1.3 Clock transcriptional regulation for C and S hubs .....	217
6.1.1.4 Implication of clock regulation in disease and ageing .....	218
6.1.2 Potential roles of EhA4/Ephrins in circadian and sleep behavior.....	219
6.2 RHY induces sleep and affects transcripts linked to sleep control .....	220
6.2.1 RHY enhances sleep time and modifies sleep oscillations in rodents .....	220
6.2.1.1. RHY modifies brain oscillations in different vigilance states.....	221
6.2.2 RHY may modulate sleep via effects on the LH.....	223
6.2.3 RHY reduces expression of HPA axis elements .....	224
6.2.4 RHY modifies genes linked to inflammatory responses.....	225
6.2.5 RHY did not modify EPHA4 phosphorylation .....	226
6.2.6 RHY modifies immediate early genes linked to the response to sleep deprivation....	228
6.2.7 Future identification of RHY targets for sleep regulation.....	229
6.3 RHY as a natural component for sleep modulation .....	230
6.4 Benefits and limitations of spatial transcriptomics .....	231
6.5 Other notions to better describe molecular mechanisms in sleep and circadian rhythms..	232
<b>Chapter 7 Conclusions .....</b>	<b>234</b>
References .....	237
Annexes .....	277

## **Chapter 2 – Cellular effects of Rhynchophylline and relevance to sleep regulation**

Table 1. Compilation of datasets showing molecular and cellular (and some electrophysiological and behavioral) effects of rhynchophylline (RHY) organized as a function of treatment type and duration, and by measurement timing.

Table 2. List of literature showing effects of RHY on sleep-related pathways under physiological (baseline) and/or pathological (disease-modeled) conditions.

## **Chapter 4 – Transcriptional regulation of EphA4 and its ligands ephrin-B2 and ephrin-A3 by the circadian clock machinery**

Table 1. Regulatory elements found in the -3kb upstream of *EphA4*, *EfnB2* and *EfnA3* transcription start sites.

Table 2. Forward and reverse primers used for cloning.

Table 3. Mutated E-boxes used in previous research.

Table S1. Differentially expressed genes (DEGs) between ZT4 and ZT14 (*see Annex*)

## **Chapter 5 – Probing pathways by which Rhynchophylline modifies sleep using spatial transcriptomics**

Table S1. Protein quantification of total and synaptoneurosomal protein fractions of thalamus/hypothalamus, cerebral cortex and hippocampus (*see Annex*)

Table S2. Differentially expressed genes (DEGs) modified by RHY at ZT4 and ZT14 in female and male brains (*see Annex*)

Table S3. Gene Ontology analysis performed for the DEG sets for bulk, white matter tracts, cerebral cortex, hippocampus, thalamus and hypothalamus (*see Annex*)

## **Annex**

Table A1. Cellular functions attributed to genes modified according to wake/sleep.

## **Chapter 1 – Introduction**

Figure 1.1. Sleep states in humans and mice

Figure 1.2. The two-process model of sleep regulation

Figure 1.3. The circadian TTFL and its many levels of regulation

Figure 1.4. EPHA4 can trigger multiple intracellular signaling.

## **Chapter 2 – Cellular effects of Rhynchophylline and relevance to sleep regulation**

Figure 1. Representation of the chemical structure of rhynchophylline (RHY) and isorhynchophylline.

Figure 2. Schematic representation of cellular pathways targeted by RHY and relevant to sleep regulation.

## **Chapter 4 – Transcriptional regulation of EphA4 and its ligands ephrin-B2 and ephrin-A3 by the circadian clock machinery**

Figure 1. *EphA4*, *EfnB2* and *EfnA3* putative promoter regions contain sleep and circadian-related regulatory elements.

Figure 2. Circadian clock transcription factors activate transcription via *EphA4* putative promoter sequences.

Figure 3. Circadian clock transcription factors activate transcription via *EfnB2* and *EfnA3* putative promoter sequences.

Figure 4. EPHA4 and EFNB2 protein levels in the mouse PFC and SCN do not show circadian oscillations.

Figure 5. *EphA4*, *EfnB2* and *EfnA3* spatial gene expression in mouse brain at ZT4 and ZT14.

## **Chapter 5 – Probing pathways by which Rhynchophylline modifies sleep using spatial transcriptomics**

Graphical abstract

Figure 1. RHY increases SWS time, reduces PS time, and promotes wake and SWS fragmentation

Figure 2. RHY modifies ECoG activity in a vigilance-state dependent manner.

Figure 3. Protein levels are not modified by RHY but correlated with sleep variables.

Figure 4. RHY modifies the mouse brain transcriptome.

Figure 5. RHY modifies the brain transcriptome in a brain region-dependent manner.

Figure 6. RHY modifies the expression of sleep-related genes.

Figure S1. Groups were similar in baseline, RHY increases SWS more prominently in females, and it modifies 24-h dynamics of ECoG oscillations in a vigilance-state dependent manner .

Figure S2. CDK5 and GLT1 levels were unchanged by RHY and pGLUR1 correlates with decreased wake alpha activity

Figure S3. CDK5 and GLT1 levels were unchanged by RHY and pGLUR1 correlates with decreased wake alpha activity.

Figure S4. Analysis of enrichment in canonical pathways and for potential upstream regulators using Ingenuity pathway analysis, and of functional gene ontology terms.

Figure S5. Spatial gene expression maps of selected DEGs found to be common between ZT4F, ZT4M, ZT14F and ZT14M.

Figure S6. Transcription factors found to be enriched in ZT4F, ZT4M, ZT14F and ZT14M DEGs, and UMAP clustering of female and male spots of brain regions.

## **Chapter 6 – Discussion and perspectives**

Figure 6.1. The core clock machinery may control EphA4 roles in sleep and circadian behavior and Rhynchophylline induces sleep

Figure 6.2. RHY induces SWS and modifies ECoG activity in *EphA4* KO mice similarly to how it does in *EphA4* WT mice.

Figure A1. Spatial gene expression of immediate early genes downregulated by RHY



## List of abbreviations

---

5-HT: serotonin or 5-hydroxytryptamine	EEG: electroencephalogram and electroencephalographic
AD: Alzheimer's disease	Efn: ephrin
ADX: adrenalectomized	EGR: early growth response
AMPA: $\alpha$ -amino-3-hydroxy-5-methyl- 4-isoxazole propionic acid	EMG: electromyogram
ATP: adenosine triphosphate	EphA4: Eph receptor A4
BDNF: brain-derived neurotrophic factor	ERK: extracellular signal-regulated kinases
BF: basal forebrain	FKHR: forkhead box O1 (or FOXO1a)
BMAL: brain and muscle aryl hydrocarbon receptor nuclear translocator-like protein	FOS: FBJ osteosarcoma oncogene
CNS: central nervous system	FRE: FOXO response elements
CA1: cornu ammonis area 1	GABA: gamma-aminobutyric acid
CA3: cornu ammonis area 3	GH: growth hormone
CAMKII: calcium/calmodulin-dependent protein kinase II	GHRH: growth hormone releasing hormone
CLOCK: circadian locomotor output cycles kaput	GLAST: glutamate/aspartate transporter (also named EAAT1)
CRE: cAMP-response element	GLT1: glutamate transporter subtype 1 (also named EAAT2)
CREB: cAMP response element (CRE)-binding protein	GLUA1: glutamate receptor AMPA1 (alpha 1) subunit (also named GluR1)
CRY: Cryptochrome	GSK3 $\beta$ : glycogen synthase kinase 3 $\beta$
CT: circadian time	Hcrt: hypocretin (orexin)
DD: dark-dark	HPA: hypothalamic-pituitary-adrenal
DEG: differentially expressed gene	IEG: immediate early gene
DNA: deoxyribonucleic acid	IL: interleukin
DR: dorsal raphe	KO: knockout
DSIP: delta sleep-inducing peptide	LC: locus coeruleus
ECoG: electrocorticogram	LD: light-dark
	LDT: laterodorsal tegmentum

LH: lateral hypothalamus  
 LL: light-light  
 LTP: long-term potentiation  
 L-VGCC: L-type VGCC  
 MAPK: mitogen-activated protein kinase  
 MEF: myocyte enhancer factor 2D  
 MEIS: meis homeobox 1  
 MESP2: mesoderm posterior 2  
 MCH: melanin concentrating hormone  
 MS/DBB: medial septum and diagonal  
     band of Broca  
 mGLUR: metabotropic glutamate receptor  
 mPFC: medial prefrontal cortex  
 mRNA: messenger RNA  
 miRNA: microRNA  
 NF- $\kappa$ B: nuclear factor kappa B  
 NGF: nerve growth factor  
 Nlgn: neuroligin  
 NMDA: N-methyl-D-aspartate  
 NMDAR: NMDA receptor  
 NPAS2: neuronal PAS domain protein 2  
 NR4A1: nuclear receptor subfamily 4,  
     group A, member 1  
 NREM: non-rapid-eye-movement  
 TNF: tumor necrosis factor  
 TSS: transcription start site  
 TTFL: transcriptional-translational  
     feedback loop  
 PACAP: pituitary adenylate cyclase activating  
     polypeptide  
 PAX3: paired box 3  
 PER: Period  
 PFC: prefrontal cortex  
 POA: preoptic area  
 PPAR: peroxisome proliferator-activated  
     receptor  
 PPT: pedunculo pontine tegmentum  
 PPRE: PPAR response element  
 PS: paradoxical sleep  
 REM: rapid-eye-movement  
 RNA: ribonucleic acid  
 RNAseq: RNA sequencing  
 RHY: rhynchophylline  
 ROR: retinoic acid-related orphan receptor  
 RORE: ROR-response elements  
 scRNAseq: single-cell RNA sequencing  
 SD: sleep deprivation  
 SCN: suprachiasmatic nuclei  
 SGK1: serum/glucocorticoid regulated kinase 1  
 Sp1: Stimulating protein 1  
 SRS: sleep regulatory substances  
 SWA: slow wave activity  
 SWS: slow wave sleep  
 TLR: Toll-like receptor  
 TMN: tuberomammillary nuclei  
 VGCC: voltage-gated calcium channel  
 VLPO: ventrolateral preoptic area  
 YKS: Yokukansan  
 ZT: *Zeitgeber* time

*“There are a hundred times more cells in our body  
than there are stars in our galaxy”  
Martin Rees*

## Acknowledgments

---

World knowledge builds on years of efforts and passion, and not a single book would be written without human exchange for the forging of new ideas. Above all, I thank my mentor, Valérie Mongrain, for opening the doors to the molecular sleep world to me, and for your generosity on scientific curiosity, rigor, self-discipline and adaptation. I also thank you for your courage and marvelous ideas. It is a treasure to build research and life career with you. This work would also not had been done without Julien. Thanks for your patience, calm answers and advice, for coming at dark circadian hours and for bringing chords and rockets to the bench. I want to deeply thank Tanya as well, for her severity in science and unique inspiring strength. This research would neither had been possible without Yousra's clarity and transparency in teamwork. Thanks also to Lydia, for your blue-pink meticulousness, great help and for sharing my first lab experience so tastefully. To Emma, for her honest advice in the form of cups of wine, and to Erika and Pierre-Gabriel, for their fantastic work and contribution to my learning. I thank Benoit (you should have arrived earlier), Rama, Romina, Thomas, Audrey, Morgane, Nicolas, Christina, Bong-Soo, and Simon, for being fantastic science peers. I express deep gratitude to Jannic and Numa, for their availability and valuable feedback all these years, and to my jury members for accepting to evaluate and enrich this work. I thank Nicolas Cermakian as well, for offering his lab and advice, and for teaching me so much about devotion for the scientific community, and I thank all the members of the student associations, scientific societies and meeting organizers with who I had the truly inspiring privilege to work with.

This work would also not be possible without the scientific:human discussions with Eve, Claudia Piccard, Cassandra, Matt, Sana, Maryam and Samir. Thanks for your scientific drive, arty motivation, values and friendship. I also have a gigantic debt to my previous professors. I thank Cristina Nicolau and Rubén Rial, for accepting me in their project in 2013 and for transmitting to me their beautiful passion for sleep and rhythms so early in my career, but I also thank A. Gamundí, P. Montoya, M. Ribas-Carbo, A. Miralles, S. Esteban, J. García, R. Alemany, S. Aparicio, J. Flexas, G.M. Vicens, and many, many other professors at UIB. Pursuing my biology degree at UIB made my real happiness appear. I also thank high school professors, especially Isabel Roca, for presenting to me Darwin and a molecular pathway for the first time (without books), and to

Antònia Sitjar, who taught me that people can be sponges of knowledge... and I have never stopped since then. It is very fun.

I also want to thank my father for suggesting to me very early to choose wisely how I want to spend my waking hours, and to my mother, who showed me how to build life flexibility and strength. You both insisted on defining one's priorities without following conventions. I am also immensely grateful to Coloma, for your endless support (since my efforts in understanding derivatives), and for your serenity and amusement when hearing my "curolles". Cheers to the ones who dream (and get frustrated, sometimes). Thanks also to my brother, my unending source of goodness, and to my grandparents Joana, Onofre, Susana and Tomeu, for nurturing perseverance and values. I deeply thank my friends Laetitia, Camil, Alberto Osa, Joan, Duncan, François, Maria Binimelis, Rosa, Maria Marin, Toni, Nati, Miquel Àngel, Victòria Burguera, Clàudia, Elvira, Catina, Aina, Josep, Rafel Cantallops, Angie, Michel, Alberto Herrero and Salva. You all make the world a better place. And I thank Sam Harris, whose work keeps me rooted to humanity's fundamentals. Thanks also to Malcolm Gladwell for entertaining my sleep scorings, to Petra, Susy Daigle, Arcade Fire, and all the researchers who pose questions and discuss out loud openly in congresses. I thank the Vanier Canada Graduate Scholarships program, the online sport trainers, the creators of zoom, and all the researchers of the many (successful and unsuccessful) COVID vaccines.

# Chapter 1

Introduction

---

Life has adapted its biological functioning to the Earth's rotation and orbit around the Sun. Some of the most robust adjustments are the ones developed according to the biphasic distribution of sunlight and heat every 24 hours. Unicellular organisms like cyanobacteria developed internal rhythms to schedule functions at the appropriate moment: for instance, they conduct nitrogen fixation with an approximate 24-hour period in order to protect the nitrogenase enzyme from heightened oxygen levels during photosynthesis taking place during the daytime (*Huang et al., 1990*). These are considered circadian rhythms of the cell because they occur even under constant lighting conditions. Other ancient organisms show endogenous circadian rhythms in activity patterns such as the swimming velocity of paramecium or the grow of mycelia in fungi (*Nakajima and Nakaoka, 1989; Baker et al., 2012*). Sponges also show daily rhythms of contractility (*Nickel, 2004*). Interestingly, 24-hour rhythms of activity-rest behavior have been found from jellyfish, nematodes, molluscs, arthropods to all vertebrates, and they are also regulated by endogenous circadian rhythms (well reviewed in *Jaggard et al., 2021; Pennisi, 2021*). This highlights that biological functions require a resting phase adequately timed since early stages of evolution.

Humans do not escape from this rule. Sleep is a circadian rhythm, occupies a third of our lifetime, and sleep deprivation strongly impairs metabolic, immune, cardiovascular and cognitive functions, as well as augments mortality risks (*Grandner, 2017*). Enough time and quality of sleep is fundamental to sustain attention, for memory consolidation and mood regulation (*Van Dongen et al., 2003; Banks and Dinges, 2007*). Unfortunately, insomnia symptoms affect one in every three individuals over a year, and inadequate sleep is calculated to cost more than \$600 billion per year worldwide (*Ferrie et al., 2011; Hafner et al., 2017; Hillman et al., 2018*). Moreover, sleep disturbances are the most prevalent comorbidity of neuropsychiatric disorders such as depression, Alzheimer's or Parkinson's disease, and suppose an aggravating factor for patients' symptomatology (*Gan-Or et al., 2018; Irwin and Vitiello, 2019; Riemann et al., 2020*). In addition, sleep is necessary for brain development (*Wintler et al., 2020; Mason et al., 2021*), and sleep disturbances in ageing are associated with cognitive impairments (*Yaffe et al., 2014; Scullin and Bliwise, 2015*). Meanwhile, chronodisruption (a misalignment of the environmental time with the phase of body functions), which often appear with night shifts, time-zone travel or sleep disturbances, has been associated with higher risk of obesity, diabetes, cardiovascular diseases, and cancer (*Reiter et al., 2007; Reiter et al., 2012; Chellappa et al., 2019*). Thus, understanding how

sleep and circadian machineries work and interact in cells and the brain is essential for today's society to maximize health.

Latest technologies in animal mutagenesis, microscopy and omics studies are allowing an increasing understanding of sleep and circadian regulation at the molecular level (*Bruning et al., 2019; Hor et al., 2019; Li et al., 2022a; Smyllie et al., 2022*). Research points that both circadian oscillations and sleep need modifies gene expression, molecule location and protein levels and activation. However, the interactions between circadian and sleep regulation, as well as potential interplay with other neuronal processes and inflammatory/metabolic factors, still needs to be united. EPHA4 is a cell adhesion molecule tyrosine kinase involved in cell growth, neuronal development, and neurotransmission (*Flanagan and Vanderhaeghen, 1998; Murai and Pasquale, 2011*). Its roles in synapses and peripheral tissues (e.g., epithelial cells) have linked it to multiple diseases, including multiple cancers and Alzheimer's disease (*Chen et al., 2012; Kou and Kandpal, 2018; Chen et al., 2021*). Interestingly, our group has shown that mice lacking the *EphA4* gene show altered sleep and circadian behaviors (*Freyburger et al., 2016; Freyburger et al., 2017; Kiessling et al., 2018*). Therefore, this thesis aims at testing EphA4 roles in both sleep and circadian physiology. On the one hand, it will be assessed if the transcription of the *EphA4* gene and the genes of its ligands is regulated by the clock machinery. On the second hand, we will investigate if a repressor of EPHA4 activity modulates sleep in normally developed adult mice. We expect with this to reveal potential mechanisms underlying roles of EphA4 in sleep and rhythms, as well as to expand the description of molecular components regulating sleep and circadian behavior.

Chapter 1 describes mechanisms governing sleep and circadian rhythms, with a focus on mammalian physiology. It includes neuronal circuitry underlying the different arousal states, how sleep is regulated by both homeostatic and circadian processes, and the contribution of multitudinous molecular elements. Research shows that targeting single molecules can largely modify sleep and rhythms. The chapter will also concentrate on describing the Eph/Ephrin cell adhesion system, its functions and potential implications for sleep and circadian physiology. It will finally present the modulator of EPHA4 activity rhynchophylline (RHY), and the potential relevance for sleep modulation. The significance of RHY highlighted at the end of Chapter 1, will be more extensively presented in a review article which composes Chapter 2.



## 1.1 Sleep

Sleep is a process of lowered behavioral activity fundamental for organisms not only to recover from activity but also to consolidate experience. It is defined as a process of decreased locomotor activity in which organisms increase the sensory threshold for arousal. These characteristics have been found in cnidaria, nematodes, arthropods, molluscs, and vertebrates (*Nath et al., 2017; Kanaya et al., 2020; Pennisi, 2021*). Sleep benefits the recovery of processes which have been accumulated or depleted during wakefulness, such as oxidative stress or energy levels (*Frank and Heller, 2019; Kempf et al., 2019*). For example, it fosters processes of DNA repair, waste clearance, protein synthesis, and pathogen fight (*Imeri and Opp, 2009; Seibt et al., 2012; Xie et al., 2013; Bellesi et al., 2016*). Thus, sleep is not only necessary for survival in mammals, but it also allows proper immune, metabolic and cognitive functions such as memory consolidation and mood (*Imeri and Opp, 2009; Frank and Heller, 2019*).

It has been suggested that repeated and synchronized neuronal silencing is another common feature of sleep present in *C. elegans*, drosophila, fishes, and the rest of vertebrates (*Nath et al., 2017; Leung et al., 2019; Niethard et al., 2021; Tainton-Heap et al., 2021*). Thus, in birds, reptiles and mammals, it is characterized by an increased neuronal synchronization detected by slower frequencies in the electroencephalogram (EEG) (*Abel et al., 2013; Rattenborg et al., 2016; Shein-Idelson et al., 2016*).

### 1.1.1 The sleep states

In reptiles, birds and mammals, sleep is composed of two main states defined as non-rapid-eye-movement (NREM) sleep (similar to slow wave sleep [SWS] in rodents and other non-primate species), and rapid-eye-movement (REM) sleep (correspondent to paradoxical sleep (PS) in non-primates) (*Abel et al., 2013; Rattenborg et al., 2016; Shein-Idelson et al., 2016*) (**Figure 1.1**). Interestingly, quiet sleep (comparable to SWS) and active sleep (potentially comparable to PS) have also been described in flies, fishes and cuttlefishes (*Frank et al., 2012; Leung et al., 2019; Tainton-Heap et al., 2021*). Human NREM sleep is subdivided in three states (NREM N1-N3)

according to their EEG frequencies and sleep depth, and which occur in a sequential order: N1 and N2 are light sleep, and N3 is deep sleep (Carskadon and Dement, 2005).

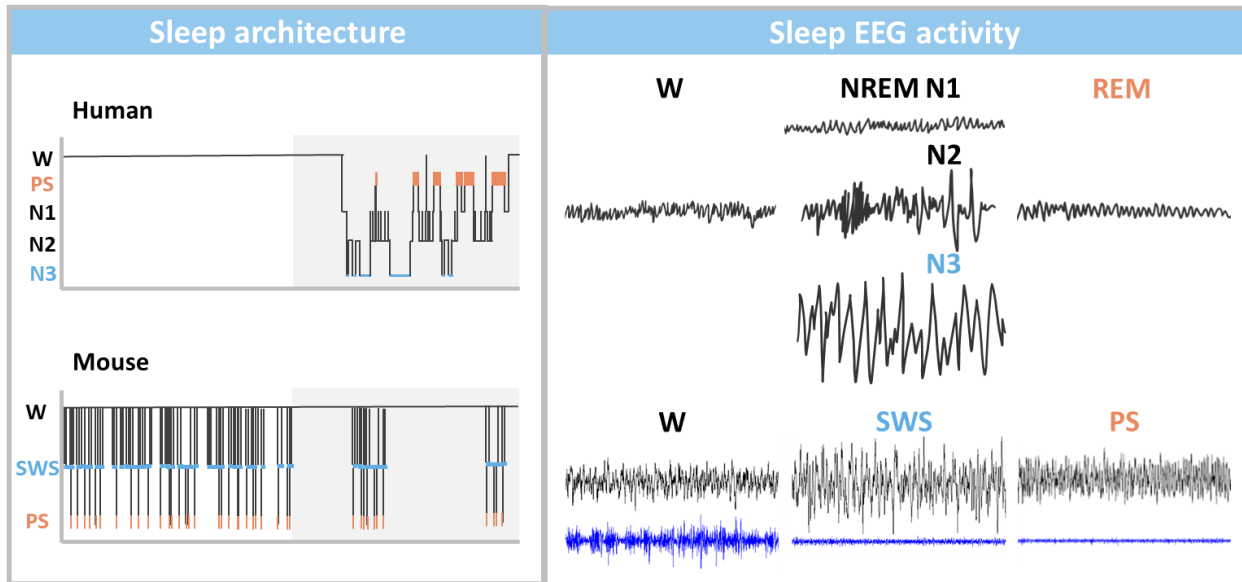


**Figure 1.1. Sleep states in humans and mice.** Sleep in humans is monophasic, occur during the night and is organized in 5-6 cycles. Sleep in nocturnal mice is more scattered throughout the 24 hours but concentrated in the light period (they are nocturnal animals). Sleep in humans is divided in wake, NREM sleep (N1-N3) and REM sleep, while in rodents it is divided into wake, SWS and PS. Figure adapted from Carskadon and Dement (2005).

Wakefulness is characterized by irregular high frequency activity determined by the cognitive processing occurring at each moment (Montgomery *et al.*, 2008; Headley and Pare, 2017). The EEG during wakefulness is predominated by alpha (generally 8-13Hz in human), beta (13-30Hz) and gamma activity (>30Hz). During active (physically or cognitively engaged) wake, theta (4-9Hz), beta and gamma activity can become more prominent, while slower frequencies are enriched in quiet wake (Gronli *et al.*, 2016; Del Percio *et al.*, 2017; Vassalli and Franken, 2017). SWS is characterized by low muscle activity and high neuronal synchronization, which is reflected with low amplitude electromyogram (EMG) and high EEG power in the slow wave activity range (SWA; 0.5-4.5 Hz; also more prominent in human N3) (Amzica and Steriade, 1998; Timofeev *et al.*, 2012; Hubbard *et al.*, 2020). SWA, which comprises slow oscillations (<1Hz) and delta activity (1-4Hz), is a product of a synchronized pattern of neuronal firing (up state or burst firing) alternating with neuronal silencing (down state or hyperpolarization) of cortical and thalamocortical neurons (Steriade *et al.*, 2001). Thalamocortical sleep spindles (10-15 Hz; distinctive of human N2) and hippocampal sharp-wave ripples are also characteristic of SWS, and

are both linked to cognitive processing (*Axmacher et al., 2008; Girardeau et al., 2009; Bandarabadi et al., 2020; Fernandez and Luthi, 2020*). PS is predominated by muscle atonia and theta activity (originating from the connections between the medial septum and diagonal band of Broca complex [MS/DBB] of the BF and the hippocampus) (*Mitchell et al., 1982; Lee et al., 1994; Montgomery et al., 2008; Boyce et al., 2016; Peever and Fuller, 2017; Bandarabadi et al., 2019*). Although the quality of the three vigilance states is defined by the brain activity quantified within these multiple EEG frequency ranges, the transition between states and the time spent in each state is determined by the activation and inhibition of different brain centers and circuits (covered in *section 1.2.1*). In addition, all sleep defining features (e.g., position of sleep during the day or sleep schedule, the duration of the sleep episode, and the quality of the EEG activity in different frequencies during sleep) are regulated by two main processes: the circadian system and the homeostatic regulation of sleep (see *section 1.3*).

### **1.1.2 Some sleep variables are influenced by sex**

Studies in both humans and mice suggest that some sleep phenotypes differ between males and females, and reviews on the topic suggest that most of these differences depend on gonadal hormones (*Mong et al., 2011; Gervais et al., 2017; Dib et al., 2021*). For instance, even though women tend to have worst subjective perception of their sleep and higher risk for insomnia than men, quantitative measures suggest that women have a longer sleep duration and higher EEG power in delta, theta and high sigma (14-15Hz) frequencies during sleep (*Dijk et al., 1989; Carrier et al., 2001; Redline et al., 2004; Mongrain et al., 2005; Zhang and Wing, 2006; Bixler et al., 2009; Suh et al., 2018*). In contrast, most studies suggest that female mice have less total sleep and SWS (*Franken et al., 2006; Koehl et al., 2006; Paul et al., 2006; Ehlen et al., 2013; Sare et al., 2020*), which highly depends on gonadal hormones and the time of the day (*Paul et al., 2006; Ehlen et al., 2013; Cusmano et al., 2014; Swift et al., 2020*). Interestingly, the aforementioned sex differences in human sleep EEG oscillations seem to better correspond to sex differences found in rodents, as female mice show higher delta and sigma activity during sleep (*Franken et al., 2006; Koehl et al., 2006*), an effect which seems also modulated by gonadal hormones and time-of-day in rats (*Schwierin et al., 1998; Swift et al., 2020; Smith et al., 2022*). This suggests that even though some of the gonadal effects may differ between species, studies in rodents may help identifying sex differences in sleep or sleep variables that depend on gonadal hormones with relevance to human.

Moreover, it is important to highlight that some sex differences in sleep might be influenced by other factors such as age, genotype or disease. For example, sex differences in slow wave activity can be modulated by age in humans and rats (*Hume et al., 1998; Robillard et al., 2010; Luca et al., 2015; Kostin et al., 2020; Rosinvil et al., 2021*). Furthermore, the effects of some mutations differ between sexes: female mice knockout (KO) for *Npas2* (a circadian gene which will be discussed in section 1.3) have more SWS delta power than wildtype females, while KO males have less (*Franken et al., 2006*). Elevated levels of prenatal kynurenin (which is found elevated in schizophrenia and bipolar disorder), reduces REM sleep in the rat male offspring, but induced hyperarousal in females (*Rentschler et al., 2021*). An hypocretin receptor antagonist (receptor involved in the activation of wake-regulatory cells) was more efficient in inducing SWS in males than females of a mouse model of Alzheimer's disease (*Keenan et al., 2022*). These examples highlight that the treatment for some sleep disorders or other disease might depend on the sex, and that it is necessary to study drug efficacy in both sexes. Thus, females and males will be considered throughout the research presented in this thesis.

## 1.2 Brain systems controlling sleep

### 1.2.1. Brain circuits

The changes in EEG activity and sensory arousal thresholds that occur across vigilance states are achieved by activation/inhibition of a collective of brain nuclei, which also determines the transition between the three vigilance states (*Saper et al., 2005a; Jones, 2020*). The idea that different brain areas could have distinct control of arousal was raised by early studies showing that lesions in the hypothalamus and brainstem, but not thalamic lesions impaired wakefulness maintenance (*Von Economo, 1930*). Nevertheless, the development of optogenetics, chemogenetic and *in vivo* single cell imaging tools have revealed that these brain regions are often heterogenous and that particular cell types inside these regions dictate SWS, PS or wakefulness (*Jones, 2020*). As will be extended below, during wakefulness, wake promoting neurons induce/sustain wakefulness and/or inhibit sleep promoting centers. Sleep promoting neurons are active during sleep and can inhibit wake-promoting centers as well.

Wakefulness is maintained by the ascending arousal circuits (*Saper and Fuller, 2017; Jones, 2020*). In the dorsal arousal circuit, neurons from the reticular formation (mainly laterodorsal tegmentum (LDT), pedunculopontine tegmentum (PPT)) project to thalamic nuclei, which in turn send broad connections to the cortex and allow cortical activation (*Steriade et al., 1993; Cisse et al., 2018; Gent et al., 2018*). The ascending ventral pathway consist of neurons from the basal forebrain (BF), lateral hypothalamus (LH), and tuberomammillary nuclei (TMN), which not only induce cortical activation but also control state occurrence (*Adamantidis et al., 2007; Han et al., 2014; Anaclet et al., 2015; Fujita et al., 2017*). BF, LH, and TMN receive modulatory input from the reticular activating neurons (e.g., the locus coeruleus; LC) (*Samuels and Szabadi, 2008; Carter et al., 2012*). Principal sleep promoting neurons are GABAergic neurons in the hypothalamus, including the ventrolateral preoptic area (VLPO), the medial preoptic area (mPO), but also in the parafacial zone and GABAergic neurons of the basal forebrain, and they can contribute to inhibit wake-promoting centers (*Szymusiak et al., 1998; Suntsova et al., 2002; Modirrousta et al., 2004; Takahashi et al., 2009; Sakai, 2011; Anaclet et al., 2014*). Main PS-inducing neurons are neurons in the LDT and PPT, which allow cortical activation while behavioral sleep is maintained (*Shouse and Siegel, 1992; Van Dort et al., 2015*). Thus, the behavioral wake or sleep states result from the sum of the activity of multiple cell populations.

One of the most well characterized sleep/wake regulating center is the LH, which contains multiple neuronal populations involved in sleep regulation. LH hypocretin (Hcrt, or orexin) cells are crucial for wakefulness, given that their light-evoked activation induce arousal, and their inhibition induces cortical synchronization and SWS (*Adamantidis et al., 2007; Tsunematsu et al., 2011*). Furthermore, the firing rate of LH Hcrt<sup>+</sup> cells is higher during active wake, lower during quiet wake, becomes almost null during SWS and PS (with particular sporadic discharges in PS) (*Lee et al., 2005; Mileykovskiy et al., 2005*). They fire particularly high at the sleep to wake transition (*Lee et al., 2005*). Hcrt cells also received scientific attention given that their number is reduced in the brain of narcoleptic patients and Hcrt expression is reduced in the CSF in both narcolepsy and hypersomnia (*Thannickal et al., 2000; Ebrahim et al., 2003; Thannickal et al., 2009*). Moreover, Hcrt modulating drugs have been approved for insomnia and are under study for narcolepsy (*Michelson et al., 2014; Barateau and Dauvilliers, 2019*). Interestingly, Hcrt<sup>+</sup> cells in the LH are intermingled with another cell type having contrasting roles in sleep regulation: the melanin concentrating hormone (MCH) cells. MCH cells are almost silent during wake and have their maximum firing during PS (*Hassani et al., 2009*). Light-induced activation of MCH cells in the general hypothalamic region was shown to induce both SWS and PS, or solely PS, which likely depended on the duration of the stimulation, the MCH subpopulation targeted in the hypothalamus and/or the moment of stimulation (dark vs light period, or stimulation during wakefulness vs SWS) (*Jego et al., 2013; Konadhode et al., 2013; Tsunematsu et al., 2014; Blanco-Centurion et al., 2016; Varin et al., 2018*). In fact, the silencing of hypothalamic MCH neurons lowered the frequency and amplitude of hippocampal theta rhythm (*Jego et al., 2013*), and the inhibition MCH inputs into the ventrolateral periaqueductal gray (vlPAG) and the LPT reduced the number of transitions to PS (*Kroeger et al., 2019*). Moreover, Hcrt<sup>+</sup> and MCH cell types seem to respond to the time spent in wakefulness. While sleep deprivation (SD) increases the number of c-FOS<sup>+</sup> Hcrt cells, MCH c-FOS<sup>+</sup> cells increased with sleep recovery (*Modirrousta et al., 2005*). Moreover, SD reduces the apposition of glutamate transporter subtype 1 (GLT1 or EAAT2) on Hcrt<sup>+</sup> cells, but increases its apposition on MCH cells (*Briggs et al., 2018*). Interestingly, inhibition of MCH neurons exclusively during PS did not alter sleep architecture but impaired hippocampal-dependent memory (*Izawa et al., 2019*). In sum, research supports that Hcrt<sup>+</sup> cells are sufficient and necessary to induce wakefulness. In contrast, MCH cells are sufficient but unnecessary to modulate sleep, and they are required for adequate sleep.

Although the activation of wake/sleep-activating centers usually results in a change in the global vigilance state, more local and/or transitory sleep features have also been found in mammals (*Vyazovskiy et al., 2004; Vyazovskiy et al., 2011; Bersagliere et al., 2018; Thomas et al., 2020*). For example, transitions between wake and SWS or between SWS and PS show gradual changes of cortical activity reminiscent of the prior and/or emerging state (*Ferrara and De Gennaro, 2011; Bjorness et al., 2018*). Moreover, birds, dolphins and other aquatic mammals, have frequent uni-hemispheric sleep, especially during migrations (*Mukhametov, 1987; Rattenborg et al., 2016*). Interestingly, local increases in SWA in specific areas of the cortex have been found in rodents and humans (*Huber et al., 2004; Vyazovskiy et al., 2006*). Although these local regulations seem to follow the level of prior use (*Vyazovskiy et al., 2004; Vyazovskiy et al., 2011; Bersagliere et al., 2018; Thomas et al., 2020*), this suggests that sleep characteristics can be regulated locally, but that the sleep state requires an integrated change in brain state.

## **1.2.2 Molecular systems within circuits**

Previous sections cover how the transition between vigilant states and brain oscillations relies on coordinated neurotransmission. Accordingly, identifying which molecules and intracellular pathways drive cell responses in sleep-regulatory neuronal populations is crucial to understand the sleep behavior. This section presents animal research which, by modulating specific cellular elements with genetic or chemical approaches, proves that single proteins at the cell membrane and proteins of intracellular cascades can dictate sleep phenotypes.

### **1.2.2.1 Channels, receptors and adhesion molecules**

It is reviewed by us and others that components of cellular membranes including ion channels, receptors, adhesion molecules and components of the extracellular matrix may modulate sleep (*O'Callaghan et al., 2017; Ode et al., 2017a; Cooper et al., 2018*). Given the importance of neuronal communication and synchronization for sleep, it is unsurprising that ion channels which modulate the membrane potential are contributing to shape EEG activity during sleep and control alternations between sleep states. Ion channels involved in neuronal depolarization and hyperpolarization states may be especially relevant, because mice KO for voltage-gated  $\text{Ca}^{2+}$  channels (*Cacna1g, Cacna1h*) and  $\text{Ca}^{2+}$ -dependent  $\text{K}^+$  channels (*Kcnn2, Kcnn3*) show a shorter sleep duration (*Tatsuki et al., 2016; Ode et al., 2017a*). Voltage-gated  $\text{Ca}^{2+}$  channels (VGCC) are important for cortical and hippocampal oscillations and mouse KO for *Cacna1c* (subunit of L-type

VGCC) show reduced gamma activity (20–64 Hz) during wakefulness and PS, as well as decreased PS after SD (Hansen *et al.*, 2014; Kumar *et al.*, 2015; Plumbly *et al.*, 2019). *CACNA1C* polymorphisms have also been linked to sleep latency in infants (Kantojarvi *et al.*, 2017). Nevertheless, it remains to be defined whether the role of these channels in regulating the sleep latency or states duration relies exclusively on their function in specific cell types or neuronal populations. For example, recent research shows that the loss of voltage-gated K<sup>+</sup> channels *KCNQ2/3* in LH Hcrt neurons induce sleep fragmentation (Li *et al.*, 2022a).

Similarly, neurotransmitter receptors highly influence sleep characteristics. Gamma aminobutyric acid type A (GABA<sub>A</sub>) receptors have been extensively studied in sleep, and agonists, such as benzodiazepines, are important sedatives (Lancel, 1999; Winsky-Sommerer, 2009; Jones, 2020). Targeting these type A receptors have been suggested to target more thalamic and cortical neurons (Winsky-Sommerer, 2009). However, it should be investigated whether GABA<sub>A</sub> receptors agonist also modulate the effects of other GABAergic populations involved in sleep regulation, such as PS-modulating neurons in the PPT or wake-inducing GABAergic cells in the LH (Venner *et al.*, 2016; Kroeger *et al.*, 2017), or GABAergic neurons in the MS/DBB, which regulate theta activity and PS-dependent memory consolidation (Boyce *et al.*, 2016). Glutamatergic receptors are also involved in sleep regulation in a cell population-dependent manner. Glutamate or N-methyl-D-aspartate (NMDA) injections in the BF or TMN increases wake time, but injections in pontine regions induce cortical desynchronization and PS (see section 2.2 in Chapter 2 for details, Ballester *et al.*, 2021; Datta and Siwek, 1997; Manfredi *et al.*, 1999; Datta *et al.*, 2001; Yin *et al.*, 2019). Likewise, in line with the implication of dorsal and ventral arousal circuits, Hcrt, acetylcholine (ACh), serotonin and dopamine receptors modify sleep variables (see section 2.8 in Chapter 2; Jones, 2020). Receptor subtypes must not be neglected in the context of wake/sleep regulation. KO mouse models suggest that Hcrt receptor (HCRTR) 2 might be more involved in reducing SWS than HCRTR1, which is likely caused by the receptor distribution in sleep regulatory neurons (Mieda *et al.*, 2011). While single KO of *Chrm1* or *Chrm3* (genes for the cholinergic muscarinic receptors) reduced SWS time and induced PS fragmentation, *Chrm1/Chrm3* double-KOs had a complete abolishment of PS sleep (Niwa *et al.*, 2018). Similarly, noradrenaline in the BF excites ACh cells through Aα1Rs, but inhibits GABAergic neurons through Aα2Rs (Manns *et al.*, 2003); and serotonin (5-HT) receptor subtypes can have contrasting roles in sleep regulation (see section



2.8 in Chapter 2). Therefore, understanding the location and regulation of receptors should be as relevant as identifying ligand levels to fully comprehend the regulation of sleep behavior.

Cell adhesion molecules (CAMs) include immunoglobulin super family, integrins, cadherins, neuroligins/neuroleptins and Ephrins/Eph receptors, and their role in modulating synaptic strength and stability makes them relevant for sleep (*O'Callaghan et al., 2017*). Previous research from our group showed that the different mouse models KO for Neuroligin-1 (Nlgn1), Neuroligin-2 (Nlgn2) or the Eph receptor A4 (EphA4) have altered sleep architecture and EEG activity (*El Helou et al., 2013; Massart et al., 2014; Freyburger et al., 2016; Freyburger et al., 2017; Seok et al., 2018*). For instance, mice KO for *Nlgn1* (involved in NMDA receptor [NMDAR] recruitment) are sleepier than wildtype mice, and mice lacking *Nlgn2* (with roles in GABAergic neurotransmission) had more wakefulness than wildtypes (*El Helou et al., 2013; Seok et al., 2018*). Potential implications of EphA4 in sleep regulation will be discussed in section 1.4. In addition, as suggested by Cooper et al., the extracellular matrix also provides a structural environment for cell-cell interactions which may be relevant for sleep regulation, and this link remains mainly unexplored (*Cooper et al., 2018*). Moreover, it will be pertinent to investigate whether CAMs and other membrane molecules are implicated in sleep regulation via roles in particular sleep circuits or nuclei.

In conclusion, membrane components modulating synaptic strength and structure, neuronal responses and firing can determine sleep transitions, oscillations, as well as proper responses to sustained wakefulness. Even though the literature showcases the relevance of receptor subtypes for sleep physiology, there is scarce information on the relevance of different subtypes of adhesion molecules (e.g., different isoforms of Neuroligin 1) (*El Helou et al., 2013*). Furthermore, CAMs such as Nlgn1 or EphA4 have been linked to cognitive disorders such as major depressive disorder (MDD) or Alzheimer's disease (*Simon et al., 2009; Williams et al., 2009; Zhang et al., 2017; Dufort-Gervais et al., 2020; Li et al., 2022b*), and the sleep phenotypes described above may explain sleep disturbances or sleep comorbidities in these pathologies. Thus, understanding the relevance of cell components in sleep brain regulatory centers will contribute to identify not only new sleep mechanisms but also novel therapeutic avenues.

### 1.2.2.2 Intracellular pathways

Comparable to findings on membrane molecules, the levels and activation of intracellular components also appear to control sleep. As will be discussed in section 1.3.2.2, recent theories suggest that kinases and the phosphorylation levels of some proteins may be linked to sleep need and onset (*Honda et al., 2018; Wang et al., 2018b; Bruning et al., 2019; Ode and Ueda, 2020*). Related to some of the studies pointing at the relevance of ion channels and receptors for sleep regulation (see previous section), it is suggested that kinases that respond to intracellular  $\text{Ca}^{2+}$  levels may determine sleep duration given that mouse models KO for *Camk2a* and *Camk2b* (calcium/calmodulin-dependent protein kinase II alpha and beta) show a shorter time spent asleep (*Tatsuki et al., 2016; Ode et al., 2017a*). Moreover, the phosphorylation state of CaMKII $\beta$  determines sleep duration in mice (*Tone et al., 2022*). The loss or mutation of a phosphorylation site for PKA in the salt-inducible kinase 3 (SIK3; as well as SIK2 and SIK3) increases SWS (*Funato et al., 2016; Honda et al., 2018; Park et al., 2020*). Attention has also been given to extracellular signal-regulated kinases (ERK)1/2. Overexpression of activated ERK in drosophila increases SWS, but ERK1 or ERK2 KO mice have reduced SWS (*Vanderheyden et al., 2013; Mikhail et al., 2017*). Intracellular membrane adaptor proteins, which link membrane and intracellular responses, can also drive sleep control. Mice mutant for SHANK3 (SH3 and multiple ankyrin repeat domains 3) have less sleep time and SWA than wildtypes (*Ingiosi et al., 2019*). Therefore, the implication of membrane molecules in sleep regulation cannot be fully understood without identifying the triggered downstream pathways. All these studies mentioned have focused on knocking out these intracellular components in the full brain, and studies targeting specific brain regions and cell populations will be required.

### 1.3 The two-process model of sleep regulation

Sleep is a state controlled to maintain the equilibrium in diverse physiological functions, and which responds to the demands of previous body activity. Prolonged time in wakefulness or more energetically demanding waking-experiences will increase sleepiness and enhance sleep intensity in the next sleep phase (Franken *et al.*, 1991b; Deboer *et al.*, 1994; Vassalli and Franken, 2017) (see section 1.3.2). Nevertheless, the need for recovery is not the only factor dictating when to enter in a sleep state, as the internal circadian rhythm aligns the body functions (including sleep) to the 24-hour rhythm of the environment (see below). Borbély and Daan defined this interplay as the “two-process model of sleep regulation”, to illustrate how sleep is under a balanced regulation by both homeostatic and circadian processes (Borbély, 1982; Daan *et al.*, 1984) (Figure 1.2). They modelled the contribution of both processes, where sleep homeostasis (process S) increases according to time-spent awake and dissipates once the organism enters sleep, and where the circadian regulation (process C) oscillates reaching a peak of wake drive near the late active period. Today, even though current research suggests that other processes might contribute to regulate sleep (e.g., motivation) (Sotelo *et al.*, 2022), the strong implication of processes C and S has continued to be confirmed by the community (Curie *et al.*, 2013; Muto *et al.*, 2016; Vassalli and Franken, 2017; Wang *et al.*, 2018b).

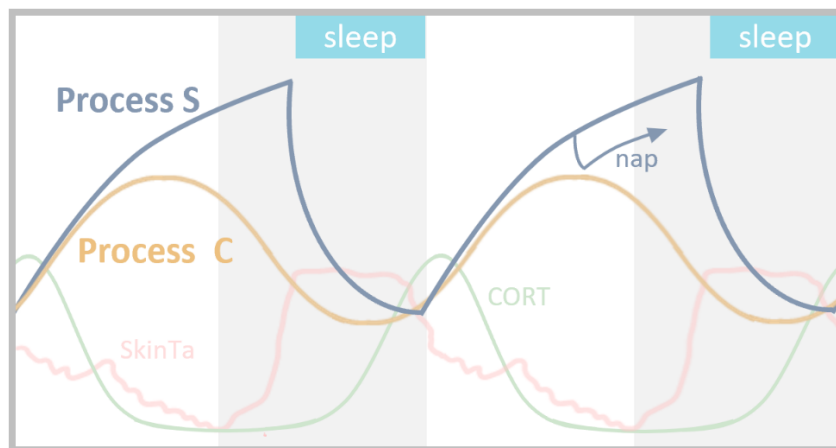


**Figure 1.2. The two-process model of sleep regulation.** Borbély and Daan proposed in 1982 that sleep need, sleep timing and sleep intensity are functions of two cooperative processes: sleep homeostasis (process S) and the circadian regulation (process C). Other processes, also regulated by processes S and C, also contribute to sleep regulation (e.g., temperature, corticosterone). Figure adapted from Borbély *et al.* (2016), Krauchi and Wirz-Justice (2001) and Oster *et al.*, (2017).

### 1.3.1 Circadian regulation (process C)

To adapt their biological functions to the environmental daily changes, organisms have developed internal circadian rhythms that oscillate with a close to 24-hour period. This circadian regulation is detected at the cellular level and is achieved by molecular feedback loops whose elements activate and repress in cycles (**Figure 1.3**). In mammals, circadian rhythms are regulated by a transcriptional translational feedback loop (TTFL) in which the proteins CLOCK (circadian locomotor output cycles kaput 1) and BMAL1 (brain and muscle Arnt [arylhydrocarbon receptor nuclear translocator]-like protein) bind in dimer to regulatory elements called E-boxes (e.g., CACGTG) to activate the transcription of the *Period* (*Per*) and *Cryptochrome* (*Cry*) genes (Gekakis *et al.*, 1998; Takahashi, 2017). Then, PER and CRY proteins form a complex with casein kinase (CK)1 $\delta$  and CK1 $\epsilon$ , translocate to the nucleus, and inhibit CLOCK and BMAL activity reducing, in consequence, their own transcription and allowing the loop to restart (Takahashi, 2017).

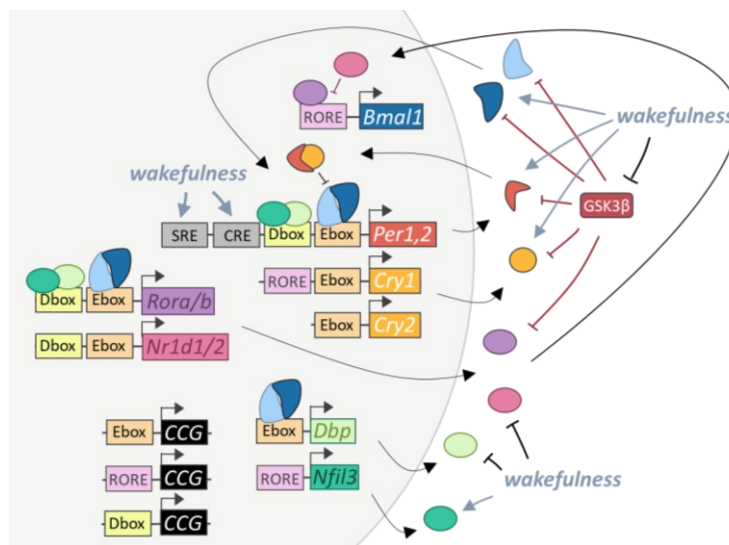


**Figure 1.3. The circadian TTFL and its many levels of regulation.** Circadian rhythms in mammals are maintained thanks to a self-sustained transcriptional translational feedback loop (TTFL). The clock transcription factors CLOCK (or its homologue NPAS2, light blue factors) dimerize with BMAL1 (or its homologue BMAL2) and activate transcription via regulatory elements called E-boxes (CACGTG or CANNTG). This induces the expression of other clock elements such as Periods (*Per*) and Cryptochromes (*Cry*). PER and CRY translocate to the nucleus and inhibit the transcriptional activation induced by CLOCK and BMAL1. Additional loops (e.g., REV-ERB $\alpha/\beta$  and ROR $\alpha/\beta/\gamma$  proteins [encoded by the *Nr1d1/2* and *Rora/b/c* genes] which act on RORE elements) and posttranslational modifications (e.g., phosphorylation by the glycogen synthase kinase 3 $\beta$  [GSK3 $\beta$ ]) adjust the period and amplitude of the rhythms. Figure adapted from Takahashi (2017).

This TTFL is expressed in most (if not all) cells of the body, and it cycles in the brain and peripheral tissues including the liver, lung, and skeletal muscle (Yamazaki *et al.*, 2000; Welsh *et al.*, 2004; Brancaccio *et al.*, 2017). In addition, mammals evolved a natural internal pacemaker that synchronizes the different tissues (and clocks) of the body to the light/dark changes of the environment, which is located in the suprachiasmatic nucleus (SCN) of the hypothalamus (Hastings *et al.*, 2018). These bilateral nuclei (each side composed of approximately 10,000 cells) are located above the optic chiasm and maintain a self-sustained rhythm of cell firing, Ca<sup>2+</sup> activity and gene expression (Noguchi *et al.*, 2017). These rhythms are “endogenous” because they persist even when isolating the SCN from external time cues or *in vitro*, which provides it with these unique pacemaker properties. Interestingly, endogenous circadian rhythms vary between species, strains and individuals (Pittendrigh and Daan, 1976; Schwartz and Zimmerman, 1990). The SCN rhythm runs in average a bit longer than 24 hours in human (~24.2 h) and a bit faster in *Mus musculus* strains (~23.5 h), but the nuclei receive multiple synchronizer signals (called *zeitgebers*) that aligns the SCN phase to the exact 24 hours of the environment (Schwartz and Zimmerman, 1990; Duffy and Wright, 2005). The most influencing *zeitgeber* (synchronizer) is the light/dark cycle of the environment, but other *zeitgebers* include temperature, food consumption and social interaction (Sharma and Chandrashekar, 2005). In fact, the SCN is particularly wired to respond to light: light stimulates retinal ganglion cells, which directly stimulates the SCN through glutamatergic and PACAP (pituitary adenylate cyclase activating polypeptide) release from the retinohypothalamic tract (Hannibal, 2002). This induces the raise of intracellular calcium in SCN neurons, and the activation of cAMP response element (CRE)-binding protein (CREB), which induces *Per* and *Cry* transcription (Gau *et al.*, 2002; Travnickova-Bendova *et al.*, 2002; Tischkau *et al.*, 2003). This triggers SCN neurons to have higher firing rates during the light period, and lower ones during the dark period, both in nocturnal and diurnal animals (Meijer *et al.*, 1997; Schwartz *et al.*, 2004; Vansteensel *et al.*, 2008), and provides to this retinohypothalamic-CREB signaling a fundamental role on resetting the circadian pacemaker (Meijer and Schwartz, 2003).

### 1.3.1.1 The circadian TTFL and clock-controlled genes

Although CLOCK, BMAL1, PER and CRY proteins compose the center of the circadian TTFL, this molecular engine has evolved additional loops which strengthen rhythmicity and/or provide additional regulation (Figure 1.3). Interestingly, CLOCK, BMAL1 and their respective homologues NPAS2 and BMAL2, vary in expression level across tissues and development (Zhou

*et al.*, 1997; DeBruyne *et al.*, 2007; Shi *et al.*, 2010; Wyse and Coogan, 2010; Ikeda and Ikeda, 2014; Landgraf *et al.*, 2016). Although the dimer CLOCK:BMAL1 (or homologues) have higher affinity for canonical E-boxes (i.e., CACGTG), they also recognize non-canonical E-boxes (CANNTG) and E'-box (CACGTT) (Gekakis *et al.*, 1998; Ueda *et al.*, 2005; Wang *et al.*, 2013). These elements are present, for instance, in promoters of components of these secondary loops, including the genes *Nr1d1* and *Nr1d2* (which encode the proteins REV-ERB $\alpha$  and REV-ERB $\beta$ ) and *Dbp* (D site albumin promoter binding protein) (Preitner *et al.*, 2002; Ripperger and Schibler, 2006; Yang *et al.*, 2013). REV-ERBs inhibit transcription via retinoic acid-related orphan receptor (ROR)-response elements (ROREs) and repress the expression of clock genes such as *Bmal1* or *Nfil3* (Mitsui *et al.*, 2001; Preitner *et al.*, 2002; Guillaumond *et al.*, 2005; Duez *et al.*, 2008; Dierickx *et al.*, 2022). In contrast, ROR $\alpha$ , ROR $\beta$  and ROR $\gamma$  compete for ROREs to (generally) induce transcription (Preitner *et al.*, 2002; Sato *et al.*, 2004). NFIL3 represses the activity of DBP via binding to D-boxes, which are found in *Nr1d*, *Ror* or *Per* genes (Mitsui *et al.*, 2001; Ueda *et al.*, 2005). In addition to this loop complexity, clock factors can be regulated by phosphorylation, acetylation, sumoylation and ubiquitylation; for example, by kinases like the glycogen synthase kinase 3 $\beta$  (GSK3 $\beta$ ) (Bellet and Sassone-Corsi, 2010). GSK3 $\beta$ , which is phosphorylated in a daily manner (Iwahana *et al.*, 2004; Besing *et al.*, 2015; Besing *et al.*, 2017; Bruning *et al.*, 2019), phosphorylates BMAL1, CRY2 and REV-ERB $\alpha$  and regulate their degradation (Harada *et al.*, 2005; Yin *et al.*, 2006; Sahar *et al.*, 2010).

Importantly, E-boxes, ROREs and D-boxes are found not exclusively in core clock transcription factors. Thus, clock factors also regulate the transcription of genes which are not necessarily involved in the TTFL (named “clock-controlled genes”), and that regulate the rhythmicity of physiological processes in mammals (Bozek *et al.*, 2009). For instance, the circadian clock may induce rhythmic levels of molecules involved in immune responses (e.g., cytokines) or synaptic transmission (e.g., receptors, CAMs) (Bozek *et al.*, 2009; Curtis *et al.*, 2014; Hannou *et al.*, 2020). We notably reviewed that the clock machinery controls the expression of synaptic components (see Hannou *et al.*, 2020). In particular, we and others have shown that neuroligins, the Eph/ephrin system, and the polysialylated form of neural cell adhesion molecule (PSA-NCAM), which are all involved in neurotransmission and neuroplasticity, are expressed in a time-dependent manner and regulate circadian or sleep behaviour (Glass *et al.*, 2000; Glass *et al.*, 2003; Prosser *et al.*, 2003; El Helou *et al.*, 2013; Massart *et al.*, 2014; Freyburger *et al.*, 2016;

*Freyburger et al., 2017; Kiessling et al., 2018; Seok et al., 2018*). Research from our lab suggests that some of these effects may be linked to the presence of E-boxes in CAM genes like neurologins (*El Helou et al., 2013; Freyburger et al., 2016; Hannou et al., 2018; Kiessling et al., 2018*). The potential control of *EphA4* transcription by the core clock factors was suggested by the finding of E-boxes in the *EphA4* putative promoter (*Freyburger et al., 2016*). This may indicate a potential rhythmic expression of *EphA4*, which will be further discussed in section 1.4 and is addressed throughout experiments in Chapter 4.

### **1.3.1.2 SCN outputs**

The SCN sends outputs to multiple brain and peripheral regions. Among these outputs, the lowered SCN activity during the night allows the nocturnal secretion of melatonin (*Reiter, 1991*). In addition, the SCN activity also influences the rhythms of glucocorticoids release, heart rate, vasodilation and the decrease in temperature that facilitate the induction of sleep in a circadian manner (*Moore and Eichler, 1972; Krauchi and Wirz-Justice, 2001; Arraj and Lemmer, 2006; Harding et al., 2018*). Both melatonin and glucocorticoids are suggested to modulate arousal/sleep rhythms (*Elder et al., 2014; Gandhi et al., 2015*). Glucocorticoids secretion follows a circadian rhythm dictated both by an adrenal-clock and the SCN (*Kiessling et al., 2014; Chung et al., 2017*). Glucocorticoids start to raise during sleep and peak just before the beginning of the active period (*Curie et al., 2013; Oster et al., 2017*). Melatonin regulates temperature and vasoconstriction reinforcing circadian regulation, and has important effects as antioxidant, on immune functions and metabolism (*Viswanathan et al., 1990; Krauchi et al., 1997; Pandi-Perumal et al., 2008; Cipolla-Neto et al., 2014*). Importantly, in contrast to other circadian modulators, melatonin raises during the dark period in both diurnal and nocturnal animals and has therefore acquired diverging roles (*Challet, 2007*). While melatonin is a sleep facilitator in humans, it is not in rodents (*Dollins et al., 1994; Huber et al., 1998*), which hinders melatonin translational research and its interpretation. Nevertheless, melatonin may regulate sleep via melatonin receptors present in sleep regulatory centers such as the VLPO, the LH and the TRN (*Ochoa-Sanchez et al., 2011; Sharma et al., 2018; Gobbi and Comai, 2019*). Moreover, the circadian system regulates sleep by sending direct SCN outputs to the subparaventricular zone, and preoptic areas (or to the LH indirectly) (*Abrahamson and Moore, 2001; Saper et al., 2005b*).

### **1.3.1.3 Some circadian variables are influenced by sex**

Circadian behavior might also be modulated by sex in humans and rodents (*Santhi et al., 2016; Dib et al., 2021*). The most frequent sex difference might concern the robustness of the circadian rhythm of locomotor activity (which is measured with lower interdaily variability). For instance, female mice have more variability in their activity onset (*Kuljis et al., 2013*). In addition, the daily rhythm of *Per1* and *Per2* in rat limbic or prefrontal cortex (PFC) regions was only significant for males, and time effect on *Bmal1* in the central and medial amygdala was different between sexes (*Chun et al., 2015*). Even though many of these differences seem to be explained by gonadal hormones, differences in brain structure may also regulate differently circadian or sleep behaviors (*Cahill, 2006; Brockman et al., 2011; Mong et al., 2011; Dib et al., 2021*). For example, the male SCN is bigger and contains more androgen receptors (*Kuljis et al., 2013; Kuljis et al., 2016*). Moreover, males have higher firing rate in the dorsal SCN during the light period (*Kuljis et al., 2013*). All these differences in SCN size and neuronal signaling may account for sex differences in circadian neuronal synchrony within the SCN and with other brain regions. Therefore, it is crucial to describe if the SCN functioning is similar in both sexes. The relevance of understanding whether protein components are distinct in female and male SCN will be considered in this thesis (Chapter 4).

### **1.3.1.4 Circadian control at the synapse**

Circadian rhythms of transcripts and proteins have been extensively documented. This section summarizes that cycling transcripts seem particularly relevant at the synapse, but that rhythmic protein activity should not be neglected (*Bruning et al., 2019; Noya et al., 2019*). Both mechanisms might contribute to provide oscillatory levels of molecules involved in neurotransmission and furnish circadian components of sleep regulation.

#### *1.3.1.4.1 Circadian regulation of the transcriptome*

Transcription is a way to control the presence of molecules in the synapse. On the one hand, core clock factors can regulate the expression of molecules involved in sleep regulation by directly acting on their E-boxes (*Hannou et al., 2020*). On the other hand, other cycling elements or CCGs might also induce rhythms in gene expression. Indeed, studies in the mouse liver show that 26% of the DNA binding of transcription factors (or DNA-binding proteins) follows a diurnal rhythms of different phases according to the molecular functions they trigger, and that RNA polymerase II is



recruited to promoters in a circadian manner (*Koike et al., 2012; Wang et al., 2018a*). The research community shows that 6-15% of genes oscillate according to circadian time in a given tissue and that 80% of protein coding genes show a 24-hour rhythm of expression in at least one tissue (*Panda et al., 2002; Storch et al., 2002; Maret et al., 2007; Menet et al., 2012; Zhang et al., 2014; Mure et al., 2018*). Thus, the circadian system seems a strong regulator of transcription. However, recent studies in the mouse forebrain revealed that while only 6% of transcripts from the full homogenate had a 24-hour rhythm of expression, 67% of transcripts from purified synapses were cycling (*Noya et al., 2019*). As suggested by the authors, this compartmentation must imply cyclic transportation and/or transcript stability. Interestingly, synaptic mRNA peaking before the dark/active periods were linked to synapse organization and transmission, while mRNA peaking before the resting period were linked to translation, lipid catabolism and cell morphology, proliferation or development. This time-segregation of functions goes in line with the compartmentation suggested for the cycling synaptic proteome and phosphoproteome (see following section). The Brown lab also showed that 30% of the oscillating transcripts in synapses remained cyclic after SD (*Noya et al., 2019*), proving that this mRNA does not oscillate because of typical wake/sleep distribution across the 24 hours. In sum, research reinforces the many transcripts cycle particularly at synapses, even if the circadian transcription might still be crucial to regulate the expression of some molecules in other cell compartments of particular brain regions. This division between the synapses and other cell compartments highlights the importance of identifying cyclic posttranscriptional modifications, which has already been suggested with 24-hour regulation of polyadenylation tail length or 3' untranslated regions (3UTR) (*Robinson et al., 1988; Kojima et al., 2003*).

#### *1.3.1.4.2 Phosphorylation as accumulative (and time) sensors*

Phosphorylation is also central in circadian regulation. To begin with, it is one of the main posttranscriptional modifications regulating the mammal core clock proteins (*Bellet and Sassone-Corsi, 2010*). In fact, the circadian clock in cyanobacteria does not rely on transcriptional loops but on the cyclic phosphorylation of its components (*Tomita et al., 2005*). Furthermore, it is suggested that the serial phosphorylation of multiple residues of CRY may function as an accumulative timer and determine the period length in mice (*Ode et al., 2017b*). Recent studies with mathematical models also support that additive phosphorylation might help increase the robustness of biological oscillations (*Tyler et al., 2022*). Interestingly, the diurnal binding of transcription factors to DNA

seems to depend more on its phosphorylation state than on its nuclear protein levels (*Wang et al., 2018a*). In fact, 24-hour rhythm is found in 11.7% of the proteome, 30% of phosphopeptides and 50% of phosphoproteins in mouse forebrain synapses (*Bruning et al., 2019; Noya et al., 2019*). The active state of proteins peaks just before the light or dark periods transitions, suggesting that they prepare the molecular environment for the activity or rest. For example, kinases involved in excitatory synaptic activity and LTP (CAMKII $\alpha$ , CAMKII $\gamma$  and PKC-linked kinases) peaked at the sleep-to-wake transition, whereas DCLK1 and ABL2 kinases (more linked to inhibitory synaptic activity) peaked at the wake-to-sleep transition (*Bruning et al., 2019*). Nevertheless, the Brown lab also demonstrated that, in contrast to the mouse brain synaptic transcriptome (whose majority remained cyclic after SD), the cycling of its synaptic phosphoproteome is 98% abolished after SD (*Bruning et al., 2019; Noya et al., 2019*). This indicates that the synaptic phosphorylation is mainly sleep/wake driven and less circadian-driven. Whether this rule applies to all brain regions, or if the cycling of the non-synaptic phosphoproteome is less alterable by sleep/wake (e.g., by SD protocols), still has to be defined. This demonstrates that some cellular processes are under both circadian and sleep regulations, but that the contribution of each factor can vary. The complexity of these sleep-circadian interactions will be discussed in section 1.3.3.

In conclusion, analysing both the circadian transcription and protein regulation provides a set of mechanisms for time-dependent neuronal functions. Furthering its description may provide mechanisms underlying some circadian regulation of sleep and may be relevant for chronotherapy. In this thesis, circadian transcriptional regulation of synaptic components will be investigated in Chapter 4, and pathways underlying sleep regulation at different times of the day will be inquired in Chapter 5.

### **1.3.2 Homeostatic regulation (process S)**

Sleep is defined to be under homeostatic regulation because prolonged time in wakefulness or more demanding waking-experiences increase the need for sleep (sleep pressure) and sleep intensity in the subsequent sleep period, while the quality of sleep determines performance in the next wake episode (*Franken et al., 1991b; Deboer et al., 1994; Nishida et al., 2009; Holz et al., 2012; Binder et al., 2013; Boyce et al., 2016; Vassalli and Franken, 2017; Peyrache and Seibt, 2020; Milinski et al., 2021*). The most explicit evidence of the homeostatic sleep regulation is detected at the level of sleep oscillations in the EEG, and it is most evident in the SWS slow wave

activity (SWA) (Deboer, 2015). Sleep pressure (and SWA) builds-up with the time spent awake (or with sleep deprivation) and according to cognitive demands of the waking experience (Dijk et al., 1987a; Dijk et al., 1987b; Franken et al., 1991b; Huber et al., 2004; Vassalli and Franken, 2017). Thus, SWA is higher at the beginning of the sleep period and dissipates along the course of sleep (Dijk et al., 1990; Hubbard et al., 2020). Moreover, napping during the active period reduces SWA in subsequent sleep (Werth et al., 1996; Cajochen et al., 2001). In fact, the increase in neuronal synchronization in slower frequencies after sleep deprivation has been shown in fish, drosophila and birds (detected by changes in calcium activity, voltage activity and EEG, respectively; Martinez-Gonzalez et al., 2008; Leung et al., 2019; Raccuglia et al., 2019), supporting that this homeostatic increase in synchronized slow activity is an intrinsic property of sleep. Moreover, the more SWA, the more difficult it is to awaken a subject (Blake and Gerard, 1937). Importantly, faster delta activity, called delta-2 (2.75-4Hz), has been recently more closely associated to the homeostatic response to sleep deprivation than the slower delta-1 (< 2Hz), which seems to be more reflecting the circadian regulation (Borbely et al., 1981; Hubbard et al., 2020). In fact, sleep need or sleep propensity (likelihood of falling asleep) is more reliably correlated with an increase in sleep intensity (defined by enhanced SWA in SWS) than sleep time (Borbely, 1982; Franken et al., 1991b; Franken et al., 1991a). Accordingly, SWA is considered the most reliable marker of homeostatic sleep pressure.

### **1.3.2.1 Potential mechanisms underlying sleep homeostasis**

As described in section 1.3.1, the brain center (SCN) and molecular basis (the clock TTFL) underlying the circadian regulation of sleep are quite well described. Intriguingly, a main mechanism driving the homeostatic regulation of sleep has not been identified. This section describes that multiple mechanisms may respond to sustained wakefulness (such as accumulated (or depleted) molecules footprint), which may all contribute in redundant manners to activate/inhibit sleep/wake-inducing neuronal populations. Some sleep regulatory substances (SRS; secreted molecules that modulate sleep) have been proposed (Krueger et al., 2008). On the other hand, genetic and protein markers known to accumulate during specific sleep or wake states can help identify processes underlying the regulation of arousal or sleep-distinctive processes (O'Callaghan et al., 2019).

#### 1.3.2.1.1 Sleep regulatory substances

Given that wakefulness is characterized by increased behavioral activity, the time spent awake is often correlated with increased cellular activity and energy consumption (e.g., oxidative levels, brain glucose consumption) in both the brain and peripheral tissues (Maquet et al., 1990; Periasamy et al., 2015; Kempf et al., 2019). Accordingly, wake-linked cellular activity in different tissues such as brain and muscle, leads to the accumulation of molecules resulting from metabolism or neurotransmission, which include adenosine, nitric oxide (NO), prostaglandin D<sub>s</sub>, interleukin-1 $\beta$  (IL1 $\beta$ ), tumor necrosis factor  $\alpha$  (TNF $\alpha$ ), growth hormone releasing hormone (GHRH), and neurotrophins such as brain-derived neurotrophic factor (BDNF) and nerve growth factor (NGF) (Obal and Krueger, 2003; Krueger et al., 2019). For instance, different natures of behavioral activity (e.g., object exploration, physical activity), external stimuli and/or neuronal activity increase adenosine secretion and protein levels of BDNF in the cortex and hippocampus, or the number of NGF<sup>+</sup> and IL1 $\beta$ <sup>+</sup> cells in the rat somatosensory cortex (Latini and Pedata, 2001; Huber et al., 2007; Hallett et al., 2010; Hsiao et al., 2014). Similarly, SD in rats rises the protein levels of IL1 $\beta$ , IL6, TNF $\alpha$  in the hippocampus, BDNF and NO levels in BF neurons, and adenosine release in the cat BF, PO, cortical and thalamic regions (Porkka-Heiskanen et al., 2000; Kalinchuk et al., 2010; Wadhwa et al., 2017; Ma et al., 2020). SD also increases the number of NGF<sup>+</sup> cells in rat somatosensory cortex, and decreases GHRH release in the rat hypothalamus (Gardi et al., 1999; Brandt et al., 2001). ATP is co-released with neurotransmitters and will activate purine type 2 receptor 7 (P2X7R) in glia, while some is converted into adenosine (Hide et al., 2000; Latini and Pedata, 2001). P2X7R activation induces IL1 $\beta$  and TNF $\alpha$  release, which in turn activates nuclear factor kappa B (NF- $\kappa$ B) (inducing NO, adenosine and the transcription of neurotransmitter receptors) (Hide et al., 2000; Suzuki et al., 2004; Krueger et al., 2008). These molecules are considered SRS not only because they increase with sleep need but also because they induce sleep. For example, adenosine perfused by microdialysis into BF or LDT induces sleep (Strecker et al., 2000), and GHRH or TNF injected into the PO induces sleep (Zhang et al., 1999; Kubota et al., 2002). IL1 $\beta$  injected intracerebroventricularly, or directly into the LC or DR induces sleep as well (De Sarro et al., 1997; Manfredi et al., 2003; Baker et al., 2005). Drugs modulating NO (which, together with adenosine, TNF and IL1, is a vasodilator) also modify sleep (Kapas et al., 1994; Kapas and Krueger, 1996). In addition, IL1 $\beta$ , TNF $\alpha$ , GHRH or BDNF injected in rat somatosensory cortex also enhance delta activity during SWS (Yoshida et al., 2004; Yasuda et al.,

2005; Szentirmai et al., 2007; Faraguna et al., 2008). Caffeine (an adenosine-receptor antagonist and NO-synthase inhibitor) importantly decreases SWA (Landolt et al., 1995). Thus, sleep regulatory neurons may integrate information about the levels of behavioral and neuronal activity. Pathways involved in the cellular response to SRS need to be investigated in sleep regulatory centers. For example, different receptors for SRS might provide additional levels of sleep regulation, like the adenosine receptors, the famous target of caffeine (Hong et al., 2005; Huang et al., 2005; Lazarus et al., 2011).

#### 1.3.2.1.2 Gene expression reflects sleep-wake history

Sleep-dependent changes in gene expression have provided an important window to processes linked to sleep homeostasis (see section 1.3.2.3). The first study that reported transcriptional differences between sleep or wake states showed that nuclear mRNA in rabbit cerebral cortex is two-fold increased during sleep, while its proportion reduces in the cytoplasm (Giuditta et al., 1980). Ensuing microarray studies suggested that the sleep state determines the expression of 4.9% of the genes in the cerebral cortex (Cirelli et al., 2004). Accumulated research with microarray and transcriptomics in the rat and mouse brain demonstrate that, relative to sleep, wakefulness or SD induces expression of genes linked to neuronal activity such as immediate early genes (IEGs)/transcription factors (e.g., *Fos*, *Arc*, *Homer1a*, *Chop*, *Ier5*, *Egr1* [NGFI-A], *Nr4a1* [Nur77, NGFI-B], *Egr2* (*Krox-20*), *N-ras*, *Stat3*); stress responses such as the unfolded protein response or apoptosis (*Bip*, *Erp72*, *Grp75*, *Hsp60*, *Hsp70*); neurotransmission (genes for synaptotagmins, neurotransmitters, receptors); positive regulation of transcription (*Fos*, *Nr4a1*, *Creb*, *Crem*), metabolism (*Slc2a1*, *Vgf*), growth factors (*Bdnf*, *Trkb*), intracellular kinases (*Jnk*, *Sgk1*) and circadian proteins (*Per1*, *Per3*, *Dbp*, *Cry*, *Cirbp*, *Nr4a1*, *Nr4a3*) (Cirelli and Tononi, 2000; Cirelli et al., 2004; Terao et al., 2006; Mackiewicz et al., 2007; Mongrain et al., 2010; Vecsey et al., 2012; Bellesi et al., 2013; Massart et al., 2014; Husse et al., 2017; Narwade et al., 2017; Guo et al., 2019; Hor et al., 2019; Gaine et al., 2021) (see **Annex Table A1**). Genes that have been the most consistently associated with wakefulness in multiple studies include *Homer1a*, *Arc*, *c-fos*, *jun-b*, *Egr1-3*, *Glut1*, *Bdnf*, *Nr4a1*, *Bip* (GRP78), *Hsp27*. On the other hand, sleep has been shown to also increase transcription of genes linked to a negative regulation of transcription (*Nf1*, *Id2*); a positive regulation of translation (*Eif2b*, *Eif4e2*), to synaptic hyperpolarization (calcineurin, *Camk*, *Kcnk1*, *Kcnk2*); but also to GABAergic signaling (*dlg3*, *gephyrin*); lipid

metabolism; and membrane trafficking (Cirelli *et al.*, 2004; Mackiewicz *et al.*, 2007; Vecsey *et al.*, 2012; Narwade *et al.*, 2017).

Transcriptomics research is also revealing SD effects on different cell types such as oligodendrocytes (Bellesi *et al.*, 2013) or specific tissues or brain regions, such as the hippocampus (Husse *et al.*, 2017; Oyola *et al.*, 2019; Wei, 2020; Gaine *et al.*, 2021). Specific PS-deprivation also modifies the brain and pituitary transcriptome, which particularly affected IEGs and genes linked to the stress responses (Narwade *et al.*, 2017; Oyola *et al.*, 2019). Therefore, even though previous sections described that transcripts oscillate in a time-dependent manner, this section stresses that sleep:wake history have a robust impact on gene expression, and that transcriptomics is an advantageous tool to screen for molecular pathways underlying sleep pressure or sleep functions. In fact, studies comparing the effect of SD on mouse gene expression reveal physiological aspects of sleep which could be relevant for ageing, Alzheimer's disease or other conditions (Guo *et al.*, 2019; Wei, 2020; Li *et al.*, 2022a). Nevertheless, other techniques also provide insights into how sleep and wake modify transcription. For instance, changes in chromatin accessibility in the murine cortex showed genes and gene functions affected by SD in agreement with transcriptomic studies (Hor *et al.*, 2019).

It is important to note that SD effects may be difficult to separate from the stress induced by keeping animals awake in some SD protocols, which have been shown to raise glucocorticoid levels in a mouse-strain dependent manner (Tartar *et al.*, 2009). This was addressed by Mongrain *et al.*, which contrasted the effects of SD in adrenalectomized (ADX) mice (Mongrain *et al.*, 2010). In that experiment, 68% of transcriptional changes induced by SD were glucocorticoid-dependent (e.g., clock genes or genes linked to cell metabolism and stress responses), while markers related to synaptic plasticity (e.g., *Fos*, *Arc*, *Egr1*, *Nr4a1*, *Homer1a*) were similarly affected by SD in ADX mice (Mongrain *et al.*, 2010). In addition, the technique used to sleep deprive the animals may also impact the wake-induced transcriptome. In fact, the expression of some genes (e.g., *c-fos*, *BIP/GRP78*) was more increased by SD induced by cage change than SD induced by gentle handling (Suzuki *et al.*, 2013). Therefore, experiments comparing the transcriptome after enhancing sleep with techniques other than SD, like we show in Chapter 5, can provide important complementary findings regarding which changes in gene expression are consistently modified with sleep need or sleep duration.

#### 1.3.2.1.3 *The phosphorylation hypothesis of sleep*

The times spent in sleep or wakefulness affects molecular pathways involved in neurotransmission (Abel et al., 2013; Puentes-Mestril and Aton, 2017). Recent studies revealed that the time spent in wakefulness is reflected at the protein phosphorylation level in the brain, suggesting that the accumulated level of phosphorylation or dephosphorylation could be involved in enhancing subsequent sleep. This has been presented as the “Phosphorylation hypothesis of Sleep” (Wang et al., 2018b; Bruning et al., 2019; Ode and Ueda, 2020). SD modifies the global phosphorylation levels in the mouse brain, increasing or decreasing it according to the phospho-sites and function of the kinase (Wang et al., 2018b; Bruning et al., 2019). Most strikingly (and as mentioned in section 1.3.1.4.2), only 1% of proteins, 2.3% of the phosphopeptides and 4.8% of the phosphoproteins found to be cycling under baseline, also cycled after SD, demonstrating that the phosphorylation state of the synapse is more dependent on wake/sleep than the circadian system *per se* (Bruning et al., 2019; Noya et al., 2019). Interestingly, as discussed in section 1.2.2, mouse mutants for specific phosphorylation sites of CaMKII or SIK have altered sleep duration, reinforcing the potential relevance of phosphorylation states to sleep control. This can be relevant for the regulation of membrane molecules such as EphA4, whose downstream pathways depend on its phosphorylation (discussed in section 1.4).

In conclusion, transcriptomic, proteomic and phosphoproteomic studies suggest that wakefulness is linked to molecules and processes related to synaptic functioning, cell metabolism and stress responses, while functions related to inhibitory signaling and protein synthesis become more activated during the sleep phase. The cycling of these cellular pathways seems strongly controlled by wake/sleep.

#### 1.3.2.2 **Sleep for the brain and the synaptic homeostasis hypothesis (SHY)**

If sleep would not account for process that cannot occur in quiet wake (rest), it might not have overcome the evolutionary cost of reducing arousal thresholds (Cirelli and Tononi, 2008). The field suggests that the environmental disconnection characteristic of sleep allows cognitive processes impossible to meet by the awake brain, which receives more (and more stochastic) stimulation. In 2003, Cirelli and Tononi proposed that, while wakefulness tends to an overall strengthening of synapses, sleep (particularly SWS) is accompanied with a homeostatic overall decrease in synaptic strength (Tononi and Cirelli, 2003, 2006, 2012). This overall downscaling

would benefit the nervous system in energetic (to decrease strength in less necessary synapses) and space (to leave room for more relevant synapses) terms. The authors defined it as SHY or the synaptic homeostasis hypothesis of sleep. Although multiple nuances due to supplementary discoveries now decorate this hypothesis, SHY continues being a main line of thought in sleep research claiming that sleep allows homeostatic synaptic regulation for adequate behavioral adaptations, including memory consolidation (*Poe et al., 2000; Wang et al., 2018b; Frank and Heller, 2019; Niethard and Born, 2019; Havekes and Aton, 2020; Thomas et al., 2020; Cirelli and Tononi, 2022*).

SHY is based on the observation that wakefulness increases and sleep decreases i) the size of synaptic apposition in rat CA1 and sensory and motor cortex (*de Vivo et al., 2017; Spano et al., 2019*), ii) the amplitude of miniature excitatory postsynaptic current (mEPSCs) in mouse and rat frontal cortex (*Liu et al., 2010; Bjorness et al., 2020; Khilghatyan et al., 2020*), and iii) GLUA1-containing AMPAR ( $\alpha$ -amino-3-hydroxy-5-methyl-4-isoxazole propionic acid receptors) in the synaptic membrane in rat cortex and hippocampus (*Vyazovskiy et al., 2008; Diering et al., 2017*). Hebbian plasticity (selective potentiation of used synapses over less required ones) and non-Hebbian plasticity (overall regulation of synapses as a function of general input) might both contribute to the overall postulate of SHY, but the mechanisms are not fully understood (*Cirelli and Tononi, 2022*). It has been suggested that the SWA up and down states or SWS sharp-wave ripples may facilitate the synaptic renormalization (*de Vivo et al., 2017; Gulati et al., 2017; Norimoto et al., 2018*). However, synapse removal can also occur during PS (*Li et al., 2017*). Additionally, research supports that sleep potentiates or downscales synapses depending on their use and brain region. For example, place cells reactivate during PS and the locking of their firing to the theta phase is indicative of synaptic strengthening (*Poe et al., 2000*), and the neuronal firing in the visual cortex induced by monocular deprivation was enhanced during PS in cats and mice (*Dumoulin Bridi et al., 2015; Clawson et al., 2018*). Indeed, in the mouse motor cortex and rat frontal cortex, sleep induces synaptic strengthening only at selected synapses according to previous wake activity, without entailing a global change in all the spines of a cell (*Yang et al., 2014; Watson et al., 2016*). In sum, sleep allows synaptic remodeling in a usage and brain-region dependent manner. Understanding this synaptic regulation is fundamental given that changes in synaptic plasticity occurring during sleep have been correlated with learning (*Miyamoto et al., 2021*).



#### 1.3.2.2.1 Potential mechanisms underlying sleep-dependent plasticity

Sleep-induced synaptic downscaling has been linked to the removal of AMPAR, which are key regulators of synaptic strength. Synaptic surface GLUA1 and its Ser845 phosphorylation (which are known to be promoted by synaptic activity and induce potentiation) is lower in sleep than wake and SD in rat cortex and hippocampus (*Hinard et al., 2012; Diering et al., 2017*). One of the suggested mechanisms underlying these observations is the myocyte enhancer factor 2 (MEF2) transcription factor, which is known to trigger *Arc* and *Homer1a*, two transcripts very consistently upregulated by SD (see section 1.3.2.1.2) (*Bjorness et al., 2020*). MEF2 transcriptional activity increases during glutamate release and wake, and it gets dephosphorylated (indicative of enhanced activation) during SD (*Flavell et al., 2006; Bjorness et al., 2020*). *Homer1a* is increased by neuronal stimulation (e.g., by glutamate or bicuculine), and it interacts in post-synaptic scaffolds regulating mGluRs activity (*Tu et al., 1998; Ango et al., 2001; Inoue et al., 2007; Hu et al., 2010*). *Arc* expression is also increased in synapses with neuronal stimulation (e.g., by electrical stimulation, mGluR activation, novel experience), and it is thought to mark less used synapses: it remains untranslated until mGluRs are activated (*Steward et al., 1998; Jakkamsetti et al., 2013*). ARC regulates the homeostatic GLUA1 levels at the synapse (*Shepherd et al., 2006*). It has been suggested that these mechanisms might be involved in sleep-dependent memory consolidation, and mGluRs and AMPAR have been involved in sleep-dependent cognitive processes (*Diering et al., 2017; Miyamoto et al., 2021*). On the other hand, processes of sleep-dependent synaptic potentiation have been linked to LTP, NMDAR, PKA and ERK signaling (*Aton et al., 2009; Dumoulin et al., 2015*). Therefore, transcription and intracellular kinases play key roles not only in modulating sleep regulation but also in regulating sleep-dependent processes. Moreover, other synaptic components discussed in previous sections and shown to modulate sleep, are also involved in synaptic plasticity and may control sleep-dependent processes (e.g. CaMKII, CAMs). For instance, GSK3 $\beta$  activation (which depends on the sleep:wake history in the hippocampus) regulates sleep-dependent plasticity (*Vyazovskiy et al., 2008; Benedetti et al., 2012; Xue et al., 2019*). Therefore, it will be relevant to further describe roles of EphA4 in sleep, given that this CAM can regulate AMPAR and can be cleaved from the membrane by activity dependent mechanisms (*Inoue et al., 2009; Fu et al., 2011*). The synaptic molecular milieu is thus relevant not only for promoting a direct regulation of sleep characteristics (sleep time, EEG frequencies) but also to optimize sleep functions.

### 1.3.3 Integrations of processes C and S

The beginning of section 1.3 describes how sleep quality and quantity are a function of the combined regulation by C and S. Even though brain regions and molecular underpinning for both processes have been presented in a segregated manner, their contribution is rarely limited to only one of the two. Research suggests that the integration of processes C and S is done at the circuit-molecular interface. Previous Section 1.3.1 had summarized how SCN outputs regulate sleep-regulatory circuits, whereas section 1.3.2 described some SRS which can modulate SCN responses as well (*Jagannath et al., 2021*). In this section, research suggesting that some molecules may be under both circadian and wake/sleep regulation will be covered. These could represent important hubs of both processes.

#### 1.3.3.1 Molecular integration of C and S

Some of the most striking examples of converged C and S interplay is the implication of core clock factors on sleep regulation. As compiled in section 1.3.2., the gene expression of clock factors is consistently affected by SD (*Cirelli et al., 2004; Maret et al., 2007; Mongrain et al., 2010; Curie et al., 2013; Massart et al., 2014; Husse et al., 2017; Guo et al., 2019; Oyola et al., 2019; Gaine et al., 2021*). In fact, the effect of SD on *Clock* and *Npas2* gene expression was modelled to be stronger than the circadian component in the mouse cerebral cortex (*Hor et al., 2019*). Interestingly, clock factors like BMAL1 and DEC2 (a transcription factors repressing E-box-induced transcriptional activation) modify sleep and the response to sleep deprivation (*Franken and Dijk, 2009; Yu et al., 2014; Hirano et al., 2018*). Clock transcription factors may directly affect the expression of peptides highly linked to sleep regulation. For instance, BMAL1 regulates the rhythmic levels of histamine in tuberomammillary neurons, which are wake promoting cells (*Yu et al., 2014*). Similarly, DEC2 represses the transcription of pre-Hcrt mRNA in the LH and regulates sleep (*Hirano et al., 2018*). Therefore, as suggested by omics studies and *Jan et al.*, clock factors outside the SCN might integrate signaling both from sleep pressure and from the cell endogenous rhythm (*Curie et al., 2013; Curie et al., 2015; Jan et al., 2020*) (**Figure 1.3**). In fact, the effect of SD on *Per2* and *Dbp* highly depended on the time-of the day (*Curie et al., 2013*). Our review on how synaptic components might be under direct regulation by the core clock machinery (*Hannou et al., 2020*), would suggest that the clock machinery may provide an integrated S and C control on the synaptic landscape. Similarly, Ode and Ueda discuss that sleep-dependent kinases seen in section 1.3.2.1.2 may be implicated in the robustness of SCN oscillations by phosphorylating

CLOCK and PER2 (Kon *et al.*, 2014; Hayasaka *et al.*, 2017; Ode and Ueda, 2020). In fact, as highlighted in previous sections, GSK3 $\beta$  modulates sleep and circadian rhythms, show daily oscillations and is linked to SD responses (Benedetti *et al.*, 2004; Iwahana *et al.*, 2004; Iitaka *et al.*, 2005; Bellet and Sassone-Corsi, 2010; Lavoie *et al.*, 2013; Bruning *et al.*, 2019). Thus, GSK3 $\beta$  might be an important integrator which has been reported to have more than 100 substrates (Beurel *et al.*, 2015). Similarly, the effects of some SRS may depend not only on sleep pressure but also on the time of the day. For example, IL1 induces sleep in rats during the dark period, but promotes wakefulness in the light period (Opp *et al.*, 1991).

In sum, *sections 1.2 and 1.3* expose that the balance of molecular components involved in neurotransmission can modulate sleep characteristics such as duration, state transitions, sleep EEG and sleep-dependent plasticity. Levels of mRNA, synaptic protein and/or protein phosphorylation might be an accumulative method to mark sleep need (or surplus) and/or time. Nevertheless, it remains to be identified which processes integrate S and C regulations and whether these processes are common throughout the brain (and potentially other tissues). In addition, some circadian and sleep processes might be more relevant at the synapse than other cell compartments or in a cell-type dependent manner (e.g., glia vs excitatory vs inhibitory neurons). Identifying synaptic components which may be regulated by both circadian and homeostatic components (e.g., clock factors) might help reveal new ways by which C and S are integrated. Here, we propose that the Eph/Ephrin system is a candidate that may be under both circadian and sleep regulation, and which might control both sleep and circadian rhythms. The following section will describe this family of CAMs and its potential implication in circadian and sleep behavior.

## 1.4 Ephrins and Eph receptors

The erythropoietin-producing hepatocellular (Eph) receptors and their ligands Ephrins (Efn) form a system of transmembrane CAMs, and the largest family of receptor tyrosine kinase (RTK) (*Yeung et al., 2021*). A particularity of this system, in contrast to other RTK, is that both ligands and receptors are anchored to the membrane, which provides them with dynamic properties for cell-to-cell communication and roles in multicellular organisms. Duplications of *Eph/Efns* genes in evolution allowed a myriad of different affinities and complex regulations of these receptors and ligands (*Arcas et al., 2020*). In mice and human, there are 9 EphA (EphA1-8, EphA10), 5 EphB (EphB1-4, EphB6), 5 Ephrins-A (EfnA1-5) and 3 Ephrins-B (EfnB1-3) (*Drescher, 2002; Arcas et al., 2020*). They are classified in these four groups based on the conservation of their sequences and ligand affinities. While most EphA receptors have affinity for Ephrins-A, and EphBs have more affinity for Ephrins-B, EPHA4 has affinity for both (except for EFNB1) (*Flanagan and Vanderhaeghen, 1998; Bowden et al., 2009; Qin et al., 2010*). Indeed, EfnA and EfnB ligands can induce the phosphorylation of EPHA4 (*Flanagan and Vanderhaeghen, 1998; Murai et al., 2003; Qin et al., 2010*).

Eph receptors are composed of an extracellular ligand-binding domain, a transmembrane and an intracellular domain (*Liang et al., 2019*). The extracellular domain includes an N-terminal ligand-binding domain, a cysteine-rich domain and two fibronectin type III repeats. The intracellular domain includes the tyrosine kinase domain, a C-terminal sterile alpha-motif (SAM), and a PDZ-binding domain (*Arcas et al., 2020*). In contrast, Ephrins are smaller. Both Ephrins-A and B have an extracellular N-terminal receptor-binding domain. Ephrins-A attach to the cellular membrane by a glycosylphosphatidylinositol (GPI)-anchor domain (*Arcas et al., 2020*). Ephrins-B contain a transmembrane domain and an intracellular PDZ-binding domain (*Lin et al., 1999*). The binding of Ephrin to receptors induces a conformational change that transduces intracellular forward (through Eph domains) and/or reverse signaling (via Ephrin domains) (*Pasquale, 2010; Murai and Pasquale, 2011*). On the forward signaling, the binding can induce receptor oligomerization and/or regulate the levels of intracellular Eph phosphorylation and protein interactions (*Pasquale, 2005*). EfnB ligands can also interact through their PDF domain and be

regulated by Src phosphorylation (Torres *et al.*, 1998; Bruckner *et al.*, 1999; Cowan and Henkemeyer, 2001; Palmer *et al.*, 2002).

Eph receptors are expressed in multiple tissues, including epithelial and blood cells, myocytes, neurons, and glia (Gale *et al.*, 2001; Murai and Pasquale, 2003; Stark *et al.*, 2011; Matsuo and Otaki, 2012; Huang *et al.*, 2016). Importantly, Eph and Ephrins have different pattern of expression in development and are involved in the patterning and segmentation of the developing central nervous system (CNS) (Flanagan and Vanderhaeghen, 1998). Their adhesion-repulsive properties seem to confer them important roles in delineating regions or cell populations, and even to allow the good cell polarization (Flanagan and Vanderhaeghen, 1998; Murai *et al.*, 2003). Genetic KOs indicate that EPHB4, EFBB1, EFNB2 and EFNB3 are involved in vascular development (Adams *et al.*, 1999; Gerety *et al.*, 1999; Goldshmit *et al.*, 2006; Royet *et al.*, 2017). They have multiple functions in the CNS, including in spinal motor neurons, and the development of retino-tectal connections and maps (Mann *et al.*, 2002; Kao *et al.*, 2012; Fiore *et al.*, 2019). Moreover, they have crucial roles in neurotransmission (see also *section 1.4.1.2.2.*). For example, EPHA4 and EPHB2 regulate LTP at CA3-CA1 synapses in a kinase-independent manner, EPHB2 (and EFNB2) regulate NMDAR and synapse formation (Dalva *et al.*, 2000; Grunwald *et al.*, 2001; Takasu *et al.*, 2002; Grunwald *et al.*, 2004), and the presence of *EfnA3*, *EphA4* or soluble EPHA2 reduces the expression of the glial glutamate/aspartate transporter (GLAST or EAAT1) and glutamate transporter subtype 1 (GLT1 or EAAT2) involved in neurotransmitter reuptake (Carmona *et al.*, 2009; Filosa *et al.*, 2009).

### **1.4.1 EphA4**

EphA4 (also known as Sek, Sek1, Cek8, Hek8, Tyro1) is expressed broadly in the body but is especially abundant in the brain (Hafner *et al.*, 2004). It is expressed in epithelial, muscle, immune and glial cells, and both in pre- and postsynaptic neurons (Martone *et al.*, 1997; Murai *et al.*, 2003; Goldshmit *et al.*, 2006; Tremblay *et al.*, 2007; Todd *et al.*, 2017). It is found in the hippocampus, cerebral cortex, striatum, brainstem, Purkinje cells, retinal ganglion cells and along axons of both sensory and motor neurons of the spinal cord (Martone *et al.*, 1997; Leighton *et al.*, 2001; Liebl *et al.*, 2003). Interestingly, *EphA4* is also expressed in the mouse and rat SCN (Freyburger *et al.*, 2016).

#### 1.4.1.1 EPHA4 activation and signaling

EPHA4 triggers both kinase-dependent and independent signaling (*Kullander et al., 2001*). The binding of EPHA4 to its ligands induces autophosphorylation of its intracellular domain (*Binns et al., 2000*). This activation might require or benefit from clustered ligands and/or from the clustering of Eph receptors (*Davis et al., 1994; Stein et al., 1998; Xu et al., 2013*). Then, the intracellular tyrosine residues phosphorylate in a sequential order (*Wybenga-Groot et al., 2001; Singla et al., 2011*), and their phosphorylation is further modulated by intracellular kinases, such as Src, and phosphatases (*Shintani et al., 2006; Warner et al., 2008*). EPHA4 regulates the activation/interaction of intracellular effectors including adaptor proteins containing the SRC homology (SH) and phosphotyrosine binding (PTB) domains; SRC; spine-associated RapGAP (SPAR)/Rap1; ERK/mitogen-activated protein kinase (MAPK); AKT; phospholipase C, gamma 1 (PLC $\gamma$ 1); c-abl oncogene 1 non-receptor tyrosine kinase (c-Abl)/Ephexin/RhoA; protein phosphatase 2B (PP2B)/slingshot protein phosphatase 1 (SSH1); integrins and the anaphase-promoting complex (APC) (*Sahin et al., 2005; Bourgin et al., 2007; Richter et al., 2007; Shin et al., 2008; Fu et al., 2011; Zhou et al., 2012; Shu et al., 2016; Zhang et al., 2017; Arcas et al., 2020; Wagner et al., 2020*) (**Figure 1.4**). Some of these pathways activated by EPHA4 (c-Abl/Ephexin/RhoA, PP2B/SSH1, PLC $\gamma$ 1), modulate cofilin activation and spine retraction (*Fu et al., 2007; Zhou et al., 2007; Zhou et al., 2012; Zhang et al., 2017*). Moreover, EPHA4:EFNA3 activation modulates spine morphology through integrin regulation via Crk-associated substrate (Cas), the tyrosine kinase focal adhesion kinase (FAK) and proline-rich tyrosine kinase 2 (Pyk2), which likely converges on cofilin modulation as well (*Bourgin et al., 2007*). SPAR/Rap1 signaling modulates spine density and growth cone collapse (*Richter et al., 2007*). Furthermore, EPHA4-ephrin interaction regulates MAPK/ERK and AKT phosphorylation, which moderates cell survival, migration and proliferation (*Shin et al., 2008; Goldshmit and Bourne, 2010; de Marcondes et al., 2016; Shu et al., 2016*). Furthermore, the SPAR/Rap1 signaling modulates spine density and cone collapse (*Richter et al., 2007*). The APC signaling induces the ubiquitin ligase and polyubiquitination of GLUA1, inducing AMPAR internalization and degradation (*Fu et al., 2011*). Besides, EPHA4 may induce reverse signaling through its ligands. For instance, Ephrins-B may trigger signaling via their PDZ domains or through SH-domain containing proteins (e.g. Grb4) (*Cowan and Henkemeyer, 2001; Lu et al., 2001; Palmer et al., 2002*), and Ephrins-A act through the Src family member FYN (*Davy et al., 1999*).

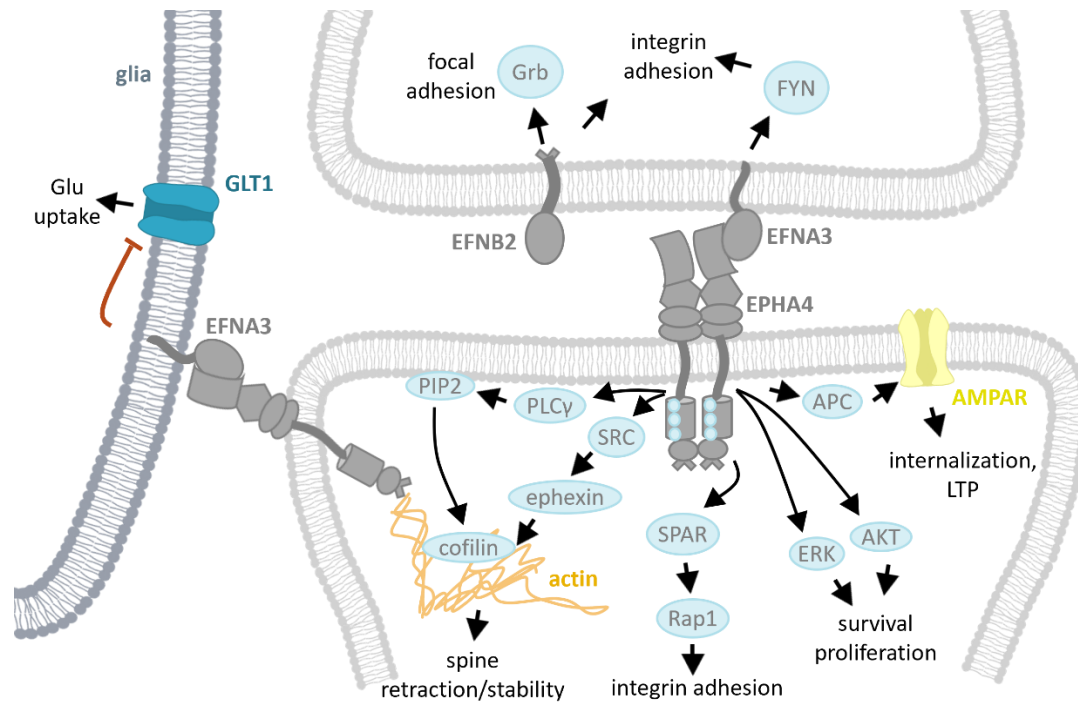


**Figure 1.4. EPHA4 can trigger multiple intracellular signaling.** EPHA4 can induce actin remodeling and regulate spine/axon retraction, it can regulate adhesion via integrin modulation as well, it can induce responses of cell survival/proliferation via MAPK/ERK and AKT, and it can induce AMPA receptor internalization and modulate synapse strength. Ephrins can also modulate kinase responses presynaptically and both Eph and Ephrins can act on astrocytes and regulate, for instance, the presence of glutamate transporters. Figure adapted from Arcas *et al.* (2020), Murai and Pasquale (2011) and Pasquale (2010).

Another level of regulation to consider is EPHA4 cleavage from the membrane, which may induce separate functions for intracellular and extracellular domains. For example, EPHA4 cleavage by  $\gamma$ -secretase (and potentially MMP9) is induced by synaptic activity and is involved in maintaining dendritic spines (Inoue *et al.*, 2009).

### 1.4.1.2 Functions of EPHA4

#### 1.4.1.2.1 CNS development

The roles of EPHA4 in cell adhesion/repulsion and cytoskeleton remodeling have contributed to its important roles in development. In neurodevelopment, EPHA4 has been involved both in modulating axonal guidance and in the segmental development of the CNS, by its patterned expression in different rhombomeres (Flanagan and Vanderhaeghen, 1998; Gatto *et al.*, 2014; Tanasic *et al.*, 2016; Fiore *et al.*, 2019). It is crucial for the development of the anterior commissure

(Dottori et al., 1998; Ho et al., 2009), of corticospinal tracts and for the regulation of midline crossing of excitatory and inhibitory neurons in the spinal cord (Dottori et al., 1998; Helmbacher et al., 2000; Leighton et al., 2001; Wegmeyer et al., 2007; Restrepo et al., 2011; Gatto et al., 2014). It has also been involved in the development of the neuromuscular junction (Yumoto et al., 2008).

*EphA4* KO mice present altered whisker innervation and representation in the barrel cortex (North et al., 2010). It is also expressed in the retina and is involved in establishing adequate retinotectal projections during development (Walkenhorst et al., 2000; Petros et al., 2006; Fiore et al., 2019; Zhu et al., 2021). Interestingly, the expression of EPHA4 in the optic chiasm was higher at P6 than P17, but absent in adult rats (Martone et al., 1997). In a similar manner, EPHA4 has been also involved in the development of thalamocortical topographic maps and topographic specificities in the hippocampus (Dufour et al., 2006; Galimberti et al., 2010). *EphA4* KO mice also present a thinner cortex, a thinner proportion of layers II-IV of mouse somatosensory cortex (North et al., 2009; Gerstmann et al., 2015), and impaired neuronal migration during cortical development (Hu et al., 2014; Steinecke et al., 2014). Moreover, it seems also relevant in adult neurogenesis, because EPHA4-ephrin contacts in adult neuroblast-astrocyte allow adequate migration from the subventricular zone (Todd et al., 2017).

#### 1.4.1.2.2 Adult neurotransmission

EPHA4 is involved in neurotransmission by regulating spine stability, myelination, neurotransmitter receptors or transporters at the membrane, and by activating intracellular pathways. EPHA4 reduces myelination in both zebrafish and rodents, and EphA4 inhibition prevents stressed-induced demyelination and reduced post-synaptic density thickness (including PSD-95 protein levels) (Harboe et al., 2018; Chen et al., 2019; Li et al., 2022b). Secondly, EPHA4 regulates synaptic strength by modulating spine retraction and AMPAR internalization (Murai et al., 2003; Fu et al., 2011). Moreover, EPHA4 has roles in neuroglia communication, which are fundamental for neurotransmission. The EPHA4 ligand EFNA3 is expressed by astrocytes but not neurites in the mouse stratum radiatum (Murai et al., 2003). When EPHA4 activates with EFNA3, it reduces the amount of GLAST and GLT1 (Filosa et al., 2009). In fact, *EfnA3*<sup>-/-</sup> mice had higher glutamate transporter current in astrocytes (Filosa et al., 2009). Thus, it was concluded that the presence of EPHA4 at the postsynaptic CA1 neurons regulates LTP at the CA3-CA1 synapse by decreasing the extracellular glutamate available in a manner that depended on glutamate uptake,



likely through GLAST or GLT1 (*Grunwald et al., 2004; Filosa et al., 2009*). The fact that EFNA2 regulates glial glutamate transporter in the mouse cortex and that EPHA4 is expressed in cortical astrocytes in primates (*Goldshmit and Bourne, 2010; Yu et al., 2013*), suggests that EPHA4 might regulate plasticity through modulating neuroglia communication outside the hippocampus as well. Finally, activation of EPHA4 by EFNA3 induces spine retraction in the hippocampus, while EphA4 or EfnA3 downregulation promotes longer spines (*Murai et al., 2003*). In fact, stimulating with soluble forms of EFNA3 reduces spine length and density, and *EphA4* KO and *EfnA3* KO mice show longer spines in the hippocampus (*Murai et al., 2003; Carmona et al., 2009*), suggesting that this EphA4 function was not compensated by other components of the Eph/Ephrin system. Therefore, changes in EPHA4 may modulate neurotransmission either by modulating the presence of receptors/transporters, by modifying the spine morphology or by modifying the levels of myelination.

#### 1.4.1.2.3 Vascular system

EPHA4 is expressed in spinal cord vessels during mouse embryonic development and lack of *EphA4* induces altered vasculature in the mouse CNS (*Goldshmit et al., 2006*). Moreover, EphA4 seems to be particularly involved in the vascular responses to insult. For example, *EphA4* is upregulated after spinal cord injury in astrocytes associated to vessels in the mouse spinal cord, but not detected in non-lesioned mice (*Goldshmit et al., 2006*). Moreover, EPHA4 has been involved in endothelial cell survival and vascularization in glioblastoma, where *EphA4* downregulation reduces apoptosis (*Royet et al., 2017*). In addition, EFNB2 (ligand of EphBs and EPHA4) is particularly expressed in arteries and necessary for mouse cardiac development (*Gerety et al., 1999*). Interestingly, EFNB2 has also been suggested to regulate lymphatic endothelial cell junctions (*Frye et al., 2020*), which highlights that the Eph/ephrin system is particularly important for adequate metabolite and cell circulation in the organisms.

#### 1.4.1.2.4 Immune system and cancer

EPHA4 expressed in endothelial cells is linked to the monocyte-endothelial cell adhesion, and it is also involved in cell-cell interaction in the context of cell migration in cancer (*Jellinghaus et al., 2013; Lu et al., 2014; Jing et al., 2016*). It was found expressed in cancer stem cells, and EphA4 inhibition was reported to reduce tumor proliferation and cytokine production, which was suggested to be via contact with Ephrin-containing monocytes (*Lu et al., 2014*). Moreover,

infection with the oncogenic Epstein-Barr virus (EBV) was shown to downregulate EPHA4 protein and mRNA levels in human B cells (*Huang et al., 2016*).

#### **1.4.1.3 EphA4 implications in diseases**

The roles of EPHA4 in cell migration, vascular and neurodevelopment has linked it to injuries and diseases. For example, EPHA4 is upregulated after cortical injury and induces astrocyte proliferation at the lesion site (*Goldshmit and Bourne, 2010*), and mice downregulated for EphA4 show faster motor recovery after stroke (*Lemmens et al., 2013*). Moreover, like multiple other Eph receptors and Ephrins (*Hafner et al., 2004*), EPHA4 has been suggested to be implicated in tumor development, including colon cancer, breast cancer, cervical carcinoma and glioblastoma (*Saintigny et al., 2012; Huang et al., 2016; Royet et al., 2017; Lee et al., 2021*). Intriguingly, it has been suggested that EPHA4 can have both tumor suppressing and promoting functions (*Fukai et al., 2008; Saintigny et al., 2012; Huang et al., 2016*). In fact, methylation of most Eph/Ephrin genes (including *EphA4, EfnA3, EfnB2*) is increased in leukemia patients and cell lines (*Kuang et al., 2010*), and *EphA4* mRNA expression is increased in human samples of melanoma, where enriched *EphA4* mutations were found (*Light et al., 2021*).

Given EPHA4 functions in neurotransmission and spine morphology, EPHA4 has been linked to cognitive disorders in both rodents and human. EPHA4 was found upregulated in the prefrontal cortex and hippocampus of a models of depression and in post-mortem brain tissue of MDD patients (*Zhang et al., 2017; Li et al., 2022b*). EphA4 shRNA reversed depression-like behavior in mice (*Zhang et al., 2017; Li et al., 2022b*). Moreover, postmortem samples from AD patients show upregulated *EphA4* mRNA expression in PFC but reduced EPHA4 protein in the hippocampus (*Simon et al., 2009; Williams et al., 2009*). Mouse models for AD also showed reduced EPHA4 levels but increased activation in the hippocampus, and EPHA4 inhibition by rhynchophylline was correlated with improved AD-like symptoms (*Simon et al., 2009; Fu et al., 2014*).

#### **1.4.1.4 EphA4 gene and transcriptional regulation**

The *EphA4* gene contains 18 exons in the mouse and 19 in human, and is found on Chromosome 1 and Chromosome 2, respectively. The introns/exon boundaries are highly conserved in the Eph/Ephrin family, underscoring the redundancy among members of the family (*Drescher, 2002*). Three transcript variants of *EphA4* have been described in the mouse and human,

but only two are translated into protein *in vivo* and require the same transcription start site (TSS) (Zhao *et al.*, 2017). Notwithstanding the high implication of EphA4 in human disease, little is known about *EphA4* transcriptional regulation. Three studies describe that transcription factors involved in development regulate *EphA4* transcription through DNA elements upstream the TSS: Krox20 (or EGR2), mesoderm posterior 2 (MESP2) and paired box 3 (PAX3)/ forkhead box O1 (FKHR, FOXO1a) (Theil *et al.*, 1998; Begum *et al.*, 2005; Nakajima *et al.*, 2006). Theil and collaborators described a 470bp enhancer region containing Krox20 binding sites, showed that Krox20 could activate the transcriptional activation of inserts containing the Krox20 enhancer, and confirmed that the mutation of Krox20 sites reduced transcriptional activity (Theil *et al.*, 1998). Interestingly, Krox20 (known to be involved in myelination) and *EphA4* follow the same pattern of expression during remyelination after nerve injury (Chen *et al.*, 2019). MESP2, involved in segmental development, can bind to an enhancer region of the *EphA4* promoter and induce its transcription (Nakajima *et al.*, 2006). The third study shows that PAX3, a transcription factor involved in neural tube development, can bind to the *EphA4* promoter either alone or fused with the protein FKHR (FOXO1a), to activate transcription (Begum *et al.*, 2005). On the other hand, stimulating protein 1 (Sp1) binds to *EphA4* promoter and decreases both *EphA4* mRNA and protein levels, a regulation which was suggested to be downstream of the ERK pathway and involved in cell proliferation (Huang *et al.*, 2016). Previous work by Mongrain *et al.*, revealed the presence of E-boxes upstream of the *EphA4* TSS (Freyburger *et al.*, 2016), which suggests that the core clock machinery may regulate the transcription of these membrane molecules. Accordingly, we will investigate the functionality of E-boxes in the putative promoters of *EphA4* and Ephrins in Chapter 4.

The 3' untranslated region (3'UTR) of transcripts may also determine mRNA location, stability and translation. The 3'UTR of *EphA4* mRNA is shown to be regulated by both microRNAs (miRNAs) and the human antigen R (HuR) (Winter *et al.*, 2008; Yan *et al.*, 2013; Cai *et al.*, 2019). First, it is suggested that *EphA4* is downregulated by acute ischemia via the binding of miR-145 to *EphA4* 3'UTR, which decreases *EphA4* mRNA and protein levels (Cai *et al.*, 2019). Secondly, miR-10a was also shown to downregulate *EphA4* transcription through its 3'UTR, which induced carcinoma cell migration, likely by reducing the cell adhering properties of EPHA4 (Yan *et al.*, 2013). Moreover, HuR, which is overexpressed in some tumors, binds to the 3'UTR of *EphA4*, *EphA3*, *EfnA2* and *EfnB2*, and, for *EphA4*, induces mRNA instability (Winter *et al.*, 2008).

Interestingly, binding motifs CPEs (cytoplasmic polyadenylation elements) and HuR in *EphA4* (and *EfnB2*) 3'UTR are highly conserved between human and mice (*Winter et al., 2008*).

Few additional studies explored the transcriptional regulation of EPHA4 ligands. A 180bp region upstream of *EfnB2* TSS which is conserved in mice and humans, is bound by Meis homeobox 1 (MEIS1), Myc-associated zinc finger protein (MAZ) and nuclear factor-Y (NF-Y) (*Sohl et al., 2009*). Moreover, SP1 binds to *EfnB2* promoter and induces its transcription (*Obi et al., 2009; Sohl et al., 2010*). It is important to note that the binding of transcription factors may require particular conditions. For example, SP1 binding to *EfnB2* could only be observed after shear stress and hypoxia conditions, but not in undisturbed conditions (*Obi et al., 2009*). Thus, the final effect of transcription factors may depend on other regulatory mechanisms. Gene methylation can also regulate *EfnB2* transcription as well (*Kuang et al., 2010*). On the other hand, *EfnA3* expression has been suggested to be reduced by miR-210 binding to its 3'UTR, which has been linked to tumor progression (*Fasanaro et al., 2008; Zhang et al., 2012*). Besides, hypoxia-inducible factor (HIF) has been shown to bind *EfnA3* promoter and induce transcription (*Husain et al., 2022*), and to induce the transcription of long non-coding RNAs (lncRNAs) at the *Ephrin* locus, which increase *EfnA3* translation by competing with 3'UTR regulating miRNAs (*Gomez-Maldonado et al., 2015*). Promoter acetylation was suggested as another regulatory mechanism of *EfnA3* transcription (*Zeng et al., 2018*).

#### **1.4.2 EphA4 and Ephrins in sleep and circadian physiology**

Previous research from my supervisor has revealed that synaptic adhesion molecules may modulate sleep characteristics (*El Helou et al., 2013; Massart et al., 2014; Freyburger et al., 2016; Freyburger et al., 2017; O'Callaghan et al., 2017; Seok et al., 2018*) and circadian physiology (*Hannou et al., 2018; Kiessling et al., 2018*). Mice KO for *Nlgn1* (*Nlgn1* KO) spend more time in SWS and have lower theta/alpha activity during wakefulness (*El Helou et al., 2013; Massart et al., 2014*). This was a first indication that anchor molecules with synapse-attaching properties involved in spine stability and neurotransmission could be relevant for sleep regulation. Subsequent studies in KO mice for the cell adhesion molecule EphA4 (*EphA4* KO) also showed altered sleep phenotypes, but different from previous *Nlgn1* KO phenotypes. *EphA4* KO mice have reduced PS and longer SWS bouts (*Freyburger et al., 2016*). Moreover, they show blunted 24-hour distribution of SWS low sigma activity (10-12Hz), and shorter duration of slow waves during SWS

(Freyburger et al., 2016; Freyburger et al., 2017). Interestingly, while *Nlgn1* KO mice had altered responses to SD, *EphA4* KOs did not show alterations in their response to SD. Further suggesting different roles of *Nlgn1* and *EphA4* in sleep regulation, SD modified the gene expression of these CAMs in different manners. On the one hand, SD decreased the levels of the *Nlgn1* transcript variant that includes an insert B, but the effect on other transcript variants depended on the mouse strain. On the other hand, SD increased *EphA4* expression in thalamus/hypothalamic regions (which was only tested in C57BL/6J mice) (Freyburger et al., 2016).

*EphA4* KO mice present altered circadian phenotypes as well. Firstly, *EphA4* KO mice have in the SCN a decreased  $PER1^+$  cell number and a decreased light-induced  $c-FOS^+$  cells. Moreover, these mice had a longer period of the running wheel activity rhythm in dark-dark (DD: constant darkness) and a shorter period in light-light (LL; constant light), suggesting that the presence of *EphA4* is required for normal endogenous circadian rhythm. Freyburger and collaborators described that the putative promoter region of the *EphA4* gene contained E-boxes, which, as presented in section 1.3.1, are regulatory elements that can be bound and activated by the circadian transcription factors CLOCK and BMAL1 (see section 1.1.3.1). Moreover, mice with the *Clock*<sup>Δ19</sup> mutation (dominant-negative function) show altered expression of *EphA4* in the mouse forebrain (Freyburger et al., 2016). In addition, the mentioned altered SWS low sigma activity in the *EphA4* KO mice, is a frequency range shown to be under circadian regulation in rats (Yasenkov and Deboer, 2011; Freyburger et al., 2016).

Therefore, research from our group suggests that *EphA4* could have relevant functions in regulating sleep and endogenous rhythms. Although some studies suggest that *EphA4* could be involved in the development of sleep regulatory brain centers such as the POA or thalamocortical projections (Takemoto et al., 2002; Zimmer et al., 2011), *EphA4* may also control sleep by regulating neurotransmission in the fully developed adult brain. Interestingly, neuronal activity modulates *EphA4* (Inoue et al., 2009), and *EGR2* (Krox20), which is a transcription factor upregulated by wakefulness or SD (Cirelli et al., 2004; Mongrain et al., 2010; Bellesi et al., 2013; Diessler et al., 2018; Guo et al., 2019; Hor et al., 2019), activates *EphA4* transcription (Theil et al., 1998). This suggests that increased behavioral or neuronal activity typical of wakefulness experience may regulate sleep through *EphA4*. Finally, astrocytes have also been shown to strongly regulate sleep and circadian rhythms (Barca-Mayo et al., 2017; Brancaccio et al., 2017; Ingiosi et

*al.*, 2020). For instance, astrocytes activity in the SCN or knocking-out components of the molecular clock uniquely in astrocytes can abolish circadian rhythms in mice (*Barca-Mayo et al.*, 2017; *Brancaccio et al.*, 2017; *Clasadonte et al.*, 2017). Modulating intracellular  $Ca^{2+}$  or connexins uniquely in astrocytes also modulates sleep or the response to sleep loss (*Clasadonte et al.*, 2017; *Ingiosi et al.*, 2020). Therefore, the presence of EPHA4 in astrocytes or reverse signaling regulating astroglia glutamate uptake through EFNA3 (*Filosa et al.*, 2009; *Todd et al.*, 2017), might have important repercussions for sleep and circadian behaviors as well. We hypothesize that one of the mechanisms that could link the Eph/Ephrin system to circadian functions could be at the level of their transcription. Chapter 4 in this thesis will aim at describing whether putative promoter regions of *EphA4*, *EfnB2* and *EfnA3* (including the already described E-boxes) are activated by the clock machinery *in vitro*, which will provide a potential level of implication of the system for rhythmic behaviors.

We suggest that EPHA4 implications in neurotransmission and plasticity have an impact in sleep and circadian physiology. However, the important effects of EPHA4 in neurodevelopment (see section 1.3.1.1.3) highlight the importance of investigating the effects of EPHA4 in fully developed adult mice. Moreover, redundant effects between different Eph molecules or compensatory mechanisms developed exclusively in *EphA4* KO mice, may have accounted for the observed sleep and circadian alterations, and needs to be further investigated.

## 1.5 Rhynchophylline may uncover EphA4 roles in sleep regulation

Rhynchophylline (RHY) is one of the main active components of *Uncaria* plants, which have been extensively used in Chinese and Japanese medicines. Interestingly RHY reduces EPHA4 phosphorylation in mice (*Fu et al., 2014; Zhang et al., 2017*). Furthermore, systemic administrations of RHY increased sleep time in the mouse and rat (*Yoo et al., 2016*), and drugs containing *Uncaria* plants were shown to increase sleep time and quality in humans (*Aizawa et al., 2002; Shinno et al., 2008b; Shinno et al., 2008a; Ozone et al., 2012; Pan et al., 2013; Sun and Liu, 2013; Ohtomo et al., 2014; Matsui et al., 2019; Ozone et al., 2020*). Therefore, given that *EphA4* KO mice show altered sleep variables (described in detail above), we propose to use RHY to downregulate EphA4 in adult mice and investigate its implication in adult sleep.

### 1.5.1 Rhynchophylline reduces EphA4 phosphorylation

Two studies have suggested that RHY prevent EPHA4 activation and the activation of downstream pathways (*Fu et al., 2014; Zhang et al., 2017*). This research further suggested that RHY allowed the recovery of spine morphology, LTP and cognitive performance through EPHA4 inhibition in mouse models of AD and depression (*Fu et al., 2014; Zhang et al., 2017*). *In vitro* and *in vivo* assays suggest that RHY reduces the EPHA4 activation induced by Ephrin ligands, which was shown both with reduced levels of EPHA4 phosphorylation and by decreased activation of downstream effectors (e.g., Ephexin) (*Fu et al., 2014; Zhang et al., 2017*). Moreover, one of the studies show that RHY was able to bind to EPHA4 by using pull-down assays (*Fu et al., 2014*). Nonetheless, as will be reviewed in Chapter 2, RHY modifies the levels or activation of numerous molecules which have been shown elsewhere to modulate sleep. Thus, we think that RHY might modify sleep via the EPHA4 receptor but that other pathways should be considered as well. For this reason, we have conducted a literature review compiling that RHY targets different cellular pathways, which have been linked to sleep regulation. This publication entitled *Cellular Effects of Rhynchophylline and Relevance to Sleep Regulation* (*Ballester Roig et al., 2021*) is included in the following Chapter 2, and will be followed by hypotheses and aims of the thesis presented under Chapter 3.

# Chapter 2

## Cellular effects of Rhynchophylline and relevance to sleep regulation

---

Cellular Effects of Rhynchophylline and Relevance to Sleep Regulation. Ballester Roig MN, Leduc T, Areal CC, Mongrain V. *Clocks Sleep*. 2021 Jun 9;3(2):312-341. doi: 10.3390/clockssleep3020020.

Published version: <https://www.mdpi.com/2624-5175/3/2/20>



# Cellular effects of Rhynchophylline and relevance to sleep regulation

Maria Neus BALLESTER ROIG<sup>1,2</sup>, Tanya LEDUC<sup>1,2</sup>, Cassandra C. AREAL<sup>1,3</sup>, Valérie MONGRAIN<sup>1,2</sup>

<sup>1</sup>Center for Advanced Research in Sleep Medicine, Recherche CIUSSS-NIM, Montreal, QC, Canada

<sup>2</sup>Department of Neuroscience, Université de Montréal, Montreal, QC, Canada

<sup>3</sup>Department of Medicine, Université de Montréal, Montreal, QC, Canada

**Manuscript submitted for publication to:** Clocks & Sleep

## **Corresponding author:**

Valérie Mongrain

Recherche CIUSSS-NIM (site Hôpital du Sacré-Coeur de Montréal)

5400 Gouin West Blvd.

Montreal, QC, H4J 1C5, Canada

valerie.mongrain@umontreal.ca

1-514-338-2222/3323

## Abstract

*Uncaria rhynchophylla* is a plant highly used in the traditional Chinese and Japanese medicines. It has numerous health benefits, which are often attributed to its alkaloid components. Recent studies in humans show that drugs containing *Uncaria* ameliorate sleep quality and increase sleep time, both in physiological and pathological conditions. Rhynchophylline (Rhy) is one of the principal alkaloids in *Uncaria* species. Although treatment with Rhy alone has not been tested in humans, observations in rodents show that Rhy increases sleep time. However, the mechanisms by which Rhy could modulate sleep have not been comprehensively described. In this review, we are highlighting cellular pathways that are shown to be targeted by Rhy and which are also known for their implications in the regulation of wakefulness and sleep. We conclude that Rhy can impact sleep through mechanisms involving ion channels, N-methyl-D-aspartate (NMDA) receptors, tyrosine kinase receptors, extracellular signal-regulated kinases (ERK)/mitogen-activated protein kinases (MAPK), phosphoinositide 3-kinase (PI3K)/RAC serine/threonine-protein kinase (AKT) and nuclear factor-kappa B (NF- $\kappa$ B) pathways. In modulating multiple cellular responses, Rhy impacts neuronal communication in a way that could have substantial effects on sleep phenotypes. Thus, understanding the mechanisms of action of Rhy will have implications for sleep pharmacology.

**Keywords:** *Uncaria rhynchophylla*, intracellular signaling pathways, neurotransmitter receptors, non-rapid eye movement sleep, rapid eye movement sleep, electroencephalographic activity

# 1. Introduction

Plant compounds have been substantially explored to treat human illnesses, especially in the traditional Chinese medicine. This includes their utilization to ameliorate sleep or induce sedation [1,2]. However, given that the use of such compounds began early in the human history, the knowledge of their beneficial effects on health is rarely accompanied by studies providing the details of the underlying mechanisms.

*Uncaria rhynchophylla* has been used in Asia as a component of numerous Chinese and Japanese treatments such as Gou-teng (or Chotoko; name given to *Uncaria* medicinal herbs), and Yi-gan-san (a blend of seven herbs also known as Yokukansan [YKS]). It has been reported to alleviate hypertension, arrhythmia, convulsions, dizziness, pain, sleep disturbances, and cognitive impairments [3-8]. Alkaloids account for 0.2% of the composition of *U. rhynchophylla* (in hook, stem, and leaves), and were proposed to underlie the majority of health benefits resulting from the use of *Uncaria* [4,9]. Rhynchophylline (Rhy) is one of the most abundant of these alkaloids, and seems to associate with nearly the same benefits as those obtained with *U. rhynchophylla* in nonhuman mammals [3,4,10].

## 1.1. Rhynchophylline pharmacology

Rhy is a tetracyclic oxindole alkaloid that represents about 10-30% of *Uncaria* alkaloids [9,11,12]. Rhy is interconvertible with its isomer isorhynchophylline (Isorhy), which accounts for another 30-50% of the alkaloid fraction [9,11,12] (**Figure 1**). Their rate of interconversion depends on pH and temperature [13,14]. Both forms are absorbed quickly by the intestine but, when provided intravenously or orally, Rhy seems more available than Isorhy in the plasma, likely because the latter is more unstable and metabolized faster by the liver and intestine [13]. Rhy easily crosses the blood-brain barrier, as it is highly detectable in the rat brain from 15 min to 6 h after oral administration [15]. Another study has shown that an *in vitro* blood-brain barrier model was more permeable to Isorhy than Rhy [16]. Therefore, even if Rhy could be more prevalent than Isorhy in the body, the administration of Rhy may trigger the presence of Isorhy, which effect should be considered.

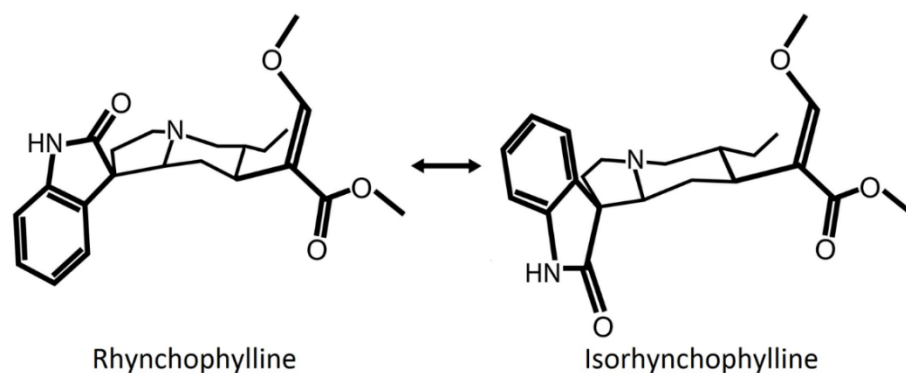


**Figure 1. Representation of the chemical structure of Rhynchophylline (Rhy) and Isorhynchophylline (Isorhy).** The position of the oxindole structure (N-C=O in the second ring) of the alkaloids Rhy and Isorhy is different. Both molecules are diastereoisomers, interconvertible with each other depending on pH and temperature. Temperature is suggested to induce a break and reclosure of the third ring that results in a twisted conformation (Wu et al., 2015).

Rhy (like Isorhy) has been proposed to mainly act on the cardiovascular system and central nervous system (CNS) [3,10]. Although there is no clinical trial investigating the effects of Rhy alone, animal research suggests that Rhy has beneficial properties such as anti-inflammatory, antihypertensive, anti-arrhythmic, anticonvulsant and neuroprotective effects [3,10]. Moreover, it seems to reduce memory impairments, mood deregulation, and addictive behaviors in rodents [17-21]. Interestingly, one study [22] and recent un-published data from our group point to an effect of Rhy on sleep in rodents, which is in line with the beneficial effects of Chotoko and YKS on human sleep time and quality (see details in section 1.3).

## 1.2 Sleep and its regulation

In mammals and other species, sleep is an essential behavior during which the organism isolates from environmental stimuli. Although the precise roles of sleep remain elusive, it could serve recovery from sustained activity (and associated oxidative stress) occurring during wakefulness in mammals and insects [23,24]. Moreover, sleep is beneficial for immune function, memory consolidation, and mood [25-28]. Mammalian sleep studies usually identify three main vigilance states: wakefulness, non-rapid eye movement (NREM) sleep (analogous to slow wave sleep in rodents), and rapid eye movement (REM) sleep (or paradoxical sleep) [29]. Wakefulness is characterized by a predominance of high frequency electroencephalographic (EEG) activity, NREM sleep by predominant low-frequency and high-amplitude EEG activity, and REM sleep by theta (4-9 Hz) EEG activity [29-33]. Delta activity (1-4 Hz) and slow oscillations (<1 Hz) during NREM sleep originate from synchronized up and down states of neuronal firing in cortical and

thalamocortical networks [34,35]. Delta activity (or slow wave activity: 0.5-4.5 Hz) was proposed to reflect a sleep homeostatic/recovery process [31,32,36-38], which relationship was recently shown to differ between slower and faster delta [32].

The transitions between vigilance states are operated by the activation/inhibition of specific brain circuits [39,40]. During wakefulness, wake-promoting brain regions contribute to sustained neuronal activity and/or inhibit sleep promoting centers. Amongst the major wake-promoting centers are Hypocretin/Orexin neurons in the lateral hypothalamus, neurons in the basal forebrain (BF), and neurons in several nuclei of the reticular formation (laterodorsal tegmentum [LDT], pedunculopontine tegmentum [PPT], raphe nucleus [RN], locus caeruleus [LC]) [39,41-46]. Sleep promoting neurons are found in the hypothalamus, with the ventrolateral preoptic area having a particular relevance [47]. During REM sleep, neurons from several nuclei of the reticular formation, including the LDT and PPT, allow cortical activation while behavioral sleep is maintained [48,49]. The knowledge of sleep neurobiology is important to refine pharmacological approaches for sleep disturbances.

### **1.3 Rhynchophylline and sleep**

Drugs containing Uncaria appear to ameliorate sleep in different ways. For instance, YKS was shown to improve sleep disturbances (sleep time, quality, and sleep-related limb movements) in adults suffering from REM sleep behavior disorder or dementia [6,50-52]. It was also reported to improve sleep quality in patients with insomnia [7], and children with nocturnal enuresis [53]. Other drugs containing Uncaria (although in smaller proportion) were also shown to increase total sleep time in healthy subjects and sleep quality in patients with Parkinson's disease or perimenopausal sleep disorder [54-56]. Fundamental research also suggests that Uncaria benefits sleep in rodents. Indeed, the administration of both YKS and a drug containing YKS was found to increase sleep time in socially isolated mice while having no impact in group-housed mice [57,58]. YKS was also shown to increase NREM sleep (and to decrease wake time) in a rat model of dementia [59], and Chotoko was reported to enhance the hypnotic-induced sleep time in mice [60]. Interestingly, Yoo and collaborators showed that Rhy increases sleep time in wild-type rats and mice [22]. This is in line with our recent observation of a longer time spent asleep after Rhy administration in mice, especially during the active (dark) period (Ballester Roig et al., in

preparation). Moreover, Rhy, Isorhy or Uncaria were all shown to reduce spontaneous locomotor activity in mice [61-63].

Very few of these studies have investigated the cellular pathways underlying modifications of sleep. Three of them suggested that the increased sleep time in mice is linked to gamma-aminobutyric acid (GABA) neurotransmission because these effects were blocked by GABA receptor antagonists and since increased levels of GABA<sub>A</sub> receptor subunits were found in hypothalamic neurons following Rhy-containing drug administration (see also section 2.9) [22,57,58]. Another study in rats with cerebral ischemia has linked the effects of YKS on sleep to a change in the mRNA level of prostaglandin receptors in the prefrontal cortex (PFC) and hypothalamus [59]. However, it appears that multiple cellular pathways impacted by Rhy may drive modifications in sleep. Therefore, this review is assembling findings on potential targets and cellular pathways affected by Rhy that are likely to impact the regulation of sleep. The literature demonstrates that Rhy could affect the activity of ion channels, N-methyl-D-aspartate (NMDA) receptors, receptor tyrosine kinases (RTK), extracellular signal-regulated kinases (ERK)/mitogen-activated protein kinases (MAPK), phosphoinositide 3-kinase (PI3K)/RAC serine/threonine-protein kinase (AKT), and nuclear factor-kappa B (NF- $\kappa$ B). A detailed overview of the effects of Rhy, including different types and durations of administration, is presented in **Table 1**. In addition, **Table 2** lists the literature reporting effects of Rhy on specific sleep-relevant targets/pathways, and **Figure 2** depicts a global scheme of the sleep-relevant pathways affected by Rhy and their interrelationships.

## **2. RHY targets and links to sleep regulation**

### **2.1 Ion channels**

#### **2.1.1. Voltage-gated Ca<sup>2+</sup> channels**

Rhy was first described as a calcium channel blocker in arteries, heart and neuronal cultures from the rat, rabbit, guinea pig, and human [10]. Some studies suggest an inhibitory effect specifically on L-type voltage-gated calcium channels (L-VGCCs; Cav1 family of calcium channels), which are high-voltage activated channels present notably in neurons, retinal photoreceptors, vascular smooth muscle cells, and cardiomyocytes [64]. For example, acute in vitro incubation of rat cortical neurons, rat ventricular myocytes, and rat and human arteries with Rhy

was shown to inhibit Ca<sup>2+</sup> influx through L-VGCCs [65-68] (**Table 1**). In vessels, this Rhy-dependent inhibition of VGCCs and the inhibition of intracellular Ca<sup>2+</sup> release were found to block the contractile response and induce vasodilation [67-69]. In cortical neurons, it was suggested that Rhy blocks L-VGCCs by decreasing the channel opening time and increasing its closing time under hypoxic conditions [65]. In neurons, L-VGCCs are mainly postsynaptic and contribute to Ca<sup>2+</sup> influx, Ca<sup>2+</sup> intracellular signaling, neuronal firing, and synaptic plasticity [70-73]. These roles affect neuronal responsiveness and synchronization, which is relevant to sleep regulation.

L-VGCCs were shown to modulate the synchronization of cortical and hippocampal neuronal oscillations, including in theta frequencies in vitro [74,75], and to affect the excitation/inhibition ratio in cortical slices [76]. In fact, Ca<sup>2+</sup> signaling and ion channels including

**Table 1. Compilation of datasets showing molecular and cellular (and some electrophysiological and behavioral) effects of rhynchophylline (Rhy) organized as a function of treatment type and duration, and by measurement timing.**

Rhy application	Timing of measurement	Rhy effect	Model	Reference #
<b>INCUBATIONS</b>				
20 s	Immediate	Attenuates epilepsy-induced ↑ in NMDAR current in EC slices	Rat brain slices	[19]
80 s	Immediate	Accelerates activation and inactivation of VGKC Accelerates activation and inactivation of Kv1.2	N2A cells HEK293	[84]
3-8 min	Immediate	↓ mAChR1- and 5-HT <sub>2</sub> -mediated currents (effect disappears after 1min) Attenuates epilepsy-induced ↑ of EC neuron discharge frequency ↓ open time and ↑ close time of L-VGCCs ↓ Ca <sup>2+</sup> influx via L-VGCCs Non-competitive inhibition of NMDAR current	Xenopus oocytes Rats Rat cortical neurons Rat cardiomyocytes Xenopus oocytes	[250] [19] [65] [66] [94]
15-30 min	Immediate	↓ EfnA1-dependent EphA4 phosphorylation and EphA4 clusters Attenuates ischemia-induced ↓ in population spike amplitude ↓ Ca <sup>2+</sup> intracellular increase via L-VGCC, promotes vasodilation	Rat cortical neurons Rat hipp. slices Human artery smooth muscle cells	[18] [250] [67]
1 h	Immediate	Attenuates ischemia-induced ↑ in ROS, MDA, LDH, mPTP, AIF, Ca <sup>2+</sup> and caspase 3 and 9 mRNA and protein Attenuates ischemia-induced ↓ in mitochondrial membrane potential, SOD, GPx, Cytc ↑ GAD65/67 and GABA <sub>A</sub> R subunits expression	Rat cardiomyocytes Rat hypothalamic neurons	[197] [22]
30 min	2 h post Rhy	Attenuates Aβ-induced ↑ in EphA4 phosphorylation and LTP impairment	Rat hipp. slices	[18]
2-6 h	Immediate	Attenuates LPS-induced ↑ in <i>Cox2</i> , <i>iNos</i> , <i>Ccl2</i> mRNAs ↑ <i>Grin1</i> mRNA (no difference in <i>Grin2b</i> )	Rat microglia Rat hipp. neurons	[161] [99]
12 h	Immediate	Improves endothelial relaxation and ↑ p-Src, p-AKT and NO (in hypertensive rat arteries) and ↑ p-eNOS (in WT arteries)	Rat intrarenal arteries	[187]
24 h	Immediate	Attenuates LPS-induced ↑ in p-ERK, p-38, p-Ikβ, NFκBp65 Attenuates LPS-induced ↓ in IkB α Attenuates LPS-induced ↑ in culture medium MCP1, PGE2, NO, IL1β, TNFα	Rat microglia	[161]

1 h	24h post Isorh	*Attenuates MPP-induced ↑ in p-GSK3 β Tyr297, p-FYN and ROS * ↑ nuclear NRF2 and ARE transcriptional activity	Human SH-SY5Y neuroblastoma cells	[205]
2 h	24h post Rhy	Attenuates MPP-induced ↓ in p-GSK3 β Ser9, p-AKT and MEF2D Attenuates MPP-induced ↑ in Bax/Bcl-2 ratio	Rat granule neurons	[188]
48 h	Immediate	↑ <i>Grin1</i> mRNA and GluN1, and ↓ <i>Grin2b</i> mRNA and GluN2B Attenuates LPS-induced ↑ in NO, iNOS, TNFα, IL-1β, p-p38, p-ERK Attenuates LPS-induced ↓ in IκBα ↓ GluN1 and ↓ ketamine-induced ↑ in GluA2/3	Rat hipp. neurons N9 mouse microglia PC12 cells	[99] [162] [296]
72 h	Immediate	↑ proliferation, GluN1, GluN2B, GluN3A ↓ BDNF, OXTR and ATP Alters proliferation/differentiation related genes	Bone mesenchymal human cells	[102]
24h	48h post Rhy	Attenuates MPP-induced ↑ ROS, LDH, Caspase-3 activity and apoptosis Attenuates MPP-induced ↓ Bcl2/Bax ratio and p-AKT	PC12 cells	[194]

#### SINGLE ADMINISTRATIONS

IC	100-600 s post Rhy	Attenuates Aβ-induced ↑ in the frequency of spontaneous discharge in CA1	Rats	[100]
IV	30 min post Rhy	Attenuates ischemia-induced ↓ in 5HIAA and DOPAC in striatum and hipp. Attenuates ischemia-induced ↑ of NE in striatum and hipp.	Rats	[297]
IP	50 min post Rhy	↓ DA in cortex, hypothalamus, and brainstem ↓ 5-HT in amygdala ↑ 5-HT in hypothalamus, and ↓ 5-HT release in hypothalamic slices ↑ 5-HT release in cortex, amygdala, and brainstem slices ↑ DA release in cortex, hypothalamus, amygdala, and brainstem slices ↓ righting reflex and spontaneous locomotor activity	Rats	[61]
Oral	0-6h post Rhy	↓ locomotor activity and sleep latency, ↑ total sleep time ↓ number of sleep/wake cycles, ↑ total sleep time and REM sleep	Mice Rats	[22]
IP	48 h post Rhy	Attenuates stress-induced ↑ p-EphA4, p-FYN, p-Cdk5, p-Ephexin in PFC, CA3, DG Attenuates stress-induced ↓ BDNF, p-TrkB, PSD95, spines in PFC, CA3, DG	Mice	[17]
IP	52 h post Rhy	Attenuates NTG-induced ↑ in EEG theta and delta activity, oxidative stress (GSH, blood CGRP), p-ERK1/2, p-JNK, p-p38, p-IκBα, and nuclear NF-κB p65 (all in trigeminal nucleus caudalis)	Rats	[116]
Hipp. inj	2 w post Rhy	Attenuates A β -induced ↑ cell death, GluN2B, and NMDA Ca <sup>2+</sup> influx in CA1	Rats	[97]

#### MULTIPLE ADMINISTRATIONS

SC for 3 days	1-3 h after last injection	Attenuates LPS-induced ↓ in stroke volume and cardiac output Attenuates LPS-induced ↑ in IL-1β, TNFα and p-IκBα in heart, macrophages and serum	Mice	[223]
IP for 3 days	3 h after last injection	* Attenuates KA-induced epileptic seizures ** Alters levels of <i>Bdnf</i> , <i>Fos</i> , <i>Nfkbia</i> , <i>Map2k3</i> , <i>Il1b</i> in cerebral cortex and hipp. Attenuates KA-induced epileptic seizures Attenuates KA-induced epileptic seizures and KA- induced ↑ in hippocampal p-JNK ** Attenuates KA-induced ↓ in cortical IL-6	Rats	[140] [166] [167]
IP for 3 days	12 h after last injection	Attenuates meth-induced ↑ in 5-HT, DA, TH, Glut, GluN2B, and locomotion Attenuates meth-induced ↑ in GluA1 and CPP Attenuates meth-induced ↑ in p-CREB and c-fos positive cells in CA1 and striatum Attenuates amph-induced ↑ in CPP, glutamic acid, DA, and NE Attenuates amph-induced ↓ in GABA, endorphin, and ACh Attenuates ketamine-induced ↑ in CPP, <i>Nr4a2</i> and <i>Bdnf</i> mRNAs, NURR1, BDNF, p-CREB (all hipp.) Attenuates amph-induced ↑ in CPP and <i>Grin2b</i> mRNA, and GluN2B protein in mPFC and CA1	Zebrafishes Rats	[101] [298] [172] [251] [141],[21] [20]



		Attenuates meth-induced ↑ in CPP and GluN2B in brain tissue	Mice	[98]
IP for 3 days	24 h after last injection	Attenuates KA-induced ↑ in IL-1β and BDNF positive cells in cortex and hipp.	Rats	[140]
		Attenuates KA-induced ↑ NO scavenging activity in blood		[166]
IP for 5 days	24 h after last injection	↓ brain infarction and neurological deficits in a stroke model. In cerebral cortex: Accentuates ischemia-induced ↑ in p-AKT and p-mTOR Attenuates ischemia-induced ↑ in TLR2,4, MyD88, caspase 3, and nuclear NF-κB Attenuates stroke-induced ↓ in p-BAD, BDNF, <i>Bdnf</i> and claudin-5		[114]
ICV infusion for 9 days	33-34 h after ICV	Attenuates epilepsy-induced ↑ EC discharge frequency, neuronal death and GluN2B and Nav1.6	Rats	[19]
1 week gavage	1 week after last gavage	Attenuates cytotoxicity-induced ↓ in TH-positive cells in substantia nigra	Mice	[194]
2 weeks gavage	Immediate	**Attenuates KA-induced neuronal death and KA-induced ↑ in spike amplitude	Rats hipp. slices	[299]
3 weeks oral	Not specified	Attenuates DOI-induced ↑ TNF α, IL-6, and IL-1B (in serum and striatum) Attenuates DOI-induced ↑ p-NF-κB p65, p-IκBα, TLR2, caspase1, MyD88, DA, D2R (in striatum) Attenuates DOI-induced ↓ in p-TrkB, BDNF (in striatum), and cell viability	Rats	[143], [222]
3 weeks gavage	24h after last gavage	*Attenuates Aβ-induced ↓ in p-AKT, p-GSK3β (in brain), Bcl2/Bax in hipp., and memory *Attenuates Aβ-induced ↑ in caspases 3 and 9 in hipp.	Rats	[189]
3-4 weeks gavage	Immediate	Attenuates p-EphA4 and rescues LTP in hipp. slices in APP mice	Mice	[18]
3 weeks gavage	5 days after last gavage	*Attenuates chronic mild stress-induced ↓ p-AKT, p-GSK3β, BDNF, NGF in cortex and hipp., and sucrose preference *Attenuates chronic mild stress-induced ↑ in TNF α, IL-6, nuclear NF-κB in cortex and hipp. and locomotion	Mice	[142]
1 day gavage/week for 4 weeks	24 h after last gavage	Attenuates asthma-induced ↑ in eosinophil recruitment, IL-13, IL-4, IL-5 in serum Attenuates asthma-induced ↑ TGF β, Smad4, p-Smad2, p-Smad3, p-ERK1/2 and p-38 in lung tissue	Mice	[164]
6 weeks in food	Immediate	*Attenuates cardiac hypertrophy-induced ↑ in TGFβ1, cTGF, Collagen1,3, p-ERK, p-38, p-JNK, and attenuates the induced ↓ in SOD2 * ↑ NRF2 and accentuates the induced ↑ in SOD3	Mice	[165]

\*Studies with Isorhynchophylline; \*\*Studies with *Uncaria rhynchophylla*; Upward arrows are indicating an increase and downward arrows a decrease; 5-HT: 5-hydroxytryptamine or serotonin; 5HIAA: 5-hydroxyindoleacetic acid; 5-HT<sub>2R</sub>: serotonin receptor 2; Aβ: amyloid β; AIF: apoptosis-inducing factor; ACh: acetylcholine; AKT: RAC serine/threonine-protein kinase; amph: amphetamine; APP: amyloid precursor protein; ARE: antioxidant response element; ATP: adenosine triphosphate; BAD: Bcl-2-associated death protein; BDNF: brain-derived neurotrophic factor; CA1: hippocampal cornu ammonis-1; CA3: hippocampal cornu ammonis-3; Cdk5: cyclin dependent kinase 5; CGRP: calcitonin gene-related peptide; Ccl2: monocyte chemoattractant protein 1 gene; Cox2: cyclooxygenase 2; CPP: conditioned place preference; CREB: cAMP response element-binding protein; cTGF: connective tissue growth factor; CytC: cytochrome c; D2R: dopamine D2 receptor; DA: Dopamine; DG: dentate gyrus; DOI: 1-(2,5-dimethoxy-4-iodophenyl)-2-aminopropane; DOPAC: 3,4-Dihydroxyphenylacetic acid; EC: entorhinal cortex; EEG: electroencephalographic; eNOS: endothelial nitric oxide synthase; EfnA1: ephrin A1; EphA4: Eph receptor A4; ERK: extracellular signal-regulated kinases; FYN: tyrosine-protein kinase Fyn; GABA<sub>A</sub>R: gamma-aminobutyric acid type A receptor; GAD: glutamic acid decarboxylase; GluA: α-amino-3-hydroxy-5-methyl-4-isoxazolepropionic acid (AMPA) receptor subunit; GluN: NMDAR subunit; GPx: glutathione peroxidase; Grin2b: glutamate ionotropic

receptor NMDA type subunit 2B; GSH: glutathione; GSK3 $\beta$ : glycogen synthase kinase-3  $\beta$ ; Hipp.: hippocampus; IC: intracerebral; ICV: intracerebroventricular; I $\kappa$ B $\alpha$ : NF-kappa-B inhibitor alpha; iNOS: inducible nitric oxide synthase; IL: interleukin; IP: intraperitoneal; IV: intravenous; JNK: c-Jun N-terminal kinase; KA: kainic acid; Kv: VGKCs subunit; LPS: lipopolysaccharide; LTP: long term potentiation; L-VGCC: L-type voltage-gated calcium channel; MCP1: monocyte chemoattractant protein 1; MDA: malondialdehyde; MEF2D: myocyte enhancer factor 2D; meth: methamphetamine; mPFC: medial prefrontal cortex; MPP: 1-methyl-4-phenylpyridinium; mPTP: mitochondrial permeability transition pore; mTOR: mechanistic target of rapamycin; MyD88: myeloid differentiation primary response protein; NAc: nucleus accumbens; Nav1.6: voltage-gated sodium channel 1.6; NE: norepinephrine; NF- $\kappa$ B: nuclear factor-kappa B; Nfkbia: I $\kappa$ B $\alpha$  gene; NGF: nerve growth factor; NMDAR: N-methyl-D-aspartate receptor; NO: nitric oxide; Nr4a2: nuclear receptor subfamily 4 group A member 2 gene; NRF2: nuclear factor E2 related factor 2; NTG: nitroglycerin; Nurr1: nuclear receptor related-1 protein or nuclear receptor subfamily 4 group A member 2; OXTR: oxytocin receptor; PC12: cell derived from pheochromocytoma of rat adrenal medulla; PSD95: postsynaptic density protein 95; REM: rapid eye movement; SC: subcutaneous; Smad: homolog of *Drosophila* mothers against decapentaplegic; SOD: superoxide dismutase; Src: proto-oncogene tyrosine-protein kinase Src; TGF $\beta$ : transforming growth factor beta; TH: tyrosine hydroxylase; TLR: toll-like receptor; TNF $\alpha$ : tumor necrosis factor  $\alpha$ ; TrkB: tropomyosin or tyrosine receptor kinase B; VGKC: voltage-gated potassium channel.

VGCCs are also proposed to be involved in the generation of the up and down states composing the slow oscillations characteristic of the NREM sleep EEG [77,78]. Cav1.2 channels represent more than 80% of L-VGCCs in the mouse brain [79]. Mice heterozygous for *Cacna1c* (gene encoding a Cav1.2 subunit) have less REM sleep during recovery after sleep deprivation (SD), as well as decreased beta and gamma activity (20-64 Hz) during wakefulness and REM sleep [80]. Moreover, *Cacna1c* genetic variants, which have also been linked to psychiatric disorders, are associated with longer sleep latency in infants [81]. Therefore, although the effect of Rhy on neuronal L-VGCCs seems to have only been studied in vitro, Rhy may impact sleep stages and EEG activity through the blockage of L-VGCC-mediated currents. Also, Cav1.2 mRNA is expressed rhythmically in the mouse suprachiasmatic nucleus (SCN), and Cav1.2 KO mice have altered circadian adjustments to light [82]. This suggests that the effect of Rhy on VGCCs may also impact the circadian regulation of wakefulness and sleep.

### 2.1.2. Potassium channels

Other ion channels targeted by Rhy which have important roles in CNS functions are voltage-gated potassium channels (VGKC). VGKC, by allowing K<sup>+</sup> efflux, regulate neuronal

repolarization and the timing of neuronal excitability [83]. Rhy was shown to speed up the inactivation of VGKC in N2A neuroblastoma cells [84] (**Table 1**). This study has also reported a specific effect on VGKC containing the Kv1.2 subunit expressed in HEK293 cells, in which Rhy accelerated Kv1.2 channels activation and inactivation times [84]. Noteworthy, the Kv1.2 subunit is highly expressed in the thalamocortical system [85,86], and potassium channels Kv1.2, Kv3.1 and Kv3.2 have been shown to regulate sleep [87-90]. In particular, Kv1.2 knockout (KO) mice spend less time in NREM sleep and more time in wakefulness [88], and Kv1.2 inhibition was reported to decrease NREM sleep and alter the NREM sleep EEG [90]. In *Drosophila*, mutation of VGKC subunits that are close to the mammalian Kv1.2 channels was also shown to induce a decrease in sleep time [24,91]. These findings suggest that the effect of Rhy on VGKCs may contribute to alterations in sleep features as well. Of note, Rhy also affects calcium-activated potassium channels in the vascular system [10]. This has not been investigated in the CNS, but might be of relevance considering that these channels can impact sleep duration [92]. Interestingly, both VGKCs and calcium-activated potassium channels are also suggested to be involved in the generation of up and down states of NREM sleep oscillations [77,78].

## 2.2 NMDA receptors

Among the most studied targets of Rhy are glutamate NMDA receptors (NMDARs), which are crucial for neurotransmission and brain plasticity [93]. Rhy was described as a non-competitive NMDAR antagonist due to its blocking effect on NMDAR current in xenopus oocytes [94]. In entorhinal cortex slices of epileptic rats, Rhy was found to cause an immediate attenuation of the potentiated NMDAR-mediated currents, which associated to a decrease of seizures in vivo [19]. Moreover, Rhy was often shown to decrease the expression of the NMDAR subunit GluN2B, which is predominant in extrasynaptic NMDARs, responds to high spreads of glutamate such as in excitotoxic conditions, and activates apoptotic pathways [95,96]. In rodents, conditions such as pilocarpine-induced status epilepticus, injections of amyloid-beta ( $A\beta$ ), and administration of amphetamine (amph) or methamphetamine (meth), are increasing GluN2B protein levels, effects that were diminished by Rhy in the medial PFC, entorhinal cortex, and hippocampal CA1 region [19,20,97,98] (**Tables 1 and 2**). This modulation of GluN2B by Rhy could depend on an effect at

**Table 2. List of literature showing effects of Rhynchophylline (Rhy) on sleep-related pathways under physiological (baseline) and/or pathological (disease-modeled) conditions.**

	Effects under baseline and/or pathological conditions	Sex(es) studied	Reference #
VGCC	<b>Baseline conditions</b>	Males	[66], [68]
	<b>Baseline conditions</b>	<b>Males and females</b>	[69]
	<b>Baseline conditions</b>	Not indicated	[67]
	Pathological conditions	Not indicated	[65]
VGKC	<b>Baseline conditions</b>	Male and female cell lines	[84]
NMDAR	<b>Baseline conditions</b>	Not indicated	[94], [99], [102]
	Pathological conditions	Males	[19], [101]
	Pathological conditions; no effect under baseline	Males	[20],[97]
	Pathological conditions	Not indicated	[98]
EPHA4	Pathological conditions; no effect under baseline	<b>Males and females</b>	[18]
	Pathological conditions; no effect under baseline	Males	[17]
BDNF/TRKB	<b>Baseline conditions</b>	Not indicated	[102]
	Pathological conditions	Males	[140], [141], [114]
	Pathological conditions; no effect under baseline	Males	[17], [142]*
	Pathological conditions	Not indicated	[21]
ERK/MAPK	Pathological conditions	Male cell line	[162]
	Pathological conditions	Not indicated	[161]
	Pathological conditions	Female	[164]
	Pathological conditions	Males	[116], [166], [167]
	Pathological conditions; no effect under baseline	Males	[165]*
CREB	Pathological conditions	Males	[141]
	Pathological conditions	Not indicated	[21] [172]
PI3K/AKT	Pathological conditions	Males	[187]
	Pathological conditions	Male cell line	[194]
	Pathological conditions	Not indicated	[197]
	Pathological conditions; no effect under baseline	Not indicated	[188]
	Pathological conditions; <b>only one effect under baseline</b>	Males	[165]*
	Pathological conditions	Males	[114]
	Pathological conditions; no effect under baseline	Males	[142]*, [189]*
NF-κB	Pathological conditions	Male cell line	[162]
	Pathological conditions	Not indicated	[161]
	Pathological conditions	Males	[114], [116], [166], [140], [222]
	Pathological conditions; no effect under baseline	Males	[223]
Other NTs	<b>Baseline conditions</b>	Not indicated	[250]
	<b>Baseline conditions</b>	<b>Males and females</b>	[61]
	Pathological conditions	Males	[101], [143]
	Pathological conditions; no effect under baseline	Not indicated	[251]
GABA <sub>A</sub> R	<b>Baseline conditions</b>	Male neurons	[22]

\*Studies with Isorhynchophylline. Lines with grey background denote *in vitro* measurements only. Studies showing Rhy effects under baseline conditions and/or including both sexes are in bold. Studies have not tested the effect of Rhy under baseline conditions if it is not indicated. AKT: RAC serine/threonine-protein kinase; BDNF: brain-derived neurotrophic factor; CREB: cAMP response element-binding protein; EphA4: Eph receptor A4; ERK: extracellular signal-regulated kinases; GABA<sub>A</sub>R: gamma-aminobutyric acid type A receptor; VGCC: voltage-gated calcium channels; NF-κB: nuclear factor-kappa B; NMDAR: N-methyl-D-aspartate receptor; NTs: neurotransmitters; PI3K: phosphoinositide 3-kinase; TrkB: tropomyosin or tyrosine receptor kinase B; VGKC: voltage-gated potassium channels.

the gene expression level because Rhy was shown to reduce Grin2b mRNA levels in rat hippocampal neurons and also after an amph-induced increase in PFC and CA1 [20,99]. Additionally, the effects of Rhy on NMDAR and GluN2B have been linked to a decrease in the frequency of discharge or population spike amplitude in brain regions including the entorhinal cortex and dentate gyrus (DG) [19,97,100]. Moreover, the Rhy-driven decreases in GluN2B are often observed in parallel with improvements in cognitive functions in rodents, such as spatial memory or drug-conditioned place preference (CPP) [20,97,98]. Similar findings were made in the zebrafish, in which Rhy was found to reduce the meth-induced increase in GluN2B protein level and CPP [101]. In contrast to the aforementioned studies, Rhy was shown to increase GluN2B protein in human mesenchymal cells [102]. Despite the fact that these last findings were from relatively long bath incubations of Rhy (72 h), they are difficult to reconcile with most of the effects reported in vivo in rodents. Also, it is important to keep in mind that only one study has reported an effect of Rhy on NMDARs in baseline conditions and this was in vitro, which may raise the question whether Rhy can modulate NMDARs under baseline conditions in vivo. Nonetheless, the literature adds up in favor of an effect of Rhy on NMDAR function.

With regard to sleep, glutamatergic signaling and NMDARs have been implicated both in arousal- and sleep-promoting pathways, with very distinct implications depending on the brain region [39]. On the one hand, NMDA or glutamate injected in the rat BF or tuberomammillary nucleus was shown to increase time spent awake [103,104], and injection of glutamate in the PPT induces neocortical desynchronization, wakefulness and REM sleep in the rat and cat [105,106]. Similarly, intraperitoneal (i.p.) injection of the MK-801 NMDAR antagonist was found to cause a delayed increase in NREM sleep time in rats [107,108]. Also, Alzheimer's disease patients treated with a non-competitive antagonist of NMDARs showed an increase in total sleep time (mainly NREM sleep) and reduced sleep fragmentation [109]. On the other hand, glutamate injection in the rat medial preoptic area (mPOA) or medial septum was shown to promote NREM sleep [110,111], and MK-801 was reported to decrease both NREM and REM sleep in mice [92]. Other data in rats have shown that peripheral administration of NMDAR antagonists induces cortical gamma activity (30-50Hz) in all vigilance states, while a specific blockade of GluN2B increases it solely in REM sleep [112]. The discrepancies between some of these studies could be explained by differences in

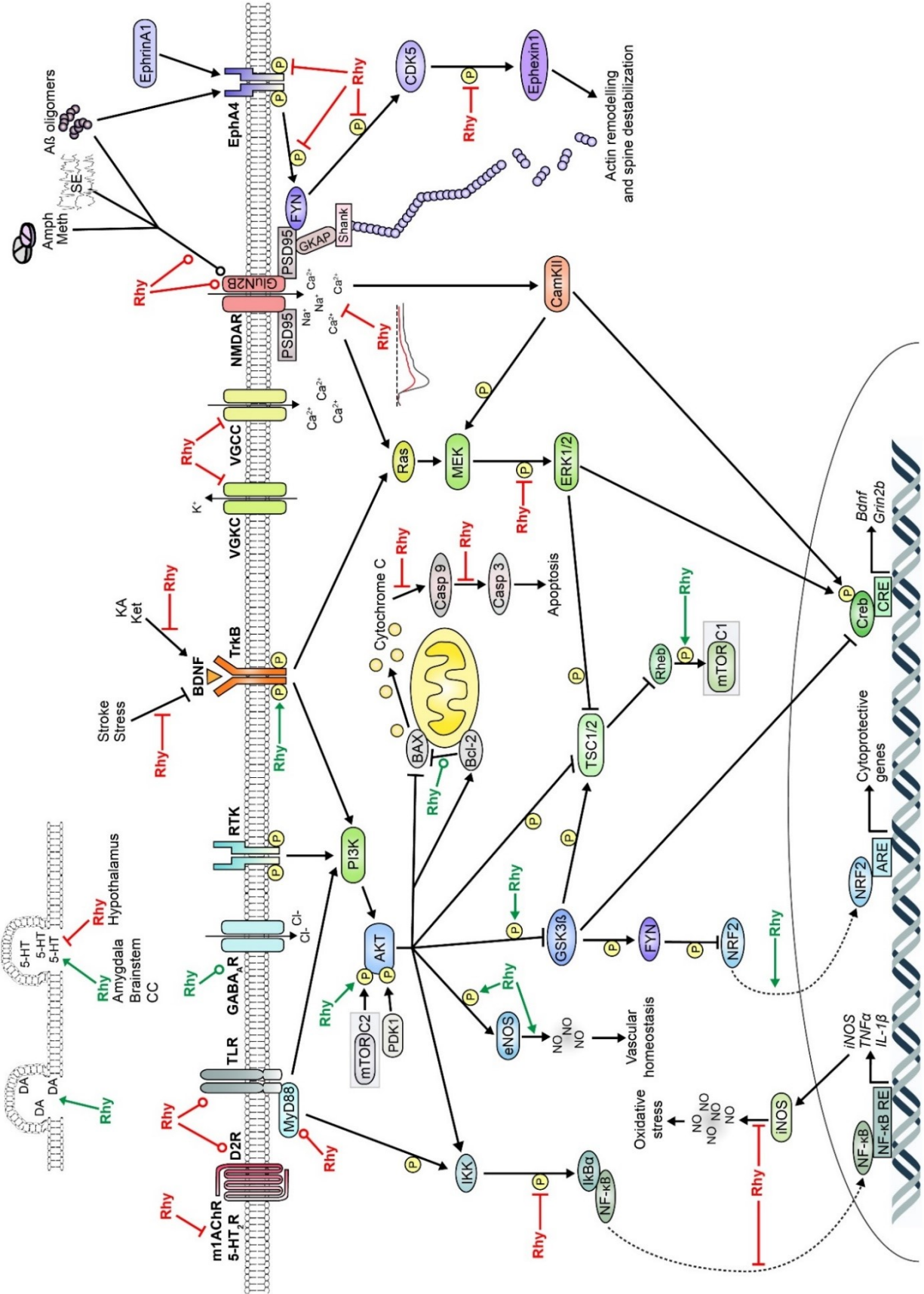


**Figure 2. Schematic representation of cellular pathways targeted by Rhy and relevant to sleep regulation.** Red flat-head lines: Rhy inhibition; Green arrows: Rhy induction; Red round-head lines: Rhy-dependent decrease in expression level; Green round-head lines: Rhy-dependent increase in expression level. Additional interactions between these cellular pathways are not represented but could also be relevant to sleep molecular physiology. For instance, L-VGCC can activate ERK/MAPK (Dolmetsch et al., 2001), and are suggested to induce CaMKII, NR2B phosphorylation and CREB activation (Wheeler et al., 2012; Kumar et al., 2019). NMDARs may also activate the PI3K/AKT pathway (Yoshii and Constantine-Paton, 2007). In addition, NF- $\kappa$ B and ERK/MAPK pathways were shown to interact with each other (Wang et al., 2014; Lai et al., 2019). 5-HT: 5-hydroxytryptamine or serotonin; 5-HT2R: serotonin receptor 2; A $\beta$ : amyloid  $\beta$ ; Amph: amphetamine; AKT: RAC serine/threonine-protein kinase; ARE: antioxidant response element; BAX: Bcl-2 associated X protein; BDNF: brain-derived neurotrophic factor; CamKII: Ca<sup>2+</sup>/calmodulin-dependent protein kinase; Casp 3: caspase 3; Casp 9: caspase 9; CC: cerebral cortex; CDK5: cyclin dependent kinase 5; CRE: cAMP response element; CREB: cAMP response element-binding protein; D2R: dopamine D2 receptor; DA: dopamine; eNOS: endothelial nitric oxide synthase; EphA4: Eph receptor A4; ERK1/2: extracellular signal-regulated kinases 1 and 2; FYN: tyrosine-protein kinase Fyn; GABAAR: gamma-aminobutyric acid type A receptor; GKAP: guanylate kinase-associated protein; GluN2B: NMDAR subunit 2B; Grin2b: glutamate ionotropic receptor NMDA type subunit 2B gene; GSK3 $\beta$ : glycogen synthase kinase-3  $\beta$ ; I $\kappa$ Ba: NF-kappa-B inhibitor alpha; IKK: I $\kappa$ B kinase; IL: interleukin; iNOS: inducible nitric oxide synthase; KA: kainic acid; Ket: ketamine; m1AChR: m1-type muscarinic acetylcholine receptor; MEF2D: myocyte enhancer factor 2D; MEK: mitogen-activated protein kinase kinase; Meth: methamphetamine; mTOR: mechanistic target of rapamycin; mTORC1: mTOR complex 1; mTORC2: mTOR complex 2; MyD88: myeloid differentiation primary response protein; NF- $\kappa$ B: nuclear factor-kappa B; NMDAR: N-methyl-D-aspartate receptor; NO: nitric oxide; NRF2: nuclear factor E2 related factor 2; PDK1: phosphoinositide-dependent protein kinase-1; PI3K: phosphoinositide 3-kinase; PSD95: postsynaptic density protein 95; RE: response element; Rheb: GTP-binding protein Rheb; Rhy: rhynchophylline; SE: status epilepticus; Shank: SH3 and multiple ankyrin repeat domains protein; TLR: toll-like receptors; TNF $\alpha$ : tumor necrosis factor  $\alpha$ ; TrkB: tropomyosin or tyrosine receptor kinase B; TSC1/2: tuberous sclerosis complex 1/2; VGCC: voltage-gated calcium channels; VGKC: voltage-gated potassium channels.

the time of administration, time of recording and/or species. Nonetheless, all support a role for NMDAR-mediated neurotransmission in sleep regulation. Therefore, the ‘generally antagonistic’ effect of Rhy on NMDARs should modulate cortical activity and show vigilance state-specific effects on wake/sleep architecture and EEG activity. Moreover, downstream effectors of NMDARs, including components of the ERK/MAPK and PI3K/AKT pathways, also seem to be altered by Rhy and involved in sleep regulation [113-118] (**Figure 2**, and sections 2.5 and 2.6). These interrelationships may reinforce the association between Rhy and NMDARs but could also imply that Rhy affects these pathways in a NMDAR-independent manner.

## 2.3 EphA4 and downstream pathways

Ephrins and their Eph RTKs are cell adhesion molecules widely expressed in neurons, glia, lymphocytes, epithelial cells, fibroblasts, myocytes, and bone cells [119-122]. In the CNS, they are crucial for axon guidance and plasticity [123]. In particular, Eph receptor A4 (EphA4) has roles in the regulation of  $\alpha$ -amino-3-hydroxy-5-methyl-4-isoxazolepropionic acid (AMPA) receptors, glial glutamate transport, and spine morphology [123-125]. In 2014, Fu and collaborators proposed that Rhy inhibits EphA4 activation by direct high-affinity interaction with its extracellular domain [18]. In this study, it was shown that Rhy inhibited both the EphrinA1-induced and A $\beta$ -induced phosphorylation of EphA4 in rat hippocampal neurons, and that oral administration of Rhy inhibited the elevated phosphorylation of EphA4 in the hippocampus of mice mutant for the amyloid precursor protein (APP) and presenilin 1 (PS1) [18]. These observations were associated with a restorative effect of Rhy on long-term potentiation and spine number. A sub-sequent study also showed that one Rhy i.p. injection reduces p-EphA4 in mice susceptible to stress, specifically in the PFC, hippocampal CA3, and DG, which correlated with an improvement of depressive-like behaviors and spine number [17]. In these same stress-susceptible mice, the phosphorylation of the tyrosine-protein kinase Fyn, cyclin de-pendent kinase 5 (Cdk5) and ephexin1 was increased, and Rhy attenuated these increments [17]. This could originate from an effect of Rhy directly on EphA4 because the Cdk5/ephexin1 pathway is downstream of EphA4 phosphorylation and linked to actin remodeling and spine destabilization [126] (**Figure 2**).

Research from our group supports a role for EphA4 in the regulation of sleep [127,128]. Indeed, we found that *EphA4* KO mice spend less time in REM sleep and have longer bouts of wakefulness and NREM sleep during the light phase in comparison to wild-type littermates [127]. Also, *EphA4* KO mice manifested a blunted 24-h rhythm of NREM sleep sigma (10-13 Hz) activity [127]. In addition, *EphA4* KO mice showed a shorter duration of slow waves (0.5-4 Hz) during NREM sleep [128]. These observations suggest that Rhy might modulate sleep through EphA4-dependent pathways, which may alter sleep variables such as REM sleep amount or EEG properties in the sigma or delta frequency ranges. In parallel, EphA4 was shown to be expressed in the mouse and rat SCN, and *EphA4* KO mice to have altered circadian responses to light [127,129]. This suggests an implication of EphA4 in the circadian timing system, and as a consequence, a potential effect of Rhy on circadian physiology.



## 2.4 BDNF/TRKB signaling

Brain-derived neurotrophic factor (BDNF) is upregulated by neuronal activity and involved in cell survival and neuroplasticity [130-134]. It generally acts on p75 neurotrophin receptor (p75NTR) and tropomyosin or tyrosine receptor kinase B (TrkB) [135], and TrkB can activate other signaling pathways including PI3K and ERK/MAPK [133,136-139]. In a rat model of epilepsy, kainic acid was found to increase BDNF protein in the cerebral cortex and hippocampus, which was attenuated by Rhy or Uncaria [140]. Similarly, ketamine-addicted rats were shown to have an increased expression of BDNF in the hippocampus, which was diminished by Rhy [21,141]. Rhy was also observed to reduce the levels of extracellular and intracellular BDNF in human bone marrow mesenchymal cells [102]. In contrast, Rhy appears to restore BDNF level when it is decreased in pathological conditions instead of increased, such as in the cortex or hippocampus of a rat stroke model [114] or of chronic/social-defeat stressed mice [17,142]. TrkB phosphorylation was also found to be increased by Rhy in the PFC, hippocampal CA3 and DG regions of stressed mice, and in the striatum of a rat model of Tourette syndrome [17,143]. Therefore, Rhy may downregulate the BDNF pathway under some conditions of neuronal activation such as epilepsy or after ketamine administration, while it may upregulate it in specific pathological conditions such as stroke, stress or Tourette syndrome (**Table 1**). This could also suggest that Rhy effects on BDNF depend on distinct upstream pathways.

Both BDNF and TrkB signaling have been linked to sleep regulation [144-146]. Firstly, BDNF has long been considered a sleep-promoting substance. For example, intracerebroventricular injection of BDNF was found to induce NREM sleep in rats and NREM and REM sleep in rabbits [147]. Studies in humans also report that lower levels of BDNF associate with shorter sleep duration or with decreased amount of deep NREM and REM sleep [148,149]. Interestingly, TrkB KO mice have more REM sleep, reduced REM sleep latency, and shorter bouts of wake and NREM sleep [150]. Secondly, the BDNF/TrkB pathway was found to impact the sleep EEG. Indeed, intracerebroventricular injection of BDNF was shown to reduce NREM sleep slow wave activity (SWA) in rabbits [147], whereas BDNF injection in the rat cortex during wakefulness was shown to increase SWA in the following NREM sleep period, and cortical injection of a BDNF antibody or a TrkB inhibitor to reduce NREM sleep SWA [151]. Moreover, the Val66Met BDNF polymorphism in humans has been linked to decreased NREM sleep delta and theta activity, and REM sleep theta, sigma and alpha activity [152,153]. Carriers of this polymorphism also lost the

positive correlation between sleep consolidation and declarative memory [154]. Thirdly, the phosphorylation of BDNF and TrkB responds to SD. Acute SD was shown to enhance BDNF levels and p-TrkB in the rat BF [155], and REM sleep deprivation (RSD) to increase BDNF in the PPT and subcœruleus nucleus, as well as in the ventromedial medulla of the spinal cord in a rat pain model [156-158]. SD was also found to increase BDNF levels in patients with major depressive disorder [159], and severe insomnia has been associated to lower BDNF [160]. Lastly, different inhibitors of TrkB were found to decrease REM sleep rebound after RSD [157]. Therefore, the literature suggests that the effects of Rhy on the BDNF/TrkB pathway could impact wakefulness and sleep phenotypes in numerous ways. However, the diverse roles of BDNF also suggest that the modulation by Rhy is likely con-text-dependent.

## 2.5 ERK/MAPK pathway

Rhy was shown to influence the phosphorylation (indicative of the activation) of ERK/MAPK. For instance, i.p. injection of Rhy diminished the elevated ERK phosphorylation (p-ERK) in trigeminal nucleus caudalis of rats stimulated with nitroglycerin (a rat migraine model) [116]. P-ERK level was also reported to be decreased by Rhy in rat and mouse microglia [161,162], and by *U. rhynchophylla* in murine macrophages [163]. In murine peripheral tissues, after several weeks of oral administration, Rhy was found to decrease the level of p-ERK in the lungs [164], and Isorhy to decrease it in the heart [165]. In contrast, others have reported that p-ERK levels were unaltered in the cortex or hippocampus after i.p. Rhy injections [166,167], which might be explained by a smaller dosage (i.e., 0.25 vs. 10-30 mg/kg). ERK and MAPK belong to a signaling cascade downstream of several membrane receptors, including NMDAR, TrkB and toll-like receptors (TLRs), and can modulate multiple cellular responses via cAMP response element-binding protein (CREB) and activity-regulated genes such as *Arc*, *Dbp*, *Homer1a* and *Bdnf* [136-139,168-171] (**Figure 2**). Therefore, the impact of Rhy on the ERK pathway may be linked to effects on both upstream and downstream elements.

CREB is a downstream effector of ERK/MAPK particularly relevant to understand the effects of Rhy. CREB is activated by neuronal activity and acts downstream of numerous other pathways including NMDAR and PI3K/AKT [137,139,170,171] (**Figure 2**). Rhy was shown to reduce p-CREB positive cells in the striatum and hippocampus in rats with meth and ketamine-

dependent p-CREB increase [21,141,172]. Rhy was also found to rescue the meth-induced decrease in the number of c-fos positive cells in the striatum and CA1, which was suggested to depend on CREB [172].

With regard to the neurophysiology of sleep, the ERK pathway was shown to associate with both wake/sleep history and regulation. Indeed, ERK phosphorylation has been reported to increase after 15 min of wakefulness and to decrease after 15 min of NREM sleep in the mouse cerebral cortex [169]. Moreover, RSD was found to decrease p-ERK level in the rat hippocampus [173]. In parallel, the deletion of Erk1 or Erk2 genes, as well as the inhibition of ERK phosphorylation, was found to increase the time spent awake in mice, generally at the expense of NREM sleep [169]. The level of p-ERK was also reported to correlate with sleep time in *Drosophila* [174]. Interestingly, the inhibition of ERK phosphorylation was shown to increase NREM sleep delta power in mice [169]. In the cat visual cortex, ERK1 phosphorylation was observed to associate with REM sleep beta-gamma activity (20-40 Hz), and has been linked to REM sleep-dependent plasticity [175]. Several datasets are also supporting that sleep is regulated by CREB in both rodents and insects. For instance, mice mutant for CREB  $\alpha$  and  $\Delta$  isoforms show an increase in NREM sleep duration and a decrease in theta activity during wake and REM sleep [176]. Likewise, a specific mutation of CREB in forebrain excitatory neurons was found to reduce time spent awake and increase NREM sleep time and bout number in rats [177]. Moreover, SD was found to increase p-CREB in the rat cerebral cortex [178,179], but RSD decreases it in the rat hippocampus [173]. In flies, SD was found to enhance CREB transcriptional activity, while the inhibition of CREB activity was found to increase rest [180]. In sum, effects of Rhy on both ERK and CREB could impact wake/sleep duration and modulate EEG activity including NREM sleep delta power.

## **2.6 PI3K/AKT signaling network**

The signaling by PI3K/AKT represents a major pathway regulating cell survival and growth [181]. Various receptors such as RTK and cytokine receptors directly stimulate PI3K upon ligand binding, which enables site-specific phosphorylation (and activation) of AKT by 3-Phosphoinositide-dependent protein kinase-1 (PDK1) and mechanistic target of rapamycin complex 2 (mTORC2) [182,183]. AKT controls numerous cellular processes such as apoptosis, anabolic metabolism, and angiogenesis notably via the phosphorylation of glycogen synthase kinase-3 (GSK3) and mTORC1 [184-186].

Both Rhy and Isorhy seem to activate the PI3K/AKT pathway [114,142,187-189] (Table 1). This pathway likely mediates neuroprotective effects of Rhy given that AKT has antiapoptotic and pro-survival effects [190-193]. In a Parkinson's disease model in which cerebellar neurons are exposed to 1-Methyl-4-phenylpyridinium (MPP<sup>+</sup>, a potent neurotoxin), pre-treatment with Rhy was shown to decrease neuronal death [188]. This effect was abolished by the addition of a specific PI3K inhibitor, indicating that the effect of Rhy on cell survival is PI3K/AKT-dependent [188]. Also, Rhy and Isorhy were shown to prevent the shift towards apoptosis as measured with the Bax to Bcl-2 ratio [188,189,194]. In similar experimental conditions, U. Rhyncophylla has been shown to favor anti-apoptotic protein over pro-apoptotic protein in vitro [195]. Also, Rhy, Isorhy and U. Rhyncophylla were all shown to prevent the increase of caspase-3 cleavage in various models of neurotoxicity [114,189,194-197]. The cleavage of caspase-3, known as an 'executor of apoptosis', is often considered the ultimate step in the apoptotic cascade [198].

GSK3, a major downstream effector of AKT [184], is a serine/threonine protein kinase particularly abundant in the CNS [199,200]. In mammals, GSK3 has two paralogs (i.e., homologous proteins derived from different genes), GSK3 $\alpha$  and GSK3 $\beta$  [201]. Unlike most enzymes, GSK3 is constitutively active and pathways converging on it tend to decrease its activity by phosphorylation. GSK3 has repeatedly been linked to mood disorders [202,203]. The literature shows that Rhy inhibits GSK3 $\beta$  under pathological conditions, which mainly depends on the activation of PI3K/AKT. Indeed, Rhy was shown to reverse the decrease in GSK3 $\beta$  phosphorylation induced by MPP<sup>+</sup> in cerebellar granule neurons, which was found to be PI3K-dependent [188]. Similarly, daily administration of Isorhy to chronically stressed mice or to A $\beta$ -treated rats was reported to revert the decrease in GSK3 $\beta$  and AKT phosphorylation in the hippocampus and/or cerebral cortex [142,189]. Of interest is also that GSK3 is part of a pathway controlling NRF2 (nuclear factor E2 related factor 2) [204], which levels and translocation to the nucleus are enhanced by Rhy in hippocampal neurons of rats subjected to subarachnoid hemorrhage [196]. Isorhy had the same effect on NRF2 [165,205], and was also shown to induce transcription of ARE (antioxidant response element)-dependent genes [205]. The transcription of those genes is activated by NRF2 under oxidative stress conditions [206,207].

Few data are directly linking PI3K/AKT to sleep regulation. AKT was shown to respond to chronic sleep restriction, which decreases its phosphorylation in the hippocampus [208], thereby

inhibiting the pathway. On the other hand, downstream targets of PI3K/AKT have been associated to sleep regulation, with in particular GSK3 $\beta$  activity that seems to impact sleep and the response to sleep loss. Firstly, mutant mice with constitutively active GSK3 $\beta$  were shown to have indications of an increased fragmentation of wakefulness and sleep states [209], and GSK3 $\beta$  knockdown in the cerebral cortex modifies the wakefulness and sleep EEG under baseline conditions and after SD in mice (Leduc et al., in preparation). Of note is that a genetic polymorphism decreasing GSK3 $\beta$  activity was found to ameliorate the clinical response to total SD in depressed patients [210,211]. Secondly, sleep-wake history appears to modify GSK3 $\beta$  activity. Chronic sleep restriction over a week was indeed shown to increase GSK3 $\beta$  phosphorylation in the hippocampus [208], and spontaneous wakefulness during the dark period to increase it in the hippocampus [212]. In a recent study, GSK3 $\beta$  activation was shown to occur at the transition to and during sleep and was proposed to act as major regulator of sleep-dependent plasticity [213]. In fact, GSK3  $\beta$  downregulation was found to abolish the SD-driven increase in mEPSCs (miniature excitatory post-synaptic currents) amplitude in the mouse PFC [214], supporting a role in wake/sleep-dependent plasticity. Thirdly, lithium, which is a direct inhibitor of GSK3 ( $\alpha$  and  $\beta$ ) [203], and the first-line treatment for bipolar disorders [215], was shown to affect sleep quality. For instance, lithium was reported to improve sleep efficiency in bipolar type I patients [216], to increase NREM sleep and decrease REM sleep in healthy volunteers [217], and to reduce REM sleep in mice [218]. The literature thus strongly supports a bidirectional relationship between GSK3 and sleep, which likely represents a key pathway by which Rhy could impact sleep architecture and EEG activity during sleep due to its inhibitory activity on GSK3 $\beta$ .

mTORC1, another serine/threonine kinase downstream of AKT [185,219], is an additional possible target of Rhy potentially underlying a role in wake/sleep regulation. In-deed, Rhy was shown to increase the phosphorylation of mTOR in a rat stroke model [114]. In parallel, sleep-wake history modifies mTORC1 activity, with sleep loss decreasing mTORC1 phosphorylation and thus attenuating mTORC1-dependent protein synthesis in the mouse hippocampus [220]. In addition, we have observed that mice heterozygous for mTOR are showing more SWA during wakefulness and REM sleep, and less the-ta activity during NREM sleep in comparison to wild-type mice (Areal et al., un-published). Globally, considering that main downstream effectors of PI3K/AKT shown to be modulated by Rhy have been linked to sleep, these represent pathways by which Rhy could impact wake/sleep phenotypes.

## 2.7 NF- $\kappa$ B and neuroinflammation

The NF- $\kappa$ B is a transcription factor with implications in multiple cellular processes including neuroinflammation [221]. It can be activated by cytokine receptors and TLRs, which drive its nuclear translocation via the phosphorylation/degradation of NF- $\kappa$ B inhibitors (I $\kappa$ Bs) [221]. The administration of Rhy has repeatedly been shown to diminish NF- $\kappa$ B activation in pathological contexts both in vitro [143,161,162,222] and in vivo [114,116,143,166,222] (**Table 1**). For example, in a rat nitroglycerin-induced migraine model, pre-treatment with Rhy almost completely prevented nuclear translocation of NF- $\kappa$ B in the trigeminal nucleus caudalis [116]. Moreover, it was shown that Rhy could decrease abnormal degradation of I $\kappa$ B $\alpha$  in pathological conditions such as treatments with lipopolysaccharide (LPS), nitroglycerin or 2,5-dimethoxy-4-iodoamphetamine [116,143,162,222,223]. In addition, there is growing literature supporting that Rhy reduces some effects associated with NF- $\kappa$ B activation: (i) the upregulation of pro-inflammatory cytokines such as interleukin-1 $\beta$  (IL-1 $\beta$ ) and tumor necrosis factor  $\alpha$  (TNF $\alpha$ ) [140,143,161,162,222,223], and (ii) the increase in oxidative stress caused, in part, by nitric oxide (NO) [116,161,162,166]. Indeed, the incubation of rat microglial cells with LPS in the presence of Rhy for 24h diminished the increase in NO, IL-1 $\beta$  and TNF $\alpha$ , and the increase in inducible NO synthase (iNOS) expression [161]. In contrast to its effect on iNOS-dependent NO synthesis, Rhy was shown to enhance endothelial NOS (eNOS)-dependent NO production in renal arteries of constitutively hypertensive rats via PI3K/AKT activation [187]. Thus, Rhy has different effects on NO synthesis depending on the context (here neuroinflammation/oxidative stress vs. vascular tone control). In pathological models such as ischemic brain injury and Tourette syndrome, Rhy was also shown to attenuate the upregulation of TLRs and MyD88 [114,222], the latter being an adaptor protein linking TLR activation to NF- $\kappa$ B nuclear translocation [224]. This led to the suggestion that the anti-inflammatory effects of Rhy in pathological contexts could result from an inhibition/downregulation of the TLR pathway [114,222]. However, a causative link remains to be defined.

The effect of Rhy on NF- $\kappa$ B and related pathways could impact sleep, at least in pathological contexts. Indeed, Rhy reduces the pathological upregulation of IL-1 $\beta$ , TNF $\alpha$  and NO, which are proposed to act as somnogenic substances [225,226]. More precisely, the administration of IL-1 $\beta$ , TNF $\alpha$  and NO (or of their precursors) was shown to increase NREM sleep duration in different mammalian species [227-232]. Moreover, the inhibition of these molecules and/or their

transcription factor NF- $\kappa$ B, was shown to decrease NREM sleep duration, again in multiple mammals [227-229,231,233-243]. In addition, SD was shown to upregulate IL-1 $\beta$ , TNF $\alpha$ , NO, and even NF- $\kappa$ B [244-247], and the inhibition of IL-1 $\beta$ , TNF $\alpha$  and NO can also reduce/block the NREM sleep rebound that is normally caused by sleep loss [234,235,238,240,248]. Finally, the administration of both IL-1 $\beta$  and TNF $\alpha$  was shown to increase slow wave amplitude during NREM sleep [230,231,249], and the inhibition of IL-1 $\beta$ , TNF $\alpha$  and NOS (non-selective NOS inhibition) was shown to reduce NREM sleep SWA [235,239,241]. The reduced NREM sleep SWA was also observed after SD for the inhibition of IL-1 $\beta$  and TNF $\alpha$  [238,240]. Accordingly, Rhy administration could, by inhibiting/downregulating NF- $\kappa$ B and IL-1 $\beta$ , TNF $\alpha$  and NO, reduce NREM sleep amount and SWA in pathological contexts. However, given that Rhy was shown not to impact IL-1 $\beta$ , TNF $\alpha$ , and p-IkBa levels in peripheral tissues (e.g., cardiomyocytes and macrophages) of healthy mice [223] (**Table 2**), support for a modulatory role of Rhy on sleep via this pathway under normal physiological conditions remains to be collected.

## 2.8 Neurotransmitters signaling

Rhy has also been suggested to affect neurotransmitter signaling. For instance, a 3-min incubation with Rhy was shown to inhibit muscarinic acetylcholine receptor 1 (mAChR1) and serotonin receptor 2 (5-HT<sub>2</sub>)-mediated currents in xenopus oocytes [250]. Also, i.p. injection of Rhy in rats was found to decrease the release of 5-HT in the hypothalamus, and to increase it in the amygdala, cerebral cortex, and brainstem [61]. In this last study, dopamine (DA) release was increased in all brain regions after Rhy administration [61]. Furthermore, Rhy was reported to rescue the amph-induced decrease of ACh, and the amph- and meth-induced increase in DA [101,251]. Rhy was also shown to attenuate the elevated DA and D2 receptor levels in the striatum of a rat Tourette syn-drome model [143]. This provides support for a direct impact of Rhy on neurotransmitters in a manner that depends on the (patho)physiological condition and brain region (**Table 1**). Importantly, mAChRs and DA receptors are metabotropic receptors, which activity has respectively been linked to Kv1.2 channels and L-VGCCs [252,253] (**Figure 2**), emphasizing that Rhy could act at multiple levels of neurotransmitter function (see section 2.1).

Interestingly, ACh, 5-HT and DA are important wake/sleep modulators, and components of the ascending arousal system [39]. Cholinergic activation in pontine regions increases cortical activation and REM sleep, and suppresses NREM sleep and SWA [44,254]. In fact, mAChR1 and

mAChR3 seem important for REM sleep regulation in both rodent and healthy subjects [255,256]. Furthermore, mAChR1 and other mAChRs modulate thalamocortical and hippocampal oscillations [257-263]. This suggests that the inhibitory effect of Rhy on mAChR1 (or its modulation of ACh release) may decrease REM sleep and cortical activation, and modify EEG activity.

5-HT, mainly originating from the RN, is another contributor to arousal [264], but its effects on wake/sleep regulation and EEG activity are more controversial. Indeed, optogenetic activation of dorsal RN 5-HT neurons was found to induce cortical activation and wakefulness [45,265], whereas the administration of 5-HT or drugs enhancing 5-HT transmission was shown to enhance EEG synchronization and sleep [264]. These opposite roles likely originate from the variety of 5-HT projections, such as to the BF [266], tegmental regions [267], and hypothalamic sleep regulatory neurons [268,269]. Moreover, different 5-HT receptors may be differently involved [270], given that the activation of 5-HT<sub>1A</sub> receptors can induce REM and theta activity [271-274], while that of 5-HT<sub>1B</sub>, 5-HT<sub>2A</sub>, 5-HT<sub>2A/2C</sub> or 5-HT<sub>7</sub> is suggested to reduce REM sleep [275-279]. Dopaminergic signaling was also found to be involved in wake/sleep regulation. Briefly, DA cells in the ventral tegmental area (VTA) discharge with different firing patterns during NREM and REM sleep [280], and DA stimulation in the VTA induces behavioral arousal [281]. Overall, more research is required to determine the mechanisms by which Rhy impacts 5-HT and DA neurotransmissions in order to eventually predict the 5-HT- and DA-dependent effects on sleep of Rhy.

Finally, the only literature directly linking Rhy and sleep (see also introduction) suggests that Rhy and Rhy-containing drugs are inducing sleep in rodents via GABA<sub>A</sub> receptors. In fact, the sleep-promoting effects of the two Uncaria-containing drugs were found to be suppressed by the GABA<sub>A</sub> receptor inhibitor bicuculline [57,58]. The only study using Rhy has linked the increased sleep time to increased level of GABA<sub>A</sub> receptor subunits and increased glutamic acid decarboxylase (GAD)65/67 ratio (indicative of increased GABA synthesis at the synapse) in hypothalamic neurons [22]. Many GABAergic neurons regulate the activity of arousal and sleep circuits [39]. The majority of sedatives/hypnotics, such as benzodiazepines, are GABA<sub>A</sub> receptor agonists and promote ‘light’ (as opposed to ‘deep’) NREM sleep [282,283]. In addition, GABAergic signaling is implicated in cell synchronization during sleep in brain circuits such as



the thalamocortical network [30,34]. Therefore, GABAergic signaling is likely a pathway by which Rhy could increase sleep time, and should be further investigated in vivo.

### 3. Conclusions

This review describes how Rhy affects diverse cellular pathways showing a particular relevance to sleep regulation, including VGCC, VGKC, NMDAR, RTK, ERK/MAPK, PI3K/AKT, NF- $\kappa$ B, and neurotransmitter signaling. The literature reveals both acute and delayed/chronic effects of Rhy on these different pathways. This suggests that Rhy may exert rapid effects on wakefulness/sleep quantity and quality, as well as effects that could last for some weeks after exposure. It is worth noting that the effects of Rhy on ion channels have only been characterized under acute conditions. This underlines the need to investigate the delayed and long-term effects of Rhy on ion channels in particular.

Interestingly, almost all studies describing effects of Rhy in vivo have reported effects solely under pathological/disturbed conditions (e.g., stress, treatments with psychostimulants, inflammation, animal models of diseases including stroke, epilepsy, and Alzheimer's disease), and not in control animals. In fact, apart from effects of Rhy under normal/undisturbed conditions reported in vitro for ion channels, neurotransmitter receptors, NMDAR and BDNF, only two in vivo studies demonstrate effects of Rhy under normal conditions. In the first, Rhy altered DA and 5-HT levels in the rat hippocampus [61], whereas the second showed that Rhy increases total sleep time and REM sleep in rats [22]. Therefore, the literature suggests that Rhy impacts molecular/cellular pathways predominantly under disturbed/diseased conditions. This suggests that Rhy could be particularly beneficial for some pathological conditions involving sleep disturbances. Nevertheless, the physiological effects (assessed under normal conditions) of Rhy on molecular/cellular targets such as ERK/MAPK, NF- $\kappa$ B (and TLR) or D2 receptors should be characterized in the CNS, given that effects have only been described in the context of neurotoxicity, inflammation or epilepsy.

Sex-dependent effects of Rhy also represent an area of need for future research. Indeed, among all studies reviewed in this article, only three have studied females. Two of these used both sexes to show effects of Rhy on EphA4 phosphorylation or neurotransmitter levels [18,61], and did not report sex-dependent effects. The last study used only females, and reported that Rhy reduces inflammatory responses and impacts the MAPK/ERK pathway in an asthma model [164], effects

that are comparable to those in males reported in other studies [116,165]. Therefore, there is a clear need to investigate whether Rhy has sex-dependent effects. This is particularly relevant with regard to Rhy targets that have been shown to be differentially involved in sleep in the two sexes. For example, genetic variants in *CACNA1C* were associated with increased sleep latency in male infants but not in females [81].

Another neglected sleep-related research area concerns the potential for effects of Rhy on circadian functions. Many of the pathways presented in this review have been linked to the circadian timing system [284]. For instance, NMDARs (including the GluN2B subunit), TrkB receptors, and D2Rs show circadian rhythms of mRNA or protein levels in specific brain regions [285-290]. This strongly suggests that the effects of Rhy on these specific targets will depend on time-of-day and/or internal circadian time. Thus, it appears crucial to consider the effects of Rhy separately, for instance, for the light and dark periods, at least for targets with known circadian regulation. Such investigation would notably help to determine the relevance of Rhy in chronotherapy.

This review has compiled the effects of Rhy with a particular focus on the CNS. However, Rhy impacts, among others, the cardiovascular and immune systems [3,10,223,291] (see also sections 2.1 and 2.6). Rhy was indeed shown to have antihypertensive roles via anti-sympathetic and vasodilatory effects that are mainly linked to ion channels [10]. Heart rate and heart rate variability differ between sleep stages [292,293], while systemic inflammation impacts sleep [28]. Thus, future research on Rhy should also consider the interplay between peripheral tissues and sleep.

As indicated in the introduction, Rhy is one of the most abundant alkaloids in *Uncaria*, which has been highly used in Chinese and Japanese traditional medicine [3,4,10]. The composition of *Uncaria* and, as a consequence, the components present in traditional treatments such as Chotoko could vary depending on the geographic region and plant growing conditions [294]. This may explain variations in the therapeutic effects of *Uncaria*, which might be overcome by the use of purified Rhy. Therefore, describing the specific mechanisms of action of Rhy will help defining the medical applications of this chemical. Nevertheless, multiple compounds in *Uncaria* may have synergistic actions in contributing to health benefits associated with the plant (e.g., chemicals helping the absorption of others; [295]). Thus, studies comparing the benefits of Rhy to those of

blends of Uncaria will help to identify the best treatment strategies for sleep disturbances and associated pathological conditions.

To conclude, Rhy may impact sleep architecture and oscillations by targeting a diversity of cellular pathways. These effects may specifically underlie the impacts of Chotoko, YKS and other Uncaria treatments on sleep. Further studies are required to precisely determine the effects of Rhy on sleep as well as on other CNS functions (e.g., memory) under undisturbed/normal conditions. A better understanding of the cellular mechanisms of action of Rhy that are relevant to sleep physiology may eventually help to determine whether this alkaloid could be used in sleep medicine.

## Acknowledgements

This work was supported by a Vanier Canada Graduate Scholarship (MNBR), a J.A. De Sève fellowship from the Research CIUSSS-NIM (TL), and the Canada Research Chair in Sleep Molecular Physiology (VM).

## References

1. Sarris, J.; Panossian, A.; Schweitzer, I.; Stough, C.; Scholey, A. Herbal medicine for depression, anxiety and insomnia: a review of psychopharmacology and clinical evidence. *Eur Neuropsychopharmacol* 2011, 21, 841-860, doi:10.1016/j.euroneuro.2011.04.002.
2. Singh, A.; Zhao, K. Treatment of insomnia with traditional chinese herbal medicine. *Int Rev Neurobiol* 2017, 135, 97-115, doi:10.1016/bs.irm.2017.02.006.
3. Yang, W.; Ip, S.P.; Liu, L.; Xian, Y.F.; Lin, Z.X. Uncaria rhynchophylla and its major constituents on central nervous system: a review on their pharmacological actions. *Curr Vasc Pharmacol* 2019, doi:10.2174/1570161117666190704092841.
4. Ndagijimana, A.; Wang, X.; Pan, G.; Zhang, F.; Feng, H.; Olaleye, O. A review on indole alkaloids isolated from Uncaria rhynchophylla and their pharmacological studies. *Fitoterapia* 2013, 86, 35-47, doi:10.1016/j.fitote.2013.01.018.
5. Shi, J.S.; Yu, J.X.; Chen, X.P.; Xu, R.X. Pharmacological actions of Uncaria alkaloids, rhynchophylline and isorhynchophylline. *Acta Pharmacol Sin* 2003, 24, 97-101.
6. Shinno, H.; Inami, Y.; Inagaki, T.; Nakamura, Y.; Horiguchi, J. Effect of Yi-Gan San on psychiatric symptoms and sleep structure at patients with behavioral and psychological symptoms of dementia. *Prog Neuropsychopharmacol Biol Psychiatry* 2008, 32, 881-885, doi:10.1016/j.pnpbp.2007.12.027.

7. Ozone, M.; Yagi, T.; Chiba, S.; Aoki, K.; Kuroda, A.; Mitsui, K.; Itoh, H.; Sasaki, M. Effect of yokukansan on psychophysiological insomnia evaluated using cyclic alternating pattern as an objective marker of sleep instability. *Sleep and Biological Rhythms* 2012, 10, 157-160.
8. Nakamura, Y.; Tajima, K.; Kawagoe, I.; Kanai, M.; Mitsuhata, H. Efficacy of traditional herbal medicine, Yokukansan on patients with neuropathic pain. *Masui* 2009, 58, 1248-1255.
9. Yamanaka, E.; Kimizuka, Y.; Aimi, N.; Sakai, S.; Haginiwa, J. Studies of plants containing indole alkaloids. IX. Quantitative analysis of tertiary alkaloids in various parts of *Uncaria rhynchophylla* MIQ. *Yakugaku Zasshi* 1983, 103, 1028-1033, doi:10.1248/yakushi1947.103.10\_1028.
10. Zhou, J.; Zhou, S. Antihypertensive and neuroprotective activities of rhynchophylline: the role of rhynchophylline in neurotransmission and ion channel activity. *J Ethnopharmacol* 2010, 132, 15-27, doi:10.1016/j.jep.2010.08.041.
11. Laus, G.; Teppner, H. The alkaloids of an *Uncaria rhynchophylla* (Rubiaceae-Coptosapelteae). *Phyton (Horn, Austria)* 1996, 36, 185-196.
12. Laus, G.; Brössner, D.; Keplinger, K. Alkaloids of peruvian *Uncaria tomentosa*. *Phytochemistry* 1997, 45, 855-860.
13. Wang, X.; Zheng, M.; Liu, J.; Huang, Z.; Bai, Y.; Ren, Z.; Wang, Z.; Tian, Y.; Qiao, Z.; Liu, W.; et al. Differences of first-pass effect in the liver and intestine contribute to the stereoselective pharmacokinetics of rhynchophylline and isorhynchophylline epimers in rats. *J Ethnopharmacol* 2017, 209, 175-183, doi:10.1016/j.jep.2017.07.039.
14. Wu, Z.F.; Wang, Y.Q.; Wan, N.; Ke, G.; Yue, P.F.; Chen, H.; Zhan, J.J.; Yang, M. Structural stabilities and transformation mechanism of Rhynchophylline and Isorhynchophylline by ultra performance liquid chromatography/time-of-flight mass spectrometry (UPLC/Q-TOF-MS). *Molecules* 2015, 20, 14849-14859, doi:10.3390/molecules200814849.
15. Lee, C.J.; Hsueh, T.Y.; Lin, L.C.; Tsai, T.H. Determination of protein-unbound rhynchophylline brain distribution by microdialysis and ultra-performance liquid chromatography with tandem mass spectrometry. *Biomed Chromatogr* 2014, 28, 901-906, doi:10.1002/bmc.3206.
16. Zhang, Y.N.; Yang, Y.F.; Xu, W.; Yang, X.W. The blood-brain barrier permeability of six indole alkaloids from *Uncariae Ramulus cum Uncis* in the MDCK-pHaMDR cell monolayer model. *Molecules* 2017, 22, doi:10.3390/molecules22111944.
17. Zhang, J.C.; Yao, W.; Qu, Y.; Nakamura, M.; Dong, C.; Yang, C.; Ren, Q.; Ma, M.; Han, M.; Shirayama, Y.; et al. Increased EphA4-ephexin1 signaling in the medial prefrontal cortex plays a role in depression-like phenotype. *Sci Rep* 2017, 7, 7133, doi:10.1038/s41598-017-07325-2.
18. Fu, A.K.; Hung, K.W.; Huang, H.; Gu, S.; Shen, Y.; Cheng, E.Y.; Ip, F.C.; Huang, X.; Fu, W.Y.; Ip, N.Y. Blockade of EphA4 signaling ameliorates hippocampal synaptic dysfunctions in mouse models of Alzheimer's disease. *Proc Natl Acad Sci U S A* 2014, 111, 9959-9964, doi:10.1073/pnas.1405803111.
19. Shao, H.; Yang, Y.; Mi, Z.; Zhu, G.X.; Qi, A.P.; Ji, W.G.; Zhu, Z.R. Anticonvulsant effect of Rhynchophylline involved in the inhibition of persistent sodium current and NMDA receptor current in the pilocarpine rat model of temporal lobe epilepsy. *Neuroscience* 2016, 337, 355-369, doi:10.1016/j.neuroscience.2016.09.029.

20. Zhou, J.Y.; Mo, Z.X.; Zhou, S.W. Rhynchophylline down-regulates NR2B expression in cortex and hippocampal CA1 area of amphetamine-induced conditioned place preference rat. *Arch Pharm Res* 2010, 33, 557-565, doi:10.1007/s12272-010-0410-3.
21. Guo, Y.; Luo, C.; Tu, G.; Li, C.; Liu, Y.; Liu, W.; Lam Yung, K.K.; Mo, Z. Rhynchophylline downregulates phosphorylated cAMP response element binding protein, nuclear receptor-related-1, and brain-derived neurotrophic factor expression in the hippocampus of ketamine-induced conditioned place preference rats. *Pharmacogn Mag* 2018, 14, 81-86, doi:10.4103/pm.pm\_90\_17.
22. Yoo, J.H.; Ha, T.W.; Hong, J.T.; Oh, K.W. Rhynchophylline, one of major constituents of *Uncariae Ramulus* et *Uncus* enhances pentobarbital-induced sleep behaviors and Rapid Eye Movement Sleep in rodents. *Natural Product Sciences* 2016, 22, 263-269.
23. Frank, M.G.; Heller, H.C. The function(s) of sleep. *Handb Exp Pharmacol* 2019, 253, 3-34, doi:10.1007/164\_2018\_140.
24. Kempf, A.; Song, S.M.; Talbot, C.B.; Miesenbock, G. A potassium channel beta-subunit couples mitochondrial electron transport to sleep. *Nature* 2019, 568, 230-234, doi:10.1038/s41586-019-1034-5.
25. Vyazovskiy, V.V.; Walton, M.E.; Peirson, S.N.; Bannerman, D.M. Sleep homeostasis, habits and habituation. *Curr Opin Neurobiol* 2017, 44, 202-211, doi:10.1016/j.conb.2017.05.002.
26. Boyce, R.; Williams, S.; Adamantidis, A. REM sleep and memory. *Curr Opin Neurobiol* 2017, 44, 167-177, doi:10.1016/j.conb.2017.05.001.
27. Timofeev, I.; Chauvette, S. Sleep slow oscillation and plasticity. *Curr Opin Neurobiol* 2017, 44, 116-126, doi:10.1016/j.conb.2017.03.019.
28. Irwin, M.R. Sleep and inflammation: partners in sickness and in health. *Nat Rev Immunol* 2019, 19, 702-715, doi:10.1038/s41577-019-0190-z.
29. Abel, T.; Havekes, R.; Saletin, J.M.; Walker, M.P. Sleep, plasticity and memory from molecules to whole-brain networks. *Curr Biol* 2013, 23, R774-788, doi:10.1016/j.cub.2013.07.025.
30. Headley, D.B.; Pare, D. Common oscillatory mechanisms across multiple memory systems. *NPJ Sci Learn* 2017, 2, doi:10.1038/s41539-016-0001-2.
31. Franken, P.; Dijk, D.J.; Tobler, I.; Borbely, A.A. Sleep deprivation in rats: effects on EEG power spectra, vigilance states, and cortical temperature. *Am J Physiol* 1991, 261, R198-208, doi:10.1152/ajpregu.1991.261.1.R198.
32. Hubbard, J.; Gent, T.C.; Hoekstra, M.M.B.; Emmenegger, Y.; Mongrain, V.; Landolt, H.P.; Adamantidis, A.R.; Franken, P. Rapid fast-delta decay following prolonged wakefulness marks a phase of wake-inertia in NREM sleep. *Nat Commun* 2020, 11, 3130, doi:10.1038/s41467-020-16915-0.
33. Montgomery, S.M.; Sirota, A.; Buzsaki, G. Theta and gamma coordination of hippocampal networks during waking and rapid eye movement sleep. *J Neurosci* 2008, 28, 6731-6741, doi:10.1523/JNEUROSCI.1227-08.2008.
34. Steriade, M.; McCormick, D.A.; Sejnowski, T.J. Thalamocortical oscillations in the sleeping and aroused brain. *Science* 1993, 262, 679-685, doi:10.1126/science.8235588.

35. Steriade, M.; Timofeev, I.; Grenier, F. Natural waking and sleep states: a view from inside neocortical neurons. *J Neurophysiol* 2001, 85, 1969-1985, doi:10.1152/jn.2001.85.5.1969.
36. Borbely, A.A. A two process model of sleep regulation. *Hum Neurobiol* 1982, 1, 195-204.
37. Daan, S.; Beersma, D.G.; Borbely, A.A. Timing of human sleep: recovery process gated by a circadian pacemaker. *Am J Physiol* 1984, 246, R161-183, doi:10.1152/ajpregu.1984.246.2.R161.
38. Dijk, D.J.; Czeisler, C.A. Contribution of the circadian pacemaker and the sleep homeostat to sleep propensity, sleep structure, electroencephalographic slow waves, and sleep spindle activity in humans. *J Neurosci* 1995, 15, 3526-3538.
39. Jones, B.E. Arousal and sleep circuits. *Neuropsychopharmacology* 2020, 45, 6-20, doi:10.1038/s41386-019-0444-2.
40. Saper, C.B.; Scammell, T.E.; Lu, J. Hypothalamic regulation of sleep and circadian rhythms. *Nature* 2005, 437, 1257-1263, doi:10.1038/nature04284.
41. Adamantidis, A.R.; Zhang, F.; Aravanis, A.M.; Deisseroth, K.; de Lecea, L. Neural substrates of awakening probed with optogenetic control of hypocretin neurons. *Nature* 2007, 450, 420-424, doi:10.1038/nature06310.
42. Carter, M.E.; Yizhar, O.; Chikahisa, S.; Nguyen, H.; Adamantidis, A.; Nishino, S.; Deisseroth, K.; de Lecea, L. Tuning arousal with optogenetic modulation of locus coeruleus neurons. *Nat Neurosci* 2010, 13, 1526-1533, doi:10.1038/nn.2682.
43. Han, Y.; Shi, Y.F.; Xi, W.; Zhou, R.; Tan, Z.B.; Wang, H.; Li, X.M.; Chen, Z.; Feng, G.; Luo, M.; et al. Selective activation of cholinergic basal forebrain neurons induces immediate sleep-wake transitions. *Curr Biol* 2014, 24, 693-698, doi:10.1016/j.cub.2014.02.011.
44. Kroeger, D.; Ferrari, L.L.; Petit, G.; Mahoney, C.E.; Fuller, P.M.; Arrigoni, E.; Scammell, T.E. Cholinergic, glutamatergic, and GABAergic neurons of the pedunculopontine tegmental nucleus have distinct effects on sleep/wake behavior in mice. *J Neurosci* 2017, 37, 1352-1366, doi:10.1523/JNEUROSCI.1405-16.2016.
45. Smith, H.R.; Leibold, N.K.; Rappoport, D.A.; Ginapp, C.M.; Purnell, B.S.; Bode, N.M.; Alberico, S.L.; Kim, Y.C.; Audero, E.; Gross, C.T.; et al. Dorsal raphe serotonin neurons mediate CO<sub>2</sub>-induced arousal from sleep. *J Neurosci* 2018, 38, 1915-1925, doi:10.1523/JNEUROSCI.2182-17.2018.
46. Boucetta, S.; Cisse, Y.; Mainville, L.; Morales, M.; Jones, B.E. Discharge profiles across the sleep-waking cycle of identified cholinergic, GABAergic, and glutamatergic neurons in the pontomesencephalic tegmentum of the rat. *J Neurosci* 2014, 34, 4708-4727, doi:10.1523/JNEUROSCI.2617-13.2014.
47. Chung, S.; Weber, F.; Zhong, P.; Tan, C.L.; Nguyen, T.N.; Beier, K.T.; Hormann, N.; Chang, W.C.; Zhang, Z.; Do, J.P.; et al. Identification of preoptic sleep neurons using retrograde labelling and gene profiling. *Nature* 2017, 545, 477-481, doi:10.1038/nature22350.
48. Van Dort, C.J.; Zachs, D.P.; Kenny, J.D.; Zheng, S.; Goldblum, R.R.; Gelwan, N.A.; Ramos, D.M.; Nolan, M.A.; Wang, K.; Weng, F.J.; et al. Optogenetic activation of cholinergic neurons in the PPT or LDT induces REM sleep. *Proc Natl Acad Sci U S A* 2015, 112, 584-589, doi:10.1073/pnas.1423136112.
49. Luppi, P.H.; Billwiller, F.; Fort, P. Selective activation of a few limbic structures during paradoxical (REM) sleep by the claustrum and the supramammillary nucleus: evidence and function. *Curr Opin Neurobiol* 2017, 44, 59-64, doi:10.1016/j.conb.2017.03.002.

50. Shinno, H.; Kamei, M.; Nakamura, Y.; Inami, Y.; Horiguchi, J. Successful treatment with Yi-Gan San for rapid eye movement sleep behavior disorder. *Prog Neuropsychopharmacol Biol Psychiatry* 2008, 32, 1749-1751, doi:10.1016/j.pnpbp.2008.06.015.
51. Matsui, K.; Sasai-Sakuma, T.; Ishigooka, J.; Nishimura, K.; Inoue, Y. Effect of Yokukansan for the treatment of idiopathic rapid eye movement sleep behavior disorder: a retrospective analysis of consecutive patients. *Journal of Clinical Sleep Medicine* 2019, 15, 1173-1178.
52. Ozone, M.; Shimazaki, H.; Ichikawa, H.; Shigeta, M. Efficacy of yokukansan compared with clonazepam for rapid eye movement sleep behaviour disorder: a preliminary retrospective study. *Psychogeriatrics* 2020, doi:10.1111/psyg.12563.
53. Ohtomo, Y.; Umino, D.; Nijama, S.; Fujinaga, S.; Shimizu, T. Yokukansan: a treatment option for nocturnal enuresis in children by improving sleep quality. *Juntendo Medical Journal* 2014, 60, 536-542.
54. Aizawa, R.; Kanbayashi, T.; Saito, Y.; Ogawa, Y.; Sugiyama, T.; Kitajima, T.; Kaneko, Y.; Abe, M.; Shimizu, T. Effects of Yoku-kan-san-ka-chimpi-hange on the sleep of normal healthy adult subjects. *Psychiatry Clin Neurosci* 2002, 56, 303-304, doi:10.1046/j.1440-1819.2002.01006.x.
55. Pan, W.; Kwak, S.; Li, G.; Chen, Y.; Cai, D. Therapeutic effect of Yang-Xue-Qing-Nao granules on sleep dysfunction in Parkinson's disease. *Chin Med* 2013, 8, 14, doi:10.1186/1749-8546-8-14.
56. Sun, Y.Z.; Liu, R. Therapeutic evaluation on needling method of regulating the conception vessel and calming the mind for perimenopausal sleep disorder. *Journal of Acupuncture and Tuina Science* 2013, 11, 142-146.
57. Egashira, N.; Nogami, A.; Iwasaki, K.; Ishibashi, A.; Uchida, N.; Takasaki, K.; Mishima, K.; Nishimura, R.; Oishi, R.; Fujiwara, M. Yokukansan enhances pentobarbital-induced sleep in socially isolated mice: possible involvement of GABA(A)-benzodiazepine receptor complex. *J Pharmacol Sci* 2011, 116, 316-320.
58. Murata, K.; Li, F.; Shinguchi, K.; Ogata, M.; Fujita, N.; Takahashi, R. Yokukansankachimpihange improves the social isolation-induced sleep disruption and allopregnanolone reduction in mice. *Front Nutr* 2020, 7, 8, doi:10.3389/fnut.2020.00008.
59. Nagao, M.; Takasaki, K.; Nogami, A.; Hirai, Y.; Moriyama, H.; Uchida, N.; Kubota, K.; Katsurabayashi, S.; Mishima, K.; Nishimura, R.; et al. Effect of Yokukansan on sleep disturbance in a rat model of cerebrovascular dementia. *Traditional & Kampo Medicine* 2014, 1, 19-26.
60. Jeenapongsa, R.; Tohda, M. Effects of Choto-san and Chotoko on thiopental-induced sleeping time. *和漢医薬学雑誌= Journal of traditional medicines* 2003, 20, 165-167.
61. Shi, J.S.; Huang, B.; Wu, Q.; Ren, R.X.; Xie, X.L. Effects of rhynchophylline on motor activity of mice and serotonin and dopamine in rat brain. *Zhongguo Yao Li Xue Bao* 1993, 14, 114-117.
62. Sakakibara, I.; Terabayashi, S.; Kubo, M.; Higuchi, M.; Komatsu, Y.; Okada, M.; Taki, K.; Kamei, J. Effect on locomotion of indole alkaloids from the hooks of *Uncaria* plants. *Phytomedicine* 1999, 6, 163-168, doi:10.1016/S0944-7113(99)80004-X.
63. Quílez, A.; Saenz, M.T.; García, M.D. *Uncaria tomentosa* (Willd. ex. Roem. & Schult.) DC. and *Eucalyptus globulus* Labill. interactions when administered with diazepam. *Phytotherapy research* 2012, 26, 458-461.

64. Lipscombe, D.; Helton, T.D.; Xu, W. L-type calcium channels: the low down. *J Neurophysiol* 2004, 92, 2633-2641, doi:10.1152/jn.00486.2004.
65. Kai, L.W., Z.F.; Xue, C.H. Effects of Rhynchophylline on L-type calcium channels in isolated rat cortical neurons during acute hypoxia. *Journal of Chinese Pharmaceutical Sciences* 1998, 7, 205-208.
66. Wang, X.L.; Zhang, L.M.; Hua, Z. Blocking effect of rhynchophylline on calcium channels in isolated rat ventricular myocytes. *Zhongguo Yao Li Xue Bao* 1994, 15, 115-118.
67. Li, P.Y.; Zeng, X.R.; Cheng, J.; Wen, J.; Inoue, I.; Yang, Y. Rhynchophylline-induced vasodilation in human mesenteric artery is mainly due to blockage of L-type calcium channels in vascular smooth muscle cells. *Naunyn Schmiedebergs Arch Pharmacol* 2013, 386, 973-982, doi:10.1007/s00210-013-0888-6.
68. Zhang, W.B.; Chen, C.X.; Sim, S.M.; Kwan, C.Y. In vitro vasodilator mechanisms of the indole alkaloids rhynchophylline and isorhynchophylline, isolated from the hook of *Uncaria rhynchophylla* (Miquel). *Naunyn Schmiedebergs Arch Pharmacol* 2004, 369, 232-238, doi:10.1007/s00210-003-0854-9.
69. Zhang, W.; Liu, G.X.; Huang, X.N. Effect of rhynchophylline on the contraction of rabbit aorta. *Zhongguo Yao Li Xue Bao* 1987, 8, 425-429.
70. Wiera, G.; Nowak, D.; van Hove, I.; Dziegiel, P.; Moons, L.; Mozrzymas, J.W. Mechanisms of NMDA receptor- and voltage-gated L-Type calcium channel-dependent hippocampal LTP critically rely on proteolysis that is mediated by distinct metalloproteinases. *J Neurosci* 2017, 37, 1240-1256, doi:10.1523/JNEUROSCI.2170-16.2016.
71. Kumar, M.; John, M.; Madhavan, M.; James, J.; Omkumar, R.V. Alteration in the phosphorylation status of NMDA receptor GluN2B subunit by activation of both NMDA receptor and L-type voltage gated calcium channel. *Neurosci Lett* 2019, 709, 134343, doi:10.1016/j.neulet.2019.134343.
72. Zamponi, G.W. Targeting voltage-gated calcium channels in neurological and psychiatric diseases. *Nat Rev Drug Discov* 2016, 15, 19-34, doi:10.1038/nrd.2015.5.
73. Lacinova, L.; Moosmang, S.; Langwieser, N.; Hofmann, F.; Kleppisch, T. Cav1.2 calcium channels modulate the spiking pattern of hippocampal pyramidal cells. *Life Sci* 2008, 82, 41-49, doi:10.1016/j.lfs.2007.10.009.
74. Hansen, A.K.; Nedergaard, S.; Andreasen, M. Intrinsic Ca<sup>2+</sup>-dependent theta oscillations in apical dendrites of hippocampal CA1 pyramidal cells in vitro. *J Neurophysiol* 2014, 112, 631-643, doi:10.1152/jn.00753.2013.
75. Plumbly, W.; Brandon, N.; Deeb, T.Z.; Hall, J.; Harwood, A.J. L-type voltage-gated calcium channel regulation of in vitro human cortical neuronal networks. *Sci Rep* 2019, 9, 13810, doi:10.1038/s41598-019-50226-9.
76. Kabir, Z.D.; Che, A.; Fischer, D.K.; Rice, R.C.; Rizzo, B.K.; Byrne, M.; Glass, M.J.; De Marco Garcia, N.V.; Rajadhyaksha, A.M. Rescue of impaired sociability and anxiety-like behavior in adult cacna1c-deficient mice by pharmacologically targeting eIF2 $\alpha$ . *Mol Psychiatry* 2017, 22, 1096-1109, doi:10.1038/mp.2017.124.
77. Ode, K.L.; Katsumata, T.; Tone, D.; Ueda, H.R. Fast and slow Ca(2+)-dependent hyperpolarization mechanisms connect membrane potential and sleep homeostasis. *Curr Opin Neurobiol* 2017, 44, 212-221, doi:10.1016/j.conb.2017.05.007.
78. Bazhenov, M.; Timofeev, I.; Steriade, M.; Sejnowski, T.J. Model of thalamocortical slow-wave sleep oscillations and transitions to activated States. *J Neurosci* 2002, 22, 8691-8704.



79. Sinnegger-Brauns, M.J.; Huber, I.G.; Koschak, A.; Wild, C.; Obermair, G.J.; Einzinger, U.; Hoda, J.C.; Sartori, S.B.; Striessnig, J. Expression and 1,4-dihydropyridine-binding properties of brain L-type calcium channel isoforms. *Mol Pharmacol* 2009, 75, 407-414, doi:10.1124/mol.108.049981.
80. Kumar, D.; Dedic, N.; Flachskamm, C.; Voule, S.; Deussing, J.M.; Kimura, M. Cacna1c (Cav1.2) modulates electroencephalographic rhythm and rapid eye movement sleep recovery. *Sleep* 2015, 38, 1371-1380, doi:10.5665/sleep.4972.
81. Kantojarvi, K.; Liuhanen, J.; Saarenpaa-Heikkila, O.; Satomaa, A.L.; Kylliainen, A.; Polkki, P.; Jaatela, J.; Toivola, A.; Milani, L.; Himanen, S.L.; et al. Variants in calcium voltage-gated channel subunit Alpha1 C-gene (CACNA1C) are associated with sleep latency in infants. *PLoS One* 2017, 12, e0180652, doi:10.1371/journal.pone.0180652.
82. Schmutz, I.; Chavan, R.; Ripperger, J.A.; Maywood, E.S.; Langwieser, N.; Jurik, A.; Stauffer, A.; Delorme, J.E.; Moosmang, S.; Hastings, M.H.; et al. A specific role for the REV-ERBalpha-controlled L-Type Voltage-Gated Calcium Channel CaV1.2 in resetting the circadian clock in the late night. *J Biol Rhythms* 2014, 29, 288-298, doi:10.1177/0748730414540453.
83. Manis, P.B. Delayed rectifier and A-Type potassium channels. In *Encyclopedia of computational neuroscience*. Springer Publishing Company, Incorporated, Jaeger, D., Jung, R., Eds.; Springer Publishing Company: New York, NY, 2015; pp. 971-985.
84. Chou, C.H.; Gong, C.L.; Chao, C.C.; Lin, C.H.; Kwan, C.Y.; Hsieh, C.L.; Leung, Y.M. Rhynchophylline from *Uncaria rhynchophylla* functionally turns delayed rectifiers into A-Type K<sup>+</sup> channels. *J Nat Prod* 2009, 72, 830-834, doi:10.1021/np800729q.
85. Sheng, M.; Tsaur, M.L.; Jan, Y.N.; Jan, L.Y. Contrasting subcellular localization of the Kv1.2 K<sup>+</sup> channel subunit in different neurons of rat brain. *J Neurosci* 1994, 14, 2408-2417.
86. Tsaur, M.L.; Sheng, M.; Lowenstein, D.H.; Jan, Y.N.; Jan, L.Y. Differential expression of K<sup>+</sup> channel mRNAs in the rat brain and down-regulation in the hippocampus following seizures. *Neuron* 1992, 8, 1055-1067, doi:10.1016/0896-6273(92)90127-y.
87. Espinosa, F.; Marks, G.; Heintz, N.; Joho, R.H. Increased motor drive and sleep loss in mice lacking Kv3-type potassium channels. *Genes Brain Behav* 2004, 3, 90-100, doi:10.1046/j.1601-183x.2003.00054.x.
88. Douglas, C.L.; Vyazovskiy, V.; Southard, T.; Chiu, S.Y.; Messing, A.; Tononi, G.; Cirelli, C. Sleep in *Kcna2* knockout mice. *BMC Biol* 2007, 5, 42, doi:10.1186/1741-7007-5-42.
89. Vyazovskiy, V.V.; Deboer, T.; Rudy, B.; Lau, D.; Borbely, A.A.; Tobler, I. Sleep EEG in mice that are deficient in the potassium channel subunit K.v.3.2. *Brain Res* 2002, 947, 204-211, doi:10.1016/s0006-8993(02)02925-6.
90. Douglas, C.L.; Vyazovskiy, V.; Southard, T.; Faraguna, U.; Cirelli, C.; Tononi, G. Voltage-dependent potassium channel Kv1.2: Effects on sleep and EEG power spectrum of intracortical injections of an anti-Kv1.2 antibody. In *Proceedings of the 20th Annual Meeting of the Associated-Professional-Sleep-Societies*, Salt Lake City, Utah, 2006.
91. Bushey, D.; Huber, R.; Tononi, G.; Cirelli, C. *Drosophila* Hyperkinetic mutants have reduced sleep and impaired memory. *J Neurosci* 2007, 27, 5384-5393, doi:10.1523/JNEUROSCI.0108-07.2007.

92. Tatsuki, F.; Sunagawa, G.A.; Shi, S.; Susaki, E.A.; Yukinaga, H.; Perrin, D.; Sumiyama, K.; Ukai-Tadenuma, M.; Fujishima, H.; Ohno, R.; et al. Involvement of Ca(2+)-dependent hyperpolarization in sleep duration in mammals. *Neuron* 2016, 90, 70-85, doi:10.1016/j.neuron.2016.02.032.
93. Malinow, R.; Malenka, R.C. AMPA receptor trafficking and synaptic plasticity. *Annu Rev Neurosci* 2002, 25, 103-126, doi:10.1146/annurev.neuro.25.112701.142758.
94. Kang, T.H.; Murakami, Y.; Matsumoto, K.; Takayama, H.; Kitajima, M.; Aimi, N.; Watanabe, H. Rhynchophylline and isorhynchophylline inhibit NMDA receptors expressed in *Xenopus* oocytes. *Eur J Pharmacol* 2002, 455, 27-34, doi:10.1016/s0014-2999(02)02581-5.
95. Liu, Y.; Wong, T.P.; Aarts, M.; Rooyackers, A.; Liu, L.; Lai, T.W.; Wu, D.C.; Lu, J.; Tymianski, M.; Craig, A.M.; et al. NMDA receptor subunits have differential roles in mediating excitotoxic neuronal death both in vitro and in vivo. *J Neurosci* 2007, 27, 2846-2857, doi:10.1523/JNEUROSCI.0116-07.2007.
96. Xu, J.; Kurup, P.; Zhang, Y.; Goebel-Goody, S.M.; Wu, P.H.; Hawasli, A.H.; Baum, M.L.; Bibb, J.A.; Lombroso, P.J. Extrasynaptic NMDA receptors couple preferentially to excitotoxicity via calpain-mediated cleavage of STEP. *J Neurosci* 2009, 29, 9330-9343, doi:10.1523/JNEUROSCI.2212-09.2009.
97. Yang, Y.; Ji, W.G.; Zhu, Z.R.; Wu, Y.L.; Zhang, Z.Y.; Qu, S.C. Rhynchophylline suppresses soluble Aβ1-42-induced impairment of spatial cognition function via inhibiting excessive activation of extrasynaptic NR2B-containing NMDA receptors. *Neuropharmacology* 2018, 135, 100-112, doi:10.1016/j.neuropharm.2018.03.007.
98. Li, J.; Liu, W.; Peng, Q.; Jiang, M.; Luo, C.; Guo, Y.; Liu, Y.; Fang, M.; Mo, Z. Effect of rhynchophylline on conditioned place preference on expression of NR2B in methamphetamine-dependent mice. *Biochem Biophys Res Commun* 2014, 452, 695-700, doi:10.1016/j.bbrc.2014.08.127.
99. He, Y.; Zeng, S.Y.; Zhou, S.W.; Qian, G.S.; Peng, K.; Mo, Z.X.; Zhou, J.Y. Effects of rhynchophylline on GluN1 and GluN2B expressions in primary cultured hippocampal neurons. *Fitoterapia* 2014, 98, 166-173, doi:10.1016/j.fitote.2014.08.002.
100. Shao, H.; Mi, Z.; Ji, W.G.; Zhang, C.H.; Zhang, T.; Ren, S.C.; Zhu, Z.R. Rhynchophylline protects against the amyloid beta-induced increase of spontaneous discharges in the hippocampal CA1 region of rats. *Neurochem Res* 2015, 40, 2365-2373, doi:10.1007/s11064-015-1730-y.
101. Jiang, M.; Chen, Y.; Li, C.; Peng, Q.; Fang, M.; Liu, W.; Kang, Q.; Lin, Y.; Yung, K.K.; Mo, Z. Inhibiting effects of rhynchophylline on zebrafish methamphetamine dependence are associated with amelioration of neurotransmitters content and down-regulation of TH and NR2B expression. *Prog Neuropsychopharmacol Biol Psychiatry* 2016, 68, 31-43, doi:10.1016/j.pnpbp.2016.03.004.
102. Kaneko, Y.; Coats, A.B.; Tuazon, J.P.; Jo, M.; Borlongan, C.V. Rhynchophylline promotes stem cell autonomous metabolic homeostasis. *Cytotherapy* 2020, 22, 106-113, doi:10.1016/j.jcyt.2019.12.008.
103. Yin, D.; Dong, H.; Wang, T.X.; Hu, Z.Z.; Cheng, N.N.; Qu, W.M.; Huang, Z.L. Glutamate activates the histaminergic tuberomammillary nucleus and increases wakefulness in rats. *Neuroscience* 2019, 413, 86-98, doi:10.1016/j.neuroscience.2019.05.032.
104. Manfredi, A.; Brambilla, D.; Mancina, M. Stimulation of NMDA and AMPA receptors in the rat nucleus basalis of Meynert affects sleep. *Am J Physiol* 1999, 277, R1488-1492, doi:10.1152/ajpregu.1999.277.5.R1488.

105. Datta, S.; Siwek, D.F. Excitation of the brain stem pedunculopontine tegmentum cholinergic cells induces wakefulness and REM sleep. *J Neurophysiol* 1997, 77, 2975-2988, doi:10.1152/jn.1997.77.6.2975.
106. Datta, S.; Spoley, E.E.; Patterson, E.H. Microinjection of glutamate into the pedunculopontine tegmentum induces REM sleep and wakefulness in the rat. *Am J Physiol Regul Integr Comp Physiol* 2001, 280, R752-759, doi:10.1152/ajpregu.2001.280.3.R752.
107. Campbell, I.G.; Feinberg, I. NREM delta stimulation following MK-801 is a response of sleep systems. *J Neurophysiol* 1996, 76, 3714-3720, doi:10.1152/jn.1996.76.6.3714.
108. Campbell, I.G.; Feinberg, I. Comparison of MK-801 and sleep deprivation effects on NREM, REM, and waking spectra in the rat. *Sleep* 1999, 22, 423-432, doi:10.1093/sleep/22.4.423.
109. Ishikawa, I.; Shinno, H.; Ando, N.; Mori, T.; Nakamura, Y. The effect of memantine on sleep architecture and psychiatric symptoms in patients with Alzheimer's disease. *Acta Neuropsychiatr* 2016, 28, 157-164, doi:10.1017/neu.2015.61.
110. Kaushik, M.K.; Kumar, V.M.; Mallick, H.N. Glutamate microinjection at the medial preoptic area enhances slow wave sleep in rats. *Behav Brain Res* 2011, 217, 240-243, doi:10.1016/j.bbr.2010.11.007.
111. Mukherjee, D.; Kaushik, M.K.; Jaryal, A.K.; Kumar, V.M.; Mallick, H.N. Glutamate microinjection in the medial septum of rats decreases paradoxical sleep and increases slow wave sleep. *Neuroreport* 2012, 23, 451-456, doi:10.1097/WNR.0b013e3283533692.
112. Kocsis, B. State-dependent increase of cortical gamma activity during REM sleep after selective blockade of NR2B subunit containing NMDA receptors. *Sleep* 2012, 35, 1011-1016, doi:10.5665/sleep.1972.
113. El Gaamouch, F.; Buisson, A.; Moustie, O.; Lemieux, M.; Labrecque, S.; Bontempi, B.; De Koninck, P.; Nicole, O. Interaction between alphaCaMKII and GluN2B controls ERK-dependent plasticity. *J Neurosci* 2012, 32, 10767-10779, doi:10.1523/JNEUROSCI.5622-11.2012.
114. Huang, H.; Zhong, R.; Xia, Z.; Song, J.; Feng, L. Neuroprotective effects of rhynchophylline against ischemic brain injury via regulation of the Akt/mTOR and TLRs signaling pathways. *Molecules* 2014, 19, 11196-11210, doi:10.3390/molecules190811196.
115. Krapivinsky, G.; Krapivinsky, L.; Manasian, Y.; Ivanov, A.; Tyzio, R.; Pellegrino, C.; Ben-Ari, Y.; Clapham, D.E.; Medina, I. The NMDA receptor is coupled to the ERK pathway by a direct interaction between NR2B and RasGRF1. *Neuron* 2003, 40, 775-784, doi:10.1016/s0896-6273(03)00645-7.
116. Lai, T.; Chen, L.; Chen, X.; He, J.; Lv, P.; Ge, H. Rhynchophylline attenuates migraine in trigeminal nucleus caudalis in nitroglycerin-induced rat model by inhibiting MAPK/NF-kB signaling. *Mol Cell Biochem* 2019, 461, 205-212, doi:10.1007/s11010-019-03603-x.
117. Wang, Y.; Wang, W.; Li, D.; Li, M.; Wang, P.; Wen, J.; Liang, M.; Su, B.; Yin, Y. IGF-1 alleviates NMDA-induced excitotoxicity in cultured hippocampal neurons against autophagy via the NR2B/PI3K-AKT-mTOR pathway. *J Cell Physiol* 2014, 229, 1618-1629, doi:10.1002/jcp.24607.
118. Yoshii, A.; Constantine-Paton, M. BDNF induces transport of PSD-95 to dendrites through PI3K-AKT signaling after NMDA receptor activation. *Nat Neurosci* 2007, 10, 702-711, doi:10.1038/nn1903.

119. Gale, N.W.; Baluk, P.; Pan, L.; Kwan, M.; Holash, J.; DeChiara, T.M.; McDonald, D.M.; Yancopoulos, G.D. Ephrin-B2 selectively marks arterial vessels and neovascularization sites in the adult, with expression in both endothelial and smooth-muscle cells. *Dev Biol* 2001, 230, 151-160, doi:10.1006/dbio.2000.0112.
120. Matsuo, K.; Otaki, N. Bone cell interactions through Eph/ephrin: bone modeling, remodeling and associated diseases. *Cell Adh Migr* 2012, 6, 148-156, doi:10.4161/cam.20888.
121. Stark, D.A.; Karvas, R.M.; Siegel, A.L.; Cornelison, D.D. Eph/ephrin interactions modulate muscle satellite cell motility and patterning. *Development* 2011, 138, 5279-5289, doi:10.1242/dev.068411.
122. Murai, K.K.; Pasquale, E.B. 'Eph'ective signaling: forward, reverse and crosstalk. *J Cell Sci* 2003, 116, 2823-2832, doi:10.1242/jcs.00625.
123. Murai, K.K.; Pasquale, E.B. Eph receptors and ephrins in neuron-astrocyte communication at synapses. *Glia* 2011, 59, 1567-1578, doi:10.1002/glia.21226.
124. Carmona, M.A.; Murai, K.K.; Wang, L.; Roberts, A.J.; Pasquale, E.B. Glial ephrin-A3 regulates hippocampal dendritic spine morphology and glutamate transport. *Proc Natl Acad Sci U S A* 2009, 106, 12524-12529, doi:10.1073/pnas.0903328106.
125. Fu, A.K.; Hung, K.W.; Fu, W.Y.; Shen, C.; Chen, Y.; Xia, J.; Lai, K.O.; Ip, N.Y. APC(Cdh1) mediates EphA4-dependent downregulation of AMPA receptors in homeostatic plasticity. *Nat Neurosci* 2011, 14, 181-189, doi:10.1038/nn.2715.
126. Fu, W.Y.; Chen, Y.; Sahin, M.; Zhao, X.S.; Shi, L.; Bikoff, J.B.; Lai, K.O.; Yung, W.H.; Fu, A.K.; Greenberg, M.E.; et al. Cdk5 regulates EphA4-mediated dendritic spine retraction through an ephexin1-dependent mechanism. *Nat Neurosci* 2007, 10, 67-76, doi:10.1038/nn1811.
127. Freyburger, M.; Pierre, A.; Paquette, G.; Belanger-Nelson, E.; Bedont, J.; Gaudreault, P.O.; Drolet, G.; Laforest, S.; Blackshaw, S.; Cermakian, N.; et al. EphA4 is involved in sleep regulation but not in the electrophysiological response to sleep deprivation. *Sleep* 2016, 39, 613-624, doi:10.5665/sleep.5538.
128. Freyburger, M.; Poirier, G.; Carrier, J.; Mongrain, V. Shorter duration of non-rapid eye movement sleep slow waves in EphA4 knockout mice. *J Sleep Res* 2017, 26, 539-546, doi:10.1111/jsr.12532.
129. Kiessling, S.; O'Callaghan, E.K.; Freyburger, M.; Cermakian, N.; Mongrain, V. The cell adhesion molecule EphA4 is involved in circadian clock functions. *Genes Brain Behav* 2018, 17, 82-92, doi:10.1111/gbb.12387.
130. Korte, M.; Carroll, P.; Wolf, E.; Brem, G.; Thoenen, H.; Bonhoeffer, T. Hippocampal long-term potentiation is impaired in mice lacking brain-derived neurotrophic factor. *Proc Natl Acad Sci U S A* 1995, 92, 8856-8860, doi:10.1073/pnas.92.19.8856.
131. Kang, H.; Schuman, E.M. Long-lasting neurotrophin-induced enhancement of synaptic transmission in the adult hippocampus. *Science* 1995, 267, 1658-1662, doi:10.1126/science.7886457.
132. Lu, B. BDNF and activity-dependent synaptic modulation. *Learn Mem* 2003, 10, 86-98, doi:10.1101/lm.54603.
133. Vigers, A.J.; Amin, D.S.; Talley-Farnham, T.; Gorski, J.A.; Xu, B.; Jones, K.R. Sustained expression of brain-derived neurotrophic factor is required for maintenance of dendritic spines and normal behavior. *Neuroscience* 2012, 212, 1-18, doi:10.1016/j.neuroscience.2012.03.031.
134. Ghosh, A.; Carnahan, J.; Greenberg, M.E. Requirement for BDNF in activity-dependent survival of cortical neurons. *Science* 1994, 263, 1618-1623, doi:10.1126/science.7907431.

135. Kowianski, P.; Lietzau, G.; Czuba, E.; Waskow, M.; Steliga, A.; Morys, J. BDNF: a key factor with multipotent impact on brain signaling and synaptic plasticity. *Cell Mol Neurobiol* 2018, 38, 579-593, doi:10.1007/s10571-017-0510-4.
136. Li, W.; Keifer, J. BDNF-induced synaptic delivery of AMPAR subunits is differentially dependent on NMDA receptors and requires ERK. *Neurobiol Learn Mem* 2009, 91, 243-249, doi:10.1016/j.nlm.2008.10.002.
137. Ying, S.W.; Futter, M.; Rosenblum, K.; Webber, M.J.; Hunt, S.P.; Bliss, T.V.; Bramham, C.R. Brain-derived neurotrophic factor induces long-term potentiation in intact adult hippocampus: requirement for ERK activation coupled to CREB and upregulation of Arc synthesis. *J Neurosci* 2002, 22, 1532-1540.
138. Yasuda, M.; Fukuchi, M.; Tabuchi, A.; Kawahara, M.; Tsuneki, H.; Azuma, Y.; Chiba, Y.; Tsuda, M. Robust stimulation of TrkB induces delayed increases in BDNF and Arc mRNA expressions in cultured rat cortical neurons via distinct mechanisms. *J Neurochem* 2007, 103, 626-636, doi:10.1111/j.1471-4159.2007.04851.x.
139. Blum, R.; Konnerth, A. Neurotrophin-mediated rapid signaling in the central nervous system: mechanisms and functions. *Physiology (Bethesda)* 2005, 20, 70-78, doi:10.1152/physiol.00042.2004.
140. Ho, T.Y.; Tang, N.Y.; Hsiang, C.Y.; Hsieh, C.L. Uncaria rhynchophylla and rhynchophylline improved kainic acid-induced epileptic seizures via IL-1beta and brain-derived neurotrophic factor. *Phytomedicine* 2014, 21, 893-900, doi:10.1016/j.phymed.2014.01.011.
141. Li, C.; Tu, G.; Luo, C.; Guo, Y.; Fang, M.; Zhu, C.; Li, H.; Ou, J.; Zhou, Y.; Liu, W.; et al. Effects of rhynchophylline on the hippocampal miRNA expression profile in ketamine-addicted rats. *Prog Neuropsychopharmacol Biol Psychiatry* 2018, 86, 379-389, doi:10.1016/j.pnpbp.2018.02.009.
142. Xian, Y.F.; Ip, S.P.; Li, H.Q.; Qu, C.; Su, Z.R.; Chen, J.N.; Lin, Z.X. Isorhynchophylline exerts antidepressant-like effects in mice via modulating neuroinflammation and neurotrophins: involvement of the PI3K/Akt/GSK-3beta signaling pathway. *FASEB J* 2019, 33, 10393-10408, doi:10.1096/fj.201802743RR.
143. Long, H.; Ruan, J.; Zhang, M.; Wang, C.; Huang, Y. Rhynchophylline attenuates Tourette Syndrome via BDNF/NF-kappaB pathway in vivo and in vitro. *Neurotox Res* 2019, 36, 756-763, doi:10.1007/s12640-019-00079-x.
144. Rahmani, M.; Rahmani, F.; Rezaei, N. The brain-derived neurotrophic factor: missing link between sleep deprivation, insomnia, and depression. *Neurochem Res* 2020, 45, 221-231, doi:10.1007/s11064-019-02914-1.
145. Monteiro, B.C.; Monteiro, S.; Candida, M.; Adler, N.; Paes, F.; Rocha, N.; Nardi, A.E.; Murillo-Rodriguez, E.; Machado, S. Relationship between brain-derived neurotrophic factor (Bdnf) and sleep on depression: a critical review. *Clin Pract Epidemiol Ment Health* 2017, 13, 213-219, doi:10.2174/1745017901713010213.
146. Schmitt, K.; Holsboer-Trachsler, E.; Eckert, A. BDNF in sleep, insomnia, and sleep deprivation. *Ann Med* 2016, 48, 42-51, doi:10.3109/07853890.2015.1131327.
147. Kushikata, T.; Fang, J.; Krueger, J.M. Brain-derived neurotrophic factor enhances spontaneous sleep in rats and rabbits. *Am J Physiol* 1999, 276, R1334-1338, doi:10.1152/ajpregu.1999.276.5.R1334.
148. Deuschle, M.; Schredl, M.; Wisch, C.; Schilling, C.; Gilles, M.; Geisel, O.; Hellweg, R. Serum brain-derived neurotrophic factor (BDNF) in sleep-disordered patients: relation to sleep stage N3 and rapid eye movement (REM) sleep across diagnostic entities. *J Sleep Res* 2018, 27, 73-77, doi:10.1111/jsr.12577.

149. Fan, T.T.; Chen, W.H.; Shi, L.; Lin, X.; Tabarak, S.; Chen, S.J.; Que, J.Y.; Bao, Y.P.; Tang, X.D.; Shi, J.; et al. Objective sleep duration is associated with cognitive deficits in primary insomnia: BDNF may play a role. *Sleep* 2019, 42, doi:10.1093/sleep/zsy192.
150. Watson, A.J.; Henson, K.; Dorsey, S.G.; Frank, M.G. The truncated TrkB receptor influences mammalian sleep. *Am J Physiol Regul Integr Comp Physiol* 2015, 308, R199-207, doi:10.1152/ajpregu.00422.2014.
151. Faraguna, U.; Vyazovskiy, V.V.; Nelson, A.B.; Tononi, G.; Cirelli, C. A causal role for brain-derived neurotrophic factor in the homeostatic regulation of sleep. *J Neurosci* 2008, 28, 4088-4095, doi:10.1523/JNEUROSCI.5510-07.2008.
152. Bachmann, V.; Klein, C.; Bodenmann, S.; Schafer, N.; Berger, W.; Brugger, P.; Landolt, H.P. The BDNF Val66Met polymorphism modulates sleep intensity: EEG frequency- and state-specificity. *Sleep* 2012, 35, 335-344, doi:10.5665/sleep.1690.
153. Guindalini, C.; Mazzotti, D.R.; Castro, L.S.; D'Aurea, C.V.; Andersen, M.L.; Poyares, D.; Bittencourt, L.R.; Tufik, S. Brain-derived neurotrophic factor gene polymorphism predicts interindividual variation in the sleep electroencephalogram. *J Neurosci Res* 2014, 92, 1018-1023, doi:10.1002/jnr.23380.
154. Gosselin, N.; De Beaumont, L.; Gagnon, K.; Baril, A.A.; Mongrain, V.; Blais, H.; Montplaisir, J.; Gagnon, J.F.; Pelleieux, S.; Poirier, J.; et al. BDNF Val66Met polymorphism interacts with sleep consolidation to predict ability to create new declarative memories. *J Neurosci* 2016, 36, 8390-8398, doi:10.1523/JNEUROSCI.4432-15.2016.
155. Ma, T.; Zhang, H.; Xu, Z.P.; Lu, Y.; Fu, Q.; Wang, W.; Li, G.H.; Wang, Y.Y.; Yang, Y.T.; Mi, W.D. Activation of brain-derived neurotrophic factor signaling in the basal forebrain reverses acute sleep deprivation-induced fear memory impairments. *Brain Behav* 2020, 10, e01592, doi:10.1002/brb3.1592.
156. Xue, J.; Li, H.; Xu, Z.; Ma, D.; Guo, R.; Yang, K.; Wang, Y. Paradoxical sleep deprivation aggravates and prolongs incision-induced pain hypersensitivity via BDNF signaling-mediated descending facilitation in rats. *Neurochem Res* 2018, 43, 2353-2361, doi:10.1007/s11064-018-2660-2.
157. Barnes, A.K.; Koul-Tiwari, R.; Garner, J.M.; Geist, P.A.; Datta, S. Activation of brain-derived neurotrophic factor-tropomyosin receptor kinase B signaling in the pedunculo pontine tegmental nucleus: a novel mechanism for the homeostatic regulation of rapid eye movement sleep. *J Neurochem* 2017, 141, 111-123, doi:10.1111/jnc.13938.
158. Datta, S.; Knapp, C.M.; Koul-Tiwari, R.; Barnes, A. The homeostatic regulation of REM sleep: A role for localized expression of brain-derived neurotrophic factor in the brainstem. *Behav Brain Res* 2015, 292, 381-392, doi:10.1016/j.bbr.2015.06.038.
159. Giese, M.; Beck, J.; Brand, S.; Muheim, F.; Hemmeter, U.; Hatzinger, M.; Holsboer-Trachsler, E.; Eckert, A. Fast BDNF serum level increase and diurnal BDNF oscillations are associated with therapeutic response after partial sleep deprivation. *J Psychiatr Res* 2014, 59, 1-7, doi:10.1016/j.jpsychires.2014.09.005.
160. Giese, M.; Unternahrer, E.; Huttig, H.; Beck, J.; Brand, S.; Calabrese, P.; Holsboer-Trachsler, E.; Eckert, A. BDNF: an indicator of insomnia? *Mol Psychiatry* 2014, 19, 151-152, doi:10.1038/mp.2013.10.

161. Song, Y.; Qu, R.; Zhu, S.; Zhang, R.; Ma, S. Rhynchophylline attenuates LPS-induced pro-inflammatory responses through down-regulation of MAPK/NF-kappaB signaling pathways in primary microglia. *Phytother Res* 2012, 26, 1528-1533, doi:10.1002/ptr.4614.
162. Yuan, D.; Ma, B.; Yang, J.Y.; Xie, Y.Y.; Wang, L.; Zhang, L.J.; Kano, Y.; Wu, C.F. Anti-inflammatory effects of rhynchophylline and isorhynchophylline in mouse N9 microglial cells and the molecular mechanism. *Int Immunopharmacol* 2009, 9, 1549-1554, doi:10.1016/j.intimp.2009.09.010.
163. Kim, J.H.; Bae, C.H.; Park, S.Y.; Lee, S.J.; Kim, Y. Uncaria rhynchophylla inhibits the production of nitric oxide and interleukin-1beta through blocking nuclear factor kappaB, Akt, and mitogen-activated protein kinase activation in macrophages. *J Med Food* 2010, 13, 1133-1140, doi:10.1089/jmf.2010.1128.
164. Wang, M.; Li, H.; Zhao, Y.; Lv, C.; Zhou, G. Rhynchophylline attenuates allergic bronchial asthma by inhibiting transforming growth factor-beta1-mediated Smad and mitogen-activated protein kinase signaling transductions in vivo and in vitro. *Exp Ther Med* 2019, 17, 251-259, doi:10.3892/etm.2018.6909.
165. Zhang, Y.; Cui, Y.; Dai, S.; Deng, W.; Wang, H.; Qin, W.; Yang, H.; Liu, H.; Yue, J.; Wu, D.; et al. Isorhynchophylline enhances Nrf2 and inhibits MAPK pathway in cardiac hypertrophy. *Naunyn Schmiedebergs Arch Pharmacol* 2020, 393, 203-212, doi:10.1007/s00210-019-01716-0.
166. Hsieh, C.L.; Ho, T.Y.; Su, S.Y.; Lo, W.Y.; Liu, C.H.; Tang, N.Y. Uncaria rhynchophylla and Rhynchophylline inhibit c-Jun N-terminal kinase phosphorylation and nuclear factor-kappaB activity in kainic acid-treated rats. *Am J Chin Med* 2009, 37, 351-360, doi:10.1142/S0192415X09006898.
167. Hsu, H.C.; Tang, N.Y.; Liu, C.H.; Hsieh, C.L. Antiepileptic effect of Uncaria rhynchophylla and Rhynchophylline involved in the initiation of c-Jun N-terminal kinase phosphorylation of MAPK signal pathways in acute seizures of kainic acid-treated rats. *Evid Based Complement Alternat Med* 2013, 2013, 961289, doi:10.1155/2013/961289.
168. Cao, H.; Ren, W.H.; Zhu, M.Y.; Zhao, Z.Q.; Zhang, Y.Q. Activation of glycine site and GluN2B subunit of NMDA receptors is necessary for ERK/CREB signaling cascade in rostral anterior cingulate cortex in rats: implications for affective pain. *Neurosci Bull* 2012, 28, 77-87, doi:10.1007/s12264-012-1060-x.
169. Mikhail, C.; Vaucher, A.; Jimenez, S.; Tafti, M. ERK signaling pathway regulates sleep duration through activity-induced gene expression during wakefulness. *Sci Signal* 2017, 10, doi:10.1126/scisignal.aai9219.
170. Tian, X.; Gotoh, T.; Tsuji, K.; Lo, E.H.; Huang, S.; Feig, L.A. Developmentally regulated role for Ras-GRFs in coupling NMDA glutamate receptors to Ras, Erk and CREB. *EMBO J* 2004, 23, 1567-1575, doi:10.1038/sj.emboj.7600151.
171. Hu, X.; Paik, P.K.; Chen, J.; Yamilina, A.; Kockeritz, L.; Lu, T.T.; Woodgett, J.R.; Ivashkiv, L.B. IFN-gamma suppresses IL-10 production and synergizes with TLR2 by regulating GSK3 and CREB/AP-1 proteins. *Immunity* 2006, 24, 563-574, doi:10.1016/j.immuni.2006.02.014.
172. Liu, W.; Peng, Q.X.; Lin, X.L.; Luo, C.H.; Jiang, M.J.; Mo, Z.X.; Yung, K.K. Effect of rhynchophylline on the expression of p-CREB and sc-Fos in striatum and hippocampal CA1 area of methamphetamine-induced conditioned place preference rats. *Fitoterapia* 2014, 92, 16-22, doi:10.1016/j.fitote.2013.10.002.

173. Su, X.; Wang, C.; Wang, X.; Han, F.; Lv, C.; Zhang, X. Sweet dream liquid chinese medicine ameliorates learning and memory deficit in a rat model of paradoxical sleep deprivation through the ERK/CREB signaling pathway. *J Med Food* 2016, 19, 472-480, doi:10.1089/jmf.2015.3530.
174. Foltenyi, K.; Greenspan, R.J.; Newport, J.W. Activation of EGFR and ERK by rhomboid signaling regulates the consolidation and maintenance of sleep in *Drosophila*. *Nat Neurosci* 2007, 10, 1160-1167, doi:10.1038/nn1957.
175. Dumoulin Bridi, M.C.; Aton, S.J.; Seibt, J.; Renouard, L.; Coleman, T.; Frank, M.G. Rapid eye movement sleep promotes cortical plasticity in the developing brain. *Sci Adv* 2015, 1, e1500105, doi:10.1126/sciadv.1500105.
176. Graves, L.A.; Hellman, K.; Veasey, S.; Blendy, J.A.; Pack, A.I.; Abel, T. Genetic evidence for a role of CREB in sustained cortical arousal. *J Neurophysiol* 2003, 90, 1152-1159, doi:10.1152/jn.00882.2002.
177. Wimmer, M.; Cui, R.; Blackwell, J.; Abel, T. CREB is required in excitatory neurons in the forebrain to sustain wakefulness. *BioRxiv* 2020.
178. Cirelli, C.; Tononi, G. Differential expression of plasticity-related genes in waking and sleep and their regulation by the noradrenergic system. *J Neurosci* 2000, 20, 9187-9194.
179. Cirelli, C.; Pompeiano, M.; Tononi, G. Neuronal gene expression in the waking state: a role for the locus coeruleus. *Science* 1996, 274, 1211-1215, doi:10.1126/science.274.5290.1211.
180. Hendricks, J.C.; Williams, J.A.; Panckeri, K.; Kirk, D.; Tello, M.; Yin, J.C.; Sehgal, A. A non-circadian role for cAMP signaling and CREB activity in *Drosophila* rest homeostasis. *Nat Neurosci* 2001, 4, 1108-1115, doi:10.1038/nn743.
181. Fruman, D.A.; Chiu, H.; Hopkins, B.D.; Bagrodia, S.; Cantley, L.C.; Abraham, R.T. The PI3K pathway in human disease. *Cell* 2017, 170, 605-635, doi:10.1016/j.cell.2017.07.029.
182. Alessi, D.R.; James, S.R.; Downes, C.P.; Holmes, A.B.; Gaffney, P.R.; Reese, C.B.; Cohen, P. Characterization of a 3-phosphoinositide-dependent protein kinase which phosphorylates and activates protein kinase B $\alpha$ . *Curr Biol* 1997, 7, 261-269, doi:10.1016/s0960-9822(06)00122-9.
183. Sarbassov, D.D.; Guertin, D.A.; Ali, S.M.; Sabatini, D.M. Phosphorylation and regulation of Akt/PKB by the rictor-mTOR complex. *Science* 2005, 307, 1098-1101, doi:10.1126/science.1106148.
184. Cross, D.A.; Alessi, D.R.; Cohen, P.; Andjelkovich, M.; Hemmings, B.A. Inhibition of glycogen synthase kinase-3 by insulin mediated by protein kinase B. *Nature* 1995, 378, 785-789, doi:10.1038/378785a0.
185. Inoki, K.; Li, Y.; Zhu, T.; Wu, J.; Guan, K.L. TSC2 is phosphorylated and inhibited by Akt and suppresses mTOR signalling. *Nat Cell Biol* 2002, 4, 648-657, doi:10.1038/ncb839.
186. Manning, B.D.; Toker, A. AKT/PKB signaling: navigating the network. *Cell* 2017, 169, 381-405, doi:10.1016/j.cell.2017.04.001.
187. Hao, H.F.; Liu, L.M.; Pan, C.S.; Wang, C.S.; Gao, Y.S.; Fan, J.Y.; Han, J.Y. Rhynchophylline ameliorates endothelial dysfunction via Src-PI3K/Akt-eNOS cascade in the cultured intrarenal arteries of spontaneous hypertensive rats. *Front Physiol* 2017, 8, 928, doi:10.3389/fphys.2017.00928.
188. Hu, S.; Mak, S.; Zuo, X.; Li, H.; Wang, Y.; Han, Y. Neuroprotection against MPP(+)-induced cytotoxicity through the activation of PI3-K/Akt/GSK3 $\beta$ /MEF2D signaling pathway by Rhynchophylline, the major



- tetracyclic oxindole alkaloid isolated from *Uncaria rhynchophylla*. *Front Pharmacol* 2018, 9, 768, doi:10.3389/fphar.2018.00768.
189. Xian, Y.F.; Mao, Q.Q.; Wu, J.C.; Su, Z.R.; Chen, J.N.; Lai, X.P.; Ip, S.P.; Lin, Z.X. Isorhynchophylline treatment improves the amyloid-beta-induced cognitive impairment in rats via inhibition of neuronal apoptosis and tau protein hyperphosphorylation. *J Alzheimers Dis* 2014, 39, 331-346, doi:10.3233/JAD-131457.
  190. Brunet, A.; Bonni, A.; Zigmond, M.J.; Lin, M.Z.; Juo, P.; Hu, L.S.; Anderson, M.J.; Arden, K.C.; Blenis, J.; Greenberg, M.E. Akt promotes cell survival by phosphorylating and inhibiting a Forkhead transcription factor. *Cell* 1999, 96, 857-868, doi:10.1016/s0092-8674(00)80595-4.
  191. Coloff, J.L.; Mason, E.F.; Altman, B.J.; Gerriets, V.A.; Liu, T.; Nichols, A.N.; Zhao, Y.; Wofford, J.A.; Jacobs, S.R.; Ilkayeva, O.; et al. Akt requires glucose metabolism to suppress puma expression and prevent apoptosis of leukemic T cells. *J Biol Chem* 2011, 286, 5921-5933, doi:10.1074/jbc.M110.179101.
  192. del Peso, L.; Gonzalez-Garcia, M.; Page, C.; Herrera, R.; Nunez, G. Interleukin-3-induced phosphorylation of BAD through the protein kinase Akt. *Science* 1997, 278, 687-689, doi:10.1126/science.278.5338.687.
  193. Pugazhenti, S.; Nesterova, A.; Sable, C.; Heidenreich, K.A.; Boxer, L.M.; Heasley, L.E.; Reusch, J.E. Akt/protein kinase B up-regulates Bcl-2 expression through cAMP-response element-binding protein. *J Biol Chem* 2000, 275, 10761-10766, doi:10.1074/jbc.275.15.10761.
  194. Zheng, M.; Chen, M.; Wang, W.; Zhou, M.; Liu, C.; Fan, Y.; Shi, D. Protection by rhynchophylline against MPTP/MPP(+)-induced neurotoxicity via regulating PI3K/Akt pathway. *J Ethnopharmacol* 2021, 268, 113568, doi:10.1016/j.jep.2020.113568.
  195. Lan, Y.L.; Zhou, J.J.; Liu, J.; Huo, X.K.; Wang, Y.L.; Liang, J.H.; Zhao, J.C.; Sun, C.P.; Yu, Z.L.; Fang, L.L.; et al. *Uncaria rhynchophylla* ameliorates Parkinson's Disease by inhibiting HSP90 expression: insights from quantitative proteomics. *Cell Physiol Biochem* 2018, 47, 1453-1464, doi:10.1159/000490837.
  196. Zhang, Y.; Sun, J.; Zhu, S.; Xu, T.; Lu, J.; Han, H.; Zhou, C.; Yan, J. The role of rhynchophylline in alleviating early brain injury following subarachnoid hemorrhage in rats. *Brain Res* 2016, 1631, 92-100, doi:10.1016/j.brainres.2015.11.035.
  197. Qin, Q.J.; Cui, L.Q.; Li, P.; Wang, Y.B.; Zhang, X.Z.; Guo, M.L. Rhynchophylline ameliorates myocardial ischemia/reperfusion injury through the modulation of mitochondrial mechanisms to mediate myocardial apoptosis. *Mol Med Rep* 2019, 19, 2581-2590, doi:10.3892/mmr.2019.9908.
  198. Julien, O.; Wells, J.A. Caspases and their substrates. *Cell Death Differ* 2017, 24, 1380-1389, doi:10.1038/cdd.2017.44.
  199. Beurel, E.; Mines, M.A.; Song, L.; Jope, R.S. Glycogen synthase kinase-3 levels and phosphorylation undergo large fluctuations in mouse brain during development. *Bipolar Disord* 2012, 14, 822-830, doi:10.1111/bdi.12023.
  200. Leroy, K.; Brion, J.P. Developmental expression and localization of glycogen synthase kinase-3beta in rat brain. *J Chem Neuroanat* 1999, 16, 279-293, doi:10.1016/s0891-0618(99)00012-5.
  201. Woodgett, J.R. Molecular cloning and expression of glycogen synthase kinase-3/factor A. *EMBO J* 1990, 9, 2431-2438.

202. Beaulieu, J.M.; Gainetdinov, R.R.; Caron, M.G. Akt/GSK3 signaling in the action of psychotropic drugs. *Annu Rev Pharmacol Toxicol* 2009, 49, 327-347, doi:10.1146/annurev.pharmtox.011008.145634.
203. Beaulieu, J.M.; Sotnikova, T.D.; Yao, W.D.; Kockeritz, L.; Woodgett, J.R.; Gainetdinov, R.R.; Caron, M.G. Lithium antagonizes dopamine-dependent behaviors mediated by an AKT/glycogen synthase kinase 3 signaling cascade. *Proc Natl Acad Sci U S A* 2004, 101, 5099-5104, doi:10.1073/pnas.0307921101.
204. Jain, A.K.; Jaiswal, A.K. GSK-3beta acts upstream of Fyn kinase in regulation of nuclear export and degradation of NF-E2 related factor 2. *J Biol Chem* 2007, 282, 16502-16510, doi:10.1074/jbc.M611336200.
205. Li, Q.; Niu, C.; Zhang, X.; Dong, M. Gastrodin and Isorhynchophylline synergistically inhibit MPP(+)-induced oxidative stress in SH-SY5Y cells by targeting ERK1/2 and GSK-3beta pathways: involvement of Nrf2 nuclear translocation. *ACS Chem Neurosci* 2018, 9, 482-493, doi:10.1021/acscchemneuro.7b00247.
206. Wild, A.C.; Moinova, H.R.; Mulcahy, R.T. Regulation of gamma-glutamylcysteine synthetase subunit gene expression by the transcription factor Nrf2. *J Biol Chem* 1999, 274, 33627-33636, doi:10.1074/jbc.274.47.33627.
207. Nguyen, T.; Huang, H.C.; Pickett, C.B. Transcriptional regulation of the antioxidant response element. Activation by Nrf2 and repression by MafK. *J Biol Chem* 2000, 275, 15466-15473, doi:10.1074/jbc.M000361200.
208. Xue, R.; Wan, Y.; Sun, X.; Zhang, X.; Gao, W.; Wu, W. Nicotinic mitigation of neuroinflammation and oxidative stress after chronic sleep deprivation. *Front Immunol* 2019, 10, 2546, doi:10.3389/fimmu.2019.02546.
209. Ahnaou, A.; Drinkenburg, W.H. Disruption of glycogen synthase kinase-3-beta activity leads to abnormalities in physiological measures in mice. *Behav Brain Res* 2011, 221, 246-252, doi:10.1016/j.bbr.2011.03.004.
210. Benedetti, F.; Dallaspesza, S.; Lorenzi, C.; Pirovano, A.; Radaelli, D.; Locatelli, C.; Poletti, S.; Colombo, C.; Smeraldi, E. Gene-gene interaction of glycogen synthase kinase 3-beta and serotonin transporter on human antidepressant response to sleep deprivation. *J Affect Disord* 2012, 136, 514-519, doi:10.1016/j.jad.2011.10.039.
211. Benedetti, F.; Serretti, A.; Colombo, C.; Lorenzi, C.; Tubazio, V.; Smeraldi, E. A glycogen synthase kinase 3-beta promoter gene single nucleotide polymorphism is associated with age at onset and response to total sleep deprivation in bipolar depression. *Neurosci Lett* 2004, 368, 123-126, doi:10.1016/j.neulet.2004.06.050.
212. Vyazovskiy, V.V.; Cirelli, C.; Pfister-Genskow, M.; Faraguna, U.; Tononi, G. Molecular and electrophysiological evidence for net synaptic potentiation in wake and depression in sleep. *Nat Neurosci* 2008, 11, 200-208, doi:10.1038/nn2035.
213. Bruning, F.; Noya, S.B.; Bange, T.; Koutsouli, S.; Rudolph, J.D.; Tyagarajan, S.K.; Cox, J.; Mann, M.; Brown, S.A.; Robles, M.S. Sleep-wake cycles drive daily dynamics of synaptic phosphorylation. *Science* 2019, 366, doi:10.1126/science.aav3617.
214. Khlghatyan, J.; Evstratova, A.; Bozoyan, L.; Chamberland, S.; Chatterjee, D.; Marakhovskaia, A.; Soares Silva, T.; Toth, K.; Mongrain, V.; Beaulieu, J.M. Fxr1 regulates sleep and synaptic homeostasis. *EMBO J* 2020, 39, e103864, doi:10.15252/embj.2019103864.

215. Yatham, L.N.; Kennedy, S.H.; Parikh, S.V.; Schaffer, A.; Bond, D.J.; Frey, B.N.; Sharma, V.; Goldstein, B.I.; Rej, S.; Beaulieu, S.; et al. Canadian Network for Mood and Anxiety Treatments (CANMAT) and International Society for Bipolar Disorders (ISBD) 2018 guidelines for the management of patients with bipolar disorder. *Bipolar Disord* 2018, 20, 97-170, doi:10.1111/bdi.12609.
216. Geoffroy, P.A.; Samalin, L.; Llorca, P.M.; Curis, E.; Bellivier, F. Influence of lithium on sleep and chronotypes in remitted patients with bipolar disorder. *J Affect Disord* 2016, 204, 32-39, doi:10.1016/j.jad.2016.06.015.
217. Friston, K.J.; Sharpley, A.L.; Solomon, R.A.; Cowen, P.J. Lithium increases slow wave sleep: possible mediation by brain 5-HT<sub>2</sub> receptors? *Psychopharmacology (Berl)* 1989, 98, 139-140, doi:10.1007/BF00442020.
218. Jones, C.A.; Perez, E.; Amici, R.; Luppi, M.; Baracchi, F.; Cerri, M.; Dentico, D.; Zamboni, G. Lithium affects REM sleep occurrence, autonomic activity and brain second messengers in the rat. *Behav Brain Res* 2008, 187, 254-261, doi:10.1016/j.bbr.2007.09.017.
219. Rubinsztein, D.C.; Gestwicki, J.E.; Murphy, L.O.; Klionsky, D.J. Potential therapeutic applications of autophagy. *Nature Reviews Drug Discovery* 2007, 6, 304-312.
220. Tudor, J.C.; Davis, E.J.; Peixoto, L.; Wimmer, M.E.; van Tilborg, E.; Park, A.J.; Poplawski, S.G.; Chung, C.W.; Havekes, R.; Huang, J.; et al. Sleep deprivation impairs memory by attenuating mTORC1-dependent protein synthesis. *Sci Signal* 2016, 9, ra41.
221. Shabab, T.; Khanabdali, R.; Moghadamtousi, S.Z.; Kadir, H.A.; Mohan, G. Neuroinflammation pathways: a general review. *Int J Neurosci* 2017, 127, 624-633, doi:10.1080/00207454.2016.1212854.
222. Long, H.; Zhang, M.; Wang, C.; Hang, Y. Rhynchophylline attenuates neurotoxicity in Tourette Syndrome rats. *Neurotox Res* 2019, 36, 679-687, doi:10.1007/s12640-019-00059-1.
223. Cao, W.; Wang, Y.; Lv, X.; Yu, X.; Li, X.; Li, H.; Wang, Y.; Lu, D.; Qi, R.; Wang, H. Rhynchophylline prevents cardiac dysfunction and improves survival in lipopolysaccharide-challenged mice via suppressing macrophage I-kappaB phosphorylation. *Int Immunopharmacol* 2012, 14, 243-251, doi:10.1016/j.intimp.2012.07.010.
224. Kielian, T. Overview of toll-like receptors in the CNS. *Curr Top Microbiol Immunol* 2009, 336, 1-14, doi:10.1007/978-3-642-00549-7\_1.
225. Cespuglio, R.; Amrouni, D.; Meiller, A.; Buguet, A.; Gautier-Sauvigne, S. Nitric oxide in the regulation of the sleep-wake states. *Sleep Med Rev* 2012, 16, 265-279, doi:10.1016/j.smrv.2012.01.006.
226. Jewett, K.A.; Krueger, J.M. Humoral sleep regulation; interleukin-1 and tumor necrosis factor. *Vitam Horm* 2012, 89, 241-257, doi:10.1016/B978-0-12-394623-2.00013-5.
227. Hars, B. Endogenous nitric oxide in the rat pons promotes sleep. *Brain Res* 1999, 816, 209-219, doi:10.1016/s0006-8993(98)01183-4.
228. Fang, J.; Wang, Y.; Krueger, J.M. Effects of interleukin-1 beta on sleep are mediated by the type I receptor. *Am J Physiol* 1998, 274, R655-660, doi:10.1152/ajpregu.1998.274.3.R655.
229. Datta, S.; Patterson, E.H.; Siwek, D.F. Endogenous and exogenous nitric oxide in the pedunclopontine tegmentum induces sleep. *Synapse* 1997, 27, 69-78, doi:10.1002/(SICI)1098-2396(199709)27:1<69::AID-SYN7>3.0.CO;2-B.

230. Opp, M.R.; Obal, F., Jr.; Krueger, J.M. Interleukin 1 alters rat sleep: temporal and dose-related effects. *Am J Physiol* 1991, 260, R52-58, doi:10.1152/ajpregu.1991.260.1.R52.
231. Opp, M.R.; Krueger, J.M. Interleukin 1-receptor antagonist blocks interleukin 1-induced sleep and fever. *Am J Physiol* 1991, 260, R453-457, doi:10.1152/ajpregu.1991.260.2.R453.
232. Dickstein, J.B.; Moldofsky, H.; Lue, F.A.; Hay, J.B. Intracerebroventricular injection of TNF-alpha promotes sleep and is recovered in cervical lymph. *Am J Physiol* 1999, 276, R1018-1022, doi:10.1152/ajpregu.1999.276.4.R1018.
233. Kapas, L.; Shibata, M.; Kimura, M.; Krueger, J.M. Inhibition of nitric oxide synthesis suppresses sleep in rabbits. *Am J Physiol* 1994, 266, R151-157, doi:10.1152/ajpregu.1994.266.1.R151.
234. Opp, M.R.; Krueger, J.M. Interleukin-1 is involved in responses to sleep deprivation in the rabbit. *Brain Res* 1994, 639, 57-65, doi:10.1016/0006-8993(94)91764-7.
235. Opp, M.R.; Krueger, J.M. Anti-interleukin-1 beta reduces sleep and sleep rebound after sleep deprivation in rats. *Am J Physiol* 1994, 266, R688-695, doi:10.1152/ajpregu.1994.266.3.R688.
236. Kapas, L.; Fang, J.; Krueger, J.M. Inhibition of nitric oxide synthesis inhibits rat sleep. *Brain Res* 1994, 664, 189-196, doi:10.1016/0006-8993(94)91969-0.
237. Dzoljic, M.R.; de Vries, R.; van Leeuwen, R. Sleep and nitric oxide: effects of 7-nitro indazole, inhibitor of brain nitric oxide synthase. *Brain Res* 1996, 718, 145-150, doi:10.1016/0006-8993(96)00102-3.
238. Takahashi, S.; Kapas, L.; Seyer, J.M.; Wang, Y.; Krueger, J.M. Inhibition of tumor necrosis factor attenuates physiological sleep in rabbits. *Neuroreport* 1996, 7, 642-646, doi:10.1097/00001756-199601310-00063.
239. Takahashi, S.; Tooley, D.D.; Kapas, L.; Fang, J.; Seyer, J.M.; Krueger, J.M. Inhibition of tumor necrosis factor in the brain suppresses rabbit sleep. *Pflugers Arch* 1995, 431, 155-160, doi:10.1007/BF00410186.
240. Takahashi, S.; Fang, J.; Kapas, L.; Wang, Y.; Krueger, J.M. Inhibition of brain interleukin-1 attenuates sleep rebound after sleep deprivation in rabbits. *Am J Physiol* 1997, 273, R677-682, doi:10.1152/ajpregu.1997.273.2.R677.
241. Ribeiro, A.C.; Kapas, L. Day- and nighttime injection of a nitric oxide synthase inhibitor elicits opposite sleep responses in rats. *Am J Physiol Regul Integr Comp Physiol* 2005, 289, R521-R531, doi:10.1152/ajpregu.00605.2004.
242. Monti, J.M.; Jantos, H. Microinjection of the nitric oxide synthase inhibitor L-NAME into the lateral basal forebrain alters the sleep/wake cycle of the rat. *Prog Neuropsychopharmacol Biol Psychiatry* 2004, 28, 239-247, doi:10.1016/j.pnpbp.2003.10.001.
243. Kubota, T.; Kushikata, T.; Fang, J.; Krueger, J.M. Nuclear factor-kappaB inhibitor peptide inhibits spontaneous and interleukin-1beta-induced sleep. *Am J Physiol Regul Integr Comp Physiol* 2000, 279, R404-413, doi:10.1152/ajpregu.2000.279.2.R404.
244. Zielinski, M.R.; Kim, Y.; Karpova, S.A.; McCarley, R.W.; Strecker, R.E.; Gerashchenko, D. Chronic sleep restriction elevates brain interleukin-1 beta and tumor necrosis factor-alpha and attenuates brain-derived neurotrophic factor expression. *Neurosci Lett* 2014, 580, 27-31, doi:10.1016/j.neulet.2014.07.043.

245. Kalinchuk, A.V.; McCarley, R.W.; Porkka-Heiskanen, T.; Basheer, R. Sleep deprivation triggers inducible nitric oxide-dependent nitric oxide production in wake-active basal forebrain neurons. *J Neurosci* 2010, 30, 13254-13264, doi:10.1523/JNEUROSCI.0014-10.2010.
246. Mackiewicz, M.; Sollars, P.J.; Ogilvie, M.D.; Pack, A.I. Modulation of IL-1 beta gene expression in the rat CNS during sleep deprivation. *Neuroreport* 1996, 7, 529-533, doi:10.1097/00001756-199601310-00037.
247. Chen, Z.; Gardi, J.; Kushikata, T.; Fang, J.; Krueger, J.M. Nuclear factor-kappaB-like activity increases in murine cerebral cortex after sleep deprivation. *Am J Physiol* 1999, 276, R1812-1818, doi:10.1152/ajpregu.1999.276.6.R1812.
248. Ribeiro, A.C.; Gilligan, J.G.; Kapas, L. Systemic injection of a nitric oxide synthase inhibitor suppresses sleep responses to sleep deprivation in rats. *Am J Physiol Regul Integr Comp Physiol* 2000, 278, R1048-1056, doi:10.1152/ajpregu.2000.278.4.R1048.
249. Shoham, S.; Davenne, D.; Cady, A.B.; Dinarello, C.A.; Krueger, J.M. Recombinant tumor necrosis factor and interleukin 1 enhance slow-wave sleep. *Am J Physiol* 1987, 253, R142-149, doi:10.1152/ajpregu.1987.253.1.R142.
250. Kang, T.H.; Murakami, Y.; Takayama, H.; Kitajima, M.; Aimi, N.; Watanabe, H.; Matsumoto, K. Protective effect of rhynchophylline and isorhynchophylline on in vitro ischemia-induced neuronal damage in the hippocampus: putative neurotransmitter receptors involved in their action. *Life Sci* 2004, 76, 331-343, doi:10.1016/j.lfs.2004.08.012.
251. Zhou, J.Y.; Mo, Z.X.; Zhou, S.W. Effect of rhynchophylline on central neurotransmitter levels in amphetamine-induced conditioned place preference rat brain. *Fitoterapia* 2010, 81, 844-848, doi:10.1016/j.fitote.2010.05.007.
252. Surmeier, D.J.;argas, J.; Hemmings, H.C., Jr.; Nairn, A.C.; Greengard, P. Modulation of calcium currents by a D1 dopaminergic protein kinase/phosphatase cascade in rat neostriatal neurons. *Neuron* 1995, 14, 385-397, doi:10.1016/0896-6273(95)90294-5.
253. Huang, X.Y.; Morielli, A.D.; Peralta, E.G. Tyrosine kinase-dependent suppression of a potassium channel by the G protein-coupled m1 muscarinic acetylcholine receptor. *Cell* 1993, 75, 1145-1156, doi:10.1016/0092-8674(93)90324-j.
254. Baghdoyan, H.A.; Rodrigo-Angulo, M.L.; McCarley, R.W.; Hobson, J.A. Site-specific enhancement and suppression of desynchronized sleep signs following cholinergic stimulation of three brainstem regions. *Brain Res* 1984, 306, 39-52, doi:10.1016/0006-8993(84)90354-8.
255. Niwa, Y.; Kanda, G.N.; Yamada, R.G.; Shi, S.; Sunagawa, G.A.; Ukai-Tadenuma, M.; Fujishima, H.; Matsumoto, N.; Masumoto, K.H.; Nagano, M.; et al. Muscarinic acetylcholine receptors Chrm1 and Chrm3 are essential for REM sleep. *Cell Rep* 2018, 24, 2231-2247 e2237, doi:10.1016/j.celrep.2018.07.082.
256. Gillin, J.C.; Sutton, L.; Ruiz, C.; Golshan, S.; Hirsch, S.; Warmann, C.; Shiromani, P. Dose dependent inhibition of REM sleep in normal volunteers by biperiden, a muscarinic antagonist. *Biol Psychiatry* 1991, 30, 151-156, doi:10.1016/0006-3223(91)90169-m.
257. Kurimoto, E.; Nakashima, M.; Kimura, H.; Suzuki, M. TAK-071, a muscarinic M1 receptor positive allosteric modulator, attenuates scopolamine-induced quantitative electroencephalogram power spectral changes in cynomolgus monkeys. *PLoS One* 2019, 14, e0207969, doi:10.1371/journal.pone.0207969.

258. Ma, X.; Zhang, Y.; Wang, L.; Li, N.; Barkai, E.; Zhang, X.; Lin, L.; Xu, J. The firing of theta state-related septal cholinergic neurons disrupt hippocampal ripple oscillations via muscarinic receptors. *J Neurosci* 2020, 40, 3591-3603, doi:10.1523/JNEUROSCI.1568-19.2020.
259. Shirey, J.K.; Brady, A.E.; Jones, P.J.; Davis, A.A.; Bridges, T.M.; Kennedy, J.P.; Jadhav, S.B.; Menon, U.N.; Xiang, Z.; Watson, M.L.; et al. A selective allosteric potentiator of the M1 muscarinic acetylcholine receptor increases activity of medial prefrontal cortical neurons and restores impairments in reversal learning. *J Neurosci* 2009, 29, 14271-14286, doi:10.1523/JNEUROSCI.3930-09.2009.
260. Williams, J.H.; Kauer, J.A. Properties of carbachol-induced oscillatory activity in rat hippocampus. *J Neurophysiol* 1997, 78, 2631-2640, doi:10.1152/jn.1997.78.5.2631.
261. Cea-del Rio, C.A.; Lawrence, J.J.; Tricoire, L.; Erdelyi, F.; Szabo, G.; McBain, C.J. M3 muscarinic acetylcholine receptor expression confers differential cholinergic modulation to neurochemically distinct hippocampal basket cell subtypes. *J Neurosci* 2010, 30, 6011-6024, doi:10.1523/JNEUROSCI.5040-09.2010.
262. Fisahn, A.; Yamada, M.; Duttaroy, A.; Gan, J.W.; Deng, C.X.; McBain, C.J.; Wess, J. Muscarinic induction of hippocampal gamma oscillations requires coupling of the M1 receptor to two mixed cation currents. *Neuron* 2002, 33, 615-624, doi:10.1016/s0896-6273(02)00587-1.
263. Langmead, C.J.; Austin, N.E.; Branch, C.L.; Brown, J.T.; Buchanan, K.A.; Davies, C.H.; Forbes, I.T.; Fry, V.A.; Hagan, J.J.; Herdon, H.J.; et al. Characterization of a CNS penetrant, selective M1 muscarinic receptor agonist, 77-LH-28-1. *Br J Pharmacol* 2008, 154, 1104-1115, doi:10.1038/bjp.2008.152.
264. Ursin, R. Serotonin and sleep. *Sleep Med Rev* 2002, 6, 55-69, doi:10.1053/smr.2001.0174.
265. Ito, H.; Yanase, M.; Yamashita, A.; Kitabatake, C.; Hamada, A.; Suhara, Y.; Narita, M.; Ikegami, D.; Sakai, H.; Yamazaki, M.; et al. Analysis of sleep disorders under pain using an optogenetic tool: possible involvement of the activation of dorsal raphe nucleus-serotonergic neurons. *Mol Brain* 2013, 6, 59, doi:10.1186/1756-6606-6-59.
266. Cape, E.G.; Jones, B.E. Differential modulation of high-frequency gamma-electroencephalogram activity and sleep-wake state by noradrenaline and serotonin microinjections into the region of cholinergic basal ganglia neurons. *J Neurosci* 1998, 18, 2653-2666.
267. Horner, R.L.; Sanford, L.D.; Annis, D.; Pack, A.I.; Morrison, A.R. Serotonin at the laterodorsal tegmental nucleus suppresses rapid-eye-movement sleep in freely behaving rats. *J Neurosci* 1997, 17, 7541-7552.
268. Chowdhury, S.; Yamanaka, A. Optogenetic activation of serotonergic terminals facilitates GABAergic inhibitory input to orexin/hypocretin neurons. *Sci Rep* 2016, 6, 36039, doi:10.1038/srep36039.
269. Saito, Y.C.; Maejima, T.; Nishitani, M.; Hasegawa, E.; Yanagawa, Y.; Mieda, M.; Sakurai, T. Monoamines inhibit GABAergic neurons in ventrolateral preoptic area that make direct synaptic connections to hypothalamic arousal neurons. *J Neurosci* 2018, 38, 6366-6378, doi:10.1523/JNEUROSCI.2835-17.2018.
270. Linley, S.B.; Vertes, R.P. Serotonergic systems in sleep and waking. In *Handbook of Behavioral Neuroscience*; Elsevier: 2019; Volume 30, pp. 101-123.
271. Bjorvatn, B.; Fagerland, S.; Eid, T.; Ursin, R. Sleep/waking effects of a selective 5-HT1A receptor agonist given systemically as well as perfused in the dorsal raphe nucleus in rats. *Brain Res* 1997, 770, 81-88, doi:10.1016/s0006-8993(97)00758-0.

272. Monti, J.M.; Jantos, H.; Monti, D. Increased REM sleep after intra-dorsal raphe nucleus injection of flesinoxan or 8-OHDPAT: prevention with WAY 100635. *Eur Neuropsychopharmacol* 2002, 12, 47-55, doi:10.1016/s0924-977x(01)00133-x.
273. Portas, C.M.; Thakkar, M.; Rainnie, D.; McCarley, R.W. Microdialysis perfusion of 8-hydroxy-2-(di-n-propylamino)tetralin (8-OH-DPAT) in the dorsal raphe nucleus decreases serotonin release and increases rapid eye movement sleep in the freely moving cat. *J Neurosci* 1996, 16, 2820-2828.
274. Vertes, R.P.; Kinney, G.G.; Kocsis, B.; Fortin, W.J. Pharmacological suppression of the median raphe nucleus with serotonin1A agonists, 8-OH-DPAT and buspirone, produces hippocampal theta rhythm in the rat. *Neuroscience* 1994, 60, 441-451, doi:10.1016/0306-4522(94)90255-0.
275. Monti, J.M.; Jantos, H. Effects of activation and blockade of 5-HT<sub>2A/2C</sub> receptors in the dorsal raphe nucleus on sleep and waking in the rat. *Prog Neuropsychopharmacol Biol Psychiatry* 2006, 30, 1189-1195, doi:10.1016/j.pnpbp.2006.02.013.
276. Monti, J.M.; Leopoldo, M.; Jantos, H. The serotonin 5-HT<sub>7</sub> receptor agonist LP-44 microinjected into the dorsal raphe nucleus suppresses REM sleep in the rat. *Behav Brain Res* 2008, 191, 184-189, doi:10.1016/j.bbr.2008.03.025.
277. Monti, J.M.; Jantos, H.; Lagos, P. Activation of serotonin 5-HT<sub>1B</sub> receptor in the dorsal raphe nucleus affects REM sleep in the rat. *Behav Brain Res* 2010, 206, 8-16, doi:10.1016/j.bbr.2009.08.037.
278. Monti, J.M.; Jantos, H. Effects of the serotonin 5-HT<sub>2A/2C</sub> receptor agonist DOI and of the selective 5-HT<sub>2A</sub> or 5-HT<sub>2C</sub> receptor antagonists EMD 281014 and SB-243213, respectively, on sleep and waking in the rat. *Eur J Pharmacol* 2006, 553, 163-170, doi:10.1016/j.ejphar.2006.09.027.
279. Popa, D.; Lena, C.; Fabre, V.; Prenat, C.; Gingrich, J.; Escourrou, P.; Hamon, M.; Adrien, J. Contribution of 5-HT<sub>2</sub> receptor subtypes to sleep-wakefulness and respiratory control, and functional adaptations in knock-out mice lacking 5-HT<sub>2A</sub> receptors. *J Neurosci* 2005, 25, 11231-11238, doi:10.1523/JNEUROSCI.1724-05.2005.
280. Dahan, L.; Astier, B.; Vautrelle, N.; Urbain, N.; Kocsis, B.; Chouvet, G. Prominent burst firing of dopaminergic neurons in the ventral tegmental area during paradoxical sleep. *Neuropsychopharmacology* 2007, 32, 1232-1241, doi:10.1038/sj.npp.1301251.
281. Eban-Rothschild, A.; Rothschild, G.; Giardino, W.J.; Jones, J.R.; de Lecea, L. VTA dopaminergic neurons regulate ethologically relevant sleep-wake behaviors. *Nat Neurosci* 2016, 19, 1356-1366, doi:10.1038/nn.4377.
282. Lancel, M. Role of GABA<sub>A</sub> receptors in the regulation of sleep: initial sleep responses to peripherally administered modulators and agonists. *Sleep* 1999, 22, 33-42, doi:10.1093/sleep/22.1.33.
283. Winsky-Sommerer, R. Role of GABA<sub>A</sub> receptors in the physiology and pharmacology of sleep. *Eur J Neurosci* 2009, 29, 1779-1794, doi:10.1111/j.1460-9568.2009.06716.x.
284. Hannou, L.; Roy, P.G.; Ballester Roig, M.N.; Mongrain, V. Transcriptional control of synaptic components by the clock machinery. *Eur J Neurosci* 2020, 51, 241-267, doi:10.1111/ejn.14294.
285. Biello, S.M.; Bonsall, D.R.; Atkinson, L.A.; Molyneux, P.C.; Harrington, M.E.; Lall, G.S. Alterations in glutamatergic signaling contribute to the decline of circadian photoentrainment in aged mice. *Neurobiol Aging* 2018, 66, 75-84, doi:10.1016/j.neurobiolaging.2018.02.013.

286. Wang, L.M.; Schroeder, A.; Loh, D.; Smith, D.; Lin, K.; Han, J.H.; Michel, S.; Hummer, D.L.; Ehlen, J.C.; Albers, H.E.; et al. Role for the NR2B subunit of the N-methyl-D-aspartate receptor in mediating light input to the circadian system. *Eur J Neurosci* 2008, 27, 1771-1779, doi:10.1111/j.1460-9568.2008.06144.x.
287. Bendova, Z.; Sladek, M.; Svobodova, I. The expression of NR2B subunit of NMDA receptor in the suprachiasmatic nucleus of Wistar rats and its role in glutamate-induced CREB and ERK1/2 phosphorylation. *Neurochem Int* 2012, 61, 43-47, doi:10.1016/j.neuint.2012.04.016.
288. Bendova, Z.; Sumova, A.; Mikkelsen, J.D. Circadian and developmental regulation of N-methyl-d-aspartate-receptor 1 mRNA splice variants and N-methyl-d-aspartate-receptor 3 subunit expression within the rat suprachiasmatic nucleus. *Neuroscience* 2009, 159, 599-609, doi:10.1016/j.neuroscience.2009.01.016.
289. Coria-Lucero, C.D.; Golini, R.S.; Ponce, I.T.; Deyurka, N.; Anzulovich, A.C.; Delgado, S.M.; Navigatore-Fonzo, L.S. Rhythmic Bdnf and TrkB expression patterns in the prefrontal cortex are lost in aged rats. *Brain Res* 2016, 1653, 51-58, doi:10.1016/j.brainres.2016.10.019.
290. Cai, Y.; Ding, H.; Li, N.; Chai, Y.; Zhang, Y.; Chan, P. Oscillation development for neurotransmitter-related genes in the mouse striatum. *Neuroreport* 2010, 21, 79-83, doi:10.1097/WNR.0b013e32832ff30e.
291. Li, H.; Bi, Q.; Cui, H.; Lv, C.; Wang, M. Suppression of autophagy through JAK2/STAT3 contributes to the therapeutic action of rhynchophylline on asthma. *BMC Complementary Medicine and Therapies* 2021, 21, 1-12.
292. Boudreau, P.; Yeh, W.H.; Dumont, G.A.; Boivin, D.B. Circadian variation of heart rate variability across sleep stages. *Sleep* 2013, 36, 1919-1928, doi:10.5665/sleep.3230.
293. Trinder, J.; Waloszek, J.; Woods, M.J.; Jordan, A.S. Sleep and cardiovascular regulation. *Pflugers Arch* 2012, 463, 161-168, doi:10.1007/s00424-011-1041-3.
294. Song, M.F.; Guan, Y.H.; Li, H.T.; Wei, S.G.; Zhang, L.X.; Zhang, Z.L.; Ma, X.J. The effects of genetic variation and environmental factors on rhynchophylline and isorhynchophylline in *Uncaria macrophylla* Wall. from different populations in China. *PLoS One* 2018, 13, e0199259, doi:10.1371/journal.pone.0199259.
295. Williamson, E.M. Synergy and other interactions in phytomedicines. *Phytomedicine* 2001, 8, 401-409, doi:10.1078/0944-7113-00060.
296. Zhou, J.Y.; Chen, J.; Zhou, S.W.; Mo, Z.X. Individual and combined effects of rhynchophylline and ketamine on proliferation, NMDAR1 and GluA2/3 protein expression in PC12 cells. *Fitoterapia* 2013, 85, 125-129, doi:10.1016/j.fitote.2013.01.012.
297. Lu, Y.F.; Xie, X.L.; Wu, Q.; Wen, G.R.; Yang, S.F.; Shi, J.S. Effects of rhynchophylline on monoamine transmitter contents of striatum and hippocampus in cerebral ischemic rats. *Chin J Pharmacol Toxicol* 2004, 18, 253-258.
298. Chen, Z.; Wei, L.; Jing, L.; Zhi-jie, C.; Chan, L.; Yu-ting, Z.; Zhi-xian, M. Rhynchophylline reverses methamphetamine-induced CPP by regulating GluR1 expression in zebrafish. *Chinese Pharmacological Bulletin* 2019, 35, 620-623.
299. Lin, Y.W.; Hsieh, C.L. Oral *Uncaria rhynchophylla* (UR) reduces kainic acid-induced epileptic seizures and neuronal death accompanied by attenuating glial cell proliferation and S100B proteins in rats. *J Ethnopharmacol* 2011, 135, 313-320, doi:10.1016/j.jep.2011.03.018.



300. Dolmetsch, R.E.; Pajvani, U.; Fife, K.; Spotts, J.M.; Greenberg, M.E. Signaling to the nucleus by an L-type calcium channel-calmodulin complex through the MAP kinase pathway. *Science* 2001, 294, 333-339, doi:10.1126/science.1063395.
301. Wheeler, D.G.; Groth, R.D.; Ma, H.; Barrett, C.F.; Owen, S.F.; Safa, P.; Tsien, R.W. Ca(V)1 and Ca(V)2 channels engage distinct modes of Ca(2+) signaling to control CREB-dependent gene expression. *Cell* 2012, 149, 1112-1124, doi:10.1016/j.cell.2012.03.041.

# Chapter 3

## Hypotheses and Objectives

---

### 3.1 Overall rationale and general hypotheses

The EPHA4 receptor is crucial for regulating cell-to-cell communication in the brain, vascular and immune systems. As detailed along Chapter 1, research has shown that i) EphA4 is required for proper neurotransmission, ii) is expressed in the SCN in rodents, iii) the *EphA4* gene contain E-boxes in its putative promoter that are conserved in rodents and humans, iv) *EphA4* KO mice have altered circadian responses to light conditions and v) *EphA4* KO mice show altered sleep parameters (e.g., decreased duration of PS in the light period, and shorter duration of slow waves in SWS) (Murai and Pasquale, 2011; Freyburger et al., 2016; Freyburger et al., 2017; Kiessling et al., 2018). The presence of E-boxes upstream of *EphA4* and the fact that *Clock* mutant mice showed reduced expression of *EphA4* (Freyburger et al., 2016), suggests that this gene could be regulated by the clock transcription factors. Moreover, given that EphA4 is required for adequate CNS development, it is necessary to define whether the sleep/circadian phenotypes observed in *EphA4* KO mice originate from neurodevelopmental effects or from a role of EphA4 in adult neuronal function. Therefore, this research aims at determining if the transcription of *EphA4*, *EfnB2* and *EfnA3* genes is under circadian regulation, and at defining if the EPHA4 modulator RHY modifies sleep in adult mice. We precisely hypothesize that:

- 1- The gene transcription of *EphA4* and its Ephrin ligands *EfnB2* and *EfnA3* is regulated by core clock transcription factors.
- 2- The protein levels of EPHA4 and EFNs oscillate with circadian rhythmicity.
- 3- The EPHA4 modulator RHY modifies sleep in adult mice in manners that resemble the sleep phenotypes of *EphA4* KO mice.
- 4- RHY will have similar effects in male and female mice, given that one of the few studies providing RHY in both male and female mice did not report sex differences (Shi et al., 1993; Fu et al., 2014).
- 5- RHY modifies EPHA4 activation and downstream effectors 13h after two different doses of RHY provided via intraperitoneal injection.
- 6- RHY modifies the spatial brain transcriptome in brain regions controlling sleep.

To test these hypotheses, we have conducted two different research projects that are described in two research manuscripts presented in this thesis: i) we investigate *in vitro* if the transcription of the *EphA4* gene and its Ephrin ligands *EfnB2* and *EfnA3* is regulated by the core

clock transcription factors, and evaluate if their protein levels oscillate with circadian rhythmicity in the mouse brain (hypotheses 1 and 2, first manuscript); and ii) the effect of systemic administration of RHY on sleep will be studied in mice (hypotheses 3-6, second manuscript). Injections of RHY will be performed at two different times of the day and brains will be sampled to investigate which RHY targets and cellular pathways are associated with the effects of RHY on sleep.

## 3.2 Specific aims

### 3.2.1 Determine if EphA4 and its ephrin ligands EfnB2 and EfnA3 are under circadian regulation

Two studies suggested the implication of EphA4 receptor in circadian physiology and the potential control of *EphA4* gene by the core clock molecular loop (Freyburger *et al.*, 2016; Kiessling *et al.*, 2018). Firstly, Freyburger and collaborators found that the putative promoter region of the *EphA4* gene contained E-boxes, which are regulatory elements for circadian transcription factors. Moreover, the same study showed that *EphA4* is expressed in the mouse and rat SCN, and that the 24-hour expression of *EphA4*, *EfnB2* and *EfnA3* is modified in *Clock<sup>Δ19</sup>* mice. Moreover, SWS low sigma activity (10-12Hz) shows a blunted 24-hour rhythmicity in *EphA4* KO mice (Freyburger *et al.*, 2016). Interestingly, this frequency range has been closely associated to circadian regulation in rats, in contrast to higher sigma (12-13Hz) and SWA (Yasenkov and Deboer, 2011). In Kiessling *et al.*, 2018, it was revealed that *EphA4* KO mice have decreased PER1 expression and decreased light-induced c-FOS<sup>+</sup> cells in the SCN. Moreover, these mutants had longer periods in DD and shorter periods in LL, further supporting that the presence of EPHA4 is required for adequate endogenous circadian rhythm of locomotor activity. Therefore, the two studies suggested that one potential mechanism by which EPHA4 may be required for proper circadian responses to light may be through circadian gene expression, which may be controlled by the E-boxes found in the *EphA4* putative promoter. Interestingly, the transcriptional regulation of *EphA4* has not been extensively studied.

First, we analyzed the putative promoter regions of multiple components of Eph/Ephrin system to describe the presence of E-boxes or other regulatory elements involved in circadian/sleep physiology. To narrow down the study and given that *EphA4*, *EfnB2* and *EfnA3* expression was

modified in *Clock<sup>Δ19</sup>* mice, our first aim was to assess *in vitro* if molecular clock core components activate transcription via putative promoter regions of *Epha4*, *EfnB2* and *EfnA3* which contain E-boxes. To further investigate a circadian regulation of *Epha4* and ligands, the second aim of this study was to describe if *Epha4* and *EfnB2* protein levels show circadian rhythmicity in the mouse cerebral cortex and SCN. To avoid confounding effects of light and unmask endogenous circadian rhythms, mice were kept for two days in constant darkness and their brains were sampled at different times of the day. Both sexes were studied because research suggest that male and female mice present some differences in circadian physiology (see section 1.3.1.2 in Chapter 1) (*Kuljis et al., 2013; Chun et al., 2015; Kuljis et al., 2016*). Thus, a sub-aim was to determine if the levels of *Epha4* and *EfnB2* and their potential circadian rhythmicity is modulated by sex. On the other hand, as discussed in sections 1.2 and 1.3 of Chapter 1, brain regions can be implicated in the regulation of circadian rhythms and sleep in very different manners. Therefore, we compared spatial transcriptomic data from male and female mice sampled either at the beginning of the light/resting period (ZT4) or at the beginning of the dark/active period (ZT14) (under LD conditions) to assess potential time effects on gene expression *in vivo* and analyze potential effects in different brain regions. Thus, a final aim was to use spatial transcriptomic to measure whether *Epha4*, *EfnB2* and *EfnA3* gene expression was different between ZT4 and ZT14.

### **3.2.2 Define the effects of Rhynchophylline on sleep and the molecular mechanisms underlying its effects**

Two studies have provided data suggesting that *Epha4* may be implicated in the control of different sleep variables (*Freyburger et al., 2016; Freyburger et al., 2017*). *Epha4* KO mice have reduced PS time and increased SWS bout duration in the light period, blunted 24-hour rhythm of sigma activity and shorter duration of the positive and negative peaks of SWS slow waves (0.5-4 Hz) (*Freyburger et al., 2016; Freyburger et al., 2017*). Moreover, sleep deprivation increased *Epha4* expression in thalamus/hypothalamus tissue in mice (*Freyburger et al., 2016*), further suggesting an implication in sleep regulation. Thus, the general aim of the second study of the thesis was to inhibit *Epha4* in adult mice to investigate whether it would replicate the sleep phenotypes observed in *Epha4* KO mice. RHY is the main active component of *Uncaria* plants, which has been used in traditional medicines for its anxiolytic and anti-inflammatory properties. Two studies suggest that that RHY was able to recover spine morphology, LTP and cognitive

performance through EPHA4 inactivation in mouse models of Alzheimer's disease and depression (Fu et al., 2014; Zhang et al., 2017). Pull-down assays, and experiments *in vivo* and *ex-vivo* suggest that RHY binds to the extracellular domain of the EPHA4 receptor, avoiding the contact between EPHA4 and its extracellular ligands, and reducing EPHA4 phosphorylation (Fu et al., 2014; Zhang et al., 2017). Interestingly, RHY was shown to increase sleep time and decrease sleep latency in adult mice (Yoo et al., 2016), and plants containing Uncaria are generally increasing sleep time and quality in human (Ballester Roig et al., 2021). Therefore, the first specific aim of this study was to characterize the effect of RHY on sleep in mice. Mice were implanted with ECoG/EMG electrodes to compare their sleep under baseline recordings and after systemic RHY injections performed at two different times of the day. Given that sex differences had been found for sleep duration, fragmentation, and EEG in both human and rodents (Carrier et al., 2001; Mongrain et al., 2005; Koehl et al., 2006; Bixler et al., 2009; Cusmano et al., 2014; Swift et al., 2020, see section 1.1.2 in Chapter 1), RHY was provided to both male and female mice to determine if the effects of RHY on sleep would be different between sexes.

The next goal was to investigate what are the molecular mechanisms underlying the effects of RHY on sleep and determine if these could be linked to EPHA4 inhibition. Several studies show that RHY modifies the levels or activation of molecular components involved in neurotransmission (e.g., NR2B, EPHA4) in the rodent brain sampled 12 to 48 hours after systemic RHY administration (Zhou et al., 2010; Lee et al., 2014; Zhang et al., 2017). Thus, microdissections of the cerebral cortex, hippocampus and thalamus/hypothalamus were sampled at the end of the recordings (12 hours after the last RHY injection) to assess if RHY modifies the levels/activation of EPHA4, NR2B and GLUA1 in total and synaptoneurosomal protein fractions. Given that the effects of RHY on sleep reach its maximum in the first 2-5 hours after injection, we decided to investigate for molecular mediators of RHY effects at this moment with a technique with broader range of detection on cellular pathways and which, in addition, could provide information on multiple brain regions. Therefore, the last aim of this study was to measure the effects of RHY on the spatial transcriptome 3 to 4 hours after systemic RHY injection targeting key sleep regulatory regions of the hypothalamus.

### **3.3 Specific contributions of the candidate**

#### **3.3.1 In determining if EphA4 and its Ephrin ligands EfnB2 and EfnA3 are under circadian regulation**

For the first publication, I did the analysis of regulatory elements in *EphA4*, *EfnB2* and *EfnA3* putative promoters, and supervised the analysis of the inter-species comparison of putative promoters performed by PGR. I did part of the plasmid designs and cloning, and part of the luciferase assays. I supervised TASG on performing the luciferase assays of mutated constructs. I planned and conducted the *in vivo* experiments, brain punches, protein extractions and quantification. I performed the data analysis and wrote the manuscript.

#### **3.3.2 In defining the effects of Rhynchophylline on sleep and the molecular mechanisms underlying its effects**

I defined the adequate dose of RHY and conditions for drug dilution preparation, by comparing previous literature. I did the surgeries for ECoG implantation in all mice, and the animal follow-up, and did the totality of animal injections and brain samplings. I did most of the sleep scoring and analyzed the totality of the sleep data. I did the protein extraction (total and synaptoneurosomal fractions) and quantification of all male samples, and supervised YM who was in charge of female samples. Together with JDG, we prepared the brain tissue for Visium slides, did slide treatment and library preparation. I did the sequencing alignment to genome and conducted the full analysis of spatial transcriptomics data. I wrote the manuscript.

# Chapter 4

Transcriptional regulation of EphA4, Ephrin-B2 and Ephrin-A3  
by the circadian clock machinery

---



# Transcriptional regulation of EphA4, Ephrin-B2 and Ephrin-A3 by the circadian clock machinery

Maria Neus Ballester Roig,<sup>1,2</sup> Pierre-Gabriel Roy,<sup>1,3</sup> Lydia Hannou,<sup>2</sup> Thomas-Andrew Sully-Guerrier,<sup>2</sup> Erika Bélanger-Nelson,<sup>2,4</sup> Valérie Mongrain,<sup>1,2,\*</sup>

<sup>1</sup>Department of Neuroscience, Université de Montréal, Montréal, QC, H3T 1J4, Canada;

<sup>2</sup>Recherche CIUSSS-NIM, Montréal, QC, H4J 1C5, Canada;

<sup>3</sup>Department of Medicine, Université de Montréal, Montréal, QC, H3T 1J4, Canada;

<sup>4</sup>Pfizer, Canada;

\*Corresponding author

Valérie Mongrain  
Department of Neuroscience  
Université de Montréal  
Pavillon Paul-G.-Desmarais  
2960, chemin de la Tour, local 111  
Montreal, QC, H3T 1J4  
Canada  
valerie.mongrain@umontreal.ca  
1-514-338-2222/3323

Manuscript to submitted for publication

Content: 8128 words (excluding summary and references), 5 figures, 3 tables, 1 supplemental table

## Abstract

Circadian rhythms in mammals are generated by a molecular transcriptional translational feedback loop. The transcription factors CLOCK and BMAL1 act on gene regulatory elements called E-boxes (CANNTG) to shape biological functions in a rhythmic manner. The EPHA4 receptor and its ligands Ephrins (EFN) compose a system of cell adhesion molecules expressed in the brain and regulating neurotransmission and dendritic spine morphology. Previous studies showed the presence of E-boxes in the genes of *EphA4* and specific Ephrins, and that *EphA4* knockout mice have an altered circadian rhythm of locomotor activity. We thus hypothesized that the core clock machinery regulates the gene expression of *EphA4*, *EfnB2* and *EfnA3*. CLOCK and BMAL1 or NPAS2 and BMAL1 were found to have transcriptional activity on distal and proximal regions of *EphA4*, *EfnB2* and *EfnA3* putative promoters. A constitutively active form of glycogen synthase kinase 3 $\beta$  (GSK3 $\beta$ ; a negative regulator of CLOCK and BMAL1) blocked the transcriptional induction. Mutations of the E-boxes of *EphA4* distal promoter sequence also inhibited transcriptional induction. EPHA4 and EFNB2 protein levels did not show circadian variations in the mouse suprachiasmatic nucleus or the prefrontal cortex. The study uncovers core circadian clock factors as regulator of the expression of elements of the Eph/Ephrin system, which might contribute to circadian rhythms in biological processes in the brain or peripheral tissues.

## Introduction

Organisms have developed endogenous circadian rhythms to adapt their biological functions to the diurnal changes of the environment. The internal rhythmicity lasts approximately 24 hours, and is orchestrated by a molecular clock. In mammals, this molecular clock comprises a transcriptional-translational feedback loop (TTFL), in which the core proteins CLOCK and BMAL1 (circadian locomotor output cycles kaput 1 and brain and muscle ARNT [arylhydrocarbon receptor nuclear translocator]-like protein 1) heterodimerize to activate the transcription of the clock genes *Period (Per)* and *Cryptochrome (Cry)* (Gekakis et al., 1998; Takahashi, 2017). PER and CRY proteins translocate to the nucleus, and inhibit the activity of CLOCK and BMAL1, therefore repressing their own transcription, and allowing the loop to restart (Kume et al., 1999; Dardente et al., 2007; Takahashi, 2017). CLOCK and BMAL1 (or their homologs NPAS2 [neuronal PAS domain protein 2] and BMAL2) activate transcription by binding to regulatory elements in the DNA called E-boxes (CANNTG) (Gekakis et al., 1998; Maemura et al., 2000; Reick et al., 2001; Leclerc and Boockfor, 2005; Kiyohara et al., 2008).

The CLOCK:BMAL1 heterodimer also activates the expression of other components of the clock such as *Nr1d1/2* (coding for REV-ERB $\alpha/\beta$ ), which generate an additional negative feedback by binding to retinoic acid-related orphan receptor response element (RORE) found in *Clock* and *Bmal1* genes (Preitner et al., 2002; Guillaumond et al., 2005; Liu et al., 2008; Crumbley and Burris, 2011). In addition, rhythmic posttranslational modifications regulate the activity, transport, and degradation of core clock elements (Bellet and Sassone-Corsi, 2010; Hirano et al., 2016). For example, Glycogen synthase kinase 3 $\beta$  (GSK3 $\beta$ ) phosphorylates BMAL1, CRY2, and REV-ERB $\alpha$ , and controls, notably, their degradation or nuclear location (Harada et al., 2005; Yin et al., 2006; Sahar et al., 2010). Importantly, core clock components also control the expression of a variety of ‘clock-controlled genes’ in a rhythmic manner (via binding to E-boxes or RORE) to adapt physiological functions such as lipid/glucose metabolism or neuronal activity (Doi et al., 2010; Pan et al., 2010; Ikeda and Ikeda, 2014).

Most (if not all) mammalian cells have a functional molecular clock (TTFL) (Yamazaki et al., 2000; Zhang et al., 2014; Mure et al., 2018). In the brain, the suprachiasmatic nuclei of the hypothalamus (SCN) act as a main circadian oscillator by synchronizing the internal time to the environmental day-night time via receiving direct excitatory input from retinal ganglion cells

(Yamazaki *et al.*, 2000; Abrahamson and Moore, 2001; Brancaccio *et al.*, 2017; Hastings *et al.*, 2018). SCN output signals are, among others, driven by clock-controlled genes contributing to 24-h changes in neuronal activity/firing (Hastings *et al.*, 2018). Elsewhere in the brain, the molecular clock (and clock-controlled genes) also contributes to daily variations in behavior and neuroplasticity. Indeed, studies in mice have shown that the transcriptional control of tyrosine hydroxylase or monoamine oxidase by the molecular clock could underly time-dependent neuronal firing in the striatum and mood alterations (Hampp *et al.*, 2008; Chung *et al.*, 2014). Genes coding for cell/synaptic adhesion molecules are also candidates in bridging the molecular clock to rhythmic neuronal function given their E-box content and the roles in neurotransmission and neuroplasticity of their protein products (Girolodi *et al.*, 1997; El Helou *et al.*, 2013; Meighan *et al.*, 2015; Freyburger *et al.*, 2016; Li *et al.*, 2016; Hannou *et al.*, 2018). For instance, the *Neurologin-1* gene, which codes for a postsynaptic adhesion protein involved in glutamatergic signalling, was shown to be bound and transcribed by CLOCK and BMAL1, and to be expressed in a rhythmic manner in the mouse forebrain (El Helou *et al.*, 2013; Hannou *et al.*, 2018). Nevertheless, the potential for other cell/synaptic adhesion proteins to act as an output signal of the molecular circadian clock largely remains to be defined (Hannou *et al.*, 2020).

Ephrins (Efn) and their Eph receptors represent a large family of cell adhesion molecules highly expressed in brain cells (e.g., neurons, glia) (Goldshmit *et al.*, 2006; Murai and Pasquale, 2011; Chen *et al.*, 2012). The interaction between EPHA4 and its ligand EphrinA3 (EFNA3) regulates glutamate uptake (via astrocytic glutamate transporters), dendritic spine plasticity (via ACTIN remodelling), cell proliferation, and cortical development (Murai *et al.*, 2003; Filosa *et al.*, 2009; Steinecke *et al.*, 2014; Tanasic *et al.*, 2016; Zhu *et al.*, 2021). Ephrin-B2 (EFNB2), another ligand of EPHA4, has roles in vascular and cortical development, and in the regulation of neuronal plasticity and N-methyl-D-aspartate (NMDA) receptors (Bouzioukh *et al.*, 2007; Essmann *et al.*, 2008; Slack *et al.*, 2008; Hu *et al.*, 2014; Ghorri *et al.*, 2017; Xing *et al.*, 2019). We have previously reported the presence of E-boxes in the *EphA4* gene, together with a decreased mRNA expression of *EphA4*, *EfnA3* and *EfnB2* in *Clock*<sup>A19</sup> mice (Freyburger *et al.*, 2016). Moreover, we found relatively high expression of *EphA4* in the SCN of both mice and rats (Freyburger *et al.*, 2016), and altered circadian phenotypes in *Epha4* knockout (KO) mice (Kiessling *et al.*, 2018). These phenotypes notably included a longer endogenous period of wheel-running activity under constant darkness, and reduced phase-shift and number of c-FOS<sup>+</sup> cells in the SCN after a delaying

light pulse (*Kiessling et al., 2018*). Despite these observations suggesting a role for *EphA4* in circadian clock functions and the likelihood of it representing a clock-controlled gene, little is known concerning its transcriptional regulation and that of its protein partners.

The aim of this research was to determine whether *EphA4*, *EfnB2* and *EfnA3* are regulated by the circadian clock machinery. Firstly, *in vitro* assays investigating direct transcriptional activation by CLOCK and BMAL1 (or their respective homologs NPAS2 and BMAL2) of gene sequences upstream of *EphA4*, *EfnB2* and *EfnA3* transcription start sites (TSS) were conducted. Secondly, the effect of E-box mutations in *EphA4*, and the impact of GSK3 $\beta$  were assessed using similar transcriptional assays. Thirdly, protein levels were measured at six different times of the day in the SCN and prefrontal cortex (PFC), and gene expression at two times of the day in multiple brain regions to verify daily changes in the targeted Eph/Ephrin. CLOCK:BMAL1 and/or NPAS2:BMAL1 were found to induce transcriptional activation via putative promoter regions of *EphA4*, *EfnB2* and *EfnA3*, which was not linked to significant rhythms in protein level in the SCN or PFC. These findings provide support to a transcriptional regulation of elements of the Eph/Ephrin system by the circadian clock molecular machinery.

## Methods

### Promoter analysis

Gene sequences for *EphA4*, *EfnB2* and *EfnA3* and upstream sequences were obtained from mm9 in the UCSC genome browser (University of California Santa Cruz). Sequences were aligned and compared with the gene ID 13838 (*EphA4*, chr. 1, 77343819-77491763, complement), gene ID 13642 (*EfnB2*, chr. 8, 8667235-8711242, complement) and gene ID 106644 (*EfnA3*, chr. 3, 89221200-89231359, complement) in NCBI (National Centre of Biotechnology Information), and with sequences ENSMUSG00000026235 (*EphA4*), ENSMUSG00000001300 (*EfnB2*) and ENSMUST00000028039 (*EfnA3*) in the Ensemble genome browser. The number and location of exons, introns and TSS were extracted and compared with genomes mm10 and mm39. The A plasmid Editor (ApE) (by Wayne Davis) was used to screen the putative promoter regions, identified from 3000bp upstream of the TSS to the TSS, for cis-regulatory elements related to the

molecular clock: canonical E-boxes (CACGTG), non-canonical E-boxes (CANNTG, CACGNG), RORE, cAMP-response element (CRE), glucocorticoid response element (GRE), etc. The identified regulatory elements are listed in **Table 1**.

**Table 1. Regulatory elements found in the -3kb upstream of *EphA4*, *EfnB2* and *EfnA3* transcription start sites.**

Columns show the number of regulatory elements found in the cloned regions distal (D) or proximal (P). D (A, G or T), H (A, C or T), K (G or T), R (A or G), S (G or C), M (A or C), W (A or T), Y (C or T), N (any nucleotide). \* indicates T enrichment instead of AT enrichment in position “W”. AP-1 site: Activator protein 1 (Fos/Jun), ARE: antioxidant response element; CRE: cAMP response element; C/EBP: CCAAT/enhancer-binding protein sites; D-box: albumin D-site-binding protein response element; EGR2: early growth response (Krox20) site; FRE: FOXO (forkhead box proteins)-recognized element; GRE: glucocorticoids response element; NBRE: NGFI-B response element; PPRE: proliferator-activated receptor response element; NF- $\kappa$ B: nuclear factor kappa-light-chain-enhancer of activated B cells; RORE: retinoic acid-related orphan receptor response element; SRE: serum response element.

DNA element	EphA4 <sub>p</sub>	EphA4 <sub>D</sub>	EfnB2 <sub>p</sub>	EfnB2 <sub>D</sub>	EfnA3 <sub>D</sub>	Consensus site	Reference
E-box	6	5	5	9	6	CANNTG	
E-box (canonical)	-	-	-	-	-	CACGTG	<i>Gekakis et al., 1998</i>
E'-box	-	-	-	-	1	CACGTT	<i>Ueda et al., 2005; Doi et al., 2019</i>
D-Box	-	-	-	-	-	TTAYRTAA	<i>Falvey et al., 1996; Ueda et al., 2005</i>
RORE	-	1*	-	-	-	W(A/W)WN(T/N)RGGTCA	<i>Harding and Lazar, 1993; Giguere et al., 1994; Ueda et al., 2005; Matsuoka et al., 2020</i>
NBRE	-	-	-	-	-	AAAGGTC(A/R)	<i>Wilson et al., 1991; Robert et al., 2006</i>
SF-1(Nr5a1) sites	-	-	-	-	-	YCAAGGTCA	<i>Robert et al., 2006</i>
PPRE	-	-	-	-	-	AGGTCANAGGTCA	<i>Hamza et al., 2009</i>
PPRE half site	-	-	-	-	-	AGGTCA	<i>Hamza et al., 2009</i>
Egr1/Egr3 site	-	-	-	-	-	GCGKGGGCG	<i>Sun et al., 2019</i>
Egr2 (Krox20) site	-	-	-	-	-	TGCGKRGGHGK	<i>Swirnoff and Milbrandt, 1995</i>
CRE	2	-	2	-	-	HGTGGGHD	<i>Pham et al., 2012; Mendes et al., 2021</i>
Half CREB	-	-	-	-	-	TGACGTCA	<i>Montminy et al., 1986</i>
C/EBP	-	-	2	-	-	TGACG or CGTCA	<i>Yamamoto et al., 1988</i>
	-	-	-	-	-	TKWWGCAAT	<i>Mendes et al., 2021</i>
	-	-	-	-	1	TGGAGAAAG	<i>Albergaria et al., 2013</i>
GRE	-	-	-	-	-	AGAACANNNTGTTCT	<i>Krug et al., 2014</i>
SRE	-	-	-	-	-	CCWWWWWWGG	<i>Taylor et al., 1989; Wang et al., 2001; Buffet et al., 2015</i>
NF- $\kappa$ B site	1	-	-	-	-	5'-GGGRNYYCC-3'	<i>Leonard et al., 1989; Mulero et al., 2019</i>
CACC (or GC) boxes	-	-	-	-	-	CC(A/W)CACCC	<i>Hartzog and Myers, 1993; Feng et al., 1994</i>
	-	-	-	-	-	TGACTCA	<i>Gustems et al., 2014</i>
AP-1 site (Jun/Fos)	-	-	-	-	-	TGA(C/G)TCA	<i>Chinenov and Kerppola, 2001; Mendes et al., 2021</i>
	-	-	-	-	-	TGTTTCA	<i>Chinenov and Kerppola, 2001</i>
ARE	1	-	-	1	-	RGTGACnnnGC	<i>Rushmore et al., 1991; Wasserman and Fahl, 1997</i>
	-	-	-	-	-	GCTGAGTCAC	<i>Wang et al., 2016</i>
	-	-	-	-	-	(T)TGTTTAC	<i>Eijkelenboom and Burgering, 2013; Audesse et al., 2019</i>
FRE	1	-	-	1	2	(G/R)(T/W)AAA(C/Y)A(A)	<i>Hale et al., 2020; Sablon et al., 2022</i>
	-	1	-	-	-	MMAAAYAA	<i>Hale et al., 2020</i>

The *EphA4* gene (also known as *rb*, *Sek*, *Cek8*, *Hek8*, *Sek1*, *Tyrol*, *AI385584*, *2900005C20Rik*) contains 18 exons in rodents (19 in human), and one general TSS (beginning of exon 1). Another TSS after exon 11 has also been suggested (*Zhao et al.*, 2017). The 3kb upstream of the initial TSS includes 13 non-canonical E-boxes (11 CANNTG and two CACGNG; **Fig. 1**). For the *EfnB2* and *EfnA3* genes, the upstream 3kb show 16 and 18 non-canonical E-boxes CANNTG, respectively (**Fig. 1**). In addition, the *EfnA3* upstream region contains an E-box like element (E'-box: CACGTT), and one CACGNG sequence is found very close to the TSSs of both *EfnB2* and *EfnA3* (similar to the CACGNGs in *EphA4*). RORE were observed in *EphA4* and *EfnA3* putative promoters, and a half PPRE (peroxisome proliferator-activated receptors [PPAR] response element) in *EphA4* and *EfnB2* upstream regions (**Fig. 1A**). The regions were also screened for binding sites not related to the molecular clock, in particular sites linked to transcription factors that have been proposed to regulate *EphA4*, *EfnA3* or *EfnB2* transcription (such as EGR2 and Sp1 binding GC-boxes or FOXO response elements [FRE]) with fewer number of elements observed in comparison to E-boxes (**Table 1** and **Fig. 1**).

The number and position of E-boxes was also mapped for the putative promoter regions upstream of rat and human gene sequences for the three targets (ENST00000281821.7, ENST00000646441.1, ENST00000368408.4 for human; NM\_001162411.1, NM\_001107328, XM\_039103763.1 for rat). This was done to identify potential regions of higher relevance for transcriptional assay in the mouse genome. E-box position and number in the 3kb upstream of the TSS was relatively well conserved between species (**Fig. 1B**). Interestingly, for *EphA4*, there was an apparent clustering of E-boxes around a more distal and a more proximal region of the putative promoter, which seemed particularly conserved in the mouse, rat and human genomes (**Fig. 1B**). Accordingly, primers were designed to clone both of these regions, identified as *EphA4<sub>D</sub>* and *EphA4<sub>P</sub>*, respectively.

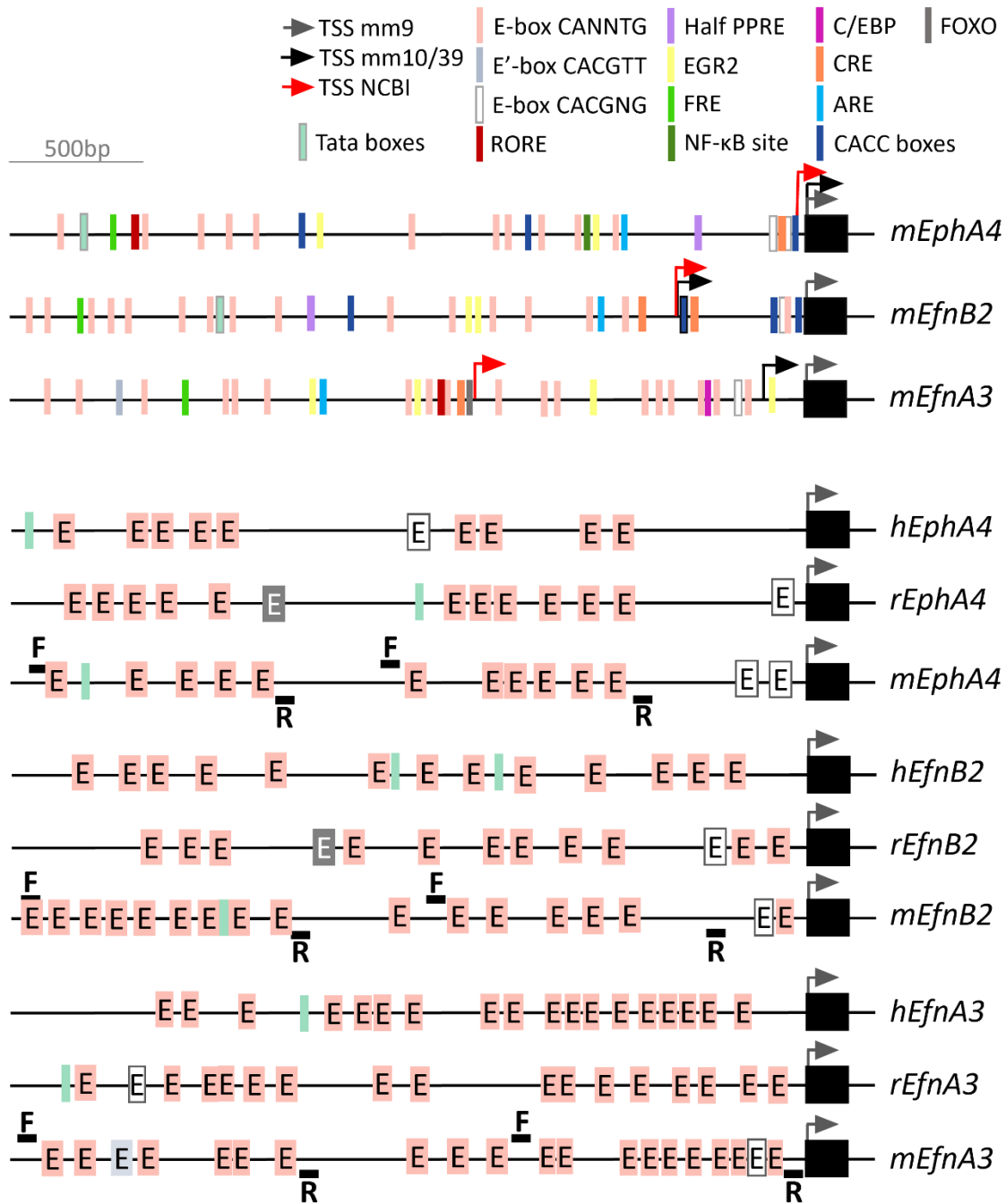


**Figure 1. *EphA4*, *EfnB2* and *EfnA3* putative promoter regions contain sleep and circadian-related regulatory elements.** Black box indicates exon 1. (A) Screening of the 3kb upstream of *EphA4*, *EfnB2* and *EfnA3* transcription start sites (TSS). Arrows indicate the transcription start sites (TSS) considered in different genome assemblies: grey in mm9, black in both mm10 and mm39; red in the NCBI tool. Colour bars indicate the regulatory elements found in these regions. AP-1 site: activator protein 1 (Fos/Jun), ARE: antioxidant response element; CRE: cAMP response element; C/EBP: CCAAT/enhancer-binding protein sites; EGR2: early growth response (Krox20) site; FRE: FOXO-recognized element; NF-κB: nuclear factor kappa-light-chain-enhancer of activated B cells; PPRE: proliferator-activated receptor response element; RORE: retinoic acid-related orphan receptor response element. (B) Alignment



and comparison of E-boxes in the 3kb upstream of the TSS for *EphA4*, *EfnB2* and *EfnA3* in the mouse, rat and human. Arrows indicate the TSS. Salmon E-boxes indicate CANNTG sequences, dark-grey E-boxes indicate CACGTG sequences (canonical E-boxes), light grey E-boxes indicate CACGTT sequences, white boxes indicate CACGNG; light green bars indicate Tata Boxes. Horizontal black bars indicate the position of forward and reverse primers used for cloning.

## Cloning

### Primer design

Five different regions of the putative promoter of *EphA4*, *EfnB2* and *EfnA3* were selected to generate reporter constructs: a 989bp proximal sequence of *EphA4* (*EphA4<sub>P</sub>*) at location -1603 to -615bp from TSS; a distal 998bp region at location -2981 to -1984 (*EphA4<sub>D</sub>*); a 1092bp proximal sequence of *EfnB2* (*EfnB2<sub>P</sub>*) at location -1392 to -301; a distal 1039bp region at location -2973 to -1935 (*EfnB2<sub>D</sub>*); and a 1081bp proximal sequence of *EfnA3* at location -2961 to -1881 (*EfnA3<sub>D</sub>*). Specific restriction enzymes were chosen to avoid cutting in the cloned sequence using NEBcutterv2.0 (New England Biolabs Inc.), and forward and reverse primers were designed for *EphA4<sub>P</sub>*, *EphA4<sub>D</sub>*, *EfnB2<sub>P</sub>*, *EfnB2<sub>D</sub>* and *EfnA3<sub>D</sub>* using the Oligo Analysis Tool (Eurofins Genomics). The sequence of used primers is provided in **Table 2**.

**Table 2. Forward (fw) and reverse (rv) primers used for cloning** with annealing temperature used for each pair. Restriction sites are indicated in bold.

Primer	5' to 3' sequence	Annealing Temperature
<i>EphA4<sub>P</sub></i> (fw)	GCTCTCGAGGGACAAGCTACTCATGAAATCC	67°C
<i>EphA4<sub>P</sub></i> (rv)	GATAAAGCTTGACCCAGTCATCTCCCCA	
<i>EphA4<sub>D</sub></i> (fw)	GTTCTCGAGGTGCTGGGACTAAAGGTGTA	67°C
<i>EphA4<sub>D</sub></i> (rv)	GCTTAAGCTTACGCAGGAATATAAGTGTGTGC	
<i>EfnB2<sub>P</sub></i> (fw)	GCTCTCGAGTGTCTCTCTGATAACGGGCA	56°C
<i>EfnB2<sub>P</sub></i> (rv)	CGCAAGCTTCCTCCTGAATCCTCGCAAC	
<i>EfnB2<sub>D</sub></i> (fw)	CCGCTCGAGTCAGTGGTTCATTGTAGC	53.5°C
<i>EfnB2<sub>D</sub></i> (rv)	GCGAAGCTTACCTTTACTGGAGAAGAGG	
<i>EfnA3<sub>D</sub></i> (fw)	CAACTCGAGGCCAGGGCTACACAGAGAA	61.5°C
<i>EfnA3<sub>D</sub></i> (rv)	GCCAAGCTTCTCCAACTGGGAATGTAC	

### DNA extraction and PCR

DNA was purified from C57BL/6J mouse ear pieces with the DNeasy Blood & Tissue Kit according to manufacturer's instructions (Qiagen, Germany). For PCR amplification, 25µL of Master Mix (2.5µL PCR Buffer 10X, 1µL of dNTP 10Mm, 1.25µL forward primer 20µM, 1.25µL reverse primer 20µM, 0.25µL Taq HotStart [5U/µL] (Qiagen), 16.08µL dH<sub>2</sub>O) were mixed with

50ng of DNA, and amplification was done using the following program: 5 minutes at 95°C (hot start); 30 cycles of 30 seconds at 94°C, 30 seconds at 53-67°C (see **Table 2**), and 1 minute at 72°C; 4 minutes at 72°C. Two and a half µL of PCR products (with 0.5µL of loading buffer) were run on an agarose gel 1% at 120V during 40 minutes for size verification, and PCR products were purified with QIAquick PCR Purification Kit according to manufacturer's protocol (Qiagen, Germany).

### **Digestion and ligation**

Purified amplicons and plasmid pGL3-basic (Promega, US) were digested with the restriction enzymes XhoI and HindIII (Thermo Fisher Scientific, US). Digestion mixes for plasmid (6µg of plasmid DNA, 3µL of each enzyme, 6µL 10X Fast Digest Green Buffer and water up to 60 µL) were incubated for 10 minutes at 37°C. Digestion mixes for insert DNA (0.4µg DNA, 1µL of each enzyme, 4µL 10X Fast Digest Green Buffer, and water up to 60 µL) were incubated for 20 minutes at 37°C. Then, 30µL of digested samples were run on a 1% agarose gel at 120V for 45 minutes, and DNA was purified using the QIAquick Gel Extraction Kit (Qiagen, Germany). Purified samples were ligated by mixing 50ng of digested plasmid with digested insert (ratio plasmid:insert 1:1 or 1:4), 4µL of ligase buffer 5X, 1µL of T4 DNA ligase and up to 20µL of dH<sub>2</sub>O, and incubated overnight (4°C). The final cloned plasmids are all 5.8 to 5.9kb and were all verified using Sanger sequencing (Genome Quebec, Montreal, Canada). *EphA4<sub>P</sub>* plasmid contained two point mutations in two cytosines (C → T at positions 198 and 837 of the insert) and *EfnA3<sub>D</sub>* contained a mutated base-pair in the fifth E-box (CAGTTG to CGGTTG), but the other plasmids did not contain any mutation.

### **Design of *EphA4<sub>D</sub>* with mutated E-boxes**

The gene sequence of *EphA4<sub>D</sub>* was then designed *in silico* with mutated E-boxes and ordered, already cloned in pGL3-basic, from Biomatik (Canada). From a literature review on E-box mutations impacting transcriptional activation and binding by CLOCK and BMAL1 (see **Table 3**), four E-boxes (CANNTG) were mutated to GCTAGT. The same restriction sites used for *EphA4<sub>D</sub>* are flanking the mutated insert (*EphA4<sub>Dmut</sub>*). The sequence of this commercial construct was also verified using Sanger sequencing (Genome Quebec, Montreal, Canada).

**Table 3. Mutated E-boxes used in previous research.** Bold indicates the mutated sequences in reference to the original E-box. Arrows indicate a decrease in comparison to wild-type sequences (↓: 10-30% reduction; ↓↓: 30-60% reduction; ↓↓↓: >60% reduction).

60-100% reduction). \* Indicates that these sequences are considered non-canonical E-boxes or E-box like sequences in other studies.

Mutated sequence	Effect regarding the original E-box	References
GCTAGT	↓↓↓ 80% transcriptional activation and binding by CLOCK/BMAL1	<i>Yoo et al., 2005; Doi et al., 2019</i>
GCTAGG	↓↓↓ transcriptional rhythm and binding CLOCK/BMAL1	<i>Nakahata et al., 2008</i>
TTTAGT	↓↓↓ 100% transcriptional activation by CLOCK/BMAL1	<i>Klemz et al., 2017</i>
ACCTGG	↓↓ 60% transcriptional activation and binding by CLOCK/BMAL1	<i>Rey et al., 2011; Hannou et al., 2018</i>
TGCGCA	↓↓↓ 70% transcriptional activation by CLOCK/BMAL1	<i>Onoue et al., 2019</i>
GGACGT	↓↓↓ 60% transcriptional activation by CLOCK/BMAL1	<i>Onoue et al., 2019</i>
TGGAAT	↓ 30% transcriptional activation by CLOCK/BMAL1	<i>Rey et al., 2011</i>
CATTG*	↓ 25-50% transcriptional activation by CLOCK/BMAL1	<i>Onoue et al., 2019</i>
CTCGAG*	↓ 15% transcriptional activation by CLOCK/BMAL1	<i>Mongrain et al., 2008</i>
GTCGCC	↓↓↓ binding of CLOCK/BMAL1	<i>Matsumura and Akashi, 2017</i>
CAGCTG*	↓↓ BMAL1 binding	<i>Chiou et al., 2016</i>
CTGAGC	Decrease binding of CLOCK/BMAL1	<i>Tamayo et al., 2015</i>

## Cell culture and transfection

Cell culture, transfection and luciferase assay were conducted similar to described previously (*Travnickova-Bendova et al., 2002; Dardente et al., 2007; Mongrain et al., 2008*). COS-7 cells were cultured in a humidified atmosphere at 37°C with 5% CO<sub>2</sub> in COS-7 media (HyClone Dulbecco's Modified Eagle Medium [DMEM]/High Modified; GE Healthcare Life Sciences, US Thermo Fisher Scientific] with 10% fetal bovine serum [FBS; Life Technologies] and 1% glutamine [Life Technologies]). For luciferase assays (see below), cells were plated on 24-well plates at 10<sup>6</sup> cells/well with 0.5mL of COS-7 media. After overnight incubation (37°C, 5% CO<sub>2</sub>; to reach 80-90% confluence), cells in each well were transfected with plasmid mixes containing: 50ng of reported constructs for selected targets (*EphA4<sub>P</sub>*, *EphA4<sub>D</sub>*, *EfnB2<sub>P</sub>*, *EfnB2<sub>D</sub>*, *EfnA3<sub>D</sub>* or *EphA4<sub>D</sub>mut*) or 25ng of positive control pGL3-*mPer1* (a 1.8-kb promoter region of *mPer1*; *Travnickova-Bendova et al., 2002*), 25ng of transfection normalizer pCR3-LacZ, 200ng of pSG5-mCLOCK or pSG5-empty, 200ng of pCS2-MTK-mBMAL1 or pCS2-MTK-empty, and completed to a total of 700ng of plasmids using pBluescript (Stratagene). In some experiments, pSG5-NPAS2 and pCS2-MTK-BMAL2 were used to replace CLOCK and BMAL1 expressing vectors, respectively. CLOCK, NPAS2, BMAL1 and BMAL2 expressing vectors were the same as those previously described (*Travnickova-Bendova et al., 2002; Dardente et al., 2007; Hannou et al., 2018*). For transfection, each well was treated with 0.7μL of Plus Reagent (ThermoFisher Scientific) diluted in 50μL of OPTI-MEM (Gibco, Life Technologies), and incubated 5 minutes at

room temperature. Cells were then immediately transfected using 2 $\mu$ L of Lipofectamine LTX (diluted in 50 $\mu$ L OPTI-MEM), and incubated for 30 minutes at room temperature. After 5 hours of incubation at 37°C, 0.5mL of COS-7 media was added per well, and plates were incubated overnight (37°C, 5% CO<sub>2</sub>) before luciferase assay. Transfection conditions were always conducted in triplicates (i.e., 3 wells per condition per plate).

The implication of the circadian clock machinery in the transcriptional control of *EphA4* and *EfnB2* was further investigated using luciferase assays conducted with the addition of the negative regulator of the clock machinery GSK3 $\beta$ . Assays were performed with a wild-type form of GSK3 $\beta$  (GSK3 $\beta$ -WT) or with a constitutively active form to prevent inactivation by intracellular mechanisms (GSK3 $\beta$ -S9A, which inactivation via serine-9 phosphorylation is rendered impossible by a substitution to alanine; (*Stambolic and Woodgett, 1994; Beaulieu, 2012*). Transfection conditions and plasmid mixes were similar as described above but included 50ng of pcDNA3-HA-GSK3 $\beta$ -WT (Addgene, Cambridge, MA; Jim Woodgett, Mont Sinai Hospital, Toronto, ON) or pcDNA3-GSK3 $\beta$ -S9A (*Stambolic and Woodgett, 1994*) or pcDNA3.1(+)-empty (#V790-20, Invitrogen).

## Luciferase assays

Media was removed, and cells were rinsed with PBS 1X. One hundred fifty  $\mu$ L of lysis buffer (25mM Tris, 2mM EDTA, 1mM dithiothreitol [DTT], 10% (v/v) glycerol, and 1% Triton X-100) was added to each well, and plates were incubated at room temperature in a Rocking Shaker (model 55, Reliable Scientific) at half its maximum speed for 10 minutes. Cells lysates were scratched and centrifuged at 13000rpm for 2 minutes to precipitate debris. For each well, 12 $\mu$ L of supernatant was transferred into a white 96-well plate. An EnSpire Multimodel Plate Reader (PerkinElmer) was used to inject 50 $\mu$ L of luciferase buffer (20mM Tris/Phosphate pH 7.8, 1mM MgCl<sub>2</sub>, 2.7mM MgSO<sub>4</sub>, 0.1mM EDTA, 33.3mM DTT, 530 $\mu$ M ATP, 270 $\mu$ M Co-enzyme A, 470 $\mu$ M D-Luciferin) per well, immediately followed by reading of luminescence counts at 560nm.

Luminescence counts were normalized to the total amount of protein and the transfection efficiency using, respectively, a DC (Lowry) protein assay (Bio-Rad) and a  $\beta$ -galactosidase assay. The DC protein assay was performed according to manufacturer's instructions (Bio-Rad Laboratories, US), and absorbance reads were done at 750nm using the EnSpire Multimodel Plate Reader. For the  $\beta$ -galactosidase assay, 30 $\mu$ L of the lysate supernatant was mixed with 750 $\mu$ L of  $\beta$ -

Mercaptoethanol in buffer Z (60mM Na<sub>2</sub>HPO<sub>4</sub>·7H<sub>2</sub>O, 40mM NaH<sub>2</sub>PO<sub>4</sub>·H<sub>2</sub>O, 10mM KCl, 1mM MgSO<sub>4</sub>·7H<sub>2</sub>O), and incubated 5 minutes at 37°C. Then, 150µL of buffer Z containing 4mg/mL o-nitrophenyl α-D-galactopyranoside (ONPG; Sigma Aldrich) was added to each condition, and incubated at 37°C until a yellow coloration appeared. A volume of 375-µL of 1M NaCO<sub>3</sub> was added to stop the reaction, and absorbance was measured at 420nm using the EnSpire Multimodel Plate Reader. Luminescence (luciferase) counts normalized with DC protein and β-galactosidase assay absorbances were finally expressed as relative values over the respective negative control condition (i.e., empty plasmids).

### **Brain tissue punches and protein extraction**

Males and females were studied for *in vivo* experiments given the reported sex differences in circadian rhythms (*Dib et al., 2021*), including in gene expression rhythms in the rodent brain (*Kuljis et al., 2013; Chun et al., 2015; Kuljis et al., 2016*). Thirty-six male and 36 female C57BL/6J mice were habituated to individual housing, a 12:12 hours light:dark cycle, and food/water available *ad libitum* for two weeks. Then, to unmask endogenous circadian rhythmicity, animals were exposed to constant darkness (DD) for two complete days followed which they were sacrificed under dim red-light at six different times: CT0, CT4, CT8, CT12, CT16 and CT20 (six mice per sex per time-point), with CT12 representing the start of the active period (usually occurring at dark onset). Full brains were immediately frozen and kept at -80°C. This experiment was performed in accordance with guidelines of the Canadian Council on Animal Care, and approved by the *Comité d'éthique de l'expérimentation animale* of the *Hôpital du Sacré-Coeur de Montréal* (CIUSSS-NIM).

Protein levels were measured for the SCN and PFC. The SCN was targeted given its roles in the circadian system, and because *EphA4* is expressed in this area (*Freyburger et al., 2016*), and the PFC given the reported rhythmic levels of BMAL1 and PER1 (*Angeles-Castellanos et al., 2007; Coria-Lucero et al., 2016*). PFC and SCN regions were sampled using tissue punches prepared using a cryostat (HM525 NX, Thermo Scientific, lame S35 - Feather®) with magnifying glasses. A 20G needle, cutted to obtain a flat end with a diameter <0.9µm, was kept in the cryostat (-12 to -13°C), and used to collect SCN and PFC punches. Brains were first sectioned in 500µm coronal slices at -12 to -13°C (starting +2mm (anterior) from the Bregma for PFC and -0.3mm (posterior) from Bregma for SCN). For PFC, five punches from the same brain section were

sampled per animal, while for the SCN, five punches each from a different mouse were pooled per time point. Each punch was immediately released in 40 $\mu$ L of ice-cold modified RIPA buffer (100mM HEPES, 0.25M EDTA, 10% SDS, 10% IGEPAL, 10% sodium deoxycholate, protease and phosphatase inhibitors [Sigma-Aldrich]). After the addition of five punches to the 40ul cold RIPA buffer, tissues were mechanically homogenized on ice with a Pellet Pestle (Sigma Aldrich) until translucent (one 30-second and one 20-second interval). Samples were immediately centrifuged at 8000rpm for 40 min (4°C), and the supernatants were kept at -80°C for subsequent analysis.

### **Immunoblotting and protein quantification**

Twenty  $\mu$ g of protein were loaded on 8% acrylamide gels, and separated by SDS-PAGE using a 65min migration at 100V. Proteins were then transferred to a PVDF membrane (Bio-Rad) for 60min at 100V. Membranes were blocked with blocking buffer (5% dry milk diluted in Tris-buffered saline [TBS: 15mM Tris-HCl, 5mM Tris base, 150mM NaCl]) for 1h at room temperature, and then incubated overnight at 4°C with primary antibodies against EPHA4 (1:1000; Invitrogen #37-1600) and EFNB2 (1:1000; R&D Systems Inc. #AF496) diluted in 5% dry milk in TBS-T (TBS with 0.1% Tween 20). After TBS-T washes, membranes were incubated for 1.5h at room temperature with secondary antibodies (1:15000 IRDye® 680RD goat anti-mouse IgG (H+L) #926-68070, IRDye® 800CW donkey anti-goat IgG (H + L) #926-32214; LI-COR) diluted in 5% dry milk TBS-T. Membranes were revealed using an Odyssey CLx imaging system (LI-COR). After image acquisition, membranes were stripped with 10% NaOH for 30min, washed in TBS-T, and blocked again with 5% dry milk TBS-T for 1h at room temperature. Membranes were then incubated overnight at 4°C with a second set of primary antibodies, namely targeting PER1 (1:1000; Abcam #2201) or PER2 (1:1000; Novus Biologicals #100-125) together with ACTIN (1:8000; Sigma Aldrich #A5441), diluted in 5% dry milk TBS-T. After TBS-T washes, membranes were incubated for 1.5h at room temperature with secondary antibodies (1:15000 IRDye® 680RD goat anti-mouse IgG (H+L) #926-68070, IRDye® 800CW goat anti-rabbit IgG (H+L), #926-32211; LI-COR) diluted in 5% dry milk TBS-T. Membranes were again revealed using an Odyssey CLx imaging system. Bands were quantified using ImageJ (NIH) (*Schneider et al., 2012*). Values were normalized to ACTIN, then to a control sample included on each different membrane, and finally to the mean CT0 level for each tissue.

## Spatial gene expression quantification

The gene expression of *EphA4*, *EfnB2* and *EfnA3* was compared between the early rest period (Zeitgeber time 4: ZT4; with ZT0 representing light onset, and ZT12 light offset) and the early active period (ZT14) for different brain regions using the 10x Genomics Visium Spatial Gene Expression kit (10x Genomics). Coronal 10 $\mu$ m brain slices (1.5mm posterior to Bregma) were prepared from C57BL/6J mice injected with saline 3-4 hours before sacrifice (control samples from Ballester Roig et al., in preparation), and processed for spatial transcriptomics according to manufacturer's instructions. Briefly, slices were fixed, stained with hematoxylin-eosin and permeabilized, following which cDNA libraries were prepared using the Visium Spatial Gene Expression kit. Libraries were sequenced using a NovaSeq6000 platform (Illumina) at Genome Québec. Sequencing reads in the FASTQ format were aligned to the mouse genome and compared between ZT4 and ZT14 using Space Ranger and Loupe Browser 5.0 (10x Genomics). Differentially expressed genes were defined as having a false discovery rate (FDR) < 0.05 (*Benjamini and Hochberg, 1995*). The dataset included one male and one female brain sampled at ZT4 and one male and one female brain sampled at ZT14, and only the gene expression of *EphA4*, *EfnB2* and *EfnA3* is reported here together with that of the circadian control gene *Per2*, *Rev-Erba*, and *Dbp*. Data will be publicly available at GEO (#GSE218537 and #GSE217058) upon publication. This experiment was also performed in accordance with guidelines of the Canadian Council on Animal Care, and approved by the *Comité d'éthique de l'expérimentation animale* of the *Hôpital du Sacré-Coeur de Montréal* (CIUSSS-NIM).

## Statistical analysis

Except for the spatial transcriptomic dataset, Prism 7 (GraphPad Software Inc., USA) was used to conduct statistical analyses and prepare figures. One-way analyses of variance (ANOVA) were used for comparisons of luciferase data between conditions, and of protein levels between time points. Post-Hoc Tukey's Multiple Comparison tests were used to decompose significant effects found in ANOVAs. Data are presented as means  $\pm$  SEM, and the threshold for statistical significance was set to 0.05. For graphical representation, curves were fitted with cosine analysis using Graphpad (constraint to a 24-hour period) and the significance of the fit was calculated with Circwavebatch v3.3 (both with initial values of tau = 24 and with tau minimum = 21 to tau maximum = 27).

## Results

### Transcriptional activation of *EphA4* by clock transcription factors

The activation of proximal (*EphA4<sub>P</sub>*) and distal (*EphA4<sub>D</sub>*) regions of the putative promoter of *EphA4* by CLOCK, BMAL1 and homologs NPAS2 and BMAL2 was investigated using luciferase assays conducted with COS-7 cells similar to previously performed for other target genes (*Dardente et al., 2007; Mongrain et al., 2008; Hannou et al., 2018*). When transfected alone, none of the core clock transcription factors induced a transcriptional activation, which applies to both the proximal and distal regions (**Fig. 2A**). In contrast, co-transfection of CLOCK and BMAL1 and/or of NPAS2 and BMAL1 induced a significant transcriptional activation via *EphA4<sub>P</sub>* and *EphA4<sub>D</sub>* (*EphA4<sub>P</sub>*  $F_{8,158} = 13.24$ ,  $p < 0.0001$  for CLOCK and BMAL1; *EphA4<sub>D</sub>*  $F_{8,202} = 28.9$ ,  $p < 0.0001$  for CLOCK and BMAL1 and  $F_{8,202} = 28.9$ ,  $p < 0.0001$  for NPAS2 and BMAL1). More precisely, CLOCK and BMAL1 induced a 2-fold transcriptional activation via *EphA4<sub>P</sub>* and 3.2-fold activation via *EphA4<sub>D</sub>*. Moreover, NPAS2 and BMAL1 also induced a 2-fold transcriptional activation via *EphA4<sub>D</sub>*. No significant transcriptional activation was found for NPAS2 and BMAL1 for *EphA4<sub>P</sub>*, or for any combination with the BMAL1 homolog BMAL2.

The implication of the core circadian clock molecular loop in the control of *EphA4* gene expression was assessed with luciferase assays in the presence of GSK3 $\beta$ , a negative regulator of the CLOCK:BMAL1 heterodimer. These assays using, an additional plasmid, showed significant transcriptional activation by CLOCK and BMAL1 and by NPAS2 and BMAL1 via both *EphA4<sub>P</sub>* and *EphA4<sub>D</sub>* ( $F_{6,65} = 28.7$ ,  $p < 0.0001$  and  $F_{6,54} = 14.6$ ,  $p < 0.0001$ , respectively; **Fig. 2B**). These activations were completely abolished by the constitutively active form of the kinase GSK3 $\beta$  (i.e., GSK3 $\beta$ -S9A), whereas GSK3 $\beta$ -WT was not impacting CLOCK:BMAL1- and NPAS2:BMAL1-driven transcriptional activation (**Fig. 2B**).

To verify the implication of specific E-boxes of *EphA4<sub>D</sub>* in the CLOCK:BMAL1-driven transcriptional activation, luciferase assays were conducted with a reporter constructs containing four mutated E-boxes in the *EphA4<sub>D</sub>* sequence (*EphA4<sub>D</sub>mut*; **Fig. 2C**). CLOCK:BMAL1 transcriptional activation via *EphA4<sub>D</sub>mut* showed a 1.7-fold induction, which was significantly different from CLOCK:BMAL1 transcriptional activation via *EphA4<sub>D</sub>* ( $F_{3,42} = 17.5$ ,  $p < 0.001$ ; **Fig. 2D**). In fact, in comparison to the wild-type *EphA4<sub>D</sub>* sequence (3.4-fold induction), transcriptional activation via *EphA4<sub>D</sub>mut* showed a 50% reduction. This suggests an implication of at least one of



the four mutated E-boxes in the transcriptional activation of *EphA4* by core clock transcription factors.

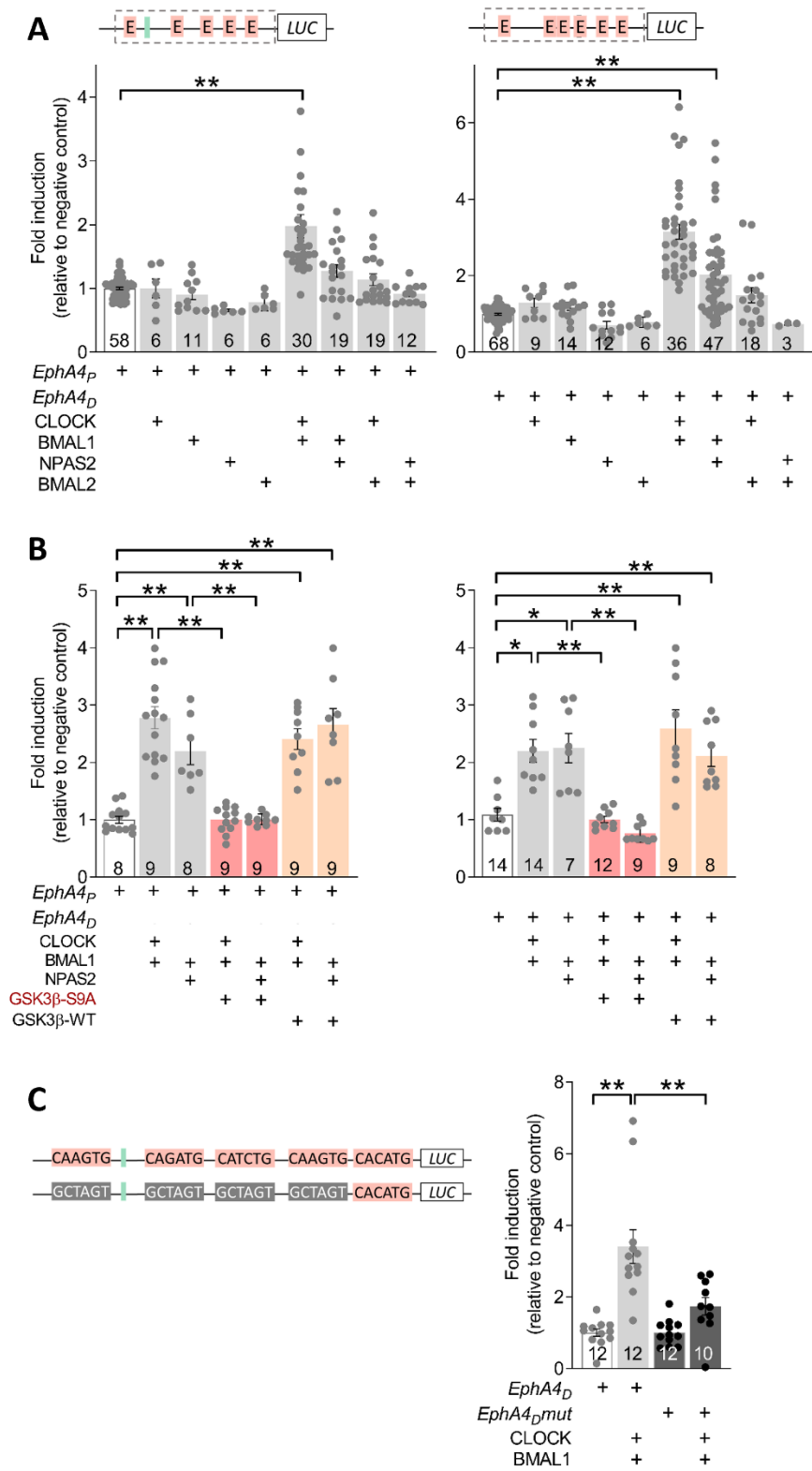


**Figure 2. Circadian clock transcription factors activate transcription via *Epha4* putative promoter sequences.**

(A) Transcriptional activation by different combinations of CLOCK, BMAL1, NPAS2 and BMAL2 via *Epha4<sub>P</sub>* (left) and *Epha4<sub>D</sub>* (right). Upper schematics represent the inserts cloned inside PGL3 plasmids and used for assays. (B) Transcriptional activation by different combinations of CLOCK, BMAL1, NPAS2, GSK3 $\beta$ -S9A and GSK3 $\beta$ -WT via *Epha4<sub>P</sub>* (left) and *Epha4<sub>D</sub>* (right). (C) Left schematic illustrates mutated E-boxes of *Epha4<sub>D</sub>* in grey in comparison to the native sequence in salmon. Right graph shows transcriptional activation by CLOCK and BMAL1 via *Epha4<sub>D</sub>* and mutated *Epha4<sub>D</sub>* (*Epha4<sub>Dmut</sub>*). + indicate transfection of plasmids containing circadian clock transcription factor or luciferase reporter (absence of + indicates transfection with corresponding empty plasmids). The numbers on bars indicate the numbers of replicates. Transcriptional activation is expressed relative to the negative control (shown in white). \* indicate  $p < 0.05$  and \*\*  $p < 0.01$  between indicated bars (post hoc comparisons).

**Transcriptional activation of *EfnB2* and *EfnA3* by clock transcription factors**

To assess whether the circadian clock molecular machinery also activates the gene expression of EPHA4 ligands, luciferase assays were conducted using proximal and distal sequences of *EfnB2* (*EfnB2<sub>P</sub>*, *EfnB2<sub>D</sub>*), and a distal sequence of *EfnA3* (*EfnA3<sub>D</sub>*). Significant transcriptional activations were found for all three gene sequences (*EfnB2<sub>P</sub>*  $F_{4,28} = 49.7$ ,  $p < 0.0001$ ; *EfnB2<sub>D</sub>*  $F_{4,56} = 46.3$ ,  $p < 0.01$ ; *EfnA3<sub>D</sub>*  $F_{4,53} = 5.2$ ,  $p < 0.005$ ; **Fig. 3A**). Simultaneous transfection of CLOCK and BMAL1 induced a 4.3-fold transcriptional activation via *EfnB2<sub>P</sub>*, whereas NPAS2:BMAL1 and NPAS2:BMAL2 co-transfections induced 4.8-fold and 2.6-fold transcriptional activation via the same sequence. Transcriptional activations via *EfnB2<sub>D</sub>* were more modest, although significant, reaching 1.4-fold for CLOCK:BMAL1 and 1.8-fold for NPAS2:BMAL1. Finally, transcriptional activation via *EfnA3<sub>D</sub>* was only induced by NPAS2:BMAL1 (2.8-fold; **Fig. 3A**).

Assays with *EfnB2* promoter sequences were then conducted in the presence of GSK3 $\beta$ -S9A and GSK3 $\beta$ -WT. The constitutively active GSK3 $\beta$ -S9A (but not GSK3 $\beta$ -WT) blocked the effect of CLOCK:BMAL1 and NPAS2:BMAL1 on *EfnB2<sub>D</sub>* ( $F_{6,38} = 16.3$ ,  $p < 0.01$ ; **Fig. 3B**). Intriguingly, GSK3 $\beta$ -WT induced 7.0-fold transcriptional activation via *EfnB2<sub>P</sub>* when co-transfected with CLOCK:BMAL1 (5.0-fold more than co-transfecting CLOCK:BMAL1 without GSK3 $\beta$ ), and the transcriptional activation of NPAS2:BMAL1 via *EfnB2<sub>P</sub>* was potentiated by GSK3 $\beta$ -WT (8.3-fold with GSK3 $\beta$ -WT compared to 3.8-fold without). In sum, concerning *EfnB2<sub>D</sub>*, the transcriptional activation by CLOCK:BMAL1 and NPAS2:BMAL1 were both abolished by the constitutively active GSK3 $\beta$ -S9A, but not by GSK3 $\beta$ -WT, which is reminiscent of observations made for *Epha4* promoter sequences. In sum, these results support that core clock transcription

factors can activate the transcription via putative promoter sequences of *EfnB2* and *EfnA3*, which is under modulations by GSK3 $\beta$ .

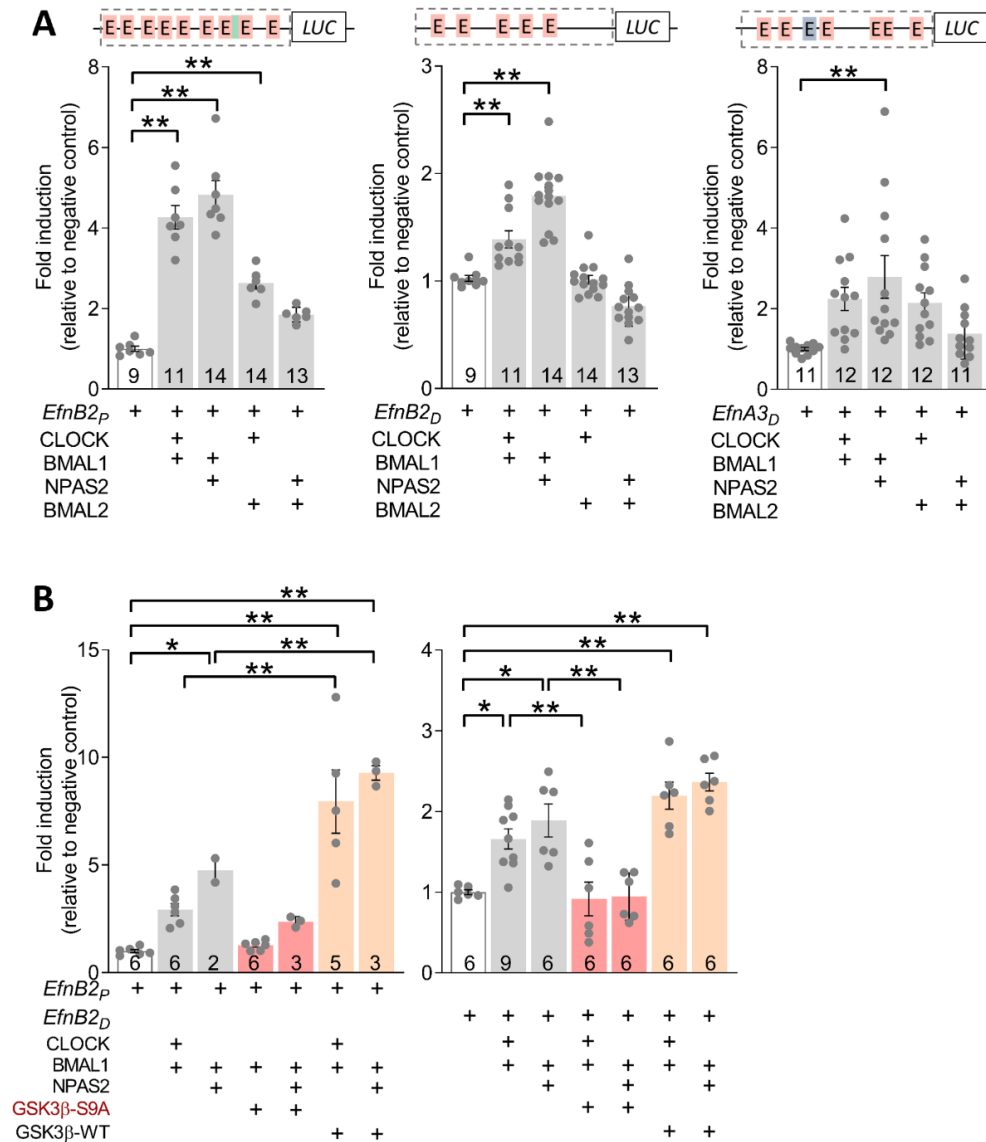


**Figure 3. Circadian clock transcription factors activate transcription via *EfnB2* and *EfnA3* putative promoter sequences.** (A) Transcriptional activation by different combinations of CLOCK, BMAL1, NPAS2 and BMAL2 via *EfnB2<sub>p</sub>* (left), and *EfnB2<sub>D</sub>* (middle) and *EfnA3<sub>D</sub>* (right). Upper schematics represent the inserts cloned inside PGL3 plasmids and used for assays. (B) Transcriptional activation by different combinations of CLOCK, BMAL1, NPAS2, GSK3 $\beta$ -S9A and GSK3 $\beta$ -WT via *EfnB2<sub>p</sub>* (left) and *EfnB2<sub>D</sub>* (right). + indicate transfection of plasmids containing circadian clock transcription factor or luciferase reporter (absence of + indicates transfection with corresponding empty plasmids). The numbers on bars indicate the numbers of replicates. Transcriptional activation is expressed relative to the negative control (shown in white). \* indicate  $p < 0.05$  and \*\*  $p < 0.01$  between indicated bars (post hoc comparisons).

## Absence of EPHA4 and EFNB2 circadian rhythm in the PFC and SCN

To assess whether the implication of the core clock transcription factors in the transcriptional regulation of *Epha4* and *Efnb2* results in a circadian rhythm of their respective protein product, EPHA4 and EFNB2 protein level was measured at six different circadian times in the SCN and PFC in male and female mice. For both males and females, no significant circadian oscillation on the level of EPHA4 and EFNB2 was found in the PFC ( $R^2 < 0.13$ ,  $p > 0.24$ ; **Fig. 4A and B**). Similar observations were made when pooling PFC punches of five different animals per time (**Fig. 4A and B**). PER1 and PER2 were also measured in the PFC, but no significant circadian curve fit was found for PER1 ( $R^2 < 0.08$ ,  $p > 0.42$ ) and merged samples for PER1 do not allow statistical comparison (**Fig. 4A, B**). In the SCN, circadian time does not seem to change the expression of EPHA4 and PER2 levels (without statistical comparison; **Fig. 4A bottom and C**). A potential circadian variation in PER2 was observed in the female SCN (without statistical comparison;). The level of EFNB2 in the SCN was too low to allow a reliable quantification. These results suggest that, although core clock transcription factors act on *Epha4* and *Efnb2* putative promoter regions, EPHA4 and EFNB2 proteins are not showing robust variations at a circadian scale in the PFC and SCN when mice are kept in constant darkness.

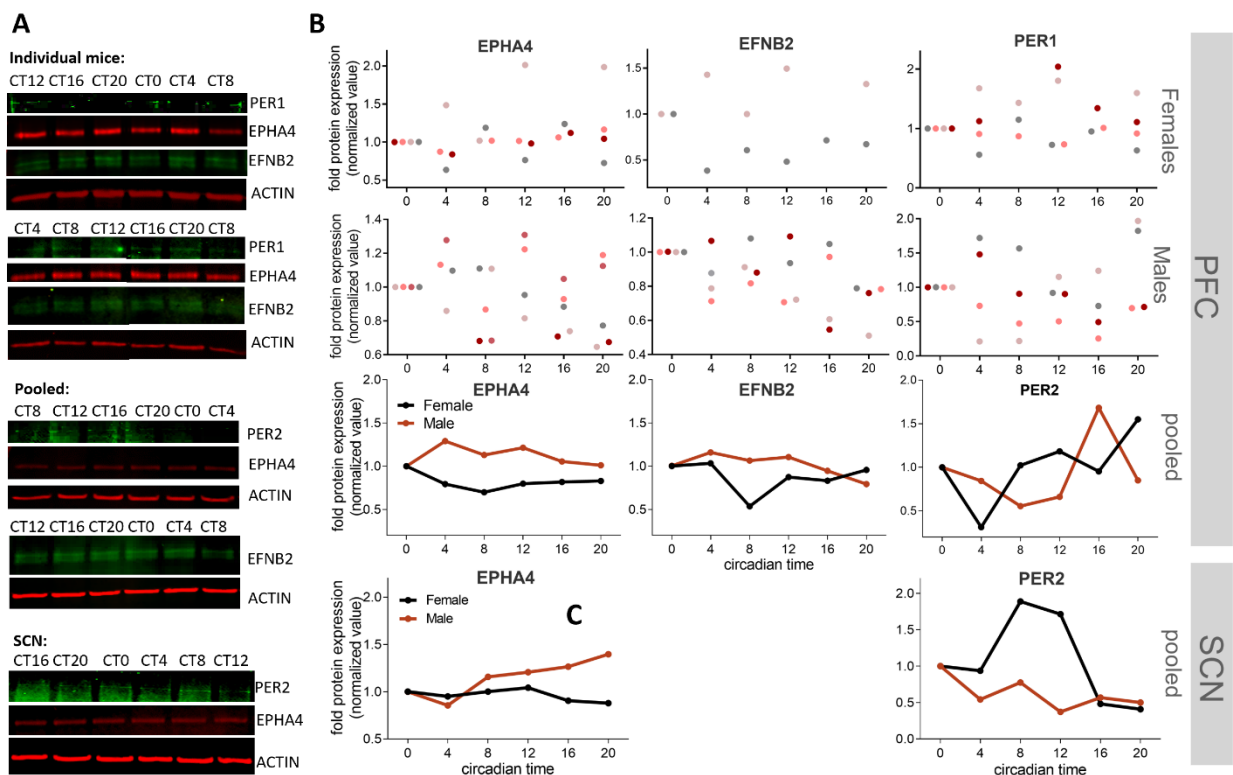


**Figure 4. EPHA4 and EFNB2 protein levels in the mouse PFC and SCN do not show circadian oscillations.** (A) Representative blots of PFC samples of individual mice (top), of PFC samples of pooled female mice (middle), and of SCN samples of pooled female mice (bottom). (B) The top two rows show quantifications of EPHA4, EFNB2 and PER1 in PFC punches from individual mice (dots of the same colour are from the same blot). The third row shows EPHA4, EFNB2, and PER2 band quantifications of PFC pooled samples. Non-significant cosine waves fitted to the data are also shown (same in panel C). P-values were calculated fitting data to a 24-h cosine curve. (C) Protein quantification of EPHA4 and PER2 for SCN punches (each point represents a pool of SCN from 5 different mice).

### ***EphA4* and *EfnB2* expression pattern in different brain regions**

We previously reported that the diurnal variations in the gene expression of components of the Ephrin/Eph system is dependent on brain region (*Freyburger et al., 2016*). We here investigated whether the mRNA expression of *EphA4*, *EfnB2* and *EfnA3* differed between the early light (ZT4) and the early dark (ZT14) period using a spatial transcriptomic strategy applied on a mouse coronal slice comprising the cerebral cortex, hippocampus, thalamus, hypothalamus, amygdala, and striatum (**Fig. 5A** and **5B**). The expression of *EphA4* and *EfnA3* was found to be particularly high in the pyramidal layer of hippocampal CA1-CA3 regions and granular layer of the dentate gyrus. *EphA4* expression was also generally elevated in the thalamic region, and that of *EfnA3* in cortical regions. In contrast, the expression of *EfnB2* was lower, especially in the hippocampus, thalamus and hypothalamus. Globally, these expression patterns matched with those reported by the Allen Brain Atlas and previous literature (Allen Mouse Brain Atlas; *Liebl et al., 2003*). *EphA4*, *EfnB2* and *EfnA3* were not comprised in the list of differentially expressed genes (DEGs, FDR < 0.05) between ZT4 and ZT14 when considering the complete brain slice or the specific regions of interest targeted (**Fig. 5A** and **5B**), although there could be a trend for a higher *EphA4* expression at ZT14 in layers I-IV of the auditory and entorhinal cortices. For comparison, the known cycling transcripts *Per2*, *Rev-Erba* and *Dbp* are shown in **Fig. 5C** (see also full DEG list in **Table S1**).

## **Discussion**

The present study provides support to a role for the circadian clock molecular machinery in the regulation of the gene expression of elements of the Eph/Ephrin system. More precisely, CLOCK and BMAL1 or NPAS2 and BMAL1 were found to induce transcription via sequences upstream of the TSS of *EphA4*, *EfnB2* and *EfnA3* using *in vitro* assays. This transcriptional

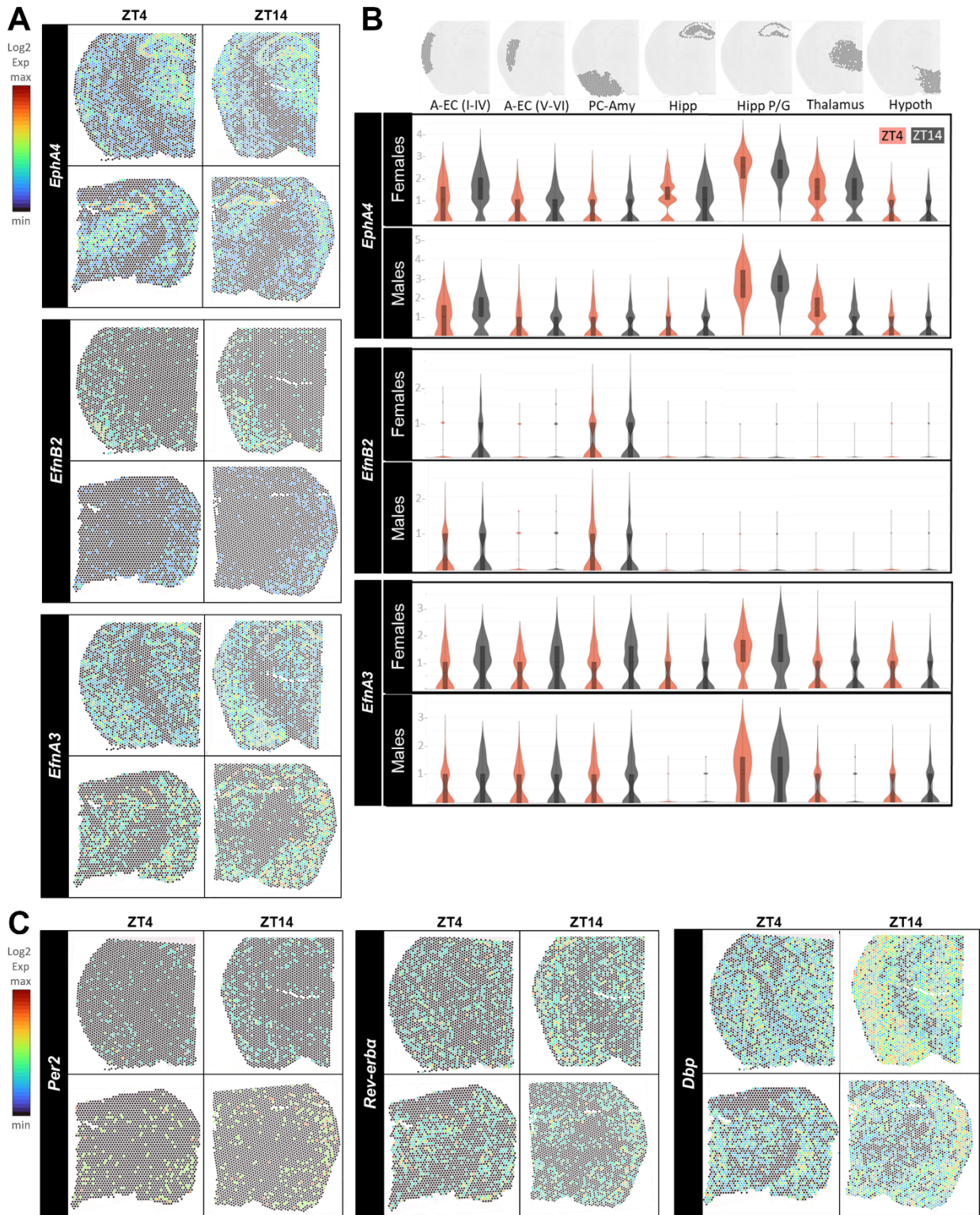


**Figure 5.** *EphA4*, *EfnB2* and *EfnA3* gene expression in the mouse brain at ZT4 and ZT14. (A) Spatial pattern of gene expression in the mouse brain for a selected coronal slice sampled at ZT4 (left) or ZT14 (right). Upper panels are from female mice, and lower panels from male mice (also in C). Black to red colors indicate spots with minimum to

maximum gene expression, respectively (also in C). (B) Violin plots of *Epha4*, *EfnB2* and *EfnA3* gene expression in spots grouped for specific regions of interest: layers I-IV or layers V-VI of auditory and entorhinal cortices (A-EC), piriform cortex and amygdala (PC-Amy), hippocampus (Hipp), pyramidal and granular layers of the hippocampus (Hipp P/G), thalamus and hypothalamus. Orange denotes expression at ZT4, and grey at ZT14. (C) Spatial pattern of *Per2*, *Rev-Erba* and *Dbp* gene expression in the mouse brain for the selected coronal slice sampled at ZT4 or ZT14.

activation was found to be repressed by the circadian clock regulator GSK3 $\beta$ , when a constitutively active form of this kinase was used. For *Epha4* in particular, mutating E-boxes in the promoter sequence reduced CLOCK:BMAL1-driven transcriptional activation. Although robust rhythms in protein level or gene expression were not detected in different brain regions, current *in vitro* findings combined to our previous observations of modified Eph/Ephrin gene expression in *Clock* mutant mice and altered circadian phenotypes in *Epha4* KO mice (Freyburger et al., 2016; Kiessling et al., 2018) are supporting a relationship between the molecular circadian clock and components of the Eph/Ephrin system.

Our findings emphasize the importance of non-canonical E-boxes in the transcriptional control by core clock transcription factors. Indeed, CLOCK:BMAL1- and NPAS2:BMAL1-induced transcriptional activation occurred via sequences of the *Epha4* and *EfnB2* putative promoter with the only presence of CANNTG non-canonical E-boxes (i.e., without the presence of the canonical sequence CACGTG). CANNTG sequences are predicted to randomly appear every 256bp in the genome but have nevertheless been reported to be important for transcriptional regulation in previous studies (Leclerc and Boockfor, 2005; Kiyohara et al., 2008; Hannou et al., 2018). For instance, CATGTG could robustly activate the transcription of the *Dbp* gene (Kiyohara et al., 2008), whereas CATTTG appeared a key sequence in the transcriptional control of *Prolactin* by CLOCK and BMAL1 (Leclerc and Boockfor, 2005). One CATGTG was present amongst the six E-boxes of *Epha4<sub>P</sub>*, and four CATTTG amongst the nine E-boxes of *EfnB2<sub>D</sub>*. However, some of the E-boxes included in our studied gene sequences (e.g., CAGATG) were reported not to be bound by core clock transcription factors in another study (Oishi et al., 2005). It is also important to underline that the functionality of E-boxes can depend on the flanking DNA or other regulatory elements, as already evoked previously (Nakahata et al., 2008). In aiming at considering the cooperative nature of E-boxes, four were mutated in the distal region of *Epha4*, which led to a 50% decrease in transcriptional activation by CLOCK and BMAL1. This result supports a role for at least one of these elements or their overall combination in the observed effect. Mutating each E-

box separately will be required to pinpoint the exact DNA sequence(s) responsible for the transcriptional activation of *Eph/Ephrin* genes by clock transcription factors.

GSK3 $\beta$  was able to shape CLOCK:BMAL1- and NPAS2:BMAL1-mediated transcriptional activation of *EphA4* and *EfnB2*. Given the roles of GSK3 $\beta$  in the regulation of the molecular clock (*Sahar et al., 2010; Besing et al., 2015*), this further supports an implication of core clock mechanisms in the gene regulation of Eph and Ephrins. Interestingly, *EphA4* KO mice and *GSK3 $\beta$*  haploinsufficient mice have both been shown to express a longer endogenous period of wheel-running activity under DD conditions (*Lavoie et al., 2013; Kiessling et al., 2018*). Thus, the downregulation of GSK3 $\beta$  and *EPHA4* could impact the circadian system similarly, at least at the level of output pathways affecting the locomotor activity rhythm. Besides roles in the circadian system, GSK3 $\beta$  is notably regulated by neurotransmission and insulin pathways (*Beurel et al., 2015; Patel and Woodgett, 2017*), and has been associated to neurodegeneration and neurological conditions (*Inoki et al., 2006; Patel and Woodgett, 2017; Liu and Klein, 2018*). Our findings therefore imply that the regulation of Eph/Ephrin gene expression by GSK3 $\beta$  could serve cellular responses in ‘non-circadian’ contexts.

A limitation of the present dataset could reside in luciferase assays conducted only using COS-7 cells. Previous research from our group has nevertheless supported the suitability of this model system for transcriptional studies related to the circadian clock (*Mongrain et al., 2008; Hannou et al., 2018*). Our results could be expanded with continuous bioluminescence recordings to investigate whether transcriptional activation by CLOCK and BMAL1 via *EphA4/Ephrin* promoter sequences shows circadian oscillations. Besides, the cloned sequences used here do not recapitulate the complexity of *in vivo* transcriptional regulation notably because reporter plasmids lack surrounding DNA as well as long distance regulatory elements, which contribute to DNA folding and can impact the binding by the circadian clock molecular machinery. In fact, gene sequence positioned 7 to 11kb upstream of *EphA4* TSS were shown to have roles in its transcriptional regulation (*Theil et al., 1998; Nakajima et al., 2006*). In parallel, the promoter analysis highlighted potential sites of interactions with other transcription factors that have not been interrogated with the used experimental design. Only few studies have investigated the transcriptional regulation of *Eph* and *Ephrin* genes. On the one hand, the transcription factors with roles in development EGR2 (Krox20), MESP2, and PAX/FOXO1a (PAX/FKHD) were shown to



bind *EphA4* promoter regions and activate transcription (*Theil et al., 1998; Begum et al., 2005; Nakajima et al., 2006*), while stimulating protein 1 (SP1) binds *EphA4* promoter to reduce mRNA and protein expression in the context of cell proliferation regulation (*Huang et al., 2016*). On the other hand, the *EfnB2* promoter was shown to be bound by Meis homeobox 1 (MEIS1), Myc-associated zinc finger protein (MAZ), and nuclear factor-Y (NF-Y), and SP1 was found to activate *EfnB2* gene expression (*Obi et al., 2009; Sohl et al., 2009, 2010*). The cooperative regulation of *Eph/Ephrin* gene expression by different transcription factors should be considered in future research, even when focusing on the circadian clock machinery.

The level of EPHA4 and EFNB2 measured in the mouse SCN and PFC did not show 24h variations under constant darkness. It is possible that measurements performed under light-dark conditions could have resulted in rhythmic levels given the presence of CREs in gene sequences upstream of TSS, and the role of CRE in the entrainment of clock gene expression to light (*Tischkau et al., 2003; Ikegami et al., 2020*). Additionally, cell type-specific rhythms could be missed in the present study sampling total proteins in the tissue. A recent study interrogating cell type-specific gene expression in a microdissection of the mouse SCN region reported a significant circadian rhythm of *EphA4* expression in astrocytes and neuronal populations outside/surrounding the SCN the SCN (*Wen et al., 2020*). Astrocytes have crucial roles in the maintenance of circadian rhythms via crosstalk with SCN neurons (*Barca-Mayo et al., 2017; Brancaccio et al., 2017*), and the Eph/Ephrin system is well recognized for its involvement in astrocyte-neuron communication (*Murai and Pasquale, 2011*). Moreover, SCN cholecystokinin/complement C1q-like 3 ( $Cck^+/C1ql3^+$ ) neurons were shown to rhythmically express *EfnB3*, and *EfnB1* and *EfnA2* were rhythmically expressed in neurons outside/surrounding the SCN (*Wen et al., 2020*), which provides further support to an implication of the Eph/Ephrin system in circadian physiology.

Our spatial transcriptomic approach did not identify *EphA4*, *EfnB2* and *EfnA3* as genes significantly changed between the early light and early dark period in areas covered by the targeted coronal slice. This finding is in line with our previous observations of rhythmic expression being significant only for *EfnA3* when considering the cerebral cortex, hippocampus and a region covering the thalamus and hypothalamus (*Freyburger et al., 2016*). Moreover, other transcriptomic studies targeting the mouse hippocampus or forebrain did not detect diurnal rhythms in the expression of *EphA4*, *EfnA3* and *EfnB2* (*Noya et al., 2019; Debski et al., 2020*), which also applies

to the post-mortem human dorsolateral PFC (*Seney et al., 2019*). This likely implies a lack of robust circadian oscillation for the expression of these genes in the multiple brain regions. Nevertheless, transcriptional regulation by clock transcription factors may drive rhythmic gene expression of these Eph/Ephrins in other brain regions or peripheral tissues, such as the cerebellum or cardiovascular tissues that show high levels of EphA4 protein and mRNA (*Martone et al., 1997; Liebl et al., 2003; Goldshmit and Bourne, 2010; Li et al., 2021*). In fact, rhythmic *EphA4* expression was reported in baboon muscle and cornea, and in human tibial artery and heart atrial tissue; and of *EfnB2* in baboon muscle and adipose tissue (*Mure et al., 2018; Ruben et al., 2018*). Tissue-specific (and cell type-specific) rhythmic expression of elements of the Eph/Ephrin system is reminiscent of reports that 6-10% of mRNA are expressed rhythmically in a given a tissue, whereas 80% are showing rhythms of expression in at least one tissue (*Panda et al., 2002; Storch et al., 2002; Maret et al., 2007; Menet et al., 2012; Zhang et al., 2014; Mure et al., 2018*). In sum, the transcriptional regulation of *EphA4* and *EfnB2* by core clock transcription factors does not appear to translate into strong gene expression rhythms for most brain regions.

In conclusion, we reported that putative promoter regions of *Epha4*, *EfnB2* and *EfnA3* can be activated by core transcription factors from the circadian system. The Eph/Ephrin system have important roles in cell-cell communication and cytoskeleton remodelling, which have implicated EphA4 (as well as EfnA3 and EfnB2) in multiple diseases/pathological conditions, including cancer, injury/stroke and Alzheimer's disease (*Goldshmit and Bourne, 2010; Chen et al., 2012; Lemmens et al., 2013; Fu et al., 2014; Huang et al., 2016; Chen et al., 2021*). Therefore, understanding the transcriptional regulation of these transmembrane molecules by the circadian clock molecular machinery should help reveal the contribution of the circadian system to cell adhesion, intracellular signalling and plasticity, and could also contribute to understand mechanisms underlying diseases.

## References

Abrahamson, E.E., Moore, R.Y. (2001). Suprachiasmatic nucleus in the mouse: retinal innervation, intrinsic organization and efferent projections. *Brain Res* 916, 172-191.

- Albergaria, A., Resende, C., Nobre, A.R., Ribeiro, A.S., Sousa, B., Machado, J.C., Seruca, R., Paredes, J., Schmitt, F. (2013). CCAAT/enhancer binding protein beta (C/EBPbeta) isoforms as transcriptional regulators of the pro-invasive CDH3/P-cadherin gene in human breast cancer cells. *PLoS One* 8, e55749.
- Allen Mouse Brain Atlas. In. [381] <http://mouse.brain-map.org/experiment/show/381>; [79591635] <http://mouse.brain-map.org/experiment/show/79591635>; [72079959] <http://mouse.brain-map.org/experiment/show/72079959>.
- Angeles-Castellanos, M., Mendoza, J., Escobar, C. (2007). Restricted feeding schedules phase shift daily rhythms of c-Fos and protein Per1 immunoreactivity in corticolimbic regions in rats. *Neuroscience* 144, 344-355.
- Audesse, A.J., Dhakal, S., Hassell, L.A., Gardell, Z., Nemtsova, Y., Webb, A.E. (2019). FOXO3 directly regulates an autophagy network to functionally regulate proteostasis in adult neural stem cells. *PLoS Genet* 15, e1008097.
- Barca-Mayo, O., Pons-Espinal, M., Follert, P., Armirotti, A., Berdondini, L., De Pietri Tonelli, D. (2017). Astrocyte deletion of Bmal1 alters daily locomotor activity and cognitive functions via GABA signalling. *Nat Commun* 8, 14336.
- Beaulieu, J.M. (2012). A role for Akt and glycogen synthase kinase-3 as integrators of dopamine and serotonin neurotransmission in mental health. *J Psychiatry Neurosci* 37, 7-16.
- Begum, S., Emami, N., Cheung, A., Wilkins, O., Der, S., Hamel, P.A. (2005). Cell-type-specific regulation of distinct sets of gene targets by Pax3 and Pax3/FKHR. *Oncogene* 24, 1860-1872.
- Bellet, M.M., Sassone-Corsi, P. (2010). Mammalian circadian clock and metabolism - the epigenetic link. *J Cell Sci* 123, 3837-3848.
- Benjamini, Y., Hochberg, Y. (1995). Controlling the false discovery rate: a practical and powerful approach to multiple testing. *Journal of the Royal statistical society: series B (Methodological)* 57, 289-300.
- Besing, R.C., Paul, J.R., Hablitz, L.M., Rogers, C.O., Johnson, R.L., Young, M.E., Gamble, K.L. (2015). Circadian rhythmicity of active GSK3 isoforms modulates molecular clock gene rhythms in the suprachiasmatic nucleus. *J Biol Rhythms* 30, 155-160.
- Beurel, E., Grieco, S.F., Jope, R.S. (2015). Glycogen synthase kinase-3 (GSK3): regulation, actions, and diseases. *Pharmacol Ther* 148, 114-131.
- Bouzioukh, F., Wilkinson, G.A., Adelmann, G., Frotscher, M., Stein, V., Klein, R. (2007). Tyrosine phosphorylation sites in ephrinB2 are required for hippocampal long-term potentiation but not long-term depression. *J Neurosci* 27, 11279-11288.
- Brancaccio, M., Patton, A.P., Chesham, J.E., Maywood, E.S., Hastings, M.H. (2017). Astrocytes Control Circadian Timekeeping in the Suprachiasmatic Nucleus via Glutamatergic Signaling. *Neuron* 93, 1420-1435 e1425.
- Buffet, C., Catelli, M.G., Hecale-Perlemonne, K., Bricaire, L., Garcia, C., Gallet-Dierick, A., Rodriguez, S., Cormier, F., Groussin, L. (2015). Dual Specificity Phosphatase 5, a Specific Negative Regulator of ERK Signaling, Is Induced by Serum Response Factor and Elk-1 Transcription Factor. *PLoS One* 10, e0145484.
- Chen, X., Zhang, L., Hua, F., Zhuang, Y., Liu, H., Wang, S. (2021). EphA4 Obstructs Spinal Cord Neuron Regeneration by Promoting Excessive Activation of Astrocytes. *Cell Mol Neurobiol*.
- Chen, Y., Fu, A.K., Ip, N.Y. (2012). Eph receptors at synapses: implications in neurodegenerative diseases. *Cell Signal* 24, 606-611.

- Chinenov, Y., Kerppola, T.K. (2001). Close encounters of many kinds: Fos-Jun interactions that mediate transcription regulatory specificity. *Oncogene* *20*, 2438-2452.
- Chiou, Y.Y., Yang, Y., Rashid, N., Ye, R., Selby, C.P., Sancar, A. (2016). Mammalian Period represses and de-represses transcription by displacing CLOCK-BMAL1 from promoters in a Cryptochrome-dependent manner. *Proc Natl Acad Sci U S A* *113*, E6072-E6079.
- Chun, L.E., Woodruff, E.R., Morton, S., Hinds, L.R., Spencer, R.L. (2015). Variations in Phase and Amplitude of Rhythmic Clock Gene Expression across Prefrontal Cortex, Hippocampus, Amygdala, and Hypothalamic Paraventricular and Suprachiasmatic Nuclei of Male and Female Rats. *J Biol Rhythms* *30*, 417-436.
- Chung, S., Lee, E.J., Yun, S., Choe, H.K., Park, S.B., Son, H.J., Kim, K.S., Dluzen, D.E., Lee, I., Hwang, O., Son, G.H., Kim, K. (2014). Impact of circadian nuclear receptor REV-ERB $\alpha$  on midbrain dopamine production and mood regulation. *Cell* *157*, 858-868.
- Coria-Lucero, C.D., Golini, R.S., Ponce, I.T., Deyurka, N., Anzulovich, A.C., Delgado, S.M., Navigatore-Fonzo, L.S. (2016). Rhythmic Bdnf and TrkB expression patterns in the prefrontal cortex are lost in aged rats. *Brain Res* *1653*, 51-58.
- Crumbley, C., Burris, T.P. (2011). Direct regulation of CLOCK expression by REV-ERB. *PLoS One* *6*, e17290.
- Dardente, H., Fortier, E.E., Martineau, V., Cermakian, N. (2007). Cryptochromes impair phosphorylation of transcriptional activators in the clock: a general mechanism for circadian repression. *Biochem J* *402*, 525-536.
- Debski, K.J., Ceglia, N., Ghestem, A., Ivanov, A.I., Brancati, G.E., Broer, S., Bot, A.M., Muller, J.A., Schoch, S., Becker, A., Loscher, W., Guye, M., Sassone-Corsi, P., Lukasiuk, K., Baldi, P., Bernard, C. (2020). The circadian dynamics of the hippocampal transcriptome and proteome is altered in experimental temporal lobe epilepsy. *Sci Adv* *6*.
- Dib, R., Gervais, N.J., Mongrain, V. (2021). A review of the current state of knowledge on sex differences in sleep and circadian phenotypes in rodents. *Neurobiol Sleep Circadian Rhythms* *11*, 100068.
- Doi, M., Shimatani, H., Atobe, Y., Murai, I., Hayashi, H., Takahashi, Y., Fustin, J.M., Yamaguchi, Y., Kiyonari, H., Koike, N., Yagita, K., Lee, C., Abe, M., Sakimura, K., Okamura, H. (2019). Non-coding cis-element of Period2 is essential for maintaining organismal circadian behaviour and body temperature rhythmicity. *Nat Commun* *10*, 2563.
- Doi, R., Oishi, K., Ishida, N. (2010). CLOCK regulates circadian rhythms of hepatic glycogen synthesis through transcriptional activation of Gys2. *J Biol Chem* *285*, 22114-22121.
- Eijkelenboom, A., Burgering, B.M. (2013). FOXOs: signalling integrators for homeostasis maintenance. *Nat Rev Mol Cell Biol* *14*, 83-97.
- El Helou, J., Belanger-Nelson, E., Freyburger, M., Dorsaz, S., Curie, T., La Spada, F., Gaudreault, P.O., Beaumont, E., Pouliot, P., Lesage, F., Frank, M.G., Franken, P., Mongrain, V. (2013). Neuroligin-1 links neuronal activity to sleep-wake regulation. *Proc Natl Acad Sci U S A* *110*, 9974-9979.
- Essmann, C.L., Martinez, E., Geiger, J.C., Zimmer, M., Traut, M.H., Stein, V., Klein, R., Acker-Palmer, A. (2008). Serine phosphorylation of ephrinB2 regulates trafficking of synaptic AMPA receptors. *Nat Neurosci* *11*, 1035-1043.

- Falvey, E., Marcacci, L., Schibler, U. (1996). DNA-binding specificity of PAR and C/EBP leucine zipper proteins: a single amino acid substitution in the C/EBP DNA-binding domain confers PAR-like specificity to C/EBP. *Biol Chem* 377, 797-809.
- Feng, W.C., Southwood, C.M., Bieker, J.J. (1994). Analyses of beta-thalassemia mutant DNA interactions with erythroid Kruppel-like factor (EKLF), an erythroid cell-specific transcription factor. *J Biol Chem* 269, 1493-1500.
- Filosa, A., Paixao, S., Honsek, S.D., Carmona, M.A., Becker, L., Feddersen, B., Gaitanos, L., Rudhard, Y., Schoepfer, R., Klopstock, T., Kullander, K., Rose, C.R., Pasquale, E.B., Klein, R. (2009). Neuron-glia communication via EphA4/ephrin-A3 modulates LTP through glial glutamate transport. *Nat Neurosci* 12, 1285-1292.
- Freyburger, M., Pierre, A., Paquette, G., Belanger-Nelson, E., Bedont, J., Gaudreault, P.O., Drolet, G., Laforest, S., Blackshaw, S., Cermakian, N., Doucet, G., Mongrain, V. (2016). EphA4 is Involved in Sleep Regulation but Not in the Electrophysiological Response to Sleep Deprivation. *Sleep* 39, 613-624.
- Fu, A.K.Y., Hung, K.W., Huang, H., Gu, S., Shen, Y., Cheng, E.Y., Ip, F.C., Huang, X., Fu, W.Y., Ip, N.Y. (2014). Blockade of EphA4 signaling ameliorates hippocampal synaptic dysfunctions in mouse models of Alzheimer's disease. *Proc Natl Acad Sci U S A* 111, 9959-9964.
- Gekakis, N., Staknis, D., Nguyen, H.B., Davis, F.C., Wilsbacher, L.D., King, D.P., Takahashi, J.S., Weitz, C.J. (1998). Role of the CLOCK protein in the mammalian circadian mechanism. *Science* 280, 1564-1569.
- Ghori, A., Freimann, F.B., Nieminen-Kelha, M., Kremenetskaia, I., Gertz, K., Endres, M., Vajkoczy, P. (2017). EphrinB2 Activation Enhances Vascular Repair Mechanisms and Reduces Brain Swelling After Mild Cerebral Ischemia. *Arterioscler Thromb Vasc Biol* 37, 867-878.
- Giguere, V., Tini, M., Flock, G., Ong, E., Evans, R.M., Otulakowski, G. (1994). Isoform-specific amino-terminal domains dictate DNA-binding properties of ROR alpha, a novel family of orphan hormone nuclear receptors. *Genes Dev* 8, 538-553.
- Giroldi, L.A., Bringuier, P.P., de Weijert, M., Jansen, C., van Bokhoven, A., Schalken, J.A. (1997). Role of E boxes in the repression of E-cadherin expression. *Biochem Biophys Res Commun* 241, 453-458.
- Goldshmit, Y., Bourne, J. (2010). Upregulation of EphA4 on astrocytes potentially mediates astrocytic gliosis after cortical lesion in the marmoset monkey. *J Neurotrauma* 27, 1321-1332.
- Goldshmit, Y., Galea, M.P., Bartlett, P.F., Turnley, A.M. (2006). EphA4 regulates central nervous system vascular formation. *J Comp Neurol* 497, 864-875.
- Guillaumond, F., Dardente, H., Giguere, V., Cermakian, N. (2005). Differential control of Bmal1 circadian transcription by REV-ERB and ROR nuclear receptors. *J Biol Rhythms* 20, 391-403.
- Gustems, M., Woellmer, A., Rothbauer, U., Eck, S.H., Wieland, T., Lutter, D., Hammerschmidt, W. (2014). c-Jun/c-Fos heterodimers regulate cellular genes via a newly identified class of methylated DNA sequence motifs. *Nucleic Acids Res* 42, 3059-3072.
- Hale, A.E., Collins-McMillen, D., Lenarcic, E.M., Igarashi, S., Kamil, J.P., Goodrum, F., Moorman, N.J. (2020). FOXO transcription factors activate alternative major immediate early promoters to induce human cytomegalovirus reactivation. *Proc Natl Acad Sci U S A* 117, 18764-18770.

- Hampff, G., Ripperger, J.A., Houben, T., Schmutz, I., Blex, C., Perreau-Lenz, S., Brunk, I., Spanagel, R., Ahnert-Hilger, G., Meijer, J.H., Albrecht, U. (2008). Regulation of monoamine oxidase A by circadian-clock components implies clock influence on mood. *Curr Biol* 18, 678-683.
- Hamza, M.S., Pott, S., Vega, V.B., Thomsen, J.S., Kandhadayar, G.S., Ng, P.W., Chiu, K.P., Pettersson, S., Wei, C.L., Ruan, Y., Liu, E.T. (2009). De-novo identification of PPARgamma/RXR binding sites and direct targets during adipogenesis. *PLoS One* 4, e4907.
- Hannou, L., Roy, P.G., Ballester Roig, M.N., Mongrain, V. (2020). Transcriptional control of synaptic components by the clock machinery. *Eur J Neurosci* 51, 241-267.
- Hannou, L., Belanger-Nelson, E., O'Callaghan, E.K., Dufort-Gervais, J., Ballester Roig, M.N., Roy, P.G., Beaulieu, J.M., Cermakian, N., Mongrain, V. (2018). Regulation of the Neuroigin-1 Gene by Clock Transcription Factors. *J Biol Rhythms* 33, 166-178.
- Harada, Y., Sakai, M., Kurabayashi, N., Hirota, T., Fukada, Y. (2005). Ser-557-phosphorylated mCRY2 is degraded upon synergistic phosphorylation by glycogen synthase kinase-3 beta. *J Biol Chem* 280, 31714-31721.
- Harding, H.P., Lazar, M.A. (1993). The orphan receptor Rev-ErbA alpha activates transcription via a novel response element. *Mol Cell Biol* 13, 3113-3121.
- Hartzog, G.A., Myers, R.M. (1993). Discrimination among potential activators of the beta-globin CACCC element by correlation of binding and transcriptional properties. *Mol Cell Biol* 13, 44-56.
- Hastings, M.H., Maywood, E.S., Brancaccio, M. (2018). Generation of circadian rhythms in the suprachiasmatic nucleus. *Nat Rev Neurosci* 19, 453-469.
- Hirano, A., Fu, Y.H., Ptacek, L.J. (2016). The intricate dance of post-translational modifications in the rhythm of life. *Nat Struct Mol Biol* 23, 1053-1060.
- Hu, Y., Li, S., Jiang, H., Li, M.T., Zhou, J.W. (2014). Ephrin-B2/EphA4 forward signaling is required for regulation of radial migration of cortical neurons in the mouse. *Neurosci Bull* 30, 425-432.
- Huang, Y.C., Lin, S.J., Lin, K.M., Chou, Y.C., Lin, C.W., Yu, S.C., Chen, C.L., Shen, T.L., Chen, C.K., Lu, J., Chen, M.R., Tsai, C.H. (2016). Regulation of EBV LMP1-triggered EphA4 downregulation in EBV-associated B lymphoma and its impact on patients' survival. *Blood* 128, 1578-1589.
- Ikeda, M., Ikeda, M. (2014). Bmal1 is an essential regulator for circadian cytosolic Ca(2)(+) rhythms in suprachiasmatic nucleus neurons. *J Neurosci* 34, 12029-12038.
- Ikegami, K., Nakajima, M., Minami, Y., Nagano, M., Masubuchi, S., Shigeyoshi, Y. (2020). cAMP response element induces Per1 in vivo. *Biochem Biophys Res Commun* 531, 515-521.
- Inoki, K., Ouyang, H., Zhu, T., Lindvall, C., Wang, Y., Zhang, X., Yang, Q., Bennett, C., Harada, Y., Stankunas, K., Wang, C.Y., He, X., MacDougald, O.A., You, M., Williams, B.O., Guan, K.L. (2006). TSC2 integrates Wnt and energy signals via a coordinated phosphorylation by AMPK and GSK3 to regulate cell growth. *Cell* 126, 955-968.
- Kiessling, S., O'Callaghan, E.K., Freyburger, M., Cermakian, N., Mongrain, V. (2018). The cell adhesion molecule EphA4 is involved in circadian clock functions. *Genes Brain Behav* 17, 82-92.

- Kiyohara, Y.B., Nishii, K., Ukai-Tadenuma, M., Ueda, H.R., Uchiyama, Y., Yagita, K. (2008). Detection of a circadian enhancer in the mDbp promoter using prokaryotic transposon vector-based strategy. *Nucleic Acids Res* 36, e23.
- Klemz, R., Reischl, S., Wallach, T., Witte, N., Jurchott, K., Klemz, S., Lang, V., Lorenzen, S., Knauer, M., Heidenreich, S., Xu, M., Ripperger, J.A., Schupp, M., Stanewsky, R., Kramer, A. (2017). Reciprocal regulation of carbon monoxide metabolism and the circadian clock. *Nat Struct Mol Biol* 24, 15-22.
- Krug, R.G., 2nd, Poshusta, T.L., Skuster, K.J., Berg, M.R., Gardner, S.L., Clark, K.J. (2014). A transgenic zebrafish model for monitoring glucocorticoid receptor activity. *Genes Brain Behav* 13, 478-487.
- Kuljis, D.A., Gad, L., Loh, D.H., MacDowell Kaswan, Z., Hitchcock, O.N., Ghiani, C.A., Colwell, C.S. (2016). Sex Differences in Circadian Dysfunction in the BACHD Mouse Model of Huntington's Disease. *PLoS One* 11, e0147583.
- Kuljis, D.A., Loh, D.H., Truong, D., Vosko, A.M., Ong, M.L., McClusky, R., Arnold, A.P., Colwell, C.S. (2013). Gonadal- and sex-chromosome-dependent sex differences in the circadian system. *Endocrinology* 154, 1501-1512.
- Kume, K., Zylka, M.J., Sriram, S., Shearman, L.P., Weaver, D.R., Jin, X., Maywood, E.S., Hastings, M.H., Reppert, S.M. (1999). mCRY1 and mCRY2 are essential components of the negative limb of the circadian clock feedback loop. *Cell* 98, 193-205.
- Lavoie, J., Hebert, M., Beaulieu, J.M. (2013). Glycogen synthase kinase-3beta haploinsufficiency lengthens the circadian locomotor activity period in mice. *Behav Brain Res* 253, 262-265.
- Leclerc, G.M., Boockfor, F.R. (2005). Pulses of prolactin promoter activity depend on a noncanonical E-box that can bind the circadian proteins CLOCK and BMAL1. *Endocrinology* 146, 2782-2790.
- Lemmens, R., Jaspers, T., Robberecht, W., Thijs, V.N. (2013). Modifying expression of EphA4 and its downstream targets improves functional recovery after stroke. *Hum Mol Genet* 22, 2214-2220.
- Leonard, J., Parrott, C., Buckler-White, A.J., Turner, W., Ross, E.K., Martin, M.A., Rabson, A.B. (1989). The NF-kappa B binding sites in the human immunodeficiency virus type 1 long terminal repeat are not required for virus infectivity. *J Virol* 63, 4919-4924.
- Li, J., Dong, W., Gao, X., Chen, W., Sun, C., Li, J., Gao, S., Zhang, Y., He, J., Lu, D., Jiang, R., Ma, M., Wang, X., Zhang, L. (2021). EphA4 is highly expressed in the atria of heart and its deletion leads to atrial hypertrophy and electrocardiographic abnormalities in rats. *Life Sci* 278, 119595.
- Li, S., Qin, X., Chai, S., Qu, C., Wang, X., Zhang, H. (2016). Modulation of E-cadherin expression promotes migration ability of esophageal cancer cells. *Sci Rep* 6, 21713.
- Liebl, D.J., Morris, C.J., Henkemeyer, M., Parada, L.F. (2003). mRNA expression of ephrins and Eph receptor tyrosine kinases in the neonatal and adult mouse central nervous system. *J Neurosci Res* 71, 7-22.
- Liu, A.C., Tran, H.G., Zhang, E.E., Priest, A.A., Welsh, D.K., Kay, S.A. (2008). Redundant function of REV-ERBalpha and beta and non-essential role for Bmal1 cycling in transcriptional regulation of intracellular circadian rhythms. *PLoS Genet* 4, e1000023.
- Liu, X., Klein, P.S. (2018). Glycogen synthase kinase-3 and alternative splicing. *Wiley Interdiscip Rev RNA* 9, e1501.

- Maemura, K., de la Monte, S.M., Chin, M.T., Layne, M.D., Hsieh, C.M., Yet, S.F., Perrella, M.A., Lee, M.E. (2000). CLIF, a novel cycle-like factor, regulates the circadian oscillation of plasminogen activator inhibitor-1 gene expression. *J Biol Chem* 275, 36847-36851.
- Maret, S., Dorsaz, S., Gurcel, L., Pradervand, S., Petit, B., Pfister, C., Hagenbuchle, O., O'Hara, B.F., Franken, P., Tafti, M. (2007). Homer1a is a core brain molecular correlate of sleep loss. *Proc Natl Acad Sci U S A* 104, 20090-20095.
- Martone, M.E., Holash, J.A., Bayardo, A., Pasquale, E.B., Ellisman, M.H. (1997). Immunolocalization of the receptor tyrosine kinase EphA4 in the adult rat central nervous system. *Brain Res* 771, 238-250.
- Matsumura, R., Akashi, M. (2017). Multiple circadian transcriptional elements cooperatively regulate cell-autonomous transcriptional oscillation of Period3, a mammalian clock gene. *J Biol Chem* 292, 16081-16092.
- Matsuoka, H., Tokunaga, R., Katayama, M., Hosoda, Y., Miya, K., Sumi, K., Ohishi, A., Kamishikiryo, J., Shima, A., Michihara, A. (2020). Retinoic acid receptor-related orphan receptor alpha reduces lipid droplets by upregulating neutral cholesterol ester hydrolase 1 in macrophages. *BMC Mol Cell Biol* 21, 32.
- Meighan, C.M., Kann, A.P., Egress, E.R. (2015). Transcription factor hlh-2/E/Daughterless drives expression of alpha integrin ina-1 during DTC migration in *C. elegans*. *Gene* 568, 220-226.
- Mendes, K., Schmidhofer, S., Minderjahn, J., Glatz, D., Kiesewetter, C., Raithel, J., Wimmer, J., Gebhard, C., Rehli, M. (2021). The epigenetic pioneer EGR2 initiates DNA demethylation in differentiating monocytes at both stable and transient binding sites. *Nat Commun* 12, 1556.
- Menet, J.S., Rodriguez, J., Abruzzi, K.C., Rosbash, M. (2012). Nascent-Seq reveals novel features of mouse circadian transcriptional regulation. *Elife* 1, e00011.
- Mongrain, V., Ruan, X., Dardente, H., Fortier, E.E., Cermakian, N. (2008). Clock-dependent and independent transcriptional control of the two isoforms from the mouse Rorgamma gene. *Genes Cells* 13, 1197-1210.
- Montminy, M.R., Sevarino, K.A., Wagner, J.A., Mandel, G., Goodman, R.H. (1986). Identification of a cyclic-AMP-responsive element within the rat somatostatin gene. *Proc Natl Acad Sci U S A* 83, 6682-6686.
- Mulero, M.C., Wang, V.Y., Huxford, T., Ghosh, G. (2019). Genome reading by the NF-kappaB transcription factors. *Nucleic Acids Res* 47, 9967-9989.
- Murai, K.K., Pasquale, E.B. (2011). Eph receptors and ephrins in neuron-astrocyte communication at synapses. *Glia* 59, 1567-1578.
- Murai, K.K., Nguyen, L.N., Irie, F., Yamaguchi, Y., Pasquale, E.B. (2003). Control of hippocampal dendritic spine morphology through ephrin-A3/EphA4 signaling. *Nat Neurosci* 6, 153-160.
- Mure, L.S., Le, H.D., Benegiamo, G., Chang, M.W., Rios, L., Jillani, N., Ngotho, M., Kariuki, T., Dkhissi-Benyahya, O., Cooper, H.M., Panda, S. (2018). Diurnal transcriptome atlas of a primate across major neural and peripheral tissues. *Science* 359.
- Nakahata, Y., Yoshida, M., Takano, A., Soma, H., Yamamoto, T., Yasuda, A., Nakatsu, T., Takumi, T. (2008). A direct repeat of E-box-like elements is required for cell-autonomous circadian rhythm of clock genes. *BMC Mol Biol* 9, 1.
- Nakajima, Y., Morimoto, M., Takahashi, Y., Koseki, H., Saga, Y. (2006). Identification of EphA4 enhancer required for segmental expression and the regulation by Mesp2. *Development* 133, 2517-2525.



- Noya, S.B., Colameo, D., Bruning, F., Spinnler, A., Mircsof, D., Opitz, L., Mann, M., Tyagarajan, S.K., Robles, M.S., Brown, S.A. (2019). The forebrain synaptic transcriptome is organized by clocks but its proteome is driven by sleep. *Science* 366.
- Obi, S., Yamamoto, K., Shimizu, N., Kumagaya, S., Masumura, T., Sokabe, T., Asahara, T., Ando, J. (2009). Fluid shear stress induces arterial differentiation of endothelial progenitor cells. *J Appl Physiol* (1985) 106, 203-211.
- Oishi, K., Shirai, H., Ishida, N. (2005). CLOCK is involved in the circadian transactivation of peroxisome-proliferator-activated receptor alpha (PPARalpha) in mice. *Biochem J* 386, 575-581.
- Onoue, T., Nishi, G., Hikima, J.I., Sakai, M., Kono, T. (2019). Circadian oscillation of TNF-alpha gene expression regulated by clock gene, BMAL1 and CLOCK1, in the Japanese medaka (*Oryzias latipes*). *Int Immunopharmacol* 70, 362-371.
- Pan, X., Zhang, Y., Wang, L., Hussain, M.M. (2010). Diurnal regulation of MTP and plasma triglyceride by CLOCK is mediated by SHP. *Cell Metab* 12, 174-186.
- Panda, S., Antoch, M.P., Miller, B.H., Su, A.I., Schook, A.B., Straume, M., Schultz, P.G., Kay, S.A., Takahashi, J.S., Hogenesch, J.B. (2002). Coordinated transcription of key pathways in the mouse by the circadian clock. *Cell* 109, 307-320.
- Patel, P., Woodgett, J.R. (2017). Glycogen Synthase Kinase 3: A Kinase for All Pathways? *Curr Top Dev Biol* 123, 277-302.
- Pham, T.H., Benner, C., Lichtinger, M., Schwarzfischer, L., Hu, Y., Andreesen, R., Chen, W., Rehli, M. (2012). Dynamic epigenetic enhancer signatures reveal key transcription factors associated with monocytic differentiation states. *Blood* 119, e161-171.
- Preitner, N., Damiola, F., Lopez-Molina, L., Zakany, J., Duboule, D., Albrecht, U., Schibler, U. (2002). The orphan nuclear receptor REV-ERBalpha controls circadian transcription within the positive limb of the mammalian circadian oscillator. *Cell* 110, 251-260.
- Reick, M., Garcia, J.A., Dudley, C., McKnight, S.L. (2001). NPAS2: an analog of clock operative in the mammalian forebrain. *Science* 293, 506-509.
- Rey, G., Cesbron, F., Rougemont, J., Reinke, H., Brunner, M., Naef, F. (2011). Genome-wide and phase-specific DNA-binding rhythms of BMAL1 control circadian output functions in mouse liver. *PLoS Biol* 9, e1000595.
- Robert, N.M., Martin, L.J., Tremblay, J.J. (2006). The orphan nuclear receptor NR4A1 regulates insulin-like 3 gene transcription in Leydig cells. *Biol Reprod* 74, 322-330.
- Ruben, M.D., Wu G., Smith D.F., Schmidt R.E., Francey L.J., Lee Y.Y., Anafi R.C., Hogenesch J.B. (2018). A database of tissue-specific rhythmically expressed human genes has potential applications in circadian medicine. *Sci Transl Med* 10, 458.
- Rushmore, T.H., Morton, M.R., Pickett, C.B. (1991). The antioxidant responsive element. Activation by oxidative stress and identification of the DNA consensus sequence required for functional activity. *J Biol Chem* 266, 11632-11639.
- Sablon, A., Bollaert, E., Pirson, C., Velghe, A.I., Demoulin, J.B. (2022). FOXO1 forkhead domain mutants in B-cell lymphoma lack transcriptional activity. *Sci Rep* 12, 1309.

- Sahar, S., Zocchi, L., Kinoshita, C., Borrelli, E., Sassone-Corsi, P. (2010). Regulation of BMAL1 protein stability and circadian function by GSK3beta-mediated phosphorylation. *PLoS One* 5, e8561.
- Schneider, C.A., Rasband, W.S., Eliceiri, K.W. (2012). NIH Image to ImageJ: 25 years of image analysis. *Nat Methods* 9, 671-675.
- Seney, M.L., Cahill, K., Enwright, J.F., 3rd, Logan, R.W., Huo, Z., Zong, W., Tseng, G., McClung, C.A. (2019). Diurnal rhythms in gene expression in the prefrontal cortex in schizophrenia. *Nat Commun* 10, 3355.
- Slack, S., Battaglia, A., Cibert-Goton, V., Gavazzi, I. (2008). EphrinB2 induces tyrosine phosphorylation of NR2B via Src-family kinases during inflammatory hyperalgesia. *Neuroscience* 156, 175-183.
- Sohl, M., Lanner, F., Farnebo, F. (2009). Characterization of the murine Ephrin-B2 promoter. *Gene* 437, 54-59.
- Sohl, M., Lanner, F., Farnebo, F. (2010). Sp1 mediate hypoxia induced ephrinB2 expression via a hypoxia-inducible factor independent mechanism. *Biochem Biophys Res Commun* 391, 24-27.
- Stambolic, V., Woodgett, J.R. (1994). Mitogen inactivation of glycogen synthase kinase-3 beta in intact cells via serine 9 phosphorylation. *Biochem J* 303 ( Pt 3), 701-704.
- Steinecke, A., Gampe, C., Zimmer, G., Rudolph, J., Bolz, J. (2014). EphA/ephrin A reverse signaling promotes the migration of cortical interneurons from the medial ganglionic eminence. *Development* 141, 460-471.
- Storch, K.F., Lipan, O., Leykin, I., Viswanathan, N., Davis, F.C., Wong, W.H., Weitz, C.J. (2002). Extensive and divergent circadian gene expression in liver and heart. *Nature* 417, 78-83.
- Sun, Z., Xu, X., He, J., Murray, A., Sun, M.A., Wei, X., Wang, X., McCoig, E., Xie, E., Jiang, X., Li, L., Zhu, J., Chen, J., Morozov, A., Pickrell, A.M., Theus, M.H., Xie, H. (2019). EGR1 recruits TET1 to shape the brain methylome during development and upon neuronal activity. *Nat Commun* 10, 3892.
- Swirnoff, A.H., Milbrandt, J. (1995). DNA-binding specificity of NGFI-A and related zinc finger transcription factors. *Mol Cell Biol* 15, 2275-2287.
- Takahashi, J.S. (2017). Transcriptional architecture of the mammalian circadian clock. *Nat Rev Genet* 18, 164-179.
- Tamayo, A.G., Duong, H.A., Robles, M.S., Mann, M., Weitz, C.J. (2015). Histone monoubiquitination by Clock-Bmal1 complex marks Per1 and Per2 genes for circadian feedback. *Nat Struct Mol Biol* 22, 759-766.
- Tanasic, S., Mattusch, C., Wagner, E.M., Eder, M., Rupprecht, R., Rammes, G., Di Benedetto, B. (2016). Desipramine targets astrocytes to attenuate synaptic plasticity via modulation of the ephrinA3/EphA4 signalling. *Neuropharmacology* 105, 154-163.
- Taylor, M., Treisman, R., Garrett, N., Mohun, T. (1989). Muscle-specific (CArG) and serum-responsive (SRE) promoter elements are functionally interchangeable in *Xenopus* embryos and mouse fibroblasts. *Development* 106, 67-78.
- Theil, T., Frain, M., Gilardi-Hebenstreit, P., Flenniken, A., Charnay, P., Wilkinson, D.G. (1998). Segmental expression of the EphA4 (Sek-1) receptor tyrosine kinase in the hindbrain is under direct transcriptional control of Krox-20. *Development* 125, 443-452.
- Tischkau, S.A., Mitchell, J.W., Tyan, S.H., Buchanan, G.F., Gillette, M.U. (2003). Ca<sup>2+</sup>/cAMP response element-binding protein (CREB)-dependent activation of Per1 is required for light-induced signaling in the suprachiasmatic nucleus circadian clock. *J Biol Chem* 278, 718-723.

- Travnickova-Bendova, Z., Cermakian, N., Reppert, S.M., Sassone-Corsi, P. (2002). Bimodal regulation of mPeriod promoters by CREB-dependent signaling and CLOCK/BMAL1 activity. *Proc Natl Acad Sci U S A* *99*, 7728-7733.
- Ueda, H.R., Hayashi, S., Chen, W., Sano, M., Machida, M., Shigeyoshi, Y., Iino, M., Hashimoto, S. (2005). System-level identification of transcriptional circuits underlying mammalian circadian clocks. *Nat Genet* *37*, 187-192.
- Wang, D., Chang, P.S., Wang, Z., Sutherland, L., Richardson, J.A., Small, E., Krieg, P.A., Olson, E.N. (2001). Activation of cardiac gene expression by myocardin, a transcriptional cofactor for serum response factor. *Cell* *105*, 851-862.
- Wang, X., Campbell, M.R., Lacher, S.E., Cho, H.Y., Wan, M., Crowl, C.L., Chorley, B.N., Bond, G.L., Kleeberger, S.R., Slattery, M., Bell, D.A. (2016). A Polymorphic Antioxidant Response Element Links NRF2/sMAF Binding to Enhanced MAPT Expression and Reduced Risk of Parkinsonian Disorders. *Cell Rep* *15*, 830-842.
- Wasserman, W.W., Fahl, W.E. (1997). Functional antioxidant responsive elements. *Proc Natl Acad Sci U S A* *94*, 5361-5366.
- Wayne Davis, M. ApE - A plasmid Editor. In. <https://jorgensen.biology.utah.edu/wayned/apE/>.
- Wen, S., Ma, D., Zhao, M., Xie, L., Wu, Q., Gou, L., Zhu, C., Fan, Y., Wang, H., Yan, J. (2020). Spatiotemporal single-cell analysis of gene expression in the mouse suprachiasmatic nucleus. *Nat Neurosci* *23*, 456-467.
- Wilson, T.E., Fahrner, T.J., Johnston, M., Milbrandt, J. (1991). Identification of the DNA binding site for NGFI-B by genetic selection in yeast. *Science* *252*, 1296-1300.
- Xing, S., Pan, N., Xu, W., Zhang, J., Li, J., Dang, C., Liu, G., Pei, Z., Zeng, J. (2019). EphrinB2 activation enhances angiogenesis, reduces amyloid-beta deposits and secondary damage in thalamus at the early stage after cortical infarction in hypertensive rats. *J Cereb Blood Flow Metab* *39*, 1776-1789.
- Yamamoto, K.K., Gonzalez, G.A., Biggs, W.H., 3rd, Montminy, M.R. (1988). Phosphorylation-induced binding and transcriptional efficacy of nuclear factor CREB. *Nature* *334*, 494-498.
- Yamazaki, S., Numano, R., Abe, M., Hida, A., Takahashi, R., Ueda, M., Block, G.D., Sakaki, Y., Menaker, M., Tei, H. (2000). Resetting central and peripheral circadian oscillators in transgenic rats. *Science* *288*, 682-685.
- Yin, L., Wang, J., Klein, P.S., Lazar, M.A. (2006). Nuclear receptor Rev-erbalpha is a critical lithium-sensitive component of the circadian clock. *Science* *311*, 1002-1005.
- Yoo, S.H., Ko, C.H., Lowrey, P.L., Buhr, E.D., Song, E.J., Chang, S., Yoo, O.J., Yamazaki, S., Lee, C., Takahashi, J.S. (2005). A noncanonical E-box enhancer drives mouse Period2 circadian oscillations in vivo. *Proc Natl Acad Sci U S A* *102*, 2608-2613.
- Zhang, R., Lahens, N.F., Ballance, H.I., Hughes, M.E., Hogenesch, J.B. (2014). A circadian gene expression atlas in mammals: implications for biology and medicine. *Proc Natl Acad Sci U S A* *111*, 16219-16224.
- Zhao, J., Boyd, A.W., Bartlett, P.F. (2017). The identification of a novel isoform of EphA4 and ITS expression in SOD1(G93A) mice. *Neuroscience* *347*, 11-21.
- Zhu, R.L., Fang, Y., Yu, H.H., Chen, D.F., Yang, L., Cho, K.S. (2021). Absence of ephrin-A2/A3 increases retinal regenerative potential for Muller cells in Rhodopsin knockout mice. *Neural Regen Res* *16*, 1317-1322.

# Chapter 5

Probing pathways by which Rhynchophylline modifies sleep  
using spatial transcriptomics

---

# Probing pathways by which Rhynchophylline modifies sleep using spatial transcriptomics

**Maria Neus Ballester Roig,<sup>1,2</sup> Tanya Leduc,<sup>1,2</sup> Julien Dufort-Gervais,<sup>1</sup> Yousra Maghmoul,<sup>2,3</sup> Olivier Tastet,<sup>4</sup> Valérie Mongrain,<sup>1,2,\*</sup>**

<sup>1</sup>Department of Neuroscience, Université de Montréal, Montréal, QC, H3T 1J4, Canada;

<sup>2</sup>Center for Advanced Research in Sleep Medicine, Recherche CIUSSS-NIM, Montréal, QC, H4J 1C5, Canada;

<sup>3</sup>Department of Medicine, Université de Montréal, Montréal, QC, H3T 1J4, Canada;

<sup>4</sup>Neuroimmunology Research Laboratory, Centre de Recherche du Centre Hospitalier de l'Université de Montréal, Montreal, QC, H2X 0A9, Canada.

\*Corresponding author

Valérie Mongrain, Ph.D.

Recherche CIUSSS-NIM

(site Hôpital du Sacré-Coeur de Montréal)

5400 Gouin West blvd.

Montreal, QC, H4J 1C5

Canada

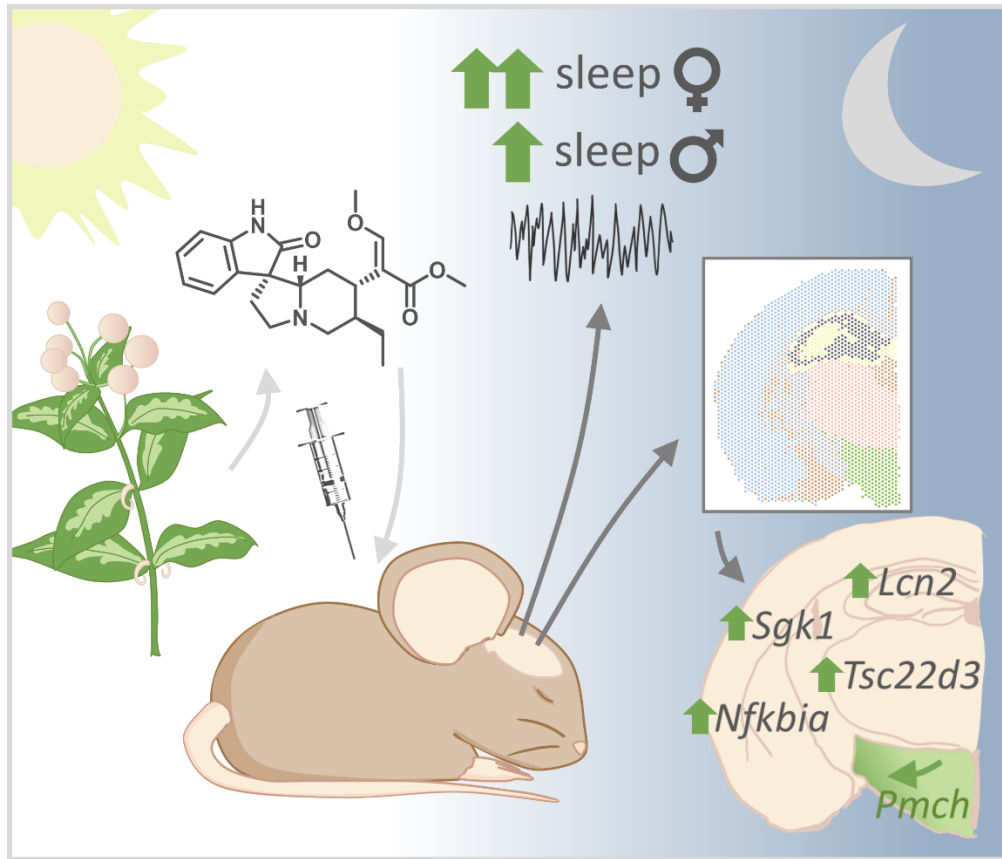
valerie.mongrain@umontreal.ca

1-514-338-2222/3323

Manuscript to submitted to: Current Biology

Content: 6842 words (excluding Summary, Methods and List of References), 6 figures, 10 supplemental figures, 4 supplemental tables

## Graphical abstract



### Highlights

- The alkaloid RHY (component of *Uncaria* plants) induces slow wave sleep in mice
- RHY's effects on paradoxical sleep differ in morning or evening injections
- RHY alter brain oscillations linked to cognitive processes during sleep and wake
- RHY affects some transcripts brain-wide and sleep-related mRNAs in the hypothalamus

### eTOC blurb

Research shows that the plant derivative RHY induces sleep and modifies brain oscillations in a vigilance state-dependent manner. Results highlight the importance of the time-of-injection and that treatments can have distinct impact in females vs males. The brain spatial transcriptome suggests that RHY impacts immune/apoptotic responses brain-wide but sleep-related transcript in the hypothalamus.

## Summary

Rhynchophylline (RHY) is an alkaloid component of *Uncaria*, which are plants extensively used in traditional Asian medicines. *Uncaria* treatments increase sleep time and quality in humans, and RHY induces sleep in rodents. However, like many traditional natural treatments, the mechanisms of action of RHY and *Uncaria* remain evasive. Moreover, it is unknown whether RHY modifies key brain oscillations during sleep. We thus aimed at defining the effects of RHY on sleep architecture and oscillations throughout a 24-h cycle, as well as identifying the underlying molecular mechanisms. Mice received systemic RHY injections at two times of the day (beginning and end of the light period), and vigilance states were studied by electrocorticographic recordings. RHY enhanced slow wave sleep (SWS) after both injections, suppressed paradoxical sleep (PS) in the light but enhanced PS in the dark period. Furthermore, RHY modified brain oscillations during both wakefulness and SWS (including delta activity dynamics) in a time-dependent manner. Interestingly, most effects were larger in females. A brain spatial transcriptomic analysis showed that RHY modifies the expression of genes linked to cell movement, apoptosis/necrosis, and transcription/translation in a brain region-independent manner, and changes those linked to sleep regulation (e.g., *Hcrt*, *Pmch*) in a brain region-specific manner (e.g., in the hypothalamus). The findings provide support to the sleep-inducing effect of RHY, expose the relevance to shape wake/sleep oscillations, and highlight its effects on the transcriptome with a high spatial resolution. The exposed molecular mechanisms underlying the effect of a natural compound should benefit sleep- and brain-related medicine.

## Introduction

Traditional Asian medicines have been used for centuries/millennia to alleviate disease symptoms and ameliorate essential behaviors and states such as sleep (*Yu et al., 2006*). Their natural origin is appealing for the general population, but the absence of solid empirical evidence and mechanisms of action has prevented their widespread use in the medical context (*Park et al., 2012*). *Uncaria* plants, in particular, were shown to have anticonvulsant, sedative and hypnotic effects, including positive impacts on sleep amount and quality in humans and mice (*Aizawa et al., 2002; Jeenapongsa and Tohda, 2003; Shinno et al., 2008b; Ozone et al., 2012*). Rhynchophylline (RHY) is an alkaloid component of *Uncaria* plants, and studies in rodents tend to support its hypnotic properties. For instance, RHY reduces locomotor activity, and was shown to increase sleep time when co-administered with pentobarbital in mice (*Shi et al., 1993; Yoo et al., 2016*). Determining how RHY precisely affect wake/sleep states and their characteristic brain oscillations, as well as identifying the underlying mechanisms of action has definite value to support the use of *Uncaria* plants or RHY for sleep disturbances or other brain ailments.

Some studies have reported that RHY impacts neuronal firing in the rodent hippocampus and cerebral cortex (*Kang et al., 2004; Hsieh et al., 2009; Fu et al., 2014; Shao et al., 2015; Shao et al., 2016*), which suggests an effect on synchronized neuronal activity of the cerebral cortex occurring during wakefulness and sleep. Neuronal synchronization is generally reflected in the activity measured in slower frequencies of the electrocorticogram (ECoG); slow wave activity (SWA; 0.5-4.5Hz) predominates during slow wave sleep (SWS), and theta activity (4-9 Hz) during paradoxical sleep (PS) (*Amzica and Steriade, 1998; Timofeev et al., 2012; Peever and Fuller, 2017; Hubbard et al., 2020*). Oscillatory activities not only represent defining features of wakefulness and sleep but also underly the role of sleep in brain function given, for instance, the established contributions of SWS SWA and PS theta activity to memory consolidation (*Poe et al., 2000; Boyce et al., 2016; Gulati et al., 2017*). Accordingly, it is crucial to determine the impact of sleep-inducing drugs on key oscillatory activities during sleep, and no such research exists for RHY.

RHY was shown to alter the cerebral cortex transcriptome in the APP/PS1 mouse model of Alzheimer's disease, targeting molecular pathways related to the ubiquitin system, microglial function, and angiogenesis (*Fu et al., 2021*). The effect of RHY on the genome-wide gene expression landscape of different brain regions in normal/healthy organisms remains to be established to adequately define the underlying mechanisms of its effect on the brain.



Transcriptomic studies have proven particularly useful in the context of sleep research revealing gene expression signatures of wakefulness and sleep with, for instance, the mRNA level of genes linked to protein translation being increased by sleep, whereas that of immediate early genes associated to neurotransmission (e.g., *Fos*, *Arc*, *Homer1a*, *Egr1*), and of genes involved in stress responses (e.g., chaperones, heat shock proteins) being increased by sleep deprivation/extended wakefulness (Cirelli and Tononi, 2000; Cirelli et al., 2004; Mackiewicz et al., 2007; Maret et al., 2007; Mongrain et al., 2010; Vecsey et al., 2012; Bellesi et al., 2013; Noya et al., 2019; Guo et al., 2020). Moreover, the wake/sleep-dependent gene expression signature depends on the brain region (Terao et al., 2003; Conti et al., 2007; Guo et al., 2020; Jha et al., 2022). Understanding effects of sleep-inducing compounds on the transcriptomic profile of brain regions controlling wake/sleep alternations and characteristic oscillations, such as the lateral hypothalamus (*LH*; Adamantidis et al., 2007; Jones, 2020; Li et al., 2022), is required to understand the suitability of these compounds for sleep medicine.

We have here investigated how RHY modifies wake/sleep amount, alternation and ECoG oscillations, and interrogated underlying molecular mechanisms using a high spatial resolution transcriptomic approach. We uncovered that RHY increases the time spent in SWS at the expense of wakefulness, and changes the dynamics of key brain oscillations during SWS and wakefulness. The spatial transcriptome revealed that RHY alters the expression of genes related to inflammation, apoptosis and the response to glucocorticoids; with some transcripts modified throughout the brain, and others for which changes were restricted to specific brain regions (e.g., genes linked to sleep regulation in the hypothalamus). This study demonstrates the relevance of traditional medicine for sleep disturbances, and of spatial transcriptomics to identify brain region-specific and sleep-relevant mechanisms.

## Results

### RHY increases SWS and state fragmentation

Mice were submitted to ECoG recording before and after RHY treatment to investigate effects on vigilance states. Two doses of RHY were studied, 50 mg/kg (RHY50) and 100 mg/kg (RHY100), and compared to vehicle administration. Similar doses were previously reported to impact behavior, synaptic plasticity, and brain protein levels in mice (*Fu et al., 2014; Lee et al., 2014*). Given the short (3-4 h) half-life/availability of RHY reported for the mouse and rat brain tissue (*Wang et al., 2010; Lee et al., 2014; Fu et al., 2021*), animals received two i.p. injection during the 24-h cycle, the first at light onset (Zeitgeber time 0: ZT0) and the second one hour before light offset (ZT11; with ZT12 representing light offset). This strategy also allowed to investigate time of day-dependent effects of RHY. Importantly, experiments were conducted in both female and male mice, and the effects of RHY was assessed in each sex to take into consideration the well-known sex differences in wake/sleep amount, alternation, and ECoG activity (*Robillard et al., 2010; Swift et al., 2020; reviewed by Dib et al., 2021*). Sleep distribution and consolidation was equivalent between groups before RHY administration (**Figure 1A** left column, and **Figure S1**).

RHY was found to decrease time spent awake and increase time spent in SWS for 4 to 7 h after injection in both females and males (**Figure 1A**). These effects were more prominent during the dark period (i.e., active period) for the two sexes (**Figures 1A** and **S1B**), and larger in females than males (**Figure S1A**). Interestingly, a dose-dependent effect was found for females, with RHY100 showing larger wake-suppressing and SWS-inducing effects than RHY50, while both doses impacted wake and SWS mostly in a similar manner in males (**Figures 1A** and **S1A**). The effect of RHY on PS was highly dependent on time of day; with RHY reducing time spent in PS during the light period and increasing it during the dark period (**Figure 1A**; only significant for the dark period in males).

The mean duration and the number of individual bouts of wakefulness/sleep were interrogated to identify whether SWS was enhanced by prolonging individual bouts of SWS, by increasing the occurrence of SWS bouts or both. RHY was observed to significantly reduce the mean duration of wake and SWS bouts in both female and male mice (**Figure 1B**). In parallel, RHY increased the number of wake and SWS bouts for about 4-6 h after injection (**Figure 1C**), with a highly similar time course for wakefulness and SWS. This effect was more prominent for

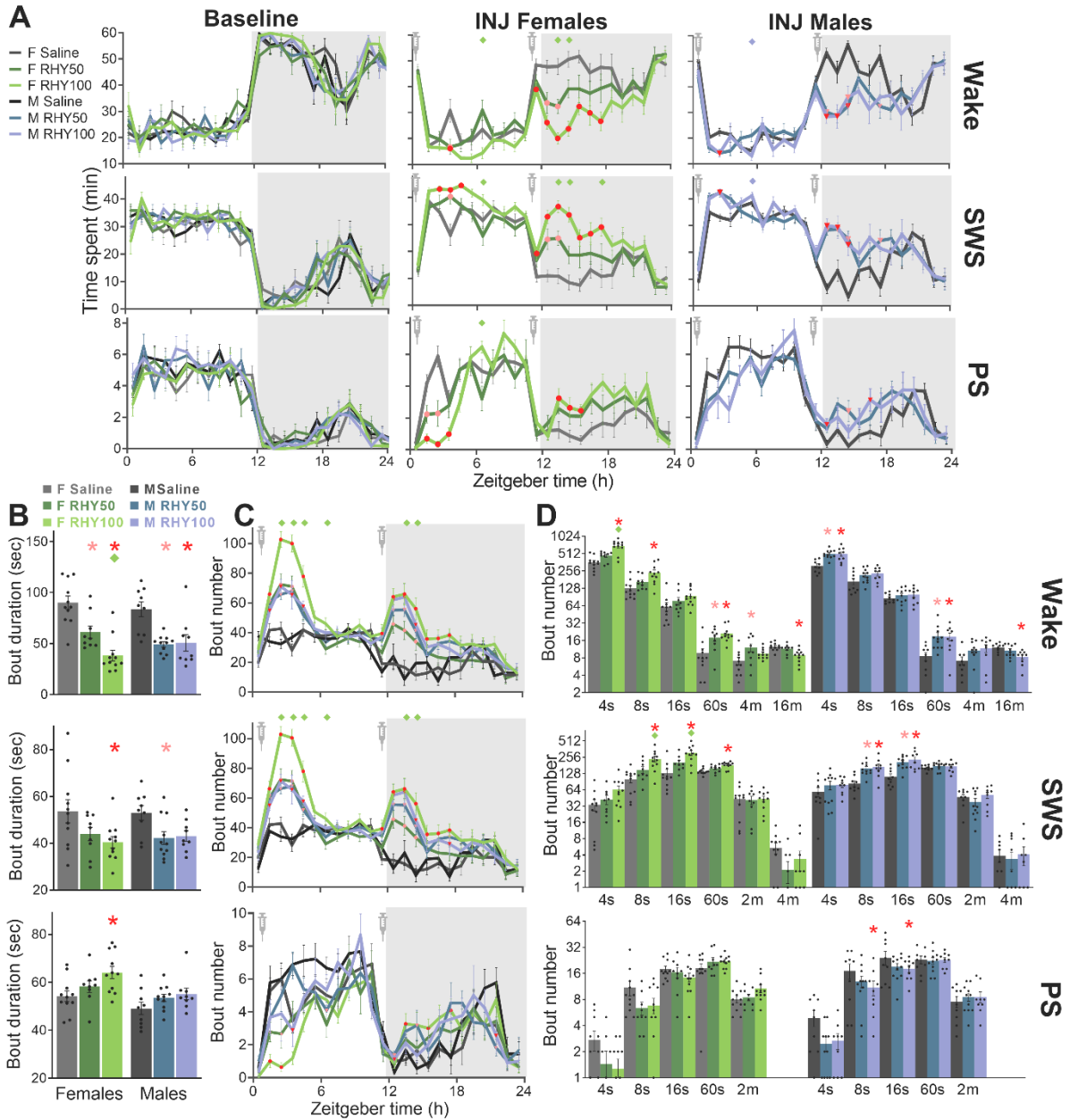


**Figure 1. RHY increases SWS time, reduces PS time, and promotes wake and SWS fragmentation.**

(A) Time course of minutes spent in each vigilance state (wake, SWS and PS) per hour during the baseline (BL) and injection (INJ) 24-h recordings. Significant interactions between RHY treatment and hour were found for wake, SWS and PS for both females (rANOVA:  $F_{46,644} > 2.0$ ,  $p_{adj} < 0.01$ ) and males (rANOVA:  $F_{46,598} > 1.9$ ,  $p_{adj} < 0.01$ ). Red and pink datapoints indicate significant differences compared to the saline group for each hour for the RHY100 and RHY50 groups, respectively (post-hoc comparisons  $p < 0.05$ ; same for panel C). Diamonds at the top of graphs indicate significant differences between RHY100 and RHY50 (post-hoc comparison  $p < 0.05$ ; also in B). Grey backgrounds represent the dark period (also in C).

(B) Mean duration of individual vigilance state bouts during the INJ day. Significant treatment effects were found for wake and SWS (females:  $F_{2,28} > 3, 6, p < 0.05$ ; males:  $F_{2,26} > 4.6, p < 0.02$ ). Red and pink stars indicate significant differences compared to the saline group of the same sex for RHY100 and RHY50, respectively (post-hoc comparison  $p < 0.05$ ; same for panel D). Diamonds at the top of graphs indicate significant differences between RHY100 and RHY50 (post-hoc comparison  $p < 0.05$ ).

(C) Time course of the number of state bouts per hour for the INJ day. Significant interaction was found between RHY treatment and hour for all three states for females (rANOVA:  $F_{46,644} > 2.2, p_{adj} < 0.001$ ) and males (rANOVA:  $F_{46,598} > 1.8, p_{adj} < 0.01$ ). Diamonds at the top of graphs indicate significant differences between RHY100 and RHY50 for females (post-hoc comparison  $p < 0.05$ ).

(D) Number of bouts of different duration for the INJ day. Significant treatment effects were found for specific duration during wake, SWS and PS (females:  $F_{2,28} > 3.7, p < 0.05$ ; males:  $F_{2,26} > 3.8, p < 0.05$ ).

shorter wake and SWS bouts ( $\leq 60$  sec) in comparison to longer SWS bouts (**Figures 1D and S1E**), and also showed a dose-dependent effect for females in particular (**Figures 1B - 1D**). Interestingly, RHY100 increased PS bout duration in females but decreased the number of short PS bouts in males (**Figures 1B and 1D**). In sum, RHY shows wake-suppressing and SWS-inducing effects in mice, and impacts PS in a time of day-dependent manner. The SWS-inducing effect is driven by a higher occurrence of short individual bouts of SWS, resulting in an overall fragmentation of SWS. These effects are generally larger during the dark period, and in females.

## **RHY impacts the ECoG in a state-dependent manner**

ECoG activity during wake, SWS or PS defines state quality and contributes to cognitive functioning, but has never been investigated after Uncaria or RHY treatments. Spectral analysis of the ECoG signal was here used to assess the impact of RHY on the 24-h power spectrum between 0 and 30 Hz of the three vigilance states. The ECoG spectral signature of wakefulness, SWS and PS was unaltered by saline in both females and males (**Figure 2A**, first column). However, RHY100 was found to significantly affect the spectral composition of the ECoG during wakefulness: the contribution of high theta/low alpha activity during wake was particularly decreased by RHY100 (i.e., 8.25-12 Hz in females and 8.25-10.5 Hz in males; **Figure 2A**, third column). RHY100 also reduced delta power (1-4 Hz) during SWS in females. In PS, the higher dose RHY100 in females and the lower RHY50 in males increased the power of frequencies in the theta/sigma (6-12Hz) and low beta (15-20Hz) ranges (**Figure 2A**). Thus, RHY globally impacted the wake ECoG in frequencies generally linked to active wakefulness, and linked to cognitive

processes occurring during sleep (Poe et al., 2000; Boyce et al., 2016; Gronli et al., 2016; Del Percio et al., 2017; Gulati et al., 2017; Vassalli and Franken, 2017).

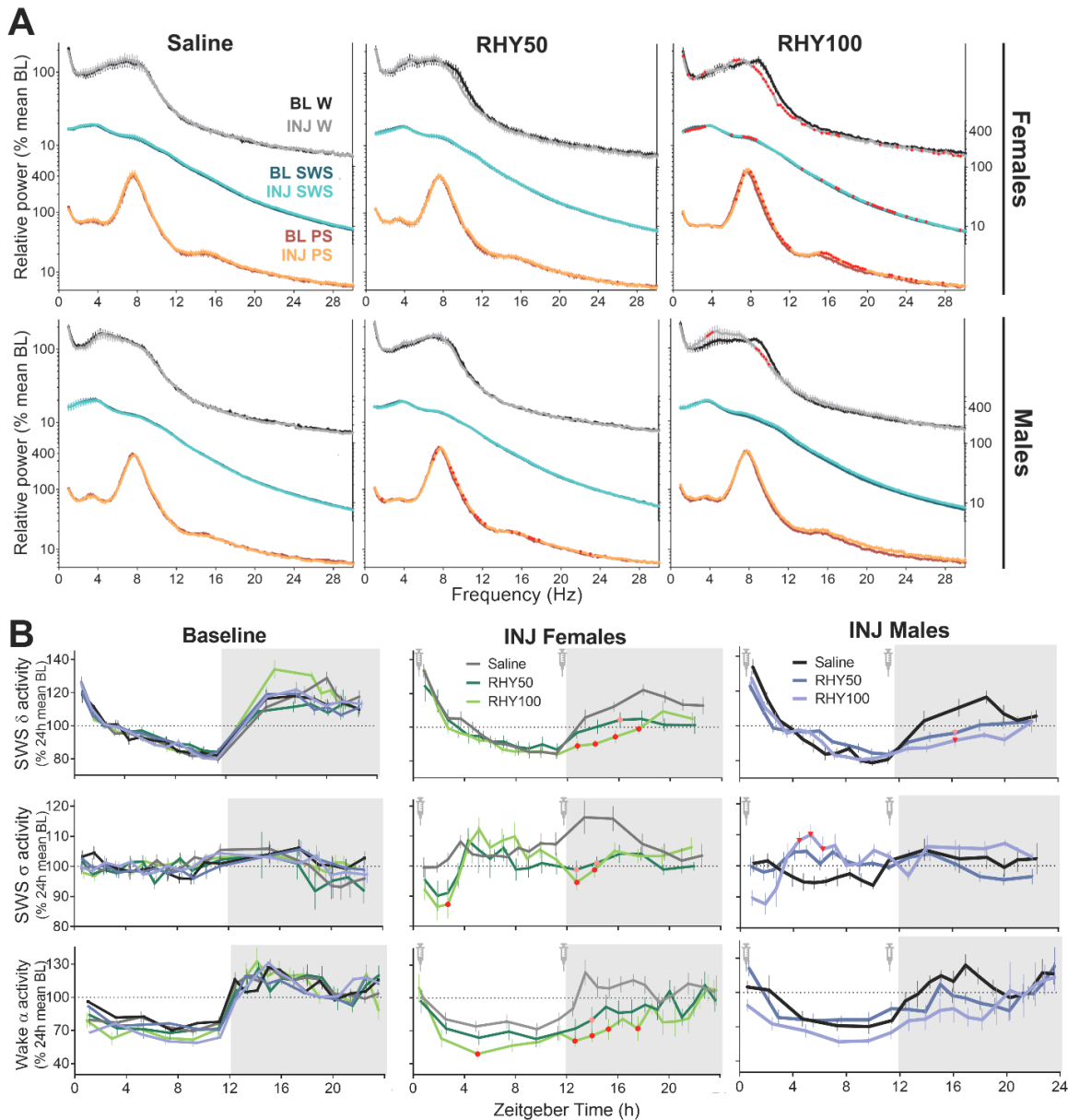


**Figure 2. RHY modifies ECoG activity in a vigilance state-dependent manner.**

(A) Power spectra of the 24-h average for each vigilance state during baseline (BL) and injection (INJ) recordings. Wake and PS spectral powers are plotted on the left axis, and SWS spectra is plotted on the right axis; always in logarithmic scale. Significant interactions between the recording day (BL vs INJ) \* frequency bin were found during wake for females RHY100 (rANOVA:  $F_{116,928} > 6.1$ ,  $p_{adj} < 0.003$ ), and males RHY100 (rANOVA:  $F_{116,928} > 4.8$ ,  $p_{adj} = 0.020$ ); and during SWS and PS for females RHY100 (rANOVA:  $F_{116,928} > 6.0$ ,  $p_{adj} < 0.004$ ) and during PS for males RHY50 (rANOVA:  $F_{116,1044} > 2.7$ ,  $p_{adj} = 0.030$ ). Parts of INJ curves in red indicate significant difference between BL and INJ (post-hoc comparisons  $p < 0.05$ ).

(B) 24-h time course of SWS delta activity (1-4 Hz; first row), SWS sigma activity (10-13 Hz; second row), and wake alpha activity (8-12 Hz; third row). For SWS, significant treatment by interval interactions were found for both sexes (delta: females  $F_{34,442} = 2.7$ ,  $p_{\text{adj}} = 0.001$ ; males  $F_{34,391} = 3.1$ ,  $p_{\text{adj}} = 0.002$ ; sigma: females  $F_{34,442} = 2.5$ ,  $p_{\text{adj}} = 0.007$ ; males  $F_{34,391} = 3.0$ ,  $p_{\text{adj}} < 0.001$ ). For wake alpha activity, a significant treatment by interval interaction was only found for females (females  $F_{34,442} = 1.6$ ,  $p_{\text{adj}} = 0.03$ ; males main treatment effect  $F_{2,21} = 1.9$ ,  $p = 0.2$ ; males treatment by interval interaction  $F_{34,357} = 1.2$ ,  $p_{\text{adj}} = 0.3$ ). Red and pink datapoints indicate significant differences compared to the saline group for each interval for the RHY100 and RHY50 groups, respectively (post-hoc comparisons  $p < 0.05$ ).

The 24-h dynamics of ECoG activity in different frequency bands were then analyzed after RHY treatment. RHY significantly modified the dynamics of delta (1-4 Hz), theta (6-9 Hz) and sigma (10-13 Hz) activity during SWS (**Figures 2B** and **S1F**). More precisely, SWS delta activity was decreased by RHY at a time matching with the strongest SWS-inducing effect (i.e., first half of the dark period). A dose-dependent effect was particularly prominent for females (and for faster delta; **Figures 2B** and **S1F**). RHY impacted SWS theta and sigma activity in a similar manner: decreasing activity in the early light and dark periods in females, and increasing their power in the mid-light period in males (**Figures 2B** and **S1F**). With regard to wakefulness, RHY modified the time course of alpha activity by generally decreasing it throughout the 24-h cycle (only significant in females). In sum, RHY alters ECoG activity during SWS and wakefulness in a manner that depends on time of day and sex.

## Specific RHY targets correlate with sleep variables

To identify mechanisms underlying the widespread effects of RHY on wake/sleep quantity and quality, specific targets of RHY were investigated in the same mice submitted to ECoG recording, which were sacrificed 24 h after the first RHY injection. Total and synaptic protein levels were quantified for three brain regions selected for their contribution to the regulation of ECoG activity and/or sleep amount (i.e., cerebral cortex, hippocampus, and a region covering the thalamus and hypothalamus). Four targets recently proposed as contributor of sleep-related effects of RHY (*Ballester Roig et al., 2021*) were examined (i.e., EPHA4, NR2B, GLUR1, and CDK5) together with GLT1, an astrocytic glutamate transporter regulated by EPHA4 (*Carmona et al., 2009; Filosa et al., 2009*). RHY did not significantly impact the protein level of these targets neither the phosphorylated level of EPHA4 (**Figures 3A, S2A** and **S2B**, and **Tables S1**), but

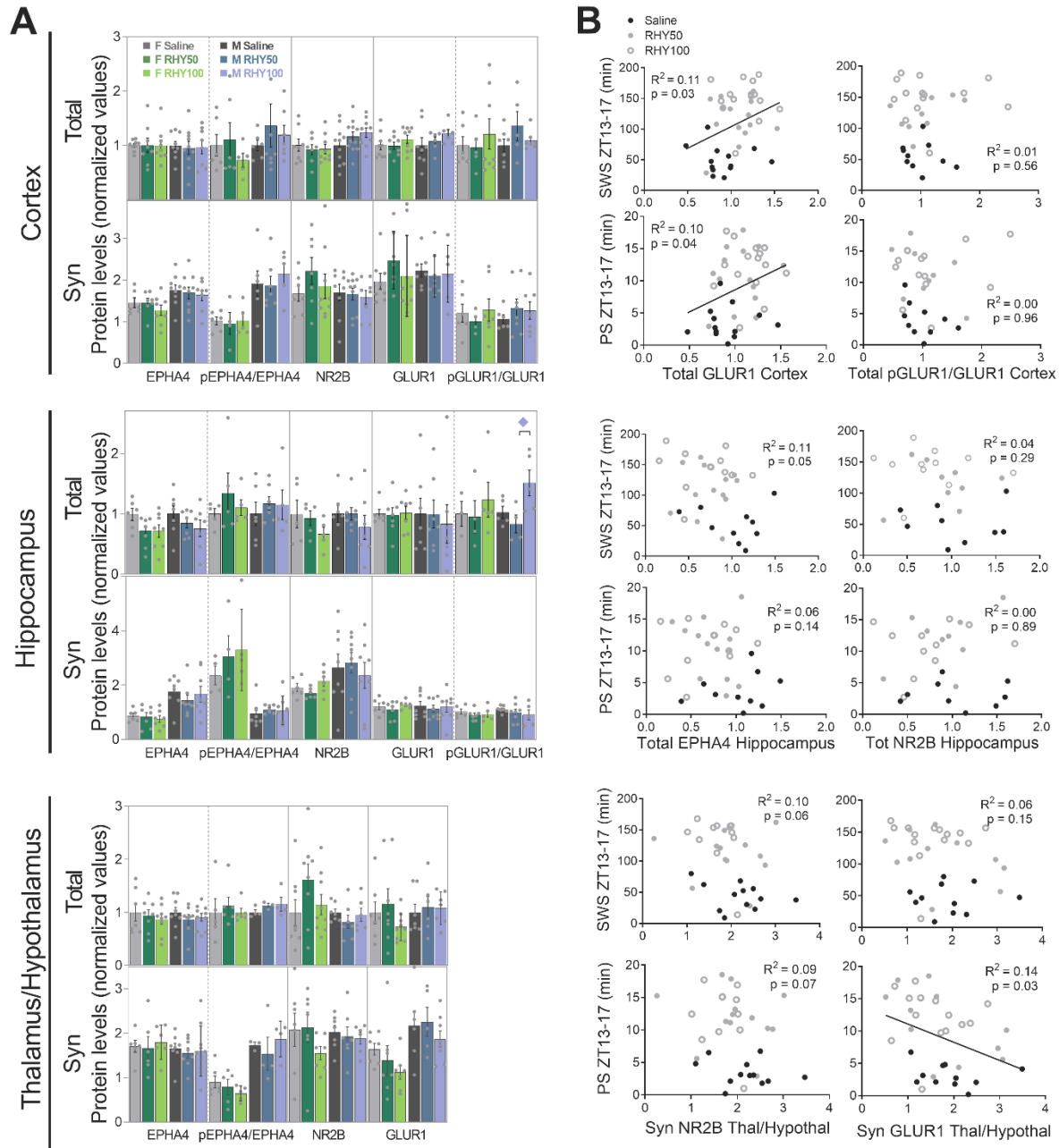


**Figure 3. Protein levels are not modified by RHY but correlated with sleep variables.**

(A) Protein levels in total and synaptoneurosomal (Syn) fractions were quantified for the cerebral cortex, hippocampus, and a thalamus/hypothalamus spanning region. No significant treatment effect was found (see **Figure S2A** for all results of one-way ANOVAs;  $n = 3-11$  per group), except for pGLUR1/GLUR1 in the total fraction of male hippocampus ( $F_{2,11} = 4.73$ ,  $p = 0.03$ ; diamond indicates significant differences between RHY100 and RHY50, post-hoc comparison  $p < 0.05$ ).

(B) Correlations (including both female and male data) between protein levels and sleep variables showed significant correlations between cerebral cortex GLUR1 level (total fraction) and time spent in SWS or PS between ZT13 and ZT17; and between thalamic/hypothalamic GLUR1 (Syn fraction) and time in PS between ZT13 and ZT17.

increased the phosphorylation of GLUR1 (Ser845) in the hippocampus of male mice ( $F_{2,11} = 4.73$ ,  $p = 0.03$ ).

To tackle the large variability in protein measurements and simultaneously investigate relationships with specific sleep features, protein levels were correlated with sleep variables selected for their considerable/highest alteration by RHY (e.g., time spent in SWS between ZT13 and ZT17). Total GLUR1 level in the cerebral cortex was significantly associated with more time spent in SWS or PS at the beginning of the dark period, whereas synaptic GLUR1 in the thalamus/hypothalamus was found to be significantly associated with less time spent in PS at the same time (**Figure 3B**). Total phosphorylated GLUR1 in the cerebral cortex was also negatively correlated with wake alpha activity measured in the dark period (**Figure S3C**). In brief, even if the effect of RHY may not be captured by the targeted proteins when measured more than 12 h after RHY administration, some of these targets could still contribute to alterations in specific sleep variables, including ECoG activity, under RHY treatment.

## **RHY shapes the brain transcriptome in injection-time- and sex-dependent ways**

To precisely capture the mechanisms by which RHY impacts sleep and the time-dependency of these effects, a spatial transcriptomic approach was applied on brain slices of mice sacrificed 3 to 4 h after RHY100 administration. This delay corresponds to the peak time of RHY effects (**Figures 1 and 2**), and led to brains being sampled at ZT4 and ZT14 in females (F) and males (M) administered with saline (S) or RHY (R) (i.e., ZT4FS, ZT4FR, ZT14FS, ZT14FR, ZT4MS, ZT4MR, ZT14MS, ZT14MR). Coronal sections covering the cerebral cortex, hippocampus, and sleep-regulatory regions of the hypothalamus (e.g., LH) were processed using the 10x Genomics Visium Spatial Gene Expression kit coupled to RNA sequencing (RNAseq). The total number of reads and the mean number of reads per spatial spot under tissue were in the same order of magnitude between the eight different conditions (188 to 258M, and 67 to 121K, respectively), as well as the percent reads confidently mapping to the genome (95 to 98 %).



Transcriptome-wide gene expression data were first compared between RHY and saline for the full slice (i.e., all spatial spots, hereafter identified as bulk) for each time point and sex, resulting in four different sets of comparisons (i.e., ZT4F, ZT14F, ZT4M, ZT14M). This generated four sets of significant (i.e., Benjamini-Hochberg False Discovery Rate [FDR] < 0.05) differentially expressed genes (DEGs). RHY administration in the early light period resulted in 575 DEGs in females (ZT4F: 247 increased by RHY100, 328 decreased) and 457 DEGs in males (ZT4M: 126 increased, 331 decreased), and RHY administration in the evening generated 117 DEGs in females (ZT14F: 77 increased by RHY, 44 decreased), and 641 in males (ZT14M: 464 increased, 177 decreased; **Figures 4A** and **S3A**, **Table S2**). A clustered heatmap compiling the fold change in expression of DEGs for ZT4F, ZT4M, ZT14F, and ZT14M identified seven distinct clusters (C1-C7; **Figures 4B** and **S3B**). C1 and C4 comprised genes generally increased by RHY in the four comparisons (**Figures 4C** and **S3B**); C3 featured six genes decreased by RHY in most comparisons (*Tshb*, *Cga*, *Prl*, *Oxt*, *Gh*, *Avp*; **Figures 4D** and **S3B**); C2 and C7 genes generally increased or decreased by RHY in only one comparison or changed in opposite directions between ZT4 and ZT14; and C5 and C6 genes modified by RHY in different directions between ZT4 and ZT14 mainly for males (**Figure S3B**). For instance, *Sgkl* and *Lcn2* belonging to cluster C1 were increased by RHY100 throughout the brain, with a particularly striking increase of *Sgkl* expression in white matter tracts (**Figure 4E**). *Tsc22d3*, an example of C4 genes, was increased for ZT4F and ZT4M; while *Uba52* from C2 was decreased by RHY at ZT4 and increased at ZT14 (**Figure 4E**).

Of importance is that even if C1, C3 and C4 comprised genes for which RHY impacted the expression in a generally consistent manner across the four different comparisons, the impact of RHY was highly dependent on time and sex. Indeed, the majority of DEGs were found in one single comparison (i.e., 310 for ZT4F, 218 for ZT4M, 24 for ZT14F, and 432 for ZT14M; **Figure 4F**). An overlap of 90 DEGs was found between females and males at ZT4, whereas only 10 DEGs were common between sexes at ZT14 (**Figure 4F**). In addition, fold changes in expression after RHY administration were significantly correlated between ZT4F and ZT4M samples and between ZT14F and ZT14M samples, whereas the correlations between time points within sex reached significance for females, but not for males (**Figure S3C**). Interestingly, only 18 DEGs overlapped among the four comparisons, and the impact of RHY for seven of these was generally opposite at ZT4 in comparison to ZT14 (**Figures 4F-G**).

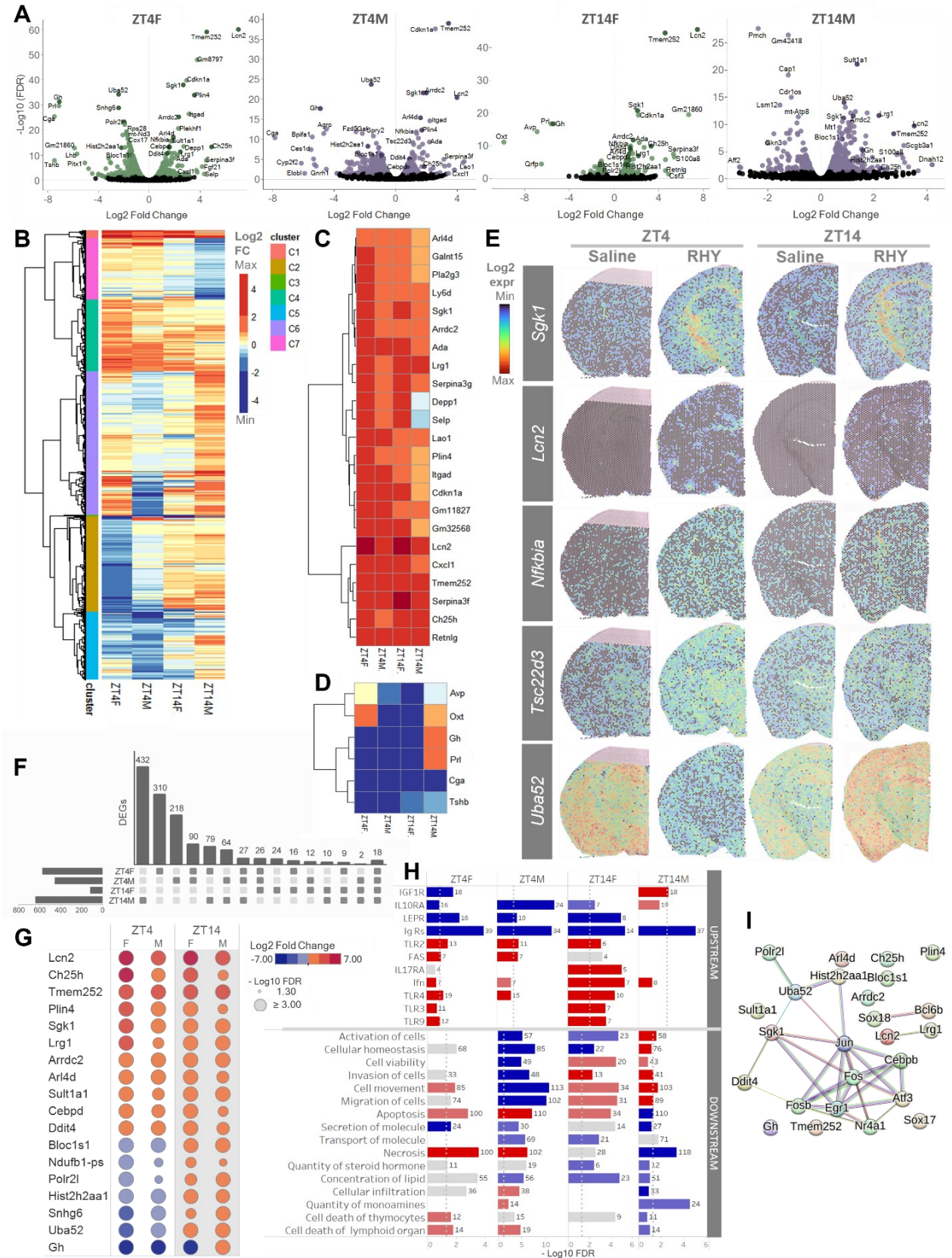


Figure 4. RHY modifies the mouse brain transcriptome.

- (A) Volcano plots showing gene expression changes between RHY and saline conditions in female (F) and male (M) mice at ZT4 or ZT14. Green (female) and purple (males) datapoints indicate differentially expressed genes (DEGs;  $FDR < 0.05$ ) between RHY100 and saline. Note that RHY changes gene expression in both directions. Black datapoints indicate transcripts with no significant change.
- (B) Heatmap of the Log<sub>2</sub> fold change in expression of the DEGs found for ZT4F, ZT4M, ZT14F, and ZT14M. The 1324 DEGs found in at least one of the four comparisons are shown. Automated hierarchical clustering showing seven DEG clusters (C1-C7) is also represented.
- (C) Zoom of cluster C1 showing 22 DEGs generally increased by RHY for ZT4F, ZT4M, ZT14F, and ZT14M.
- (D) Zoom of cluster C3 showing 6 DEGs generally decreased by RHY for ZT4F, ZT4M, ZT14F, and ZT14M.
- (E) Spatial maps of Log<sub>2</sub> gene expression under saline and RHY treatments for female mice shown for *Sgk1*, *Lcn2*, *Nfkbia*, *Tsc22d3*, and *Uba52*.
- (F) Bar diagram illustrating the number of overlapping and non-overlapping DEGs among ZT4F, ZT4M, ZT14F, and ZT14M.
- (G) Table showing the fold change and significance level of the 18 genes common in all four comparisons. Hot colors indicate increases by RHY, and cold colors decreases.
- (H) Functional analysis of ZT4F, ZT4M, ZT14F and ZT14M DEGs showing enrichment of upstream receptors (top 11) and biological functions (bottom 16) extracted from Ingenuity pathway analysis (IPA). Hot colors indicate pathways predicted to be increased by RHY, and cold colors those decreased. Grey indicates no specific direction. The number of genes associated with each specific term is shown. Dotted grey lines indicate the significance threshold for enrichment ( $FDR < 0.05$ ).
- (I) Representation of the protein-protein interaction network of the enriched transcription factors made including the 18 DEGs common in the ZT4F, ZT4M, ZT14F and ZT14M comparisons.

## Gene ontology analysis of RHY time- and sex-dependent effects

The biological functions analysis (Ingenuity Pathway Analysis: IPA) in ZT4F, ZT4M, ZT14F and ZT14M revealed that bulk DEGs were globally significantly enriched for genes linked to cell movement/migration, apoptosis, and necrosis (**Figure 4H**). There was no overlap between all four DEG sets in gene enrichment for IPA canonical pathways, but some canonical pathways were significant in two out of the four comparisons (i.e., EIF2 signalling, oxidative phosphorylation, sirtuin signaling pathway, IL-17 signaling in fibroblasts, mitochondrial dysfunction, and glucocorticoid receptor signaling; **Figure S4A**). Similarly, DAVID gene ontology analysis identified low overlap between comparisons, with ZT4F DEGs enriched in ribosome, mitochondrial and cell adhesion functions; ZT4M DEGs linked to transcription, extracellular region/cell adhesion, protein binding, hormone activity, apoptotic processes, cell development, and

immune responses; ZT14F DEGs enriched in elements of the extracellular region, secretory granules and hormone activity; and ZT14M DEGs in extracellular region, mitochondria and ribosome function (**Figure S4D** and **Table S3**). DEGs overlapping between ZT4F and ZT4M comparisons showed significant enrichment in transcriptional activation and PI3K/Akt signalling pathway, while overlapping DEGs between ZT14F and ZT14M were enriched in extracellular space and steroid metabolic process (**Figure S4E**). In summary, functional analysis supports that the impact of RHY on the genome-wide gene expression signature of the targeted brain slice may vary with time of day and sex.

### **Core RHY-controlled genes are downstream of inflammation/immune pathways**

Focusing on the 18 DEGs overlapping between the four comparisons in the bulk transcriptome can reveal core effects of RHY (i.e., independent of time of day, sex, and brain region). These 18 DEGs were related to glucocorticoid response (*Sgk1*, *Ddit4*, *Sult1a1*, *Ndufb1*, *Polr2L*), PI3K/Akt signaling (*Arlid4*, *Ddit4*, *Gh*, *Sgk1*), lipid metabolism (*Cebpd*, *Ch25h*, *Lcn2*, *Plin4*), immune response (*Cebpd*, *Lcn2*, *Lrg1*), apoptosis (*Ddit4*, *Lcn2*, *Sgk1*), transcription (*Polr2L*, *Hist2h2aa1*, *Snhg6*), endosome processes (*Arrdc2*, *Bloc1s1*), oxidative phosphorylation (*Ndufb1-ps*), and ribosome assembly (*Uba52*) (**Figures 4G** and **S5**). Interestingly, *Polr2L*, *Hist2h2aa1*, *Snhg6*, *Ndufb1-ps*, *Bloc1s1* and *Uba52* (linked to transcription, ribosome assembly, or oxidative phosphorylation) were decreased by RHY at ZT4, but increased at ZT14 (**Figures 4E**, **G** and **S5**). A similar behavior was found for *Gh* in males.

A search for predicted upstream regulators of RHY-driven DEGs with IPA revealed that, globally, the four comparisons (i.e., ZT4F, ZT4M, ZT14F, and ZT14M) were enriched in genes downstream of specific transcription factors or their regulators (e.g., ESR1, NFKBIA, EGR1, SOX2, STAT1), immunoglobulin receptors, toll-like receptors (TLR) and cytokines (**Figures 4H**, **S4B**, and **S4C**). This is strongly suggestive of an implication, among others, of cellular mechanisms related to the immune system. A second transcription factor enrichment analysis was conducted using CheA3 (**Figure S6A**; Keenan *et al.*, 2019). Only two transcription factors were predicted as upstream regulators of RHY-driven transcriptomic changes by both IPA and CheA3: EGR1 and JUN (linked to the immune system and estrogen receptor signaling, respectively, and both to

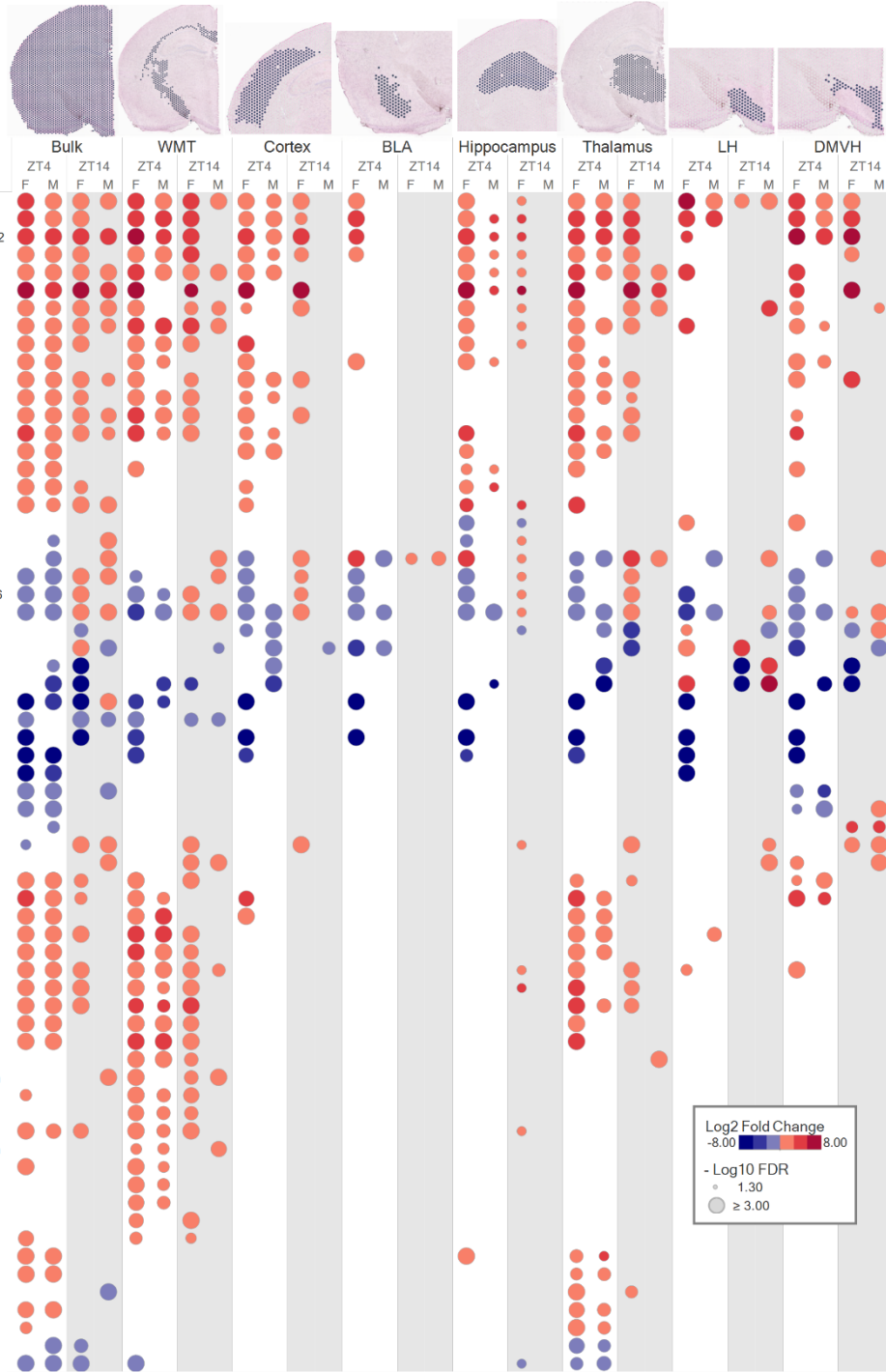
PI3K/Akt signaling). In fact, EGR1 and JUN are shown as central nodes in the protein-protein interaction networks (String analysis) build from the transcription factor enrichment analysis of the 18 common DEGs (**Figure 4I**). Overall, when considering the full mouse brain spatial landscape, RHY impacts the mRNA expression of genes downstream of inflammation/immune and estrogen receptor pathways.

## Brain region-specific effects of RHY on the transcriptome

Importantly, the platform used for spatial transcriptomics allowed the identification of specific gene sets impacted by RHY in defined regions of the brain. The 10X Genomics automated clustering pipeline defined ensembles of spatial spots belonging to the same brain region, which was adequately represented by uniform manifold approximation and projection (UMAP) for dimension reduction (**Figure S6B**). Subsequently, regions of interest of equivalent sizes and comprising spots corresponding to specific brain regions were defined in a semi-automated manner for saline and RHY brains (**Figure 5A**). In the white matter capsules and tracts (WMT), 192 and 41 DEGs between RHY100 and saline were found at ZT4, and 59 and 108 at ZT14 (in females and males, respectively). In the cerebral cortex, 143 and 17 DEGs were found at ZT4, and 20 and 2 at ZT14 (females and males, respectively); in the basolateral amygdala (BLA), 115 and 3 at ZT4, and 1 and 4 at ZT14; in the hippocampus, 149 and 10 at ZT4, and 45 and 4 at ZT14; in the thalamus, 129 and 35 at ZT4, and 31 and 554 at ZT14; in the LH, 83 and 6 at ZT4, and 5 and 57 at ZT14; and finally in a region comprising dorsal, medial and ventromedial hypothalamus (DMVH), 138 and 24 at ZT4, and 17 and 132 at ZT14 (**Table S2**). This highlights that the impact of RHY is not restricted to a limited number of brain regions.

Some DEGs were common to most/many brain regions (e.g., *Sgk1*, *Cdkn1a*, *Tmem252*, *Nfkbia*, *Lcn2*, *Uba52*; **Figure 5A**), and these were comprised in clusters C1, C4 or C7 of the previous bulk analysis. In contrast, many DEGs showed brain region specificity (**Figure 5A**, **Table S2**). Indeed, some DEGs were found in only one region, such as *Myl4* in the hippocampus; *Pomc*, *Dlk1* and *Hdc* in DMVH; and many exclusive to WMT (*Aird5b*, *Nt5c3*, *Fam214a*, and *Gpd1*). The large number of DEGs in WMT may suggest an effect of RHY on axonal functioning. Assessing the effect of RHY in smaller regions (e.g., upper cortical layers, hippocampal pyramidal layers CA1, CA2, dentate gyrus granular layer, striatum, thalamic reticular nucleus) showed no DEG,

**A**



**B**

	Bulk		WMT		Cortex		Hipp		Thalamus		Hypoth	
	ZT4	ZT14	ZT4	ZT14	ZT4	ZT14	ZT4	ZT14	ZT4	ZT14	ZT4	ZT14
Membrane/cell adhesion	20	29	82		10						14	51
Mitochondrial processes	75		93	50	43		30		22		40	87
Ribosomal processes	35		20	28	8		17		20	28	24	50
Neurodegenerative diseases	29	23	32	16	17		19		13	13	16	25
Transcription		49			46							
Glucocorticoid responses					10			5	8			
Hormone activity	9	7			7			14			6	9
Behaviour					20						9	10
Organonitrogen compound responses				49	10	16	55	28			41	9
Vesicle regulation				52					14			6
Apoptosis processes	28											71
G-protein R binding											7	4
Cell proliferation	16				22			9				18
Neurotransmission					11					16		57
												54

**Figure 5. RHY modifies the brain transcriptome in a brain region-dependent manner.**

(A) DEGs of regions of interest representing white matter tracts (WMT), cerebral cortex, basolateral amygdala (BLA), hippocampus, thalamus, lateral hypothalamus (LH) and dorsal, medial and ventromedial hypothalamus (DMVH). Bulk (full slice) data are also included for comparison. Only DEGs (FDR < 0.05) found in more than one comparison (including bulk), and in at least one brain region are shown. Circle size indicates the significance level, hot colors indicate increase, and cold colors decrease.

(B) Gene ontology enriched terms extracted from the DAVID annotation online tool for DEGs of the different brain regions. The number of DEGs enriched for the term category is indicated only for significant terms. The hypothalamus analysis includes LH and DMVH.

which could result from the fewer number of spatial spots contributing to the comparisons. Not surprisingly, some region-dependent effects of RHY were different at ZT4 versus ZT14. For instance, hippocampal *Myl4* expression was decreased at ZT4 and increased at ZT14, and some thalamic DEGs were found only at ZT4 (e.g., *Tiparp*, *Frmpd1*, *Net1*, *Fos*). DEGs found for the cerebral cortex, hippocampus, thalamus and hypothalamus (LH+DMVH) were enriched in biological/cellular/molecular functions generally in line with bulk DEGs (**Figure 5B**, **Table S3**). These functions include cell adhesion, mitochondrial and ribosomal processes, as well as neurodegenerative diseases. Interestingly, enriched terms for the cerebral cortex and hippocampus were mainly linked to ZT4F DEGs, with most significantly enriched terms found in females at ZT4. DEGs found for the hypothalamus were also found to be enriched for hormone activity, behaviour and G-protein coupled receptor binding, functions less related to other brain regions in the present dataset. No significant enrichment for biological/cellular/molecular functions was found for the BLA. In sum, the transcriptomic analysis of different brain regions indicates that RHY alters gene expression with some level of region-specificity, and further supports an important impact of time of day and sex. In addition, these findings suggest that RHY can modify wake/sleep architecture and ECoG activity by affecting the functioning of the cerebral cortex, hippocampus, thalamus and hypothalamus, together with that of main white matter tracts.

### **RHY regulates sleep-related genes**

Our genome- and brain-wide transcriptomic approach allowed for the identification of RHY-driven DEGs that are known regulators of wakefulness and sleep. First, RHY increased the expression of *Tsc22d3* in most brain regions at ZT4 (**Figures 4E** and **5A**). *Tsc22d3* codes for a

protein responding to glucocorticoids, having anti-inflammatory roles, and also called delta sleep-inducing peptide immunoreactor (DSIP) given its reported relationship with sleep amount (Friedman *et al.*, 1994; Seifritz *et al.*, 1995). In addition, RHY decreased the expression of *Hcrt* in the cerebral cortex and thalamus, and modified it with different directions depending on the injection time in the hypothalamus (LH and DMVH; **Figures 5A and 6**). RHY also generally decreased the expression of *Pmch* in several brain regions but increased it in the LH of female mice (**Figures 5A and 6**). *Hcrt*- and *Pmch*-expressing neurons are well-recognized for their contributions

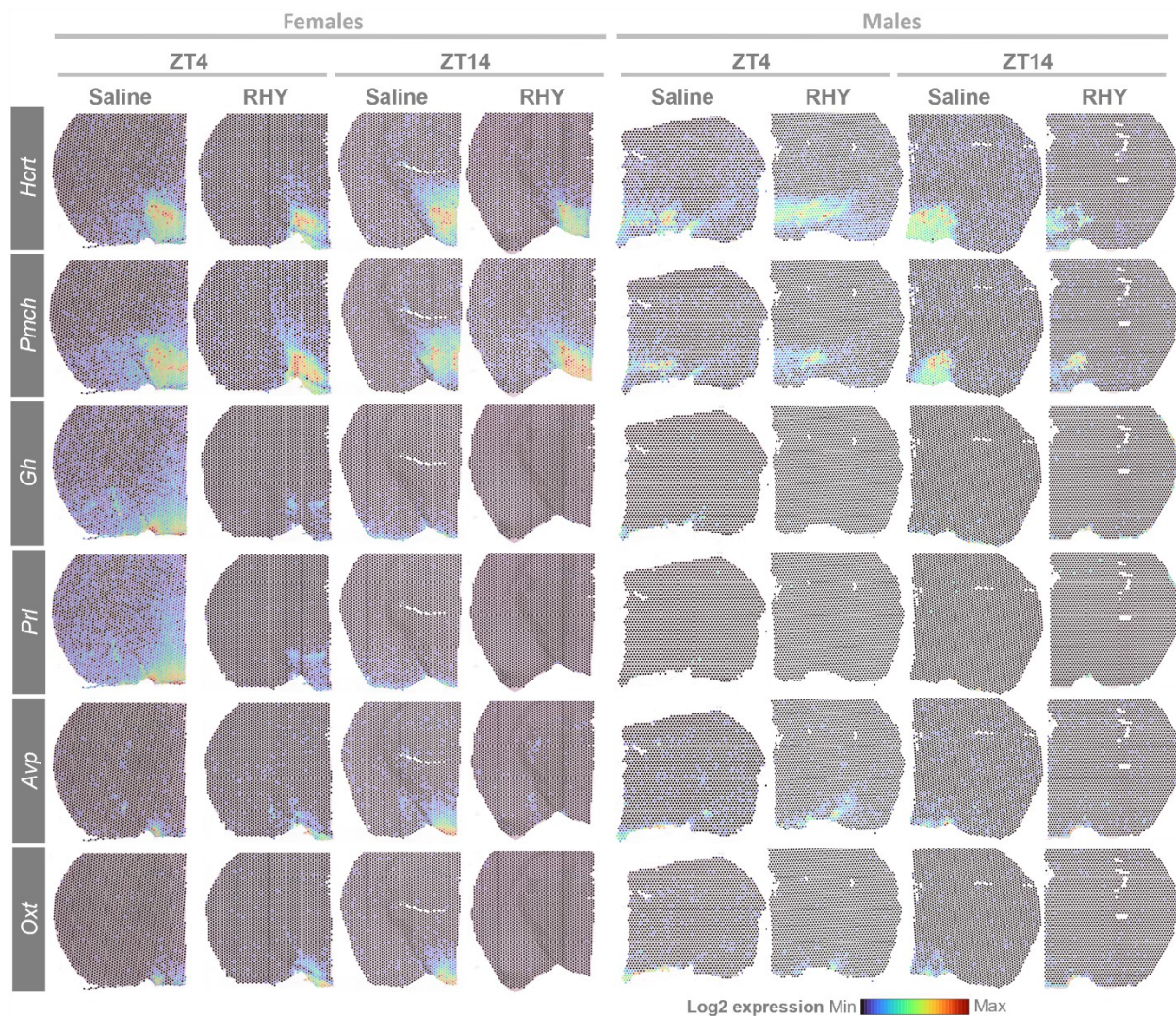


**Figure 6. RHY modifies the expression of sleep-related genes.**

Spatial map of Log2 gene expression under saline or RHY treatments conducted at two different times of the day in females (left four columns) and males (right four columns). Warm colors indicate higher gene expression and cold colors lower gene expression.



in determining wakefulness/sleep transitions and ECoG activity (*Adamantidis et al., 2007; Jengo et al., 2013; Tsunematsu et al., 2014*). Of particular interest is that RHY appears to drive a spatial reorganization in the expression pattern of *Hcrt* and *Pmch* that was particularly marked in females in which RHY apparently restricts the spatial expression map to the LH at both ZT4 and ZT14 (**Figure 6**).

RHY was also observed to alter the expression of several genes coding for peptides involved in the hypothalamic-pituitary axis (HPA). For instance, RHY generally decreased *Avp* in several studied brain regions (**Figures 5A and 6**). Similar observations were made for *Oxt*, *Gh*, *Prl*, and *Cga*. *Tshb* and *Pomc* gene expression was decreased by RHY specifically in the hypothalamus and at ZT4 (**Figure 5A**). *Pomc* codes for the precursor of several HPA peptides including corticotropin, melanocyte-stimulating hormone, and  $\beta$ -endorphin. Given the described bidirectional relationship between the HPA and sleep (*Hirotsu et al., 2015; van Daltsen and Markus, 2018*), it is expected that these alterations participate in wake-suppressing and SWS-inducing effects of RHY. In addition, the HPA is under strong circadian control, and many of these HPA-related genes are expressed in a time of day-dependent manner (*e.g., Avp, Tshb, Pomc; Mure et al., 2018*). Therefore, the modulation of the circadian control of sleep by RHY is a likely route by which changes in wake/sleep amount and alternation can be generated.

## Discussion

We here identified how a natural alkaloid component of *Uncaria* plants shapes wake/sleep amount, alternations, and ECoG activity, as well as multiple mechanisms contributing to these effects using a high spatial resolution transcriptomic strategy. Hypnotic effects of RHY reported for rats (*Yoo et al., 2016*), were first confirmed for mice in both females and males, and are in line with observations that drugs containing *Uncaria* increase sleep time in humans (*Aizawa et al., 2002; Shinno et al., 2008b; Shinno et al., 2008a; Ozone et al., 2012*). An impact of RHY on ECoG activity indicating specific changes during wakefulness, SWS or PS was reported for the first time. We then revealed that RHY changes the transcriptomic landscape of the brain, affecting multiple brain regions in a manner that highly depends on the time of injection and sex. Of importance is that RHY-driven modifications of the transcriptome comprised gene networks with key contributions to wake/sleep regulation in the hypothalamus, which represents a mechanism by which RHY can induce sleep.

The wake-suppressing and SWS-inducing effects of RHY, together with effects on ECoG activity, were found to depend on time of day or hour after injection. The larger effects found during the dark period in comparison to the light likely results from a ceiling effect related to the already high time spent in SWS during the light period in the healthy animals studied. In accordance with the well-described dynamics of homeostatic sleep pressure (*Tobler and Borbely, 1986; Franken et al., 1991*), more SWS in the early dark phase is consistent with less delta activity during SWS at this same time of the day. Alternatively, the larger effect of RHY on time spent awake/asleep during the dark could emerge from an accumulative effect of the two consecutive doses of RHY. Our observations of RHY-driven changes in PS going in opposite directions between the light and dark periods, together with the short half-life of RHY in rodents (*Wang et al., 2010; Lee et al., 2014; Fu et al., 2021*), do not support this alternative explanation. Indeed, RHY decreased PS in the early light period but increased it in the dark period. It is possible that the initial suppression of PS created a PS pressure (*Ocampo-Garces et al., 2000; Shea et al., 2008; Arthaud et al., 2020*), leading to subsequent PS rebound after the second injection. It is particularly interesting that RHY decreased wake ECoG activity in two frequency ranges previously associated with the drive for homeostatic sleep need: SWS delta and wake theta activity (*Deboer, 2015; Vassalli and Franken, 2017*). This overall suggests that RHY shapes wake/sleep quality in parallel to wake/sleep amount, which needs to be carefully considered in sleep medicine.

Mechanisms underlying the impact of RHY on wake/sleep were first investigated at the level of selected individual targets previously related to sleep (*Ballester Roig et al., 2021*). In brains sampled 13 h after the last RHY injection, no change in NR2B, GLUR1 or pEPHA4 was found. This contrasts with previous observations made using similar and longer delays between RHY administration and brain sampling (*Zhou et al., 2010; Li et al., 2014; Zhang et al., 2017a*). However, these previous studies reported effects in rodent disease models only (e.g., epilepsy, depression, addiction). It is thus possible that more subtle effects in healthy animals were not captured by the current study design, especially given findings of significant relationships between levels of GLUR1 and selected sleep variables measured about 10 h before. We thus aimed at better defining the mechanisms underlying RHY-driven wake/sleep alterations by precisely focusing on the time delays with highest effects and applying a comprehensive spatial interrogation.

RHY was found to have widespread effects on the brain transcriptome, affecting hundreds of transcripts throughout the brain, generally associated to apoptosis, necrosis, and cell

movement/migration. In addition, the core 18 genes modified by RHY independent of time of injection and sex were linked to pathways and cellular functions previously described to be impacted by RHY (e.g., PI3K/Akt signaling, immune response/inflammation; *Huang et al., 2014; Lai et al., 2019; Long et al., 2019; Ballester Roig et al., 2021; Fu et al., 2021*). Interestingly, there is a considerable overlap between the present RHY-driven DEGs and genes reported to be modulated by the wake/sleep history (*Cirelli and Tononi, 2000; Cirelli et al., 2004; Mongrain et al., 2010; Vecsey et al., 2012; Bellesi et al., 2013; Husse et al., 2017; Narwade et al., 2017; Diessler et al., 2018; Guo et al., 2019; Oyola et al., 2019; Guo et al., 2020; Wei, 2020; Gaine et al., 2021; Jha et al., 2022*). For instance, total sleep deprivation (SD) was found to increase the expression of *Sgk1, Gh, Nfkb1a*, and *Cdkn1a* in the cerebral cortex and hippocampus (*Diessler et al., 2018; Wei, 2020*), while PS restriction increased *Lcn2, Pmch, Hcrt, Oxt*, and *Pomc* (*Narwade et al., 2017; Oyola et al., 2019*). *Tsc22d3* also represents a target commonly impacted by RHY and SD (*Mongrain et al., 2010; Vecsey et al., 2012; Guo et al., 2020; Wei, 2020; Gaine et al., 2021; Jha et al., 2022*), which has a particular relevance to sleep regulation as indicated before. As a consequence, RHY alters biological functions known to respond to sleep loss (e.g., stress responses, apoptotic processes, cytokine and TNF signaling, transcriptional processes, cell differentiation; (*Cirelli and Tononi, 2000; Cirelli et al., 2004; Vecsey et al., 2012; Bellesi et al., 2013; Husse et al., 2017; Guo et al., 2019; Guo et al., 2020; Gaine et al., 2021*)). This finding that RHY impacts gene networks responding to SD reveals a route by which it can promote sleep. We hypothesize that RHY is inducing a specific molecular program encompassing multiple brain regions and favoring sleep. Importantly, RHY-driven gene expression changes might depend on time of day, which is fully in line with the well-know effect of daytime/circadian time on the brain transcriptome (*Mure et al., 2018; Noya et al., 2019*). This suggests that the molecular reprogramming induced by RHY differs between the early light and early dark periods as an adaptation to the specific internal transcriptional state of the brain.

A main discovery of the current study concerns the impact of RHY on hypothalamic regions. In the hypothalamus, RHY affected genes related to hormone activity and behaviour, which likely contributes to behavioral observations reported here and by other studies (*Shi et al., 1993; Zhou et al., 2010; Yoo et al., 2016; Zhang et al., 2017b; Yang et al., 2018*). RHY was notably found to modify the expression of *Hcrt* and *Pmch* in the LH and DMVH. HCRT neurons project to cortical and thalamic areas, and activation of these cells was found to induce behavioral arousal

and neuronal arousal/desynchronization of the cortex (Bayer *et al.*, 2004; Kirouac *et al.*, 2005; Adamantidis *et al.*, 2007). MCH neurons were shown to fire during sleep (Hassani *et al.*, 2009), and the activation of these cells induces PS (Jego *et al.*, 2013; Tsunematsu *et al.*, 2014), or both SWS and PS in the dark phase (Blanco-Centurion *et al.*, 2016). Thus, the impact of RHY on hypothalamic *Hcrt* and *Pmch* expression pattern could represent a key mechanism by which RHY modulates time spent in wakefulness/sleep. In females in particular, the spatial reorganization of hypothalamic *Pmch* expression and its increase in the LH might directly contribute to wake-suppression/SWS-induction.

Sex differences in sleep amount and synchronized cortical activity are well-known in humans and rodents (Carrier *et al.*, 2001; Mongrain *et al.*, 2005; Koehl *et al.*, 2006; Bixler *et al.*, 2009; Cusmano *et al.*, 2014; Swift *et al.*, 2020). Here, we have highlighted that many effects of RHY are different in female mice in comparison to males, which was particularly striking with regards to wake/sleep architecture, ECoG activity, and spatial transcriptome. It is interesting to note that dose-dependent effects on wake/sleep amount and ECoG were only found for females, and thus that males would not benefit from a higher dosage in the tested range. The generally larger effects of RHY on sleep variables in females was paralleled by a generally stronger impact on the transcriptome, particularly during the light period. Sex differences in sleep are often attributed to gonadal hormones (Gervais *et al.*, 2017; Dib *et al.*, 2021), but sex differences in absorption, metabolism, or downstream effectors of RHY (Tajerian *et al.*, 2015; Braun *et al.*, 2018; Zhang *et al.*, 2019; Jourova *et al.*, 2020) are also potential contributors to the generally higher effects seen in females. Our findings definitely support the need to systematically consider both females and males when investigating the potential of a drug for sleep disturbances.

In conclusion, this study depicts RHY as an alkaloid herb derivative with great promise for sleep medicine. This was done using a detailed identification of its effects on wakefulness and sleep states at the level of architecture and synchronized cortical activity, combined to an exhaustive examination of the brain transcriptome. We have exposed potential key sleep-relevant mechanisms of action of RHY in the brain, which include gene networks with roles in the immune system/inflammation and hormone signaling, and contributions of several brain regions comprising the hypothalamus. Given that the transcriptome does not always reflect changes occurring at protein and functional levels (Liu *et al.*, 2016; Gaine *et al.*, 2021; Joglekar *et al.*, 2021), future research questioning the transcriptome, proteome, and phosphoproteome will be needed to further

increase the understanding of the way by which RHY induces sleep. Furthermore, the present study has investigated a single coronal brain slice selected to represent a variety of regions with relevance to sleep, but follow-up investigations should consider other important sleep-relevant regions such as the ventrolateral preoptic hypothalamus and the brainstem to fully decipher how RHY benefits sleep.

## **Author contributions**

Conceptualization by M.N.B.R. and V.M.; mice experiments conducted by M.N.B.R., T.L. and J.D.-G.; ECoG analyzed by M.N.B.R. and T.L.; protein measurements by M.N.B.R. and Y.M.; library preparation and tissue staining by M.N.B.R. and J.D.-G.; RNAseq data analysis by M.N.B.R.; graphical representation by M.N.B.R., J.D.-G., and O.T.; manuscript written and revised by M.N.B.R., T.L. and V.M.; project administration and funding acquisition by M.N.B.R. and V.M. This work was supported by a Vanier Canada Graduate Scholarship (M.N.B.R.), a J.A. De Sève fellowship from the Recherche CIUSSS-NIM (T.L.), and the Canada Research Chair in Sleep Molecular Physiology (V.M.).

## **Acknowledgements**

The authors are thankful to Chloé Provost for help with surgeries and peri-operative care; Neil Winegarden and Patrick Lacasse from 10x Genomics for technical support regarding spatial transcriptomics; Benoît Delignat-Lavaud and Romina López Urbina for comments on the manuscript; and Sebastien Saucier, Julien Beaudry and Jean-Marc Lina for assistance with hardware.

# Star★Methods

## KEY RESOURCES TABLE

REAGENT or RESOURCE	SOURCE	IDENTIFIER
Antibodies (and dilutions)		
Mouse anti-actin (1:8000)	Sigma Aldrich	Cat# A5441
Rabbit anti-NR2B (1:1000)	Sigma Aldrich	Cat# 06-600
Rabbit anti-Glutamate receptor 1 (1:1000)	Sigma Aldrich	Cat# AB1504
Rabbit anti-phospho-Glutamate Receptor 1 (Ser845) (1:1000)	Sigma Aldrich	Cat# AB5849
Guinea pig anti-Glutamate Transporter, Glial (1:5000)	Sigma Aldrich	Cat# AB1783
Mouse anti-Cdk5 (1:1000)	Sigma Aldrich	Cat# SAB4504276
Mouse anti-EphA4 (1:1000)	Invitrogen	Cat# 37-1600
Rabbit anti-phospho-EphA4 (Tyr602) (1:500)	ECMBiosciences	Cat# EP2731
IRDye® 680RD Anti-mouse IgG (H+L) (1:15000)	LI-COR	Cat# 926-68070
IRDye® 800CW Anti-rabbit IgG (H+L) (1:15000)	LI-COR	Cat# 926-32211
IRDye® 680RD Donkey anti-Guinea Pig IgG (H+L) (1:15000)	LI-COR	Cat# 926-68077
Chemicals, peptides, and recombinant proteins		
Rhynchophylline	Baoji Herbest Bio-Tech	Cat# 76-66-4
Commercial kits		
Visium Spatial Gene Expression Slide & Reagent Kit 4	10x Genomics	Cat# 1000187
Visium Accessory Kit	10x Genomics	Cat# 1000194
Dual Index Kit TT Set A, 96 rxns	10x Genomics	Cat# 1000215
Deposited data		
Raw Visium Spatial cDNA-seq data	Gene Expression Omnibus - NCBI	GSE218537 and GSE217058
Processed Visium Spatial cDNA-seq data	Gene Expression Omnibus - NCBI	GSE218537
Experimental models: Organisms/strains		
C57BL/6J mice	The Jackson Laboratory	JAX: 000664; RRID: IMSR_JAX:000664
Software and algorithms		
Stellate Harmonie	Natus, San Carlos, CA	Version #6.2f
Statistica 6.1	StatSoft Inc.	Version #6
ImageJ	Schneider <i>et al</i> 2012	<a href="https://imagej.nih.gov/ij/">https://imagej.nih.gov/ij/</a>
Prism 7	GraphPad Software Inc.	Version #6
Space Ranger	10x Genomics	Version #1.2.2
Loupe Browser 6.0	10x Genomics	Version #6
Others		
Drill	Dremel	Cat# 8050-N/18
0.7 mm drill bit	Dremel	Cat# 628
Flat fillister head self tapping screws	MORRIS	Cat# FF00CE125
RelyX Unicem 2, Adhesive Resin Cement A2	3M	Cat# 56849
Dental acrylic cement	Yates Motloid	Cat# 44115

Gold wire 0.2 mm diameter	Delta scientific	Cat #920-862-41
Soldering iron	Weller	WES51
36-Channel EEG Wearable Headbox	LaMONT Medical	Cat# 832-000350
Conductors Awg PVC Insulation	Calmont Wire & Cables	Cat# HC-0819075R0
6-channel connector	ENA AG	Cat# BPHF2-O6S-E-3.2
Swivel connector	Crist Instrument Company Inc.	Cat# 4-TBC-9-S
Programmable Amplifier	LaMONT Medical	Cat# 815-000002-S2

## RESOURCE AVAILABILITY

### Lead Contact

Further information and requests for resources, protocols, and reagents should be directed to and will be fulfilled by the lead contact, Valérie Mongrain ([valerie.mongrain@umontreal.ca](mailto:valerie.mongrain@umontreal.ca)).

### Materials Availability

This study did not generate new unique reagents.

### Data and code Availability

Spatial transcriptomics raw and processed data have been deposited in the GEO database (<https://www.ncbi.nlm.nih.gov/geo/>), and are publicly available as of the date of publication. Accession numbers are #GSE218537 and #GSE217058. Original Western blot images and quantifications are available as supplemental material (Table S1). The code generated to create the heatmaps, box plots and Venn diagrams will be available upon request to the lead contact, Valérie Mongrain ([valerie.mongrain@umontreal.ca](mailto:valerie.mongrain@umontreal.ca)).

## EXPERIMENTAL MODEL AND SUBJECT DETAILS

### Animals

Male and female C57BL/6J were bred on site. Animals were housed in a 12 h light / 12 h dark cycle, at  $24 \pm 1^\circ\text{C}$ , with water and food available *ad libitum*. All protocols were conducted in

accordance with guidelines of the Canadian Council on Animal Care and approved by the *Comité d'éthique de l'expérimentation animale* of the CIUSSS-NIM.

## **METHOD DETAILS**

### **ECoG and EMG electrode implantation**

When mice reached 9-10 weeks-old, they were habituated to individual cages for two weeks. Subsequently, mice underwent implantation of electrodes for electrocorticography (ECoG) and electromyography (EMG) as detailed previously (*Mongrain et al., 2010; El Helou et al., 2013*). Female (n = 31 [n = 11 Saline, n = 9 RHY50, n = 11 RHY100], 12.7 ± 2.0 w old, 20.7 ± 1.7 g) and male (n = 29 [n = 9 Saline, n = 11 RHY50, n = 9 RHY100], 12.0 ± 3.2 w old, 26. ± 1.7 g) mice were implanted with electrodes under deep Ketamine/Xylazine anaesthesia (120/10 mg/kg, i.p. injection). Two gold-plated screws (diameter 1.1 mm) served as ECoG electrodes and were screwed through the skull over the right cerebral hemisphere (anterior 1.5 mm lateral to midline, 1.5 mm anterior to bregma; posterior 1.5 mm lateral to midline, 1 mm anterior to lambda). An additional screw placed on the right hemisphere (2.6 mm lateral to midline, 0.7 mm posterior to bregma) was used as a reference. Three other screws were implanted over the left hemisphere as anchors. Two gold wires were inserted in neck muscles to serve as EMG electrodes. The ECoG and EMG electrodes were soldered to a connector and, together with the anchor screws, cemented to the skull. Once awake after anesthesia, mice received a subcutaneous injection of buprenorphine (0.1 mg/kg), and were allowed to recover for 5 days.

### **RHY preparation**

It has been shown that 25-80 mg/kg of RHY modifies brain protein levels after one or several intraperitoneal injections (*Lee et al., 2014; Zhang et al., 2017a*). Moreover, RHY has been detected in the mouse brain 10 min to 3 h after 50 mg/kg oral administration, and in the rat brain 15 min to 6 h after 10 mg/kg intravenous administration (*Lee et al., 2014*), reaching maximum plasmatic concentrations 1-4 h after 37-50 mg/kg oral administration (*Wang et al., 2010; Fu et al., 2021*). Therefore, two doses of RHY were tested and compared with vehicle (saline: NaCl 0.9%): RHY 50 mg/kg (RHY50) and RHY 100 mg/kg (RHY100). RHY (Baoji Herbest Bio-Tech Co.,



Ltd, # 76-66-4) was diluted in NaCl 0.9 %, and homogenized the day before administration. RHY50 and RHY100 dilutions were kept at 4°C until use.

### **Protocols for ECoG/EMG recording**

Following recovery from implantation surgery, mice were habituated to cabling conditions for one week before experiments. Their ECoG/EMG signals were then recorded during 48 h comprising 24 h of undisturbed/baseline (BL) conditions and 24 h under injection (INJ) conditions. On the INJ day, all mice received two intraperitoneal injections, one at ZT0 (i.e., light onset) and one at ZT11 (i.e., 1 h before light offset) of saline, RHY50 or RHY100. ECoG and EMG signals were amplified (Lamont amplifier) and sampled at 256 Hz with the software Harmonie (Natus, San Carlos, CA). Mice were sacrificed at between ZT0 and ZT1 immediately after the INJ day (i.e., 24 h after the first and about 13 h after the second injection) by cervical dislocation, and brains were immediately dissected to sample the cerebral cortex, hippocampus and thalamus/hypothalamus. Brain tissues were quickly frozen on dry ice, and kept at -80°C until use.

### **Immunoblotting and protein quantification**

Brain tissues were processed to extract total and synaptoneurosomal (SYN) proteins similar to previously performed (*Seibt et al., 2012; El Helou et al., 2013*). Ice-cold modified RIPA buffer [10 mM HEPES, 2 mM EDTA, 1 mM EDTA, 0.5 mM DTT, protease and phosphatase inhibitors (Sigma-Aldrich)] was added to samples, which was followed by mechanical homogenization on ice (Pellet Pestle, Sigma Aldrich) until translucent (3 to 4 30-seconds trains). For total protein, a fraction of the homogenate was further sonicated (2 sec pulses, 5 sec pauses, 5 times) on ice, centrifuged at 13,000 rpm for 2 min at 4°C to remove cellular debris, and the supernatant was kept at -80°C for subsequent analysis. For SYN extraction, RIPA buffer was added to the remaining homogenate, vortexed, and centrifuged to remove nuclear/cell debris at 2,000 g and 4°C for 2 min. The supernatant was then passed through a 5 µm pore centrifugal filter (Ultrafree®-CL, Millipore), and centrifuged at 5,000 g and 4°C for 2 min. The filtrate was mixed and centrifuged at 5,000 g and 4°C for 15 min. The supernatants were then immediately resuspended in boiling RIPA buffer, and kept at -80°C until subsequent analysis.

For protein samples with concentration 0.6 µg/µL and above, 50 µg of protein were loaded on gels and separated by SDS-PAGE using an 8% acrylamide gel, and migration at 100 V for 65

min. Proteins were transferred to a PVDF membrane (Bio-Rad) with transfer conditions of 100 V and 60 min. Membranes were blocked with blocking buffer (5% dry milk diluted in TBS [Tris-buffered saline]) for 1 h at room temperature. Primary antibodies were diluted in TBS-T blocking buffer (5% dry milk diluted in TBS [Tris-buffered saline 0.1% Tween 20]; except anti-phospho-EphA4 diluted in 5% BSA [bovine serum albumin] diluted in TBS-T), and were incubated overnight at 4°C. After washes with TBS-T, membranes were incubated with anti-Actin antibody (diluted in TBS-T blocking buffer) for 1 h at room temperature. After washing again, membranes were incubated for 1.5 h with secondary antibodies diluted in TBS-T blocking buffer for 1 h at room temperature. Membranes were revealed using Odyssey CLx imaging system (LI-COR).

### **Protocols for spatial transcriptomics**

To study changes in the spatial transcriptome, saline and RHY100 treatments were compared. Four females and four males were used (12-13 w old): two females and two males received saline (two of each sex at ZT0 and one of each sex also at ZT11), and two females and two males received RHY100 (two of each sex at ZT0 and one of each sex also at ZT11). Mice were sacrificed at ZT4 or ZT14, and brains were immediately sampled, frozen on dry ice together with embedding in OCT compound (VWR International), and stored at -80°C until processing.

### **Tissue preparation for spatial transcriptomics**

Tissue preparation was conducted according to the 10x Genomics Visium Spatial Gene Expression protocol (CG000240 Rev C). Ten µm coronal slices were cut at -23°C with a cryostat (HM525 NX, Thermo Scientific for female brains, Leica CM3050 S Cryostat for male brains), and slices around 1.5 mm posterior to the bregma were mounted on chilled Visium Spatial Gene Expression slides (10x Genomics), and kept at -80°C for 2 to 4 days. Slides were then incubated in a thermocycler (using adaptor plate, 10x Genomics Accessory Kit, 1000194) for 1 min at 37°C, and immersed in Methanol for 30 min at -20°C. For Hematoxylin-Eosin staining (10X Genomics protocol CG000160 Rev A), slides were covered with isopropanol for 1 min at room temperature and, after air dry, covered with Hematoxylin for 7 min at room temperature. After washing, slides were covered with Bluing Buffer for 2 min at room temperature, washed, and covered with Eosin mix for 1 min at room temperature. Lastly, slides were dried using the thermocycler adaptor plate at 37°C for 5 min, and imaged using an Axio Imager M2 microscope (Zeiss, Canada).

## Library preparation

Library were prepared according to 10x Genomics Visium Spatial Gene Expression protocol (CG000239 Rev D). Immediately after imaging, brain slices were covered with permeabilization enzyme and incubated on the thermocycler adaptor plate at 37°C for 6 min. After washing with 0.1X SSC, slices were covered with a reverse transcription master mix (including reverse transcription reagent, template switch oligonucleotides, reducing agent B and reverse transcription enzyme D), and incubated on the thermocycler adaptor plate at 53°C for 45 min. Then, the resulting cDNA (on slides) was incubated with 0.08M KOH for 5 min at room temperature, washed with EB buffer and incubated with second strand synthesis mix (including second strand reagent, primers and enzyme) for 15 min at 65°C. Slices are washed again with buffer EB, and denatured by incubation in 0.08M KOH for 10 min at room temperature. Solutions containing cDNA were transferred to a tube containing Tris 1 M pH 7.0 (1:8 final volume). Samples were mixed with cDNA amplification mix (containing amplification buffer and cDNA primers), and incubated in the thermal cycler (98°C for 3 min; 15 cycles of 15 sec at 98°C, 20 sec at 63°C and 1 min at 72°C; 1 min at 72°C). Then, cDNA was cleaned with SPRIselect beads (Beckman Coulter, Cat# B23318) 0.6X, washed with ethanol 80%, and resuspended with buffer EB. For cDNA fragmentation, end repair and A-tailing, samples were incubated in fragmentation mix (containing fragmentation buffer and enzyme) for 5 min at 32°C, and 30 min at 65°C. Samples were cleaned again with SPRIselect 0.6X and 0.8X, washed with ethanol 80%, and resuspended with buffer EB. Afterwards, samples were mixed with the adaptor ligation mix (containing ligation buffer, DNA ligase and adaptor oligos), and incubated at 20°C for 15 min. Post-ligation cleanup was done again with SPRIselect 0.8X, washed with ethanol 80%, and resuspended with buffer EB. Sample indexes i5 and i7, and amplification mix were added to the samples and incubated in the thermal cycler: 45 min at 98°C; 15 cycles of 98°C for 20 sec, 67°C for 30 sec, 72°C for 20 sec; and 72°C for 1 min. Then, cDNA was purified with SPRIselect 0.6X and 0.8X, washed with ethanol 80%, and resuspended with buffer EB. Libraries were stored at -20°C.

## QUANTIFICATIONS AND STATISTICAL ANALYSES

### Sleep scoring and analysis

ECoG and EMG signals were segmented into 4-s epochs, and the bipolar ECoG signal (signal difference between the anterior and posterior electrodes) and EMG were used to visually assign a vigilance state (wakefulness, SWS or PS) to each epoch by considering ECoG/EMG frequency and amplitude. Total time spent in each vigilance state, and the mean duration of individual bouts of vigilance states were averaged for the 12 h light and dark periods. The total number of bouts of 4, 8, 16, 32, 60, 120, 240, and 960 sec was calculated for the 24 h BL or INJ, for wake, SWS and PS separately. The proportion (percent) of time spent in each vigilance state and the mean duration of individual state bouts were also calculated for full 24 h. Hourly time-courses were calculated for mean time spent in each state and the total number of bouts.

For the ECoG activity analysis, four mice were discarded because of numerous artifacts in the ECoG signal (final analyzed sample: females n = 11 saline, 9 RHY50, 9 RHY100; males n = 8 saline, 10 RHY50, 9 RHY100). For analyzed mice, artifacts were excluded, and the bipolar ECoG signal was submitted to spectral analysis conducted using a Fast Fourier transform (FFT). ECoG activity during wake, SWS and PS was calculated for the full 24 h between 0.75 and 30 Hz with a 0.25 Hz resolution. Power spectra of the 24-h INJ recording were expressed as a percent of the mean power of all 0.25-Hz bins of all states during the 24-h BL for each mouse. The time course of SWS delta (1-4 Hz), delta 1 (0.75-2 Hz), delta 2 (2.5-4 Hz), theta (6-9 Hz), and sigma (10-13 Hz) activity, and of wake theta (6-9 Hz) and alpha (8-12 Hz) activity was calculated using averages per time interval as done previously (*Curie et al., 2013; Areal et al., 2020*). In brief, to take into account the distribution of wakefulness and SWS sleep, SWS activity was average per interval for 12 equal intervals during light periods, and 6 equal intervals during dark periods; while wake activity was average for 6 equal intervals during light periods, and 12 equal intervals during dark periods. Then, relative activity was calculated for each interval as percent of the 24-h BL mean for each mouse.

### **Sleep variables statistical analyses**

Statistica 6.1 (StatSoft Inc./Tibco Software Inc., Palo Alto, CA, USA) was used to perform all statistical analysis of sleep variables. Vigilance state variables calculated for the 12-h light and dark periods were compared between treatments separately for female and male mice using one-way ANOVAs. Vigilance state variables with significant treatment effects were further decomposed with post-hoc Tukey tests. The percentage of time spent in each vigilance state was compared between treatments and sex using two-way analyses of variance (ANOVAs). State percentages with significant treatment-by-sex interaction were further decomposed with planned comparisons. Vigilance state variables calculated per hour or time interval were analyzed using two-way repeated-measure ANOVAs (rANOVA), for which the significance level was adjusted by the Huynh-Feldt correction. Relative activity per frequency bin was also analyzed using two-way rANOVA, but the significance level was adjusted by the more strict Greenhouse–Geisser correction. Significant treatment-by-time, treatment-by-intervals or recording day (BL vs INJ)-by-frequency bin interactions were decomposed using planned comparisons. Data are reported as mean and standard error of the mean (SEM), and the threshold for statistical significance was set to 0.05.

### **Protein quantification statistical analysis**

Bands from immunoblots were analyzed using ImageJ (NIH) (*Schneider et al., 2012*). Quantifications were normalized to actin, to a control sample (included on all membranes), and to the average of the total protein of the saline treatment. Values normalized to actin and the control sample for phosphorylated and non phosphorylated forms of EPHA4 and GLUR1 were used to calculate the ratios of phosphorylation and were afterwards normalized to the average of the ratio of the saline treatment. Prism 7 (GraphPad Software Inc., La Jolla, CA, USA) was used to perform statistical analyses, and to prepare figures. Protein levels were compared between treatments separately for female and male mice using one-way ANOVAs. Pearson correlations were analysed between EPHA4, pEPHA4, GLUR1, pGLUR1 and NR2B levels and vigilance-state variables at the time-interval of higher effect of RHY (between ZT13 and ZT17).

### **DNA sequencing**

Paired-end dual indexed RNAseq was conducted using an Illumina NovaSeq6000 SP100 sequencer (Genome Quebec Innovation Centre, Montreal, Canada), at a sequencing depth of approximately 150M read pairs per sample (> 40 k reads per spot under tissue). RNAseq was performed according to instructions of 10x Genomics for the Visium Spatial Gene Expression kit: read 1, 28 cycles; i7 index read, 10 cycles; i5 index read, 10 cycles; read 2, 90 cycles.

### **RNAseq processing and gene expression analyses**

Sequencing reads (demultiplexed FASTQ files) were aligned to the reference mouse genome (mm10) using the Space Ranger “spaceranger count” pipeline based on the splicing-aware aligner STAR. The pipeline initially trimmed the template switch oligo and poly-A sequences to improve the sensitivity of the alignment. The pipeline aligned reads to the genome, detected tissue spots by aligning the Hematoxylin-Eosin image using the fiducial frame of the capture area, and performed the barcode/unique molecular identifier counting. Reads mapped to the transcriptome with high confidence were used for analysis. Then, the pipeline “spaceranger aggr” was used to find genes differentially expressed between ZT4S and ZT4R samples, and between ZT14S and ZT14R samples for females and males. Gene-spot matrices were analysed using Loupe Browser, and DEGs were considered significant when  $FDR < 0.05$  (Benjamini-Hochberg correction for multiple comparisons; *Benjamini and Hochberg, 1995*). Common DEGs between time point and sex were analyzed using VIB/UGent Bioinformatics & Evolutionary Genomics Venn diagram online calculator and R version 4.1.2. Clustered heatmap was created using the Ward.D2 clustering method. “Spaceranger aggr” was run again using ZT4S, ZT4R, ZT14S, and ZT14R from females, and afterwards from males, to obtain figures of spatial gene expression normalized per slide (thus, for males and females separately).

### **Functional gene ontology analyses**

DEG lists were introduced in the DAVID annotation online tool, the Kyoto Encyclopedia of Genes and Genomes (KEGG) pathway annotation online tool, and the Ingenuity Pathway Analysis software (IPA, Qiagen) for functional analyses. Significant terms in the DAVID annotation online tool were considered when  $FDR < 0.05$ . In IPA, enrichment z-score was calculated considering transcripts Log2 fold change, and enriched terms for canonical pathway were considered when  $FDR \leq 0.01$ ; while enriched terms for predicted upstream elements were

considered when  $FDR \leq 0.0001$ , and  $z\text{-score} > 2$ ; terms for predicted upstream transcription factors when  $FDR \leq 0.01$ , and  $z\text{-score} > 1.5$ ; terms for predicted upstream receptors when  $FDR \leq 0.01$ , and  $z\text{-score} > 1.5$ ; terms for predicted downstream functions when  $FDR \leq 0.001$ . Enriched terms for biological processes ( $FDR < 0.0001$ ), molecular function ( $FDR < 0.001$ ), and KEGG ( $FDR < 0.001$ ) were also reported. Transcription factor enrichment analysis was performed with the online tool ChIP-X Enrichment Analysis Version 3 (ChEA3; (Keenan *et al.*, 2019), and subsequent analysis of functional protein association networks was done with the online database STRING (Szkłarczyk *et al.*, 2021).

## ADDITIONAL RESOURCES

Website 10x genomics: <https://www.10xgenomics.com/products/spatial-gene-expression>

Website GOA sites

Website VIB/UGent Bioinformatics & Evolutionary Genomics Venn diagram online calculator:

<https://bioinformatics.psb.ugent.be/webtools/Venn/>

Website Ingenuity Pathway Analysis (IPA): <https://digitalinsights.qiagen.com/products-overview/discovery-insights-portfolio/analysis-and-visualization/qiagen-ipa/>

Website DAVID: <https://david.ncifcrf.gov/>

Website Kyoto Encyclopedia of Genes and Genomes (KEGG) pathway annotation online tool:

<https://www.genome.jp/kegg/>

Website ChEA3: <https://maayanlab.cloud/chea3/>

Website STRING analysis: <https://string-db.org/>

## References

- Adamantidis, A.R., Zhang, F., Aravanis, A.M., Deisseroth, K., de Lecea, L. (2007). Neural substrates of awakening probed with optogenetic control of hypocretin neurons. *Nature* 450, 420-424.
- Aizawa, R., Kanbayashi, T., Saito, Y., Ogawa, Y., Sugiyama, T., Kitajima, T., Kaneko, Y., Abe, M., Shimizu, T. (2002). Effects of Yoku-kan-san-ka-chimpi-hange on the sleep of normal healthy adult subjects. *Psychiatry Clin Neurosci* 56, 303-304.

- Amzica, F., Steriade, M. (1998). Electrophysiological correlates of sleep delta waves. *Electroencephalogr Clin Neurophysiol* 107, 69-83.
- Areal, C.C., Cao, R., Sonenberg, N., Mongrain, V. (2020). Wakefulness/sleep architecture and electroencephalographic activity in mice lacking the translational repressor 4E-BP1 or 4E-BP2. *Sleep* 43.
- Arthaud, S., Libourel, P.A., Luppi, P.H., Peyron, C. (2020). Insights into paradoxical (REM) sleep homeostatic regulation in mice using an innovative automated sleep deprivation method. *Sleep* 43, zsa003.
- Ballester Roig, M.N., Leduc, T., Areal, C.C., Mongrain, V. (2021). Cellular Effects of Rhynchophylline and Relevance to Sleep Regulation. *Clocks Sleep* 3, 312-341.
- Bayer, L., Serafin, M., Eggermann, E., Saint-Mleux, B., Machard, D., Jones, B.E., Muhlethaler, M. (2004). Exclusive postsynaptic action of hypocretin-orexin on sublayer 6b cortical neurons. *J Neurosci* 24, 6760-6764.
- Bellesi, M., Pfister-Genskow, M., Maret, S., Keles, S., Tononi, G., Cirelli, C. (2013). Effects of sleep and wake on oligodendrocytes and their precursors. *J Neurosci* 33, 14288-14300.
- Benjamini, Y., Hochberg, Y. (1995). Controlling the false discovery rate: a practical and powerful approach to multiple testing. *Journal of the Royal statistical society: series B (Methodological)* 57, 289-300.
- Bixler, E.O., Papaliaga, M.N., Vgontzas, A.N., Lin, H.M., Pejovic, S., Karataraki, M., Vela-Bueno, A., Chrousos, G.P. (2009). Women sleep objectively better than men and the sleep of young women is more resilient to external stressors: effects of age and menopause. *J Sleep Res* 18, 221-228.
- Blanco-Centurion, C., Liu, M., Konadhode, R.P., Zhang, X., Pelluru, D., van den Pol, A.N., Shiromani, P.J. (2016). Optogenetic activation of melanin-concentrating hormone neurons increases non-rapid eye movement and rapid eye movement sleep during the night in rats. *Eur J Neurosci* 44, 2846-2857.
- Boyce, R., Glasgow, S.D., Williams, S., Adamantidis, A. (2016). Causal evidence for the role of REM sleep theta rhythm in contextual memory consolidation. *Science* 352, 812-816.
- Braun, M.D., Kisko, T.M., Vecchia, D.D., Andreatini, R., Schwarting, R.K.W., Wöhr, M. (2018). Sex-specific effects of *Cacna1c* haploinsufficiency on object recognition, spatial memory, and reversal learning capabilities in rats. *Neurobiol Learn Mem* 155, 543-555.
- Carmona, M.A., Murai, K.K., Wang, L., Roberts, A.J., Pasquale, E.B. (2009). Glial ephrin-A3 regulates hippocampal dendritic spine morphology and glutamate transport. *Proc Natl Acad Sci U S A* 106, 12524-12529.
- Carrier, J., Land, S., Buysse, D.J., Kupfer, D.J., Monk, T.H. (2001). The effects of age and gender on sleep EEG power spectral density in the middle years of life (ages 20-60 years old). *Psychophysiology* 38, 232-242.
- Cirelli, C., Tononi, G. (2000). Gene expression in the brain across the sleep-waking cycle. *Brain Res* 885, 303-321.
- Cirelli, C., Gutierrez, C.M., Tononi, G. (2004). Extensive and divergent effects of sleep and wakefulness on brain gene expression. *Neuron* 41, 35-43.
- Conti, B., Maier, R., Barr, A.M., Morale, M.C., Lu, X., Sanna, P.P., Bilbe, G., Hoyer, D., Bartfai, T. (2007). Region-specific transcriptional changes following the three antidepressant treatments electro convulsive therapy, sleep deprivation and fluoxetine. *Mol Psychiatry* 12, 167-189.
- Curie, T., Mongrain, V., Dorsaz, S., Mang, G.M., Emmenegger, Y., Franken, P. (2013). Homeostatic and circadian contribution to EEG and molecular state variables of sleep regulation. *Sleep* 36, 311-323.



- Cusmano, D.M., Hadjimarkou, M.M., Mong, J.A. (2014). Gonadal steroid modulation of sleep and wakefulness in male and female rats is sexually differentiated and neonatally organized by steroid exposure. *Endocrinology* *155*, 204-214.
- Deboer, T. (2015). Behavioral and electrophysiological correlates of sleep and sleep homeostasis. *Curr Top Behav Neurosci* *25*, 1-24.
- Del Percio, C., Drinkenburg, W., Lopez, S., Infarinato, F., Bastlund, J.F., Laursen, B., Pedersen, J.T., Christensen, D.Z., Forloni, G., Frasca, A., Noe, F.M., Bentivoglio, M., Fabene, P.F., Bertini, G., Colavito, V., Kelley, J., Dix, S., Richardson, J.C., Babiloni, C., PharmaCog, C. (2017). On-going electroencephalographic rhythms related to cortical arousal in wild-type mice: the effect of aging. *Neurobiol Aging* *49*, 20-30.
- Dib, R., Gervais, N.J., Mongrain, V. (2021). A review of the current state of knowledge on sex differences in sleep and circadian phenotypes in rodents. *Neurobiol Sleep Circadian Rhythms* *11*, 100068.
- Diessler, S., Jan, M., Emmenegger, Y., Guex, N., Middleton, B., Skene, D.J., Ibberson, M., Burdet, F., Gotz, L., Pagni, M., Sankar, M., Liechti, R., Hor, C.N., Xenarios, I., Franken, P. (2018). A systems genetics resource and analysis of sleep regulation in the mouse. *PLoS Biol* *16*, e2005750.
- El Helou, J., Belanger-Nelson, E., Freyburger, M., Dorsaz, S., Curie, T., La Spada, F., Gaudreault, P.O., Beaumont, E., Pouliot, P., Lesage, F., Frank, M.G., Franken, P., Mongrain, V. (2013). Neuroligin-1 links neuronal activity to sleep-wake regulation. *Proc Natl Acad Sci U S A* *110*, 9974-9979.
- Filosa, A., Paixao, S., Honsek, S.D., Carmona, M.A., Becker, L., Feddersen, B., Gaitanos, L., Rudhard, Y., Schoepfer, R., Klopstock, T., Kullander, K., Rose, C.R., Pasquale, E.B., Klein, R. (2009). Neuron-glia communication via EphA4/ephrin-A3 modulates LTP through glial glutamate transport. *Nat Neurosci* *12*, 1285-1292.
- Franken, P., Tobler, I., Borbely, A.A. (1991). Sleep homeostasis in the rat: simulation of the time course of EEG slow-wave activity. *Neurosci Lett* *130*, 141-144.
- Friedman, T.C., Garcia-Borreguero, D., Hardwick, D., Akuete, C.N., Stambuk, M.K., Dorn, L.D., Starkman, M.N., Loh, Y.P., Chrousos, G.P. (1994). Diurnal rhythm of plasma delta-sleep-inducing peptide in humans: evidence for positive correlation with body temperature and negative correlation with rapid eye movement and slow wave sleep. *J Clin Endocrinol Metab* *78*, 1085-1089.
- Fu, A.K.Y., Hung, K.W., Huang, H., Gu, S., Shen, Y., Cheng, E.Y., Ip, F.C., Huang, X., Fu, W.Y., Ip, N.Y. (2014). Blockade of EphA4 signaling ameliorates hippocampal synaptic dysfunctions in mouse models of Alzheimer's disease. *Proc Natl Acad Sci U S A* *111*, 9959-9964.
- Fu, W.Y., Hung, K.W., Lau, S.F., Butt, B., Yuen, V.W., Fu, G., Chan, I.C., Ip, F.C.F., Fu, A.K.Y., Ip, N.Y. (2021). Rhynchophylline Administration Ameliorates Amyloid-beta Pathology and Inflammation in an Alzheimer's Disease Transgenic Mouse Model. *ACS Chem Neurosci* *12*, 4249-4256.
- Gaine, M.E., Bahl, E., Chatterjee, S., Michaelson, J.J., Abel, T., Lyons, L.C. (2021). Altered hippocampal transcriptome dynamics following sleep deprivation. *Mol Brain* *14*, 125.
- Gervais, N.J., Mong, J.A., Lacreuse, A. (2017). Ovarian hormones, sleep and cognition across the adult female lifespan: An integrated perspective. *Front Neuroendocrinol* *47*, 134-153.
- Gronli, J., Rempe, M.J., Clegern, W.C., Schmidt, M., Wisor, J.P. (2016). Beta EEG reflects sensory processing in active wakefulness and homeostatic sleep drive in quiet wakefulness. *J Sleep Res* *25*, 257-268.

- Gulati, T., Guo, L., Ramanathan, D.S., Bodepudi, A., Ganguly, K. (2017). Neural reactivations during sleep determine network credit assignment. *Nat Neurosci* 20, 1277-1284.
- Guo, X., Keenan, B.T., Sarantopoulou, D., Lim, D.C., Lian, J., Grant, G.R., Pack, A.I. (2019). Age attenuates the transcriptional changes that occur with sleep in the medial prefrontal cortex. *Aging Cell* 18, e13021.
- Guo, X., Gao, X., Keenan, B.T., Zhu, J., Sarantopoulou, D., Lian, J., Galante, R.J., Grant, G.R., Pack, A.I. (2020). RNA-seq analysis of galaninergic neurons from ventrolateral preoptic nucleus identifies expression changes between sleep and wake. *BMC Genomics* 21, 633.
- Hassani, O.K., Lee, M.G., Jones, B.E. (2009). Melanin-concentrating hormone neurons discharge in a reciprocal manner to orexin neurons across the sleep-wake cycle. *Proc Natl Acad Sci U S A* 106, 2418-2422.
- Hirotsu, C., Tufik, S., Andersen, M.L. (2015). Interactions between sleep, stress, and metabolism: From physiological to pathological conditions. *Sleep Sci* 8, 143-152.
- Hsieh, C.L., Ho, T.Y., Su, S.Y., Lo, W.Y., Liu, C.H., Tang, N.Y. (2009). Uncaria rhynchophylla and Rhynchophylline inhibit c-Jun N-terminal kinase phosphorylation and nuclear factor-kappaB activity in kainic acid-treated rats. *Am J Chin Med* 37, 351-360.
- Hubbard, J., Gent, T.C., Hoekstra, M.M.B., Emmenegger, Y., Mongrain, V., Landolt, H.P., Adamantidis, A.R., Franken, P. (2020). Rapid fast-delta decay following prolonged wakefulness marks a phase of wake-inertia in NREM sleep. *Nat Commun* 11, 3130.
- Husse, J., Kiehn, J.T., Barclay, J.L., Naujokat, N., Meyer-Kovac, J., Lehnert, H., Oster, H. (2017). Tissue-Specific Dissociation of Diurnal Transcriptome Rhythms During Sleep Restriction in Mice. *Sleep* 40.
- Jeenapongsa, R., Tohda, M. (2003). Effects of Choto-san and Chotoko on thiopental-induced sleeping time. *Journal of traditional medicines* 20, 165-167.
- Jego, S., Glasgow, S.D., Herrera, C.G., Ekstrand, M., Reed, S.J., Boyce, R., Friedman, J., Burdakov, D., Adamantidis, A.R. (2013). Optogenetic identification of a rapid eye movement sleep modulatory circuit in the hypothalamus. *Nat Neurosci* 16, 1637-1643.
- Jha, P.K., Valekunja, U.K., Ray, S., Nollet, M., Reddy, A.B. (2022). Single-cell transcriptomics and cell-specific proteomics reveals molecular signatures of sleep. *Commun Biol* 5, 846.
- Joglekar, A. et al. (2021). A spatially resolved brain region- and cell type-specific isoform atlas of the postnatal mouse brain. *Nat Commun* 12, 463.
- Jones, B.E. (2020). Arousal and sleep circuits. *Neuropsychopharmacology* 45, 6-20.
- Jourova, L., Vavreckova, M., Zemanova, N., Anzenbacher, P., Langova, K., Hermanova, P., Hudcovic, T., Anzenbacherova, E. (2020). Gut Microbiome Alters the Activity of Liver Cytochromes P450 in Mice With Sex-Dependent Differences. *Front Pharmacol* 11, 01303.
- Kang, T.H., Murakami, Y., Takayama, H., Kitajima, M., Aimi, N., Watanabe, H., Matsumoto, K. (2004). Protective effect of rhynchophylline and isorhynchophylline on in vitro ischemia-induced neuronal damage in the hippocampus: putative neurotransmitter receptors involved in their action. *Life Sci* 76, 331-343.
- Keenan, A.B., Torre, D., Lachmann, A., Leong, A.K., Wojciechowicz, M.L., Utti, V., Jagodnik, K.M., Kropiwnicki, E., Wang, Z., Ma'ayan, A. (2019). ChEA3: transcription factor enrichment analysis by orthogonal omics integration. *Nucleic Acids Res* 47, W212-W224.

- Kirouac, G.J., Parsons, M.P., Li, S. (2005). Orexin (hypocretin) innervation of the paraventricular nucleus of the thalamus. *Brain Res* 1059, 179-188.
- Koehl, M., Battle, S., Meerlo, P. (2006). Sex differences in sleep: the response to sleep deprivation and restraint stress in mice. *Sleep* 29, 1224-1231.
- Lee, C.J., Hsueh, T.Y., Lin, L.C., Tsai, T.H. (2014). Determination of protein-unbound rhynchophylline brain distribution by microdialysis and ultra-performance liquid chromatography with tandem mass spectrometry. *Biomed Chromatogr* 28, 901-906.
- Li, J., Liu, W., Peng, Q., Jiang, M., Luo, C., Guo, Y., Liu, Y., Fang, M., Mo, Z. (2014). Effect of rhynchophylline on conditioned place preference on expression of NR2B in methamphetamine-dependent mice. *Biochem Biophys Res Commun* 452, 695-700.
- Li, S.B., Damonte, V.M., Chen, C., Wang, G.X., Kebschull, J.M., Yamaguchi, H., Bian, W.J., Purmann, C., Pattni, R., Urban, A.E., Mourrain, P., Kauer, J.A., Scherrer, G., de Lecea, L. (2022). Hyperexcitable arousal circuits drive sleep instability during aging. *Science* 375, eabh3021.
- Liu, Y., Beyer, A., Aebersold, R. (2016). On the Dependency of Cellular Protein Levels on mRNA Abundance. *Cell* 165, 535-550.
- Mackiewicz, M., Shockley, K.R., Romer, M.A., Galante, R.J., Zimmerman, J.E., Naidoo, N., Baldwin, D.A., Jensen, S.T., Churchill, G.A., Pack, A.I. (2007). Macromolecule biosynthesis: a key function of sleep. *Physiol Genomics* 31, 441-457.
- Maret, S., Dorsaz, S., Gurcel, L., Pradervand, S., Petit, B., Pfister, C., Hagenbuchle, O., O'Hara, B.F., Franken, P., Tafti, M. (2007). Homer1a is a core brain molecular correlate of sleep loss. *Proc Natl Acad Sci U S A* 104, 20090-20095.
- Mongrain, V., Carrier, J., Dumont, M. (2005). Chronotype and sex effects on sleep architecture and quantitative sleep EEG in healthy young adults. *Sleep* 28, 819-827.
- Mongrain, V., Hernandez, S.A., Pradervand, S., Dorsaz, S., Curie, T., Hagiwara, G., Gip, P., Heller, H.C., Franken, P. (2010). Separating the contribution of glucocorticoids and wakefulness to the molecular and electrophysiological correlates of sleep homeostasis. *Sleep* 33, 1147-1157.
- Mure, L.S., Le, H.D., Benegiamo, G., Chang, M.W., Rios, L., Jillani, N., Ngotho, M., Kariuki, T., Dkhissi-Benyahya, O., Cooper, H.M., Panda, S. (2018). Diurnal transcriptome atlas of a primate across major neural and peripheral tissues. *Science* 359.
- Narwade, S.C., Mallick, B.N., Deobagkar, D.D. (2017). Transcriptome Analysis Reveals Altered Expression of Memory and Neurotransmission Associated Genes in the REM Sleep Deprived Rat Brain. *Front Mol Neurosci* 10, 67.
- Noya, S.B., Colameo, D., Bruning, F., Spinnler, A., Mircsof, D., Opitz, L., Mann, M., Tyagarajan, S.K., Robles, M.S., Brown, S.A. (2019). The forebrain synaptic transcriptome is organized by clocks but its proteome is driven by sleep. *Science* 366.
- Ocampo-Garces, A., Molina, E., Rodriguez, A., Vivaldi, E.A. (2000). Homeostasis of REM sleep after total and selective sleep deprivation in the rat. *J Neurophysiol* 84, 2699-2702.

- Oyola, M.G., Shupe, E.A., Soltis, A.R., Sukumar, G., Paez-Pereda, M., Larco, D.O., Wilkerson, M.D., Rothwell, S., Dalgard, C.L., Wu, T.J. (2019). Sleep Deprivation Alters the Pituitary Stress Transcriptome in Male and Female Mice. *Front Endocrinol (Lausanne)* *10*, 676.
- Ozone, M., Yagi, T., Chiba, S., Aoki, K., Kuroda, A., Mitsui, K., Itoh, H., Sasaki, M. (2012). Effect of yokukansan on psychophysiological insomnia evaluated using cyclic alternating pattern as an objective marker of sleep instability. *Sleep and Biological Rhythms* *10*, 157-160.
- Park, H.L., Lee, H.S., Shin, B.C., Liu, J.P., Shang, Q., Yamashita, H., Lim, B. (2012). Traditional medicine in china, Korea, and Japan: a brief introduction and comparison. *Evid Based Complement Alternat Med* *2012*, 429103.
- Peever, J., Fuller, P.M. (2017). The Biology of REM Sleep. *Curr Biol* *27*, R1237-R1248.
- Poe, G.R., Nitz, D.A., McNaughton, B.L., Barnes, C.A. (2000). Experience-dependent phase-reversal of hippocampal neuron firing during REM sleep. *Brain Res* *855*, 176-180.
- Robillard, R., Massicotte-Marquez, J., Kawinska, A., Paquet, J., Frenette, S., Carrier, J. (2010). Topography of homeostatic sleep pressure dissipation across the night in young and middle-aged men and women. *J Sleep Res* *19*, 455-465.
- Schneider, C.A., Rasband, W.S., Eliceiri, K.W. (2012). NIH Image to ImageJ: 25 years of image analysis. *Nat Methods* *9*, 671-675.
- Seifritz, E., Muller, M.J., Schonenberger, G.A., Trachsel, L., Hemmeter, U., Hatzinger, M., Ernst, A., Moore, P., Holsboer-Trachsler, E. (1995). Human plasma DSIP decreases at the initiation of sleep at different circadian times. *Peptides* *16*, 1475-1481.
- Shao, H., Mi, Z., Ji, W.G., Zhang, C.H., Zhang, T., Ren, S.C., Zhu, Z.R. (2015). Rhynchophylline protects against the amyloid beta-induced increase of spontaneous discharges in the hippocampal CA1 region of rats. *Neurochem Res* *40*, 2365-2373.
- Shao, H., Yang, Y., Mi, Z., Zhu, G.X., Qi, A.P., Ji, W.G., Zhu, Z.R. (2016). Anticonvulsant effect of Rhynchophylline involved in the inhibition of persistent sodium current and NMDA receptor current in the pilocarpine rat model of temporal lobe epilepsy. *Neuroscience* *337*, 355-369.
- Shea, J.L., Mochizuki, T., Sagvaag, V., Aspevik, T., Bjorkum, A.A., Datta, S. (2008). Rapid eye movement (REM) sleep homeostatic regulatory processes in the rat: changes in the sleep-wake stages and electroencephalographic power spectra. *Brain Res* *1213*, 48-56.
- Shi, J.S., Huang, B., Wu, Q., Ren, R.X., Xie, X.L. (1993). Effects of rhynchophylline on motor activity of mice and serotonin and dopamine in rat brain. *Zhongguo Yao Li Xue Bao* *14*, 114-117.
- Shinno, H., Kamei, M., Nakamura, Y., Inami, Y., Horiguchi, J. (2008a). Successful treatment with Yi-Gan San for rapid eye movement sleep behavior disorder. *Prog Neuropsychopharmacol Biol Psychiatry* *32*, 1749-1751.
- Shinno, H., Inami, Y., Inagaki, T., Nakamura, Y., Horiguchi, J. (2008b). Effect of Yi-Gan San on psychiatric symptoms and sleep structure at patients with behavioral and psychological symptoms of dementia. *Prog Neuropsychopharmacol Biol Psychiatry* *32*, 881-885.
- Swift, K.M., Keus, K., Echeverria, C.G., Cabrera, Y., Jimenez, J., Holloway, J., Clawson, B.C., Poe, G.R. (2020). Sex differences within sleep in gonadally intact rats. *Sleep* *43*.

- Szklarczyk, D., Gable, A.L., Nastou, K.C., Lyon, D., Kirsch, R., Pyysalo, S., Doncheva, N.T., Legeay, M., Fang, T., Bork, P., Jensen, L.J., von Mering, C. (2021). The STRING database in 2021: customizable protein-protein networks, and functional characterization of user-uploaded gene/measurement sets. *Nucleic Acids Res* *49*, D605-D612.
- Tajerian, M., Sahbaie, P., Sun, Y., Leu, D., Yang, H.Y., Li, W., Huang, T.T., Kingery, W., David Clark, J. (2015). Sex differences in a Murine Model of Complex Regional Pain Syndrome. *Neurobiol Learn Mem* *123*, 100-109.
- Terao, A., Greco, M.A., Davis, R.W., Heller, H.C., Kilduff, T.S. (2003). Region-specific changes in immediate early gene expression in response to sleep deprivation and recovery sleep in the mouse brain. *Neuroscience* *120*, 1115-1124.
- Timofeev, I., Bazhenov, M., Seigneur, J., Sejnowski, T. (2012). Neuronal Synchronization and Thalamocortical Rhythms in Sleep, Wake and Epilepsy. In: Jasper's Basic Mechanisms of the Epilepsies (th, Noebels JL, Avoli M, Rogawski MA, Olsen RW, Delgado-Escueta AV, eds). Bethesda (MD).
- Tobler, I., Borbely, A.A. (1986). Sleep EEG in the rat as a function of prior waking. *Electroencephalogr Clin Neurophysiol* *64*, 74-76.
- Tsunematsu, T., Ueno, T., Tabuchi, S., Inutsuka, A., Tanaka, K.F., Hasuwa, H., Kilduff, T.S., Terao, A., Yamanaka, A. (2014). Optogenetic manipulation of activity and temporally controlled cell-specific ablation reveal a role for MCH neurons in sleep/wake regulation. *J Neurosci* *34*, 6896-6909.
- van Dalfsen, J.H., Markus, C.R. (2018). The influence of sleep on human hypothalamic-pituitary-adrenal (HPA) axis reactivity: A systematic review. *Sleep Med Rev* *39*, 187-194.
- Vassalli, A., Franken, P. (2017). Hypocretin (orexin) is critical in sustaining theta/gamma-rich waking behaviors that drive sleep need. *Proc Natl Acad Sci U S A* *114*, E5464-E5473.
- Vecsey, C.G., Peixoto, L., Choi, J.H., Wimmer, M., Jaganath, D., Hernandez, P.J., Blackwell, J., Meda, K., Park, A.J., Hannenhalli, S., Abel, T. (2012). Genomic analysis of sleep deprivation reveals translational regulation in the hippocampus. *Physiol Genomics* *44*, 981-991.
- Wang, W., Ma, C.M., Hattori, M. (2010). Metabolism and pharmacokinetics of rhynchophylline in rats. *Biol Pharm Bull* *33*, 669-676.
- Wei, Y. (2020). Comparative transcriptome analysis of the hippocampus from sleep-deprived and Alzheimer's disease mice. *Genet Mol Biol* *43*, e20190052.
- Yang, Y., Ji, W.G., Zhu, Z.R., Wu, Y.L., Zhang, Z.Y., Qu, S.C. (2018). Rhynchophylline suppresses soluble A $\beta$ 1-42-induced impairment of spatial cognition function via inhibiting excessive activation of extrasynaptic NR2B-containing NMDA receptors. *Neuropharmacology* *135*, 100-112.
- Yoo, J.H., Ha, T.W., Hong, J.T., Oh, K.W. (2016). Rhynchophylline, one of major constituents of *Uncariae Ramulus et Uncus* enhances pentobarbital-induced sleep behaviors and Rapid Eye Movement Sleep in rodents. *Natural Product Sciences* *22*, 263-269.
- Yu, F., Takahashi, T., Moriya, J., Kawaura, K., Yamakawa, J., Kusaka, K., Itoh, T., Morimoto, S., Yamaguchi, N., Kanda, T. (2006). Traditional Chinese medicine and Kampo: a review from the distant past for the future. *J Int Med Res* *34*, 231-239.

- Zhang, J.C., Yao, W., Qu, Y., Nakamura, M., Dong, C., Yang, C., Ren, Q., Ma, M., Han, M., Shirayama, Y., Hayashi-Takagi, A., Hashimoto, K. (2017a). Increased EphA4-ephexin1 signaling in the medial prefrontal cortex plays a role in depression-like phenotype. *Sci Rep* 7, 7133.
- Zhang, Y.N., Yang, Y.F., Xu, W., Yang, X.W. (2017b). The blood-brain barrier permeability of six indole alkaloids from *Uncariae Ramulus cum Uncis* in the MDCK-pHaMDR cell monolayer model. *Molecules* 22.
- Zhang, Z., Tremblay, J., Raelson, J., Sofer, T., Du, L., Fang, Q., Argos, M., Marois-Blanchet, F.C., Wang, Y., Yan, L., Chalmers, J., Woodward, M., Harrap, S., Hamet, P., Luo, H., Wu, J. (2019). EPHA4 regulates vascular smooth muscle cell contractility and is a sex-specific hypertension risk gene in individuals with type 2 diabetes. *J Hypertens* 37, 775-789.
- Zhou, J.Y., Mo, Z.X., Zhou, S.W. (2010). Rhynchophylline down-regulates NR2B expression in cortex and hippocampal CA1 area of amphetamine-induced conditioned place preference rat. *Arch Pharm Res* 33, 557-565.

# **Supplemental information**

## **Probing pathways by which Rhynchophylline modifies sleep using spatial transcriptomics**

**Maria Neus Ballester Roig,<sup>1,2</sup> Tanya Leduc,<sup>1,2</sup> Julien Dufort-Gervais,<sup>1</sup> Yousra Maghmoul,<sup>2,3</sup> Olivier Tastet,<sup>4</sup> Valérie Mongrain,<sup>1,2,\*</sup>**

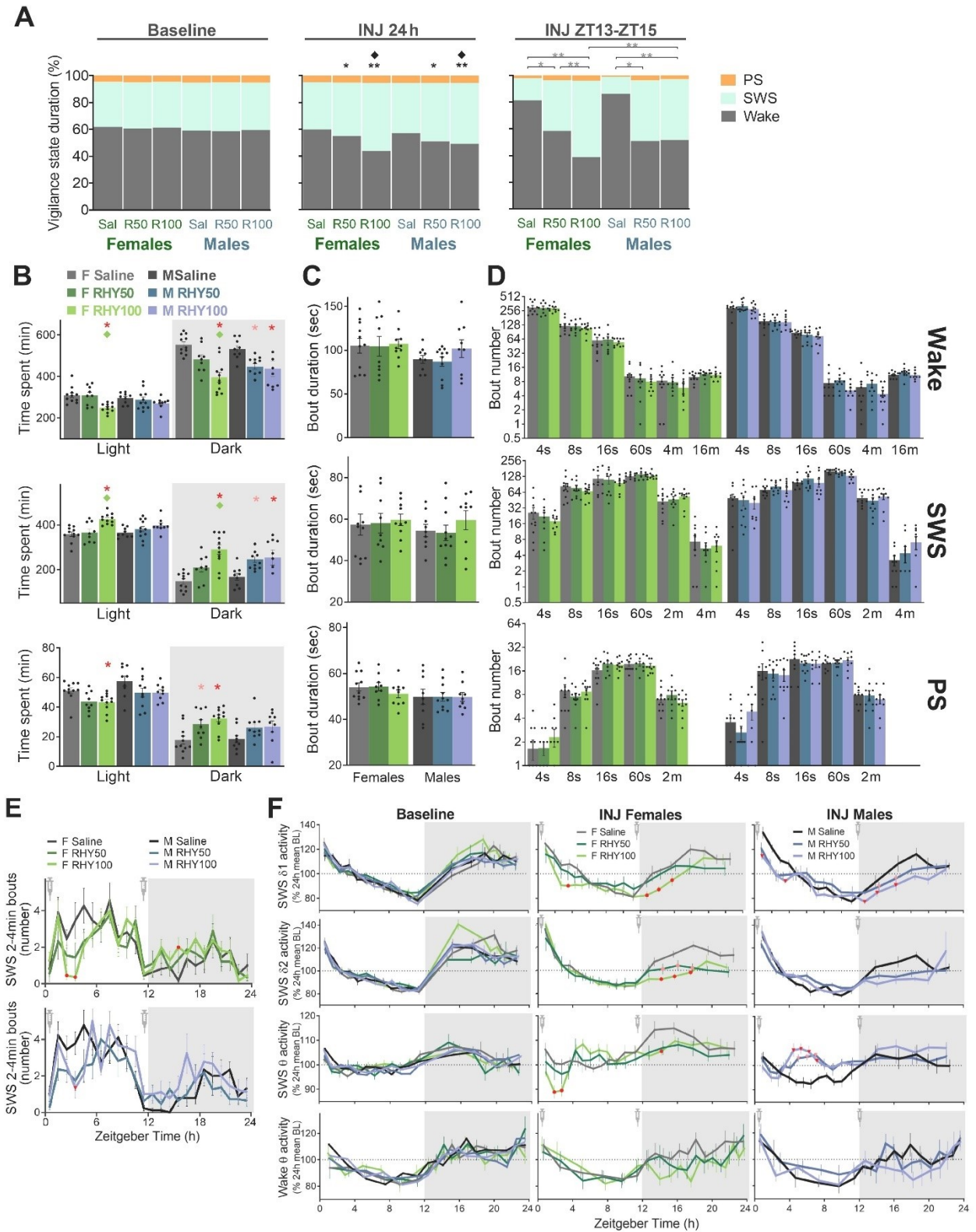


**Figure S1. Groups were similar in baseline, RHY increases SWS more prominently in females, and it modifies 24-h dynamics of ECoG oscillations in a vigilance-state dependent manner.**



(A) Percent time spent in each vigilance state for the 24-h baseline (left panel) or injection (INJ; middle panel) recordings. Significant treatment effect was found for the 24-h in the INJ day for wake and SWS ( $F_{2,54} > 19.2$ ,  $p < 0.00$ ). Black stars indicate significant differences from the vehicle group for RHY100 and RHY50 (post-hoc comparisons  $p < 0.05$ ) always for both wake and SWS; black diamonds indicate significant differences between RHY100 and RHY50 (post-hoc comparison  $p < 0.05$ ) always for both wake and SWS. Treatment-by-sex interaction was found for the average percent time spent in wake in the first hours after the evening injection (between ZT13 and ZT15 in the INJ day:  $F_{2,54} > 3.2$ ,  $p < 0.05$ ; right panel). Grey stars indicate significant post-hoc comparison for wake (\* indicates  $p < 0.05$ ; \*\* indicates  $p < 0.01$ ) between the conditions linked through bars.

(B) Total time spent in wake, SWS and PS calculated separately for the light and dark periods during the 24-h INJ recording. For females, RHY significantly changed wake, SWS and PS for both the light and dark periods ( $F_{2,28} > 4.7$ ,  $p < 0.01$ ). For males, RHY significantly affected wake and SWS only for the dark period ( $F_{2,26} > 4.4$ ,  $p < 0.05$ ). Red and pink stars indicate significant differences from the vehicle group for RHY100 and RHY50, respectively (post-hoc comparisons  $p < 0.05$ ). Green diamonds indicate significant differences between RHY100 and RHY50 (post-hoc comparison  $p < 0.05$ ) in females. Grey backgrounds represent the dark period (also in E).

(C) Mean duration of individual bouts during the baseline day.

(D) Number of bouts of different duration during the baseline day.

(E) Number of longer bouts (2-4 min) of SWS for the INJ day. A significant interaction was found between RHY treatment and hour for males (rANOVA:  $F_{46,598} = 1.8$ ,  $p_{\text{adj}} = 0.004$ ) and females (rANOVA:  $F_{46,644} = 1.5$ ,  $p_{\text{adj}} = 0.03$ ). Red datapoint indicates significant differences between the saline and RHY100 group (post-hoc comparisons  $p < 0.05$ ).

(F) RHY modifies 24-h dynamics of SWS  $\delta 1$ ,  $\delta 2$ , and  $\theta$  activity.

First row: time-course of SWS  $\delta 1$  activity (delta 1: 0.75 - 2Hz). Treatment \* interval interactions were found for both sexes (females:  $F_{34,442} = 2.5$ ,  $p_{\text{adj}} < 0.001$ ; males:  $F_{34,374} = 2.7$ ,  $p_{\text{adj}} < 0.01$ ). Second row: time-course of SWS  $\delta 2$  activity (delta 2: 2.5 - 4Hz). Treatment \* time-interval interactions were found for both sexes (females  $F_{34,442} = 2.6$ , corrected  $p = 0.003$ ; males  $F_{34,374} = 3.4$ , corrected  $p < 0.01$ ). Third row: time-course of SWS  $\theta$  activity (theta: 6 - 9Hz). Treatment \* time-interval interactions were found only for females (females  $F_{34,442} = 3.0$ , corrected  $p < 0.001$ ; males  $F_{34,374} = 2.8$ , corrected  $p = 0.002$ ). Last row: time-course of wake  $\theta$  activity. Treatment \* time-interval interactions were not significant. Red and pink datapoints indicate significant differences compared to the saline group for each interval for the RHY100 and RHY50 groups, respectively (post-hoc comparisons  $p < 0.05$ ).

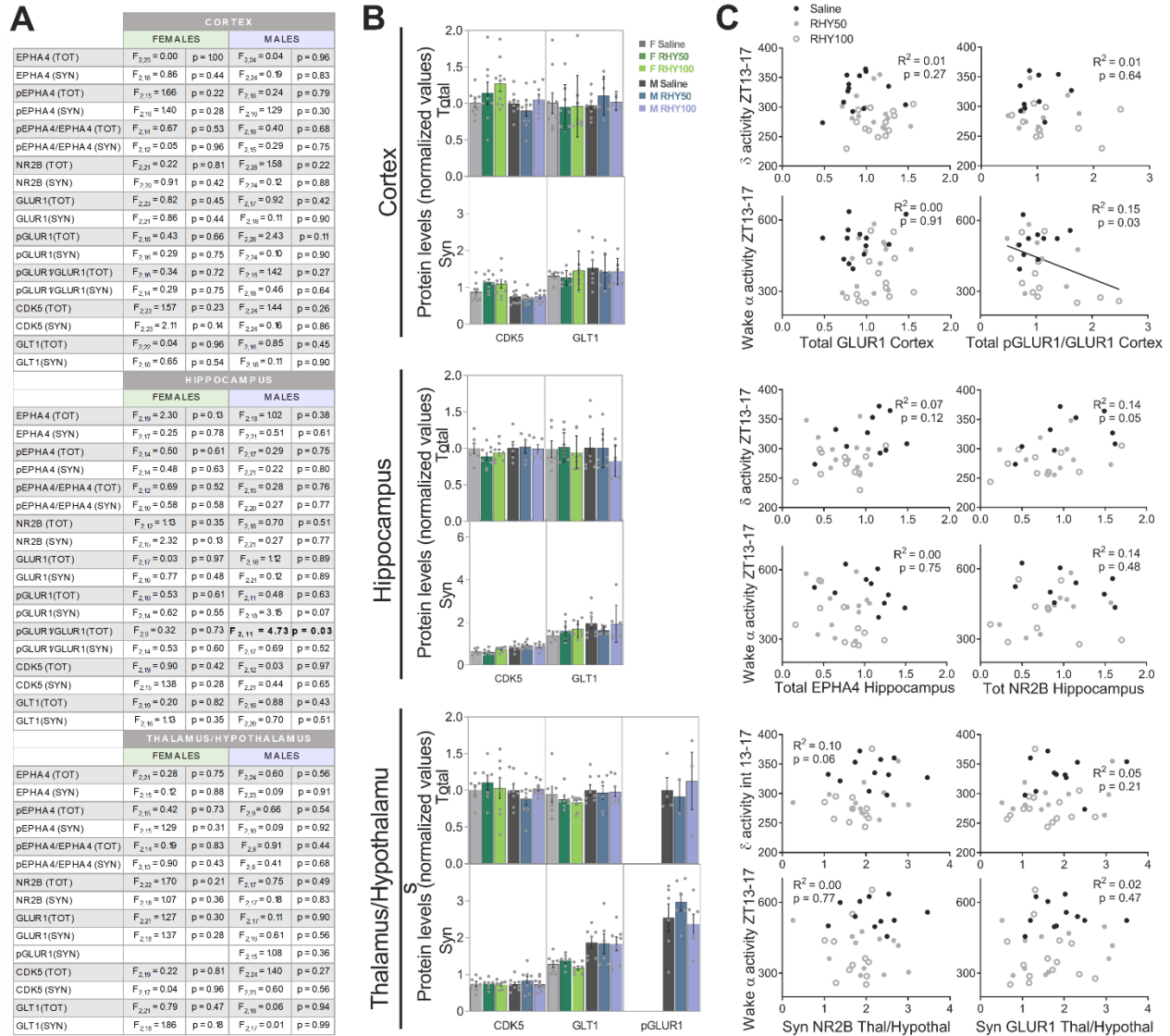


**Figure S2. CDK5 and GLT1 levels were unchanged by RHY and pGLUR1 correlates with decreased wake alpha activity**

(A) Results one-way ANOVAs of the effect of treatment (Saline, RHY50 and RHY100) on protein levels, calculated separately for female and male mice.

(B) RHY did not change the level of CDK5 or GLT1 in the total nor synaptoneurosomal (Syn) protein fractions in the cerebral cortex, hippocampus and thalamus/hypothalamus region (one-way ANOVAs,  $p > 0.05$ ).

(C) Correlations (including both female and male data) between protein levels and SWS delta activity and wake alpha activity. Phosphorylated GLUR1 in the cerebral cortex (total fraction) was negatively correlated with wake alpha activity during the dark period.

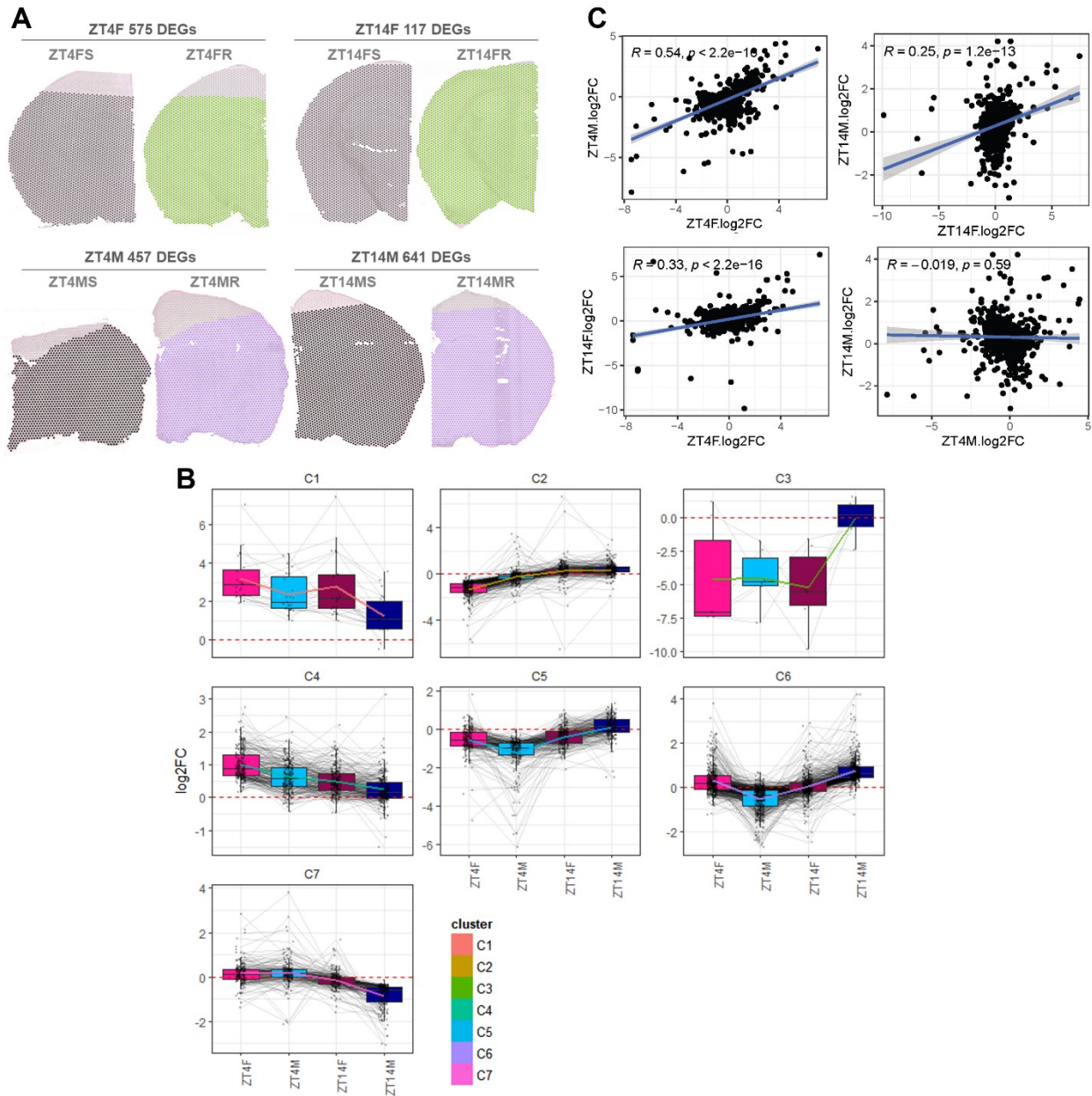


**Figure S3. Analysis of differentially expressed genes (DEGs) and hierarchical DEG clusters.**

(A) Spatial spots used to calculate differentially expressed genes (DEGs) between the different RHY and saline conditions. Common spots between slices were used to conduct comparisons. These common spots are shown in green for females and purple for males for the RHY100 conditions and in dark blue for the saline conditions. The number of DEGs obtained for each comparison is indicated in the top of each pair (FDR < 0.05).

(B) Box plots showing the behavior of genes belonging to seven clusters (C1-C7) obtained from automated clustering of Log2 fold change of DEGs from the four comparisons between RHY100 and saline conditions (ZT4F, ZT4M, ZT14F and ZT14M).

(C) Correlations of changes in gene expression between sexes or between time points. Positive correlations were found for the Log2fold change of DEGs modified by RHY at the same time of injection in different sexes, and for RHY effects on female samples taken at different time-points, but no correlation was found between ZT4M and ZT14M.



comparison datasets (ZT14 DEGs) (E). Enriched terms are colored by related functions and organized by FDR value. The number of DEGs related to each term is indicated.

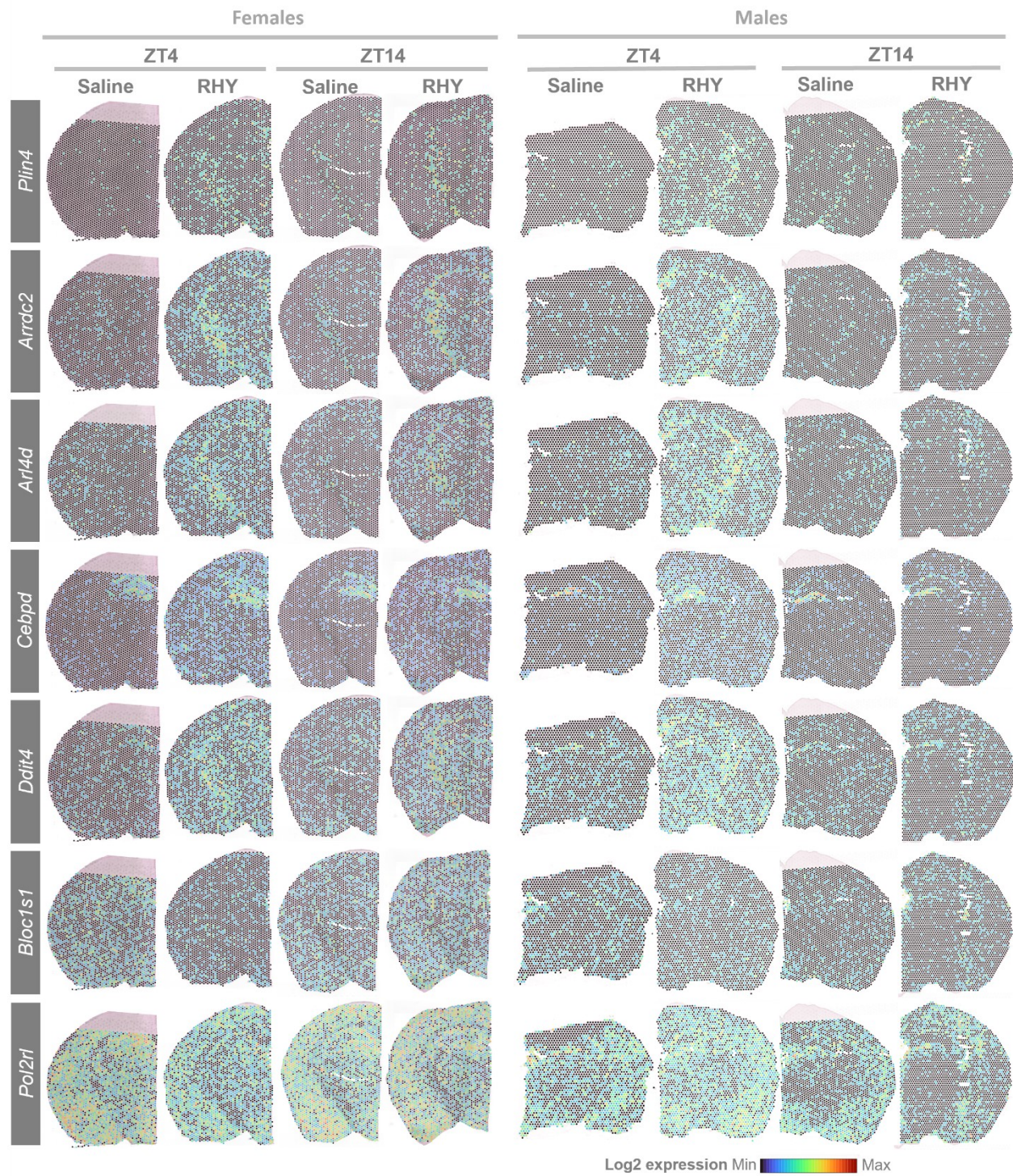


**Figure S5. Spatial gene expression maps of selected DEGs found to be common between ZT4F, ZT4M, ZT14F and ZT14M.** Color of spatial spots indicate Log<sub>2</sub> gene expression under saline and RHY treatments for female and male mice

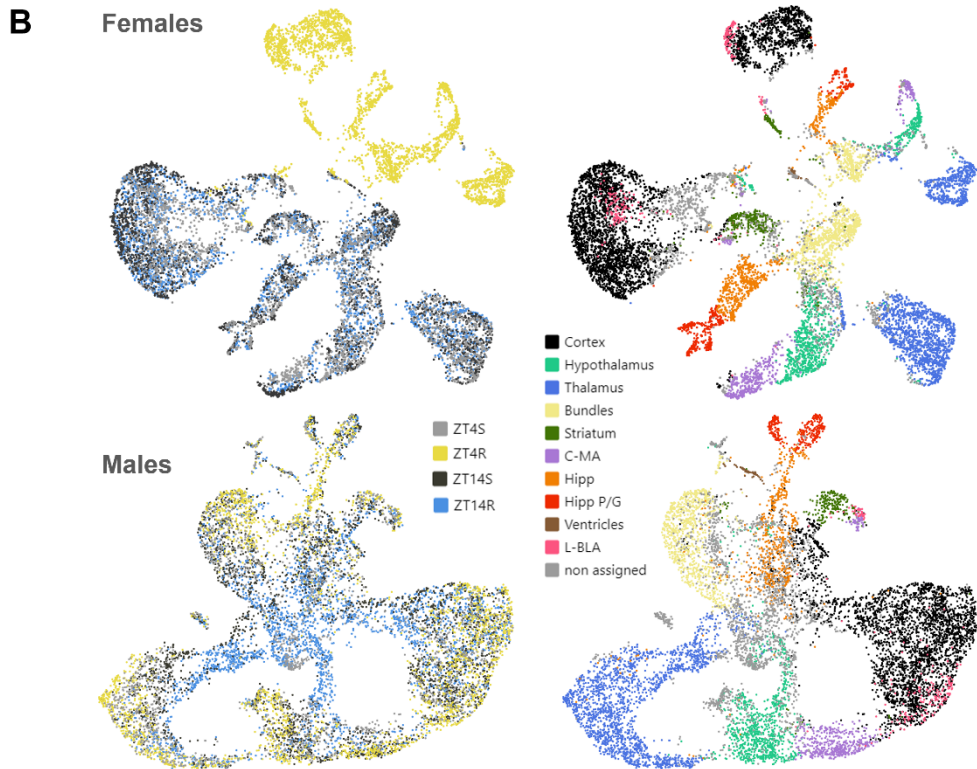
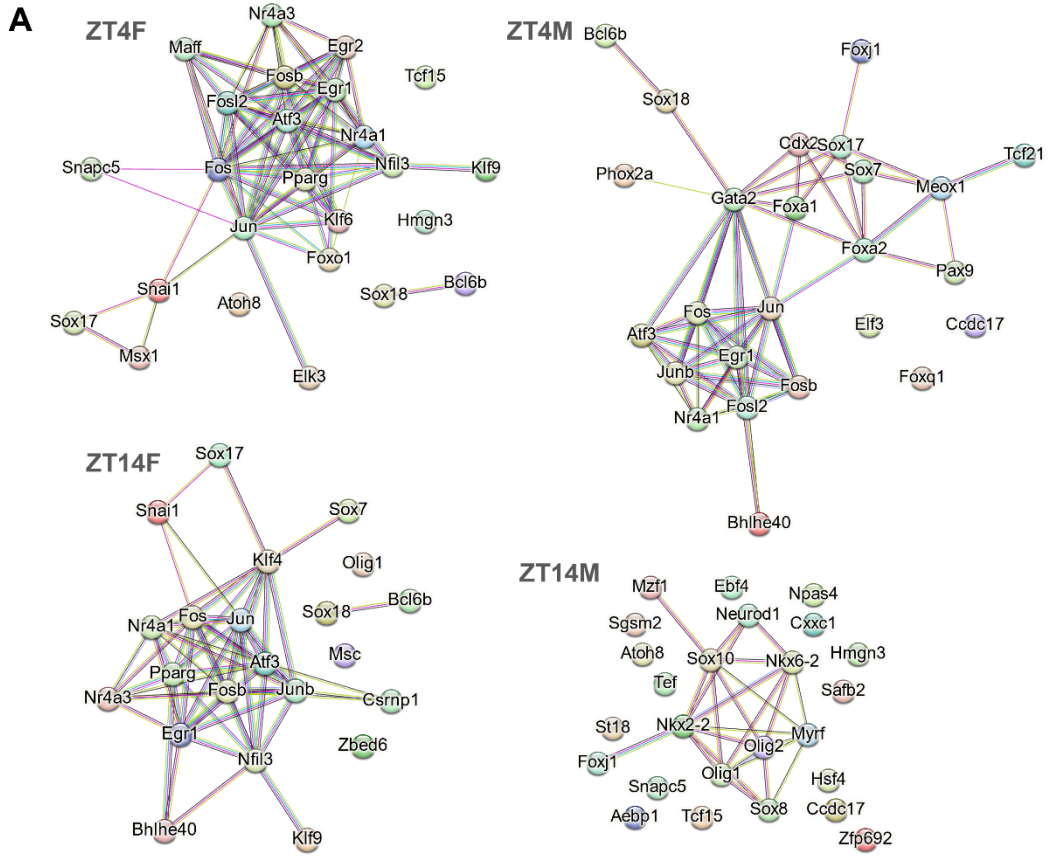




**Figure S6. Transcription factors found to be enriched in ZT4F, ZT4M, ZT14F and ZT14M DEGs, and UMAP clustering of female and male spots of brain regions.**

(A) Interaction networks of the top 25 transcription factors found to be enriched using the CheA3 analysis and ZT4F, ZT4M, ZT14F and ZT14M DEGs. Pink lines denote experimentally determined; blue lines denote links reported from curated databases; black lines denote co-expression; yellow lines denote text-mining evidence; purple lines denote homology domains.

(B) Uniform manifold approximation and projection (UMAP) adequately represents the gene expression data of known brain regions. Top: UMAPs of the four female samples (ZT4S, ZT4R, ZT14S, ZT14R) identifying the samples (left) and brain regions (right). Bottom: same for the four male samples.

# Chapter 6

Discussion

---

Previous studies suggested that the EphA4 receptor may play roles in the regulation of sleep and circadian behaviors. On the one hand, *EphA4* KO mice showed altered circadian rhythms of running wheel activity and reduced number of c-FOS<sup>+</sup> cells in the SCN after a light-pulse (*Kiessling et al., 2018*). Moreover, the 24 h expression of *EphA4*, *EfnA3* and *EfnB2* mRNAs was altered in *Clock* mutant mice, and E-boxes were described in the putative promoter of *EphA4* (*Freyburger et al., 2016*). On the other hand, *EphA4* KO mice showed altered sleep variables, such as less PS time in the light period and altered sleep ECoG oscillations (*Freyburger et al., 2016; Freyburger et al., 2017*). Thus, this thesis investigated whether the genes of *EphA4*, *EfnB2* and *EfnA3* are regulated by the molecular circadian clock machinery, and whether the EPHA4 modulator RHY modifies sleep architecture and oscillations with the additional aim of inquiring potential molecular mechanisms underlying RHY's sleep-inducing effects.

The first study shows that clock transcription factors induce transcriptional activity via upstream regions of the *EphA4*, *EfnB2* and *EfnA3* TSSs *in vitro* (Chapter 4). It supports our hypothesis 1 and signifies that the mRNA expression of these Eph/Ephrin components may be rhythmic. To assess whether this clock regulation would induce rhythmic protein levels, EPHA4 and EFNB2 were measured at different times of the day in the SCN and PFC of mice which had been maintained in constant darkness. Against hypothesis 2, neither of these proteins showed time-dependent expression in these two brain tissues, suggesting that clock transcription factors may induce their rhythmic expression in other tissues, or that the effect of clock factors in these putative promoter regions does not translate into rhythmic protein.

The second project demonstrates that systemic injections of RHY induce sleep in mice (Chapter 5) and answers our hypothesis 3. RHY enhanced SWS time, and even though it also enhanced PS in the dark (active) period, it reduced it in the light (rest) period. Moreover, RHY reduced alpha activity during wakefulness and altered the 24h distribution of SWS delta and sigma activity. All these effects on sleep architecture and the ECoG were more significant in females, which responds to our hypothesis 4. Against hypothesis 5, RHY did not modify the levels of EPHA4 or its phosphorylation 13h after injection in samples of cerebral cortex, hippocampus or thalamus-hypothalamus. Analysis of the brain transcriptome revealed that RHY modifies the expression of transcripts linked to sleep and pituitary functions in the hypothalamus, but that it also

affected the mRNA levels of genes related to apoptotic and immune responses broadly throughout the brain (results which prove our hypothesis 6).

This thesis compiles different approaches to inquire into how cell adhesion molecules, and, particularly, the Eph/Ephrin system, can have roles in circadian and sleep behaviors (**Figure 6.1**). It demonstrates that the clock machinery can act on DNA regulatory elements for synaptic components fundamental to neurotransmission. This discussion will highlight how clock transcriptional regulation can have crucial implications not only for the regulation of neuronal activity and the regulation of circadian rhythms and sleep, but also for cognition and disease. In addition, it will suggest implications of the changes on gene expression induced by RHY, suggesting potential mechanisms and follow-up experiments. We expect with this to expose the relevance of our results for understanding how *Uncaria* drugs can affect sleep and brain activity. Finally, the discussion also emphasizes advantages of using spatial transcriptomic approaches to narrow into drug mechanisms and to uncover brain region dependent processes.

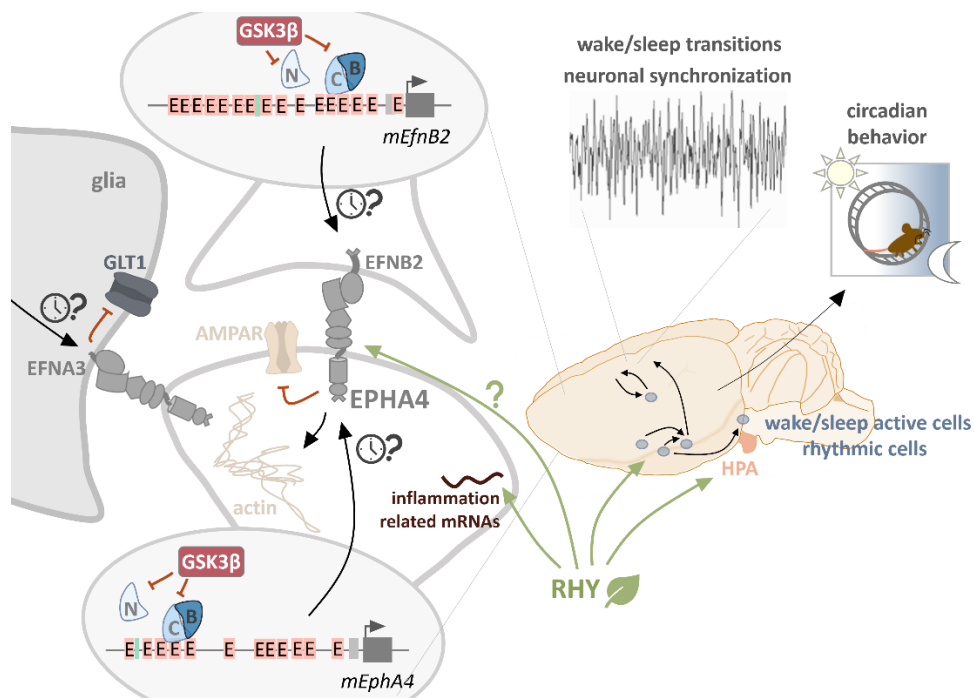


**Figure 6.1. The core clock machinery may control EphA4 roles in sleep and circadian behavior and the EphA4 modulator RHY induces sleep.** CLOCK or its homologue NPAS2 (C and N) and BMAL1 (B) increase *EphA4*, *EfnB2* and *EfnA3* mRNA *in vitro*. The negative regulator of the clock transcription factors GSK3 $\beta$  inhibits this induction. This regulation of the Eph/Ephrin system by the clock may explain previously observed circadian and sleep phenotypes in mice (Freyburger *et al.*, 2016; Freyburger *et al.*, 2017; Kiessling *et al.*, 2018). RHY, an alkaloid that reduces EPHA4 activation in mice, increases sleep time and modified sleep architecture and brain oscillations that are

indicative of cognitive processes. RHY modified transcripts linked to inflammatory pathways throughout the brain and modified the gene expression of transcripts related to sleep and for peptides involved in the hypothalamic-pituitary axis (HPA).

## 6.1 EphA4 in sleep and circadian regulation

This first section of the discussion will present the relevance of a clock regulation of the Eph/Ephrin system and how the Eph/Ephrin can impact circadian and sleep behaviours.

### 6.1.1 The molecular circadian clock regulates *EphA4*, *EfnB2* and *EfnA3*

As discussed in Chapter 1, the core clock transcription factors regulate the expression of synaptic elements, which may provide a time-dependent regulation of neurotransmission (*Hannou et al., 2020*). In fact, the expression of genes with functions linked to synaptic potentiation peaks at dusk, just before the mouse active period (*Noya et al., 2019*). Our results show that clock transcription factors may induce a rhythmic expression of *EphA4*, *EfnA3* and *EfnB2*, which are involved in neurotransmission. This supports previous findings from our group showing that *Clock<sup>Δ19</sup>* mice (dominant negative mutants) show lower expression of *EphA4*, *EfnB2* and *EfnA3* (*Freyburger et al., 2016*). Accordingly, we propose that the core clock machinery may regulate, for instance, spine morphology and the presence of glutamate receptors and transporters at the synapse by controlling the levels of Eph/Ephrin components at different times of the day. Here we further described the functionality of the E-boxes by revealing that the mutation of four E-boxes (CANNTG to GCTAGT) on distal regions of the *EphA4* promoter, reduces the transcriptional activation induced by the clock transcription factors. Nevertheless, the E-box sequences were only mutated for this distal sequence (*EphA4<sub>D</sub>*), and the effect of the clock machinery on *EfnB2* and *EfnA3* should be assessed as well with mutated inserts. We are currently performing these assays at the lab, together with additional experiments with a longer sequence of the *EphA4* promoter which englobes both the distal and proximal sequences studied in this thesis. This will demonstrate whether the studied inserts have different contributions to transcription when taking a longer proportion of the DNA, more comparable to *in vivo* conditions.

The experiments assessing the effect of the clock transcription factors were performed exclusively in COS7 cells. Therefore, it is crucial to investigate if clock dimers induce transcription of Eph/Ephrin components in other cell types and whether this regulation is functional *in vivo*. Our measures of protein levels of EPHA4 and EFNB2 suggest that the clock regulation of their genes

would not translate into rhythmic protein levels in mouse SCN and PFC. This section will discuss how a clock transcriptional regulation of the Eph/Ephrin system may depend on the brain region, cell type or cell compartment. The section also presents potential implications of GSK3 $\beta$  for the Eph/Ephrin regulation, how the clock machinery may also provide a homeostatic regulation of the Eph system, and the implication of the clock regulation for pathological conditions.

#### **6.1.1.1 Regulation by clock transcription factors may be restricted in time and space**

In mammals, the initiation of gene expression is regulated notably by chromatin modulation, by DNA sequences that determine the recruitment of the RNA polymerase II and cofactors, and by the availability of these factors and regulatory protein complexes. The promoter region is a DNA region upstream of the TSS composed of a core promoter (sufficient to trigger transcriptional initiation and, in general, immediately upstream of the TSS) plus the proximal promoter (immediately upstream of the core promoter) (*Haberle and Stark, 2018*). Enhancers (typically 100-1000bp in length) are distant regions that regulate the activity of promoters (*Spitz and Furlong, 2012; Furlong and Levine, 2018*). Eukaryote genes have alternative promoters and multiple enhancers, which provide accurate regulation across developmental stages and tissues (*Furlong and Levine, 2018; Wang et al., 2022*). Moreover, promoters of some genes can act as enhancers of others (*Dao et al., 2017*). Therefore, whether the proximal and distal promoter regions of *EphA4*, *EfnB2* and *EfnA3* have distinct functions in different tissues and developmental stages should be inquired. Differences in transcription across maturation might be particularly relevant for the EphA4/Ephrin system, which, as already discussed, is regulated by transcription factors linked to development. Our results suggest that the clock machinery may provide additional rhythmic regulation of transcription, which could likely be restricted at some stages of development and delimiting tissue boundaries. This can be further modulated by additional transcription factors and by the availability of CLOCK, BMAL1 and NPAS2. For instance, NPAS2 levels in mice, increment just before birth and peak in the first postnatal week (*Zhou et al., 1997*), which could suggest that *EphA4* and *EfnB2*, but particularly *EfnA3* are regulated by clock factors at this moment of development. Moreover, data by Wen and collaborators suggests that *EphA4* may follow a daily rhythm of expression in astrocytes and neuronal populations surrounding the SCN in the hypothalamus (*Wen et al., 2020*). Thus, clock transcription factors may induce rhythmic *EphA4*, *EfnB2* and *EfnA3* uniquely in some cell types or tissues. Astrocyte activity is in antiphase with that of neurons in the SCN, and astrocyte *Bmal1* is crucial for the SCN functioning (*Barca-Mayo et al.,*

2017; Brancaccio et al., 2017). Therefore, future studies should examine whether the effects of EphA4 in circadian behavior are mediated by transcriptional regulation of *EphA4* (or ligands like *EfnB2* or *EfnA3*) in SCN astrocytes. In fact, if protein levels were only rhythmic in astrocytes or neurons, it might explain the lack of oscillation in our homogenized SCN punches (Chapter 4).

As mentioned in other sections, rhythms of mRNA do not necessarily imply oscillating protein levels. In mouse forebrain synapses, 70% of the rhythmic mRNA shows rhythms in protein expression (Noya et al., 2019). Moreover, even though 6-15% of transcripts are rhythmic in a given tissue, studies in mouse liver show that only 20% of this rhythmicity is provided by rhythmic transcription and only 40% of rhythmic transcription may correlate with rhythmic transcripts (Koike et al., 2012; Menet et al., 2012). Therefore, our results could be complemented with, firstly, *in vitro* continued luminometry (Izumo et al., 2003), which would answer whether the transcriptional activity of clock factors induces rhythmic gene expression. Moreover, cell-type specific rhythms in mRNA and protein levels should be investigated with flow cytometry and more sensitive techniques for protein quantification such as mass spectrometry. Moreover, these techniques would allow to discern whether potential rhythms in mRNA and protein levels *in vivo* are cell-type specific. Nevertheless, even though the transcriptional effect of clock factors would not translate into rhythmic EPHA4 or EFNB2, this cell adhesion system may still have relevant roles in circadian regulation. For example, global EFNB2 phosphorylation in mouse forebrain synapses was rhythmic (Bruning et al., 2019), and future studies could investigate whether the oscillatory activity of Eph/Ephrin components is restricted to some brain regions.

### 6.1.1.2 Transcriptional modulation by GSK3

GSK3 $\beta$  regulates circadian and sleep behaviour, and our results show that this kinase regulates *EphA4* and *EfnB2* expression *in vitro*. GSK3 $\beta$ , with over a hundred substrates, has diverse roles ranging from implications in glycogen synthesis to neuroplasticity in the central nervous system (Beurel et al., 2015). It is broadly expressed in the brain and modulates synaptic plasticity by regulating axonal growth, but also potentially modulating synaptic strength, what has linked the kinase to cognitive impairments (Kim et al., 2006; Rui et al., 2013; Xing et al., 2016; Besing et al., 2017; Jaworski et al., 2019).

As discussed earlier in thesis, GSK3 $\beta$  can phosphorylate core clock components, including BMAL1, PER2, CRY2 and REV-ERB- $\alpha$ , and regulate their location or degradation (Harada et al.,

2005; Iitaka et al., 2005; Yin et al., 2006; Sahar et al., 2010). GSK3 $\beta$  phosphorylation at its serine-9 (so, GSK3 $\beta$  inhibition) follows daily variation in the mouse PFC, SCN, hippocampus and liver (Iitaka et al., 2005; Kinoshita et al., 2012), and circadian oscillation of pS9-GSK3 $\beta$  has been found in the mouse SCN and CA1 (Besing et al., 2015; Besing et al., 2017). The relevance of these regulations is confirmed by multiple studies showing that modulating GSK3 $\beta$  has effects on rhythmicity. GSK3 $\beta$ <sup>+/-</sup> mice have longer periods of running activity when housed under constant darkness (Lavoie et al., 2013). A GSK3 $\beta$  inhibitor enlarged the amplitude and shortened the PER2 period in SCN slices and in hippocampus slices and in the mouse DG (Besing et al., 2015; Besing et al., 2017; Liska et al., 2022), and modifies LTP in the dark (but not light) period (Besing et al., 2017). Likewise, the mood stabilizer lithium (inhibitor of GSK3 $\beta$ ), induces Ser-9 phosphorylation, removes rhythmicity of pS9-GSK3 $\beta$  and p-PER2 in the mouse SCN, enlengthens the PER2 period and enlengthens running wheel circadian rhythms in mice (Iwahana et al., 2004; Iitaka et al., 2005; Kinoshita et al., 2012; Li et al., 2012). Therefore, given that *EphA4* KO mice show longer periods in DD (Kiessling et al., 2018), some of the actions of GSK3 $\beta$  on maintaining circadian rhythmicity could be via its actions on EphA4/Ephrin components. This might be particularly relevant to study in some cell types in the hippocampus, given the high expression of EphA4 in this region. For instance, it could modulate EphA4 levels (in a rhythmic or non-rhythmic manner) and modulate spine retraction.

GSK3 $\beta$  has important functions in development and modulate axon growth and cell polarity (Etienne-Manneville and Hall, 2003; Jiang et al., 2005; Kim et al., 2006; Rui et al., 2013). As described earlier in this thesis, EphA4 is also crucial for development, axon growth and pathfinding. Thus, it would be interesting to determine whether some GSK3 $\beta$  functions in cell development, migration or adhesion require the regulation of *EphA4* at the transcriptional level. Furthermore, GSK3 $\alpha/\beta$  modulate LTD and LTP, dendrite growth and maturation (Peineau et al., 2007; Rui et al., 2013; Xing et al., 2016; Besing et al., 2017; Dudilot et al., 2020), and higher levels of EPHA4 activation are linked to spine retraction and AMPA receptor internalization (Murai et al., 2003; Fu et al., 2011). In addition, the downregulating effect of GSK3 $\beta$  on *EfnB2* may induce additional mechanisms for plasticity, given that EFN2 triggers NR2B phosphorylation and stabilizes AMPA receptors at the synapse (Bouzioukh et al., 2007; Essmann et al., 2008; Slack et al., 2008). Accordingly, we suggest that GSK3 $\beta$  may impact neuroplasticity by regulating the Eph/Ephrin system.



### 6.1.1.3 Clock transcriptional regulation for C and S hubs

As already discussed in the thesis, transcriptomic studies reveal that sleep deprivation (SD) modifies the expression of clock factors (including *Npas2*, *Clock*, *Per1-3*, *Dbp*) (Maret et al., 2007; Mongrain et al., 2010; Guo et al., 2019; Hor et al., 2019). SD also reduces the DNA binding of BMAL1 and CLOCK/NPAS2 to *Dbp* in the mouse cerebral cortex (Mongrain et al., 2011). In addition, CLOCK/NPAS2 dimerization with BMAL1 and their DNA-binding is modified by the redox state (which is also altered by SD and regulates CA1 membrane potential in a time-of-day dependent manner) (Rutter et al., 2001; Hsu et al., 2003; Harkness et al., 2019; Naseri Kouzehgarani et al., 2020; Vaccaro et al., 2020). Accordingly, the effect of clock factors on *EphA4*, *EfnB2*, and *EfnA3* transcription may converge information from both circadian (process C) and homeostatic (process S) regulation and may be involved in circadian and sleep phenotypes observed in *EphA4* KO mice (Freyburger et al., 2016; Freyburger et al., 2017; Kiessling et al., 2018). It could, in addition, explain why *EphA4* mRNA levels were higher in the thalamic-hypothalamic samples of sleep-deprived mice (Freyburger et al., 2016). In fact, functions linked to neurotransmission and plasticity are modulated both by sleep/wake (S) (Cirelli et al., 2004; Maret et al., 2007; Mongrain et al., 2010; Bruning et al., 2019) and by clock factors (C) (Klugmann et al., 2006; Parekh et al., 2019). Therefore, it would be provoking to investigate whether the clock control of the Eph/Ephrin system may contribute to a C and S synaptic regulation of neurotransmission. Interestingly, SD reduced the binding of NPAS2 (but not the one of CLOCK) on *Per2* (Mongrain et al., 2011). This highlights that some dimers can be more affected by SD than others, which could affect differently, for example, *EfnA3<sub>D</sub>* (which was uniquely activated by NPAS2) than *EphA4* promoter regions. Similarly, GSK3 $\beta$  shows daily expression, its activity is modified by SD and downstream of dopamine and 5-HT signaling (Benedetti et al., 2004; Iwahana et al., 2004; Iitaka et al., 2005; Beaulieu et al., 2009; Bellet and Sassone-Corsi, 2010; Lavoie et al., 2013; Bruning et al., 2019). Therefore, it would be interesting to first assess using chromatin immunoprecipitation, if clock transcription factors bind to the *EphA4*, *EfnB2*, and *EfnA3* promoters *in vivo*, and whether SD modifies their binding.

Interestingly, in our study in Chapter 5, the transcriptome was assessed under a situation of sleep surplus (after RHY-induced sleep), and the expression of clock genes was not modified. Even though it has been shown that the SD-dependent alteration of the clock transcription factors seems glucocorticoid-dependent (Mongrain et al., 2010; Curie et al., 2013), the implication of other

homeostatic mechanisms remains unknown. Therefore, it will be important to further investigate which other homeostatic processes (e.g., metabolic, inflammatory) regulate the clock machinery and how this determines the clock control of synaptic components.

#### **6.1.1.4 Implication of clock regulation in disease and ageing**

Even though this thesis has focused on circadian and sleep regulation, circadian rhythms adjust the time for many other functions in the organisms, including blood pressure, feeding and immune responses (*Takahashi et al., 2008; Cermakian et al., 2022*). For example, *BMAL1* polymorphisms are associated with susceptibility to hypertension and diabetes (*Woon et al., 2007*) and chronodisruption is considered a cancer risk (*Pariollaud and Lamia, 2020*). Therefore, considering the roles of EphA4 and Ephrins, their clock regulation may impact circadian functions in cardiovascular, immune functions and tumor growth. Moreover, circadian disruptions and clock gene polymorphisms (e.g., in *NPAS2*) have been highly linked to mental disorders including anxiety, MDD and bipolar disorder (*McChung, 2007; Soria et al., 2010*). Importantly, as mentioned in the introduction, EphA4 protein levels (or its phosphorylation) are higher in the brain of mouse models of depression and post-mortem brain tissue of MDD patients (*Zhang et al., 2017; Li et al., 2022b*), suggesting that it would be relevant to investigate whether the clock regulation of Eph/Ephrin genes contributes to these pathologies. In addition, polymorphisms in some clock genes are associated to sleep/circadian disorders, such as *PER2* and *CRY2* (linked for the familial advanced sleep phase syndrome, FASPS) and *DEC2* (associated to the human familial natural short sleep phenotype; (*Shi et al., 2017*). Therefore, alterations in the core clock machinery in these conditions may also induce altered transcription of *EphA4*, *EfnB2* and *EfnA3* in disease. Moreover, GSK3 $\beta$  activity has been implicated in depression, bipolar disorder, and Alzheimer's disease (*Li and Jope, 2010; Beurel et al., 2015*). For instance, chronic restraint stress increased GSK3 $\beta$  phosphorylation and altered *PER2* rhythms in the mouse SCN, PFC and hippocampus (*Kinoshita et al., 2012*). In addition, lithium (inhibitor of GSK3 $\beta$  and common treatment for bipolar disorder), could recover the stress-induced alterations in *PER2* and GSK3 phosphorylation, and ameliorates cognitive symptoms in Alzheimer's disease and Fragile X syndrome patients (*Kinoshita et al., 2012; Beurel et al., 2015*). Therefore, the control of *EphA4/Efns* transcription by GSK3 $\beta$  can also link this cell adhesion system to these diseases and their treatment. In sum, understanding whether the clock machinery controls the expression of EphA4 and Ephrins in particular brain regions or in

response to specific conditions such as neuronal activation, may help identify why the Eph/Ephrin system is altered in some of these pathologies.

### **6.1.2 Potential roles of EphA4/Ephrins in circadian and sleep behavior**

As suggested by the EPHA4 molecular functions, the clock-dependent regulation of this adhesion molecule may impact circadian rhythms and sleep in various manners. This section summarizes EphA4/Ephrin functions which could, according to our results, be under clock control. To begin with, EPHA4 induces spine retraction and AMPA receptor internalization; EFNB2 regulates AMPA and NMDA receptors; and the presence of EFNA3 reduces GLT1 at the synapse (*Murai et al., 2003; Essmann et al., 2008; Slack et al., 2008; Filosa et al., 2009; Fu et al., 2011*). Moreover, EPHA4 (and some ligands) can organize in lipid rafts, which determine the triggered downstream responses (*Yumoto et al., 2008; Pan et al., 2010; Averaimo et al., 2016*). A rhythm for these functions should impact neuronal synchronization, so important in circadian rhythms and sleep. Furthermore, EPHA4 receptors (like other Eph) can oligomerize in the membrane (*Light et al., 2021*), which may provide a time-escalating effect of these receptors. As discussed earlier in this thesis, recent hypotheses in circadian (and sleep) research evoke that accumulative phosphorylation in proteins may provide progressive forms of regulation (homeostatic or time-driven). Therefore, EPHA4 being a tyrosine kinase receptor with multiple phosphorylation sites (*Singla et al., 2011*), it would be relevant to investigate whether EPHA4 phosphorylation is time-dependent in some brain regions and whether this determines circadian (or sleep) behaviors. Previous research shows that EPHA4 phosphorylation was low in adult mice compared to P10, but the study did not compare different sampling times (*Murai et al., 2003*). The same authors hypothesize that EPHA4 is not constitutively engaged with Ephrins in the hippocampus, but results could vary across the 24 hours. Other activity-dependent regulatory mechanisms may also provide positive (or negative) reinforcement to the rhythms of cell activity. For instance, neuronal activity induces the cleavage of EPHA4 by the  $\gamma$ -secretase (*Inoue et al., 2009*). Moreover, all EPHA4, EFNB2 and EFNA3 are found in astrocytes (*Murai et al., 2003; Goldshmit et al., 2006; Ashton et al., 2012*). As discussed above, clock regulation of these membrane molecules could provide circadian functions to this diffuse brain matrix and have important roles in synchronizing brain functions. In fact, astrocytes are fundamental for the SCN functioning and to track sleep need (*Barca-Mayo et al., 2017; Brancaccio et al., 2017; Ingiosi et al., 2020*). It is also important that EphA4/Ephrin signaling may modify downstream effectors like kinases (e.g., CDK5,

ERK/MAPK) (Fu et al., 2007; Zhou et al., 2007; Shin et al., 2008; Goldshmit and Bourne, 2010; Zhou et al., 2012; de Marcondes et al., 2016; Shu et al., 2016; Zhang et al., 2017) but also transcription factors (e.g., MAT2B TEAD1) (Freyburger et al., 2016; Cayuso et al., 2019), which could disarrange the time for other cellular functions. Finally, it is important to remind the numerous implications of EphA4 (and many Eph/Ephrin family members including EfnB2) in development, functions which may require or benefit from being time-adjusted.

## **6.2 RHY induces sleep and affects transcripts linked to sleep control**

### **6.2.1 RHY enhances sleep time and modifies sleep oscillations in rodents**

RHY is a main oxindole alkaloid in *Uncaria* plants, which are plants highly used in traditional Chinese and Japanese medicines. Chapter 2 compiled that drugs containing *Uncaria* ameliorate sleep in humans, for instance, by enlarging sleep time and reducing latency in healthy individuals compared to a control treatment (Aizawa et al., 2002). Studies also showed that Yokukansan (YKS, a plant blend containing *Uncaria*) ameliorates sleep problems in diverse pathological conditions (although not placebo-controlled): it enhanced sleep quality in patients with insomnia and REM sleep behavior disorder; and increased sleep time and reduced sleep latency in dementia patients (Shinno et al., 2008b; Ozone et al., 2012; Matsui et al., 2019; Ozone et al., 2020). Similarly, some studies report that YKS also increases sleep time in mice and rats (Jeenapongsa and Tohda, 2003; Egashira et al., 2011; Nagao et al., 2014; Murata et al., 2020). Only one study had investigated the sleep-inducing effects of RHY and reported that RHY itself can increase sleep time in rats and enhance the sleep-inducing effect of pentobarbital in mice (Yoo et al., 2016). Our study in Chapter 5 is first showing that RHY itself induces sleep in mice, that it particularly enhances SWS and with magnified effects in the dark period, when animals are typically awake. Over the 24 hours, RHY induced a 41% increase (3.5 hours) in SWS in females and a 22% increase (2 hours) in males. These hypnotic effects go in agreement with previous research studying *Uncaria* effects. On the other hand, the effects of RHY on inducing particularly short bouts of SWS or its effects on reducing PS, should be further regarded in forthcoming investigations because human studies with *Uncaria* do not report neither reduced PS nor enhanced SWS fragmentation (Aizawa et al., 2002; Shinno et al., 2008b; Shinno et al., 2008a; Ozone et al., 2012). Given the scattered sleep of rodents (and most mammals) and the monophasic sleep of humans, it is likely that the effects on sleep fragmentation differ between mouse and human. For

instance, RHY may differently modify the levels of sleep-inducing molecules (which may accumulate at different rates in monophasic and polyphasic species) or differently affect the activity of sleep/wake-inducing neurons (which could sense homeostatic needs at different rates in distinct species) (*Phillips et al., 2010*). In any case, the sleep-inducing effects of RHY may provide restorative benefits, which should be studied under some pathological conditions with sleep comorbidities.

Both doses of RHY reduced PS in the light period (particularly in females), but increased PS in the dark. At a first glance, the reduced PS in morning injections should be detrimental for animal's memory, given that PS has roles in procedural and emotional memory (*Nishida et al., 2009; Boyce et al., 2016; Hunter, 2018; Izawa et al., 2019*). It could be intriguing to explore if there are links between this decrease in PS and the benefits of RHY observed in stress-induced depression-like symptoms (*Zhang et al., 2017*). Depression, although generally being characterized by insomnia and reduced SWA, is associated with enhanced PS, and most antidepressants reduce PS (*Riemann et al., 2020*).

#### **6.2.1.1. RHY modifies brain oscillations in different vigilance states**

Studies preceding ours did not investigate how RHY (or *Uncaria*) modifies the distribution of sleep across the 24 hours, or whether this treatment modifies neuronal synchrony during sleep. Determining whether a drug enhances sleep is not sufficient to describe its advantages and the effects on brain activity should be always characterized. This is particularly true in sleep medicine. The activity in different frequencies of brain oscillations during wakefulness and sleep can reflect changes in neuronal plasticity which are correlated with cognitive processes and performance (*Voloh et al., 2015; Gronli et al., 2016; Yu et al., 2018*). SWA and spindle activity during SWS are associated with off-line plastic processes which benefit learning in both humans and mice (*Heib et al., 2013; Kim et al., 2019; Muehlroth et al., 2019; Fernandez and Luthi, 2020*). PS theta synchronization has roles for learning and emotional memory (*Nishida et al., 2009; Boyce et al., 2016*). Interestingly, in our study RHY decreased the power of SWS delta activity (in the dark period) and altered SWS sigma and theta activity after both morning and evening injections. Interestingly, RHY causes a delayed increase of SWS sigma and theta activity between ZT5 and ZT8, in contrast to a faster increase in sleep time. Thus, it would be interesting to investigate whether the effects on this frequency range originate from impacts of RHY in particular brain

structures. Furthermore, these effects on sleep oscillations could indicate that, even though RHY enhances sleep time, the treatment could impact sleep-dependent cognitive processes and, potentially, learning. Moreover, RHY reduced alpha activity during wakefulness throughout the 24 hours. The role of alpha activity during wake is associated to physiological processes and cognitive engagement in humans and rodents (*Bazanov and Vernon, 2014*). While alpha activity in humans has been largely attributed to be characteristic of closed-eyes wakefulness and higher during less-active wakefulness, studies in both humans, rats and mice also show that alpha activity is associated to sensory processing (*Broussard and Givens, 2010; Gronli et al., 2016; van Diepen et al., 2016; Del Percio et al., 2017*). Therefore, RHY may also modify the wake-associated sensory processing or engaging.

Besides, the brain oscillatory activities can be indicative not only of cognition but also of other physiological processes. Transition from SWS into PS are characterized by more prominent sigma activity (*Franken et al., 1998; Astori et al., 2011; Wimmer et al., 2012; Carrera-Canas et al., 2019*). Thus, the decrease in PS at the beginning of the light period may be associated to the disrupted SWS sigma and theta power. Furthermore, faster delta activity (delta-2; 2.5-4Hz) has been shown to be driven more by homeostatic sleep pressure (process S) than the slower delta (delta-1; 0.75-2Hz) (*Hubbard et al., 2020*). RHY reduced the power of both delta-1 and delta-2 similarly in males and females, with a decrease in the dark period which may be indicative of both changes in neuronal synchrony and reduced sleep pressure. Interestingly, RHY decreased delta-1 activity at ZT0 (immediately after the first injection) more pronouncedly in males. This may indicate that some of the RHY downstream effectors involved in delta-1 are more critical in male mice at this time-point. This contrasts with the rest of RHY effects on sleep, which were more pronounced in females than males (e.g., percentage of time spent in SWS, delta activity in the dark phase, wake alpha activity). Therefore, even though we could not identify genes (neither associated cellular pathways) which could underly effects in particular frequency ranges, it would be interesting to analyse whether some RHY targets might have different abundance/activation between sexes. For instance, *CACNA1C* (gene for the L-VGCC subunit Cav1.2) polymorphisms were linked to sleep latency only in infant males but not female (*Kantojarvi et al., 2017*), and L-VGCCs current is modified by RHY in rat cortical neurons (*Kai, 1998*). Our lab will soon inquire with the results collected in this thesis whether the effects of RHY on reducing delta activity are linked to a decrease in amplitude (indicative of the amount of synchronized cell firing), frequency

(indicative of the duration of cortical up and down states and cell synchronization) or density (indicative of the number of slow waves per minute induced by the drug). This will be done by a semi-automated detection similarly to previous analyses performed by the group (*Freyburger et al., 2017*). Moreover, analysing how RHY modifies these parameters particularly for delta-1 may help pinpoint potential mechanisms underlying the different effects observed for this frequency range in the early light period. In any case, future research should analyse whether RHY modifies sleep oscillations in humans similarly to our findings in mice.

RHY increased SWS but did not promote higher SWA. One of the most faced difficulties in sleep pharmacology is that most sleep-inducing drugs are not able to enhance delta-rich restorative sleep (*Winsky-Sommerer, 2009*). Therefore, it is interesting to evaluate if other sleep-inducing drugs act through distinct or novel mechanisms. For instance, the optogenetic activation of the GABAergic cells in the TRN induced SWS time and SWA (*Lewis et al., 2015; Fernandez et al., 2018*), and deletion of the  $\alpha 3$  subunit of GABA<sub>A</sub> receptors in the TRN enhances thalamocortical delta power (*Uygun et al., 2022*). In agreement, activation of LH GABAergic connections into the TRN, induce arousal from SWS (but not from PS), and the inhibition of these connections enhances SWS time and SWA amplitude (*Herrera et al., 2016*). Interestingly, RHY increased the levels of GABA<sub>A</sub> subunits (including  $\alpha 3$ ) in rat hypothalamic neurons (*Yoo et al., 2016*). Thus, in our study we included the TRN to see potential mechanisms in this brain region, but the region did not show particular effects. For instance, we did not detect DEGs enriched for functions linked to GABAergic signaling. As mentioned just above for its utility on discerning distinct effects on delta-1 and delta-2, our lab will soon complement the results of Chapter 5 with additional analyses of the effects of RHY on slow wave properties (e.g., density, amplitude, properties of the negative and positive peaks). This will expand the comprehension on how the drug modifies this sleep oscillations and could support the need to consider the alkaloid for sleep medicine and, further compare its mechanisms with that of other hypnotics.

### **6.2.2 RHY may modulate sleep via effects on the LH**

Our results suggest that RHY modulates the mRNA levels of *Hcrt* and *Pmch*. As discussed, this could directly control sleep/wakefulness amount and continuity. However, Hcrt cells are suggested to converge inputs of diverse nature (*Jennings and de Lecea, 2019*). They have receptors for various neurotransmitters, and have been shown to respond to stress, fear and reward

(*Yamanaka et al., 2003; Jennings and de Lecea, 2019*). Therefore, even though *Hcrt* is considered one of the main sleep/wake regulators, the effects of RHY on *Hcrt* may be caused by other changes in the organism and not necessarily indicate that *Hcrt* cells are a first line responder to RHY. Therefore, a first future study to be pursued is to investigate whether the decrease in *Hcrt* mRNA (particularly observed in disperse spots throughout cortical and thalamic regions) translates into changes in hypocretin peptides and *Hcrt* cell activity, and to investigate whether the modulation of *Hcrt* cells dictates the effects of RHY on distinct sleep variable (e.g., sleep time, continuity, and/or SWS delta, sigma, or wake alpha). Some of the methods that would help determine the implication of *Hcrt* cells on triggering RHY effects would be to inject RHY directly in the LH. This could, in addition, be combined to optogenetic activation of *Hcrt* cells (or MCH cells), to determine whether RHY could diminish the awakening effects of *Hcrt* cells when delivered directly into this brain region. If RHY does not cause direct effects on the LH, it could also be considered that the effects seen on the LH mRNA might reflect indirect effects of RHY as well. For instance, GABAergic sleep-promoting neurons from the POA can inhibit the activity of LH *Hcrt* cells and potentially favour wake-to-sleep transitions (*Suntsova et al., 2007*). Therefore, the effects captured on the LH transcriptome might reflect effects of RHY on other neuronal populations. In sum, the localized effects of RHY on the hypothalamus raise the possibility of RHY inducing sleep through a bottom-up mechanisms via modulating sleep-regulatory neuronal populations, and require future attention.

### **6.2.3 RHY reduces expression of HPA axis elements**

In line with previous studies suggesting that RHY improves neuronal and behavioural parameters in animals subjected to stress (*Zhang et al., 2017*) and with anxiolytic effects of *Uncaria* in rats (*Jung et al., 2006*), our results from manuscript 2 (Chapter 5) show that RHY reduces the expression of multiple genes involved in the HPA axis (*Cga, Thb, Pomc, Oxt, Avp, Prl*). The effects of RHY on these transcripts was not significant in all RHY-saline comparisons, which may have been caused by differences between sexes and time-of-injection, but also by the pulsatile nature of glucocorticoids release. As already discussed in the introduction of this thesis, sleep restriction can trigger glucocorticoids and HPA stress-reactivity, which importantly depends on the SD protocol and other cognitive variables (*Meerlo et al., 2002; Roman et al., 2006; Tartar et al., 2009; Mongrain et al., 2010; McCarthy et al., 2017; Nollet et al., 2020*). Interestingly, PS deprivation highly modified the pituitary transcriptome: increasing *Pomc, Oxt, Avp, Trh* and decreasing *Cga* and *Prl* (*Narwade et al., 2017; Oyola et al., 2019*), which were all affected in our study. This



supports an association between the sleep/wake history and the expression of these hypothalamic-pituitary mRNAs. Furthermore, HPA activation also modulates sleep in rats: ADX reduces sleep bout length, corticosterone replacement reduces SWS time, and intracerebro-ventricular injection of CRH reduces SWS time and neuronal cFOS<sup>+</sup> expression in the POA (*Bradbury et al., 1998; Gvilia et al., 2015*) Accordingly, RHY may modify sleep variables throughout some of its effects on the HPA axis, it may induce sleep via mechanisms not linked to the axis, or even decrease the levels of pituitary mRNAs indirectly through its sleep-inducing effects. Therefore, RHY could be further considered for investigation for treating anxiety and sleep disorders in a synergistic manner. Moreover, the HPA axis could be linked to the altered expression of *Tsc22d3*, (also known as delta sleep-inducing peptide immunoreactor or DSIP), whose expression colocalizes with pituitary cells in multiple species (*Kovalzon and Strekalova, 2006*). Literature suggests that DSIP modifies sleep time and still debates its controversial sleep-inducing properties (*Friedman et al., 1994; Seifritz et al., 1995; Kovalzon and Strekalova, 2006; Roy et al., 2018*). In addition, DSIP is immunosuppressor and anti-inflammatory, and is induced by stress and glucocorticoids (*Yang et al., 2019*). Accordingly, it would be excellent to verify whether DSIP plays any role in RHY's sleep-inducing effects. For instance, it could be quantified if RHY enhances DSIP protein levels and whether some of RHY's effects are dampened with simultaneous administration of *Tsc22d3* inhibitory oligonucleotides.

#### **6.2.4 RHY modifies genes linked to inflammatory responses**

In our experiment, RHY also modified the expression of genes linked to inflammatory and apoptosis/necrosis pathways. The differentially expressed genes (DEGs) were predicted to be downstream of terms such as immunoglobulin or toll-like receptors (TLR), cytokines or NF- $\kappa$ B signaling. The anti-inflammatory effects of RHY on cytokines, TLR and NF- $\kappa$ B pathways had already been described in rat cardiomyocytes, cerebral cortex and hippocampus, and authors linked these pathways to RHY's benefits on decreasing reactive oxygen species, improving cell viability, as well as on attenuating pathological EEG activity in rats (*Ho et al., 2014; Lai et al., 2019; Long et al., 2019; Qin et al., 2019*). In fact, cytokines (e.g., IL1 $\beta$ ) and TLR are suggested to modulate neuronal activity (*Vezzani et al., 2013*). For instance, IL1 $\beta$  injected in the somatosensory cortex enhanced SWS SWA only in the ipsilateral hemisphere (*Yasuda et al., 2005*). Therefore, if RHY reduced the levels of pro-inflammatory cytokine, one could predict the reduced SWS SWA activity that we observed after RHY injections, or some of the other alterations in ECoG signatures.

Interestingly, links between the immune system and sleep are well described. Infection or immune activation induce sleep, and sleep fosters healing, for instance, by increasing anti-viral responses and survival to infection (well reviewed in *Irwin, 2019*). Moreover, cytokines are considered SRSs. In fact, RHY modulated rodent macrophage and microglia activity (*Yuan et al., 2009; Kim et al., 2010; Cao et al., 2012; Song et al., 2012*), and the protein abundance of components of the TLR/NF- $\kappa$ B oscillated in a diurnal manner in Kupffer cells (liver macrophages) (*Wang et al., 2018a*). Besides, the effects on these inflammatory responses may be linked to the enrichment of DEGs linked to apoptosis/necrosis (*Yang et al., 2015*). In fact, RHY reduced apoptosis in rat granule neurons and cardiomyocytes (*Hu et al., 2018; Qin et al., 2019*), and decrease neuronal death in layer III of the medial entorhinal cortex (*Shao et al., 2016*). In sum, it will be important to disentangle if RHY induces its hypnotic effects via cytokine signaling or via separated mechanisms, and whether this pathway contributes to effects of RHY that are time dependent.

### **6.2.5 RHY did not modify EPHA4 phosphorylation**

Fu and collaborators suggested RHY as a potential inhibitor of EPHA4 activity (*Fu et al., 2014*). The authors simulated docking between EPHA4 and compounds in online databases, identified RHY as a potential inhibitor and confirmed the RHY-EPHA4 binding with *in vitro* pull-down assays (*Fu et al., 2014*). As compiled in Table 1 of Chapter 2, rat hippocampal neurons treated with RHY reduced EFNA1-dependent EPHA4 phosphorylation and clusters in rat hippocampal neurons, and, *in vivo*, RHY reduced EPHA4 phosphorylation in PFC, CA3 and DG of stress-susceptible mice, and in hippocampal synaptosomal fractions of a mouse model of Alzheimer's disease (*Fu et al., 2014; Zhang et al., 2017*). In our study (Chapter 5), neither the levels of EPHA4 nor its phosphorylation was modified 13h after injection. Moreover, the transcriptome does not suggest effects of RHY downstream of EPHA4. For instance, if EPHA4 was a main driver of RHY effects, we could have expected DEGs predicted to be downstream of the transcription factors MAT2B or TEAD1, which have been suggested to be downstream of EphA4 activity (*Freyburger et al., 2016; Cayuso et al., 2019*) but which were not modified by RHY. Nevertheless, these two cited studies *in vivo* measured phosphorylation levels after 3-4 weeks of oral administration or 48h-post intraperitoneal injection, which could explain the different results. More importantly, an additional current analysis pooling male and female mice demonstrates that RHY has very similar effects on sleep architecture in *Epha4* KO mice as the effects it has in WT mice (Figures 6.1, and compare with Figure 5.1): it induces SWS of shorter

duration, it reduces PS in the light phase and enhances it in the dark phase, and increments the number of wake and SWS bouts in the 5 to 6 hours after injections. In addition, RHY modified ECoG activity similarly in *Epha4* WT and KO mice (Figure 6.2E), except for an enhanced wake alpha activity and SWS delta activity during the light period which was not affected in WTs. Even though these KO-exclusive effects may indicate that EPHA4 would be required to prevent modulations of RHY on these frequency bands, the effects may also be caused by molecular compensations (e.g., other upregulated Eph/ephrin components, *Freyburger et al., 2016*), or by neurodevelopmental changes in these mutants. Thus, the preserved effects of RHY in *Epha4* KOs, and the lack of molecular alterations linked to EPHA4 activation support that RHY does not modify sleep directly via EPHA4 interactions. Another or some others of RHY's multiple effectors (see Chapter 2, *Ballester Roig et al., 2021*) may be involved. In fact, the poor selectivity of RHY was

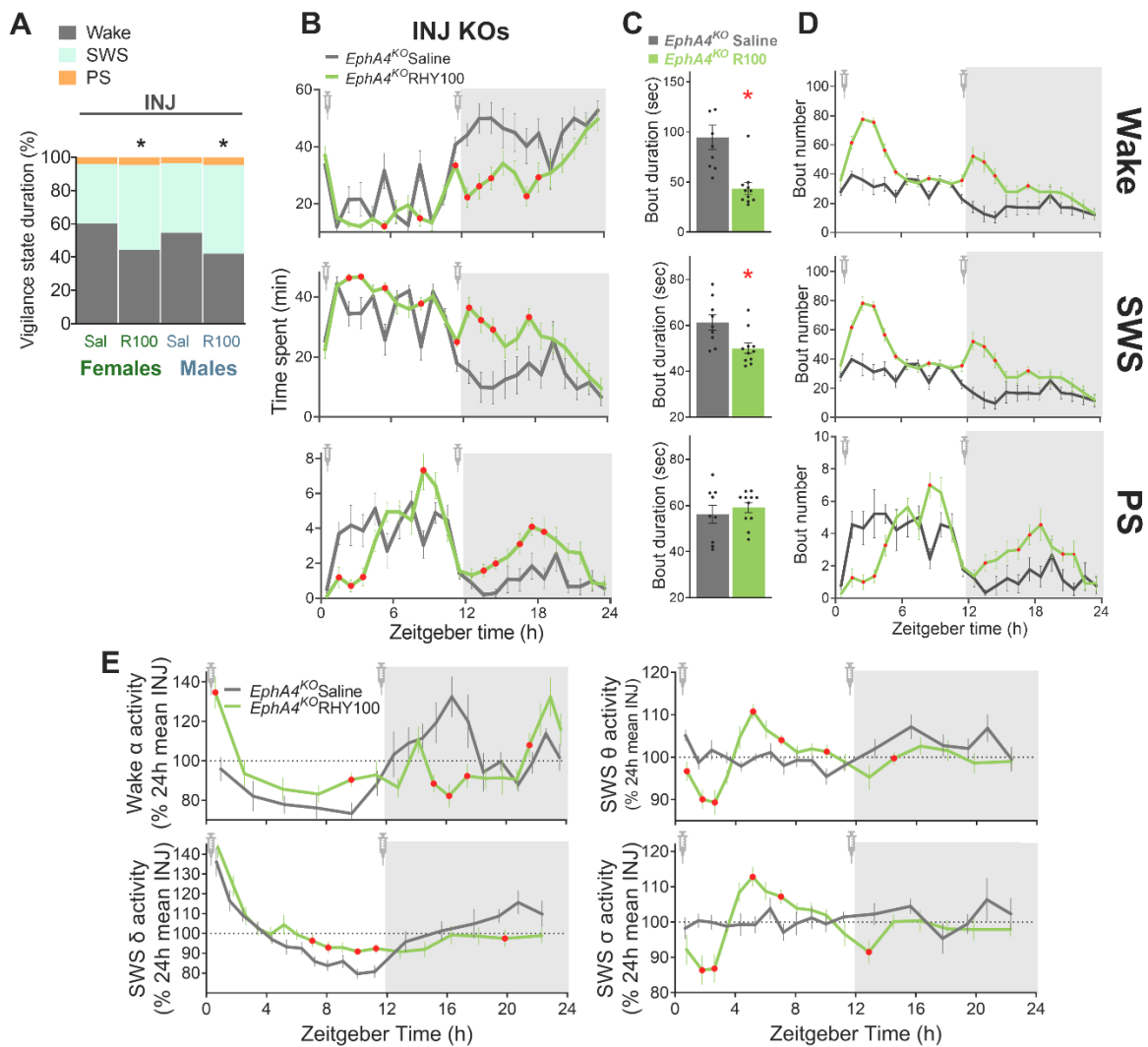


**Figure 6.2. RHY induces SWS and modifies ECoG activity in *Epha4* KO mice similarly to how it does in *Epha4* WT mice.** Male and female *Epha4*<sup>KO</sup> mice injected with RHY 100mg/kg (same protocol and statistical analysis as in Chapter 5) showed a reduction of percent of time spent in wake and enhanced the time spent in both SWS and PS compared to saline injections in the total 24-h injection recording day or INJ (A; females saline n = 4, males saline n=5, females RHY100 n = 5, males RHY100 = 6; no sex-by-treatment interaction,  $F_{1,16} > 0.19$ ,  $p_{adj} < 0.67$ ; stars indicate main treatment effect  $F_{1,16} > 15.5$ ,  $p_{adj} < 0.01$ ). Pooling male and female mice (saline n = 9; RHY100 n = 11) shows that RHY induces SWS after both injections, but that it modulates PS differently after morning and evening injections (B;  $F_{23,414} > 4.9$ ,  $p_{adj} < 0.01$ ). Red dots indicate significant post-hoc comparisons ( $p < 0.05$ ). RHY100 reduces the duration of wake and SWS bouts (C;  $t > 2.9$ ,  $p < 0.01$ ) and increases wake and SWS bout number for 5 to 6 hours after injections (D;  $F_{23,414} > 4.9$ ,  $p_{adj} < 0.01$ ). RHY also modifies ECoG activity in a vigilance state dependent manner in knockouts (E): RHY100 raised wake alpha activity (8-12 Hz) in the light period, but reduced its power during the dark phase (upper-left,  $F_{17,272} > 4.3$ ,  $p_{adj} < 0.01$ ); it enhanced SWS delta power (1-4 Hz) at the end of the light period and diminished it at the end of the dark period (lower-left,  $F_{17,289} > 3.3$ ,  $p_{adj} < 0.01$ ); and reduced both SWS sigma (10-13 Hz) and theta (6-9 Hz) activity in the first 1-3 h after injection, but enhanced these frequencies in the second half of the light period (right panels,  $F_{2,289} > 4.2$ ,  $p_{adj} < 0.01$ ).

already suggested by Dr. Tognolini, who mentioned that RHY did not block EPHA4-EFNA1 binding with ELISA-binding protocols or the Lanthanide Chelate Excite technology (*Tognolini et al., 2014*), and by Wu and collaborators, who report RHY inactivity with nuclear magnetic resonance and isothermal titration calorimetry (*Wu et al., 2017*). The latter authors suggest that the discrepancy may be due to false positives obtained with high-throughput screenings (*Baell, 2015*), like the one used by Fu *et al.* Nevertheless, RHY may still induce a decrease in EPHA4 phosphorylation via indirect mechanisms since this experimental finding has been replicated (*Zhang et al., 2017*). Alternatively, we have suggested in Ballester *et al.* (2021, Chapter 2), that RHY could impact EPHA4 only under disturbed/pathological conditions (e.g., disease models). In conclusion, our data supports that EPHA4 is not a main mediator the sleep-inducing properties of the alkaloid, but does not discard whether RHY modulates the activation of this adhesion molecule (and potentially impact sleep variables) under disturbed/pathological conditions.

## **6.2.6 RHY modifies immediate early genes linked to the response to sleep deprivation**

IEGs are a group of genes upregulated quickly (between 10 minutes to two hours) by neuronal activation and the raise of intracellular calcium. This rapid transcriptional activation regulates neuronal responses, for instance, by regulating synaptic receptors (e.g., mGLURs,

AMPA receptors and GABA receptors) and plasticity (Chen et al., 2014; Mo et al., 2015; Kim et al., 2018; Miyashita et al., 2018). As discussed in Chapter 1 (section 1.3.2.1.3), *Egr1*, *Nr1a4* and *Fos* are IEGs consistently upregulated by SD of different durations (3 to 12 hours), by different methods of SD (e.g., gentle handling, novel objects, water platforms for PS restriction), and in multiple brain regions (e.g., mPFC, hippocampus, VLPO, pituitary) (Cirelli and Tononi, 2000; Cirelli et al., 2004; Terao et al., 2006; Maret et al., 2007; Mongrain et al., 2010; Vecsey et al., 2012; Bellesi et al., 2013; Narwade et al., 2017; Diessler et al., 2018; Guo et al., 2019; Hor et al., 2019; Oyola et al., 2019; Guo et al., 2020; Wei, 2020; Gaine et al., 2021). In our study, RHY downregulates these IEGs (see **Figure A1** in Annex). Thus, in contrast to another group of genes detected to be upregulated by both SD and RHY (e.g., *Sgk1*, *Arl4d*, *Cdkn1a*, *Ddit4*, *Nfkb1a*, *Plin4*, *Tsc22d3*), RHY and sleep loss/restriction modulate *Egr1*, *Nr1a4* and *Fos* in opposite directions. While these always-upregulated genes after sleep loss may reflect mechanism linked to sleep induction, our data supports that *Egr1*, *Nr1a4* and *Fos* are reliable markers of sleep time not only when sleep is diminished but also when it is increased. Supporting the relevance of these genes, some RHY-induced DEGs (e.g., *Sgk1*, *Cebpa*, *Gh*, *Prl*, *Nfkb1a*) are predicted to be modulated by these transcription factors in enrichments analysis (Chapter 5). Interestingly, the SD-dependent increase in *Sgk1*, *Ddit4*, *Tsc22d3* and *Nfkb1a* was abolished in ADX mice, whereas the IEGs *Egr1*, *Nr4a1*, *Fos* (as well as the non-IEGs *Cdkn1a* and *Arl4a*) were upregulated in both ADX and sham mice (Mongrain et al., 2010), which suggests that *Nr4a1*, *Egr1* and *Fos* mark sleep time in a glucocorticoid independent manner. This intriguing segregation between glucocorticoids-induced and glucocorticoid-independent genes (in addition to the contradictory increase in glucocorticoids-dependent mRNAs, the downregulation HPA axis mRNAs, and the known anxiolytic effects of RHY) suggest that glucocorticoids are not the main driver of RHY effects. Nevertheless, this should be confirmed with future studies. In addition, it should be reminded that RHY induced SWS in the shape of short bouts in our study. Therefore, longer bouts of sleep might have altered these IEGs linked to sleep/wake history in different (or even more pronounced) manners, which could be further compared with effects of other sleep-inducing drugs on the transcriptome.

## 6.2.7 Future identification of RHY targets for sleep regulation

It can be compiled from this section 6.2 that RHY affected three main systems at the transcriptomics level in our study: hypothalamic, pituitary and immune responses. Accordingly, a next step will be to determine whether these systems are modified in terms of protein activity and

cell signaling. Approaches investigating targets already reported to be modulated by RHY may be good starting points: TLR2 and TLR4 have been shown to be reduced by RHY treatments, L-VGCCs are expressed in pituitary cells and modulate the secretion of GH, PRL and ACTH (Stojilkovic *et al.*, 1988; Ho *et al.*, 2014; Sosial and Nussinovitch, 2015; Long *et al.*, 2019). It has also been suggested that RHY modified neuronal firing and synaptic potentiation via NMDA and EPHA4 (Kang *et al.*, 2002; Fu *et al.*, 2014; Shao *et al.*, 2016), and was initially hypothesized that these molecules may drive effects of RHY on sleep because they have been involved in sleep and circadian phenotypes (Ballester Roig *et al.*, 2021). Nevertheless, our protein measures in the mouse cerebral cortex, hippocampus and thalamus/hypothalamus, and transcriptomic approach do not suggest effects via these two membrane receptors. Thus, it would be necessary to investigate whether some of the changes observed in the ECoG are particularly linked to hypothalamic, pituitary or inflammatory targets via some of the reported RHY targets. For instance, it would be interesting to simultaneously inject RHY with agonists of (or overexpression of) NMDARs (or particularly NR2B-containing NMDARs), EPHA4, L-VGCCs or TLRs. Delivering those directly into the brain, or even into particular brain regions such as the LH, can help provide a more exhaustive explanation. In addition, studying again potential differences between male and female regarding the role of these targets, could potentially determine why the two doses used in our study had different repercussions between sexes.

### **6.3 RHY as a natural component for sleep modulation**

It is estimated that over 30% of drugs originate from discoveries in medicinal plants (Harvey *et al.*, 2015). In fact, it is the case for drugs commonly used in today's society (e.g., aspirin, morphine), and society often debates about whether natural compounds have sometimes advantages over synthetic compounds. While modern pharmacology aims at synthesizing highly specific compounds, natural products generally provide a blend of components with often unclear mechanisms of action. On the one hand, some of the benefits of herbal medicines could be linked to the synergistic mechanisms of action of their active components, such as other components facilitating absorption (Williamson, 2001). Moreover, herbs and other vegetal vary their composition according to the cultivating region and time of the year (Song *et al.*, 2018). Given that Uncaria plants and drugs containing Uncaria (e.g., YKS) are used in Asia today, our work describes important impacts of RHY at the level of gene expression which should be considered in Uncaria

research or prescriptions. Future studies should describe whether the RHY effects discussed on inflammatory, apoptotic and hypothalamic-pituitary responses occur in humans in parallel to *Uncaria*'s sleep-inducing effects.

## 6.4 Benefits and limitations of spatial transcriptomics

The broad coverage of our spatial transcriptomic approach reveals parallel consequences of RHY on different systems (e.g., sleep-regulatory transcripts and immune and hypothalamic-pituitary responses). This might reflect that RHY, like many drugs, does not have a unique target. Therefore, further investigations of RHY mechanisms should include systems-biology avenues. Spatial transcriptomics, which was identified as the method of the year in 2020 (*Marx, 2021*), has allowed here the identification of RHY consequences that are distinct among the hypothalamus, hippocampus, cerebral cortex and white matter tracts (see Chapter 5). The platform used provides an accurate and reliable measure of gene expression in 5000 spots in a 2D-slice of tissue. The reliability of our experiment was confirmed by visualizing markers of delimited brain regions, which demonstrates that mRNA was captured in a spatially restricted manner (e.g., by confirming the previously reported distribution of *Eph/Ephrins*, or by visualizing the gene expression of markers of cortical layers such as *Cux-1*, *Rbp4*, *Camk2a.*, *Foxp1*). On the other hand, it is important to highlight that one spot (55µm) is suggested to cover 1 to 10 cells in mouse brain slices. Therefore, changes in gene expression in each spot are an average of the cell types below. There are currently ways to improve cell type resolution but keep spatial information. A first option is to align spatial RNAseq data with a complementary single cell RNA sequencing (scRNAseq) experiment (*Joglekar et al., 2021; Cable et al., 2022*). Another option is to microdissect brain regions with laser capture microdissection and perform scRNAseq of each well-defined sample (*Wen et al., 2020*). Finally, 10x Genomics is currently developing a variation of their Visium Spatial Transcriptomics product, with smaller spots covering a smaller number of cells, which the community eagerly awaits.

On the other hand, it should not be neglected that transcriptomic techniques are less reliable for less abundant transcripts. Therefore, targeted spatial transcriptomics (sequencing of a pre-set list of genes) may be beneficial to study cellular pathways of interest. Another final limitation to discuss, is that the read length of our sequencing approach could not detect isoforms (*Joglekar et al., 2021*), an analysis which can provide terrific information on the cell types or functions modified

with a set of DEGs. For instance, *Sgk1* is produced in two isoforms and, in the mouse visual cortex, one was expressed in pyramidal neurons but not in cells expressing parvalbumin or glial fibrillary acidic protein (*Arteaga et al., 2008; Martin-Batista et al., 2021*), which could have provided a hint on whether RHY targets particular cell types.

## **6.5 Other notions to better describe molecular mechanisms in sleep and circadian rhythms**

It has been highly discussed in this thesis that transcription is not the only mechanism allowing rhythmicity of synaptic components. This final section summarizes that multiple levels of regulation, redundancy in molecular processes, as well as the variability among animal models may hinder the identification of molecular mechanisms underlying sleep and circadian regulation.

Research suggests that redundant regulatory processes contribute to ensure proper rhythmicity of cellular processes. For example, changes in chromatin structure, transcription factor binding, transcripts, translation and the phosphoproteome peak at similar phases to organize the same functions (*Zhang et al., 2014; Atger et al., 2015; Mure et al., 2018; Wang et al., 2018a; Bruning et al., 2019; Hor et al., 2019; Noya et al., 2019; Lyons et al., 2020*). Similarly, it was found in the mouse liver that ubiquitination was higher in proteins coded in transcripts regulated by cycling transcription factors, suggesting redundant regulations (*Wang et al., 2018a*). Accordingly, it is difficult to identify if a molecular process is crucial to regulate a particular behavior or if it is part of a balanced assembly of convergent regulations. Thus, experiments could compare the effect of different levels of rhythmic regulation for the same function and the impact on sleep and rhythms (e.g., modify transcriptional activity and RNA stability, or RNA stability and protein activity). Potential redundant mechanisms were obtained as well when analyzing the transcriptome after RHY injections, but the diversity of functional pathways affected could also indicate consequences which are not all linked to the enhanced sleep. Therefore, when using techniques to modulate circadian rhythms, sleep amounts, depth or oscillations, diverse techniques should be compared. This has been already discussed regarding distinct methods used for sleep restriction (gentle handling, novel objects, running wheels) (*Havekes and Aton, 2020*), but it should be similarly applied in pharmacological studies which induce similar behaviors throughout different molecular mechanisms. For instance, it would have been helpful in our study to compare the effect of other sleep-inducing compounds such as benzodiazepines, to compare which pathways



overlap and the relevance of the hypothalamic effects. Likewise, organism responses and chemicals studied may be contingent upon the state of the organism (healthy, stressed, aged). For instance, recent unpublished data suggest that silencing sleep regulatory neurons in flies is more effective when flies are on a sugar diet than when they are under a protein diet (*Dissel, 2022*). Therefore, pharmacological approaches should be tested simultaneously in distinct animal models of conditions (e.g., under inflamed or sleep deprived conditions). Finally, it should not be forgotten that organism responses (e.g., responses to SD) do not only differ between different organism states, but also between mouse strains and across generations (*El Helou et al., 2013; Diessler et al., 2018*). Performing studies in mixed backgrounds, comparing strains and multiple mammal species, as well as systems genetics approaches, will help improve reproducibility and find the most relevant mechanism to extrapolate and study human health.

# Chapter 7

Conclusions

---

The cell adhesion molecule EPHA4 and its ligands Ephrins are crucial for cell communication in multiple tissues and regulate spine morphology and neurotransmission in the central nervous system. Interestingly, *EphA4* KO mice have abnormal circadian rhythms of locomotor activity and altered sleep variables (e.g., PS time and SWS delta and sigma activity). This thesis identifies that the circadian transcription factors CLOCK and BMAL1 (as well as NPAS2 and BMAL1) activate transcription via putative promoter regions of the *EphA4*, *EfnB2* and *EfnA3* genes *in vitro*. The effect of these clock factors was blocked by GSK3 $\beta$ , a kinase that negatively regulates the clock machinery which has also important roles in neurite morphology and synaptic plasticity. This clock regulation of EphA4 supports the previously observed circadian phenotypes in *EphA4* KO mice. Although protein measurements at different times of the day show no oscillation of EPHA4 and EFNB2 in PFC or SCN of mice kept in constant darkness, the regulation by clock factors might be cell type- or tissue-specific. Furthermore, although clock transcription factors are basis of circadian rhythms in mammals, they are also under strong sleep regulation, which suggests that both circadian and homeostatic processes could regulate EphA4/EfnB2/EfnA3 interactions. Future studies should determine whether the clock machinery regulates the transcription of Eph/Ephrin components *in vivo* and whether this regulation underlies responses to both homeostatic and rhythmic processes.

In the second research project, we investigated molecular mechanisms of an alkaloid (RHY) purified from plants used in traditional Asian medicines for their sedative properties. RHY, which had been shown to modulate EPHA4 activity and synaptic transmission, induces SWS in mice. Its effects on PS time, wake alpha activity, and SWS delta and sigma activity were different after morning or evening injections, suggesting that some RHY mechanisms of action may depend on (internal or external) time. Importantly, RHY effects were more pronounced and dose dependent in females, which stresses the need to explore several pharmacological doses in both sexes. The spatial transcriptome demonstrates that RHY affects the expression of some genes in a general manner throughout the brain (e.g., genes involved in apoptosis and inflammatory responses) and modifies the expression of other transcripts involved in sleep and pituitary functions particularly in the hypothalamus. Future investigations assessing which RHY targets (e.g., NMDA receptors, TLR) trigger each effect on sleep (e.g., sleep time, brain oscillations), may help understand molecular mechanisms regulating sleep, and potentially contribute to enrich possibilities for sleep medicine.

In conclusion, this thesis describes a transcriptional regulation for elements of the cell adhesion system Eph/Ephrin, and places this mechanism in the context of circadian rhythms and sleep. Moreover, we demonstrate that an alkaloid which had been suggested to affect the activity of the Eph/Ephrin system, has significant sleep-inducing properties and profound impacts on brain gene expression. This work also supports that spatial transcriptomic (and other omic) techniques are advantageous tools to describe pharmacological effects. Finally, we highlight the importance of considering cell adhesion mechanisms to better understand the neurophysiology of behaviors.

## References

---

- Abel, T., Havekes, R., Saletin, J.M., Walker, M.P. (2013). Sleep, plasticity and memory from molecules to whole-brain networks. *Curr Biol* 23, R774-788.
- Abrahamson, E.E., Moore, R.Y. (2001). Suprachiasmatic nucleus in the mouse: retinal innervation, intrinsic organization and efferent projections. *Brain Res* 916, 172-191.
- Adamantidis, A.R., Zhang, F., Aravanis, A.M., Deisseroth, K., de Lecea, L. (2007). Neural substrates of awakening probed with optogenetic control of hypocretin neurons. *Nature* 450, 420-424.
- Adams, R.H., Wilkinson, G.A., Weiss, C., Diella, F., Gale, N.W., Deutsch, U., Risau, W., Klein, R. (1999). Roles of ephrinB ligands and EphB receptors in cardiovascular development: demarcation of arterial/venous domains, vascular morphogenesis, and sprouting angiogenesis. *Genes Dev* 13, 295-306.
- Aizawa, R., Kanbayashi, T., Saito, Y., Ogawa, Y., Sugiyama, T., Kitajima, T., Kaneko, Y., Abe, M., Shimizu, T. (2002). Effects of Yoku-kan-san-ka-chimpi-hange on the sleep of normal healthy adult subjects. *Psychiatry Clin Neurosci* 56, 303-304.
- Amzica, F., Steriade, M. (1998). Electrophysiological correlates of sleep delta waves. *Electroencephalogr Clin Neurophysiol* 107, 69-83.
- Anaclet, C., Ferrari, L., Arrigoni, E., Bass, C.E., Saper, C.B., Lu, J., Fuller, P.M. (2014). The GABAergic parafacial zone is a medullary slow wave sleep-promoting center. *Nat Neurosci* 17, 1217-1224.
- Anaclet, C., Pedersen, N.P., Ferrari, L.L., Venner, A., Bass, C.E., Arrigoni, E., Fuller, P.M. (2015). Basal forebrain control of wakefulness and cortical rhythms. *Nat Commun* 6, 8744.
- Ango, F., Prezeau, L., Muller, T., Tu, J.C., Xiao, B., Worley, P.F., Pin, J.P., Bockaert, J., Fagni, L. (2001). Agonist-independent activation of metabotropic glutamate receptors by the intracellular protein Homer. *Nature* 411, 962-965.
- Arcas, A., Wilkinson, D.G., Nieto, M.A. (2020). The Evolutionary History of Ephs and Ephrins: Toward Multicellular Organisms. *Mol Biol Evol* 37, 379-394.
- Arraj, M., Lemmer, B. (2006). Circadian rhythms in heart rate, motility, and body temperature of wild-type C57 and eNOS knock-out mice under light-dark, free-run, and after time zone transition. *Chronobiol Int* 23, 795-812.
- Arteaga, M.F., Coric, T., Straub, C., Canessa, C.M. (2008). A brain-specific SGK1 splice isoform regulates expression of ASIC1 in neurons. *Proc Natl Acad Sci U S A* 105, 4459-4464.
- Ashton, R.S., Conway, A., Pangarkar, C., Bergen, J., Lim, K.I., Shah, P., Bissell, M., Schaffer, D.V. (2012). Astrocytes regulate adult hippocampal neurogenesis through ephrin-B signaling. *Nat Neurosci* 15, 1399-1406.
- Astori, S., Wimmer, R.D., Prosser, H.M., Corti, C., Corsi, M., Liaudet, N., Volterra, A., Franken, P., Adelman, J.P., Luthi, A. (2011). The Ca(V)3.3 calcium channel is the major sleep spindle pacemaker in thalamus. *Proc Natl Acad Sci U S A* 108, 13823-13828.
- Atger, F., Gobet, C., Marquis, J., Martin, E., Wang, J., Weger, B., Lefebvre, G., Descombes, P., Naef, F., Gachon, F. (2015). Circadian and feeding rhythms differentially affect rhythmic mRNA transcription and translation in mouse liver. *Proc Natl Acad Sci U S A* 112, E6579-6588.

- Aton, S.J., Seibt, J., Dumoulin, M., Jha, S.K., Steinmetz, N., Coleman, T., Naidoo, N., Frank, M.G. (2009). Mechanisms of sleep-dependent consolidation of cortical plasticity. *Neuron* *61*, 454-466.
- Averaimo, S., Assali, A., Ros, O., Couvet, S., Zagar, Y., Genescu, I., Rebsam, A., Nicol, X. (2016). A plasma membrane microdomain compartmentalizes ephrin-generated cAMP signals to prune developing retinal axon arbors. *Nat Commun* *7*, 12896.
- Axmacher, N., Elger, C.E., Fell, J. (2008). Ripples in the medial temporal lobe are relevant for human memory consolidation. *Brain* *131*, 1806-1817.
- Baell, J.B. (2015). Screening-based translation of public research encounters painful problems. *ACS Med Chem Lett* *6*, 229-234.
- Baker, C.L., Loros, J.J., Dunlap, J.C. (2012). The circadian clock of *Neurospora crassa*. *FEMS Microbiol Rev* *36*, 95-110.
- Baker, F.C., Shah, S., Stewart, D., Angara, C., Gong, H., Szymusiak, R., Opp, M.R., McGinty, D. (2005). Interleukin 1beta enhances non-rapid eye movement sleep and increases c-Fos protein expression in the median preoptic nucleus of the hypothalamus. *Am J Physiol Regul Integr Comp Physiol* *288*, R998-R1005.
- Ballester Roig, M.N., Leduc, T., Areal, C.C., Mongrain, V. (2021). Cellular Effects of Rhynchophylline and Relevance to Sleep Regulation. *Clocks Sleep* *3*, 312-341.
- Bandarabadi, M., Herrera, C.G., Gent, T.C., Bassetti, C., Schindler, K., Adamantidis, A.R. (2020). A role for spindles in the onset of rapid eye movement sleep. *Nat Commun* *11*, 5247.
- Bandarabadi, M., Boyce, R., Gutierrez Herrera, C., Bassetti, C.L., Williams, S., Schindler, K., Adamantidis, A. (2019). Dynamic modulation of theta-gamma coupling during rapid eye movement sleep. *Sleep* *42*.
- Banks, S., Dinges, D.F. (2007). Behavioral and physiological consequences of sleep restriction. *J Clin Sleep Med* *3*, 519-528.
- Barateau, L., Dauvilliers, Y. (2019). Recent advances in treatment for narcolepsy. *Ther Adv Neurol Disord* *12*, 1756286419875622.
- Barca-Mayo, O., Pons-Espinal, M., Follert, P., Armirotti, A., Berdondini, L., De Pietri Tonelli, D. (2017). Astrocyte deletion of Bmal1 alters daily locomotor activity and cognitive functions via GABA signalling. *Nat Commun* *8*, 14336.
- Bazanov, O.M., Vernon, D. (2014). Interpreting EEG alpha activity. *Neurosci Biobehav Rev* *44*, 94-110.
- Beaulieu, J.M., Gainetdinov, R.R., Caron, M.G. (2009). Akt/GSK3 signaling in the action of psychotropic drugs. *Annu Rev Pharmacol Toxicol* *49*, 327-347.
- Begum, S., Emami, N., Cheung, A., Wilkins, O., Der, S., Hamel, P.A. (2005). Cell-type-specific regulation of distinct sets of gene targets by Pax3 and Pax3/FKHR. *Oncogene* *24*, 1860-1872.
- Bellesi, M., Bushey, D., Chini, M., Tononi, G., Cirelli, C. (2016). Contribution of sleep to the repair of neuronal DNA double-strand breaks: evidence from flies and mice. *Sci Rep* *6*, 36804.
- Bellesi, M., Pfister-Genskow, M., Maret, S., Keles, S., Tononi, G., Cirelli, C. (2013). Effects of sleep and wake on oligodendrocytes and their precursors. *J Neurosci* *33*, 14288-14300.
- Bellet, M.M., Sassone-Corsi, P. (2010). Mammalian circadian clock and metabolism - the epigenetic link. *J Cell Sci* *123*, 3837-3848.

- Benedetti, F., Serretti, A., Colombo, C., Lorenzi, C., Tubazio, V., Smeraldi, E. (2004). A glycogen synthase kinase 3-beta promoter gene single nucleotide polymorphism is associated with age at onset and response to total sleep deprivation in bipolar depression. *Neurosci Lett* 368, 123-126.
- Benedetti, F., Dallaspezia, S., Lorenzi, C., Pirovano, A., Radaelli, D., Locatelli, C., Poletti, S., Colombo, C., Smeraldi, E. (2012). Gene-gene interaction of glycogen synthase kinase 3-beta and serotonin transporter on human antidepressant response to sleep deprivation. *J Affect Disord* 136, 514-519.
- Bersagliere, A., Pascual-Marqui, R.D., Tarokh, L., Achermann, P. (2018). Mapping Slow Waves by EEG Topography and Source Localization: Effects of Sleep Deprivation. *Brain Topogr* 31, 257-269.
- Besing, R.C., Paul, J.R., Hablitz, L.M., Rogers, C.O., Johnson, R.L., Young, M.E., Gamble, K.L. (2015). Circadian rhythmicity of active GSK3 isoforms modulates molecular clock gene rhythms in the suprachiasmatic nucleus. *J Biol Rhythms* 30, 155-160.
- Besing, R.C., Rogers, C.O., Paul, J.R., Hablitz, L.M., Johnson, R.L., McMahon, L.L., Gamble, K.L. (2017). GSK3 activity regulates rhythms in hippocampal clock gene expression and synaptic plasticity. *Hippocampus* 27, 890-898.
- Beurel, E., Grieco, S.F., Jope, R.S. (2015). Glycogen synthase kinase-3 (GSK3): regulation, actions, and diseases. *Pharmacol Ther* 148, 114-131.
- Binder, S., Rawohl, J., Born, J., Marshall, L. (2013). Transcranial slow oscillation stimulation during NREM sleep enhances acquisition of the radial maze task and modulates cortical network activity in rats. *Front Behav Neurosci* 7, 220.
- Binns, K.L., Taylor, P.P., Sicheri, F., Pawson, T., Holland, S.J. (2000). Phosphorylation of tyrosine residues in the kinase domain and juxtamembrane region regulates the biological and catalytic activities of Eph receptors. *Mol Cell Biol* 20, 4791-4805.
- Bixler, E.O., Papaliaga, M.N., Vgontzas, A.N., Lin, H.M., Pejovic, S., Karataraki, M., Vela-Bueno, A., Chrousos, G.P. (2009). Women sleep objectively better than men and the sleep of young women is more resilient to external stressors: effects of age and menopause. *J Sleep Res* 18, 221-228.
- Bjorness, T.E., Booth, V., Poe, G.R. (2018). Hippocampal theta power pressure builds over non-REM sleep and dissipates within REM sleep episodes. *Arch Ital Biol* 156, 112-126.
- Bjorness, T.E., Kulkarni, A., Rybalchenko, V., Suzuki, A., Bridges, C., Harrington, A.J., Cowan, C.W., Takahashi, J.S., Konopka, G., Greene, R.W. (2020). An essential role for MEF2C in the cortical response to loss of sleep in mice. *Elife* 9.
- Blake, H., Gerard, R.W. (1937). Brain potentials during sleep. *American Journal of Physiology-Legacy Content* 119, 692-703.
- Blanco-Centurion, C., Liu, M., Konadhode, R.P., Zhang, X., Pelluru, D., van den Pol, A.N., Shiromani, P.J. (2016). Optogenetic activation of melanin-concentrating hormone neurons increases non-rapid eye movement and rapid eye movement sleep during the night in rats. *Eur J Neurosci* 44, 2846-2857.
- Borbely, A.A. (1982). A two process model of sleep regulation. *Hum Neurobiol* 1, 195-204.
- Borbely, A.A., Daan, S., Wirz-Justice, A., Deboer, T. (2016). The two-process model of sleep regulation: a reappraisal. *J Sleep Res* 25, 131-143.

- Borbely, A.A., Baumann, F., Brandeis, D., Strauch, I., Lehmann, D. (1981). Sleep deprivation: effect on sleep stages and EEG power density in man. *Electroencephalogr Clin Neurophysiol* 51, 483-495.
- Bourgin, C., Murai, K.K., Richter, M., Pasquale, E.B. (2007). The EphA4 receptor regulates dendritic spine remodeling by affecting beta1-integrin signaling pathways. *J Cell Biol* 178, 1295-1307.
- Bouzioukh, F., Wilkinson, G.A., Adelman, G., Frotscher, M., Stein, V., Klein, R. (2007). Tyrosine phosphorylation sites in ephrinB2 are required for hippocampal long-term potentiation but not long-term depression. *J Neurosci* 27, 11279-11288.
- Bowden, T.A., Aricescu, A.R., Nettleship, J.E., Siebold, C., Rahman-Huq, N., Owens, R.J., Stuart, D.I., Jones, E.Y. (2009). Structural Plasticity of Eph-Receptor A4 Facilitates Cross-Class Ephrin Signaling. *Structure* 17, 1679.
- Boyce, R., Glasgow, S.D., Williams, S., Adamantidis, A. (2016). Causal evidence for the role of REM sleep theta rhythm in contextual memory consolidation. *Science* 352, 812-816.
- Bozek, K., Relogio, A., Kielbasa, S.M., Heine, M., Dame, C., Kramer, A., Herzog, H. (2009). Regulation of clock-controlled genes in mammals. *PLoS One* 4, e4882.
- Bradbury, M.J., Dement, W.C., Edgar, D.M. (1998). Effects of adrenalectomy and subsequent corticosterone replacement on rat sleep state and EEG power spectra. *Am J Physiol* 275, R555-565.
- Brancaccio, M., Patton, A.P., Chesham, J.E., Maywood, E.S., Hastings, M.H. (2017). Astrocytes Control Circadian Timekeeping in the Suprachiasmatic Nucleus via Glutamatergic Signaling. *Neuron* 93, 1420-1435 e1425.
- Brandt, J.A., Churchill, L., Guan, Z., Fang, J., Chen, L., Krueger, J.M. (2001). Sleep deprivation but not a whisker trim increases nerve growth factor within barrel cortical neurons. *Brain Res* 898, 105-112.
- Briggs, C., Hirasawa, M., Semba, K. (2018). Sleep Deprivation Distinctly Alters Glutamate Transporter 1 Apposition and Excitatory Transmission to Orexin and MCH Neurons. *J Neurosci* 38, 2505-2518.
- Brockman, R., Bunick, D., Mahoney, M.M. (2011). Estradiol deficiency during development modulates the expression of circadian and daily rhythms in male and female aromatase knockout mice. *Horm Behav* 60, 439-447.
- Broussard, J.I., Givens, B. (2010). Low frequency oscillations in rat posterior parietal cortex are differentially activated by cues and distractors. *Neurobiol Learn Mem* 94, 191-198.
- Bruckner, K., Pablo Labrador, J., Scheiffele, P., Herb, A., Seeburg, P.H., Klein, R. (1999). EphrinB ligands recruit GRIP family PDZ adaptor proteins into raft membrane microdomains. *Neuron* 22, 511-524.
- Bruning, F., Noya, S.B., Bange, T., Koutsouli, S., Rudolph, J.D., Tyagarajan, S.K., Cox, J., Mann, M., Brown, S.A., Robles, M.S. (2019). Sleep-wake cycles drive daily dynamics of synaptic phosphorylation. *Science* 366.
- Cable, D.M., Murray, E., Zou, L.S., Goeva, A., Macosko, E.Z., Chen, F., Irizarry, R.A. (2022). Robust decomposition of cell type mixtures in spatial transcriptomics. *Nat Biotechnol* 40, 517-526.
- Cahill, L. (2006). Why sex matters for neuroscience. *Nat Rev Neurosci* 7, 477-484.
- Cai, Wei, D., Chen, S., Chen, X., Li, S., Chen, W., He, W. (2019). MiR-145 protected the cell viability of human cerebral cortical neurons after oxygen-glucose deprivation by downregulating EPHA4. *Life Sci* 231, 116517.
- Cajochen, C., Knoblauch, V., Krauchi, K., Renz, C., Wirz-Justice, A. (2001). Dynamics of frontal EEG activity, sleepiness and body temperature under high and low sleep pressure. *Neuroreport* 12, 2277-2281.



- Cao, W., Wang, Y., Lv, X., Yu, X., Li, X., Li, H., Wang, Y., Lu, D., Qi, R., Wang, H. (2012). Rhynchophylline prevents cardiac dysfunction and improves survival in lipopolysaccharide-challenged mice via suppressing macrophage I-kappaB phosphorylation. *Int Immunopharmacol* *14*, 243-251.
- Carmona, M.A., Murai, K.K., Wang, L., Roberts, A.J., Pasquale, E.B. (2009). Glial ephrin-A3 regulates hippocampal dendritic spine morphology and glutamate transport. *Proc Natl Acad Sci U S A* *106*, 12524-12529.
- Carrera-Canas, C., Garzon, M., de Andres, I. (2019). The Transition Between Slow-Wave Sleep and REM Sleep Constitutes an Independent Sleep Stage Organized by Cholinergic Mechanisms in the Rostrodorsal Pontine Tegmentum. *Front Neurosci* *13*, 748.
- Carrier, J., Land, S., Buysse, D.J., Kupfer, D.J., Monk, T.H. (2001). The effects of age and gender on sleep EEG power spectral density in the middle years of life (ages 20-60 years old). *Psychophysiology* *38*, 232-242.
- Carskadon, M.A., Dement, W.C. (2005). Normal human sleep: an overview. *Principles and practice of sleep medicine*.
- Carter, M.E., Brill, J., Bonnavion, P., Huguenard, J.R., Huerta, R., de Lecea, L. (2012). Mechanism for Hypocretin-mediated sleep-to-wake transitions. *Proc Natl Acad Sci U S A* *109*, E2635-2644.
- Cayuso, J., Xu, Q., Addison, M., Wilkinson, D.G. (2019). Actomyosin regulation by Eph receptor signaling couples boundary cell formation to border sharpness. *Elife* *8*.
- Cermakian, N., Stegeman, S.K., Tekade, K., Labrecque, N. (2022). Circadian rhythms in adaptive immunity and vaccination. *Semin Immunopathol* *44*, 193-207.
- Challet, E. (2007). Minireview: Entrainment of the suprachiasmatic clockwork in diurnal and nocturnal mammals. *Endocrinology* *148*, 5648-5655.
- Chellappa, S.L., Vujovic, N., Williams, J.S., Scheer, F. (2019). Impact of Circadian Disruption on Cardiovascular Function and Disease. *Trends Endocrinol Metab* *30*, 767-779.
- Chen, R., Yang, X., Zhang, B., Wang, S., Bao, S., Gu, Y., Li, S. (2019). EphA4 Negatively Regulates Myelination by Inhibiting Schwann Cell Differentiation in the Peripheral Nervous System. *Front Neurosci* *13*, 1191.
- Chen, X., Zhang, L., Hua, F., Zhuang, Y., Liu, H., Wang, S. (2021). EphA4 Obstructs Spinal Cord Neuron Regeneration by Promoting Excessive Activation of Astrocytes. *Cell Mol Neurobiol*.
- Chen, Y., Fu, A.K., Ip, N.Y. (2012). Eph receptors at synapses: implications in neurodegenerative diseases. *Cell Signal* *24*, 606-611.
- Chen, Y., Wang, Y., Erturk, A., Kallop, D., Jiang, Z., Weimer, R.M., Kaminker, J., Sheng, M. (2014). Activity-induced Nr4a1 regulates spine density and distribution pattern of excitatory synapses in pyramidal neurons. *Neuron* *83*, 431-443.
- Chun, L.E., Woodruff, E.R., Morton, S., Hinds, L.R., Spencer, R.L. (2015). Variations in Phase and Amplitude of Rhythmic Clock Gene Expression across Prefrontal Cortex, Hippocampus, Amygdala, and Hypothalamic Paraventricular and Suprachiasmatic Nuclei of Male and Female Rats. *J Biol Rhythms* *30*, 417-436.
- Chung, S., Lee, E.J., Cha, H.K., Kim, J., Kim, D., Son, G.H., Kim, K. (2017). Cooperative roles of the suprachiasmatic nucleus central clock and the adrenal clock in controlling circadian glucocorticoid rhythm. *Sci Rep* *7*, 46404.
- Cipolla-Neto, J., Amaral, F.G., Afeche, S.C., Tan, D.X., Reiter, R.J. (2014). Melatonin, energy metabolism, and obesity: a review. *J Pineal Res* *56*, 371-381.
- Cirelli, C., Tononi, G. (2000). Gene expression in the brain across the sleep-waking cycle. *Brain Res* *885*, 303-321.

- Cirelli, C., Tononi, G. (2008). Is sleep essential? *PLoS Biol* 6, e216.
- Cirelli, C., Tononi, G. (2022). The why and how of sleep-dependent synaptic down-selection. *Semin Cell Dev Biol* 125, 91-100.
- Cirelli, C., Gutierrez, C.M., Tononi, G. (2004). Extensive and divergent effects of sleep and wakefulness on brain gene expression. *Neuron* 41, 35-43.
- Cisse, Y., Toossi, H., Ishibashi, M., Mainville, L., Leonard, C.S., Adamantidis, A., Jones, B.E. (2018). Discharge and Role of Acetylcholine Pontomesencephalic Neurons in Cortical Activity and Sleep-Wake States Examined by Optogenetics and Juxtacellular Recording in Mice. *eNeuro* 5.
- Clasadonte, J., Scemes, E., Wang, Z., Boison, D., Haydon, P.G. (2017). Connexin 43-Mediated Astroglial Metabolic Networks Contribute to the Regulation of the Sleep-Wake Cycle. *Neuron* 95, 1365-1380 e1365.
- Clawson, B.C., Durkin, J., Suresh, A.K., Pickup, E.J., Broussard, C.G., Aton, S.J. (2018). Sleep Promotes, and Sleep Loss Inhibits, Selective Changes in Firing Rate, Response Properties and Functional Connectivity of Primary Visual Cortex Neurons. *Front Syst Neurosci* 12, 40.
- Cooper, J.M., Halter, K.A., Prosser, R.A. (2018). Circadian rhythm and sleep-wake systems share the dynamic extracellular synaptic milieu. *Neurobiol Sleep Circadian Rhythms* 5, 15-36.
- Cowan, C.A., Henkemeyer, M. (2001). The SH2/SH3 adaptor Grb4 transduces B-ephrin reverse signals. *Nature* 413, 174-179.
- Curie, T., Maret, S., Emmenegger, Y., Franken, P. (2015). In Vivo Imaging of the Central and Peripheral Effects of Sleep Deprivation and Suprachiasmatic Nuclei Lesion on PERIOD-2 Protein in Mice. *Sleep* 38, 1381-1394.
- Curie, T., Mongrain, V., Dorsaz, S., Mang, G.M., Emmenegger, Y., Franken, P. (2013). Homeostatic and circadian contribution to EEG and molecular state variables of sleep regulation. *Sleep* 36, 311-323.
- Curtis, A.M., Bellet, M.M., Sassone-Corsi, P., O'Neill, L.A. (2014). Circadian clock proteins and immunity. *Immunity* 40, 178-186.
- Cusmano, D.M., Hadjimarkou, M.M., Mong, J.A. (2014). Gonadal steroid modulation of sleep and wakefulness in male and female rats is sexually differentiated and neonatally organized by steroid exposure. *Endocrinology* 155, 204-214.
- Daan, S., Beersma, D.G., Borbely, A.A. (1984). Timing of human sleep: recovery process gated by a circadian pacemaker. *Am J Physiol* 246, R161-183.
- Dalva, M.B., Takasu, M.A., Lin, M.Z., Shamah, S.M., Hu, L., Gale, N.W., Greenberg, M.E. (2000). EphB receptors interact with NMDA receptors and regulate excitatory synapse formation. *Cell* 103, 945-956.
- Dao, L.T.M., Galindo-Albarran, A.O., Castro-Mondragon, J.A., Andrieu-Soler, C., Medina-Rivera, A., Souaid, C., Charbonnier, G., Griffon, A., Vanhille, L., Stephen, T., Alomairi, J., Martin, D., Torres, M., Fernandez, N., Soler, E., van Helden, J., Puthier, D., Spicuglia, S. (2017). Genome-wide characterization of mammalian promoters with distal enhancer functions. *Nat Genet* 49, 1073-1081.
- Datta, S., Siwek, D.F. (1997). Excitation of the brain stem pedunculopontine tegmentum cholinergic cells induces wakefulness and REM sleep. *J Neurophysiol* 77, 2975-2988.
- Datta, S., Spooley, E.E., Patterson, E.H. (2001). Microinjection of glutamate into the pedunculopontine tegmentum induces REM sleep and wakefulness in the rat. *Am J Physiol Regul Integr Comp Physiol* 280, R752-759.

- Davis, S., Gale, N.W., Aldrich, T.H., Maisonpierre, P.C., Lhotak, V., Pawson, T., Goldfarb, M., Yancopoulos, G.D. (1994). Ligands for EPH-related receptor tyrosine kinases that require membrane attachment or clustering for activity. *Science* *266*, 816-819.
- Davy, A., Gale, N.W., Murray, E.W., Klinghoffer, R.A., Soriano, P., Feuerstein, C., Robbins, S.M. (1999). Compartmentalized signaling by GPI-anchored ephrin-A5 requires the Fyn tyrosine kinase to regulate cellular adhesion. *Genes Dev* *13*, 3125-3135.
- de Marcondes, P.G., Bastos, L.G., de-Freitas-Junior, J.C., Rocha, M.R., Morgado-Diaz, J.A. (2016). EphA4-mediated signaling regulates the aggressive phenotype of irradiation survivor colorectal cancer cells. *Tumour Biol* *37*, 12411-12422.
- De Sarro, G., Gareri, P., Sinopoli, V.A., David, E., Rotiroti, D. (1997). Comparative, behavioural and electrocortical effects of tumor necrosis factor-alpha and interleukin-1 microinjected into the locus coeruleus of rat. *Life Sci* *60*, 555-564.
- de Vivo, L., Bellesi, M., Marshall, W., Bushong, E.A., Ellisman, M.H., Tononi, G., Cirelli, C. (2017). Ultrastructural evidence for synaptic scaling across the wake/sleep cycle. *Science* *355*, 507-510.
- Deboer, T. (2015). Behavioral and electrophysiological correlates of sleep and sleep homeostasis. *Curr Top Behav Neurosci* *25*, 1-24.
- Deboer, T., Franken, P., Tobler, I. (1994). Sleep and cortical temperature in the Djungarian hamster under baseline conditions and after sleep deprivation. *J Comp Physiol A* *174*, 145-155.
- DeBruyne, J.P., Weaver, D.R., Reppert, S.M. (2007). CLOCK and NPAS2 have overlapping roles in the suprachiasmatic circadian clock. *Nat Neurosci* *10*, 543-545.
- Del Percio, C., Drinkenburg, W., Lopez, S., Infarinato, F., Bastlund, J.F., Laursen, B., Pedersen, J.T., Christensen, D.Z., Forloni, G., Frasca, A., Noe, F.M., Bentivoglio, M., Fabene, P.F., Bertini, G., Colavito, V., Kelley, J., Dix, S., Richardson, J.C., Babiloni, C., PharmaCog, C. (2017). On-going electroencephalographic rhythms related to cortical arousal in wild-type mice: the effect of aging. *Neurobiol Aging* *49*, 20-30.
- Dib, R., Gervais, N.J., Mongrain, V. (2021). A review of the current state of knowledge on sex differences in sleep and circadian phenotypes in rodents. *Neurobiol Sleep Circadian Rhythms* *11*, 100068.
- Dierickx, P. et al. (2022). Circadian REV-ERBs repress E4bp4 to activate NAMPT-dependent NAD(+) biosynthesis and sustain cardiac function. *Nat Cardiovasc Res* *1*, 45-58.
- Diering, G.H., Nirujogi, R.S., Roth, R.H., Worley, P.F., Pandey, A., Haganir, R.L. (2017). Homer1a drives homeostatic scaling-down of excitatory synapses during sleep. *Science* *355*, 511-515.
- Diessler, S., Jan, M., Emmenegger, Y., Guex, N., Middleton, B., Skene, D.J., Ibberson, M., Burdet, F., Gotz, L., Pagni, M., Sankar, M., Liechti, R., Hor, C.N., Xenarios, I., Franken, P. (2018). A systems genetics resource and analysis of sleep regulation in the mouse. *PLoS Biol* *16*, e2005750.
- Dijk, D.J., Beersma, D.G., Daan, S. (1987a). EEG power density during nap sleep: reflection of an hourglass measuring the duration of prior wakefulness. *J Biol Rhythms* *2*, 207-219.
- Dijk, D.J., Beersma, D.G., Bloem, G.M. (1989). Sex differences in the sleep EEG of young adults: visual scoring and spectral analysis. *Sleep* *12*, 500-507.

- Dijk, D.J., Brunner, D.P., Borbely, A.A. (1990). Time course of EEG power density during long sleep in humans. *Am J Physiol* 258, R650-661.
- Dijk, D.J., Beersma, D.G., Daan, S., Bloem, G.M., Van den Hoofdakker, R.H. (1987b). Quantitative analysis of the effects of slow wave sleep deprivation during the first 3 h of sleep on subsequent EEG power density. *Eur Arch Psychiatry Neurol Sci* 236, 323-328.
- Dissel, S. (2022). New Insights into Sleep Regulation in Flies. In: *Sleep Regulation and Function*, Gordon Research Conference. Barga, Italy.
- Dollins, A.B., Zhdanova, I.V., Wurtman, R.J., Lynch, H.J., Deng, M.H. (1994). Effect of inducing nocturnal serum melatonin concentrations in daytime on sleep, mood, body temperature, and performance. *Proc Natl Acad Sci U S A* 91, 1824-1828.
- Dottori, M., Hartley, L., Galea, M., Paxinos, G., Polizzotto, M., Kilpatrick, T., Bartlett, P.F., Murphy, M., Kontgen, F., Boyd, A.W. (1998). EphA4 (Sek1) receptor tyrosine kinase is required for the development of the corticospinal tract. *Proc Natl Acad Sci U S A* 95, 13248-13253.
- Drescher, U. (2002). Eph family functions from an evolutionary perspective. *Curr Opin Genet Dev* 12, 397-402.
- Dudilot, A., Trillaud-Doppia, E., Boehm, J. (2020). RCAN1 Regulates Bidirectional Synaptic Plasticity. *Curr Biol* 30, 1167-1176 e1162.
- Duez, H., van der Veen, J.N., Duhem, C., Pourcet, B., Touvier, T., Fontaine, C., Derudas, B., Bauge, E., Havinga, R., Bloks, V.W., Wolters, H., van der Sluijs, F.H., Vennstrom, B., Kuipers, F., Staels, B. (2008). Regulation of bile acid synthesis by the nuclear receptor Rev-erbalpha. *Gastroenterology* 135, 689-698.
- Duffy, J.F., Wright, K.P., Jr. (2005). Entrainment of the human circadian system by light. *J Biol Rhythms* 20, 326-338.
- Dufort-Gervais, J., Provost, C., Charbonneau, L., Norris, C.M., Calon, F., Mongrain, V., Brouillette, J. (2020). Neuroligin-1 is altered in the hippocampus of Alzheimer's disease patients and mouse models, and modulates the toxicity of amyloid-beta oligomers. *Sci Rep* 10, 6956.
- Dufour, A., Egea, J., Kullander, K., Klein, R., Vanderhaeghen, P. (2006). Genetic analysis of EphA-dependent signaling mechanisms controlling topographic mapping in vivo. *Development* 133, 4415-4420.
- Dumoulin Bridi, M.C., Aton, S.J., Seibt, J., Renouard, L., Coleman, T., Frank, M.G. (2015). Rapid eye movement sleep promotes cortical plasticity in the developing brain. *Sci Adv* 1, e1500105.
- Dumoulin, M.C., Aton, S.J., Watson, A.J., Renouard, L., Coleman, T., Frank, M.G. (2015). Extracellular signal-regulated kinase (ERK) activity during sleep consolidates cortical plasticity in vivo. *Cereb Cortex* 25, 507-515.
- Ebrahim, I.O., Sharief, M.K., de Lacy, S., Semra, Y.K., Howard, R.S., Kopelman, M.D., Williams, A.J. (2003). Hypocretin (orexin) deficiency in narcolepsy and primary hypersomnia. *J Neurol Neurosurg Psychiatry* 74, 127-130.
- Egashira, N., Nogami, A., Iwasaki, K., Ishibashi, A., Uchida, N., Takasaki, K., Mishima, K., Nishimura, R., Oishi, R., Fujiwara, M. (2011). Yokukansan enhances pentobarbital-induced sleep in socially isolated mice: possible involvement of GABA(A)-benzodiazepine receptor complex. *J Pharmacol Sci* 116, 316-320.

- Ehlen, J.C., Hesse, S., Pinckney, L., Paul, K.N. (2013). Sex chromosomes regulate nighttime sleep propensity during recovery from sleep loss in mice. *PLoS One* *8*, e62205.
- El Helou, J., Belanger-Nelson, E., Freyburger, M., Dorsaz, S., Curie, T., La Spada, F., Gaudreault, P.O., Beaumont, E., Pouliot, P., Lesage, F., Frank, M.G., Franken, P., Mongrain, V. (2013). Neuroligin-1 links neuronal activity to sleep-wake regulation. *Proc Natl Acad Sci U S A* *110*, 9974-9979.
- Elder, G.J., Wetherell, M.A., Barclay, N.L., Ellis, J.G. (2014). The cortisol awakening response--applications and implications for sleep medicine. *Sleep Med Rev* *18*, 215-224.
- Essmann, C.L., Martinez, E., Geiger, J.C., Zimmer, M., Traut, M.H., Stein, V., Klein, R., Acker-Palmer, A. (2008). Serine phosphorylation of ephrinB2 regulates trafficking of synaptic AMPA receptors. *Nat Neurosci* *11*, 1035-1043.
- Etienne-Manneville, S., Hall, A. (2003). Cdc42 regulates GSK-3beta and adenomatous polyposis coli to control cell polarity. *Nature* *421*, 753-756.
- Faraguna, U., Vyazovskiy, V.V., Nelson, A.B., Tononi, G., Cirelli, C. (2008). A causal role for brain-derived neurotrophic factor in the homeostatic regulation of sleep. *J Neurosci* *28*, 4088-4095.
- Fasanaro, P., D'Alessandra, Y., Di Stefano, V., Melchionna, R., Romani, S., Pompilio, G., Capogrossi, M.C., Martelli, F. (2008). MicroRNA-210 modulates endothelial cell response to hypoxia and inhibits the receptor tyrosine kinase ligand Ephrin-A3. *J Biol Chem* *283*, 15878-15883.
- Fernandez, L.M., Vantomme, G., Osorio-Forero, A., Cardis, R., Beard, E., Luthi, A. (2018). Thalamic reticular control of local sleep in mouse sensory cortex. *Elife* *7*.
- Fernandez, L.M.J., Luthi, A. (2020). Sleep Spindles: Mechanisms and Functions. *Physiol Rev* *100*, 805-868.
- Ferrara, M., De Gennaro, L. (2011). Going local: insights from EEG and stereo-EEG studies of the human sleep-wake cycle. *Curr Top Med Chem* *11*, 2423-2437.
- Ferrie, J.E., Kumari, M., Salo, P., Singh-Manoux, A., Kivimaki, M. (2011). Sleep epidemiology--a rapidly growing field. *Int J Epidemiol* *40*, 1431-1437.
- Filosa, A., Paixao, S., Honsek, S.D., Carmona, M.A., Becker, L., Feddersen, B., Gaitanos, L., Rudhard, Y., Schoepfer, R., Klopstock, T., Kullander, K., Rose, C.R., Pasquale, E.B., Klein, R. (2009). Neuron-glia communication via EphA4/ephrin-A3 modulates LTP through glial glutamate transport. *Nat Neurosci* *12*, 1285-1292.
- Fiore, L., Medori, M., Spelzini, G., Carreno, C.O., Carri, N.G., Sanchez, V., Scicolone, G. (2019). Regulation of axonal EphA4 forward signaling is involved in the effect of EphA3 on chicken retinal ganglion cell axon growth during retinotectal mapping. *Exp Eye Res* *178*, 46-60.
- Flanagan, J.G., Vanderhaeghen, P. (1998). The ephrins and Eph receptors in neural development. *Annu Rev Neurosci* *21*, 309-345.
- Flavell, S.W., Cowan, C.W., Kim, T.K., Greer, P.L., Lin, Y., Paradis, S., Griffith, E.C., Hu, L.S., Chen, C., Greenberg, M.E. (2006). Activity-dependent regulation of MEF2 transcription factors suppresses excitatory synapse number. *Science* *311*, 1008-1012.
- Frank, M.G., Heller, H.C. (2019). The Function(s) of Sleep. *Handb Exp Pharmacol* *253*, 3-34.
- Frank, M.G., Waldrop, R.H., Dumoulin, M., Aton, S., Boal, J.G. (2012). A preliminary analysis of sleep-like states in the cuttlefish *Sepia officinalis*. *PLoS One* *7*, e38125.

- Franken, P., Dijk, D.J. (2009). Circadian clock genes and sleep homeostasis. *Eur J Neurosci* 29, 1820-1829.
- Franken, P., Tobler, I., Borbely, A.A. (1991a). Sleep homeostasis in the rat: simulation of the time course of EEG slow-wave activity. *Neurosci Lett* 130, 141-144.
- Franken, P., Malafosse, A., Tafti, M. (1998). Genetic variation in EEG activity during sleep in inbred mice. *Am J Physiol* 275, R1127-1137.
- Franken, P., Dijk, D.J., Tobler, I., Borbely, A.A. (1991b). Sleep deprivation in rats: effects on EEG power spectra, vigilance states, and cortical temperature. *Am J Physiol* 261, R198-208.
- Franken, P., Dudley, C.A., Estill, S.J., Barakat, M., Thomason, R., O'Hara, B.F., McKnight, S.L. (2006). NPAS2 as a transcriptional regulator of non-rapid eye movement sleep: genotype and sex interactions. *Proc Natl Acad Sci U S A* 103, 7118-7123.
- Freyburger, M., Poirier, G., Carrier, J., Mongrain, V. (2017). Shorter duration of non-rapid eye movement sleep slow waves in EphA4 knockout mice. *J Sleep Res* 26, 539-546.
- Freyburger, M., Pierre, A., Paquette, G., Belanger-Nelson, E., Bedont, J., Gaudreault, P.O., Drolet, G., Laforest, S., Blackshaw, S., Cermakian, N., Doucet, G., Mongrain, V. (2016). EphA4 is Involved in Sleep Regulation but Not in the Electrophysiological Response to Sleep Deprivation. *Sleep* 39, 613-624.
- Friedman, T.C., Garcia-Borreguero, D., Hardwick, D., Akuete, C.N., Stambuk, M.K., Dorn, L.D., Starkman, M.N., Loh, Y.P., Chrousos, G.P. (1994). Diurnal rhythm of plasma delta-sleep-inducing peptide in humans: evidence for positive correlation with body temperature and negative correlation with rapid eye movement and slow wave sleep. *J Clin Endocrinol Metab* 78, 1085-1089.
- Frye, M., Stritt, S., Orsater, H., Hernandez Vasquez, M., Kaakinen, M., Vicente, A., Wiseman, J., Eklund, L., Martinez-Torrecuadrada, J.L., Vestweber, D., Mäkinen, T. (2020). EphrinB2-EphB4 signalling provides Rho-mediated homeostatic control of lymphatic endothelial cell junction integrity. *Elife* 9.
- Fu, A.K.Y., Hung, K.W., Fu, W.Y., Shen, C., Chen, Y., Xia, J., Lai, K.O., Ip, N.Y. (2011). APC(Cdh1) mediates EphA4-dependent downregulation of AMPA receptors in homeostatic plasticity. *Nat Neurosci* 14, 181-189.
- Fu, A.K.Y., Hung, K.W., Huang, H., Gu, S., Shen, Y., Cheng, E.Y., Ip, F.C., Huang, X., Fu, W.Y., Ip, N.Y. (2014). Blockade of EphA4 signaling ameliorates hippocampal synaptic dysfunctions in mouse models of Alzheimer's disease. *Proc Natl Acad Sci U S A* 111, 9959-9964.
- Fu, W.Y., Chen, Y., Sahin, M., Zhao, X.S., Shi, L., Bikoff, J.B., Lai, K.O., Yung, W.H., Fu, A.K., Greenberg, M.E., Ip, N.Y. (2007). Cdk5 regulates EphA4-mediated dendritic spine retraction through an ephexin1-dependent mechanism. *Nat Neurosci* 10, 67-76.
- Fujita, A., Bonnavion, P., Wilson, M.H., Mickelsen, L.E., Bloit, J., de Lecea, L., Jackson, A.C. (2017). Hypothalamic Tuberomammillary Nucleus Neurons: Electrophysiological Diversity and Essential Role in Arousal Stability. *J Neurosci* 37, 9574-9592.
- Fukai, J., Yokote, H., Yamanaka, R., Arai, T., Nishio, K., Itakura, T. (2008). EphA4 promotes cell proliferation and migration through a novel EphA4-FGFR1 signaling pathway in the human glioma U251 cell line. *Mol Cancer Ther* 7, 2768-2778.
- Funato, H. et al. (2016). Forward-genetics analysis of sleep in randomly mutagenized mice. *Nature* 539, 378-383.
- Furlong, E.E.M., Levine, M. (2018). Developmental enhancers and chromosome topology. *Science* 361, 1341-1345.

- Gaine, M.E., Bahl, E., Chatterjee, S., Michaelson, J.J., Abel, T., Lyons, L.C. (2021). Altered hippocampal transcriptome dynamics following sleep deprivation. *Mol Brain* *14*, 125.
- Gale, N.W., Baluk, P., Pan, L., Kwan, M., Holash, J., DeChiara, T.M., McDonald, D.M., Yancopoulos, G.D. (2001). Ephrin-B2 selectively marks arterial vessels and neovascularization sites in the adult, with expression in both endothelial and smooth-muscle cells. *Dev Biol* *230*, 151-160.
- Galimberti, I., Bednarek, E., Donato, F., Caroni, P. (2010). EphA4 signaling in juveniles establishes topographic specificity of structural plasticity in the hippocampus. *Neuron* *65*, 627-642.
- Gan-Or, Z., Alcalay, R.N., Rouleau, G.A., Postuma, R.B. (2018). Sleep disorders and Parkinson disease; lessons from genetics. *Sleep Med Rev* *41*, 101-112.
- Gandhi, A.V., Mosser, E.A., Oikonomou, G., Prober, D.A. (2015). Melatonin is required for the circadian regulation of sleep. *Neuron* *85*, 1193-1199.
- Gardi, J., Obal, F., Jr., Fang, J., Zhang, J., Krueger, J.M. (1999). Diurnal variations and sleep deprivation-induced changes in rat hypothalamic GHRH and somatostatin contents. *Am J Physiol* *277*, R1339-1344.
- Gatto, G., Morales, D., Kania, A., Klein, R. (2014). EphA4 receptor shedding regulates spinal motor axon guidance. *Curr Biol* *24*, 2355-2365.
- Gau, D., Lemberger, T., von Gall, C., Kretz, O., Le Minh, N., Gass, P., Schmid, W., Schibler, U., Korf, H.W., Schutz, G. (2002). Phosphorylation of CREB Ser142 regulates light-induced phase shifts of the circadian clock. *Neuron* *34*, 245-253.
- Gekakis, N., Staknis, D., Nguyen, H.B., Davis, F.C., Wilsbacher, L.D., King, D.P., Takahashi, J.S., Weitz, C.J. (1998). Role of the CLOCK protein in the mammalian circadian mechanism. *Science* *280*, 1564-1569.
- Gent, T.C., Bandarabadi, M., Herrera, C.G., Adamantidis, A.R. (2018). Thalamic dual control of sleep and wakefulness. *Nat Neurosci* *21*, 974-984.
- Gerety, S.S., Wang, H.U., Chen, Z.F., Anderson, D.J. (1999). Symmetrical mutant phenotypes of the receptor EphB4 and its specific transmembrane ligand ephrin-B2 in cardiovascular development. *Mol Cell* *4*, 403-414.
- Gerstmann, K., Pensold, D., Symmank, J., Khundadze, M., Hubner, C.A., Bolz, J., Zimmer, G. (2015). Thalamic afferents influence cortical progenitors via ephrin A5-EphA4 interactions. *Development* *142*, 140-150.
- Gervais, N.J., Mong, J.A., Lacreuse, A. (2017). Ovarian hormones, sleep and cognition across the adult female lifespan: An integrated perspective. *Front Neuroendocrinol* *47*, 134-153.
- Girardeau, G., Benchenane, K., Wiener, S.I., Buzsaki, G., Zugaro, M.B. (2009). Selective suppression of hippocampal ripples impairs spatial memory. *Nat Neurosci* *12*, 1222-1223.
- Giuditta, A., Rutigliano, B., Vitale-Neugebauer, A. (1980). Influence of synchronized sleep on the biosynthesis of RNA in neuronal and mixed fractions isolated from rabbit cerebral cortex. *J Neurochem* *35*, 1267-1272.
- Glass, J.D., Shen, H., Fedorkova, L., Chen, L., Tomasiewicz, H., Watanabe, M. (2000). Polysialylated neural cell adhesion molecule modulates photic signaling in the mouse suprachiasmatic nucleus. *Neurosci Lett* *280*, 207-210.
- Glass, J.D., Watanabe, M., Fedorkova, L., Shen, H., Ungers, G., Rutishauser, U. (2003). Dynamic regulation of polysialylated neural cell adhesion molecule in the suprachiasmatic nucleus. *Neuroscience* *117*, 203-211.

- Gobbi, G., Comai, S. (2019). Differential Function of Melatonin MT1 and MT2 Receptors in REM and NREM Sleep. *Front Endocrinol (Lausanne)* *10*, 87.
- Goldshmit, Y., Bourne, J. (2010). Upregulation of EphA4 on astrocytes potentially mediates astrocytic gliosis after cortical lesion in the marmoset monkey. *J Neurotrauma* *27*, 1321-1332.
- Goldshmit, Y., Galea, M.P., Bartlett, P.F., Turnley, A.M. (2006). EphA4 regulates central nervous system vascular formation. *J Comp Neurol* *497*, 864-875.
- Gomez-Maldonado, L., Tiana, M., Roche, O., Prado-Cabrero, A., Jensen, L., Fernandez-Barral, A., Guijarro-Munoz, I., Favaro, E., Moreno-Bueno, G., Sanz, L., Aragonés, J., Harris, A., Volpert, O., Jimenez, B., del Peso, L. (2015). EFNA3 long noncoding RNAs induced by hypoxia promote metastatic dissemination. *Oncogene* *34*, 2609-2620.
- Grandner, M.A. (2017). Sleep, Health, and Society. *Sleep Med Clin* *12*, 1-22.
- Gronli, J., Rempe, M.J., Clegern, W.C., Schmidt, M., Wisor, J.P. (2016). Beta EEG reflects sensory processing in active wakefulness and homeostatic sleep drive in quiet wakefulness. *J Sleep Res* *25*, 257-268.
- Grunwald, I.C., Korte, M., Wolfer, D., Wilkinson, G.A., Unsicker, K., Lipp, H.P., Bonhoeffer, T., Klein, R. (2001). Kinase-independent requirement of EphB2 receptors in hippocampal synaptic plasticity. *Neuron* *32*, 1027-1040.
- Grunwald, I.C., Korte, M., Adelmann, G., Plueck, A., Kullander, K., Adams, R.H., Frotscher, M., Bonhoeffer, T., Klein, R. (2004). Hippocampal plasticity requires postsynaptic ephrinBs. *Nat Neurosci* *7*, 33-40.
- Guillaumond, F., Dardente, H., Giguere, V., Cermakian, N. (2005). Differential control of Bmal1 circadian transcription by REV-ERB and ROR nuclear receptors. *J Biol Rhythms* *20*, 391-403.
- Gulati, T., Guo, L., Ramanathan, D.S., Bodepudi, A., Ganguly, K. (2017). Neural reactivations during sleep determine network credit assignment. *Nat Neurosci* *20*, 1277-1284.
- Guo, X., Keenan, B.T., Sarantopoulou, D., Lim, D.C., Lian, J., Grant, G.R., Pack, A.I. (2019). Age attenuates the transcriptional changes that occur with sleep in the medial prefrontal cortex. *Aging Cell* *18*, e13021.
- Guo, X., Gao, X., Keenan, B.T., Zhu, J., Sarantopoulou, D., Lian, J., Galante, R.J., Grant, G.R., Pack, A.I. (2020). RNA-seq analysis of galaninergic neurons from ventrolateral preoptic nucleus identifies expression changes between sleep and wake. *BMC Genomics* *21*, 633.
- Gvilia, I., Suntsova, N., Kumar, S., McGinty, D., Szymusiak, R. (2015). Suppression of preoptic sleep-regulatory neuronal activity during corticotropin-releasing factor-induced sleep disturbance. *Am J Physiol Regul Integr Comp Physiol* *309*, R1092-1100.
- Haberle, V., Stark, A. (2018). Eukaryotic core promoters and the functional basis of transcription initiation. *Nat Rev Mol Cell Biol* *19*, 621-637.
- Hafner, C., Schmitz, G., Meyer, S., Bataille, F., Hau, P., Langmann, T., Dietmaier, W., Landthaler, M., Vogt, T. (2004). Differential gene expression of Eph receptors and ephrins in benign human tissues and cancers. *Clin Chem* *50*, 490-499.
- Hafner, M., Stepanek, M., Taylor, J., Troxel, W.M., van Stolk, C. (2017). Why Sleep Matters-The Economic Costs of Insufficient Sleep: A Cross-Country Comparative Analysis. *Rand Health Q* *6*, 11.



- Hallett, H., Churchill, L., Taishi, P., De, A., Krueger, J.M. (2010). Whisker stimulation increases expression of nerve growth factor- and interleukin-1beta-immunoreactivity in the rat somatosensory cortex. *Brain Res* 1333, 48-56.
- Han, Y., Shi, Y.F., Xi, W., Zhou, R., Tan, Z.B., Wang, H., Li, X.M., Chen, Z., Feng, G., Luo, M., Huang, Z.L., Duan, S., Yu, Y.Q. (2014). Selective activation of cholinergic basal forebrain neurons induces immediate sleep-wake transitions. *Curr Biol* 24, 693-698.
- Hannibal, J. (2002). Neurotransmitters of the retino-hypothalamic tract. *Cell Tissue Res* 309, 73-88.
- Hannou, L., Roy, P.G., Ballester Roig, M.N., Mongrain, V. (2020). Transcriptional control of synaptic components by the clock machinery. *Eur J Neurosci* 51, 241-267.
- Hannou, L., Belanger-Nelson, E., O'Callaghan, E.K., Dufort-Gervais, J., Ballester Roig, M.N., Roy, P.G., Beaulieu, J.M., Cermakian, N., Mongrain, V. (2018). Regulation of the Neurologin-1 Gene by Clock Transcription Factors. *J Biol Rhythms* 33, 166-178.
- Hansen, A.K., Nedergaard, S., Andreasen, M. (2014). Intrinsic Ca<sup>2+</sup>-dependent theta oscillations in apical dendrites of hippocampal CA1 pyramidal cells in vitro. *J Neurophysiol* 112, 631-643.
- Harada, Y., Sakai, M., Kurabayashi, N., Hirota, T., Fukada, Y. (2005). Ser-557-phosphorylated mCRY2 is degraded upon synergistic phosphorylation by glycogen synthase kinase-3 beta. *J Biol Chem* 280, 31714-31721.
- Harboe, M., Torvund-Jensen, J., Kjaer-Sorensen, K., Laursen, L.S. (2018). Ephrin-A1-EphA4 signaling negatively regulates myelination in the central nervous system. *Glia* 66, 934-950.
- Harding, E.C., Yu, X., Miao, A., Andrews, N., Ma, Y., Ye, Z., Lignos, L., Miracca, G., Ba, W., Yustos, R., Vyssotski, A.L., Wisden, W., Franks, N.P. (2018). A Neuronal Hub Binding Sleep Initiation and Body Cooling in Response to a Warm External Stimulus. *Curr Biol* 28, 2263-2273 e2264.
- Harkness, J.H., Bushana, P.N., Todd, R.P., Clegern, W.C., Sorg, B.A., Wisor, J.P. (2019). Sleep disruption elevates oxidative stress in parvalbumin-positive cells of the rat cerebral cortex. *Sleep* 42.
- Harvey, A.L., Edrada-Ebel, R., Quinn, R.J. (2015). The re-emergence of natural products for drug discovery in the genomics era. *Nat Rev Drug Discov* 14, 111-129.
- Hassani, O.K., Lee, M.G., Jones, B.E. (2009). Melanin-concentrating hormone neurons discharge in a reciprocal manner to orexin neurons across the sleep-wake cycle. *Proc Natl Acad Sci U S A* 106, 2418-2422.
- Hastings, M.H., Maywood, E.S., Brancaccio, M. (2018). Generation of circadian rhythms in the suprachiasmatic nucleus. *Nat Rev Neurosci* 19, 453-469.
- Havekes, R., Aton, S.J. (2020). Impacts of Sleep Loss versus Waking Experience on Brain Plasticity: Parallel or Orthogonal? *Trends Neurosci* 43, 385-393.
- Hayasaka, N., Hirano, A., Miyoshi, Y., Tokuda, I.T., Yoshitane, H., Matsuda, J., Fukada, Y. (2017). Salt-inducible kinase 3 regulates the mammalian circadian clock by destabilizing PER2 protein. *Elife* 6.
- Headley, D.B., Pare, D. (2017). Common oscillatory mechanisms across multiple memory systems. *NPJ Sci Learn* 2.
- Heib, D.P., Hoedlmoser, K., Anderer, P., Zeitlhofer, J., Gruber, G., Klimesch, W., Schabus, M. (2013). Slow oscillation amplitudes and up-state lengths relate to memory improvement. *PLoS One* 8, e82049.
- Helmbacher, F., Schneider-Maunoury, S., Topilko, P., Tiret, L., Charnay, P. (2000). Targeting of the EphA4 tyrosine kinase receptor affects dorsal/ventral pathfinding of limb motor axons. *Development* 127, 3313-3324.

- Herrera, C.G., Cadavieco, M.C., Jago, S., Ponomarenko, A., Korotkova, T., Adamantidis, A. (2016). Hypothalamic feedforward inhibition of thalamocortical network controls arousal and consciousness. *Nat Neurosci* *19*, 290-298.
- Hide, I., Tanaka, M., Inoue, A., Nakajima, K., Kohsaka, S., Inoue, K., Nakata, Y. (2000). Extracellular ATP triggers tumor necrosis factor- $\alpha$  release from rat microglia. *J Neurochem* *75*, 965-972.
- Hillman, D., Mitchell, S., Streatfeild, J., Burns, C., Bruck, D., Pezzullo, L. (2018). The economic cost of inadequate sleep. *Sleep* *41*.
- Hinard, V., Mikhail, C., Pradervand, S., Curie, T., Houtkooper, R.H., Auwerx, J., Franken, P., Tafti, M. (2012). Key electrophysiological, molecular, and metabolic signatures of sleep and wakefulness revealed in primary cortical cultures. *J Neurosci* *32*, 12506-12517.
- Hirano, A., Hsu, P.K., Zhang, L., Xing, L., McMahon, T., Yamazaki, M., Ptacek, L.J., Fu, Y.H. (2018). DEC2 modulates orexin expression and regulates sleep. *Proc Natl Acad Sci U S A* *115*, 3434-3439.
- Ho, S.K., Kovacevic, N., Henkelman, R.M., Boyd, A., Pawson, T., Henderson, J.T. (2009). EphB2 and EphA4 receptors regulate formation of the principal inter-hemispheric tracts of the mammalian forebrain. *Neuroscience* *160*, 784-795.
- Ho, T.Y., Tang, N.Y., Hsiang, C.Y., Hsieh, C.L. (2014). *Uncaria rhynchophylla* and rhynchophylline improved kainic acid-induced epileptic seizures via IL-1 $\beta$  and brain-derived neurotrophic factor. *Phytomedicine* *21*, 893-900.
- Holz, J., Piosczyk, H., Feige, B., Spiegelhalter, K., Baglioni, C., Riemann, D., Nissen, C. (2012). EEG Sigma and slow-wave activity during NREM sleep correlate with overnight declarative and procedural memory consolidation. *J Sleep Res* *21*, 612-619.
- Honda, T., Fujiyama, T., Miyoshi, C., Ikkyu, A., Hotta-Hirashima, N., Kanno, S., Mizuno, S., Sugiyama, F., Takahashi, S., Funato, H., Yanagisawa, M. (2018). A single phosphorylation site of SIK3 regulates daily sleep amounts and sleep need in mice. *Proc Natl Acad Sci U S A* *115*, 10458-10463.
- Hong, Z.Y., Huang, Z.L., Qu, W.M., Eguchi, N., Urade, Y., Hayaishi, O. (2005). An adenosine A receptor agonist induces sleep by increasing GABA release in the tuberomammillary nucleus to inhibit histaminergic systems in rats. *J Neurochem* *92*, 1542-1549.
- Hor, C.N., Yeung, J., Jan, M., Emmenegger, Y., Hubbard, J., Xenarios, I., Naef, F., Franken, P. (2019). Sleep-wake-driven and circadian contributions to daily rhythms in gene expression and chromatin accessibility in the murine cortex. *Proc Natl Acad Sci U S A* *116*, 25773-25783.
- Hsiao, Y.H., Hung, H.C., Chen, S.H., Gean, P.W. (2014). Social interaction rescues memory deficit in an animal model of Alzheimer's disease by increasing BDNF-dependent hippocampal neurogenesis. *J Neurosci* *34*, 16207-16219.
- Hsu, J.C., Lee, Y.S., Chang, C.N., Chuang, H.L., Ling, E.A., Lan, C.T. (2003). Sleep deprivation inhibits expression of NADPH-d and NOS while activating microglia and astroglia in the rat hippocampus. *Cells Tissues Organs* *173*, 242-254.

- Hu, J.H., Park, J.M., Park, S., Xiao, B., Dehoff, M.H., Kim, S., Hayashi, T., Schwarz, M.K., Haganir, R.L., Seeburg, P.H., Linden, D.J., Worley, P.F. (2010). Homeostatic scaling requires group I mGluR activation mediated by Homer1a. *Neuron* 68, 1128-1142.
- Hu, S., Mak, S., Zuo, X., Li, H., Wang, Y., Han, Y. (2018). Neuroprotection against MPP(+)-induced cytotoxicity through the activation of PI3-K/Akt/GSK3beta/MEF2D signaling pathway by Rhynchophylline, the major tetracyclic oxindole alkaloid isolated from *Uncaria rhynchophylla*. *Front Pharmacol* 9, 768.
- Hu, Y., Li, S., Jiang, H., Li, M.T., Zhou, J.W. (2014). Ephrin-B2/EphA4 forward signaling is required for regulation of radial migration of cortical neurons in the mouse. *Neurosci Bull* 30, 425-432.
- Huang, T.C., Tu, J., Chow, T.J., Chen, T.H. (1990). Circadian Rhythm of the Prokaryote *Synechococcus* sp. RF-1. *Plant Physiol* 92, 531-533.
- Huang, Y.C., Lin, S.J., Lin, K.M., Chou, Y.C., Lin, C.W., Yu, S.C., Chen, C.L., Shen, T.L., Chen, C.K., Lu, J., Chen, M.R., Tsai, C.H. (2016). Regulation of EBV LMP1-triggered EphA4 downregulation in EBV-associated B lymphoma and its impact on patients' survival. *Blood* 128, 1578-1589.
- Huang, Z.L., Qu, W.M., Eguchi, N., Chen, J.F., Schwarzschild, M.A., Fredholm, B.B., Urade, Y., Hayaishi, O. (2005). Adenosine A2A, but not A1, receptors mediate the arousal effect of caffeine. *Nat Neurosci* 8, 858-859.
- Hubbard, J., Gent, T.C., Hoekstra, M.M.B., Emmenegger, Y., Mongrain, V., Landolt, H.P., Adamantidis, A.R., Franken, P. (2020). Rapid fast-delta decay following prolonged wakefulness marks a phase of wake-inertia in NREM sleep. *Nat Commun* 11, 3130.
- Huber, R., Tononi, G., Cirelli, C. (2007). Exploratory behavior, cortical BDNF expression, and sleep homeostasis. *Sleep* 30, 129-139.
- Huber, R., Deboer, T., Schwierin, B., Tobler, I. (1998). Effect of melatonin on sleep and brain temperature in the Djungarian hamster and the rat. *Physiol Behav* 65, 77-82.
- Huber, R., Ghilardi, M.F., Massimini, M., Tononi, G. (2004). Local sleep and learning. *Nature* 430, 78-81.
- Hume, K.I., Van, F., Watson, A. (1998). A field study of age and gender differences in habitual adult sleep. *J Sleep Res* 7, 85-94.
- Hunter, A.S. (2018). REM deprivation but not sleep fragmentation produces a sex-specific impairment in extinction. *Physiol Behav* 196, 84-94.
- Husain, A., Chiu, Y.T., Sze, K.M., Ho, D.W., Tsui, Y.M., Suarez, E.M.S., Zhang, V.X., Chan, L.K., Lee, E., Lee, J.M., Cheung, T.T., Wong, C.C., Chung, C.Y., Ng, I.O. (2022). Ephrin-A3/EphA2 axis regulates cellular metabolic plasticity to enhance cancer stemness in hypoxic hepatocellular carcinoma. *J Hepatol*.
- Husse, J., Kiehn, J.T., Barclay, J.L., Naujokat, N., Meyer-Kovac, J., Lehnert, H., Oster, H. (2017). Tissue-Specific Dissociation of Diurnal Transcriptome Rhythms During Sleep Restriction in Mice. *Sleep* 40.
- Iitaka, C., Miyazaki, K., Akaike, T., Ishida, N. (2005). A role for glycogen synthase kinase-3beta in the mammalian circadian clock. *J Biol Chem* 280, 29397-29402.
- Ikeda, M., Ikeda, M. (2014). Bmal1 is an essential regulator for circadian cytosolic Ca(2)(+) rhythms in suprachiasmatic nucleus neurons. *J Neurosci* 34, 12029-12038.
- Imeri, L., Opp, M.R. (2009). How (and why) the immune system makes us sleep. *Nat Rev Neurosci* 10, 199-210.

- Ingiosi, A.M., Hayworth, C.R., Harvey, D.O., Singletary, K.G., Rempe, M.J., Wisor, J.P., Frank, M.G. (2020). A Role for Astroglial Calcium in Mammalian Sleep and Sleep Regulation. *Curr Biol* *30*, 4373-4383 e4377.
- Ingiosi, A.M., Schoch, H., Wintler, T., Singletary, K.G., Righelli, D., Roser, L.G., Medina, E., Risso, D., Frank, M.G., Peixoto, L. (2019). Shank3 modulates sleep and expression of circadian transcription factors. *Elife* *8*.
- Inoue, E., Deguchi-Tawarada, M., Togawa, A., Matsui, C., Arita, K., Katahira-Tayama, S., Sato, T., Yamauchi, E., Oda, Y., Takai, Y. (2009). Synaptic activity prompts gamma-secretase-mediated cleavage of EphA4 and dendritic spine formation. *J Cell Biol* *185*, 551-564.
- Inoue, Y., Udo, H., Inokuchi, K., Sugiyama, H. (2007). Homer1a regulates the activity-induced remodeling of synaptic structures in cultured hippocampal neurons. *Neuroscience* *150*, 841-852.
- Irwin, M.R. (2019). Sleep and inflammation: partners in sickness and in health. *Nat Rev Immunol* *19*, 702-715.
- Irwin, M.R., Vitiello, M.V. (2019). Implications of sleep disturbance and inflammation for Alzheimer's disease dementia. *Lancet Neurol* *18*, 296-306.
- Iwahana, E., Akiyama, M., Miyakawa, K., Uchida, A., Kasahara, J., Fukunaga, K., Hamada, T., Shibata, S. (2004). Effect of lithium on the circadian rhythms of locomotor activity and glycogen synthase kinase-3 protein expression in the mouse suprachiasmatic nuclei. *Eur J Neurosci* *19*, 2281-2287.
- Izawa, S., Chowdhury, S., Miyazaki, T., Mukai, Y., Ono, D., Inoue, R., Ohmura, Y., Mizoguchi, H., Kimura, K., Yoshioka, M., Terao, A., Kilduff, T.S., Yamanaka, A. (2019). REM sleep-active MCH neurons are involved in forgetting hippocampus-dependent memories. *Science* *365*, 1308-1313.
- Izumo, M., Johnson, C.H., Yamazaki, S. (2003). Circadian gene expression in mammalian fibroblasts revealed by real-time luminescence reporting: temperature compensation and damping. *Proc Natl Acad Sci U S A* *100*, 16089-16094.
- Jagannath, A. et al. (2021). Adenosine integrates light and sleep signalling for the regulation of circadian timing in mice. *Nat Commun* *12*, 2113.
- Jaggard, J.B., Wang, G.X., Mourrain, P. (2021). Non-REM and REM/paradoxical sleep dynamics across phylogeny. *Curr Opin Neurobiol* *71*, 44-51.
- Jakkamsetti, V., Tsai, N.P., Gross, C., Molinaro, G., Collins, K.A., Nicoletti, F., Wang, K.H., Osten, P., Bassell, G.J., Gibson, J.R., Huber, K.M. (2013). Experience-induced Arc/Arg3.1 primes CA1 pyramidal neurons for metabotropic glutamate receptor-dependent long-term synaptic depression. *Neuron* *80*, 72-79.
- Jan, M., O'Hara, B.F., Franken, P. (2020). Recent advances in understanding the genetics of sleep. *F1000Res* *9*.
- Jaworski, T., Banach-Kasper, E., Gralec, K. (2019). GSK-3beta at the Intersection of Neuronal Plasticity and Neurodegeneration. *Neural Plast* *2019*, 4209475.
- Jeenapongsa, R., Tohda, M. (2003). Effects of Choto-san and Chotoko on thiopental-induced sleeping time. *Journal of traditional medicines* *20*, 165-167.
- Jego, S., Glasgow, S.D., Herrera, C.G., Ekstrand, M., Reed, S.J., Boyce, R., Friedman, J., Burdakov, D., Adamantidis, A.R. (2013). Optogenetic identification of a rapid eye movement sleep modulatory circuit in the hypothalamus. *Nat Neurosci* *16*, 1637-1643.

- Jellinghaus, S., Poitz, D.M., Ende, G., Augstein, A., Weinert, S., Stutz, B., Braun-Dullaeus, R.C., Pasquale, E.B., Strasser, R.H. (2013). Ephrin-A1/EphA4-mediated adhesion of monocytes to endothelial cells. *Biochim Biophys Acta* 1833, 2201-2211.
- Jennings, K.J., de Lecea, L. (2019). Chapter 1 – Hypocretins (Orexins): Twenty years of dissecting arousal circuits. In: *The Orexin/Hypocretin System* (J.A. B, J.R. F, eds), pp 1-29. Cambridge: Academic Press.
- Jiang, H., Guo, W., Liang, X., Rao, Y. (2005). Both the establishment and the maintenance of neuronal polarity require active mechanisms: critical roles of GSK-3beta and its upstream regulators. *Cell* 120, 123-135.
- Jing, X., Sonoki, T., Miyajima, M., Sawada, T., Terada, N., Takemura, S., Sakaguchi, K. (2016). EphA4-deleted microenvironment regulates cancer development and leukemoid reaction of the isografted 4T1 murine breast cancer via reduction of an IGF1 signal. *Cancer Med* 5, 1214-1227.
- Joglekar, A. et al. (2021). A spatially resolved brain region- and cell type-specific isoform atlas of the postnatal mouse brain. *Nat Commun* 12, 463.
- Jones, B.E. (2020). Arousal and sleep circuits. *Neuropsychopharmacology* 45, 6-20.
- Jung, J.W., Ahn, N.Y., Oh, H.R., Lee, B.K., Lee, K.J., Kim, S.Y., Cheong, J.H., Ryu, J.H. (2006). Anxiolytic effects of the aqueous extract of *Uncaria rhynchophylla*. *J Ethnopharmacol* 108, 193-197.
- Kai, L.W., Z.F.; Xue, C.H. (1998). Effects of Rhynchophylline on L-type calcium channels in isolated rat cortical neurons during acute hypoxia. *Journal of Chinese Pharmaceutical Sciences* 7, 205-208.
- Kalinchuk, A.V., McCarley, R.W., Porkka-Heiskanen, T., Basheer, R. (2010). Sleep deprivation triggers inducible nitric oxide-dependent nitric oxide production in wake-active basal forebrain neurons. *J Neurosci* 30, 13254-13264.
- Kanaya, H.J., Park, S., Kim, J.H., Kusumi, J., Krenenou, S., Sawatari, E., Sato, A., Lee, J., Bang, H., Kobayakawa, Y., Lim, C., Itoh, T.Q. (2020). A sleep-like state in Hydra unravels conserved sleep mechanisms during the evolutionary development of the central nervous system. *Sci Adv* 6.
- Kang, T.H., Murakami, Y., Matsumoto, K., Takayama, H., Kitajima, M., Aimi, N., Watanabe, H. (2002). Rhynchophylline and isorhynchophylline inhibit NMDA receptors expressed in *Xenopus* oocytes. *Eur J Pharmacol* 455, 27-34.
- Kantojarvi, K., Liuhanen, J., Saarenpaa-Heikkila, O., Satomaa, A.L., Kylliainen, A., Polkki, P., Jaatela, J., Toivola, A., Milani, L., Himanen, S.L., Porkka-Heiskanen, T., Paavonen, J., Paunio, T. (2017). Variants in calcium voltage-gated channel subunit Alpha1 C-gene (CACNA1C) are associated with sleep latency in infants. *PLoS One* 12, e0180652.
- Kao, T.J., Law, C., Kania, A. (2012). Eph and ephrin signaling: lessons learned from spinal motor neurons. *Semin Cell Dev Biol* 23, 83-91.
- Kapas, L., Krueger, J.M. (1996). Nitric oxide donors SIN-1 and SNAP promote nonrapid-eye-movement sleep in rats. *Brain Res Bull* 41, 293-298.
- Kapas, L., Shibata, M., Kimura, M., Krueger, J.M. (1994). Inhibition of nitric oxide synthesis suppresses sleep in rabbits. *Am J Physiol* 266, R151-157.

- Keenan, R.J., Daykin, H., Chu, J., Cornthwaite-Duncan, L., Allocca, G., Hoyer, D., Jacobson, L.H. (2022). Differential sleep/wake response and sex differences following acute suvorexant, MK-1064 and zolpidem administration in the rTg4510 mouse model of tauopathy. *Br J Pharmacol*.
- Kempf, A., Song, S.M., Talbot, C.B., Miesenbock, G. (2019). A potassium channel beta-subunit couples mitochondrial electron transport to sleep. *Nature* 568, 230-234.
- Khlghatyan, J., Evstratova, A., Bozoyan, L., Chamberland, S., Chatterjee, D., Marakhovskaia, A., Soares Silva, T., Toth, K., Mongrain, V., Beaulieu, J.M. (2020). Fxr1 regulates sleep and synaptic homeostasis. *EMBO J* 39, e103864.
- Kiessling, S., Sollars, P.J., Pickard, G.E. (2014). Light stimulates the mouse adrenal through a retinohypothalamic pathway independent of an effect on the clock in the suprachiasmatic nucleus. *PLoS One* 9, e92959.
- Kiessling, S., O'Callaghan, E.K., Freyburger, M., Cermakian, N., Mongrain, V. (2018). The cell adhesion molecule EphA4 is involved in circadian clock functions. *Genes Brain Behav* 17, 82-92.
- Kim, J., Gulati, T., Ganguly, K. (2019). Competing Roles of Slow Oscillations and Delta Waves in Memory Consolidation versus Forgetting. *Cell* 179, 514-526 e513.
- Kim, J.H., Bae, C.H., Park, S.Y., Lee, S.J., Kim, Y. (2010). Uncaria rhynchophylla inhibits the production of nitric oxide and interleukin-1beta through blocking nuclear factor kappaB, Akt, and mitogen-activated protein kinase activation in macrophages. *J Med Food* 13, 1133-1140.
- Kim, S., Kim, H., Um, J.W. (2018). Synapse development organized by neuronal activity-regulated immediate-early genes. *Exp Mol Med* 50, 1-7.
- Kim, W.Y., Zhou, F.Q., Zhou, J., Yokota, Y., Wang, Y.M., Yoshimura, T., Kaibuchi, K., Woodgett, J.R., Anton, E.S., Snider, W.D. (2006). Essential roles for GSK-3s and GSK-3-primed substrates in neurotrophin-induced and hippocampal axon growth. *Neuron* 52, 981-996.
- Kinoshita, C., Miyazaki, K., Ishida, N. (2012). Chronic stress affects PERIOD2 expression through glycogen synthase kinase-3beta phosphorylation in the central clock. *Neuroreport* 23, 98-102.
- Klugmann, M., Leichtlein, C.B., Symes, C.W., Klaussner, B.C., Brooks, A.I., Young, D., During, M.J. (2006). A novel role of circadian transcription factor DBP in hippocampal plasticity. *Mol Cell Neurosci* 31, 303-314.
- Koehl, M., Battle, S., Meerlo, P. (2006). Sex differences in sleep: the response to sleep deprivation and restraint stress in mice. *Sleep* 29, 1224-1231.
- Koike, N., Yoo, S.H., Huang, H.C., Kumar, V., Lee, C., Kim, T.K., Takahashi, J.S. (2012). Transcriptional architecture and chromatin landscape of the core circadian clock in mammals. *Science* 338, 349-354.
- Kojima, S., Hirose, M., Tokunaga, K., Sakaki, Y., Tei, H. (2003). Structural and functional analysis of 3' untranslated region of mouse Period1 mRNA. *Biochem Biophys Res Commun* 301, 1-7.
- Kon, N., Yoshikawa, T., Honma, S., Yamagata, Y., Yoshitane, H., Shimizu, K., Sugiyama, Y., Hara, C., Kameshita, I., Honma, K., Fukada, Y. (2014). CaMKII is essential for the cellular clock and coupling between morning and evening behavioral rhythms. *Genes Dev* 28, 1101-1110.
- Konadhode, R.R., Pelluru, D., Blanco-Centurion, C., Zayachkivsky, A., Liu, M., Uhde, T., Glen, W.B., Jr., van den Pol, A.N., Mulholland, P.J., Shiromani, P.J. (2013). Optogenetic stimulation of MCH neurons increases sleep. *J Neurosci* 33, 10257-10263.

- Kostin, A., Alam, M.A., Siegel, J.M., McGinty, D., Alam, M.N. (2020). Sex- and Age-dependent Differences in Sleep-wake Characteristics of Fisher-344 Rats. *Neuroscience* 427, 29-42.
- Kou, C.J., Kandpal, R.P. (2018). Differential Expression Patterns of Eph Receptors and Ephrin Ligands in Human Cancers. *Biomed Res Int* 2018, 7390104.
- Kovalzon, V.M., Strekalova, T.V. (2006). Delta sleep-inducing peptide (DSIP): a still unresolved riddle. *J Neurochem* 97, 303-309.
- Krauchi, K., Wirz-Justice, A. (2001). Circadian clues to sleep onset mechanisms. *Neuropsychopharmacology* 25, S92-96.
- Krauchi, K., Cajochen, C., Wirz-Justice, A. (1997). A relationship between heat loss and sleepiness: effects of postural change and melatonin administration. *J Appl Physiol* (1985) 83, 134-139.
- Kroeger, D., Bandaru, S.S., Madara, J.C., Vetrivelan, R. (2019). Ventrolateral periaqueductal gray mediates rapid eye movement sleep regulation by melanin-concentrating hormone neurons. *Neuroscience* 406, 314-324.
- Kroeger, D., Ferrari, L.L., Petit, G., Mahoney, C.E., Fuller, P.M., Arrigoni, E., Scammell, T.E. (2017). Cholinergic, Glutamatergic, and GABAergic Neurons of the Pedunculopontine Tegmental Nucleus Have Distinct Effects on Sleep/Wake Behavior in Mice. *J Neurosci* 37, 1352-1366.
- Krueger, J.M., Nguyen, J.T., Dykstra-Aiello, C.J., Taishi, P. (2019). Local sleep. *Sleep Med Rev* 43, 14-21.
- Krueger, J.M., Rector, D.M., Roy, S., Van Dongen, H.P., Belenky, G., Panksepp, J. (2008). Sleep as a fundamental property of neuronal assemblies. *Nat Rev Neurosci* 9, 910-919.
- Kuang, S.Q., Bai, H., Fang, Z.H., Lopez, G., Yang, H., Tong, W., Wang, Z.Z., Garcia-Manero, G. (2010). Aberrant DNA methylation and epigenetic inactivation of Eph receptor tyrosine kinases and ephrin ligands in acute lymphoblastic leukemia. *Blood* 115, 2412-2419.
- Kubota, T., Li, N., Guan, Z., Brown, R.A., Krueger, J.M. (2002). Intrapreoptic microinjection of TNF-alpha enhances non-REM sleep in rats. *Brain Res* 932, 37-44.
- Kuljis, D.A., Gad, L., Loh, D.H., MacDowell Kaswan, Z., Hitchcock, O.N., Ghiani, C.A., Colwell, C.S. (2016). Sex Differences in Circadian Dysfunction in the BACHD Mouse Model of Huntington's Disease. *PLoS One* 11, e0147583.
- Kuljis, D.A., Loh, D.H., Truong, D., Vosko, A.M., Ong, M.L., McClusky, R., Arnold, A.P., Colwell, C.S. (2013). Gonadal- and sex-chromosome-dependent sex differences in the circadian system. *Endocrinology* 154, 1501-1512.
- Kullander, K., Mather, N.K., Diella, F., Dottori, M., Boyd, A.W., Klein, R. (2001). Kinase-dependent and kinase-independent functions of EphA4 receptors in major axon tract formation in vivo. *Neuron* 29, 73-84.
- Kumar, D., Dedic, N., Flachskamm, C., Voule, S., Deussing, J.M., Kimura, M. (2015). *Cacna1c* (Cav1.2) modulates electroencephalographic rhythm and rapid eye movement sleep recovery. *Sleep* 38, 1371-1380.
- Lai, T., Chen, L., Chen, X., He, J., Lv, P., Ge, H. (2019). Rhynchophylline attenuates migraine in trigeminal nucleus caudalis in nitroglycerin-induced rat model by inhibiting MAPK/NF-kB signaling. *Mol Cell Biochem* 461, 205-212.
- Lancel, M. (1999). Role of GABAA receptors in the regulation of sleep: initial sleep responses to peripherally administered modulators and agonists. *Sleep* 22, 33-42.

- Landgraf, D., Wang, L.L., Diemer, T., Welsh, D.K. (2016). NPAS2 Compensates for Loss of CLOCK in Peripheral Circadian Oscillators. *PLoS Genet* 12, e1005882.
- Landolt, H.P., Dijk, D.J., Gaus, S.E., Borbely, A.A. (1995). Caffeine reduces low-frequency delta activity in the human sleep EEG. *Neuropsychopharmacology* 12, 229-238.
- Latini, S., Pedata, F. (2001). Adenosine in the central nervous system: release mechanisms and extracellular concentrations. *J Neurochem* 79, 463-484.
- Lavoie, J., Hebert, M., Beaulieu, J.M. (2013). Glycogen synthase kinase-3beta haploinsufficiency lengthens the circadian locomotor activity period in mice. *Behav Brain Res* 253, 262-265.
- Lazarus, M., Shen, H.Y., Cherasse, Y., Qu, W.M., Huang, Z.L., Bass, C.E., Winsky-Sommerer, R., Semba, K., Fredholm, B.B., Boison, D., Hayaishi, O., Urade, Y., Chen, J.F. (2011). Arousal effect of caffeine depends on adenosine A2A receptors in the shell of the nucleus accumbens. *J Neurosci* 31, 10067-10075.
- Lee, C.J., Hsueh, T.Y., Lin, L.C., Tsai, T.H. (2014). Determination of protein-unbound rhynchophylline brain distribution by microdialysis and ultra-performance liquid chromatography with tandem mass spectrometry. *Biomed Chromatogr* 28, 901-906.
- Lee, H.H. et al. (2021). Human ribonuclease 1 serves as a secretory ligand of ephrin A4 receptor and induces breast tumor initiation. *Nat Commun* 12, 2788.
- Lee, M.G., Hassani, O.K., Jones, B.E. (2005). Discharge of identified orexin/hypocretin neurons across the sleep-waking cycle. *J Neurosci* 25, 6716-6720.
- Lee, M.G., Chrobak, J.J., Sik, A., Wiley, R.G., Buzsaki, G. (1994). Hippocampal theta activity following selective lesion of the septal cholinergic system. *Neuroscience* 62, 1033-1047.
- Leighton, P.A., Mitchell, K.J., Goodrich, L.V., Lu, X., Pinson, K., Scherz, P., Skarnes, W.C., Tessier-Lavigne, M. (2001). Defining brain wiring patterns and mechanisms through gene trapping in mice. *Nature* 410, 174-179.
- Lemmens, R., Jaspers, T., Robberecht, W., Thijs, V.N. (2013). Modifying expression of EphA4 and its downstream targets improves functional recovery after stroke. *Hum Mol Genet* 22, 2214-2220.
- Leung, L.C., Wang, G.X., Madelaine, R., Skariah, G., Kawakami, K., Deisseroth, K., Urban, A.E., Mourrain, P. (2019). Neural signatures of sleep in zebrafish. *Nature* 571, 198-204.
- Lewis, L.D., Voigts, J., Flores, F.J., Schmitt, L.I., Wilson, M.A., Halassa, M.M., Brown, E.N. (2015). Thalamic reticular nucleus induces fast and local modulation of arousal state. *Elife* 4, e08760.
- Li, J., Lu, W.Q., Beesley, S., Loudon, A.S., Meng, Q.J. (2012). Lithium impacts on the amplitude and period of the molecular circadian clockwork. *PLoS One* 7, e33292.
- Li, S.B., Damonte, V.M., Chen, C., Wang, G.X., Kebschull, J.M., Yamaguchi, H., Bian, W.J., Purmann, C., Pattni, R., Urban, A.E., Mourrain, P., Kauer, J.A., Scherrer, G., de Lecea, L. (2022a). Hyperexcitable arousal circuits drive sleep instability during aging. *Science* 375, eabh3021.
- Li, W., Ma, L., Yang, G., Gan, W.B. (2017). REM sleep selectively prunes and maintains new synapses in development and learning. *Nat Neurosci* 20, 427-437.
- Li, X., Jope, R.S. (2010). Is glycogen synthase kinase-3 a central modulator in mood regulation? *Neuropsychopharmacology* 35, 2143-2154.



- Li, Y., Su, P., Chen, Y., Nie, J., Yuan, T.F., Wong, A.H., Liu, F. (2022b). The Eph receptor A4 plays a role in demyelination and depression-related behavior. *J Clin Invest*.
- Liang, L.Y., Patel, O., Janes, P.W., Murphy, J.M., Lucet, I.S. (2019). Eph receptor signalling: from catalytic to non-catalytic functions. *Oncogene* 38, 6567-6584.
- Liebl, D.J., Morris, C.J., Henkemeyer, M., Parada, L.F. (2003). mRNA expression of ephrins and Eph receptor tyrosine kinases in the neonatal and adult mouse central nervous system. *J Neurosci Res* 71, 7-22.
- Light, T.P., Gomez-Soler, M., Wang, Z., Karl, K., Zapata-Mercado, E., Gehring, M.P., Lechtenberg, B.C., Pogorelov, T.V., Hristova, K., Pasquale, E.B. (2021). A cancer mutation promotes EphA4 oligomerization and signaling by altering the conformation of the SAM domain. *J Biol Chem* 297, 100876.
- Lin, D., Gish, G.D., Songyang, Z., Pawson, T. (1999). The carboxyl terminus of B class ephrins constitutes a PDZ domain binding motif. *J Biol Chem* 274, 3726-3733.
- Liska, K., Sladek, M., Houdek, P., Shrestha, N., Luzna, V., Ralph, M.R., Sumova, A. (2022). High Sensitivity of the Circadian Clock in the Hippocampal Dentate Gyrus to Glucocorticoid- and GSK3-Beta-Dependent Signals. *Neuroendocrinology* 112, 384-398.
- Liu, Z.W., Faraguna, U., Cirelli, C., Tononi, G., Gao, X.B. (2010). Direct evidence for wake-related increases and sleep-related decreases in synaptic strength in rodent cortex. *J Neurosci* 30, 8671-8675.
- Long, H., Zhang, M., Wang, C., Hang, Y. (2019). Rhynchophylline attenuates neurotoxicity in Tourette Syndrome rats. *Neurotox Res* 36, 679-687.
- Lu, H., Clauser, K.R., Tam, W.L., Frose, J., Ye, X., Eaton, E.N., Reinhardt, F., Donnenberg, V.S., Bhargava, R., Carr, S.A., Weinberg, R.A. (2014). A breast cancer stem cell niche supported by juxtacrine signalling from monocytes and macrophages. *Nat Cell Biol* 16, 1105-1117.
- Lu, Q., Sun, E.E., Klein, R.S., Flanagan, J.G. (2001). Ephrin-B reverse signaling is mediated by a novel PDZ-RGS protein and selectively inhibits G protein-coupled chemoattraction. *Cell* 105, 69-79.
- Luca, G., Haba Rubio, J., Andries, D., Tobback, N., Vollenweider, P., Waeber, G., Marques Vidal, P., Preisig, M., Heinzer, R., Tafti, M. (2015). Age and gender variations of sleep in subjects without sleep disorders. *Ann Med* 47, 482-491.
- Lyons, L.C., Chatterjee, S., Vanrobaeys, Y., Gaine, M.E., Abel, T. (2020). Translational changes induced by acute sleep deprivation uncovered by TRAP-Seq. *Mol Brain* 13, 165.
- Ma, T., Zhang, H., Xu, Z.P., Lu, Y., Fu, Q., Wang, W., Li, G.H., Wang, Y.Y., Yang, Y.T., Mi, W.D. (2020). Activation of brain-derived neurotrophic factor signaling in the basal forebrain reverses acute sleep deprivation-induced fear memory impairments. *Brain Behav* 10, e01592.
- Mackiewicz, M., Shockley, K.R., Romer, M.A., Galante, R.J., Zimmerman, J.E., Naidoo, N., Baldwin, D.A., Jensen, S.T., Churchill, G.A., Pack, A.I. (2007). Macromolecule biosynthesis: a key function of sleep. *Physiol Genomics* 31, 441-457.
- Manfridi, A., Brambilla, D., Mancina, M. (1999). Stimulation of NMDA and AMPA receptors in the rat nucleus basalis of Meynert affects sleep. *Am J Physiol* 277, R1488-1492.

- Manfridi, A., Brambilla, D., Bianchi, S., Mariotti, M., Opp, M.R., Imeri, L. (2003). Interleukin-1beta enhances non-rapid eye movement sleep when microinjected into the dorsal raphe nucleus and inhibits serotonergic neurons in vitro. *Eur J Neurosci* *18*, 1041-1049.
- Mann, F., Ray, S., Harris, W., Holt, C. (2002). Topographic mapping in dorsoventral axis of the *Xenopus* retinotectal system depends on signaling through ephrin-B ligands. *Neuron* *35*, 461-473.
- Manns, I.D., Lee, M.G., Modirrousta, M., Hou, Y.P., Jones, B.E. (2003). Alpha 2 adrenergic receptors on GABAergic, putative sleep-promoting basal forebrain neurons. *Eur J Neurosci* *18*, 723-727.
- Maquet, P., Dive, D., Salmon, E., Sadzot, B., Franco, G., Poirrier, R., von Frenckell, R., Franck, G. (1990). Cerebral glucose utilization during sleep-wake cycle in man determined by positron emission tomography and [<sup>18</sup>F]2-fluoro-2-deoxy-D-glucose method. *Brain Res* *513*, 136-143.
- Maret, S., Dorsaz, S., Gurcel, L., Pradervand, S., Petit, B., Pfister, C., Hagenbuchle, O., O'Hara, B.F., Franken, P., Tafti, M. (2007). Homer1a is a core brain molecular correlate of sleep loss. *Proc Natl Acad Sci U S A* *104*, 20090-20095.
- Martin-Batista, E., Maglio, L.E., Armas-Capote, N., Hernandez, G., Alvarez de la Rosa, D., Giraldez, T. (2021). SGK1.1 limits brain damage after status epilepticus through M current-dependent and independent mechanisms. *Neurobiol Dis* *153*, 105317.
- Martinez-Gonzalez, D., Lesku, J.A., Rattenborg, N.C. (2008). Increased EEG spectral power density during sleep following short-term sleep deprivation in pigeons (*Columba livia*): evidence for avian sleep homeostasis. *J Sleep Res* *17*, 140-153.
- Martone, M.E., Holash, J.A., Bayardo, A., Pasquale, E.B., Ellisman, M.H. (1997). Immunolocalization of the receptor tyrosine kinase EphA4 in the adult rat central nervous system. *Brain Res* *771*, 238-250.
- Marx, V. (2021). Method of the Year: spatially resolved transcriptomics. *Nat Methods* *18*, 9-14.
- Mason, G.M., Lokhandwala, S., Riggins, T., Spencer, R.M.C. (2021). Sleep and human cognitive development. *Sleep Med Rev* *57*, 101472.
- Massart, R., Freyburger, M., Suderman, M., Paquet, J., El Helou, J., Belanger-Nelson, E., Rachalski, A., Koumar, O.C., Carrier, J., Szyf, M., Mongrain, V. (2014). The genome-wide landscape of DNA methylation and hydroxymethylation in response to sleep deprivation impacts on synaptic plasticity genes. *Transl Psychiatry* *4*, e347.
- Matsui, K., Sasai-Sakuma, T., Ishigooka, J., Nishimura, K., Inoue, Y. (2019). Effect of Yokukansan for the treatment of idiopathic rapid eye movement sleep behavior disorder: a retrospective analysis of consecutive patients. *Journal of Clinical Sleep Medicine* *15*, 1173-1178.
- Matsuo, K., Otaki, N. (2012). Bone cell interactions through Eph/ephrin: bone modeling, remodeling and associated diseases. *Cell Adh Migr* *6*, 148-156.
- McCarthy, A., Loomis, S., Eastwood, B., Wafford, K.A., Winsky-Sommerer, R., Gilmour, G. (2017). Modelling maintenance of wakefulness in rats: comparing potential non-invasive sleep-restriction methods and their effects on sleep and attentional performance. *J Sleep Res* *26*, 179-187.
- McClung, C.A. (2007). Circadian genes, rhythms and the biology of mood disorders. *Pharmacol Ther* *114*, 222-232.

- Meerlo, P., Koehl, M., van der Borght, K., Turek, F.W. (2002). Sleep restriction alters the hypothalamic-pituitary-adrenal response to stress. *J Neuroendocrinol* *14*, 397-402.
- Meijer, J.H., Schwartz, W.J. (2003). In search of the pathways for light-induced pacemaker resetting in the suprachiasmatic nucleus. *J Biol Rhythms* *18*, 235-249.
- Meijer, J.H., Schaap, J., Watanabe, K., Albus, H. (1997). Multiunit activity recordings in the suprachiasmatic nuclei: in vivo versus in vitro models. *Brain Res* *753*, 322-327.
- Menet, J.S., Rodriguez, J., Abruzzi, K.C., Rosbash, M. (2012). Nascent-Seq reveals novel features of mouse circadian transcriptional regulation. *Elife* *1*, e00011.
- Michelson, D., Snyder, E., Paradis, E., Chengan-Liu, M., Snavely, D.B., Hutzelmann, J., Walsh, J.K., Krystal, A.D., Benca, R.M., Cohn, M., Lines, C., Roth, T., Herring, W.J. (2014). Safety and efficacy of suvorexant during 1-year treatment of insomnia with subsequent abrupt treatment discontinuation: a phase 3 randomised, double-blind, placebo-controlled trial. *Lancet Neurol* *13*, 461-471.
- Mieda, M., Hasegawa, E., Kisanuki, Y.Y., Sinton, C.M., Yanagisawa, M., Sakurai, T. (2011). Differential roles of orexin receptor-1 and -2 in the regulation of non-REM and REM sleep. *J Neurosci* *31*, 6518-6526.
- Mikhail, C., Vaucher, A., Jimenez, S., Tafti, M. (2017). ERK signaling pathway regulates sleep duration through activity-induced gene expression during wakefulness. *Sci Signal* *10*.
- Mileykovskiy, B.Y., Kiyashchenko, L.I., Siegel, J.M. (2005). Behavioral correlates of activity in identified hypocretin/orexin neurons. *Neuron* *46*, 787-798.
- Milinski, L., Fisher, S.P., Cui, N., McKillop, L.E., Blanco-Duque, C., Ang, G., Yamagata, T., Bannerman, D.M., Vyazovskiy, V.V. (2021). Waking experience modulates sleep need in mice. *BMC Biol* *19*, 65.
- Mitchell, S.J., Rawlins, J.N., Steward, O., Olton, D.S. (1982). Medial septal area lesions disrupt theta rhythm and cholinergic staining in medial entorhinal cortex and produce impaired radial arm maze behavior in rats. *J Neurosci* *2*, 292-302.
- Mitsui, S., Yamaguchi, S., Matsuo, T., Ishida, Y., Okamura, H. (2001). Antagonistic role of E4BP4 and PAR proteins in the circadian oscillatory mechanism. *Genes Dev* *15*, 995-1006.
- Miyamoto, D., Marshall, W., Tonomi, G., Cirelli, C. (2021). Net decrease in spine-surface GluA1-containing AMPA receptors after post-learning sleep in the adult mouse cortex. *Nat Commun* *12*, 2881.
- Miyashita, T., Kikuchi, E., Horiuchi, J., Saitoe, M. (2018). Long-Term Memory Engram Cells Are Established by c-Fos/CREB Transcriptional Cycling. *Cell Rep* *25*, 2716-2728 e2713.
- Mo, J., Kim, C.H., Lee, D., Sun, W., Lee, H.W., Kim, H. (2015). Early growth response 1 (Egr-1) directly regulates GABAA receptor alpha2, alpha4, and theta subunits in the hippocampus. *J Neurochem* *133*, 489-500.
- Modirrousta, M., Mainville, L., Jones, B.E. (2004). Gabaergic neurons with alpha2-adrenergic receptors in basal forebrain and preoptic area express c-Fos during sleep. *Neuroscience* *129*, 803-810.
- Modirrousta, M., Mainville, L., Jones, B.E. (2005). Orexin and MCH neurons express c-Fos differently after sleep deprivation vs. recovery and bear different adrenergic receptors. *Eur J Neurosci* *21*, 2807-2816.
- Mong, J.A., Baker, F.C., Mahoney, M.M., Paul, K.N., Schwartz, M.D., Semba, K., Silver, R. (2011). Sleep, rhythms, and the endocrine brain: influence of sex and gonadal hormones. *J Neurosci* *31*, 16107-16116.

- Mongrain, V., Carrier, J., Dumont, M. (2005). Chronotype and sex effects on sleep architecture and quantitative sleep EEG in healthy young adults. *Sleep* 28, 819-827.
- Mongrain, V., La Spada, F., Curie, T., Franken, P. (2011). Sleep loss reduces the DNA-binding of BMAL1, CLOCK, and NPAS2 to specific clock genes in the mouse cerebral cortex. *PLoS One* 6, e26622.
- Mongrain, V., Hernandez, S.A., Pradervand, S., Dorsaz, S., Curie, T., Hagiwara, G., Gip, P., Heller, H.C., Franken, P. (2010). Separating the contribution of glucocorticoids and wakefulness to the molecular and electrophysiological correlates of sleep homeostasis. *Sleep* 33, 1147-1157.
- Montgomery, S.M., Sirota, A., Buzsaki, G. (2008). Theta and gamma coordination of hippocampal networks during waking and rapid eye movement sleep. *J Neurosci* 28, 6731-6741.
- Moore, R.Y., Eichler, V.B. (1972). Loss of a circadian adrenal corticosterone rhythm following suprachiasmatic lesions in the rat. *Brain Res* 42, 201-206.
- Muehlroth, B.E., Sander, M.C., Fandakova, Y., Grandy, T.H., Rasch, B., Shing, Y.L., Werkle-Bergner, M. (2019). Precise Slow Oscillation-Spindle Coupling Promotes Memory Consolidation in Younger and Older Adults. *Sci Rep* 9, 1940.
- Mukhametov, L.M. (1987). Unihemispheric slow-wave sleep in the Amazonian dolphin, *Inia geoffrensis*. *Neurosci Lett* 79, 128-132.
- Murai, K.K., Pasquale, E.B. (2003). 'Eph'ective signaling: forward, reverse and crosstalk. *J Cell Sci* 116, 2823-2832.
- Murai, K.K., Pasquale, E.B. (2011). Eph receptors and ephrins in neuron-astrocyte communication at synapses. *Glia* 59, 1567-1578.
- Murai, K.K., Nguyen, L.N., Irie, F., Yamaguchi, Y., Pasquale, E.B. (2003). Control of hippocampal dendritic spine morphology through ephrin-A3/EphA4 signaling. *Nat Neurosci* 6, 153-160.
- Murata, K., Li, F., Shinguchi, K., Ogata, M., Fujita, N., Takahashi, R. (2020). Yokukansankachimpihange improves the social isolation-induced sleep disruption and allopregnanolone reduction in mice. *Front Nutr* 7, 8.
- Mure, L.S., Le, H.D., Benegiamo, G., Chang, M.W., Rios, L., Jillani, N., Ngotho, M., Kariuki, T., Dkhissi-Benyahya, O., Cooper, H.M., Panda, S. (2018). Diurnal transcriptome atlas of a primate across major neural and peripheral tissues. *Science* 359.
- Muto, V., Jaspard, M., Meyer, C., Kusse, C., Chellappa, S.L., Degueldre, C., Balteau, E., Shaffii-Le Bourdieu, A., Luxen, A., Middleton, B., Archer, S.N., Phillips, C., Collette, F., Vandewalle, G., Dijk, D.J., Maquet, P. (2016). Local modulation of human brain responses by circadian rhythmicity and sleep debt. *Science* 353, 687-690.
- Nagao, M., Takasaki, K., Nogami, A., Hirai, Y., Moriyama, H., Uchida, N., Kubota, K., Katsurabayashi, S., Mishima, K., Nishimura, R., Iwasaki, K. (2014). Effect of Yokukansan on sleep disturbance in a rat model of cerebrovascular dementia. *Traditional & Kampo Medicine* 1, 19-26.
- Nakajima, K., Nakaoka, Y. (1989). Circadian change of photosensitivity in *Paramecium bursaria*. *Journal of experimental biology* 144, 43-51.
- Nakajima, Y., Morimoto, M., Takahashi, Y., Koseki, H., Saga, Y. (2006). Identification of Epha4 enhancer required for segmental expression and the regulation by Mesp2. *Development* 133, 2517-2525.

- Narwade, S.C., Mallick, B.N., Deobagkar, D.D. (2017). Transcriptome Analysis Reveals Altered Expression of Memory and Neurotransmission Associated Genes in the REM Sleep Deprived Rat Brain. *Front Mol Neurosci* *10*, 67.
- Naseri Kouzehgarani, G., Bothwell, M.Y., Gillette, M.U. (2020). Circadian rhythm of redox state regulates membrane excitability in hippocampal CA1 neurons. *Eur J Neurosci* *51*, 34-46.
- Nath, R.D., Bedbrook, C.N., Abrams, M.J., Basinger, T., Bois, J.S., Prober, D.A., Sternberg, P.W., Gradinaru, V., Goentoro, L. (2017). The Jellyfish *Cassiopea* Exhibits a Sleep-like State. *Curr Biol* *27*, 2984-2990 e2983.
- Nickel, M. (2004). Kinetics and rhythm of body contractions in the sponge *Tethya wilhelma* (Porifera: Demospongiae). *J Exp Biol* *207*, 4515-4524.
- Niethard, N., Born, J. (2019). Back to baseline: sleep recalibrates synapses. *Nat Neurosci* *22*, 149-151.
- Niethard, N., Brodt, S., Born, J. (2021). Cell-Type-Specific Dynamics of Calcium Activity in Cortical Circuits over the Course of Slow-Wave Sleep and Rapid Eye Movement Sleep. *J Neurosci* *41*, 4212-4222.
- Nishida, M., Pearsall, J., Buckner, R.L., Walker, M.P. (2009). REM sleep, prefrontal theta, and the consolidation of human emotional memory. *Cereb Cortex* *19*, 1158-1166.
- Niwa, Y., Kanda, G.N., Yamada, R.G., Shi, S., Sunagawa, G.A., Ukai-Tadenuma, M., Fujishima, H., Matsumoto, N., Masumoto, K.H., Nagano, M., Kasukawa, T., Galloway, J., Perrin, D., Shigeyoshi, Y., Ukai, H., Kiyonari, H., Sumiyama, K., Ueda, H.R. (2018). Muscarinic Acetylcholine Receptors *Chrm1* and *Chrm3* Are Essential for REM Sleep. *Cell Rep* *24*, 2231-2247 e2237.
- Noguchi, T., Leise, T.L., Kingsbury, N.J., Diemer, T., Wang, L.L., Henson, M.A., Welsh, D.K. (2017). Calcium Circadian Rhythmicity in the Suprachiasmatic Nucleus: Cell Autonomy and Network Modulation. *eNeuro* *4*.
- Nollet, M., Wisden, W., Franks, N.P. (2020). Sleep deprivation and stress: a reciprocal relationship. *Interface Focus* *10*, 20190092.
- Norimoto, H., Makino, K., Gao, M., Shikano, Y., Okamoto, K., Ishikawa, T., Sasaki, T., Hioki, H., Fujisawa, S., Ikegaya, Y. (2018). Hippocampal ripples down-regulate synapses. *Science* *359*, 1524-1527.
- North, H.A., Karim, A., Jacquin, M.F., Donoghue, M.J. (2010). EphA4 is necessary for spatially selective peripheral somatosensory topography. *Dev Dyn* *239*, 630-638.
- North, H.A., Zhao, X., Kolk, S.M., Clifford, M.A., Ziskind, D.M., Donoghue, M.J. (2009). Promotion of proliferation in the developing cerebral cortex by EphA4 forward signaling. *Development* *136*, 2467-2476.
- Noya, S.B., Colameo, D., Bruning, F., Spinnler, A., Mirsof, D., Opitz, L., Mann, M., Tyagarajan, S.K., Robles, M.S., Brown, S.A. (2019). The forebrain synaptic transcriptome is organized by clocks but its proteome is driven by sleep. *Science* *366*.
- O'Callaghan, E.K., Ballester Roig, M.N., Mongrain, V. (2017). Cell adhesion molecules and sleep. *Neurosci Res* *116*, 29-38.
- O'Callaghan, E.K., Green, E.W., Franken, P., Mongrain, V. (2019). Omics Approaches in Sleep-Wake Regulation. *Handb Exp Pharmacol* *253*, 59-81.
- Obal, F., Jr., Krueger, J.M. (2003). Biochemical regulation of non-rapid-eye-movement sleep. *Front Biosci* *8*, d520-550.

- Obi, S., Yamamoto, K., Shimizu, N., Kumagaya, S., Masumura, T., Sokabe, T., Asahara, T., Ando, J. (2009). Fluid shear stress induces arterial differentiation of endothelial progenitor cells. *J Appl Physiol* (1985) *106*, 203-211.
- Ochoa-Sanchez, R., Comai, S., Lacoste, B., Bambico, F.R., Dominguez-Lopez, S., Spadoni, G., Rivara, S., Bedini, A., Angeloni, D., Fraschini, F., Mor, M., Tarzia, G., Descarries, L., Gobbi, G. (2011). Promotion of non-rapid eye movement sleep and activation of reticular thalamic neurons by a novel MT2 melatonin receptor ligand. *J Neurosci* *31*, 18439-18452.
- Ode, K.L., Ueda, H.R. (2020). Phosphorylation Hypothesis of Sleep. *Front Psychol* *11*, 575328.
- Ode, K.L., Katsumata, T., Tone, D., Ueda, H.R. (2017a). Fast and slow Ca(2+)-dependent hyperpolarization mechanisms connect membrane potential and sleep homeostasis. *Curr Opin Neurobiol* *44*, 212-221.
- Ode, K.L., Ukai, H., Susaki, E.A., Narumi, R., Matsumoto, K., Hara, J., Koide, N., Abe, T., Kanemaki, M.T., Kiyonari, H., Ueda, H.R. (2017b). Knockout-Rescue Embryonic Stem Cell-Derived Mouse Reveals Circadian-Period Control by Quality and Quantity of CRY1. *Mol Cell* *65*, 176-190.
- Ohtomo, Y., Umino, D., Nijama, S., Fujinaga, S., Shimizu, T. (2014). Yokukansan: a treatment option for nocturnal enuresis in children by improving sleep quality. *Juntendo Medical Journal* *60*, 536-542.
- Opp, M.R., Obal, F., Jr., Krueger, J.M. (1991). Interleukin 1 alters rat sleep: temporal and dose-related effects. *Am J Physiol* *260*, R52-58.
- Oster, H., Challet, E., Ott, V., Arvat, E., de Kloet, E.R., Dijk, D.J., Lightman, S., Vgontzas, A., Van Cauter, E. (2017). The Functional and Clinical Significance of the 24-Hour Rhythm of Circulating Glucocorticoids. *Endocr Rev* *38*, 3-45.
- Oyola, M.G., Shupe, E.A., Soltis, A.R., Sukumar, G., Paez-Pereda, M., Larco, D.O., Wilkerson, M.D., Rothwell, S., Dalgard, C.L., Wu, T.J. (2019). Sleep Deprivation Alters the Pituitary Stress Transcriptome in Male and Female Mice. *Front Endocrinol (Lausanne)* *10*, 676.
- Ozone, M., Shimazaki, H., Ichikawa, H., Shigeta, M. (2020). Efficacy of yokukansan compared with clonazepam for rapid eye movement sleep behaviour disorder: a preliminary retrospective study. *Psychogeriatrics*.
- Ozone, M., Yagi, T., Chiba, S., Aoki, K., Kuroda, A., Mitsui, K., Itoh, H., Sasaki, M. (2012). Effect of yokukansan on psychophysiological insomnia evaluated using cyclic alternating pattern as an objective marker of sleep instability. *Sleep and Biological Rhythms* *10*, 157-160.
- Palmer, A., Zimmer, M., Erdmann, K.S., Eulenburg, V., Porthin, A., Heumann, R., Deutsch, U., Klein, R. (2002). EphrinB phosphorylation and reverse signaling: regulation by Src kinases and PTP-BL phosphatase. *Mol Cell* *9*, 725-737.
- Pan, W., Kwak, S., Li, G., Chen, Y., Cai, D. (2013). Therapeutic effect of Yang-Xue-Qing-Nao granules on sleep dysfunction in Parkinson's disease. *Chin Med* *8*, 14.
- Pan, X., Zhang, Y., Wang, L., Hussain, M.M. (2010). Diurnal regulation of MTP and plasma triglyceride by CLOCK is mediated by SHP. *Cell Metab* *12*, 174-186.
- Panda, S., Antoch, M.P., Miller, B.H., Su, A.I., Schook, A.B., Straume, M., Schultz, P.G., Kay, S.A., Takahashi, J.S., Hogenesch, J.B. (2002). Coordinated transcription of key pathways in the mouse by the circadian clock. *Cell* *109*, 307-320.

- Pandi-Perumal, S.R., Trakht, I., Srinivasan, V., Spence, D.W., Maestroni, G.J., Zisapel, N., Cardinali, D.P. (2008). Physiological effects of melatonin: role of melatonin receptors and signal transduction pathways. *Prog Neurobiol* 85, 335-353.
- Parekh, P.K., Logan, R.W., Ketchesin, K.D., Becker-Krail, D., Shelton, M.A., Hildebrand, M.A., Barko, K., Huang, Y.H., McClung, C.A. (2019). Cell-Type-Specific Regulation of Nucleus Accumbens Synaptic Plasticity and Cocaine Reward Sensitivity by the Circadian Protein, NPAS2. *J Neurosci* 39, 4657-4667.
- Pariollaud, M., Lamia, K.A. (2020). Cancer in the Fourth Dimension: What Is the Impact of Circadian Disruption? *Cancer Discov* 10, 1455-1464.
- Park, M., Miyoshi, C., Fujiyama, T., Kakizaki, M., Ikkyu, A., Honda, T., Choi, J., Asano, F., Mizuno, S., Takahashi, S., Yanagisawa, M., Funato, H. (2020). Loss of the conserved PKA sites of SIK1 and SIK2 increases sleep need. *Sci Rep* 10, 8676.
- Pasquale, E.B. (2005). Eph receptor signalling casts a wide net on cell behaviour. *Nat Rev Mol Cell Biol* 6, 462-475.
- Pasquale, E.B. (2010). Eph receptors and ephrins in cancer: bidirectional signalling and beyond. *Nat Rev Cancer* 10, 165-180.
- Paul, K.N., Dugovic, C., Turek, F.W., Laposky, A.D. (2006). Diurnal sex differences in the sleep-wake cycle of mice are dependent on gonadal function. *Sleep* 29, 1211-1223.
- Peever, J., Fuller, P.M. (2017). The Biology of REM Sleep. *Curr Biol* 27, R1237-R1248.
- Peineau, S., Taghibiglou, C., Bradley, C., Wong, T.P., Liu, L., Lu, J., Lo, E., Wu, D., Saule, E., Bouschet, T., Matthews, P., Isaac, J.T., Bortolotto, Z.A., Wang, Y.T., Collingridge, G.L. (2007). LTP inhibits LTD in the hippocampus via regulation of GSK3beta. *Neuron* 53, 703-717.
- Pennisi, E. (2021). The simplest of slumbers. *Science* 374, 526-529.
- Periasamy, S., Hsu, D.Z., Fu, Y.H., Liu, M.Y. (2015). Sleep deprivation-induced multi-organ injury: role of oxidative stress and inflammation. *EXCLI J* 14, 672-683.
- Petros, T.J., Williams, S.E., Mason, C.A. (2006). Temporal regulation of EphA4 in astroglia during murine retinal and optic nerve development. *Mol Cell Neurosci* 32, 49-66.
- Peyrache, A., Seibt, J. (2020). A mechanism for learning with sleep spindles. *Philos Trans R Soc Lond B Biol Sci* 375, 20190230.
- Phillips, A.J., Robinson, P.A., Kedziora, D.J., Abeyesuriya, R.G. (2010). Mammalian sleep dynamics: how diverse features arise from a common physiological framework. *PLoS Comput Biol* 6, e1000826.
- Pittendrigh, C.S., Daan, S. (1976). A functional analysis of circadian pacemakers in nocturnal rodents. *Journal of comparative physiology*. I. The Stability and Lability of Spontaneous Frequency. *Journal of comparative physiology* 106, 223-252.
- Plumbly, W., Brandon, N., Deeb, T.Z., Hall, J., Harwood, A.J. (2019). L-type voltage-gated calcium channel regulation of in vitro human cortical neuronal networks. *Sci Rep* 9, 13810.
- Poe, G.R., Nitz, D.A., McNaughton, B.L., Barnes, C.A. (2000). Experience-dependent phase-reversal of hippocampal neuron firing during REM sleep. *Brain Res* 855, 176-180.

- Porkka-Heiskanen, T., Strecker, R.E., McCarley, R.W. (2000). Brain site-specificity of extracellular adenosine concentration changes during sleep deprivation and spontaneous sleep: an in vivo microdialysis study. *Neuroscience* *99*, 507-517.
- Preitner, N., Damiola, F., Lopez-Molina, L., Zakany, J., Duboule, D., Albrecht, U., Schibler, U. (2002). The orphan nuclear receptor REV-ERB $\alpha$  controls circadian transcription within the positive limb of the mammalian circadian oscillator. *Cell* *110*, 251-260.
- Prosser, R.A., Rutishauser, U., Ungers, G., Fedorkova, L., Glass, J.D. (2003). Intrinsic role of polysialylated neural cell adhesion molecule in photic phase resetting of the Mammalian circadian clock. *J Neurosci* *23*, 652-658.
- Puentes-Mestril, C., Aton, S.J. (2017). Linking Network Activity to Synaptic Plasticity during Sleep: Hypotheses and Recent Data. *Front Neural Circuits* *11*, 61.
- Qin, H., Noberini, R., Huan, X., Shi, J., Pasquale, E.B., Song, J. (2010). Structural characterization of the EphA4-Ephrin-B2 complex reveals new features enabling Eph-ephrin binding promiscuity. *J Biol Chem* *285*, 644-654.
- Qin, Q.J., Cui, L.Q., Li, P., Wang, Y.B., Zhang, X.Z., Guo, M.L. (2019). Rhynchophylline ameliorates myocardial ischemia/reperfusion injury through the modulation of mitochondrial mechanisms to mediate myocardial apoptosis. *Mol Med Rep* *19*, 2581-2590.
- Raccuglia, D., Huang, S., Ender, A., Heim, M.M., Laber, D., Suarez-Grimalt, R., Liotta, A., Sigrist, S.J., Geiger, J.R.P., Oswald, D. (2019). Network-Specific Synchronization of Electrical Slow-Wave Oscillations Regulates Sleep Drive in *Drosophila*. *Curr Biol* *29*, 3611-3621 e3613.
- Rattenborg, N.C., Voirin, B., Cruz, S.M., Tisdale, R., Dell'Omo, G., Lipp, H.P., Wikelski, M., Vyssotski, A.L. (2016). Evidence that birds sleep in mid-flight. *Nat Commun* *7*, 12468.
- Redline, S., Kirchner, H.L., Quan, S.F., Gottlieb, D.J., Kapur, V., Newman, A. (2004). The effects of age, sex, ethnicity, and sleep-disordered breathing on sleep architecture. *Arch Intern Med* *164*, 406-418.
- Reiter, R.J. (1991). Pineal melatonin: cell biology of its synthesis and of its physiological interactions. *Endocr Rev* *12*, 151-180.
- Reiter, R.J., Tan, D.X., Korkmaz, A., Ma, S. (2012). Obesity and metabolic syndrome: association with chronodisruption, sleep deprivation, and melatonin suppression. *Ann Med* *44*, 564-577.
- Reiter, R.J., Tan, D.X., Korkmaz, A., Erren, T.C., Piekarski, C., Tamura, H., Manchester, L.C. (2007). Light at night, chronodisruption, melatonin suppression, and cancer risk: a review. *Crit Rev Oncog* *13*, 303-328.
- Rentschler, K.M., Baratta, A.M., Ditty, A.L., Wagner, N.T.J., Wright, C.J., Milosavljevic, S., Mong, J.A., Pocivavsek, A. (2021). Prenatal Kynurenine Elevation Elicits Sex-Dependent Changes in Sleep and Arousal During Adulthood: Implications for Psychotic Disorders. *Schizophr Bull* *47*, 1320-1330.
- Restrepo, C.E., Margaryan, G., Borgius, L., Lundfald, L., Sargsyan, D., Kiehn, O. (2011). Change in the balance of excitatory and inhibitory midline fiber crossing as an explanation for the hopping phenotype in EphA4 knockout mice. *Eur J Neurosci* *34*, 1102-1112.
- Richter, M., Murai, K.K., Bourgin, C., Pak, D.T., Pasquale, E.B. (2007). The EphA4 receptor regulates neuronal morphology through SPAR-mediated inactivation of Rap GTPases. *J Neurosci* *27*, 14205-14215.



- Riemann, D., Krone, L.B., Wulff, K., Nissen, C. (2020). Sleep, insomnia, and depression. *Neuropsychopharmacology* 45, 74-89.
- Ripperger, J.A., Schibler, U. (2006). Rhythmic CLOCK-BMAL1 binding to multiple E-box motifs drives circadian Dbp transcription and chromatin transitions. *Nat Genet* 38, 369-374.
- Robillard, R., Massicotte-Marquez, J., Kawinska, A., Paquet, J., Frenette, S., Carrier, J. (2010). Topography of homeostatic sleep pressure dissipation across the night in young and middle-aged men and women. *J Sleep Res* 19, 455-465.
- Robinson, B.G., Frim, D.M., Schwartz, W.J., Majzoub, J.A. (1988). Vasopressin mRNA in the suprachiasmatic nuclei: daily regulation of polyadenylate tail length. *Science* 241, 342-344.
- Roman, V., Hagewoud, R., Luiten, P.G., Meerlo, P. (2006). Differential effects of chronic partial sleep deprivation and stress on serotonin-1A and muscarinic acetylcholine receptor sensitivity. *J Sleep Res* 15, 386-394.
- Rosinvil, T., Bouvier, J., Dube, J., Lafreniere, A., Bouchard, M., Cyr-Cronier, J., Gosselin, N., Carrier, J., Lina, J.M. (2021). Are age and sex effects on sleep slow waves only a matter of electroencephalogram amplitude? *Sleep* 44.
- Roy, K., Chauhan, G., Kumari, P., Wadhwa, M., Alam, S., Ray, K., Panjwani, U., Kishore, K. (2018). Phosphorylated delta sleep inducing peptide restores spatial memory and p-CREB expression by improving sleep architecture at high altitude. *Life Sci* 209, 282-290.
- Royet, A., Broutier, L., Coissieux, M.M., Malleval, C., Gadot, N., Maillet, D., Gratadou-Hupon, L., Bernet, A., Nony, P., Treilleux, I., Honnorat, J., Liebl, D., Pelletier, L., Berger, F., Meyronet, D., Castets, M., Mehlen, P. (2017). Ephrin-B3 supports glioblastoma growth by inhibiting apoptosis induced by the dependence receptor EphA4. *Oncotarget* 8, 23750-23759.
- Rui, Y., Myers, K.R., Yu, K., Wise, A., De Blas, A.L., Hartzell, H.C., Zheng, J.Q. (2013). Activity-dependent regulation of dendritic growth and maintenance by glycogen synthase kinase 3beta. *Nat Commun* 4, 2628.
- Rutter, J., Reick, M., Wu, L.C., McKnight, S.L. (2001). Regulation of clock and NPAS2 DNA binding by the redox state of NAD cofactors. *Science* 293, 510-514.
- Sahar, S., Zocchi, L., Kinoshita, C., Borrelli, E., Sassone-Corsi, P. (2010). Regulation of BMAL1 protein stability and circadian function by GSK3beta-mediated phosphorylation. *PLoS One* 5, e8561.
- Sahin, M., Greer, P.L., Lin, M.Z., Poucher, H., Eberhart, J., Schmidt, S., Wright, T.M., Shamah, S.M., O'Connell, S., Cowan, C.W., Hu, L., Goldberg, J.L., Debant, A., Corfas, G., Krull, C.E., Greenberg, M.E. (2005). Eph-dependent tyrosine phosphorylation of ephexin1 modulates growth cone collapse. *Neuron* 46, 191-204.
- Saintigny, P., Peng, S., Zhang, L., Sen, B., Wistuba, II, Lippman, S.M., Girard, L., Minna, J.D., Heymach, J.V., Johnson, F.M. (2012). Global evaluation of Eph receptors and ephrins in lung adenocarcinomas identifies EphA4 as an inhibitor of cell migration and invasion. *Mol Cancer Ther* 11, 2021-2032.
- Sakai, K. (2011). Sleep-waking discharge profiles of median preoptic and surrounding neurons in mice. *Neuroscience* 182, 144-161.
- Samuels, E.R., Szabadi, E. (2008). Functional neuroanatomy of the noradrenergic locus coeruleus: its roles in the regulation of arousal and autonomic function part II: physiological and pharmacological manipulations and pathological alterations of locus coeruleus activity in humans. *Curr Neuropharmacol* 6, 254-285.

- Santhi, N., Lazar, A.S., McCabe, P.J., Lo, J.C., Groeger, J.A., Dijk, D.J. (2016). Sex differences in the circadian regulation of sleep and waking cognition in humans. *Proc Natl Acad Sci U S A* *113*, E2730-2739.
- Saper, C.B., Fuller, P.M. (2017). Wake-sleep circuitry: an overview. *Curr Opin Neurobiol* *44*, 186-192.
- Saper, C.B., Scammell, T.E., Lu, J. (2005a). Hypothalamic regulation of sleep and circadian rhythms. *Nature* *437*, 1257-1263.
- Saper, C.B., Lu, J., Chou, T.C., Gooley, J. (2005b). The hypothalamic integrator for circadian rhythms. *Trends Neurosci* *28*, 152-157.
- Sare, R.M., Lemons, A., Song, A., Smith, C.B. (2020). Sleep Duration in Mouse Models of Neurodevelopmental Disorders. *Brain Sci* *11*.
- Sato, T.K., Panda, S., Miraglia, L.J., Reyes, T.M., Rudic, R.D., McNamara, P., Naik, K.A., FitzGerald, G.A., Kay, S.A., Hogenesch, J.B. (2004). A functional genomics strategy reveals Rora as a component of the mammalian circadian clock. *Neuron* *43*, 527-537.
- Schwartz, M.D., Nunez, A.A., Smale, L. (2004). Differences in the suprachiasmatic nucleus and lower subparaventricular zone of diurnal and nocturnal rodents. *Neuroscience* *127*, 13-23.
- Schwartz, W.J., Zimmerman, P. (1990). Circadian timekeeping in BALB/c and C57BL/6 inbred mouse strains. *J Neurosci* *10*, 3685-3694.
- Schwierin, B., Borbely, A.A., Tobler, I. (1998). Sleep homeostasis in the female rat during the estrous cycle. *Brain Res* *811*, 96-104.
- Scullin, M.K., Bliwise, D.L. (2015). Sleep, cognition, and normal aging: integrating a half century of multidisciplinary research. *Perspect Psychol Sci* *10*, 97-137.
- Seibt, J., Dumoulin, M.C., Aton, S.J., Coleman, T., Watson, A., Naidoo, N., Frank, M.G. (2012). Protein synthesis during sleep consolidates cortical plasticity in vivo. *Curr Biol* *22*, 676-682.
- Seifritz, E., Muller, M.J., Schonenberger, G.A., Trachsel, L., Hemmeter, U., Hatzinger, M., Ernst, A., Moore, P., Holsboer-Trachslar, E. (1995). Human plasma DSIP decreases at the initiation of sleep at different circadian times. *Peptides* *16*, 1475-1481.
- Seok, B.S., Cao, F., Belanger-Nelson, E., Provost, C., Gibbs, S., Jia, Z., Mongrain, V. (2018). The effect of Neurologin-2 absence on sleep architecture and electroencephalographic activity in mice. *Mol Brain* *11*, 52.
- Shao, H., Yang, Y., Mi, Z., Zhu, G.X., Qi, A.P., Ji, W.G., Zhu, Z.R. (2016). Anticonvulsant effect of Rhynchophylline involved in the inhibition of persistent sodium current and NMDA receptor current in the pilocarpine rat model of temporal lobe epilepsy. *Neuroscience* *337*, 355-369.
- Sharma, R., Sahota, P., Thakkar, M.M. (2018). Melatonin promotes sleep in mice by inhibiting orexin neurons in the perifornical lateral hypothalamus. *J Pineal Res* *65*, e12498.
- Sharma, V.K., Chandrashekar, M.K. (2005). Zeitgebers (time cues) for biological clocks. *Current Science* *1136-1146*.
- Shein-Idelson, M., Ondracek, J.M., Liaw, H.P., Reiter, S., Laurent, G. (2016). Slow waves, sharp waves, ripples, and REM in sleeping dragons. *Science* *352*, 590-595.
- Shepherd, J.D., Rumbaugh, G., Wu, J., Chowdhury, S., Plath, N., Kuhl, D., Haganir, R.L., Worley, P.F. (2006). Arc/Arg3.1 mediates homeostatic synaptic scaling of AMPA receptors. *Neuron* *52*, 475-484.

- Shi, G., Wu, D., Ptacek, L.J., Fu, Y.H. (2017). Human genetics and sleep behavior. *Curr Opin Neurobiol* *44*, 43-49.
- Shi, J.S., Huang, B., Wu, Q., Ren, R.X., Xie, X.L. (1993). Effects of rhynchophylline on motor activity of mice and serotonin and dopamine in rat brain. *Zhongguo Yao Li Xue Bao* *14*, 114-117.
- Shi, S., Hida, A., McGuinness, O.P., Wasserman, D.H., Yamazaki, S., Johnson, C.H. (2010). Circadian clock gene *Bmal1* is not essential; functional replacement with its paralog, *Bmal2*. *Curr Biol* *20*, 316-321.
- Shin, J., Gu, C., Kim, J., Park, S. (2008). Transient activation of the MAP kinase signaling pathway by the forward signaling of EphA4 in PC12 cells. *BMB Rep* *41*, 479-484.
- Shinno, H., Kamei, M., Nakamura, Y., Inami, Y., Horiguchi, J. (2008a). Successful treatment with Yi-Gan San for rapid eye movement sleep behavior disorder. *Prog Neuropsychopharmacol Biol Psychiatry* *32*, 1749-1751.
- Shinno, H., Inami, Y., Inagaki, T., Nakamura, Y., Horiguchi, J. (2008b). Effect of Yi-Gan San on psychiatric symptoms and sleep structure at patients with behavioral and psychological symptoms of dementia. *Prog Neuropsychopharmacol Biol Psychiatry* *32*, 881-885.
- Shintani, T., Ihara, M., Sakuta, H., Takahashi, H., Watakabe, I., Noda, M. (2006). Eph receptors are negatively controlled by protein tyrosine phosphatase receptor type O. *Nat Neurosci* *9*, 761-769.
- Shouse, M.N., Siegel, J.M. (1992). Pontine regulation of REM sleep components in cats: integrity of the pedunculopontine tegmentum (PPT) is important for phasic events but unnecessary for atonia during REM sleep. *Brain Res* *571*, 50-63.
- Shu, Y., Xiao, B., Wu, Q., Liu, T., Du, Y., Tang, H., Chen, S., Feng, L., Long, L., Li, Y. (2016). The Ephrin-A5/EphA4 Interaction Modulates Neurogenesis and Angiogenesis by the p-Akt and p-ERK Pathways in a Mouse Model of TLE. *Mol Neurobiol* *53*, 561-576.
- Simon, A.M., de Maturana, R.L., Ricobaraza, A., Escribano, L., Schiapparelli, L., Cuadrado-Tejedor, M., Perez-Mediavilla, A., Avila, J., Del Rio, J., Frechilla, D. (2009). Early changes in hippocampal Eph receptors precede the onset of memory decline in mouse models of Alzheimer's disease. *J Alzheimers Dis* *17*, 773-786.
- Singla, N., Erdjument-Bromage, H., Himanen, J.P., Muir, T.W., Nikolov, D.B. (2011). A semisynthetic Eph receptor tyrosine kinase provides insight into ligand-induced kinase activation. *Chem Biol* *18*, 361-371.
- Slack, S., Battaglia, A., Cibert-Goton, V., Gavazzi, I. (2008). EphrinB2 induces tyrosine phosphorylation of NR2B via Src-family kinases during inflammatory hyperalgesia. *Neuroscience* *156*, 175-183.
- Smith, P.C., Phillips, D.J., Pocivavsek, A., Byrd, C.A., Viechweg, S.S., Hampton, B., Mong, J.A. (2022). Estradiol influences adenosinergic signaling and nonrapid eye movement sleep need in adult female rats. *Sleep* *45*.
- Smyllie, N.J., Bagnall, J., Koch, A.A., Niranjana, D., Polidarova, L., Chesham, J.E., Chin, J.W., Partch, C.L., Loudon, A.S.I., Hastings, M.H. (2022). Cryptochrome proteins regulate the circadian intracellular behavior and localization of PER2 in mouse suprachiasmatic nucleus neurons. *Proc Natl Acad Sci U S A* *119*.
- Sohl, M., Lanner, F., Farnebo, F. (2009). Characterization of the murine Ephrin-B2 promoter. *Gene* *437*, 54-59.
- Sohl, M., Lanner, F., Farnebo, F. (2010). Sp1 mediate hypoxia induced ephrinB2 expression via a hypoxia-inducible factor independent mechanism. *Biochem Biophys Res Commun* *391*, 24-27.
- Song, M.F., Guan, Y.H., Li, H.T., Wei, S.G., Zhang, L.X., Zhang, Z.L., Ma, X.J. (2018). The effects of genetic variation and environmental factors on rhynchophylline and isorhynchophylline in *Uncaria macrophylla* Wall. from different populations in China. *PLoS One* *13*, e0199259.

- Song, Y., Qu, R., Zhu, S., Zhang, R., Ma, S. (2012). Rhynchophylline attenuates LPS-induced pro-inflammatory responses through down-regulation of MAPK/NF-kappaB signaling pathways in primary microglia. *Phytother Res* 26, 1528-1533.
- Soria, V., Martinez-Amoros, E., Escaramis, G., Valero, J., Perez-Egea, R., Garcia, C., Gutierrez-Zotes, A., Puigdemont, D., Bayes, M., Crespo, J.M., Martorell, L., Vilella, E., Labad, A., Vallejo, J., Perez, V., Menchon, J.M., Estivill, X., Gratacos, M., Urretavizcaya, M. (2010). Differential association of circadian genes with mood disorders: CRY1 and NPAS2 are associated with unipolar major depression and CLOCK and VIP with bipolar disorder. *Neuropsychopharmacology* 35, 1279-1289.
- Sosial, E., Nussinovitch, I. (2015). Multiple Ca<sup>2+</sup> channel-dependent components in growth hormone secretion from rat anterior pituitary somatotrophs. *J Neuroendocrinol* 27, 166-176.
- Sotelo, M.I., Tyan, J., Markunas, C., Sulaman, B.A., Horwitz, L., Lee, H., Morrow, J.G., Rothschild, G., Duan, B., Eban-Rothschild, A. (2022). Lateral hypothalamic neuronal ensembles regulate pre-sleep nest-building behavior. *Curr Biol* 32, 806-822 e807.
- Spano, G.M., Banningh, S.W., Marshall, W., de Vivo, L., Bellesi, M., Loschky, S.S., Tononi, G., Cirelli, C. (2019). Sleep Deprivation by Exposure to Novel Objects Increases Synapse Density and Axon-Spine Interface in the Hippocampal CA1 Region of Adolescent Mice. *J Neurosci* 39, 6613-6625.
- Spitz, F., Furlong, E.E. (2012). Transcription factors: from enhancer binding to developmental control. *Nat Rev Genet* 13, 613-626.
- Stark, D.A., Karvas, R.M., Siegel, A.L., Cornelison, D.D. (2011). Eph/ephrin interactions modulate muscle satellite cell motility and patterning. *Development* 138, 5279-5289.
- Stein, E., Lane, A.A., Cerretti, D.P., Schoecklmann, H.O., Schroff, A.D., Van Etten, R.L., Daniel, T.O. (1998). Eph receptors discriminate specific ligand oligomers to determine alternative signaling complexes, attachment, and assembly responses. *Genes Dev* 12, 667-678.
- Steinecke, A., Gampe, C., Zimmer, G., Rudolph, J., Bolz, J. (2014). EphA/ephrin A reverse signaling promotes the migration of cortical interneurons from the medial ganglionic eminence. *Development* 141, 460-471.
- Steriade, M., McCormick, D.A., Sejnowski, T.J. (1993). Thalamocortical oscillations in the sleeping and aroused brain. *Science* 262, 679-685.
- Steriade, M., Timofeev, I., Grenier, F. (2001). Natural waking and sleep states: a view from inside neocortical neurons. *J Neurophysiol* 85, 1969-1985.
- Steward, O., Wallace, C.S., Lyford, G.L., Worley, P.F. (1998). Synaptic activation causes the mRNA for the IEG Arc to localize selectively near activated postsynaptic sites on dendrites. *Neuron* 21, 741-751.
- Stojilkovic, S.S., Izumi, S., Catt, K.J. (1988). Participation of voltage-sensitive calcium channels in pituitary hormone release. *J Biol Chem* 263, 13054-13061.
- Storch, K.F., Lipan, O., Leykin, I., Viswanathan, N., Davis, F.C., Wong, W.H., Weitz, C.J. (2002). Extensive and divergent circadian gene expression in liver and heart. *Nature* 417, 78-83.
- Strecker, R.E., Morairty, S., Thakkar, M.M., Porkka-Heiskanen, T., Basheer, R., Dauphin, L.J., Rainnie, D.G., Portas, C.M., Greene, R.W., McCarley, R.W. (2000). Adenosinergic modulation of basal forebrain and

- preoptic/anterior hypothalamic neuronal activity in the control of behavioral state. *Behav Brain Res* 115, 183-204.
- Suh, S., Cho, N., Zhang, J. (2018). Sex Differences in Insomnia: from Epidemiology and Etiology to Intervention. *Curr Psychiatry Rep* 20, 69.
- Sun, Y.Z., Liu, R. (2013). Therapeutic evaluation on needling method of regulating the conception vessel and calming the mind for perimenopausal sleep disorder. *Journal of Acupuncture and Tuina Science* 11, 142-146.
- Suntsova, N., Szymusiak, R., Alam, M.N., Guzman-Marin, R., McGinty, D. (2002). Sleep-waking discharge patterns of median preoptic nucleus neurons in rats. *J Physiol* 543, 665-677.
- Suntsova, N., Guzman-Marin, R., Kumar, S., Alam, M.N., Szymusiak, R., McGinty, D. (2007). The median preoptic nucleus reciprocally modulates activity of arousal-related and sleep-related neurons in the perifornical lateral hypothalamus. *J Neurosci* 27, 1616-1630.
- Suzuki, A., Sinton, C.M., Greene, R.W., Yanagisawa, M. (2013). Behavioral and biochemical dissociation of arousal and homeostatic sleep need influenced by prior wakeful experience in mice. *Proc Natl Acad Sci U S A* 110, 10288-10293.
- Suzuki, T., Hide, I., Ido, K., Kohsaka, S., Inoue, K., Nakata, Y. (2004). Production and release of neuroprotective tumor necrosis factor by P2X7 receptor-activated microglia. *J Neurosci* 24, 1-7.
- Swift, K.M., Keus, K., Echeverria, C.G., Cabrera, Y., Jimenez, J., Holloway, J., Clawson, B.C., Poe, G.R. (2020). Sex differences within sleep in gonadally intact rats. *Sleep* 43.
- Szentirmai, E., Yasuda, T., Taishi, P., Wang, M., Churchill, L., Bohnet, S., Magrath, P., Kacsoh, B., Jimenez, L., Krueger, J.M. (2007). Growth hormone-releasing hormone: cerebral cortical sleep-related EEG actions and expression. *Am J Physiol Regul Integr Comp Physiol* 293, R922-930.
- Szymusiak, R., Alam, N., Steininger, T.L., McGinty, D. (1998). Sleep-waking discharge patterns of ventrolateral preoptic/anterior hypothalamic neurons in rats. *Brain Res* 803, 178-188.
- Tainton-Heap, L.A.L., Kirszenblat, L.C., Notaras, E.T., Grabowska, M.J., Jeans, R., Feng, K., Shaw, P.J., van Swinderen, B. (2021). A Paradoxical Kind of Sleep in *Drosophila melanogaster*. *Curr Biol* 31, 578-590 e576.
- Takahashi, J.S. (2017). Transcriptional architecture of the mammalian circadian clock. *Nat Rev Genet* 18, 164-179.
- Takahashi, J.S., Hong, H.K., Ko, C.H., McDearmon, E.L. (2008). The genetics of mammalian circadian order and disorder: implications for physiology and disease. *Nat Rev Genet* 9, 764-775.
- Takahashi, K., Lin, J.S., Sakai, K. (2009). Characterization and mapping of sleep-waking specific neurons in the basal forebrain and preoptic hypothalamus in mice. *Neuroscience* 161, 269-292.
- Takasu, M.A., Dalva, M.B., Zigmond, R.E., Greenberg, M.E. (2002). Modulation of NMDA receptor-dependent calcium influx and gene expression through EphB receptors. *Science* 295, 491-495.
- Takemoto, M., Fukuda, T., Sonoda, R., Murakami, F., Tanaka, H., Yamamoto, N. (2002). Ephrin-B3-EphA4 interactions regulate the growth of specific thalamocortical axon populations in vitro. *Eur J Neurosci* 16, 1168-1172.
- Tanasic, S., Mattusch, C., Wagner, E.M., Eder, M., Rupprecht, R., Rammes, G., Di Benedetto, B. (2016). Desipramine targets astrocytes to attenuate synaptic plasticity via modulation of the ephrinA3/EphA4 signalling. *Neuropharmacology* 105, 154-163.

- Tartar, J.L., Ward, C.P., Cordeira, J.W., Legare, S.L., Blanchette, A.J., McCarley, R.W., Strecker, R.E. (2009). Experimental sleep fragmentation and sleep deprivation in rats increases exploration in an open field test of anxiety while increasing plasma corticosterone levels. *Behav Brain Res* 197, 450-453.
- Tatsuki, F., Sunagawa, G.A., Shi, S., Susaki, E.A., Yukinaga, H., Perrin, D., Sumiyama, K., Ukai-Tadenuma, M., Fujishima, H., Ohno, R., Tone, D., Ode, K.L., Matsumoto, K., Ueda, H.R. (2016). Involvement of Ca<sup>2+</sup>-Dependent Hyperpolarization in Sleep Duration in Mammals. *Neuron* 90, 70-85.
- Terao, A., Wisor, J.P., Peyron, C., Apte-Deshpande, A., Wurts, S.W., Edgar, D.M., Kilduff, T.S. (2006). Gene expression in the rat brain during sleep deprivation and recovery sleep: an Affymetrix GeneChip study. *Neuroscience* 137, 593-605.
- Thannickal, T.C., Nienhuis, R., Siegel, J.M. (2009). Localized loss of hypocretin (orexin) cells in narcolepsy without cataplexy. *Sleep* 32, 993-998.
- Thannickal, T.C., Moore, R.Y., Nienhuis, R., Ramanathan, L., Gulyani, S., Aldrich, M., Cornford, M., Siegel, J.M. (2000). Reduced number of hypocretin neurons in human narcolepsy. *Neuron* 27, 469-474.
- Theil, T., Frain, M., Gilardi-Hebenstreit, P., Flenniken, A., Charnay, P., Wilkinson, D.G. (1998). Segmental expression of the EphA4 (Sek-1) receptor tyrosine kinase in the hindbrain is under direct transcriptional control of Krox-20. *Development* 125, 443-452.
- Thomas, C.W., Guillaumin, M.C., McKillop, L.E., Achermann, P., Vyazovskiy, V.V. (2020). Global sleep homeostasis reflects temporally and spatially integrated local cortical neuronal activity. *Elife* 9.
- Timofeev, I., Bazhenov, M., Seigneur, J., Sejnowski, T. (2012). Neuronal Synchronization and Thalamocortical Rhythms in Sleep, Wake and Epilepsy. In: Jasper's Basic Mechanisms of the Epilepsies (th, Noebels JL, Avoli M, Rogawski MA, Olsen RW, Delgado-Escueta AV, eds). Bethesda (MD).
- Tischkau, S.A., Mitchell, J.W., Tyan, S.H., Buchanan, G.F., Gillette, M.U. (2003). Ca<sup>2+</sup>/cAMP response element-binding protein (CREB)-dependent activation of Per1 is required for light-induced signaling in the suprachiasmatic nucleus circadian clock. *J Biol Chem* 278, 718-723.
- Todd, K.L., Baker, K.L., Eastman, M.B., Kolling, F.W., Trausch, A.G., Nelson, C.E., Conover, J.C. (2017). EphA4 Regulates Neuroblast and Astrocyte Organization in a Neurogenic Niche. *J Neurosci* 37, 3331-3341.
- Tognolini, M., Incerti, M., Lodola, A. (2014). Are we using the right pharmacological tools to target EphA4? *ACS Chem Neurosci* 5, 1146-1147.
- Tomita, J., Nakajima, M., Kondo, T., Iwasaki, H. (2005). No transcription-translation feedback in circadian rhythm of KaiC phosphorylation. *Science* 307, 251-254.
- Tone, D. et al. (2022). Distinct phosphorylation states of mammalian CaMKIIbeta control the induction and maintenance of sleep. *PLoS Biol* 20, e3001813.
- Tononi, G., Cirelli, C. (2003). Sleep and synaptic homeostasis: a hypothesis. *Brain Res Bull* 62, 143-150.
- Tononi, G., Cirelli, C. (2006). Sleep function and synaptic homeostasis. *Sleep Med Rev* 10, 49-62.
- Tononi, G., Cirelli, C. (2012). Time to be SHY? Some comments on sleep and synaptic homeostasis. *Neural Plast* 2012, 415250.

- Torres, R., Firestein, B.L., Dong, H., Staudinger, J., Olson, E.N., Haganir, R.L., Brecht, D.S., Gale, N.W., Yancopoulos, G.D. (1998). PDZ proteins bind, cluster, and synaptically colocalize with Eph receptors and their ephrin ligands. *Neuron* 21, 1453-1463.
- Travnickova-Bendova, Z., Cermakian, N., Reppert, S.M., Sassone-Corsi, P. (2002). Bimodal regulation of mPeriod promoters by CREB-dependent signaling and CLOCK/BMAL1 activity. *Proc Natl Acad Sci U S A* 99, 7728-7733.
- Tremblay, M.E., Riad, M., Bouvier, D., Murai, K.K., Pasquale, E.B., Descarries, L., Doucet, G. (2007). Localization of EphA4 in axon terminals and dendritic spines of adult rat hippocampus. *J Comp Neurol* 501, 691-702.
- Tsunematsu, T., Kilduff, T.S., Boyden, E.S., Takahashi, S., Tominaga, M., Yamanaka, A. (2011). Acute optogenetic silencing of orexin/hypocretin neurons induces slow-wave sleep in mice. *J Neurosci* 31, 10529-10539.
- Tsunematsu, T., Ueno, T., Tabuchi, S., Inutsuka, A., Tanaka, K.F., Hasuwa, H., Kilduff, T.S., Terao, A., Yamanaka, A. (2014). Optogenetic manipulation of activity and temporally controlled cell-specific ablation reveal a role for MCH neurons in sleep/wake regulation. *J Neurosci* 34, 6896-6909.
- Tu, J.C., Xiao, B., Yuan, J.P., Lanahan, A.A., Leoffert, K., Li, M., Linden, D.J., Worley, P.F. (1998). Homer binds a novel proline-rich motif and links group 1 metabotropic glutamate receptors with IP3 receptors. *Neuron* 21, 717-726.
- Tyler, J., Lu, Y., Dunlap, J., Forger, D.B. (2022). Evolution of the repression mechanisms in circadian clocks. *Genome Biol* 23, 17.
- Ueda, H.R., Hayashi, S., Chen, W., Sano, M., Machida, M., Shigeyoshi, Y., Iino, M., Hashimoto, S. (2005). System-level identification of transcriptional circuits underlying mammalian circadian clocks. *Nat Genet* 37, 187-192.
- Uygun, D.S., Yang, C., Tilli, E.R., Katsuki, F., Hodges, E.L., McKenna, J.T., McNally, J.M., Brown, R.E., Basheer, R. (2022). Knockdown of GABAA alpha3 subunits on thalamic reticular neurons enhances deep sleep in mice. *Nat Commun* 13, 2246.
- Vaccaro, A., Kaplan Dor, Y., Nambara, K., Pollina, E.A., Lin, C., Greenberg, M.E., Rogulja, D. (2020). Sleep Loss Can Cause Death through Accumulation of Reactive Oxygen Species in the Gut. *Cell* 181, 1307-1328 e1315.
- van Diepen, R.M., Miller, L.M., Mazaheri, A., Geng, J.J. (2016). The Role of Alpha Activity in Spatial and Feature-Based Attention. *eNeuro* 3.
- Van Dongen, H.P., Maislin, G., Mullington, J.M., Dinges, D.F. (2003). The cumulative cost of additional wakefulness: dose-response effects on neurobehavioral functions and sleep physiology from chronic sleep restriction and total sleep deprivation. *Sleep* 26, 117-126.
- Van Dort, C.J., Zachs, D.P., Kenny, J.D., Zheng, S., Goldblum, R.R., Gelwan, N.A., Ramos, D.M., Nolan, M.A., Wang, K., Weng, F.J., Lin, Y., Wilson, M.A., Brown, E.N. (2015). Optogenetic activation of cholinergic neurons in the PPT or LDT induces REM sleep. *Proc Natl Acad Sci U S A* 112, 584-589.
- Vanderheyden, W.M., Gerstner, J.R., Tanenhaus, A., Yin, J.C., Shaw, P.J. (2013). ERK phosphorylation regulates sleep and plasticity in *Drosophila*. *PLoS One* 8, e81554.
- Vansteensel, M.J., Michel, S., Meijer, J.H. (2008). Organization of cell and tissue circadian pacemakers: a comparison among species. *Brain Res Rev* 58, 18-47.

- Varin, C., Luppi, P.H., Fort, P. (2018). Melanin-concentrating hormone-expressing neurons adjust slow-wave sleep dynamics to catalyze paradoxical (REM) sleep. *Sleep* 41.
- Vassalli, A., Franken, P. (2017). Hypocretin (orexin) is critical in sustaining theta/gamma-rich waking behaviors that drive sleep need. *Proc Natl Acad Sci U S A* 114, E5464-E5473.
- Vecsey, C.G., Peixoto, L., Choi, J.H., Wimmer, M., Jaganath, D., Hernandez, P.J., Blackwell, J., Meda, K., Park, A.J., Hannenhalli, S., Abel, T. (2012). Genomic analysis of sleep deprivation reveals translational regulation in the hippocampus. *Physiol Genomics* 44, 981-991.
- Venner, A., Anaclet, C., Broadhurst, R.Y., Saper, C.B., Fuller, P.M. (2016). A Novel Population of Wake-Promoting GABAergic Neurons in the Ventral Lateral Hypothalamus. *Curr Biol* 26, 2137-2143.
- Vezzani, A., Friedman, A., Dingledine, R.J. (2013). The role of inflammation in epileptogenesis. *Neuropharmacology* 69, 16-24.
- Viswanathan, M., Laitinen, J.T., Saavedra, J.M. (1990). Expression of melatonin receptors in arteries involved in thermoregulation. *Proc Natl Acad Sci U S A* 87, 6200-6203.
- Voloh, B., Valiante, T.A., Everling, S., Womelsdorf, T. (2015). Theta-gamma coordination between anterior cingulate and prefrontal cortex indexes correct attention shifts. *Proc Natl Acad Sci U S A* 112, 8457-8462.
- Von Economo, C. (1930). Sleep as a problem of localization. *J Nerv Ment Dis* 71, 249-259.
- Vyazovskiy, V.V., Welker, E., Fritschy, J.M., Tobler, I. (2004). Regional pattern of metabolic activation is reflected in the sleep EEG after sleep deprivation combined with unilateral whisker stimulation in mice. *Eur J Neurosci* 20, 1363-1370.
- Vyazovskiy, V.V., Ruijgrok, G., Deboer, T., Tobler, I. (2006). Running wheel accessibility affects the regional electroencephalogram during sleep in mice. *Cereb Cortex* 16, 328-336.
- Vyazovskiy, V.V., Cirelli, C., Pfister-Genskow, M., Faraguna, U., Tononi, G. (2008). Molecular and electrophysiological evidence for net synaptic potentiation in wake and depression in sleep. *Nat Neurosci* 11, 200-208.
- Vyazovskiy, V.V., Olcese, U., Hanlon, E.C., Nir, Y., Cirelli, C., Tononi, G. (2011). Local sleep in awake rats. *Nature* 472, 443-447.
- Wadhwa, M., Prabhakar, A., Ray, K., Roy, K., Kumari, P., Jha, P.K., Kishore, K., Kumar, S., Panjwani, U. (2017). Inhibiting the microglia activation improves the spatial memory and adult neurogenesis in rat hippocampus during 48 h of sleep deprivation. *J Neuroinflammation* 14, 222.
- Wagner, M.J., Hsiung, M.S., Gish, G.D., Bagshaw, R.D., Doodnauth, S.A., Soliman, M.A., Jorgensen, C., Tucholska, M., Rottapel, R. (2020). The Shb scaffold binds the Nck adaptor protein, p120 RasGAP, and Chimaerins and thereby facilitates heterotypic cell segregation by the receptor EphB2. *J Biol Chem* 295, 3932-3944.
- Walkenhorst, J., Dutting, D., Handwerker, C., Huai, J., Tanaka, H., Drescher, U. (2000). The EphA4 receptor tyrosine kinase is necessary for the guidance of nasal retinal ganglion cell axons in vitro. *Mol Cell Neurosci* 16, 365-375.
- Wang, J., Zhang, S., Lu, H., Xu, H. (2022). Differential regulation of alternative promoters emerges from unified kinetics of enhancer-promoter interaction. *Nat Commun* 13, 2714.



- Wang, Y., Song, L., Liu, M., Ge, R., Zhou, Q., Liu, W., Li, R., Qie, J., Zhen, B., Wang, Y., He, F., Qin, J., Ding, C. (2018a). A proteomics landscape of circadian clock in mouse liver. *Nat Commun* 9, 1553.
- Wang, Z., Wu, Y., Li, L., Su, X.D. (2013). Intermolecular recognition revealed by the complex structure of human CLOCK-BMAL1 basic helix-loop-helix domains with E-box DNA. *Cell Res* 23, 213-224.
- Wang, Z. et al. (2018b). Quantitative phosphoproteomic analysis of the molecular substrates of sleep need. *Nature* 558, 435-439.
- Warner, N., Wybenga-Groot, L.E., Pawson, T. (2008). Analysis of EphA4 receptor tyrosine kinase substrate specificity using peptide-based arrays. *FEBS J* 275, 2561-2573.
- Watson, B.O., Levenstein, D., Greene, J.P., Gelinas, J.N., Buzsaki, G. (2016). Network Homeostasis and State Dynamics of Neocortical Sleep. *Neuron* 90, 839-852.
- Wegmeyer, H., Egea, J., Rabe, N., Gezelius, H., Filosa, A., Enjin, A., Varoqueaux, F., Deininger, K., Schnutgen, F., Brose, N., Klein, R., Kullander, K., Betz, A. (2007). EphA4-dependent axon guidance is mediated by the RacGAP alpha2-chimaerin. *Neuron* 55, 756-767.
- Wei, Y. (2020). Comparative transcriptome analysis of the hippocampus from sleep-deprived and Alzheimer's disease mice. *Genet Mol Biol* 43, e20190052.
- Welsh, D.K., Yoo, S.H., Liu, A.C., Takahashi, J.S., Kay, S.A. (2004). Bioluminescence imaging of individual fibroblasts reveals persistent, independently phased circadian rhythms of clock gene expression. *Curr Biol* 14, 2289-2295.
- Wen, S., Ma, D., Zhao, M., Xie, L., Wu, Q., Gou, L., Zhu, C., Fan, Y., Wang, H., Yan, J. (2020). Spatiotemporal single-cell analysis of gene expression in the mouse suprachiasmatic nucleus. *Nat Neurosci* 23, 456-467.
- Werth, E., Dijk, D.J., Achermann, P., Borbely, A.A. (1996). Dynamics of the sleep EEG after an early evening nap: experimental data and simulations. *Am J Physiol* 271, R501-510.
- Williams, C., Mehrian Shai, R., Wu, Y., Hsu, Y.H., Sitzer, T., Spann, B., McCleary, C., Mo, Y., Miller, C.A. (2009). Transcriptome analysis of synaptoneurosome identifies neuroplasticity genes overexpressed in incipient Alzheimer's disease. *PLoS One* 4, e4936.
- Williamson, E.M. (2001). Synergy and other interactions in phytomedicines. *Phytomedicine* 8, 401-409.
- Wimmer, R.D., Astori, S., Bond, C.T., Rovo, Z., Chatton, J.Y., Adelman, J.P., Franken, P., Luthi, A. (2012). Sustaining sleep spindles through enhanced SK2-channel activity consolidates sleep and elevates arousal threshold. *J Neurosci* 32, 13917-13928.
- Winsky-Sommerer, R. (2009). Role of GABAA receptors in the physiology and pharmacology of sleep. *Eur J Neurosci* 29, 1779-1794.
- Winter, J., Roepcke, S., Krause, S., Muller, E.C., Otto, A., Vingron, M., Schweiger, S. (2008). Comparative 3'UTR analysis allows identification of regulatory clusters that drive Eph/ephrin expression in cancer cell lines. *PLoS One* 3, e2780.
- Wintler, T., Schoch, H., Frank, M.G., Peixoto, L. (2020). Sleep, brain development, and autism spectrum disorders: Insights from animal models. *J Neurosci Res* 98, 1137-1149.

- Woon, P.Y., Kaisaki, P.J., Braganca, J., Bihoreau, M.T., Levy, J.C., Farrall, M., Gauguier, D. (2007). Aryl hydrocarbon receptor nuclear translocator-like (BMAL1) is associated with susceptibility to hypertension and type 2 diabetes. *Proc Natl Acad Sci U S A* *104*, 14412-14417.
- Wu, B., De, S.K., Kulinich, A., Salem, A.F., Koeppen, J., Wang, R., Barile, E., Wang, S., Zhang, D., Ethell, I., Pellecchia, M. (2017). Potent and Selective EphA4 Agonists for the Treatment of ALS. *Cell Chem Biol* *24*, 293-305.
- Wybenga-Groot, L.E., Baskin, B., Ong, S.H., Tong, J., Pawson, T., Sicheri, F. (2001). Structural basis for autoinhibition of the Ephb2 receptor tyrosine kinase by the unphosphorylated juxtamembrane region. *Cell* *106*, 745-757.
- Wyse, C.A., Coogan, A.N. (2010). Impact of aging on diurnal expression patterns of CLOCK and BMAL1 in the mouse brain. *Brain Res* *1337*, 21-31.
- Xie, L., Kang, H., Xu, Q., Chen, M.J., Liao, Y., Thiyagarajan, M., O'Donnell, J., Christensen, D.J., Nicholson, C., Iliff, J.J., Takano, T., Deane, R., Nedergaard, M. (2013). Sleep drives metabolite clearance from the adult brain. *Science* *342*, 373-377.
- Xing, B., Li, Y.C., Gao, W.J. (2016). GSK3beta Hyperactivity during an Early Critical Period Impairs Prefrontal Synaptic Plasticity and Induces Lasting Deficits in Spine Morphology and Working Memory. *Neuropsychopharmacology* *41*, 3003-3015.
- Xu, K., Tzvetkova-Robev, D., Xu, Y., Goldgur, Y., Chan, Y.P., Himanen, J.P., Nikolov, D.B. (2013). Insights into Eph receptor tyrosine kinase activation from crystal structures of the EphA4 ectodomain and its complex with ephrin-A5. *Proc Natl Acad Sci U S A* *110*, 14634-14639.
- Xue, R., Wan, Y., Sun, X., Zhang, X., Gao, W., Wu, W. (2019). Nicotinic mitigation of neuroinflammation and oxidative stress after chronic sleep deprivation. *Front Immunol* *10*, 2546.
- Yaffe, K., Falvey, C.M., Hoang, T. (2014). Connections between sleep and cognition in older adults. *Lancet Neurol* *13*, 1017-1028.
- Yamanaka, A., Beuckmann, C.T., Willie, J.T., Hara, J., Tsujino, N., Mieda, M., Tominaga, M., Yagami, K., Sugiyama, F., Goto, K., Yanagisawa, M., Sakurai, T. (2003). Hypothalamic orexin neurons regulate arousal according to energy balance in mice. *Neuron* *38*, 701-713.
- Yamazaki, S., Numano, R., Abe, M., Hida, A., Takahashi, R., Ueda, M., Block, G.D., Sakaki, Y., Menaker, M., Tei, H. (2000). Resetting central and peripheral circadian oscillators in transgenic rats. *Science* *288*, 682-685.
- Yan, Y., Luo, Y.C., Wan, H.Y., Wang, J., Zhang, P.P., Liu, M., Li, X., Li, S., Tang, H. (2013). MicroRNA-10a is involved in the metastatic process by regulating Eph tyrosine kinase receptor A4-mediated epithelial-mesenchymal transition and adhesion in hepatoma cells. *Hepatology* *57*, 667-677.
- Yang, F., Inoue, I., Kumagai, M., Takahashi, S., Nakajima, Y., Ikeda, M. (2013). Real-time analysis of the circadian oscillation of the Rev-Erb beta promoter. *J Atheroscler Thromb* *20*, 267-276.
- Yang, G., Lai, C.S., Cichon, J., Ma, L., Li, W., Gan, W.B. (2014). Sleep promotes branch-specific formation of dendritic spines after learning. *Science* *344*, 1173-1178.
- Yang, H. et al. (2019). Stress-glucocorticoid-TSC22D3 axis compromises therapy-induced antitumor immunity. *Nat Med* *25*, 1428-1441.

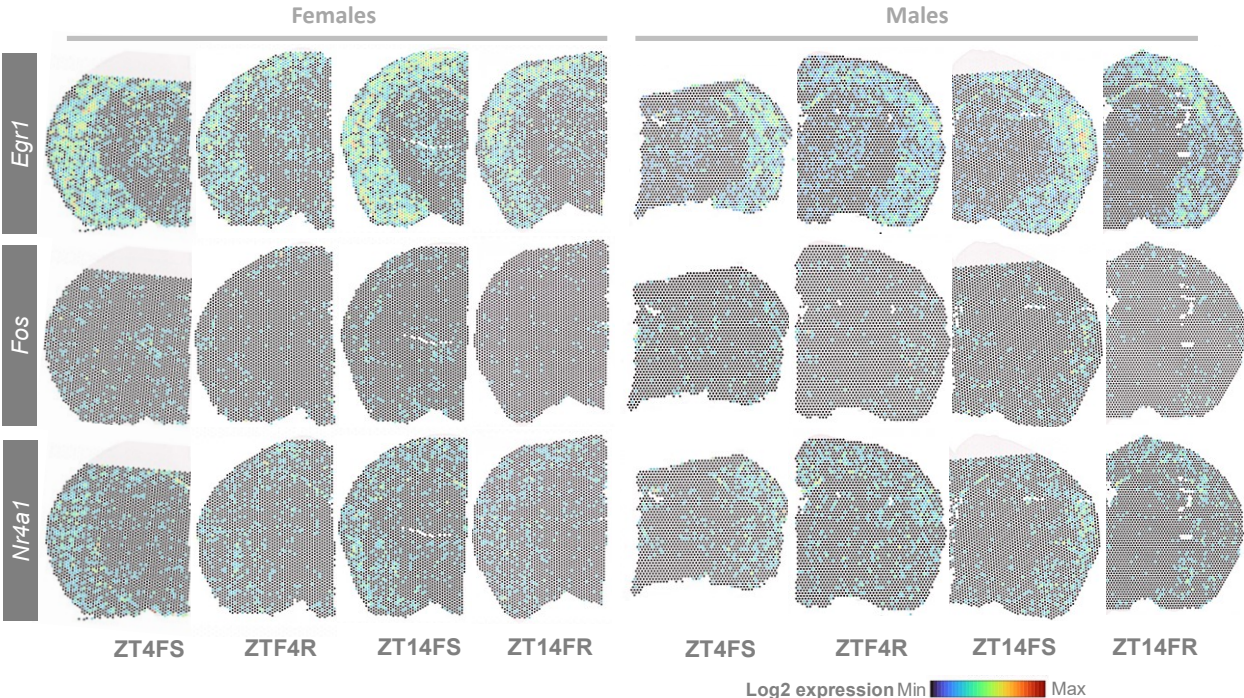
- Yang, Y., Jiang, G., Zhang, P., Fan, J. (2015). Programmed cell death and its role in inflammation. *Mil Med Res* 2, 12.
- Yasenkov, R., Deboer, T. (2011). Interrelations and circadian changes of electroencephalogram frequencies under baseline conditions and constant sleep pressure in the rat. *Neuroscience* 180, 212-221.
- Yasuda, T., Yoshida, H., Garcia-Garcia, F., Kay, D., Krueger, J.M. (2005). Interleukin-1beta has a role in cerebral cortical state-dependent electroencephalographic slow-wave activity. *Sleep* 28, 177-184.
- Yeung, W., Kwon, A., Taujale, R., Bunn, C., Venkat, A., Kannan, N. (2021). Evolution of Functional Diversity in the Holozoan Tyrosine Kinome. *Mol Biol Evol* 38, 5625-5639.
- Yin, D., Dong, H., Wang, T.X., Hu, Z.Z., Cheng, N.N., Qu, W.M., Huang, Z.L. (2019). Glutamate activates the histaminergic tuberomammillary nucleus and increases wakefulness in rats. *Neuroscience* 413, 86-98.
- Yin, L., Wang, J., Klein, P.S., Lazar, M.A. (2006). Nuclear receptor Rev-erbalpha is a critical lithium-sensitive component of the circadian clock. *Science* 311, 1002-1005.
- Yoo, J.H., Ha, T.W., Hong, J.T., Oh, K.W. (2016). Rhynchophylline, one of major constituents of *Uncaria Ramulus* et *Uncus* enhances pentobarbital-induced sleep behaviors and Rapid Eye Movement Sleep in rodents. *Natural Product Sciences* 22, 263-269.
- Yoshida, H., Peterfi, Z., Garcia-Garcia, F., Kirkpatrick, R., Yasuda, T., Krueger, J.M. (2004). State-specific asymmetries in EEG slow wave activity induced by local application of TNFalpha. *Brain Res* 1009, 129-136.
- Yu, C., Li, Y., Stitt, I.M., Zhou, Z.C., Sellers, K.K., Frohlich, F. (2018). Theta Oscillations Organize Spiking Activity in Higher-Order Visual Thalamus during Sustained Attention. *eNeuro* 5.
- Yu, X., Wang, G., Gilmore, A., Yee, A.X., Li, X., Xu, T., Smith, S.J., Chen, L., Zuo, Y. (2013). Accelerated experience-dependent pruning of cortical synapses in ephrin-A2 knockout mice. *Neuron* 80, 64-71.
- Yu, X., Zecharia, A., Zhang, Z., Yang, Q., Yustos, R., Jager, P., Vyssotski, A.L., Maywood, E.S., Chesham, J.E., Ma, Y., Brickley, S.G., Hastings, M.H., Franks, N.P., Wisden, W. (2014). Circadian factor BMAL1 in histaminergic neurons regulates sleep architecture. *Curr Biol* 24, 2838-2844.
- Yuan, D., Ma, B., Yang, J.Y., Xie, Y.Y., Wang, L., Zhang, L.J., Kano, Y., Wu, C.F. (2009). Anti-inflammatory effects of rhynchophylline and isorhynchophylline in mouse N9 microglial cells and the molecular mechanism. *Int Immunopharmacol* 9, 1549-1554.
- Yumoto, N., Wakatsuki, S., Kurisaki, T., Hara, Y., Osumi, N., Frisen, J., Sehara-Fujisawa, A. (2008). Meltrin beta/ADAM19 interacting with EphA4 in developing neural cells participates in formation of the neuromuscular junction. *PLoS One* 3, e3322.
- Zeng, L., Zhang, D., McLoughlin, H.S., Zalon, A.J., Aravind, L., Paulson, H.L. (2018). Loss of the Spinocerebellar Ataxia type 3 disease protein ATXN3 alters transcription of multiple signal transduction pathways. *PLoS One* 13, e0204438.
- Zhang, B., Wing, Y.K. (2006). Sex differences in insomnia: a meta-analysis. *Sleep* 29, 85-93.
- Zhang, J., Obal, F., Jr., Zheng, T., Fang, J., Taishi, P., Krueger, J.M. (1999). Intraoptotic microinjection of GHRH or its antagonist alters sleep in rats. *J Neurosci* 19, 2187-2194.

- Zhang, J.C., Yao, W., Qu, Y., Nakamura, M., Dong, C., Yang, C., Ren, Q., Ma, M., Han, M., Shirayama, Y., Hayashi-Takagi, A., Hashimoto, K. (2017). Increased EphA4-ephexin1 signaling in the medial prefrontal cortex plays a role in depression-like phenotype. *Sci Rep* 7, 7133.
- Zhang, R., Lahens, N.F., Ballance, H.I., Hughes, M.E., Hogenesch, J.B. (2014). A circadian gene expression atlas in mammals: implications for biology and medicine. *Proc Natl Acad Sci U S A* 111, 16219-16224.
- Zhang, Y., Fei, M., Xue, G., Zhou, Q., Jia, Y., Li, L., Xin, H., Sun, S. (2012). Elevated levels of hypoxia-inducible microRNA-210 in pre-eclampsia: new insights into molecular mechanisms for the disease. *J Cell Mol Med* 16, 249-259.
- Zhao, J., Boyd, A.W., Bartlett, P.F. (2017). The identification of a novel isoform of EphA4 and ITS expression in SOD1(G93A) mice. *Neuroscience* 347, 11-21.
- Zhou, J.Y., Mo, Z.X., Zhou, S.W. (2010). Rhynchophylline down-regulates NR2B expression in cortex and hippocampal CA1 area of amphetamine-induced conditioned place preference rat. *Arch Pharm Res* 33, 557-565.
- Zhou, L., Jones, E.V., Murai, K.K. (2012). EphA signaling promotes actin-based dendritic spine remodeling through slingshot phosphatase. *J Biol Chem* 287, 9346-9359.
- Zhou, L., Martinez, S.J., Haber, M., Jones, E.V., Bouvier, D., Doucet, G., Corera, A.T., Fon, E.A., Zisch, A.H., Murai, K.K. (2007). EphA4 signaling regulates phospholipase Cgamma1 activation, cofilin membrane association, and dendritic spine morphology. *J Neurosci* 27, 5127-5138.
- Zhou, Y.D., Barnard, M., Tian, H., Li, X., Ring, H.Z., Francke, U., Shelton, J., Richardson, J., Russell, D.W., McKnight, S.L. (1997). Molecular characterization of two mammalian bHLH-PAS domain proteins selectively expressed in the central nervous system. *Proc Natl Acad Sci U S A* 94, 713-718.
- Zhu, R.L., Fang, Y., Yu, H.H., Chen, D.F., Yang, L., Cho, K.S. (2021). Absence of ephrin-A2/A3 increases retinal regenerative potential for Muller cells in Rhodopsin knockout mice. *Neural Regen Res* 16, 1317-1322.
- Zimmer, G., Rudolph, J., Landmann, J., Gerstmann, K., Steinecke, A., Gampe, C., Bolz, J. (2011). Bidirectional ephrinB3/EphA4 signaling mediates the segregation of medial ganglionic eminence- and preoptic area-derived interneurons in the deep and superficial migratory stream. *J Neurosci* 31, 18364-18380.

**Table A1. Cellular functions attributed to genes modified according to wake/sleep reported by literature.** Studies compare gene expression associated to wake time (studied by sleep deprivation [SD] most of the time) and gene expression associated to sleep conditions. \* indicates studies that used paradoxical sleep deprivation (PSD).

WAKE/SD UP	Cirelli and Tononi, 2000	Cirelli et al., 2004	Terao et al., 2006	Mackiewicz et al., 2007	Maret et al., 2007	Mongrain et al., 2010	Vecsey et al., 2012	Bellesi et al., 2013	Massart et al., 2014	Narwade et al., 2017	Husse et al., 2017	Diessler et al., 2018	Oyola et al., 2019	Hor et al., 2019	Guo et al., 2019	Guo et al., 2020	Wei, 2020	Gainet al., 2021	Cortex
Immediate early genes/TFs (neurotransmission/potential)	✓	✓	✓	✓	✓	✓	✓	✓	✓	✓	✓	✓	✓	✓	✓	✓	✓	✓	Cortex
Circadian genes						✓			✓				✓		✓				Cortex
Energy metabolism	✓	✓				✓													Cortex
Positive regulation of transcription		✓					✓		✓		✓								Cortex/Hypothalamus
Negative regulation of translation		✓																	Brain
Growth factors /adhesion molecules	✓		✓					✓				✓			✓				Forebrain
Stress responses (unfolded protein response, apoptosis)	✓	✓				✓	✓	✓	✓	✓	✓	✓	✓		✓	✓			Hippocampus
Vesicle and synapse related genes	✓																		Oligodendrocytes
Neurotransmitter/hormone receptors	✓	✓	✓	✓	✓	✓		✓	✓				✓	✓	✓				Cortex
Neurotransmitter/hormone transporters	✓																		Brain *
Depolarization sensitive		✓																	Hypothalamus
Lipid, cholesterol						✓		✓											Cortex
Enzymes	✓					✓									✓				Pituitary *
<b>UPREGULATED IN SLEEP</b>																			Cortex
Synaptic plasticity (consolidation/depression)		✓					✓			✓									mPFC
Membrane trafficking and maintenance		✓						✓											VLPO galanin neurons
Metabolism				✓															Hippocampus
Antioxidant enzymes				✓															Hippocampus
Cholesterol biosynthesis		✓		✓				✓											Hippocampus
Negative regulation of transcription		✓		✓			✓			✓						✓			Hippocampus
Positive regulation of translation		✓		✓			✓									✓			Hippocampus
Hyperpolarization promoting (leakage)		✓																	Hippocampus
Maintenance of vesicle pools				✓															Hippocampus
Response to temperature				✓															Hippocampus
Neurohypophysis										✓									Hippocampus
GABAergic neurotransmission		✓																	Hippocampus

Figure A1. Spatial gene expression of immediate early genes downregulated by RHY but upregulated by SD









ENSMUSG00000020732	Rab37	0.173301240	0.823843351	0.015441439
ENSMUSG00000075514	Gm13375	0.018061171	-1.228282339	0.015479572
ENSMUSG000000095687	Rnaset2a	0.072244686	0.951801461	0.016745758
ENSMUSG00000028656	Cap1	0.461849954	-0.678632319	0.016768931
ENSMUSG00000020216	Jsrp1	0.076974992	-0.818248466	0.016956597
ENSMUSG00000089661	Mia	0.261886985	1.056353527	0.017347879
ENSMUSG00000027860	Vang11	0.069234490	0.981919916	0.018351649
ENSMUSG00000070306	Ccdc153	0.188782244	1.198798733	0.018351649
ENSMUSG00000022353	Mtss1	0.289838798	0.712626519	0.018891292
ENSMUSG00000011154	Cfap161	0.037842454	1.181933681	0.019216739
ENSMUSG00000045005	Fzd5	0.040422622	1.150524976	0.019240527
ENSMUSG00000039943	Plcb4	0.910369043	0.673990704	0.019240527
ENSMUSG00000027716	Trpc3	0.119977781	0.819181455	0.019240527
ENSMUSG00000057315	Arhgap24	0.089875829	0.879877386	0.019240527
ENSMUSG00000037029	Zfp146	0.012900837	-1.289562757	0.019240527
ENSMUSG00000021108	Prkh	0.208993555	0.758019476	0.019240527
ENSMUSG00000066687	Zbtb16	0.007310474	-1.854267689	0.019299967
ENSMUSG00000054256	Msi1	0.089875829	0.914093102	0.019382526
ENSMUSG00000038059	Smim3	0.090735885	-0.813806809	0.020628708
ENSMUSG00000029697	Fezf1	0.030531980	-1.140176561	0.020957802
ENSMUSG00000034227	Foxj1	0.119977781	0.937362881	0.020957802
ENSMUSG00000089682	Bcl2l2	0.289838798	0.706394566	0.021178337
ENSMUSG00000062760	Shisa1	0.477330958	0.696435182	0.021464251
ENSMUSG00000028298	Cga	0.279948156	3.104969087	0.021546318
ENSMUSG00000029516	Cit	0.675573815	0.674186717	0.021546318
ENSMUSG00000072847	A530017D24Rik	0.032682120	1.222965044	0.021546318
ENSMUSG00000020799	Tekt1	0.053323458	1.087022034	0.021546318
ENSMUSG00000039004	Bmp6	0.086435606	0.916952756	0.021546318
ENSMUSG00000045394	Epcam	0.026661729	2.557949292	0.021546318
ENSMUSG00000056973	Ces1d	0.076974992	2.750594369	0.022076181
ENSMUSG00000019982	Myb	0.012470809	2.072522464	0.022076181
ENSMUSG00000036962	Cfap221	0.041712705	1.136485523	0.022687762
ENSMUSG00000021647	Cartpt	1.030776852	-0.990996310	0.022773065
ENSMUSG00000039270	Megf9	0.588708181	0.654854709	0.025423807
ENSMUSG00000076609	Igkc	0.038272482	1.299932960	0.025614612
ENSMUSG00000021913	Ogdhl	0.246405981	0.704829952	0.025614612
ENSMUSG00000024897	Apba1	0.485501488	0.658482749	0.026333714
ENSMUSG00000097162	Z310010J17Rik	0.136318841	0.771155692	0.026340188
ENSMUSG00000000303	Cdh1	0.007740502	2.828596881	0.026945868
ENSMUSG00000018569	Cldn7	0.007740502	2.828596881	0.026945868
ENSMUSG00000027134	Lpcat4	0.193082523	0.722025217	0.027030853
ENSMUSG00000070866	Zfp804a	0.141049148	0.766024410	0.027830979
ENSMUSG00000074754	Smim26	0.758999226	0.636751934	0.028126755
ENSMUSG00000032238	Rora	0.904778680	0.653528125	0.028126755
ENSMUSG00000023952	Gtpbp2	0.223614503	0.702931397	0.028410137
ENSMUSG00000023266	Frs3	0.098046359	0.824926567	0.028559214
ENSMUSG00000025316	Banp	0.237375395	-0.668676297	0.029192518
ENSMUSG00000072663	Spef2	0.024511590	1.379756674	0.029331677
ENSMUSG00000046470	Sox18	0.020211311	1.502666856	0.029677311
ENSMUSG00000086915	Gm16364	0.014190920	1.793663091	0.030263119
ENSMUSG00000035517	Tdrd7	0.205123303	0.708946672	0.030708565
ENSMUSG00000097604	Gm17322	0.012900837	-1.220021824	0.030877309
ENSMUSG00000005994	Tyrrp1	0.018491199	1.537600646	0.031556009
ENSMUSG00000021702	Thbs4	0.057193709	1.123196602	0.031584390
ENSMUSG00000032303	Chrna3	0.124278060	1.126372438	0.031875879
ENSMUSG00000048416	Mlf1	0.076544964	0.962947119	0.033378606
ENSMUSG00000052539	Magi3	0.075254881	0.870175985	0.033378606
ENSMUSG00000052861	Dnah6	0.034402231	1.147929867	0.033378606
ENSMUSG00000063594	Gng8	0.236945367	0.869014862	0.033378606
ENSMUSG000000108634	Gm38534	0.034402231	1.147929867	0.033378606
ENSMUSG00000001506	Col1a1	0.042142733	1.122563147	0.033378606
ENSMUSG00000020723	Cacng4	0.272207654	0.673070999	0.034156833
ENSMUSG00000056586	Zar1l	0.017201116	1.616293278	0.034805932

ENSMUSG00000020262	Adarb1	1.517998451	0.622818047	0.034877722
ENSMUSG00000009210	Prrr29	0.019781283	1.472293207	0.035448991
ENSMUSG00000043448	Gjc2	0.224904586	0.743727650	0.035505279
ENSMUSG00000002831	Plin4	0.050313263	-0.888363021	0.037077546
ENSMUSG00000072473	1700024G13Rik	0.038272482	1.372082746	0.037247818
ENSMUSG00000010825	Grid2ip	0.032682120	1.147016191	0.038073646
<b>ENSMUSG00000055116</b>	<b>Arntl</b>	<b>0.202113108</b>	<b>0.692068293</b>	<b>0.038073646</b>
ENSMUSG00000039720	Got11l	0.023651534	1.329130601	0.038073646
ENSMUSG00000043102	Qrfp	0.001290084	-2.692349126	0.038088520
ENSMUSG00000035681	Kcnc2	0.986914007	0.622317065	0.038088520
ENSMUSG00000037254	Itih2	0.030531980	1.248094029	0.039178203
ENSMUSG00000072647	Adam1a	0.030962008	1.185531426	0.039178203
ENSMUSG00000039391	Ccdc81	0.021071367	1.417170636	0.039178203
ENSMUSG00000040624	Plekhhg1	0.406806384	0.675641954	0.039178203
ENSMUSG00000061544	Zfp229	0.021071367	1.417170636	0.039178203
ENSMUSG000000066196	Spag8	0.038272482	1.072522464	0.039520335
ENSMUSG00000015312	Gadd45b	0.110517168	-0.705783925	0.039996040
ENSMUSG00000048583	Igf2	0.327681252	0.789886401	0.040542870
ENSMUSG00000045690	Wdr89	0.097186303	0.792508011	0.041007052
ENSMUSG00000070529	Wfdc10	0.006020390	3.072522464	0.041202915
ENSMUSG00000032637	Atxn2l	0.246836009	0.664165030	0.043307561
ENSMUSG00000025491	Ifftm1	0.070524574	-0.816774071	0.043307561
ENSMUSG00000063550	Nup98	0.071814658	0.857509573	0.044210103
ENSMUSG00000015305	Sash1	0.392185436	0.638159145	0.044214564
ENSMUSG00000046711	Hmga1	0.218024140	-0.644965066	0.044244736
ENSMUSG00000052974	Cyp2f2	0.033972203	3.317634962	0.045067397
ENSMUSG00000037946	Fgd3	0.036552371	1.068334667	0.045067397
ENSMUSG00000079666	1700015F17Rik	0.001720112	-2.212879755	0.045208708
ENSMUSG00000066113	Adamts1l	0.039992594	1.076364531	0.045961216
ENSMUSG00000037206	Islr	0.055473598	1.038252562	0.045961216
ENSMUSG00000035383	Pmch	9.937084481	-1.002814865	0.045961216
ENSMUSG00000071753	Cdr1os	0.394335575	-0.646653816	0.045961216
ENSMUSG00000075703	Selenoi	0.160400403	0.735246405	0.047574068
ENSMUSG00000022194	Pabpn1	0.284248435	-0.626072053	0.047625599
ENSMUSG00000056888	Glipr1	0.015911032	-1.110002574	0.049158967
ENSMUSG00000042743	Sgtb	0.022791478	-0.986371225	0.049388605
ENSMUSG00000044748	Defb1	0.040852650	1.258741273	0.049652643















TOTAL PHOSPHO-EPHA4 PROTEIN (females)								
Thalamus/Hypo	Female	Total protein phospho-EphA4						
	Sample	Actin	Peak 1+2	Peak 1+2/A	Peak 1+2	Peak 1+2	Norm Tot	Saline
	526	2752.527	3973.912	1.4437323	1.62976	1.225383		
	<b>538</b>	<b>3014.234</b>	<b>3143.154</b>	<b>1.0427704</b>	<b>1.177133</b>	<b>0.885062</b>	Average Peak 1 + 2 Thalamus No	
	<b>757</b>	<b>3486.648</b>	<b>2392.841</b>	<b>0.6862869</b>	<b>0.774716</b>	<b>0.582493</b>	<b>Saline</b>	<b>50 100</b>
							1.177133	
	<b>771</b>	<b>4099.477</b>	-	-	-	-	<b>stripe on p</b>	0.774716
	CTRL	5968.548	5287.276	0.8858563	1	0.75188		1.478614
	649	3606.648	3990.518	1.106434	1.249	0.939098		1.773615
	715	3091.82	2671.376	0.8640141	0.975344	0.733341		0.762833
	<b>716</b>	<b>3411.648</b>	<b>4468.711</b>	<b>1.3098394</b>	<b>1.478614</b>	<b>1.11174</b>		2.018962
							<b>Norm Tot</b>	<b>Saline 1.331</b>
	36	2775.184	2740.468	0.9874906	1.341699	1.008796		
	<b>3</b>	<b>2087.577</b>	<b>2725.083</b>	<b>1.3053808</b>	<b>1.773615</b>	<b>1.333545</b>	Average Peak 1+2 Thalamus No	
	34	2622.284	1973.669	0.7526526	1.022626	0.768892	Females	
	<b>78</b>	<b>2034.284</b>	<b>2125.255</b>	<b>1.0447189</b>	<b>1.419455</b>	<b>1.067259</b>	<b>spot on p</b>	<b>Saline 50 100</b>
	CTRL	4305.284	3169.962	0.7362957	1.000402	0.752182	0.885062	1.225383 0.939098
	<b>42</b>	-	-	-	-	-	<b>stripe on p</b>	0.582493 0.733341 0.768892
	<b>44</b>	<b>2233.113</b>	<b>1253.77</b>	<b>0.5614449</b>	<b>0.762833</b>	<b>0.573558</b>		1.11174 1.008796 <b>0.92927</b>
	400	3056.355	1490.648	0.4877208	0.662664	0.498244	1.333545	0.498244 <b>1.394009</b>
							0.573558	2.040355 0.884978
	<b>134</b>	<b>2524.719</b>	-	-	-	-	<b>stripe on p</b>	1.514689 1.517899 0.901278
	<b>133</b>	<b>1964.305</b>	-	-	-	-	<b>spot on pEphA4 band</b>	
	61	3528.941	4787.64	1.356679	2.719886	2.045027		
	<b>277</b>	<b>2552.598</b>	-	-	-	-	<b>spot on pEphA4 band</b>	
	CTRL	6166.598	3076.184	0.4988462	1.000093	0.751949		
	104	2906.527	1802.012	0.619988	1.242959	0.934556	repeated, average was done	
	-	-	-	-	-	-	not a total thalamus sample	
	771	3053.406	2183.669	0.7151584	1.433758	1.078013	repeated, average was done	
	130	2755.648	2568.761	0.9321804	1.868846	1.405147		
							<b>Norm Tot</b>	<b>Saline</b>
	104	3029.406	1980.548	0.6537744	1.228899	0.923984	repeated earlier, average was done	
	277	3242.698	2030.497	0.6261752	1.177021	0.884978		
	CTRL	4463.82	2374.568	0.5319587	0.999922	0.751821		
	134	2818.113	1797.134	0.6377083	1.1987	0.901278		
	771	2387.991	2889.305	1.2099313	2.274307	1.710005	repeated earlier, average was done	
	<b>133</b>	<b>2049.577</b>	<b>2201.255</b>	<b>1.0740045</b>	<b>2.018806</b>	<b>1.517899</b>		

SYNAPTONEUROSOMAL PHOSPHO-EPHA4 PROTEIN (females)													
Thalam/Hypo	Female	SYNAPTONEUROSOMAL protein phospho-EphA4							Average Peak 1+2 Thalamus No				
	Sample	Actin	Peak 1+2	Peak 1+2/A	Peak 1+2	Peak 1+2	Norm Tot	Saline	Females				
	130	4493.891	2250.497	0.50079	0.856301	0.643835			Average Peak 1 + 2 Thalamus No				
	<b>133</b>	<b>4188.648</b>	<b>4492.539</b>	<b>1.072551</b>	<b>1.833954</b>	<b>1.378912</b>		<b>Saline</b>	<b>50</b>	<b>100</b>			
	134	3742.062	3144.589	0.840336	1.436889	1.080368		1.378912	0.643835	1.080368			
	<b>277</b>	<b>4163.406</b>	<b>5814.368</b>	-	-	-	<b>spot on pE</b>	1.443586	1.454439	1.433768			
	CTRL	5077.648	2969.539	0.584826	0.999993	0.751874		1.515456	1.414136	1.030988			
	<b>66</b>	<b>3677.82</b>	<b>4129.66</b>	<b>1.122855</b>	<b>1.919969</b>	<b>1.443586</b>		1.353343	2.365905	1.302683			
	104	4105.77	4578.832	1.115219	1.906911	1.433768		1.535678	1.620729	1.336457			
	<b>61</b>	-	<b>5857.589</b>	-	-	-	<b>damaged actin</b>	2.895563	1.319056	1.281767			
							<b>Norm Tot</b>	<b>Saline</b>					
	526	2909.648	4263.539	1.465311	1.934404	1.454439							
	<b>538</b>	<b>4052.82</b>	<b>6187.782</b>	<b>1.526784</b>	<b>2.015557</b>	<b>1.515456</b>	Average Peak 1+2 Thalamus No						
	<b>757</b>	<b>3249.698</b>	<b>4430.832</b>	<b>1.36346</b>	<b>1.799947</b>	<b>1.353343</b>	Females						
	771	3576.891	3715.296	1.038694	1.371213	1.030988							
	CTRL	3852.87	2918.569	0.757505	1.000007	0.751885							
	649	3586.991	4707.64	1.31242	1.732568	1.302683							
	715	3546.406	5052.589	1.424707	1.880801	1.414136							
	<b>716</b>	<b>2799.284</b>	<b>4330.933</b>	<b>1.547157</b>	<b>2.042452</b>	<b>1.535678</b>							
							<b>Sample</b>	<b>Actin</b>	<b>Peak 1+2</b>	<b>Peak 1+2/A</b>	<b>Peak 1+2</b>	<b>Norm Tot</b>	<b>Saline</b>
	36	3751.598	5253.217	1.400261	3.146654	2.365905							
	<b>3</b>	<b>4630.012</b>	<b>7934.631</b>	<b>1.713739</b>	<b>3.851098</b>	<b>2.895563</b>	Average Peak 1+2 Thalamus No						
	34	3625.598	2867.782	0.790982	1.777487	1.336457	Females						
	78	2557.648	2453.368	0.959228	2.155569	1.620729							
	CTRL	5878.134	2617.489	0.445293	1.000657	0.752374							
	42	3637.062	2759.125	0.758614	1.70475	1.281767							
	<b>44</b>	<b>2921.355</b>	-	-	-	-	<b>spot on pEphA band</b>						
	400	3941.891	3077.368	0.780683	1.754344	1.319056							

Cortex		Total protein phospho-EphA4						Average Cortex peak 1+2			Cortex		SYNAPTONEUROSOMAL protein phospho-EphA4						Average Peak 1+2 Cortex Normal						
2021-10-22	Male	Sample	Actin	Peak 1+2	Peak 1+2/Actin	Peak 1+2 Nor	Norm Tot	Saline	50	100	2020-10-30	Male	Sample	Actin	Peak 1+2	Peak 1+2/Actin	Peak 1+2 Nor	Norm Tot	Saline	50	100	Saline	50	100	
			215	2801.284	3241.409	1.157115	0.737016211	1.188736	0.626796						215	4662.527	3808.711	0.816877	3.713077206	5.988834			5.24654046		
			100	3651.406	4480.581	1.227084	0.781582012	1.260616	0.611162						100	4226.527	1987.912	0.4703417	2.137916932	3.448253			3.44825312		
			954	3993.82	3930.196	0.984069	0.626795788	1.010961	0.516634						954	4593.355	3287.134	0.7156281	3.252855088	5.24654			5.26703076		
			129	4199.527	4178.51	0.994995	0.633755025	1.022186	0.731628						129	4476.406	2291.527	0.5119122	2.326873795	3.753022			2.92379156		
			137	3226.042	4096.933	1.269956	0.808889489	1.30466	0.43985						137	3939.113	4483.841	1.138287	5.17403168	8.345212			4.1200492		
			CTRL	4409.82	6931.995	1.571945	1.001238926	1.614901	0.877862						CTRL	4821.527	1067.82	0.2214693	1.006678439	1.623675			2.41918721		
			958	3167.577	3039.367	0.959524	0.611161954	0.985745	0.537029						958	4619.113	3318.477	0.718423	3.265559072	5.267031			3.129		
			138	4102.698	3800.125	0.92625	0.589968305	0.951562	0.620137						138	3935.527	2774.477	0.7049823	3.204465143	5.168492			4.230		
			2021-10-22	Sample	Actin	Peak 1+2	Peak 1+2/Actin	Peak 1+2 Nor	Norm Tot	Saline	50	100	2020-11-04	Sample	Actin	Peak 1+2	Peak 1+2/Actin	Peak 1+2 Nor	Norm Tot	Saline	50	100	Saline	50	100
			801	3529.527	2045.861	0.579642	0.356838727	0.575546	0.620137						535	3703.577	1546.69	0.4176206	1.291803167	2.083553			1.91594164		
			720	2736.991	2296.912	0.839211	0.51663444	0.833281	Normalized Peak 1 +2 Cortex						59	3127.456	2504.154	0.8007	2.476761971	3.994777					
			766	3163.749	2943.861	0.930498	0.572832494	0.923923	Saline						71	3528.698	2067.941	0.5860351	1.812750769	2.923792					
			768	3184.991	2976.397	0.934507	0.575300849	0.927905	1.010961						CTRL	3991.545	1290.406	0.3232848	0.999999474	1.612902					
			CTRL	3043.87	4944.397	1.624379	0.999999908	1.612902	0.985745						860	2862.87	2364.184	0.8258091	2.554430505	4.120049					
			763	3051.284	3626.276	1.188443	0.731628459	1.180046	0.833281						74	3211.456	3089.841	0.9621309	2.97610741	4.800173					
			767	2770.577	3086.326	1.113965	0.685778617	1.106095	1.180046						72	4194.991	2150.87	0.5127234	1.585979518	2.558031					
			779	2695.284	2467.154	0.91536	0.563513198	0.908892	0.709436						891	4552.598	2207.527	0.4848939	1.499896067	2.419187					
			2020-11-04	Sample	Actin	Peak 1+2	Peak 1+2/Actin	Peak 1+2 Nor	Norm Tot	Saline	50	100	2021-07-28	Sample	Actin	Peak 1+2	Peak 1+2/Actin	Peak 1+2 Nor	Norm Tot	Saline	50	100	Saline	50	100
			535	2816.213	1866.74	0.662855	0.439850492	0.709436	1.415907						801	4395.841	4022.711	0.9151175	1.994	3.216					
			59	2474.385	2821.225	1.140172	0.756584077	1.220297	0.866176						720	4630.941	4122.074	0.8901159	1.940	3.129					
			71	2375.213	2829.225	1.191146	0.790408629	1.274853	1.454707						766	4538.991	3970.246	0.8746979	1.906	3.074					
			CTRL	3161.749	4764.761	1.507002	1.000001103	1.612905							768	3838.577	3549.64	0.9247281	2.015	3.250			Stripe on pEphA4		
			860	2545.042	3366.933	1.322938	0.877862037	1.415907							763	4567.577	5496.853	1.2034505	2.623	4.230					
			74	2625.042	3567.933	1.359191	0.901918264	1.454707							767	4785.991	2608.882	0.545108	1.188	1.916					
			72	3414.406	2745.811	0.804184	0.533632445	0.860697							779	4009.163	2816.296	0.7024648	1.531	2.469					
			891	3960.991	3205.64	0.809303	0.537028879	0.866176							CTRL	4742.406	2176.225	0.4588863	1.000	1.61289					

Cortex Female Total protein phospho-EphA4							Average Cortex Female			Cortex Female SYNAPTONEUROSOMAL protein phospho-EphA4							Average Peak 1+2 Cortex Norm Female		
Sample	Actin	Peak 1+2	Peak 1+2/A	Peak 1+2	Norm Tot	Saline	Saline	50	100	Sample	Actin	Peak 1+2	Peak 1+2/A	Peak 1+2	Norm Tot	Saline	Saline	50	100
526	3229.426	3895.539	1.2062636	0.78365	0.462058					803	2709.941	2410.518	0.889509	2.328924	1.373187				
538	3467.841	5257.368	1.5160349	0.984893	0.580715	0.984893				78	2705.82	2071.033	0.765399	2.003978	1.181591	1.373187	1.181591	1.623906	
539	4211.083	5175.953	1.2291263	0.798503	0.470815	0.927221				76	4357.527	4583.761	1.051918	2.754145	1.623906	1.289189	1.503174	0.953288	
61	3751.062	4573.539	1.2192651	0.792096	0.467038	1.160017				130	-	3388.154	-	-	-	1.439603	0.815322	1.051491	
CTRL	3398.941	5231.953	1.5392891	1	0.589623	1.29505				CTRL	3012.991	1150.791	0.381943	1.000008	0.589627	1.2759	0.495901	1.242743	
66	3539.527	5051.832	1.4272619	0.927222	0.546711	2.341858				133	3905.113	3261.154	0.835098	2.186465	1.289189	1.474604		1.181037	
104	3536.941	5459.61	1.5435966	1.002798	0.591273	2.698176				277	3482.163	2150.276	0.617512	1.616776	0.953288	0.785675		1.222331	
650	-	-	-	-	-	2.464515	spot on ac			716	3639.113	3393.59	0.932532	2.441567	1.439603	1.913455		2.1534	
649	3708.184	5249.711	-	-	-	1.696	Part of ac			Sample	Actin	Peak 1+2	Peak 1+2/A	Peak 1+2	Norm Tot	Saline			
803	3198.941	4732.417	1.4793699	1.160108	0.684026	1.592701				3	3024.82	3877.417	1.281867	2.163927	1.2759				
78	2416.698	3511.518	1.4530231	1.139447	0.671844	1.454774				44	4026.062	5964.611	1.4815	2.500929	1.474604				
76	4159.698	7329.439	1.7620123	1.381754	0.814713	0.671844				34	3189.113	3369.004	1.056408	1.783328	1.051491				
130	3897.527	5755.246	1.4766404	1.157968	0.682764	0.580715	0.462058	0.470815		399	4023.234	6075.904	1.510204	2.549384	1.503174				
CTRL	3899.991	4973.661	1.2753006	1.000079	0.589669	0.546711	0.467038	0.591273		CTRL	3312.527	1962.275	0.59238	1	0.589623				
133	3743.577	6012.146	1.6059897	1.259402	0.742572	0.684026	0.671844	0.814713		771	4561.648	5695.468	1.248555	2.107693	1.242743				
277	3718.406	4484.782	1.2061034	0.945815	0.557674	0.742572	0.682764	0.557674		757	3503.234	2765.276	0.789349	1.332505	0.785675				
716	-	-	-	-	-	1.382371	1.131553	1.043724	Part of ac	42	4627.062	-	-	-	-	1.382786	0.815322		Part of actin lost at the end of the gel
3	4266.991	3451.368	0.8088529	2.344501	1.382371	1.592701	0.760157			Sample	Actin	Peak 1+2	Peak 1+2/A	Peak 1+2	Norm Tot	Saline			
44	3470.698	3234.418	0.9319215	2.701222	1.592701	1.454774				538	2098.577	1953.275	0.930762	3.24522	1.913455				
34	2739.749	1673.175	0.6107038	1.770156	1.043724					526	2918.749	704.063	0.241221	0.841047	0.495901				
399	3831.527	2536.832	0.6620943	1.919114	1.131553					539	2515.749	1445.276	0.574491	2.003038	1.181037				
CTRL	4354.719	1504.074	0.3453894	1.001129	0.590288					104	2989.799	1777.669	0.594578	2.073073	1.222331				
771	4798.669	2134.368	0.4447833	1.289227	0.760157					CTRL 104	2996.92	859.548	0.28681	1.000002	0.589624				
757	4148.548	3531.317	0.8512176	2.467297	1.454774					61	2980.627	-	-	-	-	1.382786	0.815322		spot on pEphA band
400	3556.154	3537.781	0.9948335	2.883575	1.700221	spot on actin				66	2844.749	1815.326	0.638132	2.22493	1.311869				
42	2884.861	5403.853	1.8731762	5.429496	3.201354	Part of actin lost at the end of the gel				725	3693.406	3868.761	1.047478	3.652166	2.1534				
										715	3853.062	-	-	-	-				damaged pEphA4 band

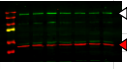
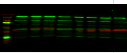




TOTAL NR2B PROTEIN (males)											
Thalamus/Hypothal	Male	TOTAL protein NR2B				Average Thalamus					
2020-08-21	Sample	Actin	NR2B	NR2B/Actin	Norm NR2B	Norm to TotalSaline	Male				
							Saline	50	100		
	535	3941.598	1451.163	0.36816616	0.58718686	1.260844987					
	497	4026.255	1680.163	0.41730169	0.66555293	1.4291176	0.58718686				
	557	4097.234	1412.749	0.34480554	0.5499291	1.180842754	0.4679883				
	CTRL	7071.962	4436.648	0.62735744	1.00057009	2.148487758	0.45036937				
	553	4441.083	1302.335	0.29324717	0.4679883	1.004272685	0.56364106				
	552	4632.719	1429.698	0.30860883	0.49219909	1.056881216	0.3980669				
	679	4086.305	1730.577	0.42350657	0.6754907	1.450367224	0.382				
	556	3582.305	1011.577	0.2823816	0.45036937	0.967061771	0.411				
	2020-08-22	Sample	Actin	NR2B	NR2B/Actin	Norm NR2B	Norm to TotalSaline	0.465708			
		766	3990.891	721.213	0.18071478	0.34487554	0.740538705				
		768	3547.305	818.335	0.23069203	0.44025197	0.945337046				
		647	3666.012	1082.749	0.29534791	0.56364106	1.210285949	Average Thalamus - norm to saline			
		767	3264.477	370.556	0.1135116	0.21662519	0.465151385	Male			
		779	4422.841	767.213	0.1734661	0.33104218	0.710834844	Saline			
		CTRL	6136.962	3212.991	0.52354748	0.99913642	2.145409291	50			
		720	4015.719	837.627	0.20858706	0.3980669	0.854754576	100			
		861	4733.598	763.213	0.16123317	0.30769688	0.660706331	1.26084499			
		2020-08-25	Sample	Actin	NR2B	NR2B/Actin	Norm NR2B	Norm to TotalSaline	1.4291176		
		763	3677.891	667.385	0.18145861	0.38201813	0.820293644	1.18084275			
		801	3927.477	639.092	0.1627233	0.34257536	0.73559961	1.45036722			
		954	3851.012	644.385	0.16732874	0.35227104	0.756418792	0.94533705			
		CTRL	6087.548	2892.577	0.47516291	1.00034296	2.14800062	0.85475458			
		851	4428.012	863.92	0.19510336	0.41074391	0.881975454	0.73559961			
		858	2358.698	261.092	0.11069327	0.23303847	0.500395028	0.66070633			
		74	4347.426	792.335	0.18225382	0.38369225	0.823888425	0.82029364			
		Synaptoneurosomal	74	-	2075.163			0.75641879			

SYNAPTONEUROSONAL NR2B PROTEIN (males)											
Thalamus/Hypothal	Male	SYNAPTONEUROSONAL protein NR2B				Average Thalamus NormTotSal					
2020-08-21	Sample	Actin	NR2B	NR2B/Actin	Norm NR2B	Norm to TotalSaline	Male				
							Saline	50	100		
	535	4265.669	2604.355	0.610538464	1.16293	2.49711817					
	497	4022.134	2874.234	0.714604237	1.361151	2.92274989	2.49711817				
	557	4989.184	2411.234	0.483292258	0.920557	1.97667789	1.74153716				
	CTRL	6070.841	3188.113	0.525151787	1.000289	2.14788445	1.8533627				
	553	5483.477	2334.87	0.425801002	0.81105	1.74153716	2.35160998				
	552	4420.012	1800.577	0.407369256	0.775941	1.66615084	2.13570243				
	679	5060.477	2691.527	0.531872193	1.01309	2.17537108	1.8185927				
	556	4883.012	2212.698	0.453142036	0.863128	1.8533627	2.26886526				
	2020-08-22	Sample	Actin	NR2B	NR2B/Actin	Norm NR2B	Norm to TotalSaline	1.84709737			
		766	4209.012	2191.941	0.520773284	1.082689	2.32481816				
		768	4074.184	1953.577	0.479501417	0.996884	2.14057371				
		647	4842.891	2551.113	0.526774813	1.095166	2.35160998	Average Thalamus - norm to saline			
		767	4496.134	1123.749	0.249936723	0.519619	1.11575891	Male			
		779	4262.719	1526.577	0.358122832	0.744538	1.59871961	Saline			
		CTRL	6733.255	3239.113	0.481061983	1.000129	2.14754034	50			
		720	4861.305	2325.698	0.478410221	0.994616	2.13570243	100			
		861	3652.255	1688.991	0.462451554	0.961438	2.0644603	1.26084499			
		2020-08-25	Sample	Actin	NR2B	NR2B/Actin	Norm NR2B	Norm to TotalSaline	1.4291176		
		763	7245.912	1583.577	0.218547645	0.643544	1.38185927	1.18084275			
		801	6638.205	1835.577	0.276517071	0.814243	1.74839532	1.45036722			
		954	7353.912	1597.749	0.217265178	0.639768	1.37375034	0.94533705			
		CTRL	9441.276	3206.284	0.339602825	1.000008	2.1472815	0.85475458			
		851	6183.255	2218.749	0.358831877	1.056631	2.26886526	0.73559961			
		858	9562.589	2869.991	0.300126984	0.883766	1.89767891	0.66070633			
		71	9277.004	3454.062	0.37232516	1.096364	2.3541822	Part of actin lost at the end of the gel			
		CTRL	6087.548	2892.577	0.475162906	0.965778	2.07378055	0.82029364			
		74	5078.719	2075.163	0.408599688	0.86021	1.84709737	0.75641879			



Cortex	Male	TOTAL protein NR2B					Average Cortex			Cortex	Male	SYNAPTONEUROSOMAL protein NR2B					Average Cortex - normalized to salin		
		2020-10-21	Sample	Actin	NR2B	Norm NR2B Rest	Norm to Saline	Saline	50			100	2020-10-21	Sample	Actin	NR2B	Norm NR2B Rest	Norm to Total Saline	Saline
		556	3371.648	1779.749	0.5278573	0.95281101	0.783699539				556	4500.113	2977.406	0.661629164	1.912223	1.57282849			
		552	3466.113	2179.87	0.6289091	1.13521498	0.933729196	0.95281101			552	4008.991	2909.456	0.72532734	2.097493	1.72521585	1.57282849	1.72521585	1.71606948
		557	2442.284	2657.749	1.08822275	1.96430098	1.615663302	0.56915497			557	4398.698	3175.355	0.721885203	2.086373	1.71606948	2.2339252	1.83460468	1.36606357
		CTRL	3287.749	1822.92	0.55445838	1.00082741	0.823139366	1.12259145			CTRL	5137.941	1779.506	0.346346134	1.001	0.82333594	2.19598441	1.98783332	2.09010487
		647	4768.698	1503.627	0.31531185	0.56915497	0.46813742	1.33089409			647	4280.284	3254.284	0.760296279	2.197388	1.8073805	2.05206827	0.9212117	0.92637312
		646	3303.87	1469.627	0.44481986	0.80292394	0.660415463	0.75787462			646	4996.527	3856.062	0.771748456	2.230487	1.83460468	1.02104178	1.10664526	0.93297454
		679	3088.406	1656.627	0.53640195	0.96823457	0.796385619	1.88034275			679	5073.648	2915.577	0.57465102	1.660841	1.36606357	0.51721173	1.07703279	1.75508949
		535	3007.87	2172.355	0.7222237	1.12259145	0.923346179	1.75889243			535	4941.648	3274.82	0.66269795	2.715975	2.2339252	1.85349516	2.00819785	1.81373166
		59	2502.749	2073.234	0.82838271	1.28759955	1.059067508	1.47619611			59	4282.698	2731.698	0.637845115	2.614119	2.1501474	2.10117606	1.84303525	
		71	2549.042	2104.648	0.82566235	1.28337115	1.055589588	1.32881494			71	5510.82	3404.698	0.617820578	2.532052	2.08264558			1.98087795
		CTRL	3530.9442	2271.648	0.64335426	0.99999994	0.822513056	0.80279909			CTRL	4477.698	1094.163	0.244358373	1.001469	0.82372117			
		860	1988.042	1702.234	0.85623644	1.33089409	1.094677833	1.21578603			860	3809.991	2481.991	0.651442746	2.669847	2.19598441			
		74	2314.042	1685.82	0.72851746	1.13237365	0.931392171			74	4428.406	2611.406	0.589694351	2.41678	1.98783332				
		72	3009.042	2340.477	0.77781467	1.20899894	0.994417472			72	4330.87	2685.284	0.620033388	2.54112	2.09010487				
		891	3804.577	1855.042	0.48758167	0.75787462	0.623361807			891	4891.698	2977.82	0.608749763	2.494876	2.05206827				
		215	5695.276	1744.87	0.30637146	1.57438941	1.294955922			215	4648.113	2501.941	0.538270262	1.119996	0.9212117				
		100	8664.033	2674.234	0.30865926	1.58614603	1.304625893			100	4099.163	2218.82	0.541286111	1.126272	0.92637312				
		954	7082.104	2591.406	0.36590906	1.88034275	1.546606551			954	3839.577	2290.698	0.596601657	1.241368	1.02104178				
		129	9017.569	3665.82	0.40651976	2.08903406	1.718257894			129	4229.406	2734.82	0.646620353	1.345444	1.10664526				
		137	8515.69	2829.113	0.33222358	1.70723895	1.404226409			137	4153.113	2264.042	0.545143366	1.134297	0.93297454				
		CTRL	11094.175	2154.042	0.19415973	0.99775294	0.820664865			CTRL	4758.406	2286.99	0.480621031	1.000044	0.8225491				
		958	8187.225	2802.284	0.34227519	1.75889243	1.446712077			958	4573.113	1382.042	0.302210332	0.628819	0.51721173				
		138	7812.054	1987.92	0.25446829	1.30766809	1.07557414			138	4485.991	2823.113	0.62931758	1.309441	1.07703279				
		801	6012.477	3083.234	0.51280595	1.62075206	1.333089813			801	5453.477	3301.477	0.605389369	2.441539	2.00819785				
		720	4390.941	2050.87	0.46706845	1.47619611	1.214190644			720	5133.062	2868.113	0.558752846	2.253454	1.85349516				
		766	5471.355	2806.698	0.51298042	1.62130348	1.333543363			766	4749.062	2638.577	0.555599611	2.240737	1.84303525				
		768	5543.355	3249.991	0.58628592	1.85298964	1.524108263			768	5141.234	2720.163	0.529087569	2.133813	1.75508949				
		CTRL	7185.305	2273.456	0.31640355	1.00001122	0.82252233			CTRL	6031.184	1495.456	0.247953967	1	0.822513				
		763	6389.891	2816.87	0.44083225	1.39327511	1.145987039			763	5058.062	3203.87	0.633418491	2.554581	2.10117606				
		767	5978.77	2278.991	0.38118058	1.20474266	0.990916625			767	4618.648	2758.042	0.597153539	2.408324	1.98087795				
		553	-	-	-	-	-			553	-	-	-	-	-				
		497	4258.527	2846.577	0.66844169	1.75582268	1.444187163			497	4258.527	2846.577	0.66844169	1.75582268	1.444187163				
		570	4017.698	2049.456	0.51010703	1.33991865	1.102100652			570	4017.698	2049.456	0.51010703	1.33991865	1.102100652				
		CTRL	5879.698	2238.627	0.38073843	1.00010095	0.822596139			CTRL	5879.698	2238.627	0.38073843	1.00010095	0.822596139				
		959	4923.598	2490.749	0.50587985	1.32881494	1.092967699			959	4923.598	2490.749	0.50587985	1.32881494	1.092967699				
		779	4277.991	2613.577	0.6109356	1.60476911	1.319943624			779	4277.991	2613.577	0.6109356	1.60476911	1.319943624				
		997	4428.477	1353.456	0.30562561	0.80279909	0.660312772			997	4428.477	1353.456	0.30562561	0.80279909	0.660312772				



Cortex		Female						TOTAL protein NR2B			Average Cortex		
Sample	Actin	NR2B	NR2B/Actin	Norm NR2B	Rest	Norm to Saline	Saline	50	100	Saline	50	100	
526	4688.598	4016.255	0.85660042	1.22739707	-	0.92285494							
538	4917.891	-	-	-	-	-	1.34706134						
539	5351.012	3392.012	0.63390103	0.90829779	0.68293067	-	1.28318163						
61	4757.477	-	-	-	-	-	0.88622375						
CTRL	5256.184	3668.548	0.69794893	1.00007011	0.75193241	-	2.05625533						
66	3657.456	3438.426	0.94011411	1.34706134	1.01282808	-	1.85591623						
104	4156.406	3058.548	0.73586363	1.05439695	0.79277966	-	1.30039799						
649	4364.477	2993.255	0.68582215	0.98269401	0.73886768	-	1.02505942						
650	3730.891	3341.134	0.89553246	1.28318163	0.96479822	-	0.94379257						
Sample	Actin	NR2B	NR2B/Actin	Norm NR2B	Norm to TotalSaline		1.33723603						
803	-	-	-	-	-	-	damaged actin						
78	-	-	-	-	-	-	damaged actin						
76	3720.234	3079.305	0.8277181	1.00238704	0.75367447	-	Average Cortex - normalized to saline						
133	3327.113	2434.77	0.73179661	0.88622375	0.66633365	-	Females						
CTRL	4560.941	3766.184	0.82574714	1.00000017	0.75187983	-	Saline	50	100				
130	3166.82	1764.234	0.55709955	0.67466131	0.50726414	-	1.01282808	0.92285494	0.68293067				
277	2895.698	2587.891	0.89370197	1.08229514	0.81375575	-	0.96479822	0.50726414	0.79277966				
715	2514.991	1980.77	0.78758532	0.95378527	0.71713178	-	0.66633365	0.71713178	0.73886768				
716	-	-	-	-	-	-	1.54605664	0.96925832	0.75367447				
Sample	Actin	NR2B	NR2B/Actin	Norm NR2B	Norm to TotalSaline		1.39542574	1.13121281	0.81375575				
3	3910.234	2524.698	0.64566417	2.05625533	1.54605664	-	0.97774285	1.23266552	1.43532285				
36	3855.355	1560.577	0.40478166	1.28911357	0.96925832	-	0.77072137	0.96790072	1.21906676				
34	3837.234	2300.113	0.59941953	1.90897939	1.43532285	-	0.70961847		0.89691058				
44	4076.648	2375.698	0.5827577	1.85591623	1.39542574	-			1.06172886				
CTRL	5584.376	1754.113	0.31411083	1.00035297	0.75214509	-							
400	5575.205	3198.82	0.57375827	1.82725565	1.37387643	-							
42	4698.648	2392.113	0.50910666	1.6213588	1.21906676	-							
399	4924.598	2535.113	0.51478578	1.63944514	1.23266552	-							
771	4212.698	1577.941	0.37456779	1.19289107	0.89691058	-							
Sample	Actin	NR2B	NR2B/Actin	Norm NR2B	Norm to TotalSaline								
803	2591.87	2455.719	0.94746997	1.30039799	0.97774285	-							
716	3483.456	2601.648	0.74685829	1.02505942	0.77072137	-							
776	4044.991	2781.527	0.68764727	0.94379257	0.70961847	-							
78	1618.627	1518.163	0.93793258	1.28730796	0.96790072	-							
CTRL	3959.698	2885.113	0.72861946	1.0000267	0.75189978	-							
725	3467.991	3568.062	1.02885561	1.41209938	1.06172886	-							
400	3306.406	2846.941	0.86103794	1.18177043	0.8885492	-							
repeated earlier, so average was done													

Cortex		Female						SYNAPTONEUROSOMAL protein NR2B			Average Cortex - normalized to saline		
Sample	Actin	NR2B	NR2B/Actin	Norm NR2B	Rest	Norm to Saline	Saline	50	100	Saline	50	100	
526	3869.891	-	-	-	-	-				stripe on NR			
538	4411.719	-	-	-	-	-				stripe on NR			
539	4584.891	2970.113	0.6478045	1.59165724	1.19673476	-				1.16109203	2.97413408	1.19673476	
61	4536.376	-	-	-	-	-				1.11972868	1.49832503	1.11111311	
CTRL	4592.062	1870.163	0.40725996	1.00063873	0.75235995	-				1.53696877	2.15780447	1.36263311	
66	3914.113	2460.062	0.62851073	1.5442524	1.16109203	-				1.87650087	3.32540632	1.5582217	
104	3714.991	2234.406	0.60145664	1.47778044	1.11111311	-				2.0487869	1.81600751	1.32905624	
649	4291.598	1785.991	0.4161599	1.0225059	0.76880143	-				2.41480037	2.80659606	3.77769248	
650	-	2867.527	-	-	-	-				all damaged			
Sample	Actin	NR2B	NR2B/Actin	Norm NR2B	Norm to TotalSaline								
78	3590.527	2816.527	0.78443276	3.42547056	2.57554178	-				repeated later, so average was done			
803	3491.062	1190.577	0.34103577	1.48923915	1.11972868	-							
76	5495.548	3324.82	0.60500245	2.64193209	1.98641511	-							
130	4316.891	1969.991	0.45634486	1.9927723	1.49832503	-							
CTRL	4754.77	1089.042	0.22904199	1.00018338	0.75201758	-							
133	4635.598	2169.991	0.46811458	2.04416846	1.53696877	-							
277	3607.941	1712.284	0.47458758	2.07243486	1.5582217	-							
715	3699.184	2431.113	0.65720251	2.86987994	2.15780447	-							
716	-	2754.527	-	-	-	-				Part of actin lost at the end of the gel			
Sample	Actin	NR2B	NR2B/Actin	Norm NR2B	Norm to TotalSaline								
650	2616.598	1324.577	0.50622105	2.06649264	1.55375386	-							
61	2941.406	919.042	0.3124499	1.27548114	0.95900838	-							
649	3293.577	1426.163	0.43301341	1.76764481	1.32905624	-				repeated later, so average was done			
716	3122.941	1909.284	0.6113737	2.49574616	1.87650087	-							
CTRL	4441.598	1088.042	0.24496634	1.00000016	0.75187982	-							
78	2563.577	2816.991	1.09885172	4.48572608	3.37272638	-				repeated earlier, so average was done			
725	2415.749	2973.284	1.23079178	5.024331	3.77769248	-							
526	2633.284	2852.991	1.0834346	4.4227904	3.32540632	-							
757	-	-	-	-	-	-				damaged actin			
Sample	Actin	NR2B	NR2B/Actin	Norm NR2B	Norm to TotalSaline								
3	3777.355	2630.82	0.69647147	2.72488658	2.0487869	-							
42	3535.698	3360.527	0.95045646	3.71858167	2.79592606	-							
400	3907.941	2412.527	0.61733967	2.41528999	1.81600751	-							
36	3821.406	3645.941	0.95408365	3.73277276	2.80659606	-							
CTRL	4086.82	1044.577	0.25559653	1.00000011	0.75187978	-							
771	4304.698	2251.113	0.52294331	2.04597209	1.53832488	-							
757	3507.284	2879.113	0.82089531	3.21168449	2.41480037	-							
34	3632.284	2653.82	0.73062018	2.85849056	2.14924102	-							
649	3305.698	1568.991	0.47463229	1.85695926	1.39620997	-				repeated earlier, so average was done			



TOTAL GLUR1 PROTEIN (males)									
Thalamus/Hypot	Male	Total protein GluR1					Average Thalamus		
2020-08-29	Sample	Actin	GluR1	GluR1/Actir	Norm Glur	Norm toTotalSaline	Male		
							Saline	50	100
	535	8423.933	706.355	0.083851	0.1621876	0.687235			
	497	6770.64	727.284	0.1074173	0.2077704	0.880383			0.162188
	557	6500.276	702.941	0.1081402	0.2091686	0.886308			0.223725
	CTRL	9678.518	5004.083	0.5170299	1.0000578	4.237533			0.159728
	553	6271.569	725.406	0.1156658	0.2237249	0.947987			0.167932
	552	6668.861	413.627	0.0620236	0.1199683	0.50834			0.375211
	679	6682.983	857.648	0.1283331	0.2482265	1.051807			0.185711
	556	7145.154	590.042	0.0825793	0.1597279	0.676813			0.37625
2020-09-01	Sample	Actin	GluR1	GluR1/Actir	Norm Glur	Norm toTotalSaline	0.235821		
	766	3629.134	1066.64	0.2939103	0.455322	1.92933	Average Thalamus NormTotSal		
	768	3711.648	349.719	0.094222	0.1459675	0.618506	Male		
	647	4018.426	435.598	0.1084002	0.1679321	0.711577	Saline 50 100		
	767	4180.355	844.912	0.2021149	0.3131137	1.326753			
	779	5196.891	1107.569	0.2131215	0.3301649	1.399004	0.687235	0.880383	0.886308
	CTRL	5892.891	3803.912	0.6455086	1.0000134	4.237345	0.947987	0.50834	0.618506
	720	3777.234	914.841	0.2421987	0.3752109	1.589877	0.676813	1.92933	1.399004
	861	3397.406	745.841	0.2195325	0.3400968	1.441088	0.711577	1.326753	1.441088
2020-09-02	Sample	Actin	GluR1	GluR1/Actir	Norm Glur	Norm toTotalSaline	1.589877	0.736891	1.234115
	72	3911.941	1230.506	0.3145513	0.2912512	1.234115	0.786912	1.205253	1.140441
	860	3489.941	699.971	0.2005681	0.1857112	0.786912	1.594279		0.833521
	129	4058.234	762.213	0.1878189	0.1739064	0.736891			
	137	3391.406	985.799	0.2906756	0.2691441	1.140441			
	CTRL	5585.77	6045.234	1.0822562	1.002089	4.24614			
	891	4290.355	1743.385	0.4063498	0.3762498	1.594279			
	138	3476.527	1067.971	0.3071948	0.2844396	1.205253			
	100	3386.406	719.435	0.2124479	0.1967111	0.833521			

SYNAPTONEUROSOMAL GLUR1 PROTEIN (males)									
	Male	SYNAPTONEUROSOMAL protein GluR1					Average Thalamus NormTotSal		
2020-08-29	Sample	Actin	GluR1	GluR1/Act Norm Glur	Norm toTotalSaline	Male			
						Saline	50	100	
	535	7691.64	1204.991	0.156662	0.2514646	1.065528			
	497	6105.861	1540.87	0.252359	0.4050709	1.716402	1.065528	1.716402	1.605211
	557	6085.154	1436.163	0.236011	0.3788298	1.605211	2.31619	1.456574	1.250531
	CTRL	8385.104	5226.012	0.62325	1.0004005	4.238985	1.607755	3.064902	1.304706
	553	7830.033	2666.477	0.340545	0.5466209	2.31619	2.098353	2.107566	1.720638
	552	6314.447	1352.284	0.214157	0.3437515	1.456574	3.490787	2.961019	1.824436
	679	6365.912	1170.456	0.183863	0.2951253	1.250531	2.48835		2.177477
	556	5349.861	1264.627	0.236385	0.3794302	1.607755			2.740153
2020-09-01	Sample	Actin	GluR1	GluR1/Act Norm Glur	Norm toTotalSaline	2.36081			
	766	3202.77	2209.941	0.690009	1.0781395	4.568388			
	768	3352.113	660.577	0.197063	0.3079107	1.304706			
	647	1979.577	217.678	0.109962	0.1718154	0.728031	Part of sample lost outside the gel		
	767	2797.577	1295.062	0.462923	0.7233168	3.064902			
	779	2999.698	779.577	0.259885	0.4060706	1.720638			
	CTRL	5342.184	3422.648	0.640683	1.0010676	4.241812			
	720	3073.698	974.163	0.316935	0.4952112	2.098353			
	861	2248.406	619.577	0.275563	0.4305668	1.824436			
2020-09-02	Sample	Actin	GluR1	GluR1/Act Norm Glur	Norm toTotalSaline				
	72	3313.234	1293.991	0.390552	0.5138845	2.177477			
	860	3117.113	1951.648	0.626108	0.8238257	3.490787			
	129	3775.941	1427.355	0.378013	0.4973856	2.107566			
	137	3304.577	1624.113	0.491474	0.646676	2.740153			
	CTRL	5063.941	3848.77	0.760035	1.0000454	4.237481			
	891	2533.163	1130.577	0.44631	0.5872505	2.48835			
	138	2075.749	1102.406	0.531088	0.6988004	2.961019			
	570	3291.698	1393.82	0.423435	0.5571513	2.36081			



Cortex		Male	Total protein GluR1					Average Cortex			Cortex		Male	SYNAPTONEUROSOMAL protein GluR1					Average Cortex - norm to TOTSaline		
2020-10-30		Sample	Actin	GluR1	GluR1/Actin Norm	Glur1	Norm to saline	Male			2020-10-30		Sample	Actin	GluR1	GluR1/Act Norm	Glur1	Norm to TotalSaline	Male		
		215	5228.376	2549.376	0.4876038	0.7354567	1.231921	Saline	50	100	215	5523.184	2860.113	0.517838	0.9738368	1.631217	1.631217	Saline	50	100	
		100	7622.205	3442.598	0.4516538	0.681233	1.141094	0.582716			100	3950.234	1476.113	0.373677	0.7027313	1.177104	1.177104	2.137463			
		954	8160.79	3152.82	0.3863376	0.5827161	0.976074	0.91104			954	4482.406	3041.527	0.678548	1.2760656	2.137463	2.137463	2.416434			
		129	9509.205	3714.497	0.3906212	0.589177	0.986896	0.577337			129	4715.355	2972.82	0.630455	1.1856233	1.985969	1.985969	1.763064			
		137	7923.548	3976.648	0.5018772	0.7569853	1.267982	0.457213			137	4604.355	3468.527	0.753314	1.4166703	2.372982	2.372982	2.366937			
		CTRL	9129.548	6052.841	0.6629946	1	1.675042	0.285228			CTRL	5069.715	2695.82	0.53175	0.9999996	1.675041	1.675041	1.858456			
		958	6143.426	3710.719	0.6040146	0.91104	1.52603	0.546557			958	5322.891	4083.234	0.767108	1.4426109	2.416434	2.416434	2.084787			
		138	7051.912	3395.548	0.4815074	0.7262615	1.216518	0.979726			138	4520.841	2552.355	0.564575	1.0617306	1.778443	1.778443	3.006822			
2020-11-04		Sample	Actin	GluR1	GluR1/Actin Norm	Glur1	Norm to saline	0.437512			2020-11-04		Sample	Actin	GluR1	GluR1/Act Norm	Glur1	Norm to TotalSaline	2.108014		
		535	4923.355	1840.477	0.3738258	0.5773371	0.967064	0.597166					535	3872.991	2267.234	0.585396	1.0525489	1.763064			
		59	4611.477	2132.648	0.4624653	0.7142321	1.196369						59	3199.284	3336.648	1.042936	1.8752106	3.141056			
		71	5047.941	2042.355	0.4045917	0.624852	1.046653						71	3899.991	3315.698	0.850181	1.528635	2.560528			
		CTRL	5216.527	3377.719	0.6475034	1.0000053	1.675051	Average Cortex - Norm to saline					CTRL	4416.456	2456.284	0.556166	0.9999934	1.675031			
		860	4017.234	1189.284	0.2960455	0.4572131	0.765851	Male					860	3192.87	2509.284	0.785902	1.4130614	2.366937			
		74	4137.82	1221.456	0.2951931	0.4558967	0.763646	Saline					74	3712.87	2149.87	0.579032	1.0411059	1.743896			
		72	4589.941	1831.991	0.3991317	0.6164196	1.032529	1.231921					72	3489.456	1842.456	0.528007	0.949362	1.590221			
		891	4921.184	908.87	0.1846852	0.2852282	0.477769	0.986896					891	3753.406	2316.113	0.61707	1.1094983	1.858456			
2020-07-06		Sample	Actin	GluR1	GluR1/Actin Norm	Glur1	Norm to saline	0.765851			2021-07-11		Sample	Actin	GluR1	GluR1/Act Norm	Glur1	Norm to TotalSaline			
		553	3782.991	1445.991	0.3822349	0.5465573	0.915506	1.196369					801	5144.891	2564.234	0.498404	1.1087717	1.857239			
		497	4141.406	1887.284	0.4557109	0.6516207	1.091492	0.763646					720	4356.648	2437.406	0.559468	1.2446179	2.084787			
		570	3490.042	2271.284	0.6507899	0.9305639	1.558734	1.558734					766	5127.305	3546.234	0.691637	1.5386466	2.577297			
		CTRL	5032.991	3519.82	0.6993496	0.9999994	1.675041	0.915506					768	5107.598	2887.113	0.565258	1.2574992	2.106364			
		959	3606.991	2471.406	0.6851711	0.9797256	1.641081	1.641081					CTRL	6188.548	2781.82	0.449511	1.0000021	1.675045			
		779	4575.042	2354.406	0.5146195	0.7358541	1.232586	0.732851					763	5819.134	4695.477	0.806903	1.7950725	3.006822			
		997	3692.698	1129.87	0.3059741	0.4375121	0.732851	1.232586					767	5212.376	2948.648	0.565701	1.2584844	2.108014			
								1.032529					779	4499.77	3726.355	0.828121	1.8422754	3.085888			

Cortex	Females	Total protein GluR1					Average Cortex			Cortex	Females	SYNAPTONEUROSONAL protein GluR1					Average Cortex - norm to TOTSal				
		Sample	Actin	GluR1	GluR1/Act Norm	Norm to saline	Saline	50	100			Sample	Actin	GluR1	GluR1/Act Norm	Norm to TotalSaline	Saline	50	100		
		526	4688.598	4516.426	0.963279	1.208782	1.162291				526	3869.891	4687.255	1.211211	1.695187	1.629988	repeated				
		538	4917.891	3178.941	0.646403	0.811147	0.779949				538	4411.719	5470.255	1.239937	1.735392	1.668646		1.668646	2.370964	1.416473393	
		539	5351.012	3398.891	0.635187	0.797072	0.766415				539	4584.891	4825.841	1.052553	1.473132	1.416473		1.687799	2.562922	1.507576694	
		61	4757.477	3487.184	0.73299	0.919802	0.884425				61	4536.376	4308.255	0.949713	1.329199	1.278076	damaged	1.467259	3.133961	1.21837446	
		CTRL	5256.184	4188.477	0.796867	0.999958	0.961498				CTRL	4592.062	3281.134	0.714523	1.000032	0.961569		3.11076	3.592893	3.823685961	
		66	3657.456	3268.77	0.893728	1.121506	1.078371				66	3914.113	4908.962	1.25417	1.755311	1.687799		2.16071	1.959885	2.067017022	
		104	4156.406	3405.648	0.819373	1.028201	0.988655				104	3714.991	4161.719	1.12025	1.56788	1.507577		1.900526	1.616587	3.675156837	
		649	4364.477	3274.77	0.750324	0.941553	0.905339				649	4291.598	4580.255	1.067261	1.493717	1.436267	repeated	1.52763	2.080375	1.848198021	
		650	3730.891	3069.648	0.822765	1.032458	0.992748				650	-	4568.861	-	-	-	damaged	2.221518		1.521699159	
		Sample	Actin	GluR1	GluR1/Act Norm	Norm to saline				0.823377	Sample	Actin	GluR1	GluR1/Act Norm	Norm to saline					1.797677789	
		803	-	1888.113	-	-	-	damaged	1.040469		78	3590.527	1473.941	0.410508	2.568888	2.470084	repeated later, so average was done				
		78	-	1328.82	-	-	-	damaged actin			803	3491.062	851.284	0.243847	1.525949	1.467259					
		76	3720.234	4238.134	1.139212	1.371718	1.318959				76	5495.548	3492.234	0.635466	3.976633	3.823686					
		133	3327.113	2865.184	0.861162	1.03692	0.997039				130	4316.891	2248.406	0.520839	3.259319	3.133961					
		CTRL	4560.941	3787.77	0.83048	0.999976	0.961515				CTRL	4813.184	769.163	0.159803	1.000021	0.961559					
		130	3166.82	2484.941	0.78468	0.944829	0.908489				133	4635.598	2396.527	0.516983	3.23519	3.11076					
		277	2895.698	2214.355	0.764705	0.920777	0.885362				277	3607.941	1239.406	0.343522	2.149698	2.067017					
		715	2514.991	1548.355	0.61565	0.741301	0.712789				715	3699.184	2208.82	0.59711	3.736609	3.592893					
		716	-	-	-	-	-	Part of act	0.997039	0.712789	1.318959	716	-	943.941	-	-	-	Part of actin lost at the end of the gel			
		Sample	Actin	GluR1	GluR1/Act Norm	Norm to saline			1.26657	1.258075	0.885362	Sample	Actin	GluR1	GluR1/Act Norm	Norm to saline					
		3	3910.234	3888.77	0.994511	1.317233	1.26657		1.468965	1.08811	1.321377	650	2616.598	3708.426	1.41727	2.247138	2.16071				
		36	3855.355	3808.477	0.987841	1.308398	1.258075		0.837666	1.089474	1.230212	61	2941.406	3781.305	1.285543	2.03828	1.959885				
		34	3837.234	3981.305	1.037546	1.374232	1.321377		0.791043	0.830877	1.334244	649	3293.577	3734.276	1.133806	1.797694	1.728552	damaged band, repeated in other westerns			
		44	4076.648	4702.134	1.153431	1.527724	1.468965		0.791709	1.250616		716	3122.941	3893.083	1.246608	1.976547	1.900526				
		CTRL	5584.376	4217.083	0.755157	1.000209	0.961739				CTRL	4441.598	2801.305	0.630698	0.999996	0.961535					
		400	5575.205	4773.426	0.856188	1.134024	1.090408	repeated later, so average was done				78	2563.577	4465.719	1.741987	2.761991	2.65576	repeated earlier, so average was done			
		42	4698.648	4538.719	0.965963	1.279421	1.230212				725	2415.749	5823.497	2.410638	3.822163	3.675157					
		399	4924.598	4212.77	0.855455	1.133052	1.089474				526	2633.284	5375.083	2.041209	3.236418	3.111941	repeated earlier, so average was done				
		771	4212.698	4413.426	1.047648	1.387614	1.334244				757	-	6062.79	-	-	-	damaged GLUR1 band				
		Sample	Actin	GluR1	GluR1/Act Norm	Norm to saline					Sample	Actin	GluR1	GluR1/Act Norm	Norm to saline						
		803	2591.87	2115.941	0.816376	0.871173	0.837666				3	3777.355	3969.205	1.05079	1.588735	1.52763					
		716	3483.456	2685.527	0.770938	0.822684	0.791043				42	3535.698	4494.912	1.271294	1.922126	1.848198					
		776	4044.991	3121.062	0.771587	0.823377	0.791709				400	3907.941	4345.548	1.111979	1.68125	1.616587					
		78	1618.627	1310.698	0.809759	0.864112	0.830877				36	3821.406	5468.426	1.430998	2.16359	2.080375					
		CTRL	3959.698	3710.648	0.937104	1.000004	0.961542				CTRL	4086.82	2702.941	0.66138	0.99997	0.961509					
		725	3467.991	4226.891	1.21883	1.30064	1.250616				771	4304.698	4505.77	1.04671	1.582567	1.521699					
		400	3306.406	3498.891	1.058216	1.129245	1.085813	repeated earlier, so average was done			757	3507.284	5359.426	1.528084	2.310379	2.221518					
											34	3632.284	4491.477	1.236543	1.869585	1.797678					
											649	3305.698	2274.941	0.688188	1.040502	1.000482	repeated earlier, so average was done				

Hippocampus Male Total protein GluR1							Average Hippocampus Male			Hippocampus Male SYNAPTONEUROSOMAL protein GluR1							Average Hipp - Norm to saline Male				
2020-04-07	Sample	Actin	GluR1	GluR1/Actin	Norm Glur1	Norm to Saline	Saline	50	100	2020-04-07	Sample	Actin	GluR1	GluR1/Act	Norm Glur	Norm to TotalSaline	Saline	50	100		
	997	2847.012	5295.619	1.8600621	4.7693899	1.096916	Average Hippocampus Male				59	4472.719	5001.619	1.11825	6.5779425	1.512866	Average Hipp - Norm to saline Male				
	129	3888.012	6039.083	1.5532573	3.982711	0.915987	Average Hippocampus Male				997	4196.891	2796.841	0.666408	3.920046	0.901575	Average Hipp - Norm to saline Male				
	137	4353.305	5714.719	1.3127311	3.3659773	0.774144	Average Hippocampus Male				129	5268.184	5967.205	1.132687	6.6628663	1.532398	Average Hipp - Norm to saline Male				
	CTRL	5298.477	2071.062	0.3908787	1.0022532	0.230509	Average Hippocampus Male				CTRL	6035.598	1036.991	0.171812	1.0106616	0.232443	Average Hipp - Norm to saline Male				
	761	4142.355	5399.376	1.3034556	3.342194	0.768674	Average Hippocampus Male				137	6394.134	7038.619	1.100793	6.4752539	1.489249	Average Hipp - Norm to saline Male				
	766	4218.598	5620.912	1.3324123	3.4164419	0.78575	Average Hippocampus Male				CTRL	6035.598	1036.991	0.171812	1.0106616	0.232443	Average Hipp - Norm to saline Male				
	954	4157.598	4230.912	1.0176337	2.6093173	0.600119	Average Hippocampus Male				761	5404.719	7137.154	1.320541	7.7678893	1.786543	Average Hipp - Norm to saline Male				
	767	4696.305	3546.619	0.7551935	1.9363936	0.445353	Average Hippocampus Male				766	3794.77	2051.184	0.540529	3.1795835	0.731275	Average Hipp - Norm to saline Male				
	2020-04-21	Sample	Actin	GluR1	GluR1/Actin	Norm Glur1	Norm to TotalSaline	Average Hipp - Norm to saline Male				954	4967.891	5130.205	1.032673	6.0745448	1.397089	Average Hipp - Norm to saline Male			
	720	2550.891	5636.497	2.2096189	2.3142217	0.53225	Average Hipp - Norm to saline Male				767	4214.598	3496.548	0.829628	4.880164	1.122393	Average Hipp - Norm to saline Male				
	557	2795.234	579.163	0.2071966	0.2170052	0.049909	Average Hipp - Norm to saline Male				2020-04-21	Sample	Actin	GluR1	GluR1/Act	Norm Glur	Norm to TotalSaline	Average Hipp - Norm to saline Male			
	CTRL	3615.184	3452.012	0.9548648	1.0000679	0.230006	Average Hipp - Norm to saline Male				72	3527.113	5871.912	1.664793	3.8538028	0.886339	Average Hipp - Norm to saline Male				
	891	3395.113	5970.669	1.7586069	1.8418589	0.423611	Average Hipp - Norm to saline Male				720	4647.355	7347.276	1.580959	3.6597366	0.841706	Average Hipp - Norm to saline Male				
	74	3415.891	6827.669	1.9987959	2.0934184	0.481467	Average Hipp - Norm to saline Male				646	3582.698	5662.447	1.580498	3.6586703	0.841461	Average Hipp - Norm to saline Male				
	71	4965.426	6567.376	1.3226209	1.3852334	0.318591	Average Hipp - Norm to saline Male				CTRL	5013.113	2165.598	0.431987	0.9999992	0.229991	Average Hipp - Norm to saline Male				
	767	5331.477	3969.305	0.7445038	0.7797485	0.179335	Average Hipp - Norm to saline Male				557	3560.577	1038.77	0.291742	0.6753491	0.155324	Average Hipp - Norm to saline Male				
	2020-04-27	Sample	Actin	GluR1	GluR1/Actin	Norm Glur1	Norm to TotalSaline	Average Hipp - Norm to saline Male				CTRL	5013.113	2165.598	0.431987	0.9999992	0.229991	Average Hipp - Norm to saline Male			
	535	4691.598	1265.598	0.2697584	1.8375913	0.422629	Average Hipp - Norm to saline Male				891	3001.698	4263.083	1.420224	3.2876541	0.75613	Average Hipp - Norm to saline Male				
	858	5418.841	2563.912	0.4731477	3.2230768	0.741278	Average Hipp - Norm to saline Male				74	4812.941	8071.347	1.677009	3.8820829	0.892843	Average Hipp - Norm to saline Male				
	861	6134.669	1774.669	0.2892852	1.9706077	0.453222	Average Hipp - Norm to saline Male				71	3999.062	6695.74	1.674328	3.875875	0.891416	Average Hipp - Norm to saline Male				
	CTRL	5459.184	801.406	0.1467996	0.9999972	0.22999	Average Hipp - Norm to saline Male				556	3544.648	6718.033	1.895261	4.3873102	1.009041	Average Hipp - Norm to saline Male				
	2020-07-06	Sample	Actin	GluR1	GluR1/Actin	Norm Glur1	Norm to TotalSaline	Average Hipp - Norm to saline Male				2020-04-27	Sample	Actin	GluR1	GluR1/Act	Norm Glur	Norm to TotalSaline	Average Hipp - Norm to saline Male		
	553	3655.648	2305.163	0.6305758	6.3057576	1.450266	Average Hipp - Norm to saline Male				535	3709.648	3511.912	0.946697	7.0125691	1.612826	Average Hipp - Norm to saline Male				
	497	3609.012	2481.163	0.6874909	6.8749093	1.581166	Average Hipp - Norm to saline Male				497	3786.648	1683.305	0.444537	3.2928664	0.757329	Average Hipp - Norm to saline Male				
	570	3579.698	4054.113	1.1325293	11.325293	2.604713	Average Hipp - Norm to saline Male				779	4172.012	4958.033	1.188403	8.8029877	2.024606	Average Hipp - Norm to saline Male				
	CTRL	3953.991	401.385	0.1015139	1.0151389	0.233473	Average Hipp - Norm to saline Male				CTRL	5778.941	780.698	0.135094	1.0006934	0.23015	Average Hipp - Norm to saline Male				
	556	3673.698	3683.698	1.0027221	10.027221	2.306168	Average Hipp - Norm to saline Male				860	3482.406	2151.255	0.61775	4.5759231	1.05242	Average Hipp - Norm to saline Male				
	552	4699.527	4239.991	0.9022165	9.0221654	2.075015	Average Hipp - Norm to saline Male				858	4297.527	4004.426	0.931798	6.9022056	1.587444	Average Hipp - Norm to saline Male				
	679	4249.941	1918.577	0.4514361	4.5143615	1.038262	Average Hipp - Norm to saline Male				861	3827.234	3011.719	0.786918	5.8290216	1.340621	Average Hipp - Norm to saline Male				
							Average Hipp - Norm to saline Male				2020-04-27	Sample	Actin	GluR1	GluR1/Act	Norm Glur	Norm to TotalSaline	Average Hipp - Norm to saline Male			
							Average Hipp - Norm to saline Male				CTRL	5976.376	801.406	0.134096	1.0007138	0.230155	Average Hipp - Norm to saline Male				
							Average Hipp - Norm to saline Male				851	5276.497	5818.205	1.102664	8.2288382	1.892557	Average Hipp - Norm to saline Male				
							Average Hipp - Norm to saline Male				679	5049.012	4135.083	0.818989	6.1118548	1.40567	Average Hipp - Norm to saline Male				





TOTAL phospho-GLUR1 PROTEIN (males)											
Thalamus	Male	Total protein p-GluR1					Average Thalamus				
2020-08-21	Sample	Actin	p-GluR1	pGluR/Acti	Norm pGlu	Norm to saline	Male				
	535	3941.598	444.577	0.1127911	0.2044798	0.7834895	Saline	50	100		
	497	4026.255	662.87	0.1646369	0.2984715	1.1436302				0.20448	
	557	4097.234	571.163	0.1394021	0.2527232	0.9683399	spot on p-			0.208305	
	CTRL	7071.962	3900.912	0.5516025	1.0000046	3.8316406				0.39219	
	553	4441.083	510.284	0.1149008	0.2083046	0.7981446				0.23897	
	552	4632.719	166.021	0.0358366	0.0649685	0.2489348	band not			0.260986	
	679	4086.305	289.678	0.07089	0.128517	0.4924286	band not observed				
	556	3582.305	136.778	0.0381816	0.0692197	0.2652236	band not observed				
2020-08-22	Sample	Actin	p-GluR1	pGluR/Acti	Norm pGlu	Norm to saline	Average Thalamus - Norm to S				
	766	3990.891	1772.719	0.4441913	0.5464597	2.0938276	spot on p				
	768	3547.305	999.941	0.2818875	0.3467879	1.3287606					
	647	3666.012	1168.698	0.3187927	0.39219	1.5027243					
	767	3264.477	473.627	0.1450851	0.1784888	0.6839018		0.78349	1.14363	1.328761	
	779	4422.841	1572.134	0.355458	0.4372968	1.6755567		0.798145	0.683902	1.675557	
	CTRL	6136.962	4988.447	0.8128528	1.0000001	3.8316233		1.502724		0.37124	
	720	4015.719	780.042	0.1942472	0.2389697	0.9156417		0.915642			
	861	4733.598	372.799	0.0787559	0.0968883	0.3712396					

SYNAPTONEUROSOMAL phospho-GLUR1 PROTEIN (males)										
Thalamus	Male	SYNAPTONEUROSOMAL protein p-GluR1					Average Thalamus			
2020-08-21	Sample	Actin	p-GluR1	pGluR/Act	Norm pGluR	Norm to saline	Male			
	535	4265.669	2539.205	0.595265	0.88845576	3.404228				
	497	4022.134	2493.962	0.620059	0.92546179	3.546021		3.404228	3.546021	2.76121
	557	4989.184	2408.912	0.482827	0.72063709	2.76121		3.299304	3.160387	1.978018
	CTRL	6070.841	4064.64	0.669535	0.99930584	3.828963		1.913933	3.606112	2.063029
	553	5483.477	3163.518	0.576918	0.86107203	3.299304		3.071267	2.051184	2.708568
	552	4420.012	2442.619	0.552627	0.82481677	3.160387		2.475218	2.744177	3.297269
	679	5060.477	1750.305	0.345877	0.51623504	1.978018		1.061459	2.746001	1.365011
	556	4883.012	1634.205	0.334672	0.49950972	1.913933				
2020-08-22	Sample	Actin	p-GluR1	pGluR/Act	Norm pGluR	Norm to saline	Average Thalamus - Norm to S			
	766	4209.012	2297.548	0.545864	0.94114478	3.606112				
	768	4074.184	1272.305	0.312285	0.53842176	2.063029				
	647	4842.891	2251.477	0.464904	0.80155777	3.071267				
	767	4496.134	1396.012	0.310492	0.53533041	2.051184				
	779	4262.719	1747.719	0.410001	0.70689825	2.708568				
	CTRL	6733.255	3903.719	0.579767	0.99959826	3.830084				
	720	4861.305	1821.426	0.374678	0.64599725	2.475218				
	861	3652.255	1822.891	0.499114	0.8605411	3.297269				
2020-08-25	Sample	Actin	p-GluR1	pGluR/Act	Norm pGluR	Norm to saline	Average Thalamus - Norm to S			
	763	7245.912	3352.104	0.46262	1.05855439	4.055982	spot on pGLUR1 band			
	801	6638.205	2077.74	0.312997	0.71619171	2.744177				
	954	7353.912	1144.941	0.155691	0.35624882	1.365011				
	CTRL	9441.276	4126.134	0.437031	1.00000319	3.831635				
	851	6183.255	748.598	0.121069	0.27702582	1.061459				
	858	9562.589	2995.054	0.313205	0.71666784	2.746001				
	71	9584.66	5617.095	0.586051	1.34098465	5.138148	Part of actin lost at the end of the gel			

TOTAL phospho-GLUR1 PROTEIN (females)										
Thalamus/Hypoth	Female	Total protein p-GluR1					Average Thalamus			
Sample	Actin	p-GluR1	pGluR/Act	Norm pGlu	Norm to saline	Females				
not measured						Saline	50	100		

SYNAPTONEUROSOMAL phospho-GLUR1 PROTEIN (females)										
Thalamus/Hypoth	Female	SYNAPTONEUROSOMAL protein p-GluR1					Average Thalamus			
Sample	Actin	p-GluR1	pGluR/Act	Norm pGlu	Norm to saline	Females				
not measured						Saline	50	100		



CORTEX		Total protein p-GluR1					Average Cortex			CORTEX		SYNAPTONEUROSOMAL protein p-GluR1					Average Cortex - Norm to Salin		
Female	Sample	Actin	p-GluR1	pGluR/Act Norm pGI	Norm to saline	Females			Female	Sample	Actin	p-GluR1	pGluR/Act Norm pGI	Norm to saline	Females				
						Saline	50	100							Saline	50	100		
	3	3033.477	2952.861	0.973425	0.99038	0.853776				3	2605.648	2652.548	1.017999	2.252211	1.941561				
	44	4070.184	5063.711	1.244099	1.265769	1.09118				44	3864.82	5207.326	1.347366	2.980898	2.569739	1.941561	2.287353	1.51727	
	34	4071.255	4420.004	1.085661	1.104572	0.952217				34	3428.355	2727.376	0.795535	1.760033	1.51727	2.569739	2.066006	1.573165	
	399	4298.598	4503.983	1.04778	1.06603	0.918991				399	4380.941	5254.083	1.199305	2.653329	2.287353	2.054179	2.012757	2.028526	
	CTRL	3408.648	3350.276	0.982875	0.999995	0.862065				CTRL	3189.648	1441.891	0.452053	1.000118	0.862171	3.178761	2.125233	3.030187	
	771	4038.77	3251.154	0.804986	0.819008	0.706041				771	3760.234	3101.598	0.824842	1.824871	1.573165	2.698439	1.780374	3.401528	
	757	3601.234	4233.861	1.17567	1.196148	1.031162				757	2705.941	2914.426	1.077047	2.382848	2.054179	1.383659		3.458936	
	400	3999.82	3845.548	0.96143	0.978177	0.843256				400	3179.991	3444.719	1.083248	2.396566	2.066006	1.496448		1.490325	
	42	2837.113	2885.991	1.017228	1.034946	0.892195				42	2881.648	3064.912	1.063597	2.353091	2.028526				
							1.164199												
	538	3284.163	2383.749	0.725832	1.409601	1.215173	Average Cortex - Norm to Salin			538	2956.113	3226.477	1.091459	3.687362	3.178761				
	526	3210.284	3327.749	1.03659	2.013109	1.735439	Females			526	2633.82	1820.234	0.6911	2.334799	2.012757				
	539	3596.234	3430.355	0.953874	1.852471	1.596958	Saline	50	100	539	3032.698	3155.355	1.040445	3.515016	3.030187				
	104	2824.527	2802.113	0.992065	1.926638	1.660895	0.847442	0.912174	0.945153	104	2982.456	3483.355	1.167948	3.945772	3.401528				
	CTRL	3146.991	1620.456	0.514922	1.000005	0.862073	1.083085	0.837	0.700803	CTRL	3108.991	921.698	0.296462	1.001561	0.863415				
	61	2944.891	2325.577	0.789699	1.533634	1.322098	1.023512	1.722549	0.885576	61	3749.87	2736.355	0.72972	2.46527	2.125233				
	66	3177.991	2711.335	0.85316	1.656879	1.428344	1.206147	1.312278	1.585096	66	3747.042	3471.77	0.926536	3.13019	2.698439				
	649	2758.477	3591.184	1.301872	2.5283	2.179569	1.417734	0.884938	1.648558	725	3942.113	4681.891	1.18766	4.012366	3.458936				
	650	-	1986.406	-	-	-	Too much	1.417734	0.884938	1.648558	650	-	-	-	-	-	-	Damaged p-GLUR1 band	
	803	2419.577	1937.891	0.800921	0.663014	0.571564	0.567328	0.419187	2.163379	803	1679.87	2162.406	1.287246	1.605045	1.383659				
	78	1572.456	1964.477	1.249305	1.034193	0.891546	0.854751	0.844891	0.73489	78	2172.577	3598.477	1.656317	2.065234	1.780374				
	76	4497.355	5364.305	1.192769	0.987391	0.8512				76	4323.698	5994.719	1.38648	1.728778	1.490325				
	133	3081.284	3601.598	1.168863	0.967602	0.834139				133	2845.406	3961.305	1.392176	1.73588	1.496448				
	CTRL	2935.577	3546.134	1.207985	0.999988	0.862059				CTRL	2685.991	2155.355	0.802443	1.000553	0.862545				
	716	4090.527	3733.841	-	-	-	Not cortex sample			716	3193.406	-	-	-	-	-	-	Not cortex sample	
	725	4456.113	4478.184	1.004953	0.831915	0.717168	spot on p-GLUR1 band			725	3727.284	-	-	-	-	-	-	Damaged p-GLUR1 band	
	130	3855.163	2281.426	0.591785	0.489888	0.422317				130	-	-	-	-	-	-	-	Part of bands lost at the end of gel	

Hippocampus		Male	Total protein p-GluR1					Average Hippocampus		
2020-08-13	Sample	Actin	p-GluR1	pGluR/Actin	Norm pGlu	Norm to saline	Male			
	997	3026.284	4785.891	1.5814415	3.1377807	1.2706066	Saline	50	100	
	129	3103.335	3620.77	1.1667351	2.3149507	0.9374114	3.137781			
	137	3062.213	5127.184	1.6743394	3.3221021	1.3452453	2.868111			
	CTRL	3446.042	1737.406	0.5041744	1.0003459	0.4050781	2.186449			
	761	2444.335	3533.355	1.4455281	2.8681114	1.1614072	2.170862			
	766	3048.163	2832.234	0.9291609	1.8435733	0.7465328	1.984369			
	954	2814.506	4910.891	1.7448501	3.4620041	1.4018969	2.469514			
	767	3228.163	1959.234	0.6069192	1.2042047	0.4876282				
2020-08-13		Sample	Actin	p-GluR1	pGluR/Actin	Norm pGlu	Norm to saline	Average Hipp - Norm to Saline		
	720	2595.749	3445.012	1.3271745	2.186449	0.8853762	Male			
	557	2247.213	546.163	0.2430402	0.4003956	0.1621354	Saline	50	100	
	CTRL	3792.698	2304.184	0.6075316	1.0008758	0.4052926	1.270607	0.937411	1.345245	
	891	3119.456	4110.548	1.3177131	2.1708618	0.8790644	1.161407	0.746533	1.401897	
	74	3994.941	5766.669	1.4434929	2.3780773	0.9629738	0.885376	0.487628	0.162135	
	71	3694.456	6066.497	1.6420542	2.7051964	1.0954367	0.879064	0.962974	1.095437	
	535	3182.698	3833.598	1.204512	1.9843691	0.8035464	0.803546		0.820556	
	861	2969.234	3652.184	1.2300088	2.0263737	0.8205557				

Hippocampus		Male	Synaptoneurosomal protein p-GluR1					Average Hipp - Norm to Saline		
2020-08-13	Sample	Actin	p-GluR1	pGluR/Act	Norm pGluR	Norm to saline	Male			
	59	3164.456	5324.012	1.682441	3.43671018	1.391654	Saline	50	100	
	997	2314.749	4683.134	2.023171	4.1327166	1.673494	1.673494	1.391654	1.238158	
	129	2421.335	4007.891	1.65524	3.38114633	1.369155	1.289511	1.369155	1.277389	
	137	3555.698	5322.426	1.496872	3.05764956	1.238158	2.586805	1.25237	0.37214	
	CTRL	3189.749	1561.527	0.489545	0.99999064	0.404934	1.568009	1.556742	1.793634	
	761	3195.284	4981.305	1.558955	3.18446598	1.289511	2.128785	1.500993	1.854041	
	766	3030.284	4588.012	1.514053	3.09274531	1.25237	2.415178	1.926043		
	954	3558.87	5495.962	1.5443	3.15452913	1.277389	3.292262	1.937114		
	767	3508.941	6603.912	1.882024	3.84439635	1.556742	1.932905	2.663611		
2020-08-13		Sample	Actin	p-GluR1	pGluR/Act	Norm pGluR	Norm to saline	Average Hipp - Norm to Saline		
	553	700.627	1700.77	2.427497	6.38815022	2.586805	Male			
	646	3053.284	4300.719	1.408555	3.70672416	1.500993	Saline	50	100	
	557	1990.113	694.991	0.349222	0.91900494	0.37214	1.270607	0.937411	1.345245	
	CTRL	3793.991	1444.77	0.380805	1.00211791	0.405796	1.161407	0.746533	1.401897	
	891	3064.991	4509.962	1.471444	3.87222052	1.568009	0.879064	0.962974	1.095437	
	74	3259.698	5891.669	1.807428	4.75638912	1.926043	0.803546		0.820556	
	71	3458.991	5822.083	1.683174	4.42940472	1.793634				
	556	3137.234	6267.205	1.997685	5.25706554	2.128785				
2021-08-19		Sample	Actin	p-GluR1	pGluR/Act	Norm pGluR	Norm to saline	Average Hipp - Norm to Saline		
	535	3430.406	3149.719	0.918177	5.96431674	2.415178	Male			
	497	2416.749	1779.77	0.736431	4.78373096	1.937114	Saline	50	100	
	851	3384.335	4235.891	1.251617	8.13028637	3.292262	1.673494	1.391654	1.238158	
	779	2963.163	5141.134	1.735016	11.2703601	4.563797	1.289511	1.369155	1.277389	
	CTRL	4209.234	647.991	0.153945	1.00000073	0.404938	2.586805	1.25237	0.37214	
	860	3065.698	2252.77	0.734831	4.77333479	1.932905	1.568009	1.556742	1.793634	
	858	3560.941	3605.891	1.012623	6.57782369	2.663611	2.128785	1.500993	1.854041	
	861	3629.577	2558.305	0.704849	4.57857906	1.854041				

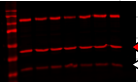
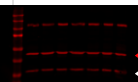
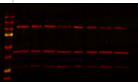
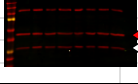
Hippocampus		Female		Total protein p-GluR1					Average Hippocampus		
2021-08-18	Sample	Actin	p-GluR1	pGluR/Act	Norm pGI	Norm to saline	Female				
							Saline	50	100		
	78	2896.456	3247.184	1.121089	0.918925	0.88614					
	500	3100.213	3158.477	1.018794	0.835077	0.805283					
	757	2540.799	2212.527	0.8708	0.71377	0.688304	1.001752				
	old CTRL	2382.506	1080.698	0.453597	0.371801	0.358536	1.37331				
	771	2194.506	2551.113	1.1625	0.952869	0.918872	1.059158				
becomes CTRL in H	776	2461.213	3007.941	1.222138	1.001752	0.966012	1.036998				
	134	2759.627	2626.062	0.9516	0.78	0.752171					
	277	3250.335	5458.305	1.679305	1.37648	1.32737					
2021-08-18	Sample	Actin	p-GluR1	pGluR/Act	Norm pGI	Norm to saline	Average Hipp - Norm to Saline				
							Male				
							Saline	50	100		
	76	3460.113	4818.234	1.392508	1.822654	1.757625					
	61	3039.749	2147.577	0.706498	0.924736	0.891743	0.688304	0.88614	0.918872		
	66	3018.456	3166.991	1.049209	1.37331	1.324313	0.966012	0.805283	0.752171		
	CTRL	2956.627	2259.577	0.764241	1.000316	0.964627	1.324313	1.32737	1.757625		
	34	3554.991	2975.991	0.83713	1.09572	1.056627	1.021369	0.891743	1.056627		
	36	3401.749	1492.335	0.438696	0.57421	0.553723					
	44	3037.456	2399.991	0.790132	1.059158	1.021369		0.553723			

Hippocampus		Female		Synaptonerosomal protein p-GluR1					Average Hipp - Norm to Saline		
2021-08-19	Sample	Actin	p-GluR1	pGluR/Act	Norm pGI	Norm to saline	Male				
							Saline	50	100		
	526	4184.941	5008.962	1.196901	1.554775	1.499304					
	539	4309.113	4689.305	1.08823	1.41361	1.363176	1.480361	1.499304	1.363176		
	803	3989.406	4714.598	1.181779	1.535131	1.480361	1.421287	1.481976	1.242238		
	old CTRL	4226.113	1005.527	0.237932	0.309073	0.298046	1.947791	0.982954	1.967128		
	CTRL	3580.82	2756.598	0.769823	1	0.964322	0.832554	1.057349	0.955168		
	694	2989.335	2964.477	0.991684	1.288198	1.242238	0.901853	0.631133	0.92252		
	715	3643.284	4310.255	1.183069	1.536806	1.481976		1.283529			
	716	3525.527	4000.134	1.13462	1.473871	1.421287		0.624166			
2021-08-19	Sample	Actin	p-GluR1	pGluR/Act	Norm pGI	Norm to saline	Average Hipp - Norm to Saline				
							Male				
							Saline	50	100		
	78	4269.355	1386.163	0.324677	1.019322	0.982954					
	500	4077.77	1424.163	0.34925	1.096469	1.057349					
	CTRL	4173.82	1329.456	0.318523	0.999999	0.964321					
	757	4022.82	2588.163	0.64337	2.019855	1.947791					
	771	3180.163	2066.335	0.649758	2.039908	1.967128					
	776	2782.163	765.092	0.274999	0.863357	0.832554					
	134	3916.577	1235.678	0.315499	0.990508	0.955168					
	277	4170.648	4666.577	1.118909	3.512805	3.387476					
2021-08-19	Sample	Actin	p-GluR1	pGluR/Act	Norm pGI	Norm to saline	Average Hipp - Norm to Saline				
							Male				
							Saline	50	100		
	61	3412.477	2058.305	0.60317	0.654483	0.631133					
	399	3910.82	4797.255	1.226662	1.331017	1.283529					
	34	3255.749	2870.426	0.881648	0.956652	0.92252					
	CTRL	2381.799	2195.062	0.921598	1	0.964322					
	36	2933.335	1749.77	0.596512	0.647259	0.624166					
	44	2954.163	2546.184	0.861897	0.93522	0.901853					





Cortex							Average Cortex			Cortex							Average Cortex - norm to TOTS			
2020-10-21	Male	Total protein Cdk5					Total Saline	Male			2020-10-21	Male	SYNAPTONEUROSOMAL protein Cdk5					Male		
Sample	Actin	Cdk5	Cdk5/Actin	Cdk Norm	Norm to Total Saline	Saline		50	100	Sample	Actin	Cdk5	Cdk5/Actin	Cdk Norm	Norm to Total Saline	Saline	50	100		
	556	5412.355	4076.962	0.7532695	0.9744754	1.031	0.974475			556	5903.426	6164.276	1.0441862	0.71033075	0.751315	0.751315				
	552	6111.841	4232.012	0.6924284	0.8957676	0.947				552	6239.305	5446.569	0.8729448	0.59384002	0.628103	0.751315	0.628103	0.842008		
	557	5449.184	3921.184	0.719591	0.9309069	0.985	0.877693			557	5210.062	6096.983	1.1702323	0.79607642	0.842008	0.586525	0.709183	0.639884		
	CTRL	6691.376	5173.012	0.7730864	1.0001118	1.058	0.846123			CTRL	5414.012	7973.811	1.47281	1.00191156	1.059719	0.524283	1.07247	0.90946		
	647	5751.305	3902.012	0.6784568	0.8776931	0.928	1.229948			647	5386.062	4390.497	0.815159	0.55452994	0.586525	1.145816	0.782895	0.915399		
	646	5392.426	3862.598	0.7163006	0.9266502	0.98	0.963222			646	5513.134	5433.912	0.9856303	0.67049681	0.709183	0.564496	0.547334	0.60223		
	679	4904.77	4266.74	0.8699164	1.125377	1.19	0.915627			679	5227.305	4648.74	0.8893187	0.6049787	0.639884	0.777256	0.683346	0.771692		
2020-10-22	Sample	Actin	Cdk5	Cdk5/Actin	Cdk Norm	Norm to Total Saline	1.064884		2020-10-22	Sample	Actin	Cdk5	Cdk5/Actin	Cdk Norm	Norm to Total Saline	0.918246	0.52009	0.794504		
	535	4959.234	4024.083	0.8114324	0.8461234	0.895	0.967234			535	4448.113	2087.648	0.4693334	0.49568344	0.524283	0.586563	0.69525	0.522636		
	59	4876.82	4340.548	0.8900365	0.9280882	0.982	0.669813			59	2801.577	2689.698	0.9600657	1.01396719	1.07247	0.886528	0.773692			
	71	4668.355	3344.012	0.7163148	0.7469394	0.79				71	3733.991	3039.991	0.8141399	0.85984857	0.90946		0.700669			
	CTRL	4534.307	4349.012	0.959135	1.0001407	1.058	0.945447			CTRL	4448.906	4212.406	0.946841	0.99999997	1.057697					
	860	2917.941	3441.77	1.1795201	1.2299479	1.301				860	2803.698	2875.82	1.0257239	1.08331165	1.145816					
	74	4094.062	2838.77	0.6933872	0.7230314	0.765				74	3615.82	2534.113	0.7008405	0.74018813	0.782895					
	72	4797.062	4562.012	0.9510013	0.9916593	1.049				72	4245.991	3479.406	0.8194568	0.86546395	0.915399					
	891	4803.891	4437.497	0.9237297	0.9632218	1.019				891	4566.941	2307.82	0.5053317	0.53370279	0.564496					
	Sample	Actin	Cdk5	Cdk5/Actin	Cdk Norm	Norm to Total Saline	Average Cortex - norm to TOTSa			Sample	Actin	Cdk5	Cdk5/Actin	Cdk Norm	Norm to Total Saline					
	215	3034.648	1259.355	0.4149921	0.4626652	0.489	1.0307	0.947451	0.984618		215	4143.284	2210.305	0.5334669	0.5174769	0.547334				
	100	3607.284	3963.77	1.0988239	1.2250536	1.296	0.928334	0.980115	1.190308		100	4839.284	2840.527	0.5869726	0.56937877	0.60223				
	954	3085.92	2534.406	0.8212805	0.9156268	0.968	0.894943	0.981636	0.790036		954	4610.527	3492.77	0.7575642	0.73485707	0.777256				
	129	2900.87	3146.234	1.0845829	1.2091766	1.279	1.300913	0.764748	1.048875		129	4931.406	3284.477	0.6660326	0.64606903	0.683346				
	137	3298.87	3716.062	1.1264651	1.2558701	1.328	1.018797	0.48936	1.295736		137	4161.698	3130.184	0.7521411	0.72959654	0.771692				
	CTRL	4404.025	3950.234	0.8969599	1	1.058	0.968456	1.278943	1.328331		CTRL	4386.698	4522.305	1.0309132	1.00001283	1.057711				
	958	3207.042	3063.234	0.9551587	1.0648845	1.126	1.126326	1.046765	0.861869		958	4116.163	3683.891	0.8949818	0.86815579	0.918246				
	138	3722.426	3304.355	0.8876886	0.9896636	1.047	1.023041	0.706833	0.932018		138	3812.82	1932.77	0.5069135	0.49171939	0.52009				
2020-10-28	Sample	Actin	Cdk5	Cdk5/Actin	Cdk Norm	Norm to Total Saline	0.708459	0.76383		2020-10-28	Sample	Actin	Cdk5	Cdk5/Actin	Cdk Norm	Norm to Total Saline				
	801	5069.234	2716.891	0.5359569	0.6682755	0.707		1.038014			801	4985.941	3909.912	0.7841874	0.65732387	0.69525				
	720	3477.82	2697.82	0.7757216	0.9672339	1.023					720	4757.941	3147.841	0.6615973	0.55456607	0.586563				
	766	4925.577	2852.77	0.5791748	0.7221631	0.764					766	4312.234	3763.134	0.8726646	0.73148752	0.773692				
	768	5294.82	3460.234	0.6535131	0.8148542	0.862					768	4009.577	3593.134	0.8961379	0.75116339	0.794504				
	CTRL	4870.527	3907.234	0.802222	1.0002743	1.058					CTRL	4699.82	5607.548	1.193141	1.0001182	1.057822				
	763	5446.527	2925.82	0.53719	0.669813	0.708					763	4930.062	4929.74	0.9999347	0.83816822	0.866528				
	767	3956.062	3113.719	0.7870754	0.9813907	1.038					767	4107.406	3246.083	0.7903	0.66244762	0.700669				
	779	4607.841	3256.376	0.7067032	0.8811761	0.932					779	4359.82	2688.548	0.6166649	0.49412648	0.522636				









TOTAL GLT1 PROTEIN (males)									
Thalamus/Hypothalamus	Male	Total protein GLT1				Average Thalamus			
2020-08-29	Sample	Actin	GLT1	GLT1/Actin Norm GLT1	Norm to Total Saline	Male			
	535	8423.933	11276.07	1.338575	0.7757606	0.891679			
	497	6770.64	12251.82	1.8095517	1.0487115	1.205416	0.775761		
	557	6500.276	11960.22	1.8399553	1.0663316	1.225669	1.031929		
	CTRL	9678.518	16700.14	1.7254849	0.9999913	1.149415	1.177208		
	553	6271.569	11167.12	1.7805937	1.0319291	1.186125	0.750889		
	552	6668.861	11938.46	1.7901796	1.0374846	1.192511	0.850063		
	679	6682.983	12480.65	1.8675271	1.0823107	1.244035	0.718198		
	556	7145.154	14513.75	2.0312721	1.1772078	1.353112	0.805218		
2020-09-01	Sample	Actin	GLT1	GLT1/Actin Norm GLT1	Norm to Total Saline	0.872752			
	766	3629.134	6715.61	1.8504718	0.5784532	0.664889			
	768	3711.648	9185.288	2.4747196	0.7735916	0.889186			
	647	4018.426	9652.631	2.4020925	0.7508886	0.86309			
	767	4180.355	10654.17	2.5486273	0.796695	0.915741			
	779	5196.891	11812.7	2.2730325	0.7105447	0.816718			
	CTRL	5892.891	18852.55	3.1992024	1.0000633	1.149498			
	720	3777.234	10271.63	2.7193526	0.8500633	0.977084			
	861	3397.406	8588.924	2.5280829	0.7902729	0.90836			
2020-09-02	Sample	Actin	GLT1	GLT1/Actin Norm GLT1	Norm to Total Saline	1.353112	0.664889	0.889186	
	72	3911.941	7180.953	1.8356496	0.7232662	0.83134	0.86309	0.915741	0.816718
	860	3489.941	6361.418	1.8227867	0.7181981	0.825515	0.977084	0.711221	0.90836
	129	4058.234	6373.125	1.5704183	0.6187621	0.711221	0.825515	1.110597	0.83134
	137	3391.406	6367.125	1.8774293	0.7397279	0.850262	0.925538		0.850262
	CTRL	5585.77	14176.2	2.5379126	0.9999656	1.149386			1.048433
	891	4290.355	8767.953	2.0436428	0.8052178	0.925538			
	138	3476.527	8525.368	2.4522657	0.9662197	1.110597			
	100	3386.406	7839.539	2.3150027	0.9121366	1.048433			

SYNAPTONEUROSONAL GLT1 PROTEIN (males)									
Thalamus/Hypothalamus	Male	SYNAPTONEUROSONAL protein GLT1				Average Thalamus NormTotSal			
2020-08-29	Sample	Actin	GLT1	GLT1/Actin Norm GLT1	Norm to Total Saline	Male			
	535	7691.64	16194.69	2.105493	1.311017	1.506916			
	497	6105.861	10818.48	1.771819	1.10325	1.268103	1.506916	1.268103	1.162075
	557	6085.154	9880.309	1.623674	1.011005	1.162075	1.438652	1.280047	1.238992
	CTRL	8385.104	13463.43	1.605637	0.999774	1.149165	1.385785	1.908877	1.746877
	553	7830.033	15739.26	2.010114	1.251628	1.438652	2.158493	2.17986	1.981709
	552	6314.447	11293.43	1.788507	1.11364	1.280047	2.144361	1.447466	2.095861
	679	6365.912	11020.31	1.731144	1.077923	1.238992	2.411981	2.930521	2.558468
	556	5349.861	10358.65	1.936247	1.205633	1.385785	2.025634		2.050544
2020-09-01	Sample	Actin	GLT1	GLT1/Actin Norm GLT1	Norm to Total Saline				
	766	3202.77	13244.1	4.1352	1.660723	1.908877			
	768	3352.113	12685.27	3.78426	1.519783	1.746877			
	647	1979.577	9256.388	4.675942	1.877889	2.158493			
	767	2797.577	13210.8	4.72223	1.896478	2.17986			
	779	2999.698	12877.63	4.292976	1.724087	1.981709			
	CTRL	5342.184	13320.46	2.493448	1.001385	1.151017			
	720	3073.698	14278.34	4.645329	1.865594	2.144361			
	861	2248.406	13578.39	6.039117	2.425348	2.787757			Part of actin lost at the end of the gel
2020-09-02	Sample	Actin	GLT1	GLT1/Actin Norm GLT1	Norm to Total Saline				
	72	3313.234	11966.7	3.611789	1.823399	2.095861			
	860	3117.113	12956.46	4.156557	2.098424	2.411981			
	129	3775.941	9418.752	2.494412	1.259295	1.447466			
	137	3304.577	14569.87	4.408998	2.225867	2.558468			
	CTRL	5063.941	10030.63	1.980795	0.999998	1.149423			
	891	2533.163	8842.681	3.490767	1.762301	2.025634			
	138	2075.749	10482.85	5.050154	2.549553	2.930521			
	570	3291.698	11631.85	3.533694	1.783973	2.050544			

TOTAL GLT1 PROTEIN (females)							Average Thalamus			
Thalamus/Hypothalam	Female	Total protein GLT1					Female			
Sample	Actin	GLT1	GLT1/Acti	Norm GLT1	Norm toTotalSaline	Saline	50	100		
130	4242.234	15033.26	3.543713	1.104993	0.945651	<b>repeated</b>				
133	<b>4561.719</b>	<b>15172.62</b>	<b>3.326076</b>	<b>1.037131</b>	<b>0.887574</b>	<b>stripe on</b>				
134	4275.577	13990.67	3.27223	1.02034	0.873205	1.192683				
277	4850.527	11898.02	2.452933	0.764868	0.654573	0.851408				
CTRL	6702.841	21496.4	3.207058	1.000018	0.855814	0.933025				
61	4851.548	12594.48	2.595971	0.80947	0.692743	<b>repeated</b>				
66	<b>4904.77</b>	<b>11233.7</b>	<b>2.290363</b>	<b>0.714176</b>	<b>0.61119</b>	1.200631				
104	4932.527	16054.89	3.254902	1.014937	0.868581	1.752396				
Sample	Actin	GLT1	GLT1/Acti	Norm GLT1	Norm toTotalSaline	1.168494				
526	3045.82	12287.75	4.0343	0.996123	0.852481					
538	<b>2227.335</b>	<b>10756.17</b>	<b>4.829164</b>	<b>1.192386</b>	<b>1.020442</b>					
757	<b>2112.163</b>	<b>7282.56</b>	<b>3.447916</b>	<b>0.851337</b>	<b>0.728573</b>					
771	2836.284	11980.34	4.223956	1.042952	0.892556					
CTRL	4489.991	18179.95	4.048994	0.999752	0.855585					
649	2450.577	10538.75	4.300519	1.061856	0.908735					
715	2251.87	9874.167	4.384874	1.082685	0.926556					
716	<b>2753.82</b>	<b>11399.46</b>	<b>4.139508</b>	<b>1.022101</b>	<b>0.874712</b>	<b>spot on ac</b>				
Sample	Actin	GLT1	GLT1/Acti	Norm GLT1	Norm toTotalSaline	0.61119	1.154832	0.873205		
36	5991.426	15208.19	2.538325	0.89064	0.762208	<b>repeated</b>				
3	<b>5002.305</b>	<b>13290.53</b>	<b>2.656881</b>	<b>0.932239</b>	<b>0.797808</b>	0.924171 0.789661 0.908735				
34	-	<b>13059.8</b>	-	-	-	<b>Damaged</b>				
78	-	-	-	-	-	<b>Compress</b>				
CTRL	5999.134	17082.87	2.847557	0.999143	0.855064	0.871924 0.882203 0.689288				
42	4521.77	12248.34	2.708749	0.950438	0.813383					
44	<b>4718.841</b>	<b>14523.17</b>	<b>3.077698</b>	<b>1.079894</b>	<b>0.924171</b>					
400	5034.79	12240.34	2.431152	0.853036	0.730026					
Sample	Actin	GLT1	GLT1/Acti	Norm GLT1	Norm toTotalSaline	0.728573	0.852481	0.868581		
397	<b>2467.062</b>	<b>12537.77</b>	<b>5.082066</b>	<b>1.200583</b>	<b>1.027456</b>	0.797808 0.926556 0.892556				
399	3141.648	12809.07	4.077181	0.963189	0.824296	0.924171 0.789661 0.908735				
34	2436.527	13398.31	5.498937	1.299064	1.111736	<b>repeated later, so average was done</b>				
61	2764.77	13782.48	4.985037	1.17766	1.00784	<b>repeated earlier, so average was done</b>				
CTRL	5089.305	21542.16	4.232829	0.99996	0.855763					
78	2629.234	11339.26	4.312761	1.018843	0.871924					
76	3187.477	13908.89	4.363606	1.030854	0.882203					
36	3309.941	13377.65	4.041659	0.954798	0.817114	<b>repeated earlier, so average was done</b>				
133	<b>1699.163</b>	<b>12603.7</b>	<b>7.417594</b>	<b>1.752326</b>	<b>1.499637</b>					
Sample	Actin	GLT1	GLT1/Acti	Norm GLT1	Norm toTotalSaline	0.728573	0.852481	0.868581		
CTRL	5922.062	17428.48	2.942975	0.999991	0.855791					
130	2332.749	10942.22	4.690696	1.593849	1.364012	<b>repeated earlier, so average was done</b>				
725	4071.648	9651.388	2.370389	0.805433	0.689288					
34	4044.82	9278.388	2.293894	0.779441	0.667044	<b>repeated earlier, so average was done</b>				

SYNAPTONEUROSOMAL GLT1 PROTEIN (females)							Average Thalamus NormTotSal				
Thalamus/Hypothalam	Female	SYNAPTONEUROSOMAL protein GLT1					Female				
Sample	Actin	GLT1	GLT1/Acti	Norm GLT1	Norm toTotalSaline	Saline	50	100			
130	2820.355	13146.53	4.661303	1.601272	1.370366						
133	<b>2933.527</b>	<b>9751.045</b>	<b>3.324</b>	<b>1.141876</b>	<b>0.977215</b>	0.977215 1.370366 0.977183					
134	2767.941	9200.338	3.323892	1.141839	0.977183	1.159348 1.03492 0.963092					
CTRL	5261.184	15313.41	2.910639	0.999876	0.855692	1.715696 1.1926 1.302565					
277	3449.062	11299	3.275962	1.125373	0.963092	1.311642 1.551302 1.176344					
61	3939.234	13867.22	3.520283	1.209304	1.03492	1.326615 1.462953 1.434702					
66	<b>3842.648</b>	<b>15153.58</b>	<b>3.943526</b>	<b>1.354698</b>	<b>1.159348</b>	1.294526 1.37261 1.326558					
104	3857.184	17089.95	4.430679	1.522047	1.302565	1.635554 1.336364 1.26571					
Sample	Actin	GLT1	GLT1/Acti	Norm GLT1	Norm toTotalSaline	36	3962.477	14743.53	3.720786	1.393553	1.1926
3	<b>2937.941</b>	<b>15726.19</b>	<b>5.352792</b>	<b>2.004791</b>	<b>1.715696</b>						
34	3754.648	13779.82	3.670071	1.374558	1.176344						
78	<b>3423.719</b>	<b>13193.46</b>	<b>3.853546</b>	<b>1.443276</b>	<b>1.235152</b>	<b>damaged actin, was repeated later</b>					
CTRL	5265.477	14067.58	2.671663	1.000623	0.856331						
42	3777.355	16907.89	4.47612	1.676449	1.434702						
44	<b>4015.891</b>	<b>16433.77</b>	<b>4.092186</b>	<b>1.532654</b>	<b>1.311642</b>						
400	2401.355	10960.41	4.56426	1.709461	1.462953						
Sample	Actin	GLT1	GLT1/Acti	Norm GLT1	Norm toTotalSaline	526	2880.355	13859.36	4.811684	1.603895	1.37261
538	<b>3034.355</b>	<b>14111.12</b>	<b>4.65045</b>	<b>1.55015</b>	<b>1.326615</b>						
771	3198.941	14875.87	4.65025	1.550083	1.326558						
757	<b>3244.305</b>	<b>14722.53</b>	<b>4.537961</b>	<b>1.512654</b>	<b>1.294526</b>						
CTRL	4378.77	13138.24	3.00044	1.000147	0.855924						
649	3289.941	14597.29	4.436945	1.478982	1.26571						
715	2748.113	12873.87	4.684623	1.561541	1.336364						
716	<b>3053.82</b>	<b>17508.87</b>	<b>5.733434</b>	<b>1.911145</b>	<b>1.635554</b>						
78	<b>995.991</b>	-	-	-	-	<b>Part of actin lost at the end of the gel</b>					
Sample	Actin	GLT1	GLT1/Acti	Norm GLT1	Norm toTotalSaline	5948.062	14602.65	2.455027	1.000011	0.855807	
CTRL	5948.062	14602.65	2.455027	1.000011	0.855807						
78	2688.82	11965.7	4.450168	1.812696	1.551302						
399	<b>3516.841</b>	-	-	-	-	<b>Part of bands lost at the end of the gel</b>					

Cortex	Male	Total protein GLT1					Average Cortex			Cortex	Male	SYNAPTO NEURO SOMAL protein GLT1					Average Cortex - norm to TOTS		
2020-10-30	Sample	Actin	GLT1	GLT1/Actin Norm GLT1	Norm to Total Saline	Male			2020-10-30	Sample	Actin	GLT1	GLT1/Actin Norm GLT1	Norm to Total Saline	Male				
	215	5228.376	23267.54	4.4502429	1.6919358	1.442032	<b>Saline</b>	<b>50</b>	<b>100</b>		215	5523.184	25150.35	4.553596	1.060448	0.903817	<b>Saline</b>	<b>50</b>	<b>100</b>
	100	7622.205	27258.74	3.576227	1.3596441	1.15882	1.323762			100	3950.234	22184.09	5.615892	1.307837	1.114666	1.129434	0.903817	1.114666	
	954	8160.79	28414.64	3.4818486	1.3237624	1.128239	1.483681			954	4482.406	25506.23	5.690299	1.325165	1.129434	0.874266	1.06572	1.109514	
	129	9509.205	27984.22	2.9428559	1.118843	0.953586	1.044612			129	4715.355	25318.13	5.369294	1.250409	1.06572	1.741164	1.034471	2.047324	
	137	7923.548	23908.44	3.0173909	1.1471805	0.977738	1.109972			137	4604.355	25738.06	5.589938	1.301793	1.109514	2.358048	2.278681	1.606599	
	CTRL	9129.548	24013.15	2.630267	1	0.852297	1.208775			CTRL	5069.715	21769.5	4.294029	1	0.852297	1.951409	1.914185	1.249101	
	958	6143.426	23974.58	3.9024779	1.4836813	1.264537	1.139549			958	5322.891	23445.82	4.404714	1.025776	0.874266	1.373854	1.410664	1.482951	
	138	7051.912	29144.69	4.132877	1.5712766	1.339194	0.939285			138	4520.841	23561.99	5.211859	1.213745	1.034471	1.244408	1.441865		
2020-11-04	Sample	Actin	GLT1	GLT1/Actin Norm GLT1	Norm to Total Saline	Average Cortex - norm to TOTS			2020-11-04	Sample	Actin	GLT1	GLT1/Actin Norm GLT1	Norm to Total Saline	Male				
	535	4923.355	13371.69	2.7159717	1.0446119	0.89032	1.173333			535	3872.991	12799.51	3.304813	2.042908	1.741164	1.319816			
	59	4611.477	10876.65	2.3586048	0.9071621	0.773172			59	3199.284	13837.05	4.325044	2.673576	2.278681					
	71	5047.941	14623.53	2.8969297	1.1142116	0.949639			71	3899.991	15155.05	3.885918	2.402125	2.047324					
	CTRL	5216.527	13562.87	2.5999816	1	0.852297			CTRL	4416.456	7144.489	1.617697	0.999998	0.852296					
	860	4017.234	11593.36	2.8859058	1.1099716	0.946025			860	3192.87	14290.29	4.475687	2.766698	2.358048					
	74	4137.82	15255.43	3.6868278	1.4180207	1.208575			74	3712.87	13489.65	3.633214	2.245913	1.914185					
	72	4589.941	12654.43	2.7569919	1.060389	0.903766			72	3489.456	10640.75	3.049401	1.885023	1.606599					
	891	4921.184	15466.26	3.1427921	1.2087747	1.030235			891	3753.406	13902.12	3.703867	2.289588	1.951409					
2020-07-06	Sample	Actin	GLT1	GLT1/Actin Norm GLT1	Norm to Total Saline	Average Cortex - norm to TOTS			2021-07-28	Sample	Actin	GluR1	GluR1/Act Norm GluR1	Norm to Total Saline	Male				
	553	3738.477	12727.58	3.4044829	1.1395492	0.971234	1.128239	1.442032	1.15882		801	5144.891	23106.74	4.491202	1.655132	1.410664			
	497	3655.234	11808.63	3.2306088	1.08135	0.921631	1.264537	0.953586	0.977738	720	4356.648	19056.02	4.374009	1.611943	1.373854				
	570	3480.991	13269.22	3.8119079	1.2759225	1.087465	0.89032	1.339194	0.949639	766	5127.305	23537.09	4.590538	1.69174	1.441865				
	CTRL	4921.698	14703.92	2.9875714	1.0000005	0.852297	1.030235	1.208575	1.087465	768	5107.598	20312.02	3.976824	1.46557	1.249101				
	959	4536.891	12731.34	2.8061811	0.9392855	0.80055	0.971234	0.921631		CTRL	5574.134	15125.53	2.713521	1.000008	0.852304				
	779	3797.991	13348.34	3.5145786	1.1764004	1.002642 bubble on	0.80055			763	5819.134	23054.72	3.961882	1.460063	1.244408				
	997	3872.77	10056.8	2.5967984	0.8692009	0.740817	0.740817			767	5212.376	21902.21	4.201962	1.54854	1.319816				



HIPPOCAMPUS						Average Hippocampus					
2020-04-07	Sample	Actin	GLT1	GLT1/Actin Norm Eph	Norm to TotalSaline	Male					
	997	2847.012	10558.65	3.7086784	1.5354939	1.435041	Saline	50	100		
	129	3888.012	11244	2.8919651	1.1973523	1.119021	1.535494				
	137	4353.305	12724.7	2.922998	1.2102008	1.131029	0.954754				
	CTRL	5298.477	12797.46	2.415309	1.0000037	0.934583	0.831778				
	761	4142.355	9552.338	2.3060163	0.9547536	0.892293	0.882229				
	766	4218.598	8018.681	1.9007929	0.78698	0.735495	1.773036				
	954	4157.598	6318.146	1.5196626	0.6291817	0.58802	0.799219				
	767	4696.305	21634.36	4.6066767	1.9072897	1.782514	repeated 0.776444				
							1.078993				
2020-04-21						Average Hipp - norm to TOTSal					
2020-04-21	Sample	Actin	GLT1	GLT1/Actin Norm Eph	Norm to TotalSaline	Male					
	720	2550.891	9467.288	3.7113652	0.8317783	0.777363	Saline	50	100		
	557	2795.234	7975.267	2.8531661	0.6394417	0.597609	1.435041				
	CTRL	3615.184	16130.82	4.4619646	1	0.934579	0.892293				
	891	3395.113	13364.77	3.9364737	0.8822288	0.824513	0.777363				
	74	3415.891	12489.36	3.6562522	0.8194265	0.765819	1.194237				
	71	4965.426	16778.48	3.3790615	0.7573035	0.70776	1.194237				
	767	5331.477	15424.19	2.893042	0.6483785	0.605961	repeated 1.194237				
2020-04-27						Average Hipp - norm to TOTSal					
2020-04-27	Sample	Actin	GLT1	GLT1/Actin Norm Eph	Norm to TotalSaline	Male					
	535	4691.598	7107.217	1.5148819	1.773036	1.657043	Saline	50	100		
	858	5418.841	7266.167	1.340908	1.5694147	1.466743	0.765819				
	861	6134.669	5843.146	0.9524794	1.1147933	1.041863	0.765819				
	CTRL	5459.184	4664.489	0.8544297	1.0000348	0.934612	0.725648				
2020-07-06						Average Hipp - norm to TOTSal					
2020-07-06	Sample	Actin	GLT1	GLT1/Actin Norm Eph	Norm to TotalSaline	Male					
	553	3655.648	11847.34	3.2408312	0.7992185	0.746933	Saline	50	100		
	497	3609.012	13741.8	3.8076357	0.9389977	0.877568	0.746933				
	570	3579.698	12911.97	3.6070009	0.8895193	0.831326	0.746933				
	CTRL	3953.991	16033.75	4.0550806	1.0000199	0.934598	0.725648				
	556	3673.698	11566.56	3.1484787	0.7764436	0.725648	0.725648				
	552	4699.527	17219.29	3.664047	0.9035874	0.844474	0.844474				
	679	4249.941	16075.53	3.7825302	0.9328065	0.871782	0.871782				

HIPPOCAMPUS						SYNAPTONEUROSOMAL protein GLT1					
2020-04-07	Sample	Actin	GLT1	GLT1/Actin Norm Eph	Norm to TotalSaline	Male					
	59	4472.719	21003.59	4.695934	1.542909	1.429944	Saline	50	100		
	997	4196.891	17991.42	4.286845	1.38688	1.285338	1.285338				
	129	5268.184	24979.4	4.741558	1.5579	1.443837	1.375906				
	137	6394.134	25897.08	4.050131	1.330722	1.233292	1.520366				
	CTRL	6035.598	18369.69	3.043558	1	0.934579	1.54773				
	761	5404.719	24421.08	4.518473	1.484602	1.375906	1.891328				
	766	3794.77	18171.69	4.788615	1.573361	1.458166	2.444776				
	954	4967.891	22527.35	4.53459	1.489898	1.380813	2.279267				
	767	4214.598	25208.64	5.981267	1.935059	1.793382	3.151163				
2020-04-21						Average Hipp - norm to TOTSal					
2020-04-21	Sample	Actin	GLT1	GLT1/Actin Norm Eph	Norm to TotalSaline	Male					
	72	3527.113	17593.72	4.988137	2.185624	2.04264	Saline	50	100		
	720	4647.355	17254.43	3.712742	1.626792	1.520366	1.520366				
	646	3582.698	14810.07	4.133775	1.811273	1.692779	1.692779				
	557	3560.577	11794	3.312383	1.451369	1.356419	1.356419				
	CTRL	5013.113	11441.17	2.282248	1	0.934579	1.54773				
	891	3001.698	11345.12	3.779566	1.656072	1.54773	1.54773				
	74	4812.941	17524.43	3.641106	1.595403	1.491031	1.491031				
	71	3999.062	16682.43	4.171586	1.827841	1.708262	1.708262				
	556	3544.648	16371.43	4.618634	2.023721	1.891328	1.891328				
2020-04-27						Average Hipp - norm to TOTSal					
2020-04-27	Sample	Actin	EphA4	EphA4/Ac Norm Eph	Norm to TotalSaline	Male					
	535	3709.648	14809.72	3.992218	2.637913	2.444776	Saline	50	100		
	497	3786.648	11441.48	3.021533	1.996519	1.850342	1.850342				
	779	4172.012	13333.79	3.19601	2.108186	1.953833	Bubble on GLT1 band				
	CTRL	5778.941	8745.752	1.513383	0.999989	0.934569	0.934569				
	860	3482.406	12983.6	3.728342	2.459329	2.279267	2.279267				
	858	4297.527	11632.95	2.706893	1.788617	1.657662	1.657662				
	861	3827.234	12282.43	3.209218	2.120536	1.965279	1.965279				
2020-04-27						Average Hipp - norm to TOTSal					
2020-04-27	Sample	Actin	GLT1	GLT1/Actin Norm Eph	Norm to TotalSaline	Male					
	CTRL	5976.376	4664.489	0.780488	1.000625	0.935164	Saline	50	100		
	851	5276.497	13993.7	2.652082	3.400105	3.151163	3.151163				
	679	5049.012	15920.77	3.153245	4.042622	3.746638	3.746638				



HIPPOCAMPUS						Female			Total protein GLT1					Average Hippocampus			HIPPOCAMPUS						Female			SYNAPTONEUROSOMAL protein GLT1					Average Hipp - norm to TOTSal								
						Sample			Actin	GLT1	GLT1/Actin Norm GLT1	Norm to Total Saline	Female									Sample			Actin	GLT1	GLT1/Actin Norm GLT1	Norm to Total Saline	Female								Saline	50	100
						526	4728.134	14140.36	2.990685	0.821617	0.810273		0.827494									526	6129.255	24234.84	3.953962	2.415371	2.382023	1.593665			2.382023								
						539	4241.305	14159.95	3.338582	0.917193	0.904529		0.70226									539	5825.426	21463.62	3.684473	2.250747	2.219671	1.593665			2.382023								
						803	3651.184	10997.65	3.012078	0.827494	0.816069		0.882503									803	5165.426	13664.38	2.645354	1.615977	1.593665	1.553562			1.573655								
						CTRL	4628.941	16858.24	3.641921	1.000528	0.986714		0.878417									CTRL	5282.062	8647.995	1.637238	1.000146	0.986337	1.546517			1.240156								
						694	3442.355	16468.05	4.783947	1.314271	1.296125		1.309458									715	5234.891	13674.26	2.612138	1.595686	1.573655	1.324322			1.045706								
						715	3574.82	17950.95	5.021496	1.379532	1.360485		1.384174									716	5391.305	13903.02	2.578785	1.575311	1.553562	1.058716			1.555446								
						78	4381.598	13586.24	3.10075	1.066649	1.051922		0.997384									78	4172.305	17564.09	4.209684	1.811942	1.786925	1.39244											
						500	4185.355	10945.41	2.615169	0.899611	0.88719		Average Hipp - norm to TOTSal									500	4511.426	13180.55	2.921593	1.257519	1.240156	1.18379			1.786925								
						757	4945.477	10096.05	2.04147	0.70226	0.692564		Female									757	4968.426	13855.97	2.788804	1.200363	1.18379	1.546517			1.240156								
						CTRL	5079.648	14768.87	2.90746	1.000158	0.986349		Saline									CTRL	5065.062	11767.7	2.323309	1.000004	0.986197	1.546517			1.240156								
						771	4262.062	11134.58	2.612487	0.898688	0.88628		0.816069									771	4725.012	13011.6	2.753771	1.185284	1.16892	1.546517			1.240156								
						776	5166.376	11722.46	2.268991	0.780527	0.76975	Stripe on	0.692564									776	4454.598	16229.55	3.643326	1.568168	1.546517	1.546517			1.240156								
						134	5333.548	14496.75	2.718032	0.934995	0.922086		0.692564									134	3166.941	15650.97	4.941982	2.127139	2.09777	1.546517			1.240156								
						277	5177.305	10945.63	2.114156	0.727264	0.717223		0.870318									277	3592.184	16207.38	4.511846	1.941999	1.915186	1.546517			1.240156								
						76	4757.891	10927.22	2.296651	0.739901	0.729685		0.866289									76	4133.77	17597.21	4.256939	1.576644	1.554876	1.546517			1.240156								
						61	4096.062	10920.56	2.666112	0.858928	0.847069		1.291378									61	5277.74	15109.82	2.862934	1.060346	1.045706	1.546517			1.240156								
						CTRL	4696.941	14578.27	3.103779	0.999929	0.986123		1.384174									CTRL	5501.891	14867.75	2.702299	1.000851	0.987033	1.546517			1.240156								
						34	3553.184	9131.196	2.569863	0.82792	0.816489		0.986594									34	4042.184	15409.7	3.812222	1.411934	1.39244	1.546517			1.240156								
						36	3556.648	10472.56	2.944503	0.948616	0.935518		1.255954									36	3964.184	16881.48	4.258501	1.577222	1.555446	1.546517			1.240156								
						44	3923.184	10696.97	2.726605	0.878417	0.866289		1.255954									44	5665.012	16420.34	2.898553	1.073538	1.058716	1.546517			1.240156								
						399	3763.355	11686.2	3.10526	1.000406	0.986594		0.866289									399	4375.406	-	-	-	-	Part of band lost at the end of the gel											
						538	3481.577	8406.853	2.414668	1.108663	1.093356	had to increase a lot the exposure, so it was repeated to check. Avarage was done	0.866289									538	3224.648	13071.17	4.053517	1.510252	1.489401	repeated											
						650	2645.991	7305.439	2.760946	1.267652	1.25015	had to increase a lot the exposure, so it was repeated to check. Avarage was done	0.866289									650	3125.113	12912.63	4.131893	1.539453	1.518198	repeated											
						CTRL	4714.062	10267.2	2.177993	0.999997	0.98619		0.866289									CTRL	6039.941	16209.87	2.68378	0.999918	0.986113	1.546517			1.240156								

**Table S2. Differentially expressed genes (DEGs) between RHY100 and saline at ZT4 and ZT14 in female and male brains.**

Table S2A. DEGs at ZT4 in female and male full brains (bulk). The average number of counts per spot in the RHY condition, the log2 fold change in gene expression (RHY relative to saline), and the adjusted p-value (FDR) are shown.

ZT4 FEMALES - Bulk					ZT4 MALES - Bulk				
FeatureID	FeatureName	ZT4RF count average	ZT4RF Log2FoldChange	ZT4RF FDR	FeatureID	FeatureName	ZT4RM count average	ZT4RM Log2FoldChange	ZT4RM FDR
ENSMUSG00000026822	Lcn2	0.869514549	7.041533061	8.25433E-61	ENSMUSG00000048572	Tmem252	0.301522266	3.436333172	9.1296E-40
ENSMUSG00000048572	Tmem252	0.406429199	4.530032722	7.47375E-60	ENSMUSG00000023067	Cdkn1a	0.728708476	2.575387298	2.57076E-38
ENSMUSG000000103034	Gm8797	0.258887137	3.792684066	9.85481E-49	ENSMUSG00000090137	Uba52	1.566705425	-1.592591861	1.9628E-24
ENSMUSG00000023067	Cdkn1a	0.69285752	2.947335022	1.66595E-40	ENSMUSG00000025591	Tma16	0.512623452	1.988273614	2.35032E-22
ENSMUSG00000019970	Sgk1	3.497337024	2.687560996	9.51568E-39	ENSMUSG00000019970	Sgk1	4.075000454	1.783373553	2.35032E-22
ENSMUSG000000090137	Uba52	1.34912461	-2.401030667	5.14977E-35	ENSMUSG00000002910	Arrdc2	0.534338751	1.972320584	2.4024E-22
ENSMUSG00000002831	Plin4	0.199476867	3.566097483	1.18204E-34	ENSMUSG00000026822	Lcn2	0.318965703	3.976808511	4.16514E-21
ENSMUSG00000020713	Gh	0.127476341	-7.064504344	6.30449E-32	ENSMUSG00000020713	Gh	0.00249192	-4.908971261	2.10465E-18
ENSMUSG00000021342	Prl	0.220722924	-7.081251693	2.23951E-30	ENSMUSG00000034936	Arl4d	0.671750315	1.603404159	4.72061E-16
ENSMUSG00000098234	Snhg6	0.114886085	-2.386385158	1.31535E-29	ENSMUSG00000070369	Ilgad	0.129223828	2.216207357	2.98866E-15
ENSMUSG00000070369	Ilgad	0.159345426	3.151600826	5.24894E-27	ENSMUSG00000005705	Agpr	0.004983839	-4.510227569	3.50875E-13
ENSMUSG00000028298	Cga	0.018491938	-7.447204959	3.47791E-26	ENSMUSG0000002831	Plin4	0.238868289	1.677518709	5.54416E-13
ENSMUSG00000002910	Arrdc2	0.566954961	2.328043661	6.44245E-26	ENSMUSG00000045005	Fzd5	0.00961169	-2.579389594	1.37469E-12
ENSMUSG00000038489	Poir2l	0.499675781	-1.987088892	5.278E-24	ENSMUSG00000021025	Nfkbia	0.856864339	1.340768081	1.37469E-12
ENSMUSG00000013902	Ndufb1-ps	3.111366991	-1.934297638	1.40121E-23	ENSMUSG00000027301	Oxt	0.108932484	-4.69224172	4.48353E-12
ENSMUSG00000060143	Gm10076	5.250136714	-1.902615352	7.10562E-23	ENSMUSG00000030880	Poir3e	0.77320704	1.370673745	4.48353E-12
ENSMUSG00000074170	Plekhh1	0.270297057	2.317786142	2.535E-21	ENSMUSG00000024907	Gal	0.187961932	-2.177349175	4.48353E-12
ENSMUSG00000067288	Rps28	5.370924481	-1.780213169	4.0999E-20	ENSMUSG00000022114	Spry2	0.076181541	-1.450285029	1.73023E-11
ENSMUSG00000028998	Tomm7	1.962899585	-1.767832341	9.48946E-20	ENSMUSG00000027483	Bpifa1	0.000355989	-5.417118165	2.99229E-11
ENSMUSG00000104960	Snhg8	0.660201544	-1.74573269	8.21573E-19	ENSMUSG00000028298	Cga	0.001423954	-7.861166751	4.38548E-11
ENSMUSG00000097383	1500026H17Rik	0.05941027	-2.058365498	8.21573E-19	ENSMUSG00000074170	Plekhh1	0.279450979	1.45531296	6.23744E-11
ENSMUSG00000064360	mt-Nd3	10.14420525	-1.719382457	8.21573E-19	ENSMUSG00000017697	Ada	0.07155369	2.182199629	4.90995E-10
ENSMUSG00000034936	Arl4d	0.535085876	1.900401307	5.34175E-18	ENSMUSG00000031431	Tsc22d3	2.740755525	1.11920956	6.33229E-10
ENSMUSG00000016427	Ndufa1	1.936145291	-1.659049331	1.88339E-17	ENSMUSG00000009630	Ppp2cb	0.106796552	-1.263871905	1.28236E-09
ENSMUSG00000046516	Cox17	1.957784794	-1.64535227	3.4674E-17	ENSMUSG00000031962	Cdh15	0.106796552	1.757607823	1.67321E-09
ENSMUSG00000030711	Sult1a1	0.318690853	1.827894918	1.92996E-16	ENSMUSG00000025509	Pnpla2	0.626183786	1.17771458	2.59802E-09
ENSMUSG00000021025	Nfkbia	0.755415354	1.711700349	2.58374E-16	ENSMUSG00000064220	Hist2h2aa1	0.021003322	-1.807908118	5.91358E-09
ENSMUSG00000079641	Rpl39	5.942994234	-1.560340603	1.34817E-15	ENSMUSG00000024066	Xdh	0.141327438	1.519066737	9.67857E-09
ENSMUSG00000074754	Smim26	0.540987559	-1.594941394	1.78564E-15	ENSMUSG00000041378	Cldn5	0.380551715	-1.087303393	1.2652E-08
ENSMUSG00000090733	Rps27	6.487522802	-1.550998544	2.17679E-15	ENSMUSG00000000567	Sox9	0.158414886	-1.137164273	1.59906E-08
ENSMUSG00000034892	Rps29	14.23525153	-1.516695694	9.24708E-15	ENSMUSG00000005693	Ces1d	0.002135931	-5.50861652	4.77881E-08
ENSMUSG00000071528	Atp5md	11.92572646	-1.513851646	9.87152E-15	ENSMUSG00000034579	Pla2g3	0.072265667	1.795875558	1.76116E-07
ENSMUSG00000038803	Ost4	0.446560639	-1.551390547	1.09321E-14	ENSMUSG00000025217	Btrc	0.445697612	1.092692821	2.16421E-07
ENSMUSG00000021290	Atp5mpl	4.967249401	-1.507785787	1.40945E-14	ENSMUSG00000040856	Dlk1	0.199709553	-1.11979411	2.36065E-07
ENSMUSG00000020018	Snrpf	0.538626886	-1.556548426	1.46713E-14	ENSMUSG00000024659	Anxa1	0.009967678	-2.4499081	2.52211E-07
ENSMUSG00000048489	Depp1	0.072000526	2.717646113	4.31224E-14	ENSMUSG00000022146	Osmr	0.074757587	1.719018523	3.65805E-07
ENSMUSG00000024222	Fkbp5	0.474101824	1.595521958	4.9092E-14	ENSMUSG00000019960	Dusp6	0.184758036	-1.021676146	3.91831E-07
ENSMUSG00000050370	Ch25h	0.033442867	4.942277007	4.9398E-14	ENSMUSG00000024222	Fkbp5	0.51547136	1.042977372	5.347E-07
ENSMUSG00000030880	Poir3e	0.710562568	1.632643164	5.23942E-14	ENSMUSG00000089661	Mia	0.124595978	-1.612842636	5.3474E-07
ENSMUSG00000057322	Rpl38	16.00024803	-1.471016733	5.23942E-14	ENSMUSG00000038059	Smim3	0.285146795	1.128802235	6.07004E-07
ENSMUSG000000025739	Gng13	1.678045045	-1.487478096	5.2036E-14	ENSMUSG00000096768	Gm47283	1.410782458	-0.6882580924	7.69614E-07
ENSMUSG00000035674	Ndufa3	4.461671937	-1.470225982	5.94352E-14	ENSMUSG00000090247	Bloc1s1	0.29582645	-0.940680121	1.17646E-06
ENSMUSG00000060981	Hist1h4h	0.044065896	-1.886201207	7.61688E-14	ENSMUSG00000026051	Ecrq4	0.220356887	-1.537598541	1.37974E-06
ENSMUSG000000071637	Cebpδ	0.68066071	1.593922162	8.03251E-14	ENSMUSG00000066687	Zbtb16	0.046990483	2.05320177	1.37974E-06
ENSMUSG00000064220	Hist2h2aa1	0.022819839	-2.161040441	1.22362E-13	ENSMUSG00000020954	Strn3	0.158770875	1.244054902	1.79836E-06
ENSMUSG00000095366	Gm21860	0	-5.876305171	1.52615E-13	ENSMUSG00000048108	Tmem72	0.008899713	-2.301640948	1.96757E-06
ENSMUSG00000041841	Rpl37	14.41269545	-1.419407427	4.65333E-13	ENSMUSG000000048450	Msx1	0.043074609	-1.377151758	2.75133E-06
ENSMUSG00000017778	Cox7c	11.1010647	-1.413577968	5.82646E-13	ENSMUSG00000023043	Krt18	0.025631173	-1.537148869	3.27024E-06
ENSMUSG00000062997	Rpl35	6.179848423	-1.409445665	7.17019E-13	ENSMUSG00000021250	Fos	0.064077931	-1.158858265	4.39028E-06
ENSMUSG00000050856	Atp5k	7.013952877	-1.404559388	8.58855E-13	ENSMUSG00000003962	Kcne2	0.024563207	-2.051600802	4.76489E-06
ENSMUSG00000042737	Dpm3	0.733775852	-1.443213218	1.05969E-12	ENSMUSG00000056174	Col8a2	0.020647333	-1.564222459	4.80369E-06
ENSMUSG00000078974	Sec61g	2.879234148	-1.388304776	2.04433E-12	ENSMUSG00000098234	Snhg6	0.198285599	-0.934446545	5.64636E-06
ENSMUSG00000028407	Smim27	0.158951981	-1.527265997	2.39313E-12	ENSMUSG00000021903	Hist15	0.072265667	1.554867459	5.64636E-06
ENSMUSG00000039001	Rps21	18.02098411	-1.371409727	3.1534E-12	ENSMUSG00000056380	Gpr50	0.009967678	-2.144099671	5.64636E-06

ENSMUSG00000037095	Lrg1	0.082230109	2.457668266	5.0485E-12	ENSMUSG00000060143	Gm10076	4.767042114	-0.807162958	6.59757E-06
ENSMUSG00000025591	Tma16	0.346232037	1.557543474	6.07736E-12	ENSMUSG00000061517	Sox21	0.03346292	-1.349762897	6.59757E-06
ENSMUSG00000038059	Smim3	0.360789521	1.475719546	1.64738E-11	ENSMUSG00000062960	Kdr	0.035598851	-1.440730722	6.64928E-06
ENSMUSG00000023153	Tmem52	0.092066246	2.000211776	1.80994E-11	ENSMUSG00000005057	Sh2b2	0.140615461	1.212238455	7.118E-06
ENSMUSG00000020108	Ddit4	0.682234492	1.433334527	1.83573E-11	ENSMUSG00000020108	Ddit4	0.792074431	0.913042782	7.43314E-06
ENSMUSG00000005057	Sh2b2	0.153443744	1.769485045	2.17421E-11	ENSMUSG00000021506	Pitx1	0.000355989	-5.35571762	9.15131E-06
ENSMUSG00000031431	Tsc22d3	2.495624788	1.322760872	3.24659E-11	ENSMUSG00000086765	Gm11827	0.021715299	3.122040646	1.15526E-05
ENSMUSG00000100916	Lhb	0.000393445	-5.680384961	3.33812E-11	ENSMUSG00000027525	Phactr3	1.849716289	0.859359069	1.21847E-05
ENSMUSG00000027364	Usp50	0.052328251	-1.643507692	3.82257E-11	ENSMUSG00000048489	Depp1	0.056602173	1.734884928	1.27795E-05
ENSMUSG00000073412	Lst1	0.094033474	-1.50980404	4.54067E-11	ENSMUSG00000064360	mt-Nd3	16.7403596	-0.784468461	1.33429E-05
ENSMUSG00000017697	Ada	0.069246407	2.246652208	8.54096E-11	ENSMUSG00000021848	Otx2	0.046990483	-1.203137984	1.34594E-05
ENSMUSG00000093565	Rab26os	0.03934455	-1.704338138	8.54096E-11	ENSMUSG00000078640	Gm11627	0.171586461	1.11739343	1.39575E-05
ENSMUSG00000021903	Galnt15	0.056262706	2.226505635	1.03519E-10	ENSMUSG00000016024	Lbp	0.061942	-1.226434603	2.17263E-05
ENSMUSG00000090247	Bloc1s1	0.23764108	-1.374195906	1.09E-10	ENSMUSG00000045337	Defb11	0.009255701	-1.910158176	2.17263E-05
ENSMUSG00000038570	Saxo2	0.143214161	-1.406863322	1.59074E-10	ENSMUSG00000021390	Ogn	0.033818908	-1.366134236	2.18737E-05
ENSMUSG00000016252	Atp5e	7.407398375	1.271103734	1.6124E-10	ENSMUSG00000021453	Gadd45g	0.756831568	0.884826752	2.23606E-05
ENSMUSG00000042541	Sem1	1.563552406	-1.281022485	1.61632E-10	ENSMUSG00000095845	Gm5741	0.246344048	-1.518272117	2.25552E-05
ENSMUSG00000064356	mt-Atp8	1.61824133	-1.285016592	1.61632E-10	ENSMUSG00000048583	Igf2	0.212525139	-1.100007086	2.26312E-05
ENSMUSG00000057278	Snrpg	1.47581406	-1.274398194	2.13945E-10	ENSMUSG00000066196	Spag8	0.019223379	-1.510227569	2.82838E-05
ENSMUSG00000089665	Fcor	0.204591659	-1.355685117	2.98945E-10	ENSMUSG00000036169	Sostdc1	0.087217185	-1.315905914	3.1342E-05
ENSMUSG00000079523	Tmsb10	10.82329218	-1.255320642	3.35808E-10	ENSMUSG00000020660	Pomc	0.146311277	-1.69061957	3.15718E-05
ENSMUSG00000046330	Rpl37a	8.860392595	-1.249458433	3.58252E-10	ENSMUSG00000066363	Serpina3f	0.013527563	4.453246555	4.10844E-05
ENSMUSG00000056023	Gm9989	0.035016649	-1.687942921	4.18119E-10	ENSMUSG00000034227	Foxj1	0.079029449	-1.134543573	4.12766E-05
ENSMUSG00000087687	Pet100	0.983220297	-1.251557804	5.86739E-10	ENSMUSG00000028294	Cfap206	0.018867391	-1.503532917	4.29179E-05
ENSMUSG00000024778	Fas	0.083803891	1.79804762	7.9994E-10	ENSMUSG00000031875	Cmtm3	0.97317726	0.505313E-05	5.05313E-05
ENSMUSG00000025509	Pnpla2	0.643676833	1.314288986	8.39378E-10	ENSMUSG00000051367	Six1	0.001423954	-3.154083759	5.33756E-05
ENSMUSG00000090101	Snhg9	0.084984227	-1.43897021	8.66369E-10	ENSMUSG00000038418	Egr1	0.549646257	-0.814303788	5.72994E-05
ENSMUSG00000014313	Cox6c	15.7456888	-1.223496121	8.76123E-10	ENSMUSG00000024610	Cd74	0.072265667	-1.50402623	5.85769E-05
ENSMUSG00000036372	Tmem258	1.217320368	-1.242329735	9.04911E-10	ENSMUSG00000005994	Tyfp1	0.005339828	-2.189707669	6.04408E-05
ENSMUSG00000034579	Pla2g3	0.068066071	2.020356292	1.43156E-09	ENSMUSG00000066720	Cldn9	0.003915874	-2.861903008	6.06954E-05
ENSMUSG00000096956	Snhg18	0.056262706	-1.539671881	2.05925E-09	ENSMUSG00000099553	Gm29538	0.006407793	-2.04365979	8.82731E-05
ENSMUSG00000047721	Bola2	1.661126889	-1.208119541	2.20024E-09	ENSMUSG00000025915	Sgk3	0.273399174	0.934505161	8.88497E-05
ENSMUSG00000057863	Rpl36	7.552579763	-1.198733477	2.21783E-09	ENSMUSG00000039202	Abhd2	0.171586461	-0.858790791	9.47284E-05
ENSMUSG00000045394	Epcam	0.003934455	-3.167514083	2.41404E-09	ENSMUSG00000022595	Lypd2	0.00249192	-3.002806666	9.56135E-05
ENSMUSG00000031760	Mt3	16.58136703	-1.186344046	3.43045E-09	ENSMUSG00000028341	Nr4a3	0.092201024	-0.954446094	9.77541E-05
ENSMUSG00000021040	Slirp	0.707415004	-1.199787942	4.83897E-09	ENSMUSG00000024903	Lao1	0.012815586	4.377297701	9.77541E-05
ENSMUSG00000093674	Rpl41	15.30857085	-1.174366262	5.10875E-09	ENSMUSG00000075224	Rrc55	0.153774036	-1.059774387	0.000101629
ENSMUSG00000097162	2310010J17Rik	0.079082545	-1.393098607	7.19531E-09	ENSMUSG00000032246	Calml4	0.112848357	-1.253982329	0.000101629
ENSMUSG00000070394	Tmem256	1.918046799	-1.173919808	7.36663E-09	ENSMUSG00000043020	Wdr63	0.004627851	-2.516653839	0.000112127
ENSMUSG00000027857	Tshb	0.001967227	-7.457445961	1.17424E-08	ENSMUSG00000024835	Coro1b	0.061230023	-1.034152057	0.000122781
ENSMUSG00000067847	Romo1	1.99476867	-1.15845149	1.22189E-08	ENSMUSG00000087627	A230059L01Rik	0.030971	-1.255367095	0.000123194
ENSMUSG00000024066	Xdh	0.127869787	1.507188401	1.35919E-08	ENSMUSG00000023964	Calcr	0.015307506	-1.542649047	0.000123194
ENSMUSG00000073616	Cops9	5.005413615	-1.146708051	1.50878E-08	ENSMUSG00000001827	Folr1	0.084369276	-1.346728837	0.000123194
ENSMUSG00000030677	Kif22	0.10662373	-1.311408293	1.51529E-08	ENSMUSG00000032231	Anxa2	0.122104058	-0.93367916	0.000123194
ENSMUSG00000066363	Serpina3f	0.024393621	4.493292175	1.51529E-08	ENSMUSG00000052974	Cyp2f2	0.000355989	-6.154083759	0.000126909
ENSMUSG00000091050	9330020H09Rik	0.059803716	-1.416424464	1.75697E-08	ENSMUSG00000092035	Peg10	0.071909679	-1.012309798	0.000127046
ENSMUSG00000004131	Ccnb1	0.014557483	-1.917884275	1.99112E-08	ENSMUSG00000030087	Klf15	0.487704256	0.844023354	0.000127046
ENSMUSG000000224175	Tekt4	0.068066071	1.762558535	2.04384E-08	ENSMUSG00000020424	Castor1	0.104304633	1.158063315	0.000140193
ENSMUSG00000065947	mt-Nd4l	2.777331764	-1.13767356	2.42635E-08	ENSMUSG00000041323	Ak7	0.022427276	-1.587043166	0.000144921
ENSMUSG00000031875	Cmtm3	0.303346478	1.267167035	2.6655E-08	ENSMUSG00000073421	H2-Ab1	0.028123092	-1.498912256	0.000184153
ENSMUSG00000035048	Anapc13	1.048138804	-1.14252972	2.6655E-08	ENSMUSG00000052384	Nrros	0.134919645	1.051199417	0.000186427
ENSMUSG00000112639	A730063M14Rik	0.028328076	-1.616091284	3.00992E-08	ENSMUSG00000118506	1700094D03Rik	0.122104058	-1.106330628	0.000188448
ENSMUSG00000068240	Gm11808	0.335215564	-1.17594599	3.15183E-08	ENSMUSG00000028645	Slc2a1	1.699489138	0.76342051	0.000192821
ENSMUSG00000058351	Smim4	0.310428497	-1.181709025	3.68849E-08	ENSMUSG00000059325	Hopx	0.184402047	-0.843232072	0.000192821
ENSMUSG00000050288	Fzd2	0.175870137	1.34608725	4.37185E-08	ENSMUSG00000054360	Bsx	0.002135931	-2.72524046	0.000214234
ENSMUSG00000037152	Ndufc1	4.966069065	-1.106169324	5.60726E-08	ENSMUSG00000031167	Rbm3	2.736127674	0.746252951	0.000223529
ENSMUSG00000060636	Rpl35a	11.53975643	-1.104369	5.60726E-08	ENSMUSG00000038007	Acer2	0.166602622	0.986006013	0.000228951
ENSMUSG00000078747	Gm20878	0.044065896	-1.445168499	6.60183E-08	ENSMUSG00000033737	Fndc3c1	0	-5.291587283	0.000236008
ENSMUSG00000078784	Rbis	1.390436387	-1.109239496	6.6794E-08	ENSMUSG00000045394	Epcam	0.004627851	-3.002806666	0.000264381
ENSMUSG00000020163	Uqcrr11	7.338545413	-1.091994166	8.61124E-08	ENSMUSG00000024053	Emilin2	0.119968127	1.109292153	0.000285141
ENSMUSG00000033715	Akr1c14	0.003147564	-3.051028341	8.7689E-08	ENSMUSG00000034467	Dynlrb2	0.090421081	-1.272430455	0.000296056
ENSMUSG00000109118	Gm32031	0.042492114	-1.439179953	1.13337E-07	ENSMUSG00000054160	Nkx2-4	0.006407793	-1.976545574	0.000307222
ENSMUSG00000021506	Pitx1	0	-5.068950249	1.15238E-07	ENSMUSG00000031737	Irx5	0.011391632	-1.620651559	0.000314815

ENSMUSG00000027525	Phactr3	1.80434105	1.103178062	1.34584E-07	ENSMUSG00000068323	Slc4a5	0.019223379	-1.477060706	0.000351498
ENSMUSG00000022146	Osmr	0.063738171	1.749263189	1.358E-07	ENSMUSG00000110500	Gm32568	0.013527563	3.453246555	0.000376839
ENSMUSG00000058626	Capn11	0.002360673	-2.998560921	1.43649E-07	ENSMUSG00000024175	Tekt4	0.082589334	1.174049485	0.000421777
ENSMUSG000000038690	Atp5j2	8.296191753	-1.063626771	2.15611E-07	ENSMUSG00000074637	Sox2	0.373787934	-0.7371246649	0.000431586
ENSMUSG00000085035	Gm12031	0.014164038	-1.829123234	2.4187E-07	ENSMUSG00000050105	Grrp1	0.151651105	0.975199258	0.000431586
ENSMUSG00000079435	Rpl36a	4.480950767	-1.058979843	2.67751E-07	ENSMUSG00000089809	Rasgef1b	0.26485545	-0.756625454	0.000431586
ENSMUSG00000028645	Slc2a1	1.499814235	1.087042838	3.3358E-07	ENSMUSG00000071497	Nutf2-ps1	0.022427276	-1.291587283	0.000434378
ENSMUSG00000028655	Mfsd2a	0.464659132	1.12311373	3.71767E-07	ENSMUSG00000022194	Pabpn1	0.701297361	0.763828242	0.00045181
ENSMUSG00000046768	Rhoj	0.110164739	1.467216748	4.32626E-07	ENSMUSG00000035615	Frrmpd1	0.211813162	0.887166969	0.000568897
ENSMUSG000000087336	Gm15860	0.049967578	-1.341968743	4.40353E-07	ENSMUSG00000027857	Tshb	0.001423954	-5.168439052	0.000585174
ENSMUSG00000106918	Mrp133	1.156336316	-1.052720307	4.54798E-07	ENSMUSG00000023153	Tmem52	0.067281828	1.245846848	0.000586609
ENSMUSG00000110156	Gm42067	0.180984929	-1.151064646	4.55776E-07	ENSMUSG00000022376	Adcy8	0.101812713	-0.862005592	0.000627491
ENSMUSG00000023089	Ndufa5	5.289087818	-1.039316174	4.88508E-07	ENSMUSG00000042607	Asb4	0.027055127	-1.209225313	0.000679898
ENSMUSG00000020424	Castor1	0.116853313	1.34286335	5.89433E-07	ENSMUSG00000068566	Myadm	0.103592656	-0.851784471	0.000685141
ENSMUSG000000087590	Epb411aaos	0.279739748	-1.099248849	5.90408E-07	ENSMUSG00000033453	Soxh15	0.048414437	-1.0195258	0.000685141
ENSMUSG000000019689	Fmc1	1.135090259	-1.04237929	6.24909E-07	ENSMUSG00000043102	Qrfp	0.022783265	3.190212149	0.000693471
ENSMUSG00000053113	Socs3	0.062164389	1.658970206	6.24909E-07	ENSMUSG00000045903	Npas4	0.021715299	-1.28735029	0.000718836
ENSMUSG00000006360	Crip1	0.212067123	-1.305017607	6.76147E-07	ENSMUSG00000034640	Tiparp	0.198997576	0.887736416	0.000728276
ENSMUSG000000028862	Map3k6	0.132197687	1.297907189	6.89845E-07	ENSMUSG00000050335	Lgals3	0.026699138	-1.198937995	0.000728276
ENSMUSG00000025362	Rps26	7.840581867	-1.020553956	8.50403E-07	ENSMUSG00000050370	Ch25h	0.031682977	1.85234251	0.000764233
ENSMUSG00000059534	Uqcr10	6.645294447	-1.013983329	1.05263E-06	ENSMUSG00000047793	Sned1	0.032038966	-1.131715946	0.00076572
ENSMUSG000000085255	Taco1os	0.036590431	-1.394284945	1.11407E-06	ENSMUSG00000020922	Lsm12	0.259159634	0.838415552	0.00076572
ENSMUSG00000041481	Serpina3g	0.033049422	2.340440687	1.15979E-06	ENSMUSG00000045382	Cxcr4	0.003203897	-2.317582492	0.000813882
ENSMUSG00000030087	Klf15	0.472134597	1.085442482	1.22572E-06	ENSMUSG00000075514	Gm13375	0.06443392	1.249374221	0.000813882
ENSMUSG00000025058	Rplp2	6.015388206	-1.006321193	1.31949E-06	ENSMUSG00000019997	Ccn2	0.065857874	-1.08741272	0.000815926
ENSMUSG00000025915	Sgk3	0.249444445	1.197268413	1.34258E-06	ENSMUSG00000017723	Wfdc2	0.025275184	-1.507720714	0.000886336
ENSMUSG00000052384	Nrros	0.127869787	1.28983157	1.39616E-06	ENSMUSG00000046470	Sox18	0.009255701	-1.662230663	0.000886336
ENSMUSG000000086765	Gm11827	0.024000175	2.595739444	1.83032E-06	ENSMUSG00000096225	Lhx8	0.036666816	1.698359052	0.000900497
ENSMUSG00000017662	Gm4013	0.016131265	-1.666579161	1.99355E-06	ENSMUSG00000054256	Msi1	0.067281828	-0.955787013	0.000989788
ENSMUSG000000085241	Snhg3	0.340330355	-1.040914096	2.36533E-06	ENSMUSG00000027435	Cd9j	0.02634315	-1.188299475	0.001005291
ENSMUSG00000034634	Ly6d	0.030688749	2.234830499	2.36533E-06	ENSMUSG00000079436	Kcnj13	0.038446759	-1.321359182	0.001044993
ENSMUSG00000010406	Mrp152	1.613126538	-0.993156682	2.48107E-06	ENSMUSG00000032303	Chrna3	0.077961483	-1.225721633	0.001111663
ENSMUSG00000062006	Rpl34	10.31810816	-0.978616387	2.95411E-06	ENSMUSG00000021806	Nid2	0.012103609	-1.560853643	0.001121292
ENSMUSG000000084786	Ubl5	4.550197174	-0.980208298	2.96554E-06	ENSMUSG00000022425	Enpp2	3.57946445	-0.788756498	0.001127579
ENSMUSG00000102014	2900009J06Rik	0.038557659	-1.335757818	2.99722E-06	ENSMUSG00000030125	Lrrc23	0.021715299	-1.252998785	0.001128426
ENSMUSG00000053332	Gas5	5.640434647	-0.978123652	3.20372E-06	ENSMUSG00000027597	Ahcy	0.081877357	-0.869149872	0.001256925
ENSMUSG000000108668	Gm32816	0.003541009	-2.50783449	3.24725E-06	ENSMUSG00000039155	Cdh26	0.008187736	-1.706624782	0.001256925
ENSMUSG00000030827	Fgf21	0.012983701	4.188437594	4.52289E-06	ENSMUSG00000048416	Mif1	0.054466242	-1.049184901	0.001271011
ENSMUSG00000045106	Ccdc73	0.030688749	-1.402599421	4.6959E-06	ENSMUSG00000017144	Rnd3	0.068705782	-0.897578739	0.00139399
ENSMUSG000000041378	Cldn5	0.288788995	-1.048965874	4.72941E-06	ENSMUSG00000036598	Ccdc113	0.039158736	-1.037739798	0.00139399
ENSMUSG00000024018	Ccdc167	0.277772521	-1.020298631	5.5073E-06	ENSMUSG00000020182	Ddc	0.378415784	0.771915659	0.001396689
ENSMUSG00000050105	Grrp1	0.15816509	1.17064828	5.59129E-06	ENSMUSG00000071637	Cebpd	0.44142575	0.765651636	0.001396689
ENSMUSG00000002289	Angptl4	0.097967929	1.338838583	6.40808E-06	ENSMUSG00000015652	Steap1	0.017443437	-1.358224476	0.001402833
ENSMUSG00000021453	Gadd45g	0.871088331	0.9840453	7.96896E-06	ENSMUSG00000027985	Lef1	0.187605944	-0.767901123	0.001424238
ENSMUSG00000114639	Gm31946	0.017311602	-1.567043488	8.11466E-06	ENSMUSG00000031492	Chrn3	0.020291345	-1.259576888	0.001424238
ENSMUSG00000002416	Ndufb2	4.409343686	-0.939200546	8.13328E-05	ENSMUSG00000006386	Tek	0.046990483	-0.986326594	0.001500136
ENSMUSG00000096887	Gm20594	0.012590256	-1.700121179	1.06054E-05	ENSMUSG00000070436	Serpinh1	0.166246633	-0.765921966	0.001500136
ENSMUSG00000084883	Ccdc85c	0.06295128	-1.175438683	1.07705E-05	ENSMUSG00000022096	Hr	0.159482852	0.890953129	0.001500136
ENSMUSG000000086943	4732414G09Rik	0.022426393	-1.458896767	1.09512E-05	ENSMUSG00000000530	Acvr11	0.07155369	-0.881303314	0.001580084
ENSMUSG000000098120	Gm5914	0.149902734	-1.042695608	1.0983E-05	ENSMUSG00000028023	Pitx2	0.006763782	-2.064816421	0.001602432
ENSMUSG00000050423	Ppp1r3g	0.207345777	1.100974753	1.13638E-05	ENSMUSG000000052957	Gas1	0.046634495	-0.977586104	0.001609231
ENSMUSG00000046991	Wdr27	0.038951104	-1.277536871	1.13638E-05	ENSMUSG00000062456	Rpl9-ps6	0.108220506	-0.803491906	0.001660928
ENSMUSG00000070637	Srarp	0.166427445	1.13540825	1.2508E-05	ENSMUSG00000026546	Cfap45	0.033818908	-1.080083178	0.001673196
ENSMUSG00000014294	Ndufa2	4.822854904	-0.92127175	1.64541E-05	ENSMUSG00000045690	Wdr89	0.07867346	-0.85791876	0.001763808
ENSMUSG00000000739	Sult5a1	0.019278829	-1.5125569	2.11233E-05	ENSMUSG00000050423	Ppp1r3g	0.184758036	0.859295271	0.001857368
ENSMUSG000000084843	B230312C02Rik	0.029114967	-1.32841804	2.34453E-05	ENSMUSG00000030888	Rr2b	0.161974771	0.871451333	0.001920228
ENSMUSG00000054312	Mrs21	2.19660621	-0.913037722	2.35774E-05	ENSMUSG00000036594	H2-Aa	0.032750943	-1.42227987	0.001920228
ENSMUSG00000038357	Camp	0	-4.757006243	2.47341E-05	ENSMUSG00000075602	Ly6a	1.323921262	0.690194859	0.001984644
ENSMUSG00000028967	Erfri1	0.381642132	1.015873616	2.49489E-05	ENSMUSG00000084989	Crocc2	0.002847908	-2.306086853	0.002085562
ENSMUSG00000074218	Cox7a1	0.121968104	-1.050796378	2.51183E-05	ENSMUSG00000064057	Scgb3a1	0.01673146	2.430878316	0.002085562
ENSMUSG00000024038	Ndufv3	3.736158441	-0.907733771	2.51183E-05	ENSMUSG00000017754	Pltp	0.673174269	-0.686239901	0.002099188
ENSMUSG00000052974	Cyp2f2	0.000786891	-3.401525588	2.88874E-05	ENSMUSG00000003477	Inmt	0.012103609	-1.484232361	0.002110706
ENSMUSG000000087627	A230059L01Rik	0.013770592	-1.599464966	3.00443E-05	ENSMUSG00000058488	Kl	0.117832196	-1.14361676	0.002201363

ENSMUSG00000034390	Cmip	0.142820715	1.100974753	3.67067E-05	ENSMUSG00000039543	Cfap70	0.006407793	-1.793681517	0.002201363
ENSMUSG00000024517	Grp	0.301772696	1.06022841	4.26963E-05	ENSMUSG00000035202	Lars2	1.8493603	-0.629160652	0.002504385
ENSMUSG000000048603	Gm9828	0.02360673	-1.369167346	4.71687E-05	ENSMUSG00000034738	Nostrin	0.084369276	1.040294286	0.002515591
ENSMUSG000000087269	D330023K18Rik	0.120787768	-1.007278138	4.8092E-05	ENSMUSG00000024176	Sox8	0.368448106	0.745860771	0.002515972
ENSMUSG000000062960	Kdr	0.026754294	-1.337395251	5.35042E-05	ENSMUSG00000052861	Dnah6	0.02135931	-1.223346422	0.002533174
ENSMUSG000000080727	C920021113Rik	0.024787066	-1.341968743	5.42366E-05	ENSMUSG00000019982	Myb	0.004271862	-2.038606542	0.002593861
ENSMUSG000000086841	2410006H16Rik	1.120532776	-0.890136156	5.42366E-05	ENSMUSG00000024778	Fas	0.066213863	1.129776295	0.002593861
ENSMUSG00000056313	Tcim	0.041311777	1.543492988	6.832E-05	ENSMUSG00000025795	Rassf3	0.190097863	-0.708339797	0.002892749
ENSMUSG00000045996	Poir2k	1.397518406	-0.874660699	7.82529E-05	ENSMUSG00000097451	Rian	2.419297902	0.642907993	0.002892749
ENSMUSG00000038393	Txnip	0.333641782	0.981972556	7.89443E-05	ENSMUSG00000044177	Wfikkn2	0.015307506	-1.326920356	0.00297103
ENSMUSG00000038717	Atp5l	8.397700691	-0.863512856	7.98101E-05	ENSMUSG00000049382	Krt8	0.010679655	-1.521815544	0.003016929
ENSMUSG00000022820	Ndufb4	5.208824937	-0.864342215	8.01877E-05	ENSMUSG00000073079	Srp54a	0.213949093	-0.69393301	0.0030698
ENSMUSG00000004328	Hif3a	0.049180687	1.434398486	8.91632E-05	ENSMUSG00000037235	Mxd4	0.904566799	0.661010473	0.003077909
ENSMUSG00000073702	Rpl3l	5.579450595	-0.858115841	9.46912E-05	ENSMUSG00000043164	Tmem212	0.111068415	-1.225131401	0.003114902
ENSMUSG00000078879	Zfp973	0.003541009	-2.277536871	0.000100197	ENSMUSG00000030093	Wnt7a	0.077249506	-0.832155664	0.003200154
ENSMUSG000000047369	Dnah14	0.055475815	1.57829653	0.000104079	ENSMUSG00000018569	Cldn7	0.001067966	-3.080083178	0.003200154
ENSMUSG00000052296	Ppp6r1	0.209313004	-0.925841912	0.000105902	ENSMUSG00000061808	Ttr	28.66526265	-1.313820279	0.003200154
ENSMUSG00000024903	Lao1	0.009442692	3.744830942	0.000110064	ENSMUSG00000023267	Gabbr2	0.039514724	1.390236757	0.00344292
ENSMUSG00000072844	G530011O06Rik	0.079869436	1.218811243	0.000113581	ENSMUSG00000015812	Degs2	0.004271862	-4.515420239	0.00344292
ENSMUSG00000047021	Cfap65	0.033049422	1.652384694	0.000116238	ENSMUSG00000026638	Irf6	0.001067966	-2.919618506	0.00346215
ENSMUSG00000022114	Spry2	0.049967578	-1.108478613	0.000126035	ENSMUSG00000031170	Slc38a5	0.029191058	-1.086472853	0.00346215
ENSMUSG00000042312	S100a13	0.841579918	-0.871460239	0.000136403	ENSMUSG00000021263	Degs2	0.019935356	-1.247193164	0.003530133
ENSMUSG000000063714	Sp3os	0.18964073	-0.922725083	0.000136573	ENSMUSG00000032135	Mcarn	0.110356438	-0.780203585	0.003535109
ENSMUSG00000079480	Pin4	0.998171226	-0.853698233	0.000146024	ENSMUSG00000059991	Nptx2	0.404758934	-0.65571879	0.003682426
ENSMUSG00000039960	Rhou	0.774300738	0.879315222	0.000146285	ENSMUSG00000026579	F5	0.025987161	-1.377589801	0.004050323
ENSMUSG00000026500	Cox20	0.920662463	-0.853638973	0.000154244	ENSMUSG00000000275	Trim25	0.030971	-1.045149388	0.004050323
ENSMUSG00000022861	Dgkg	0.029114967	1.744830942	0.000155836	ENSMUSG00000044988	Ucn3	0.017799425	2.255307177	0.004050323
ENSMUSG00000032807	Alox12b	0.032655976	1.63531118	0.000161436	ENSMUSG00000037086	Prr32	0.019223379	-1.24062051	0.004149169
ENSMUSG00000020954	Strn3	0.111345076	1.100974753	0.000169339	ENSMUSG00000021913	Ogdhl	0.223916772	-0.675054703	0.004271098
ENSMUSG00000039911	Spsb1	0.202624431	0.993260935	0.000172519	ENSMUSG00000048234	Rnf149	0.060518046	1.126265232	0.004479799
ENSMUSG00000070858	Gm1673	2.592018935	-0.837748455	0.000174248	ENSMUSG00000050288	Fzd2	0.217864967	0.769376117	0.004479799
ENSMUSG00000051243	Islr2	0.254559237	0.933030115	0.000189654	ENSMUSG00000087211	Lhx1os	0.07155369	1.044696105	0.004513917
ENSMUSG00000055148	Klf2	0.281706976	0.939345635	0.000191847	ENSMUSG00000039004	Bmp6	0.066213863	-0.870223705	0.004513917
ENSMUSG00000051439	Cd14	0.061377498	1.351201382	0.00019471	ENSMUSG00000027654	Fam83d	0.06443392	1.15207702	0.004573007
ENSMUSG00000054256	Msi1	0.026754294	-1.249932409	0.000213737	ENSMUSG00000043415	Otd1d	0.117120219	-0.741957855	0.004582828
ENSMUSG00000066687	Zbtb16	0.022426393	1.958955748	0.000220351	ENSMUSG0000003469	Phyhip	0.689905729	-0.613231262	0.004894825
ENSMUSG00000028936	Rpl22	3.488681223	-0.825093164	0.000230581	ENSMUSG00000096211	Smm22	0.020291345	-1.183628035	0.004894825
ENSMUSG00000009630	Ppp2cb	0.121968104	-0.937926598	0.000248744	ENSMUSG00000046768	Rhoj	0.108576495	0.901670222	0.005033352
ENSMUSG00000022194	Pabpn1	0.705841222	0.85004695	0.00025596	ENSMUSG00000030711	Sult1a1	0.278027025	0.729020584	0.005064698
ENSMUSG00000029062	Cdk11b	0.43515072	-0.852001875	0.000261776	ENSMUSG00000032081	Apo3c	0.031682977	-1.510272569	0.005064698
ENSMUSG00000032330	Cox7a2	10.38381356	-0.815681795	0.000266864	ENSMUSG00000046242	Nme9	0.023495242	-1.305225285	0.005064698
ENSMUSG00000030790	Adm	0.076721872	1.161095745	0.000270422	ENSMUSG00000090698	Apo1d1	0.076181541	1.00914659	0.005115579
ENSMUSG00000059412	Fxyd2	0.1703619	-0.900686382	0.000280856	ENSMUSG00000012123	Crybg2	0.058738104	1.116619012	0.005165727
ENSMUSG00000036781	Rps27l	0.755415354	-0.832947992	0.000281941	ENSMUSG00000041616	Nppa	0.033106931	-1.243351097	0.005166392
ENSMUSG00000027456	Sdcbp2	0.037377322	1.476483888	0.000282284	ENSMUSG00000015112	Slc25a13	0.087217185	1.179621503	0.005166392
ENSMUSG00000033685	Ucp2	0.56184017	0.865802963	0.000290139	ENSMUSG00000048154	Kmt2d	0.13598761	-0.718560632	0.005166392
ENSMUSG000000041789	2700046A07Rik	0.092066246	1.170136777	0.000312281	ENSMUSG00000015970	Chdh	0.025631173	-1.085274601	0.005371662
ENSMUSG00000020660	Pomc	0.273838066	-1.208062769	0.00033871	ENSMUSG00000028967	Erfri1	0.0348851	0.670521099	0.005578178
ENSMUSG00000110834	Gm39469	0.129443569	-0.916407326	0.000355028	ENSMUSG00000028998	Tom7	2.696968938	-0.579101933	0.005578178
ENSMUSG00000005580	Adcy9	0.040918332	1.645295269	0.000355669	ENSMUSG00000031537	Ikbkb	0.309354014	-0.637139682	0.005678313
ENSMUSG000000042699	Dhx9	0.202230986	-0.877860637	0.000366251	ENSMUSG000000104960	Snhg8	1.074017329	-0.59091188	0.005692166
ENSMUSG00000029313	Aff1	0.108590957	1.054845582	0.000407986	ENSMUSG00000091705	H2-Q2	0.043430598	-0.977104	0.005851028
ENSMUSG00000008090	Fgfr1	0.05508237	-1.030936923	0.000409763	ENSMUSG00000031762	Mt2	4.544549296	0.608917451	0.005856246
ENSMUSG000000027133	Nop10	2.076605334	-0.803855592	0.000410839	ENSMUSG00000021095	Gsc	0.008543724	3.811700525	0.005856246
ENSMUSG00000054514	Atad3aos	0.020852611	-1.293884865	0.000411113	ENSMUSG00000027400	Pdyn	0.347800773	-0.712246201	0.006015617
ENSMUSG00000037235	Mxd4	0.808137051	0.823967404	0.000417412	ENSMUSG00000039391	Ccdc81	0.011391632	-1.431617735	0.006015617
ENSMUSG00000016394	Tmprss6	0.025573957	1.753051449	0.000417412	ENSMUSG00000090101	Snhg9	0.19080984	-0.670267982	0.006118532
ENSMUSG00000079017	Ifi2712a	0.066885735	-1.60270625	0.000470096	ENSMUSG00000068240	Gm11808	0.530422877	-0.605240684	0.006149497
ENSMUSG00000040429	Mterf1a	0.051934806	-1.038499666	0.000490845	ENSMUSG00000029380	Cxcl1	0.008543724	3.811700525	0.006149497
ENSMUSG00000027654	Fam83d	0.044852787	1.487033185	0.000501026	ENSMUSG00000024206	Rfx2	0.02135931	-1.14934584	0.006241133
ENSMUSG00000000791	Il12rb1	0.022426393	1.958955748	0.000572874	ENSMUSG00000090061	Nwd2	0.324661519	-0.788847503	0.00630159
ENSMUSG00000014198	Zfp385c	0.036590431	1.446110239	0.000577166	ENSMUSG00000026525	Opn3	0.080097414	-0.786763762	0.006358853
ENSMUSG00000106583	4930447N08Rik	0.012590256	-1.469340972	0.000612318	ENSMUSG00000031927	1700012B09Rik	0.037734782	-1.188720761	0.006358853

ENSMUSG00000041957	Pkp2	0.189247284	0.91057628	0.000618255	ENSMUSG00000096887	Gm20594	0.017087448	-1.239813633	0.006577867
ENSMUSG00000046470	Sox18	0.008655801	-1.642249832	0.000632867	ENSMUSG00000047712	Ust	0.088997127	-0.767502706	0.006646939
ENSMUSG000000078572	Ndufa8	0.849055383	-0.79621634	0.000632867	ENSMUSG00000035621	Midn	0.105372598	-0.736777616	0.00692716
ENSMUSG000000039221	Rpl2l1	6.019322661	-0.780728249	0.000656288	ENSMUSG00000027217	Tspan18	0.071909679	-0.806982252	0.006982252
ENSMUSG000000086601	Rab25	0.002754118	-2.390878344	0.000656288	ENSMUSG00000019929	Dcn	0.117476208	-0.827790472	0.00721717
ENSMUSG000000096215	Sminm22	0.016918156	-1.416873552	0.000667518	ENSMUSG00000035539	Ccdc180	0.004983839	-1.832155664	0.007333016
ENSMUSG000000095385	D630033011Rik	0.007868991	-1.864259829	0.000670749	ENSMUSG00000033006	Sox10	0.336765129	-0.638422006	0.007333016
ENSMUSG000000029570	Lfng	0.183739047	0.91064354	0.000671056	ENSMUSG00000052539	Magi3	0.062653977	-0.823981733	0.007504628
ENSMUSG000000015112	Sic25a13	0.068459517	1.212335861	0.000675827	ENSMUSG00000060586	H2-Eb1	0.035242862	-1.188299475	0.007538441
ENSMUSG000000026072	Il1r1	0.054295479	1.219915825	0.000699939	ENSMUSG00000074794	Arrdc3	0.590228947	0.654489141	0.007731375
ENSMUSG000000023019	Gpd1	0.734562743	0.808382155	0.000742081	ENSMUSG00000031216	Stard8	0.05731415	-0.841033816	0.008158629
ENSMUSG000000097467	Gm26737	0.004721346	-1.926505984	0.000798246	ENSMUSG00000045930	Clec14a	0.018867391	-1.185792619	0.008336022
ENSMUSG000000078640	Gm11627	0.183345602	0.902164302	0.000798246	ENSMUSG00000084883	Ccdc85c	0.187605944	-0.658126265	0.008419133
ENSMUSG000000039903	Eva1c	0.053902033	1.209499209	0.000807349	ENSMUSG000000039304	Tnfsf10	0.005695816	-1.744692823	0.00864627
ENSMUSG000000038067	Csf3	0.009836137	3.801414471	0.000813072	ENSMUSG00000041479	Syt15	0.005695816	-1.744692823	0.00864627
ENSMUSG000000011514	Cfap161	0.032655976	1.58640158	0.000915655	ENSMUSG00000070643	Sox13	0.042362632	-0.902721682	0.008721682
ENSMUSG000000054364	Rhob	4.925937624	0.763574942	0.000952155	ENSMUSG00000042213	Zfand4	0.076181541	0.961840875	0.00898854
ENSMUSG00000104675	Gm43689	0.006688573	-1.729100246	0.000986939	ENSMUSG00000032595	Cdhr4	0.038446759	-1.263643684	0.009019491
ENSMUSG000000034640	Tiparp	0.142033824	0.928395298	0.01005458	ENSMUSG00000033731	3300002A11Rik	0.014951517	-1.383170833	0.009341553
ENSMUSG000000068523	Gng5	1.627290576	-0.768826524	0.01063086	ENSMUSG00000057836	Xlr3a	0.033818908	1.360489414	0.009341553
ENSMUSG000000038418	Egr1	0.387543815	-0.804549562	0.01070181	ENSMUSG00000103502	9330121J05Rik	0.030259023	1.424184089	0.009352272
ENSMUSG000000035828	Pim3	0.742038208	0.788096606	0.01142191	ENSMUSG00000097842	9330104G04Rik	0.030615012	1.44086283	0.00960603
ENSMUSG000000085348	Myhas	0.021639502	1.738404673	0.0116282	ENSMUSG00000026301	lqca	0.013527563	-1.301640948	0.009609887
ENSMUSG000000026525	Opn3	0.062557834	-0.95647552	0.01174204	ENSMUSG00000026679	Enkur	0.060518046	-0.8819087	0.009609887
ENSMUSG000000037820	Tgm2	0.151476516	0.94523894	0.01177694	ENSMUSG00000064280	Ccdc146	0.013527563	-1.301640948	0.009609887
ENSMUSG000000050397	Foxl2	0.001573782	-2.621491272	0.01245381	ENSMUSG000000039477	Tnrc18	0.211457174	-0.640549368	0.009661802
ENSMUSG000000034161	Scx	0.100328602	0.98203368	0.01245381	ENSMUSG00000078302	Foxd1	0.013171575	-1.417118165	0.009815458
ENSMUSG000000032766	Gng11	0.863612866	-0.785626921	0.0126244	ENSMUSG00000037095	Lrg1	0.06443392	1.249374221	0.009815458
ENSMUSG000000041881	Ndufa7	3.91793026	-0.75118499	0.01272023	ENSMUSG00000096753	Fam181a	0.023139253	-1.073163764	0.009829558
ENSMUSG000000032278	Paqf5	0.093640028	1.024561637	0.01329385	ENSMUSG00000026840	Lamc3	0.018511402	-1.191698051	0.009958856
ENSMUSG000000046916	Myct1	0.003934455	-1.99418248	0.01341097	ENSMUSG00000029056	Pank4	0.113916323	-0.734544868	0.009958856
ENSMUSG000000080683	Rps15a	8.466947098	-0.745390007	0.01407009	ENSMUSG00000086742	Gm16201	0.025987161	-1.048967053	0.009958856
ENSMUSG000000051851	Rtl8c	0.020459166	-1.215498912	0.01407009	ENSMUSG00000032232	Cgnl1	0.039158736	-0.920382847	0.009958856
ENSMUSG000000027907	S100a11	0.064525062	-0.979786259	0.014497	ENSMUSG00000096140	Ankrd66	0.008899713	-1.489267951	0.009958856
ENSMUSG000000025730	Rab40c	0.64131616	0.776748668	0.014497	ENSMUSG00000045817	Zfp3612	0.21715299	-0.661935482	0.009958856
ENSMUSG000000024521	Pmaip1	0.06295128	1.109963536	0.01479977	ENSMUSG00000041789	2700046A07Rik	0.084013288	0.927304568	0.009958856
ENSMUSG000000031231	Cox7b	8.438619022	-0.741923691	0.01526965	ENSMUSG00000118332	Fam220a	0.010679655	-1.432548206	0.010094625
ENSMUSG000000059852	Kcng2	0.232132843	0.848557454	0.01558807	ENSMUSG00000029843	Slc13a4	0.058738104	-0.948969329	0.010240133
ENSMUSG000000020940	1700023F06Rik	0.169968455	-0.822040445	0.01567715	ENSMUSG000000052085	Dock8	0.013883552	-1.265115072	0.010620114
ENSMUSG000000026182	1700001C02Rik	0.035016649	1.734846854	0.01574113	ENSMUSG00000031075	Ano1	0.053754265	-0.832155664	0.010662893
ENSMUSG000000016179	Camk1g	0.317117071	0.81488511	0.01613383	ENSMUSG00000031871	Cdh5	0.03809077	-0.922758213	0.010715145
ENSMUSG000000041966	Dcaf17	0.077508763	-0.924304656	0.01681767	ENSMUSG000000022949	Clic6	0.133139702	-0.925265069	0.010715145
ENSMUSG00000107219	Gm42738	0.008262355	-1.568876646	0.0171941	ENSMUSG00000040562	Gstm2	0.029903035	-1.109265255	0.010726771
ENSMUSG000000038745	Nlrp6	0.014164038	2.140503117	0.0171941	ENSMUSG00000070473	Cldn3	0.006051805	-1.706624702	0.011285564
ENSMUSG000000090553	Snrpe	1.259812482	-0.745920707	0.0182178	ENSMUSG000000060429	Sntb1	0.071909679	-0.774150861	0.011601238
ENSMUSG000000018585	Atox1	2.334312134	-0.737916869	0.0182178	ENSMUSG00000039911	Spsb1	0.221424852	0.702739839	0.011916357
ENSMUSG000000103502	9330121J05Rik	0.032262531	1.476014184	0.01861413	ENSMUSG00000047804	Akap10	0.024919196	-1.039960549	0.012003659
ENSMUSG000000035615	Frmpp1	0.160525763	0.876064978	0.0187111	ENSMUSG00000079018	Lyc6c1	1.805573714	0.591534133	0.012003659
ENSMUSG000000061787	Rps17	4.797674392	-0.731095215	0.0194812	ENSMUSG00000023034	Nr4a1	0.19330176	-0.636476526	0.012096652
ENSMUSG000000074578	Zfas1	0.740857871	-0.749062741	0.01977725	ENSMUSG00000053747	Sox14	0.004627851	-1.832155664	0.012358839
ENSMUSG000000040856	Dlk1	0.238427971	-0.904954952	0.01977725	ENSMUSG00000085069	Prdm16os	0.039158736	-0.895720793	0.012787804
ENSMUSG000000059278	Naa38	2.373656684	-0.731906872	0.02035175	ENSMUSG00000037846	Rtnk2	0.044854552	1.156529022	0.012849066
ENSMUSG000000043102	Qrfp	0.000786891	-2.957918937	0.02047454	ENSMUSG00000086284	Frmpp1os	0.006407793	-1.62862227	0.0136942
ENSMUSG000000046707	Csnk2a2	0.335215564	-0.775491813	0.02076012	ENSMUSG00000027134	Lpcat4	0.182978093	-0.634298677	0.013731296
ENSMUSG00000104444	Gm33051	0.01219681	2.29361983	0.02084796	ENSMUSG00000018604	Tbx3	0.009255701	-2.077268162	0.013812396
ENSMUSG000000032083	Apoa1	0.046033123	-0.982166483	0.0210234	ENSMUSG00000090439	Gm17455	0.017799425	-1.204124442	0.014029511
ENSMUSG000000022220	Adcy4	0.008262355	-1.548118086	0.02217464	ENSMUSG00000026814	Eng	0.136343599	-0.665045678	0.014091916
ENSMUSG000000027120	Fshb	0.000393445	-4.483987748	0.02220958	ENSMUSG00000021466	Ptch1	0.320389657	-0.590419556	0.014091916
ENSMUSG000000012483	Rpa3	0.094426919	-0.859580024	0.02220958	ENSMUSG00000026303	Mlph	0.025987161	1.470407106	0.014225111
ENSMUSG000000022651	Retnlg	0.016918156	2.97544387	0.02221803	ENSMUSG00000047228	A2ml1	0.493044084	0.618713941	0.014225111
ENSMUSG000000095362	Gm14325	0.007082019	-1.628377658	0.02257272	ENSMUSG00000046886	Zfp474	0.004271862	-1.832155664	0.014225111
ENSMUSG000000027434	Nkx2-2	0.05154136	-0.957918937	0.02265266	ENSMUSG00000108634	Gm38534	0.024919196	-1.022258548	0.014620212
ENSMUSG000000001768	Rin2	0.260854365	0.810678267	0.02323849	ENSMUSG00000040420	Cdh18	0.039158736	1.2073727	0.014620212

ENSMUSG00000022096	Hr	0.099541711	0.93991232	0.002439851	ENSMUSG00000053414	Hunk	0.062653977	-0.782402629	0.014735828
ENSMUSG00000020399	Havcr2	0.032655976	1.364009158	0.002442079	ENSMUSG00000041577	Prelp	0.175502335	-0.671690992	0.014755071
ENSMUSG000000072473	1700024G13Rik	0.036196986	2.116571608	0.002479057	ENSMUSG00000016427	Ndufa1	2.621855363	-0.53527465	0.014765482
ENSMUSG000000023267	Gabbr2	0.031869085	1.504330447	0.002491956	ENSMUSG00000030376	Slc8a2	0.347088796	-0.580898426	0.01548848
ENSMUSG00000044894	Uqcrq	9.422232765	-0.71725975	0.002495463	ENSMUSG00000022805	Maats1	0.017443437	-1.142495785	0.015661122
ENSMUSG000000032394	Igdcc3	0.009442692	2.744830942	0.002627544	ENSMUSG0000001029	Icam2	0.033818908	-0.919618506	0.016245691
ENSMUSG000000034317	Trim59	0.07947599	-0.951365753	0.002642072	ENSMUSG00000027845	Dclre1b	0.103592656	0.818510083	0.016396578
ENSMUSG00000094786	Gm14403	0.016524711	-1.240944818	0.002801129	ENSMUSG00000074892	B3galt5	0.43430598	0.620791921	0.016396578
ENSMUSG000000005705	Agrrp	0.102689275	1.830617006	0.002877406	ENSMUSG00000074274	D930028M14Rik	0.034886874	1.273639	0.016503916
ENSMUSG000000042622	Maff	0.02006572	1.801414471	0.00288383	ENSMUSG00000054146	Krt15	0.002847908	-2.185792619	0.016521919
ENSMUSG00000031609	Sap30	0.138492815	0.871012168	0.002894328	ENSMUSG00000058443	Rpl10-ps3	0.053398276	-0.803204291	0.017056563
ENSMUSG00000060404	Olfr1369-ps1	0.002754118	-2.146952761	0.002895401	ENSMUSG00000070306	Ccdc153	0.136699587	-1.011625354	0.017976807
ENSMUSG000000032902	Slc16a1	0.125115668	-0.831911052	0.003001489	ENSMUSG00000053161	Daw1	0.007475759	-1.502007063	0.017979975
ENSMUSG00000035885	Cox8a	20.11529449	-0.708164853	0.003001489	ENSMUSG00000037738	Nek5	0.007475759	-1.502007063	0.017979975
ENSMUSG00000073877	Gm13306	0.005901682	-1.70638017	0.003027053	ENSMUSG00000115625	2900040C04Rik	0.085437242	-1.069013448	0.017979975
ENSMUSG000000045690	Wdr89	0.078689099	-0.8626834	0.003201153	ENSMUSG00000030551	Nrf2f	0.429678129	-0.572461384	0.018588868
ENSMUSG00000089768	Tmsb15b1	0.112525412	-0.818926709	0.003246579	ENSMUSG00000038011	Dnah10	0.013171575	-1.256653493	0.018812698
ENSMUSG00000030048	Gkn3	0.027147739	-1.179133167	0.003423778	ENSMUSG00000016028	Celsr1	0.012459598	-1.276940507	0.019007945
ENSMUSG000000086340	1810059C17Rik	0	-3.986488089	0.003464696	ENSMUSG00000056313	Tsrm	0.035242862	1.226738025	0.019142507
ENSMUSG00000057963	Itpk1	0.698759203	0.746455599	0.003464696	ENSMUSG00000039720	Got111	0.014951517	-1.187250623	0.019842744
ENSMUSG00000021520	Uqcrb	5.046725392	-0.703098903	0.003464696	ENSMUSG00000059854	Hydin	0.015307506	-1.20561406	0.019883412
ENSMUSG000000012123	Crybg2	0.052328251	1.100974753	0.003551503	ENSMUSG00000001247	Lsr	0.063009966	-0.76581317	0.020669055
ENSMUSG000000035621	Midn	0.048000351	-0.939504317	0.003576974	ENSMUSG00000039865	Slc44a3	0.000355989	-3.291587283	0.020720893
ENSMUSG00000038332	Sesn1	0.788858222	0.72456691	0.003577689	ENSMUSG00000047281	Sfn	0.005339828	-1.690136659	0.021068037
ENSMUSG000000048731	Ggnbp1	0.050361024	-0.932192111	0.003638002	ENSMUSG00000031488	Rab11fip1	0.012815586	-1.237412143	0.021465874
ENSMUSG00000026580	Selp	0.007082019	4.348902266	0.003661073	ENSMUSG00000020904	Cfap52	0.012815586	-1.237412143	0.021465874
ENSMUSG000000032595	Cdhr4	0.031082194	1.837940347	0.00369698	ENSMUSG00000004266	Ptpn6	0.02135931	-1.110871692	0.021526249
ENSMUSG000000083920	Abhd2	0.112131967	-0.842441719	0.004016473	ENSMUSG00000056315	Bcl3	0.029547046	1.312234242	0.021526249
ENSMUSG00000114018	Gm36495	0.006295128	-1.64445242	0.004016473	ENSMUSG00000032511	Scn5a	0.100744748	0.809796815	0.021526249
ENSMUSG000000030748	Il4ra	0.076721872	0.987764142	0.004061078	ENSMUSG00000038485	Socs7	0.229968576	-0.592565845	0.021526249
ENSMUSG000000079036	Ccdc153	0.142033824	1.534731449	0.004061078	ENSMUSG00000020799	Tekt1	0.041294667	-0.915987255	0.021799834
ENSMUSG00000024208	Uqcc2	5.066791112	-0.694537678	0.004147299	ENSMUSG00000015950	Ncf1	0.090065093	0.871126804	0.022105049
ENSMUSG000000048015	Neurod4	0.002754118	-2.108478613	0.004152039	ENSMUSG00000037727	Avp	0.736896212	-1.733415906	0.024579047
ENSMUSG000000034064	Poglut1	0.5854469	-0.715899301	0.004152039	ENSMUSG00000022758	P2rx6	0.013171575	-1.228084341	0.024579047
ENSMUSG00000118107	Gm34455	0.003147564	-2.086652251	0.004185082	ENSMUSG00000070866	Zfp804a	0.129935805	-0.651846181	0.024634837
ENSMUSG000000036751	Cox6b1	7.61317037	-0.690692087	0.004370487	ENSMUSG00000014158	Trpv4	0.019935356	-1.065354841	0.024669444
ENSMUSG000000028211	Trp53inp1	0.074754644	0.977963862	0.004451442	ENSMUSG00000047502	Mroh7	0.024563207	-0.988274866	0.02477868
ENSMUSG000000097032	4930539J05Rik	0.018885384	-1.166958453	0.004503077	ENSMUSG00000052387	Trpm3	0.455309302	-0.554621689	0.02477868
ENSMUSG00000070866	Zfp804a	0.06727918	-0.869365274	0.004533303	ENSMUSG00000042699	Dhx9	0.383399623	-0.552430068	0.024913243
ENSMUSG00000029380	Cxcl1	0.00786891	2.908329675	0.004680221	ENSMUSG00000039349	C130074G19Rik	0.052330311	-0.908104518	0.024913243
ENSMUSG00000026388	3110009E18Rik	0.033442867	-0.996322449	0.004715331	ENSMUSG00000030827	Fgf21	0.008899713	2.868284054	0.024913243
ENSMUSG000000113769	5033406O09Rik	0.025573957	1.501512682	0.004772365	ENSMUSG00000027276	Jag1	0.032394954	-0.90850655	0.024977884
ENSMUSG00000058600	Rpl30	10.5423721	-0.686024182	0.004792632	ENSMUSG00000057914	Cacnb2	0.200065542	-0.593010008	0.025486888
ENSMUSG000000055839	Elob	9.734235045	-0.684372061	0.004898402	ENSMUSG00000035357	Pdzrn3	0.079385437	-0.704280842	0.025486888
ENSMUSG000000027985	Lef1	0.103869611	-0.835018635	0.004919939	ENSMUSG00000027737	Slc7a11	0.181198151	-0.612589287	0.025747072
ENSMUSG00000021099	Six6	0.013377147	-1.369655073	0.005000274	ENSMUSG00000041930	Fam22a	0.113204346	-0.654294403	0.025747072
ENSMUSG000000030785	Cox6a2	0.674759028	-0.722147485	0.005018877	ENSMUSG00000051041	Olffml1	0.065501886	-0.760205822	0.025747072
ENSMUSG000000063320	1190007I07Rik	0.159738872	-0.761521724	0.005267126	ENSMUSG00000113902	Ndufb1-ps	4.088528017	-0.506171122	0.02590477
ENSMUSG00000075602	Ly6a	1.615487211	0.704498188	0.005267126	ENSMUSG00000034041	Lyl1	0.01423954	-1.175043378	0.026028871
ENSMUSG000000040055	Gjb6	1.259025591	0.695433165	0.005553065	ENSMUSG00000047420	Fam180a	0.005695816	-1.602673818	0.026031573
ENSMUSG000000091625	Lsm5	0.354494393	-0.714128037	0.005586645	ENSMUSG00000067288	Rps28	7.950291354	-0.504467008	0.026031573
ENSMUSG00000001025	S100a6	0.583479672	-0.714136613	0.005708075	ENSMUSG00000057068	Fam47e	0.008187736	-1.417118165	0.02646749
ENSMUSG000000039634	Zfp189	0.07947599	0.933420656	0.005837174	ENSMUSG00000050721	Plekho2	0.056246184	-0.767200222	0.02646749
ENSMUSG000000036915	Kirrel2	0.063738171	0.990271288	0.005837174	ENSMUSG00000057722	Lepr	0.003559885	-1.896286002	0.026558433
ENSMUSG00000048807	Slc35e4	0.412330881	0.724262727	0.005837174	ENSMUSG00000017756	Slc12a7	0.016019483	-1.141483722	0.027242939
ENSMUSG000000085691	Gm14216	0	-3.986488089	0.005874335	ENSMUSG00000050397	Foxl2	0.003915874	-1.891049353	0.027357894
ENSMUSG000000074521	Gm14327	0.019278829	-1.137812107	0.00602167	ENSMUSG00000098176	Ccdc166	0.145955288	0.711285767	0.027357894
ENSMUSG00000024176	Sox8	0.274624957	0.778633928	0.006180547	ENSMUSG00000025494	Sigirr	0.012815586	-1.207664799	0.027614442
ENSMUSG000000014846	Tppp3	1.769717846	0.737514198	0.006318625	ENSMUSG00000048655	Ccdc169	0.001423954	-2.417118165	0.027651531
ENSMUSG000000086939	Gm13530	0.007475464	-1.50783449	0.006411516	ENSMUSG00000063975	Slc01a5	0.001423954	-2.417118165	0.027651531
ENSMUSG00000097333	Zfp87	0.118033649	-0.776541241	0.006411516	ENSMUSG00000042379	Esm1	0.001423954	-2.417118165	0.027651531
ENSMUSG000000064057	Segb3a1	0.02006572	1.553486957	0.006478958	ENSMUSG00000021194	Chga	2.055477646	-0.607429728	0.027678834
ENSMUSG00000043164	Tmem212	0.100722047	1.663655806	0.00687256	ENSMUSG00000090877	Hspa1b	0.049126414	-0.790030189	0.027850204

ENSMUSG00000110500	Gm32568	0.009049246	3.100974753	0.007045714	ENSMUSG00000024033	Rsph1	0.136699587	-0.801861742	0.0281105164
ENSMUSG00000086003	B230206L02Rik	0.055475815	-0.88882948	0.007093317	ENSMUSG00000035200	Chrnb4	0.027055127	-1.08893108	0.028155257
ENSMUSG00000066170	E230001N04Rik	0.018491938	1.598474412	0.007093317	ENSMUSG00000048349	Pou4f1	0.046990483	-0.926620348	0.028405891
ENSMUSG00000048416	Mlf1	0.070820189	1.1078967543	0.007294238	ENSMUSG00000026565	Pou2f1	0.083657299	-0.628649182	0.028649182
ENSMUSG00000034855	Cxcl10	0.002360673	-3.220953342	0.007294238	ENSMUSG00000027360	Hdc	0.035598851	-1.031925177	0.02870055
ENSMUSG00000071451	Psmg4	0.465052578	-0.692199084	0.007294238	ENSMUSG00000024521	Pmaip1	0.065857874	0.899648225	0.02870055
ENSMUSG00000056501	Cebpb	0.488265862	0.708767962	0.007345006	ENSMUSG00000050199	Lgr4	0.149515173	-0.610334268	0.029142335
ENSMUSG00000025993	Slc40a1	0.025180512	-1.036528771	0.007585711	ENSMUSG00000075703	Selenoi	0.154499013	-0.606442885	0.029250306
ENSMUSG00000046683	0610025J13Rik	0.007475464	2.837940347	0.007585711	ENSMUSG00000037206	Islr	0.039870713	-0.918867298	0.029250306
ENSMUSG00000020562	Efcab10	0.175083246	-0.736561262	0.007585711	ENSMUSG00000084843	B230312C02Rik	0.043074609	-0.820281564	0.029288618
ENSMUSG00000035215	Lsm7	2.188737301	-0.667181026	0.007611373	ENSMUSG00000035686	Thrsp	0.499807866	0.582539599	0.029476393
ENSMUSG00000024535	Snx24	0.289969331	0.730606303	0.007632785	ENSMUSG00000021638	Ocln	0.058738104	-0.751736982	0.030099117
ENSMUSG00000036596	Cpz	0.000786891	-2.773494365	0.007856616	ENSMUSG00000061086	Myl4	0.259871611	-0.633577631	0.030213845
ENSMUSG00000085037	4933421O10Rik	0.096394147	-0.786233477	0.007862398	ENSMUSG00000027111	Itga6	0.111780392	-0.641472103	0.030418319
ENSMUSG00000030494	Rhpn2	0.076328426	0.980384612	0.007942138	ENSMUSG00000048807	Slc35e4	0.459225176	0.577305117	0.030418319
ENSMUSG00000033126	Ybey	0.059803716	-0.85109077	0.008305005	ENSMUSG00000030494	Rhpn2	0.114272311	0.757294227	0.031103021
ENSMUSG00000034271	Jdp2	0.321444971	0.718940063	0.008305005	ENSMUSG00000046402	Rbp1	0.357056474	-0.588532565	0.03119545
ENSMUSG00000001029	Icam2	0.029114967	-0.992134652	0.00836354	ENSMUSG00000038331	Sfb2	0.109288472	-0.647518165	0.031294552
ENSMUSG00000026335	Pam	0.320264635	-0.695974548	0.008573585	ENSMUSG00000028655	Mtd2a	0.468480877	0.573781924	0.032422791
ENSMUSG00000044734	Serp1b1a	0.218755696	-0.764755742	0.008607378	ENSMUSG00000025352	Gdf11	0.169094541	-0.59197393	0.032422791
ENSMUSG00000098332	2310009A05Rik	0.471347706	-0.682636559	0.008607821	ENSMUSG00000026875	Traf1	0.011035644	-1.258420419	0.032484524
ENSMUSG00000052336	Cx3cr1	0.070820189	-0.829631912	0.008607821	ENSMUSG00000046555	Aqp1	0.02135931	-1.091242886	0.032484524
ENSMUSG00000026126	Ptpn18	0.077115317	-0.812248805	0.008717356	ENSMUSG00000041431	Ccnb1	0.013527563	-1.2746739	0.032854392
ENSMUSG00000024033	Rsph1	0.167214336	0.965319653	0.008881633	ENSMUSG00000047109	Cldn14	0.045922518	1.020287147	0.033397244
ENSMUSG00000043773	1700048O20Rik	0.128263232	0.812065388	0.008963225	ENSMUSG00000031340	Gabre	0.031326989	-0.895581044	0.033397244
ENSMUSG00000096768	Gm47283	1.541912903	0.663116546	0.008930307	ENSMUSG00000039001	Rps21	24.63760867	-0.489045246	0.033925358
ENSMUSG00000054091	1810037117Rik	2.008539263	-0.659031399	0.008957028	ENSMUSG00000038738	Shank1	0.852948466	-0.510528476	0.033925358
ENSMUSG00000086682	Gm16023	0.003934455	-1.797145633	0.009334708	ENSMUSG00000038489	Rhp2l	0.761459419	-0.512753444	0.034477523
ENSMUSG00000043832	Clec4a3	0.005508237	-1.606844496	0.009334708	ENSMUSG00000030111	A2m	0.069773748	-0.725803683	0.034631973
ENSMUSG00000009079	Ewsr1	0.987548198	-0.662632274	0.00959201	ENSMUSG00000037868	Egr2	0.003915874	-1.77075512	0.034682608
ENSMUSG00000037279	Ovol2	0.113312303	0.892196143	0.009642095	ENSMUSG00000014686	Ceacam16	0.000711977	-2.832155664	0.035150933
ENSMUSG00000000567	Sox9	0.092459692	-0.787871668	0.009682379	ENSMUSG00000046516	Cox17	2.881014997	-0.494050825	0.035357681
ENSMUSG00000091255	Speer4e	0	-3.805915843	0.009907102	ENSMUSG00000047867	Gimap6	0.063365954	0.896772611	0.035427787
ENSMUSG00000063316	Rpl27	5.08882406	-0.64942375	0.009907102	ENSMUSG00000022861	Dgkg	0.04770246	0.996732419	0.03554528
ENSMUSG00000009585	Apobec3	0.035410095	1.182504638	0.010079016	ENSMUSG00000027434	Nkx2-2	0.067637817	-0.762521476	0.036318793
ENSMUSG00000009281	Rarres2	0.384396251	0.805846717	0.010121951	ENSMUSG00000092384	Gm4189	0.016375471	-1.084921735	0.036318793
ENSMUSG00000050621	Rps27rt	0.072000526	-0.805915843	0.010121951	ENSMUSG00000038765	Lmx1b	0.001067966	-2.639510586	0.036353834
ENSMUSG00000040564	Apoc1	0.105443393	-0.76125354	0.010392337	ENSMUSG00000022656	Nectin3	0.114272311	-0.625360098	0.037772341
ENSMUSG00000050721	Plekho2	0.047606905	-0.875178506	0.010422868	ENSMUSG00000026833	Olfn1	12.47988913	-0.495835239	0.037897383
ENSMUSG00000041870	Ankrd13a	0.501249563	0.703010767	0.010533049	ENSMUSG00000059343	Aldoart1	0.006407793	-1.491118746	0.037897383
ENSMUSG00000044145	1810024B03Rik	0.040918332	-0.899025247	0.010812764	ENSMUSG00000086013	M5706	0.118544173	0.718658614	0.037897383
ENSMUSG00000055652	Klhl25	0.093640028	0.852094441	0.01082272	ENSMUSG00000057534	Elobl	0	-5.919618506	0.037897383
ENSMUSG00000041930	Fam222a	0.069246407	-0.81512399	0.010869459	ENSMUSG00000043091	Tuba1c	0.027411115	-0.921792877	0.037897383
ENSMUSG00000022324	Matn2	0.30846127	0.703503126	0.010943689	ENSMUSG00000024513	Mbd2	0.292622554	-0.541869739	0.037897383
ENSMUSG00000020672	Sntg2	0.049967578	1.013511911	0.011011921	ENSMUSG0000008090	Fgf1r1	0.070841713	-0.696094115	0.038122198
ENSMUSG00000079657	Rab26	0.619283212	0.676351204	0.011207639	ENSMUSG00000098051	Gm27032	0.285858772	0.599727506	0.038217764
ENSMUSG00000009234	Malat1	2.290246239	0.655532629	0.011207639	ENSMUSG00000060981	Hist1h4h	0.063721943	-0.715341999	0.038217764
ENSMUSG00000078234	Klhdc7a	0.046820014	1.030585425	0.011397366	ENSMUSG00000074207	Adh1	0.003559885	-1.832155664	0.038363129
ENSMUSG00000097848	Gm807	0.011803365	2.055171063	0.011408709	ENSMUSG00000046280	She	0.007831747	-1.39605655	0.038500966
ENSMUSG00000076274	Plac9b	0.005901682	-1.65391275	0.011886155	ENSMUSG00000044921	Rassf9	0.007831747	-1.39605655	0.038500966
ENSMUSG000000110716	Gm39271	0.000786891	-2.70638017	0.012179771	ENSMUSG00000049521	Cdc42ep1	0.194369725	-0.588507683	0.038577469
ENSMUSG00000023034	Nr4a1	0.150689625	-0.723453683	0.012488316	ENSMUSG00000030849	Fgfr2	0.332493267	-0.552047745	0.038592047
ENSMUSG000000113722	Snhg10	0.078689099	-0.783248933	0.012583557	ENSMUSG00000037490	Slc2a12	0.099846805	-0.644672292	0.038628882
ENSMUSG00000033731	3300002A11Rik	0.014950929	2.386376971	0.012622281	ENSMUSG00000054364	Rhob	5.272112184	0.050002394	0.039167368
ENSMUSG00000112117	Rmst	0.107410621	0.815302543	0.012652289	ENSMUSG00000019178	Styx1l	0.001067966	-2.532595382	0.039578423
ENSMUSG00000025652	Tmem89	0.003541009	-1.862499371	0.012744598	ENSMUSG00000093507	Gm20627	0.000355989	-3.154083759	0.039805711
ENSMUSG00000009210	Prr29	0.015344374	1.963471229	0.01276659	ENSMUSG00000025094	Slc18a2	0.036310828	1.099457361	0.041032296
ENSMUSG00000074768	Bhmt	0.005901682	3.100974753	0.013102998	ENSMUSG00000021222	Dcaf4	0.252039864	0.604063151	0.041063975
ENSMUSG00000051159	Cited1	0.302559587	0.721022595	0.013522572	ENSMUSG00000089889	0610040B10Rik	0.119968127	0.710742777	0.04129384
ENSMUSG00000096974	Gm26881	0.201050649	-0.691815542	0.01388708	ENSMUSG00000055235	Wdr86	0.017087448	-1.10008887	0.04174747
ENSMUSG00000109556	Gm38843	0.011016474	-1.269862943	0.014134974	ENSMUSG00000026447	Pik3c2b	0.038446759	-0.818858842	0.0420232
ENSMUSG00000032135	Mcam	0.064525062	-0.831911052	0.014427737	ENSMUSG00000045613	Chrm2	0.038446759	-0.818858842	0.0420232
ENSMUSG00000047109	Cldn14	0.049967578	1.056580633	0.014437055	ENSMUSG00000034656	Cacna1a	0.523659096	-0.514386958	0.0420232



ENSMUSG00000091329	1700112D23Rik	0.022032948	-1.020331544	0.014917524	ENSMUSG00000028139	Riad1	0.180486174	-0.574790009	0.042286029
ENSMUSG00000118038	Gm9895	0.029901858	1.367761293	0.015202933	ENSMUSG00000040809	Chil3	0	-3.832155664	0.042286029
ENSMUSG000000001506	Col1a1	0.025573957	-1.093035867	0.015371985	ENSMUSG00000029236	Nmu	0	-3.832155664	0.042286029
ENSMUSG000000064179	Tnnt1	1.150041188	0.692117946	0.015397733	ENSMUSG00000025511	Tspan4	0.421490394	0.561532056	0.04246014
ENSMUSG00000025163	Cd7	0.013377147	1.770826151	0.015426173	ENSMUSG00000018581	Dnah11	0.006051805	-1.520211658	0.042549922
ENSMUSG00000074001	Klhl40	0.063738171	0.910544096	0.01561253	ENSMUSG00000091378	Gm4219	0.006407793	3.415771849	0.042854909
ENSMUSG00000020182	Ddc	0.24550999	0.730475649	0.015750554	ENSMUSG00000027364	Usp50	0.07867346	-0.667096418	0.042963346
ENSMUSG00000074637	Sox2	0.337182791	-0.667919006	0.015822107	ENSMUSG00000063594	Gng8	0.211101185	-0.710593684	0.042999705
ENSMUSG00000062931	Zfp938	0.266362602	-0.668809467	0.016107692	ENSMUSG00000030235	Slco1c1	0.302590232	-0.53376857	0.043977564
ENSMUSG00000029499	Pxmp2	0.206558886	0.722041227	0.016151591	ENSMUSG00000024985	Tcf7l2	1.440685493	-0.51582993	0.043977564
ENSMUSG00000046806	Cyren	0.104263057	-0.735526515	0.016287527	ENSMUSG00000022701	Ccdc191	0.037378793	-0.832155664	0.044101596
ENSMUSG00000009927	Rps25	4.976692093	-0.622700355	0.016287527	ENSMUSG00000026227	2810459M11Rik	0.043430598	-0.784458922	0.0442699
ENSMUSG000000114241	Gm30108	0.005901682	-1.542881437	0.016377427	ENSMUSG00000039485	Tspyl4	2.0569016	-0.481801956	0.044631205
ENSMUSG00000045930	Clec14a	0.015344374	-1.131686004	0.016736753	ENSMUSG00000047671	Tctex1d4	0.022071288	-1.00462286	0.044700022
ENSMUSG00000029255	Gnrhr	0	-3.70638017	0.016861241	ENSMUSG00000018919	Tm4sf5	0.050906357	0.945451914	0.044942124
ENSMUSG00000045854	Lymr2	0.354100947	-0.652548106	0.017496404	ENSMUSG00000034634	Ly6d	0.018511402	1.573836695	0.04502661
ENSMUSG00000081683	Fzd10	0.007475464	-1.409987167	0.017676424	ENSMUSG00000041624	Gucy1a2	0.007831747	2.691406292	0.046434444
ENSMUSG00000106951	5930430L01Rik	0.01219681	-1.202805996	0.018023272	ENSMUSG00000015890	Amdhd1	0.007831747	2.691406292	0.046434444
ENSMUSG00000010122	Slc47a1	0.0043279	-1.740327501	0.018203698	ENSMUSG00000025225	Nfkb2	0.15983884	-0.607089109	0.047076438
ENSMUSG00000097360	9430065F17Rik	0.013377147	-1.162059653	0.018402151	ENSMUSG00000045193	Cirbp	1.719780483	0.503873961	0.047105094
ENSMUSG00000031700	Gpt2	0.62125044	0.644534554	0.018417265	ENSMUSG00000020848	Doc2b	0.138123541	-0.590473093	0.047105094
ENSMUSG00000054428	Atp1f1	9.062230135	-0.61524862	0.018478182	ENSMUSG00000073125	Xlr3b	0.063009966	0.862218053	0.047372783
ENSMUSG00000095620	Csta2	0.007082019	-1.432457448	0.018535252	ENSMUSG00000029718	Pcolce	0.093980966	-0.671050364	0.048552824
ENSMUSG00000046500	Tafa4	0.081836663	0.865819379	0.018904209	ENSMUSG00000027744	Stoml3	0.012815586	-1.17729115	0.049399406
ENSMUSG00000084849	Gm16105	0.008655801	2.302608614	0.018904209	ENSMUSG00000027386	Fbln7	0.020647333	-0.971880428	0.049600021
ENSMUSG00000014361	Mertk	0.121968104	0.759693703	0.019537773					
ENSMUSG00000019738	Polr2i	1.152401861	-0.621043578	0.019537773					
ENSMUSG00000025810	Nrp1	0.037377322	1.071227409	0.019537773					
ENSMUSG00000053907	Mat2a	1.698504211	0.618223299	0.020182282					
ENSMUSG00000113186	A330076C08Rik	0.041705223	-0.851045219	0.020302791					
ENSMUSG00000004654	Ghrhr	0.000393445	-2.986488089	0.020552072					
ENSMUSG00000027333	Smox	0.795940241	0.632757215	0.020688326					
ENSMUSG00000071653	1810009A15Rik	0.009836137	-1.286048371	0.021137635					
ENSMUSG00000027173	Depdc7	0.013377147	-1.196006985	0.02138189					
ENSMUSG00000029056	Pank4	0.079869436	-0.754076912	0.02138189					
ENSMUSG00000020327	Fgf22	0.082623554	0.822073941	0.02138189					
ENSMUSG00000033863	Klf9	1.275156856	0.617710982	0.02138189					
ENSMUSG00000074794	Arrdc3	0.311608834	0.693232819	0.021406446					
ENSMUSG00000089996	Tmsb15b2	0.319477744	-0.642365057	0.022396808					
ENSMUSG00000020722	Cacng1	0.011409919	1.837940347	0.022423326					
ENSMUSG00000093483	AA465934	0.007475464	-1.384452075	0.022635575					
ENSMUSG000000109089	4833411C07Rik	0.010229583	2.048507333	0.022686895					
ENSMUSG00000035860	Cdhr3	0.044852787	0.992268493	0.023163753					
ENSMUSG00000025488	Cox8b	0.055869261	-1.056566524	0.023310161					
ENSMUSG00000031962	Cdh15	0.114099194	0.754468635	0.023928706					
ENSMUSG00000089809	Rasgef1b	0.231345952	-0.654003465	0.024180208					
ENSMUSG00000053198	Prx	0	-3.70638017	0.02452101					
ENSMUSG000000117674	Gm31087	0.007475464	2.422902847	0.024977107					
ENSMUSG00000032680	6820408C15Rik	0.040131441	1.006115566	0.02502793					
ENSMUSG00000031827	Cotl1	0.819940416	0.616042253	0.025322301					
ENSMUSG00000029394	Cdk2ap1	0.461118123	0.633403946	0.02571083					
ENSMUSG00000033326	Kdm4a	0.208919559	0.688651638	0.026549168					
ENSMUSG00000026032	Ndufb3	2.797004039	-0.597246852	0.026710522					
ENSMUSG00000003309	Ap1m2	0.00786891	-1.339597839	0.027586762					
ENSMUSG00000105703	Gm43305	0.057443043	0.891256161	0.027586762					
ENSMUSG00000079018	Ly6c1	1.881062922	0.607982378	0.027815412					
ENSMUSG00000003541	Ier3	0.328920436	0.647667236	0.027815412					
ENSMUSG00000052310	Slc39a1	0.108984403	-0.695963554	0.028930031					
ENSMUSG00000006386	Tek	0.038951104	-0.8550819	0.028930031					
ENSMUSG000000109080	Gm38944	0.012983701	-1.133490501	0.028930031					
ENSMUSG00000021414	Fam217a	0.01219681	1.779046658	0.029031126					
ENSMUSG00000068079	Tcf15	0.03580354	1.039574208	0.029650206					
ENSMUSG00000062077	Trim54	0.02360673	-0.956972597	0.029650206					

ENSMUSG00000025496	Drd4	0.017705047	1.454611707	0.029650206
ENSMUSG00000089736	Tgfr3l	0.04721346	-0.813052024	0.029652001
ENSMUSG00000040447	Spns2	0.376133895	0.637027653	0.029712128
ENSMUSG00000021913	Ogdhl	0.105836839	-0.695653763	0.029712128
ENSMUSG00000024076	Vit	0.054295479	0.953129285	0.029712128
ENSMUSG00000006958	Chrd	0.160525763	0.694782744	0.029848152
ENSMUSG00000059854	Hydin	0.012983701	2.018512592	0.030542443
ENSMUSG00000021215	Net1	0.214821241	0.668894769	0.030774054
ENSMUSG00000068263	Efcc1	0.011803365	1.733242968	0.031075161
ENSMUSG00000051367	Six1	0.001967227	-2.014502465	0.031308295
ENSMUSG00000025511	Tspan4	0.363150194	0.630795699	0.031312968
ENSMUSG00000071202	Ccdc78	0.009836137	2.479486376	0.031312968
ENSMUSG00000015981	Stk32c	1.16302489	0.600226144	0.03173769
ENSMUSG00000059991	Nptx2	0.365510867	-0.624778129	0.032473817
ENSMUSG00000105881	4932422M17Rik	0.003934455	-1.649046994	0.032826519
ENSMUSG00000027845	Dclre1b	0.077508763	0.835513609	0.032864447
ENSMUSG00000006205	Htra1	2.611297764	0.58774971	0.032940875
ENSMUSG00000051989	Smim11	0.417052227	-0.609367539	0.032940875
ENSMUSG00000039646	Vasn	0.092853137	0.760899311	0.033578058
ENSMUSG00000050074	Spink8	0.47449527	0.69613302	0.033584499
ENSMUSG00000038587	Akap12	0.217968805	0.670424254	0.033584499
ENSMUSG00000019947	Arid5b	0.268723275	0.654641123	0.033584499
ENSMUSG00000064141	Zfp69	0.002754118	-1.853221558	0.033961079
ENSMUSG00000097511	Gm16677	0.002754118	-1.853221558	0.033961079
ENSMUSG00000053161	Daw1	0.009049246	2.364009158	0.034172595
ENSMUSG00000059498	Fcgr3	0.289969331	0.654037169	0.034194379
ENSMUSG00000034906	Ncaph	0.021639502	1.264473485	0.03466795
ENSMUSG000000095115	Itpril2	0.015344374	-1.068950249	0.035281616
ENSMUSG000000110427	4933406817Rik	0.002754118	-1.853221558	0.036247007
ENSMUSG00000000031	H19	0.001180336	-2.29134267	0.036591775
ENSMUSG00000045662	Henmt1	0.017311602	1.422902847	0.036902636
ENSMUSG00000049517	Rps23	9.694890495	-0.574782723	0.037171529
ENSMUSG00000030708	Dnajb13	0.01219681	1.779046658	0.037397574
ENSMUSG00000020155	Kcnmb1	0.016918156	1.47294353	0.037397574
ENSMUSG00000044243	Bhlha9	0.063738171	0.834993063	0.037397574
ENSMUSG00000026344	Lypd1	1.308599723	0.619828647	0.038435906
ENSMUSG00000037419	Endod1	2.006572035	0.590593488	0.03852894
ENSMUSG00000047205	Dusp18	0.155410971	0.680482823	0.038985898
ENSMUSG00000089812	Gm15867	0.007082019	-1.351537452	0.039244597
ENSMUSG000000117437	Gm33727	0.03934455	-0.848144078	0.039282045
ENSMUSG00000049751	Rpl36al	4.539967591	-0.572244596	0.039527792
ENSMUSG000000035183	Slc24a5	0.14242727	0.691911154	0.039904457
ENSMUSG00000079484	Phyhd1	0.201050649	0.666346525	0.039939971
ENSMUSG00000087178	A230056P14Rik	0.033049422	-0.847186316	0.039939971
ENSMUSG00000038135	Crygn	0.031869085	1.288601756	0.040282757
ENSMUSG00000030888	Rrp8	0.139673151	0.687964935	0.040367955
ENSMUSG00000096753	Fam181a	0.019278829	-0.983089512	0.040797095
ENSMUSG00000010462	Gm35572	0.01219681	1.641543134	0.04103118
ENSMUSG00000005413	Hmox1	0.062164389	0.828895207	0.041259036
ENSMUSG00000085260	Med9os	0.031869085	-0.854356198	0.041777302
ENSMUSG00000047617	Paxx	1.965260258	0.571348833	0.041990945
ENSMUSG00000044197	Gpr146	0.219936033	0.641543134	0.041990945
ENSMUSG00000035673	Sbno2	0.101115493	0.790273913	0.041990945
ENSMUSG00000098087	Gm17750	0.123935332	-0.666706862	0.041990945
ENSMUSG00000067071	Hes6	0.283674203	0.625286225	0.042002165
ENSMUSG00000030747	Dgat2	0.987154752	0.587896779	0.042519654
ENSMUSG00000021091	Serpina3n	0.236067298	0.642197962	0.042963513
ENSMUSG00000020027	Socs2	0.159345426	0.668278587	0.042982871
ENSMUSG00000034923	Ly6gef	0.024787066	-0.965114438	0.042985533
ENSMUSG00000036114	Rpp25l	0.575610762	0.590151148	0.044227135
ENSMUSG00000056973	Ces1d	0.003147564	-1.773494365	0.044227135
ENSMUSG000000113707	Gm10457	0.001967227	-1.957918937	0.04425962
ENSMUSG00000095562	Gm21887	0.086558009	0.74932596	0.044684977

ENSMUSG00000092593	Gm20492	0.003541009	-1.664559994	0.045062826
ENSMUSG00000117069	Gm49894	0.000786891	-2.483987748	0.045062826
ENSMUSG00000086771	170080G11Rik	0.008655801	2.039574208	0.045213846
ENSMUSG00000110332	Gm19935	0.165640554	0.794167945	0.045213846
ENSMUSG00000046242	Nme9	0.023213284	1.54843373	0.045213846
ENSMUSG00000026874	Hc	0.009836137	1.801414471	0.045783324
ENSMUSG00000031765	Mt1	18.6851201	-0.562265232	0.04621443
ENSMUSG00000109006	B230209E15Rik	0.084590782	0.747337798	0.046568697
ENSMUSG00000025006	Sorbs1	0.077902208	0.771815088	0.047060966
ENSMUSG00000040710	St8sia4	0.05154136	-0.749448891	0.047124666
ENSMUSG00000044156	Hepacam2	0.002360673	-1.899025247	0.047124666
ENSMUSG00000015575	Atp6v0e	1.462043467	0.568580303	0.047512346
ENSMUSG00000114780	Al197445	0	-3.483987748	0.047770713
ENSMUSG00000116097	Gm36738	0.005508237	-1.418399407	0.04789418
ENSMUSG00000044786	Zfp36	0.060197161	0.859966653	0.048577925
ENSMUSG00000087466	A330041J22Rik	0.076721872	-0.693706339	0.04894278
ENSMUSG00000056043	Rgs9bp	0.005901682	2.516012252	0.049335242

Table S2B. DEGs at ZT14 in female and male full brains (bulk). The average number of counts per spot in the RHY condition, the log2 fold change in gene expression (RHY relative to saline), and the adjusted p-value (FDR) are shown.

ZT14 FEMALES - Bulk

FeatureID	FeatureName	ZT14RF count average	ZT14RF Log2FoldChange	ZT14RF FDR
ENSMUSG00000026822	Lcn2	0.553259877	7.466298495	2.3751E-46
ENSMUSG00000048572	Tmem252	0.267647257	4.57169635	3.05839E-45
ENSMUSG00000019970	Sgk1	3.198201398	2.084449132	1.75882E-21
ENSMUSG00000095366	Gm21860	0.031531047	6.670837251	2.99987E-20
ENSMUSG00000023067	Cdkn1a	0.437401613	2.182694336	3.5189E-20
ENSMUSG00000020713	Gh	0.005499601	-5.428531108	1.95465E-17
ENSMUSG00000021342	Pr1	0.005499601	-5.623855286	1.95465E-17
ENSMUSG00000037727	Avp	0.04949641	-6.88699684	4.31384E-15
ENSMUSG00000002910	Arrdc2	0.477732021	1.69703866	1.60202E-12
ENSMUSG00000027301	Oxt	0.003299761	-9.863673861	8.54863E-12
ENSMUSG00000017697	Ada	0.09459314	2.244702043	9.0161E-12
ENSMUSG00000021025	Nfkbia	0.762611362	1.476167945	1.17651E-10
ENSMUSG00000050370	Ch25h	0.042896889	3.303181883	1.32257E-10
ENSMUSG00000048489	Depp1	0.053529451	2.672678598	2.61866E-10
ENSMUSG00000020108	Ddit4	0.749412319	1.439509256	4.45124E-10
ENSMUSG00000034936	Arl4d	0.47076586	1.470638012	1.70947E-09
ENSMUSG00000002289	Angptl4	0.104125782	1.682272146	2.3496E-08
ENSMUSG00000030711	Sult1a1	0.414303288	1.340609833	2.63538E-08
ENSMUSG00000066363	Serpina3f	0.024564885	5.315356597	2.72284E-08
ENSMUSG00000037095	Lrg1	0.086160418	2.179799467	1.07656E-07
ENSMUSG00000056054	S100a8	0.039230488	5.397818757	2.56181E-07
ENSMUSG0000001637	Cebpδ	0.576724842	1.253788977	3.27299E-07
ENSMUSG00000041481	Serpina3g	0.026031446	3.397818757	6.98299E-07
ENSMUSG00000034579	Pla2g3	0.066728494	1.699199474	1.16082E-06
ENSMUSG00000029380	Cxcl1	0.015032243	4.620211178	1.66657E-06
ENSMUSG0000002831	Plin4	0.18918628	1.353170977	1.98523E-06
ENSMUSG00000031765	Mt1	57.21748388	1.081425773	3.30897E-06
ENSMUSG00000048001	Hes5	0.323009801	-1.152378326	3.9046E-06
ENSMUSG00000090137	Uba52	8.572778296	1.067205038	4.58418E-06
ENSMUSG00000103034	Gm8797	0.111091944	-1.189514648	1.29675E-05
ENSMUSG00000043102	Qrfp	0	-6.486351762	3.31648E-05
ENSMUSG00000033585	Ndn	2.106713886	-1.027295451	4.19956E-05
ENSMUSG00000034317	Trim59	0.075894496	-1.239048672	4.26826E-05
ENSMUSG00000029394	Cdk2ap1	0.201652043	-1.071339199	4.93272E-05
ENSMUSG00000064220	Hist2h2aa1	0.131990428	1.208048944	5.41386E-05
ENSMUSG00000090247	Bloc1s1	0.872970025	1.008099381	5.41386E-05
ENSMUSG00000035383	Pmch	22.13589469	1.663208759	5.6116E-05
ENSMUSG00000039634	Zfp189	0.086527058	1.296458042	5.97694E-05
ENSMUSG00000060143	Gm10076	19.89022421	0.964531407	7.51305E-05
ENSMUSG00000025591	Tma16	0.290012301	1.075890662	0.000122527

ZT14 MALES - Bulk

FeatureID	FeatureName	ZT14RM count average	ZT14RM Log2FoldChange	ZT14RM FDR
ENSMUSG00000035383	Pmch	1.998712712	-2.353167152	2.35485E-28
ENSMUSG00000098178	Gm42418	4.129713873	-1.227666651	4.22846E-27
ENSMUSG00000030711	Sult1a1	0.229550169	1.371871646	8.90599E-22
ENSMUSG00000028656	Cap1	0.169504348	-1.222523099	8.32202E-20
ENSMUSG00000071753	Cdr1os	0.156369325	-1.116405331	9.7768E-16
ENSMUSG00000090137	Uba52	1.985577689	0.882789073	9.68068E-15
ENSMUSG00000020922	Lsm12	0.031586604	-1.533201777	3.1847E-14
ENSMUSG00000095041	AC149090.1	0.823440865	0.923804219	7.65731E-14
ENSMUSG00000117465	Gm49980	0.106956618	1.312062251	4.90829E-13
ENSMUSG00000027875	Hmgcs2	0.05316557	1.759976818	8.52135E-13
ENSMUSG00000092274	Neat1	0.236743158	1.126818627	8.52135E-13
ENSMUSG00000037095	Lrg1	0.040030547	2.201348465	2.58136E-12
ENSMUSG00000002910	Arrdc2	0.116026039	1.231029153	2.69212E-12
ENSMUSG00000064356	mt-Atp8	0.618909788	-0.84869804	4.09293E-12
ENSMUSG00000019970	Sgk1	0.764645999	0.870412537	7.05283E-12
ENSMUSG00000015090	Ptgdδ	15.69697832	0.809234721	3.03677E-11
ENSMUSG00000001827	Folr1	0.110396743	1.185238988	4.01792E-11
ENSMUSG00000022949	Clic6	0.161373143	1.050336343	4.44441E-11
ENSMUSG00000018339	Gpx3	0.217353362	-0.892847556	5.89498E-11
ENSMUSG00000027570	Col9a3	0.136979529	1.075807313	1.43951E-10
ENSMUSG00000026822	Lcn2	0.03252482	3.525855104	2.0377E-10
ENSMUSG00000090101	Snhg9	0.090694208	1.262296412	2.39549E-10
ENSMUSG00000031765	Mt1	12.0054113	0.719344555	3.3024E-10
ENSMUSG00000042524	Sun2	0.110396743	1.127905813	3.41145E-10
ENSMUSG00000048583	Igf2	0.162311359	0.979828265	9.61704E-10
ENSMUSG00000024176	Sox8	0.048474491	-1.145062982	1.15979E-09
ENSMUSG00000032246	Calml4	0.133852142	1.028064451	1.21155E-09
ENSMUSG000000115625	2900040C04Rik	0.110709482	1.088906755	1.35036E-09
ENSMUSG00000062591	Tubb4a	1.214051439	-0.743815144	1.79123E-09
ENSMUSG00000020681	Ace	0.171068042	0.948303289	1.90505E-09
ENSMUSG00000021268	Meg3	3.171482649	0.704409911	2.07384E-09
ENSMUSG00000029843	Slc13a4	0.070678935	1.261782194	3.05532E-09
ENSMUSG00000050063	Klk6	0.033463036	-1.283809979	4.57522E-09
ENSMUSG00000068240	Gm11808	0.290534206	0.824314302	4.70221E-09
ENSMUSG00000011884	Gltpr	0.134164881	-0.878029646	4.70221E-09
ENSMUSG00000021647	Cartpt	0.440961496	-1.188154442	4.85206E-09
ENSMUSG00000079484	Phyh1	0.124157244	1.045386116	5.37025E-09
ENSMUSG00000030048	Gkn3	0.010633114	-1.768058615	5.37025E-09
ENSMUSG00000048572	Tmem252	0.023455399	2.759976818	5.37025E-09
ENSMUSG00000006522	Ith13	0.348703595	0.790680565	7.62815E-09

ENSMUSG00000031762	Mt2	4.716457959	0.952020423	0.000143684	ENSMUSG00000022194	Pabpn1	0.132288449	-0.868554698	8.23329E-09
ENSMUSG00000027173	Depdc7	0.012099123	-1.729037523	0.00025382	ENSMUSG00000004655	Aqp1	0.03471399	1.704694382	1.28307E-08
ENSMUSG00000050105	Grrp1	0.134923549	1.133318942	0.000349249	ENSMUSG00000025225	Nfkb2	0.120717119	1.142454776	1.709E-08
ENSMUSG000000095845	Gm5741	0.14298963	2.908181215	0.000358858	ENSMUSG000000052193	Ogdhl	0.136041313	1.051419338	1.9524E-08
ENSMUSG00000079484	Phyh1	0.273146858	1.022732726	0.000385329	ENSMUSG00000025488	Cox8b	0.056292957	1.283974737	4.76328E-08
ENSMUSG00000062960	Kdr	0.016865444	-1.474905236	0.000385329	ENSMUSG000000115783	Bc1	0.41000037	0.7147832	5.21375E-08
ENSMUSG00000074170	Plekhh1	0.188453	1.096771025	0.000403887	ENSMUSG00000020660	Pomc	0.086628606	-1.177973798	5.21375E-08
ENSMUSG00000024778	Fas	0.068928335	1.314402749	0.000411708	ENSMUSG00000090247	Bloc1s1	0.219542532	0.817145341	5.34821E-08
ENSMUSG00000044258	Ctla2a	0.32887615	0.996806238	0.000702791	ENSMUSG00000062456	Rpl9-ps6	0.055042002	1.279215136	7.27189E-08
ENSMUSG00000027875	Hmgcs2	0.085427138	1.191367879	0.000713274	ENSMUSG00000030108	Slc6a13	0.068177026	1.167895291	2.29048E-07
ENSMUSG00000060377	Rpl36a-ps1	0.020165204	-1.339790754	0.00079943	ENSMUSG00000075514	Gm13375	0.005629296	-2.021382896	2.5302E-07
ENSMUSG000000115783	Bc1	0.403670726	-0.916496154	0.000832887	ENSMUSG00000046516	Cox17	1.193723427	0.638748611	2.5302E-07
ENSMUSG00000037279	Ovol2	0.211551325	0.980754672	0.001038974	ENSMUSG00000020954	Strn3	0.018764319	-1.358113258	2.59061E-07
ENSMUSG00000027525	Phactr3	1.960424495	0.877121482	0.001170857	ENSMUSG00000035202	Lars2	0.607338458	-0.671097586	2.74678E-07
ENSMUSG00000041378	Cldn5	0.239415971	-0.932687015	0.001273736	ENSMUSG00000043164	Tmem212	0.06723881	1.127385454	2.74908E-07
ENSMUSG00000006154	Eps811	0.017598724	-1.366849766	0.001274928	ENSMUSG00000043091	Tabal1c	0.029397433	1.689587493	3.12461E-07
ENSMUSG00000037169	Mycn	0.029331206	-1.173723228	0.002309043	ENSMUSG00000022763	Aifm3	0.342448822	0.700188303	4.78133E-07
ENSMUSG00000051851	Rtl8c	0.075894496	1.108154511	0.002524497	ENSMUSG00000025739	Gng13	1.39231247	0.621383945	4.78133E-07
ENSMUSG00000034634	Ly6d	0.025664805	1.622753373	0.002661951	ENSMUSG00000058488	Kl	0.102265539	0.944788805	4.82413E-07
ENSMUSG00000074896	Ifit3	0.052429531	-1.077914674	0.003407206	ENSMUSG00000064057	Scgb3a1	0.011258591	3.136540169	8.36427E-07
ENSMUSG00000028967	Errfi1	0.383505521	0.874077082	0.003936417	ENSMUSG00000039218	Srrm2	0.395927131	0.677143056	8.99303E-07
ENSMUSG00000022651	Retnlg	0.007332802	4.620211178	0.003970881	ENSMUSG00000021750	Fam107a	1.033913977	0.62639997	1.02581E-06
ENSMUSG00000025509	Pnpla2	0.554359797	0.847110113	0.004125333	ENSMUSG00000036504	Phpt1	0.219855271	0.74506873	1.1906E-06
ENSMUSG00000066170	E230001N04Rik	0.013932323	2.191367879	0.004374364	ENSMUSG00000030088	Alpdh11	0.324935457	0.736755591	1.33083E-06
ENSMUSG00000069806	Cacng7	0.107425543	-0.914508568	0.00445269	ENSMUSG00000073616	Cops9	3.410414978	0.577677639	2.05911E-06
ENSMUSG00000071497	Nutf2-ps1	0.003299761	-2.064887994	0.00445269	ENSMUSG00000063594	Gng8	0.111647698	0.876924009	2.15525E-06
ENSMUSG00000042622	Maff	0.027498006	1.521624958	0.005078514	ENSMUSG00000061086	Myl4	0.247689011	0.710684459	2.50986E-06
ENSMUSG00000056071	S100a9	0.040330409	2.774382109	0.005314193	ENSMUSG00000021290	Atp5mpl	3.314404212	0.57378722	2.66964E-06
ENSMUSG00000039883	Lrrc17	0.065995214	-0.958760885	0.005878638	ENSMUSG00000061436	Hipk2	0.008756682	-1.641196956	2.72464E-06
ENSMUSG00000038489	Polr2l	2.035219071	0.790168661	0.005878638	ENSMUSG00000031760	Mt3	12.73440509	0.565755981	2.76693E-06
ENSMUSG00000021903	Galnt15	0.037397288	1.359805431	0.007158201	ENSMUSG00000044349	Snhg11	2.278613804	0.583686458	3.1732E-06
ENSMUSG00000053175	Bcl3	0.022731685	1.561317489	0.007360366	ENSMUSG00000055235	Wdr86	0.029084694	1.5430762	3.46799E-06
ENSMUSG00000033006	Sox10	0.242715731	-0.878010804	0.007376207	ENSMUSG00000031425	Plp1	5.605527562	-0.607230461	3.84772E-06
ENSMUSG00000027845	Dclre1b	0.096792981	1.020354462	0.007635332	ENSMUSG00000027245	Hypk	0.400305472	0.653951808	4.07452E-06
ENSMUSG00000055172	C1ra	0.021631765	1.611222395	0.007765183	ENSMUSG00000076498	Trbc2	0.164813269	0.762027557	4.10072E-06
ENSMUSG00000045664	Cdc42ep2	0.184053319	-0.867812599	0.008737317	ENSMUSG0000008682	Rpl10	2.473449983	-0.576378802	4.55077E-06
ENSMUSG00000044734	Serpinb1a	0.18955292	-0.883292278	0.009908798	ENSMUSG00000030677	Kif22	0.08569039	0.528836585	4.63103E-06
ENSMUSG00000074521	Gm14327	0.050229691	1.126964847	0.010512814	ENSMUSG00000074754	Smim26	0.284279433	0.676436122	4.73898E-06
ENSMUSG0000005892	Trh	0.105225702	-1.224233063	0.010669643	ENSMUSG00000089661	Mia	0.104767448	0.859972608	5.28161E-06
ENSMUSG00000045471	Hcrt	2.724869057	-1.2739785	0.010669643	ENSMUSG00000048756	Foxo3	0.195774395	0.724886153	5.44325E-06
ENSMUSG00000021453	Gadd45g	0.639786936	0.785843304	0.010669643	ENSMUSG00000014313	Cox6c	9.783715926	0.551220324	5.44325E-06
ENSMUSG00000021250	Fos	0.040330409	-1.000058191	0.011385147	ENSMUSG00000097767	Miat	0.299603627	0.66421956	5.69631E-06
ENSMUSG000000113902	Ndufb1-ps	12.19151586	0.740738745	0.012964105	ENSMUSG00000026830	Ernm	0.208909418	-0.680460987	5.79327E-06
ENSMUSG00000020469	Myl7	0.00146656	-2.735580369	0.013218809	ENSMUSG00000038570	Saxo2	0.087566822	0.911766004	6.21466E-06
ENSMUSG00000024066	Xdh	0.09312658	0.96485935	0.013575737	ENSMUSG00000020713	Gh	0.08569039	1.59296903	6.24537E-06
ENSMUSG00000044792	Isca1	0.837405937	0.75560508	0.014763436	ENSMUSG00000028998	Tomm7	1.16526421	0.570910736	8.21102E-06
ENSMUSG00000004328	Hif3a	0.055362652	1.100781837	0.015171531	ENSMUSG00000029697	Fezf1	0.012509546	-1.406523097	8.36044E-06
ENSMUSG00000030413	Pglyrp1	0.580391243	0.779099568	0.015171531	ENSMUSG00000086841	2410006H16Rik	0.729932009	0.584262461	8.86285E-06
ENSMUSG00000098234	Snhg6	0.454633696	0.770471535	0.015189679	ENSMUSG00000032579	Hemk1	0.160122189	0.810960746	1.24127E-05
ENSMUSG00000032854	Ugt8a	0.312377346	-0.826867202	0.015189679	ENSMUSG000000118506	1700094D03Rik	0.079435617	0.913945704	1.27317E-05
ENSMUSG000000105703	Gm43305	0.061595533	-0.906502185	0.015189679	ENSMUSG00000021133	Susd6	0.082875742	0.901995625	1.32626E-05
ENSMUSG00000031255	Syt4	0.005499601	-1.67899684	0.015221247	ENSMUSG00000073424	Cyp4f15	0.097887197	0.846668121	1.32626E-05
ENSMUSG00000049649	Gpr3	0.011732482	-1.327624967	0.01577095	ENSMUSG00000019230	Lhx9	0.06723881	0.963156058	1.77824E-05
ENSMUSG00000025652	Tmem89	0.013565683	1.890858768	0.015797176	ENSMUSG00000070306	Ccdc153	0.086628606	1.053561549	1.79897E-05
ENSMUSG00000020473	Aebp1	0.067095134	-1.023331348	0.016177023	ENSMUSG00000044258	Ctla2a	0.115087823	0.815524636	2.01407E-05
ENSMUSG00000085896	5330429C05Rik	0.011732482	2.102362873	0.016371464	ENSMUSG00000003469	Phyhip	0.491625158	0.599970799	2.42144E-05
ENSMUSG00000097383	1500026H17Rik	0.266913977	0.792224923	0.016700755	ENSMUSG00000091705	H2-Q2	0.015636932	-1.25846885	2.42144E-05
ENSMUSG00000033213	AA467197	0.030431126	1.262659174	0.018750961	ENSMUSG00000016024	Lbp	0.05354741	1.02199845	2.78065E-05
ENSMUSG00000078193	Gm2000	0.126857467	-0.815113824	0.019655474	ENSMUSG000000224245	Enpp2	2.555700248	0.63910548	2.84733E-05
ENSMUSG00000090698	Apold1	0.044730089	1.126014141	0.020746198	ENSMUSG00000030905	Crym	0.530092012	0.597015535	3.478E-05
ENSMUSG00000086765	Gm11827	0.012832403	1.938387138	0.021701922	ENSMUSG00000095366	Gm21860	0.022204444	1.594511464	3.57624E-05
ENSMUSG00000024534	Sncap1	0.013565683	-1.238424249	0.023817188	ENSMUSG00000059361	Nrsn2	0.654561994	-0.562467909	3.76873E-05
ENSMUSG00000070369	Itgad	0.086160418	0.970985452	0.024085651	ENSMUSG000000115008	4933429019Rik	0.008756682	3.048102204	3.77952E-05

ENSMUSG00000049521	Cdc42ep1	0.131990428	-0.821215651	0.024085651	ENSMUSG00000056054	S100a8	0.014073239	2.865686259	4.18574E-05
ENSMUSG00000059325	Hopx	0.217050926	-0.776963808	0.026393412	ENSMUSG00000003526	Prodh	0.214225975	0.651025717	4.80423E-05
ENSMUSG00000028128	F3	0.388271842	0.754180349	0.026972056	ENSMUSG00000061751	Kalrn	0.800298205	0.552047372	5.69023E-05
ENSMUSG00000030048	Gkn3	0.04692993	-0.994498666	0.027098366	ENSMUSG00000025006	Sorbs1	0.015949671	-1.222139205	5.85989E-05
ENSMUSG00000036362	P2ry13	0.039597128	-0.946436425	0.027166751	ENSMUSG00000035048	Anapc13	0.755576578	0.564936822	6.315E-05
ENSMUSG00000024835	Coro1b	0.150322432	0.807600531	0.032144694	ENSMUSG00000030541	Idh2	0.335568571	0.582237152	6.97845E-05
ENSMUSG00000019577	Pdk4	0.023098325	1.527454037	0.033238348	ENSMUSG00000021957	Tkt	0.275210012	0.643995822	8.17182E-05
ENSMUSG00000078879	Zfp973	0.021631765	1.379896849	0.035121677	ENSMUSG00000040147	Maob	0.160122189	0.681974306	8.17182E-05
ENSMUSG00000038067	Csf3	0.008799362	4.871749945	0.036705309	ENSMUSG00000013523	Bcas1	0.35214372	-0.570057223	8.67591E-05
ENSMUSG00000028927	Padi2	0.09385986	-0.835259973	0.039290818	ENSMUSG00000032060	Cryab	1.34133607	-0.534279747	8.74608E-05
ENSMUSG00000017754	Pltp	0.416869768	-0.743296201	0.040245447	ENSMUSG00000032595	Cdhr4	0.026895524	1.370030299	8.85379E-05
ENSMUSG00000046470	Sox18	0.005499601	-1.579461167	0.040662375	ENSMUSG00000044734	Serpinb1a	0.066926071	-0.764897409	8.85379E-05
ENSMUSG00000024650	Slc22a6	0.019798564	-1.303629486	0.040950867	ENSMUSG00000032766	Gng11	0.217353362	-0.648633545	9.55167E-05
ENSMUSG00000018604	Tbx3	0.007332802	-1.424182941	0.047608412	ENSMUSG00000079523	Tmsb10	7.101669264	0.496253676	9.82204E-05
					ENSMUSG00000022860	Chodl	0.008756682	-1.475459752	9.91667E-05
					ENSMUSG00000032115	Hyou1	0.042845195	-0.863242016	0.000104961
					ENSMUSG00000017778	Cox7c	5.767838922	0.500518901	0.000104961
					ENSMUSG00000038489	Poir2l	0.414065973	0.566413335	0.000107476
					ENSMUSG00000019874	Fabp7	0.122280812	-0.657875697	0.000108519
					ENSMUSG00000026641	Usf1	0.054729264	-0.80008547	0.000111291
					ENSMUSG00000098234	Snhg6	0.060671298	0.919707273	0.0001124
					ENSMUSG00000054667	Irs4	0.016575148	-1.167691421	0.00011502
					ENSMUSG00000096768	Gm47283	0.315240559	0.594427359	0.000116302
					ENSMUSG00000097162	2310010J17Rik	0.06254773	0.905713153	0.000120053
					ENSMUSG00000070780	Rbm47	0.014073239	1.948148419	0.000120617
					ENSMUSG00000029499	Pxmp2	0.098512675	0.765981503	0.000130584
					ENSMUSG00000093674	Rpl41	11.23169588	0.484437454	0.000135837
					ENSMUSG00000052188	Gm14964	0.054103786	0.9549928	0.000136405
					ENSMUSG00000030600	Lrfr1	0.069740719	-0.738587497	0.000151592
					ENSMUSG00000023084	Lrrc71	0.007192989	3.097011805	0.000173905
					ENSMUSG00000048108	Tmem72	0.029710172	1.23903081	0.000173905
					ENSMUSG00000035545	Leng8	0.12040438	0.70790156	0.000173905
					ENSMUSG000000104960	Snhg8	0.460038554	0.541755811	0.000182657
					ENSMUSG00000031239	Itm2a	0.246750795	-0.56787424	0.000210328
					ENSMUSG00000027562	Car2	0.913509597	-0.510728631	0.000213504
					ENSMUSG00000052861	Dnah6	0.02095349	1.470229128	0.000243966
					ENSMUSG00000052397	Ezr	0.242685192	0.588299283	0.000243966
					ENSMUSG00000037490	Slc2a12	0.068489764	0.842197906	0.000260933
					ENSMUSG00000002625	Akap8l	0.450030917	0.550631766	0.000261055
					ENSMUSG00000020018	Snrpf	0.288970513	0.567697334	0.00026617
					ENSMUSG00000063714	Sp3os	0.122906289	0.687017897	0.000267226
					ENSMUSG00000025597	Klhl4	0.038154115	-0.853775221	0.000270806
					ENSMUSG00000026575	Nme7	0.577628287	0.641844733	0.000283073
					ENSMUSG00000044988	Ucn3	0.008443944	-1.691823029	0.000283073
					ENSMUSG00000057103	Nat8f1	0.168878871	0.625749803	0.000344376
					ENSMUSG00000034209	Rasl10a	0.241434238	-0.554513362	0.000354247
					ENSMUSG00000027199	Gatm	0.401243688	-0.544145235	0.000357013
					ENSMUSG00000030329	Pianp	0.293036115	-0.55261591	0.000375308
					ENSMUSG00000105361	AY036118	0.021891705	-1.226946825	0.000375891
					ENSMUSG00000040420	Cdh18	0.003127386	-1.959256415	0.000410016
					ENSMUSG00000015806	Qdpr	1.507400293	-0.489745093	0.000418312
					ENSMUSG00000036833	Pnpla7	0.059107605	0.862736392	0.000424732
					ENSMUSG00000018217	Pmp22	0.103516493	-0.659805724	0.000424732
					ENSMUSG00000056553	Ptprn2	0.013135023	-1.201237294	0.000424732
					ENSMUSG00000026051	Ecrg4	0.242059715	0.71563911	0.000458861
					ENSMUSG00000020163	Uqcr11	4.922193612	0.458783372	0.000472897
					ENSMUSG000000110710	C78859	0.048787229	0.936305333	0.000478578
					ENSMUSG00000042541	Sem1	0.747132635	0.493456843	0.000484587
					ENSMUSG00000034059	Ypel4	0.222044441	0.599892653	0.00048802
					ENSMUSG00000033208	S100b	0.80624024	-0.485431193	0.000488474
					ENSMUSG00000022122	Ednrb	0.102265539	-0.811637103	0.00049888
					ENSMUSG00000030000	Add2	0.301792797	0.552947335	0.000532345
					ENSMUSG00000038861	Pl4kb	0.030961126	-0.883013495	0.000551735

ENSMUSG00000033731	330002A11Rik	0.017513364	1.537584396	0.000578644
ENSMUSG00000058740	Kcnt1	0.237994113	0.562134536	0.000592219
ENSMUSG00000021848	Otx2	0.035026729	1.065441726	0.000608137
ENSMUSG00000037086	Prr32	0.022204444	1.360046211	0.000608137
ENSMUSG00000038685	Rtel1	0.043783411	0.965100129	0.000608812
ENSMUSG00000073702	Rpl31	3.755365709	0.453544903	0.000646113
ENSMUSG00000068196	Col8a1	0.025644569	1.243232546	0.000646113
ENSMUSG00000061808	Ttr	37.40354254	0.866885642	0.000646113
ENSMUSG00000020889	Nr1d1	0.139481438	-0.58770152	0.000646546
ENSMUSG00000038690	Atp5j2	4.893734395	0.449976691	0.000658401
ENSMUSG00000019146	Cacng2	0.055042002	-0.734590663	0.000658401
ENSMUSG00000073982	Rhog	0.167627916	-0.580304301	0.00066331
ENSMUSG00000052353	Cemip	0.036903161	1.031827636	0.000680675
ENSMUSG00000038068	Rnf144b	0.074431799	0.769059922	0.000684822
ENSMUSG00000064220	Hist2h2aa1	0.03252482	1.097011805	0.000732423
ENSMUSG00000025350	Rdh5	0.091319686	0.712452722	0.000732423
ENSMUSG00000022982	Sod1	1.608102138	0.461877932	0.000732423
ENSMUSG00000041841	Rpl37	11.33521237	0.442088395	0.000816002
ENSMUSG00000030315	Vgll4	0.005003818	-1.629306545	0.000842971
ENSMUSG00000019890	Nts	0.121029858	-0.597121666	0.000879735
ENSMUSG00000087075	Lbhd2	0.073806321	-0.665296637	0.000880836
ENSMUSG00000022805	Maats1	0.018764319	1.442786642	0.000917948
ENSMUSG00000025199	Chuk	0.070366196	0.769985842	0.000938979
ENSMUSG00000072473	1700024G13Rik	0.019389796	1.401866386	0.000959897
ENSMUSG00000062328	Rpl17	5.359714983	-0.446709734	0.001006096
ENSMUSG00000028139	Rriad1	0.105392925	0.665001227	0.001009192
ENSMUSG00000035370	Gm49322	0.005629296	3.175014317	0.00109881
ENSMUSG00000034227	Foxj1	0.054103786	0.846468343	0.001113932
ENSMUSG0000004567	Mcoln1	0.160747666	0.589740589	0.001141786
ENSMUSG00000046711	Hmga1	0.10414197	-0.60010143	0.001266863
ENSMUSG00000016427	Ndufa1	1.032350284	0.455499385	0.001270949
ENSMUSG00000025241	Fyco1	0.10414197	0.66213392	0.001273757
ENSMUSG0000006360	Crip1	0.180137462	0.570734647	0.001278205
ENSMUSG00000064345	mt-Nd2	23.67306485	-0.438661183	0.001283671
ENSMUSG00000022843	Clcn2	0.094447072	0.678407691	0.001289247
ENSMUSG00000044709	Gemin7	0.253943784	-0.510837125	0.001352435
ENSMUSG00000032295	Man2c1	0.168566132	0.574844431	0.001368194
ENSMUSG00000024810	Il33	0.24080876	-0.512993283	0.001398486
ENSMUSG00000045027	Prss22	0.002814648	-1.920910103	0.001411778
ENSMUSG00000020634	Ubxn2a	0.052852832	-0.70791638	0.001446079
ENSMUSG00000034796	Cpne7	0.323997241	0.510658755	0.001449468
ENSMUSG00000028957	Per3	0.11821521	0.62689223	0.001529166
ENSMUSG00000045318	Adra2c	0.054729264	-0.700944419	0.001599599
ENSMUSG00000032554	Trf	1.096774445	-0.462015306	0.001599599
ENSMUSG00000029516	Cit	0.27114441	0.537198605	0.001805215
ENSMUSG00000048794	Cfap100	0.031273865	1.04097777	0.001863739
ENSMUSG00000078974	Sec61g	1.82076442	0.439808878	0.001863739
ENSMUSG00000041736	Tspo	0.091006947	0.673967866	0.001863739
ENSMUSG00000024033	Rsph1	0.085064913	0.685943208	0.001863739
ENSMUSG00000017723	Wfdc2	0.03940507	0.930878383	0.001887459
ENSMUSG00000060671	Atp8b2	0.026895524	1.122102786	0.002023926
ENSMUSG00000026579	F5	0.042219718	0.899072427	0.002059061
ENSMUSG00000023089	Ndufa5	3.329415668	0.421839177	0.002207608
ENSMUSG00000064354	mt-Co2	41.39221128	-0.424373685	0.002226792
ENSMUSG00000032399	Rpl4	5.692468907	0.441444869	0.002233973
ENSMUSG00000040506	Ambra1	0.149176336	0.573712324	0.002299903
ENSMUSG00000029817	Tra2a	0.246750795	0.608327593	0.002362108
ENSMUSG00000086370	Ftx	0.040030547	0.908566715	0.00237771
ENSMUSG00000087590	Epb41l4aos	0.212662282	0.526955511	0.002401682
ENSMUSG00000026668	Ucma	0.019077058	1.55935019	0.00241749
ENSMUSG00000021879	Dnah12	0.003752864	4.212489022	0.00241749
ENSMUSG00000060377	Rpl36a-ps1	0.012822285	1.656439213	0.00241749
ENSMUSG00000023943	Sult1c1	0.003752864	4.212489022	0.00241749

ENSMUSG00000026255	Efhd1	0.094134334	-0.589395959	0.002479335
ENSMUSG00000042073	Abhd14b	0.094134334	0.65242196	0.002550198
ENSMUSG00000028763	Hspg2	0.025019092	1.123978852	0.002721068
ENSMUSG00000026034	Clk1	0.323997241	0.481762609	0.003047218
ENSMUSG00000113722	Snhg10	0.048787229	0.817985366	0.003092719
ENSMUSG00000024516	Sec11c	0.937277734	-0.431771335	0.003096312
ENSMUSG00000064357	mt-Atp6	58.68509493	-0.41342803	0.003230619
ENSMUSG00000053475	Tnfaip6	0.06942798	-0.689865812	0.003259264
ENSMUSG00000020108	Ddit4	0.191396054	0.528618584	0.003307687
ENSMUSG00000040759	Cmtm5	0.377788289	-0.45170017	0.00331469
ENSMUSG00000029718	Pcolce	0.072868105	0.695913497	0.003346835
ENSMUSG00000024186	Rgs11	0.083813958	0.664648429	0.003346835
ENSMUSG00000060780	Lrrtm1	0.239557806	-0.48606851	0.003405484
ENSMUSG00000029060	Mib2	0.230488385	0.506196578	0.003590182
ENSMUSG00000062031	Pgggh	0.024080876	1.125026181	0.003590402
ENSMUSG00000070304	Scn2b	0.64643079	0.436619293	0.003601929
ENSMUSG00000022861	Dgkg	0.005003818	-1.509012311	0.003630065
ENSMUSG00000010044	Zmynd10	0.037215899	0.91114526	0.003747436
ENSMUSG00000026247	Ecel1	0.076620969	-0.632899032	0.003790014
ENSMUSG00000070637	Srarp	0.048787229	0.806670053	0.003790014
ENSMUSG00000033061	Resp18	1.874555468	-0.435884303	0.004007936
ENSMUSG00000037152	Ndufc1	3.04388528	0.406754755	0.004069469
ENSMUSG00000035896	Rnase1	0.001563693	-2.188390414	0.004105046
ENSMUSG00000087269	D330023K18Rik	0.065362378	0.718500182	0.004106819
ENSMUSG00000028248	Pnlsr	0.260198557	0.48800383	0.004115168
ENSMUSG00000069917	Hba-a2	1.587148649	0.582225484	0.004152621
ENSMUSG00000028495	Rps6	2.243587075	-0.412414797	0.004191268
ENSMUSG00000041354	Rgl2	0.145110734	0.552957248	0.004209367
ENSMUSG00000024985	Tcf7l2	0.413440495	0.49578425	0.004234275
ENSMUSG00000042647	Acad12	0.027521001	1.033586425	0.00423694
ENSMUSG00000023764	Sfi1	0.058794866	0.74337485	0.004238323
ENSMUSG00000027133	Nop10	1.103029218	0.42055095	0.004297469
ENSMUSG00000030499	Kctd15	0.047536275	0.803652862	0.004361118
ENSMUSG00000057322	Rpl38	11.8152662	0.396798281	0.004361118
ENSMUSG00000110332	Gm19935	0.089755993	0.632125756	0.004386174
ENSMUSG00000078771	Evi2a	0.150114552	-0.621084896	0.004386174
ENSMUSG00000036568	Bicral	0.124469983	0.574865412	0.004386174
ENSMUSG00000054091	1810037117Rik	0.911320426	0.419094571	0.004579591
ENSMUSG00000068323	Slc4a5	0.029397433	0.994442071	0.004594688
ENSMUSG00000017167	Cntnap1	0.23392851	0.492915137	0.004594688
ENSMUSG00000025266	Gnl3l	0.47723918	0.439277473	0.004594688
ENSMUSG00000039004	Bmp6	0.037215899	0.895377944	0.004714031
ENSMUSG00000036181	Hist1h1c	0.144485256	0.546738725	0.004747644
ENSMUSG00000066129	Kndc1	0.388421403	0.47877693	0.004789872
ENSMUSG00000037625	Cldn11	1.040794227	0.509451413	0.004802414
ENSMUSG00000024299	Adamts10	0.049099968	0.793462239	0.004802414
ENSMUSG00000034936	Arl4d	0.12978654	0.561437331	0.004857803
ENSMUSG00000023826	Prkn	0.035652206	0.914595859	0.004857803
ENSMUSG00000098332	2310009A05Rik	0.220793487	0.495816277	0.004878836
ENSMUSG00000028128	F3	0.150427291	0.539242267	0.004898827
ENSMUSG00000066687	Zbtb16	0.004378341	-1.558340024	0.004914447
ENSMUSG00000069833	Ahnak	0.09726172	0.61257618	0.004953329
ENSMUSG00000034317	Trim59	0.040030547	-0.710343117	0.005193189
ENSMUSG00000036138	Acaa1a	0.352769197	0.475459537	0.005193189
ENSMUSG00000021495	Fam193b	0.172006257	0.51992573	0.005193189
ENSMUSG00000036814	Slc6a20a	0.072868105	0.668168506	0.005291514
ENSMUSG00000029311	Hsd17b11	0.107269357	0.589585905	0.005306342
ENSMUSG00000040690	Col16a1	0.059107605	0.724352908	0.005314475
ENSMUSG00000028936	Rpl22	1.802625578	0.400600968	0.005314475
ENSMUSG00000020799	Tekt1	0.028146478	0.997476131	0.005329476
ENSMUSG00000009281	Rarres2	0.18295211	0.526897069	0.005392156
ENSMUSG00000059412	Fxyd2	0.117276994	0.574785059	0.005417483
ENSMUSG00000071528	Atp5md	7.404713016	0.390631963	0.005417483

ENSMUSG00000039307	Hexdc	0.137917745	0.548407804	0.005437603
ENSMUSG00000033697	Arhgap39	0.172944473	0.517267013	0.005437603
ENSMUSG00000064360	mt-Nd3	6.390814312	0.39143319	0.005437603
ENSMUSG00000039485	Tspyl4	0.629542902	0.426526079	0.005523546
ENSMUSG00000085251	Gm12326	0.01845158	1.249014898	0.005531831
ENSMUSG00000051166	Eml5	0.126346415	0.559117558	0.005651565
ENSMUSG00000103181	A330069K06Rik	0.007505728	2.155905494	0.005724428
ENSMUSG00000054312	Mrps21	1.275348215	0.404073425	0.005751477
ENSMUSG00000029455	Aldh2	0.485370385	0.431653007	0.005751477
ENSMUSG00000028234	Rps20	7.411906005	0.38867587	0.005766315
ENSMUSG00000034467	Dynlrb2	0.060671298	0.709988682	0.005813463
ENSMUSG00000001930	Vwfv	0.060671298	0.880974879	0.005981742
ENSMUSG00000048058	Ldlrad3	0.016575148	-0.952231714	0.006131202
ENSMUSG00000038300	Pth2	0.004065602	3.319404226	0.006482931
ENSMUSG00000015341	Golga7	0.279901092	-0.452085243	0.00659525
ENSMUSG00000031189	Aff2	0.000312739	-3.072913197	0.00659525
ENSMUSG00000053644	Aldh7a1	0.233303033	0.477697799	0.006651213
ENSMUSG00000029994	Anxa4	0.021578967	1.117770365	0.006674756
ENSMUSG00000025492	Ifitm3	0.159183973	0.520560804	0.006674756
ENSMUSG00000038060	Dlec1	0.011884069	1.54952401	0.006908452
ENSMUSG00000017639	Rab11fip4	0.413440495	0.428376016	0.006997291
ENSMUSG00000053646	Plxnb1	0.22235718	0.479988095	0.007247688
ENSMUSG00000041607	Mbp	9.074111929	-0.404119105	0.007315756
ENSMUSG00000047230	Cldn2	0.021891705	1.107207572	0.007438197
ENSMUSG00000037111	Setd7	0.3196189	0.444550543	0.007442326
ENSMUSG00000031762	Mt2	1.265653316	0.39470906	0.007873786
ENSMUSG00000025422	Agap2	0.139168699	-0.499228101	0.007955964
ENSMUSG00000030279	C2cd5	0.091632424	0.597979483	0.008002615
ENSMUSG00000028907	Utp11	0.083813958	-0.558595391	0.008102249
ENSMUSG00000075266	Cenpw	0.059420343	0.697160709	0.008102249
ENSMUSG00000074207	Adh1	0.008131205	1.945008711	0.008261413
ENSMUSG00000052387	Trpm3	0.22704826	0.585318958	0.008261413
ENSMUSG00000049721	Gal3st1	0.090694208	-0.543866685	0.008330034
ENSMUSG00000048731	Ggnbp1	0.038779593	1.002100158	0.008335117
ENSMUSG00000015647	Lama5	0.032212081	0.908708274	0.008482808
ENSMUSG00000062115	Rai1	0.124157244	0.575026737	0.008482808
ENSMUSG00000058669	Nkx2-9	0.001876432	-1.965997993	0.008697969
ENSMUSG00000057969	Sema3b	0.034088513	0.884018082	0.008716591
ENSMUSG00000025645	Ccdc51	0.02783374	0.959508281	0.008716591
ENSMUSG00000005580	Adcy9	0.008131205	-1.208796625	0.008716591
ENSMUSG00000015401	Cltrn	0.010945853	1.594514464	0.008716591
ENSMUSG00000015652	Steap1	0.020640751	1.118706876	0.008727626
ENSMUSG00000031170	Slc38a5	0.026270047	0.990702903	0.008781444
ENSMUSG00000099632	2900093K20Rik	0.103516493	0.569676122	0.008827779
ENSMUSG00000024579	Pcyox1l	0.06723881	0.659606493	0.008850278
ENSMUSG00000062488	Ifit3b	0.012196807	-1.036387321	0.008850278
ENSMUSG00000072214	Sept5	0.063798685	-0.593105442	0.00908676
ENSMUSG00000023150	Ivns1abp	0.680519302	0.430249995	0.009100859
ENSMUSG00000047228	A2ml1	0.12509546	-0.500488162	0.009635033
ENSMUSG00000024897	Apba1	0.181388417	0.487429337	0.009673476
ENSMUSG00000047904	Sstr2	0.046598059	-0.647149291	0.009727428
ENSMUSG00000004980	Hnrnpa2b1	1.593403422	0.384773673	0.009771878
ENSMUSG00000044033	Ccdc141	0.053478309	0.709495368	0.00980997
ENSMUSG00000039001	Rps21	12.74472546	0.370987549	0.00980997
ENSMUSG00000031537	Ikbkb	0.174195428	0.73228877	0.00980997
ENSMUSG00000025451	Paip1	0.156056586	-0.479268453	0.00980997
ENSMUSG00000085133	B930095G15Rik	0.150740029	0.551411736	0.00980997
ENSMUSG00000032988	Slc16a8	0.016575148	1.266936806	0.00980997
ENSMUSG00000017344	Vtn	0.397803563	0.428391375	0.009928461
ENSMUSG00000079304	Tex52	0.000312739	-3.011512652	0.01004527
ENSMUSG00000113029	Gm40578	0.016575148	-0.912972284	0.01004527
ENSMUSG00000032968	Inha	0.09507255	0.574890178	0.010312591
ENSMUSG00000037820	Tgm2	0.054103786	0.745539434	0.010366569



ENSMUSG00000030638	Sh3gl3	0.232052078	-0.44558788	0.010366569
ENSMUSG00000070394	Tmem256	1.115226026	0.387361285	0.010372018
ENSMUSG00000054428	Atpif1	4.641354304	0.37306198	0.010486643
ENSMUSG00000047557	Lxn	0.326811889	-0.423067844	0.01070306
ENSMUSG00000026500	Cox20	0.499756363	0.414379483	0.010771197
ENSMUSG00000092626	9130230N09Rik	0.013760501	1.360046211	0.010795301
ENSMUSG00000040618	Pck2	0.131662972	0.522342059	0.010795301
ENSMUSG00000020439	Smtn	0.032837558	0.900119756	0.010799323
ENSMUSG00000091955	Gm9844	0.037528638	0.816202697	0.010841174
ENSMUSG00000031775	Plip	0.384668539	-0.416476888	0.011092754
ENSMUSG00000087211	Lhx1os	0.00688025	-1.249790959	0.011092754
ENSMUSG00000059970	Hspa2	0.258322125	0.448905321	0.011092754
ENSMUSG00000036561	Ppp6r2	0.072555367	-0.56040249	0.011148143
ENSMUSG00000023043	Krt18	0.031273865	0.884858568	0.011148143
ENSMUSG00000113186	A330076C08Rik	0.004065602	-1.513485788	0.011268067
ENSMUSG00000037126	Psd	1.381366617	0.38222525	0.011340628
ENSMUSG00000002007	Srpk3	0.026895524	1.024255462	0.011376076
ENSMUSG00000017009	Sdc4	0.386232233	0.444775949	0.011393838
ENSMUSG00000029068	Ccnl2	0.290846944	0.44247191	0.011418854
ENSMUSG00000042628	Zfyve1	0.053791048	0.698750018	0.012001943
ENSMUSG00000024903	Lao1	0.007818466	1.890560927	0.01218157
ENSMUSG00000045690	Wdr89	0.036277683	0.827825172	0.01218157
ENSMUSG00000047842	Diras2	0.816560615	0.391821352	0.01218157
ENSMUSG00000042369	Rbm45	0.014385978	-0.9445891	0.012310462
ENSMUSG00000112343	Sfta3-ps	0.002814648	-1.689584557	0.012310462
ENSMUSG00000030111	A2m	0.03002291	0.902508781	0.012481948
ENSMUSG00000092627	D130058E05Rik	0.021578967	1.05636982	0.012805292
ENSMUSG00000060424	Pantr1	0.822189911	0.385056354	0.012849484
ENSMUSG00000037852	Cpe	12.01104059	0.362463557	0.012849484
ENSMUSG00000038564	Ift172	0.14354704	0.502670972	0.0130844
ENSMUSG00000020272	Stk10	0.019077058	1.256792249	0.01328819
ENSMUSG00000025856	Pdgfa	0.14604895	-0.470895532	0.013289554
ENSMUSG00000087196	Gm13373	0.010320375	1.599512145	0.013347744
ENSMUSG00000042707	Dnal1	0.02095349	1.075950189	0.013347744
ENSMUSG00000046160	Olig1	0.60921489	-0.394298359	0.013347744
ENSMUSG00000074922	Fam122a	0.009694898	-1.087863538	0.013347744
ENSMUSG00000017677	Wsb1	0.202967384	0.461882517	0.013352036
ENSMUSG00000015850	Adamts14	0.008756682	-1.121822797	0.013723489
ENSMUSG00000024076	Vit	0.029397433	0.892080354	0.01405896
ENSMUSG00000036687	Tmem184a	0.005942034	2.249014898	0.014126143
ENSMUSG00000050370	Ch25h	0.005942034	2.249014898	0.014126143
ENSMUSG00000056201	Cfl1	4.720477183	-0.366783563	0.014192459
ENSMUSG00000038354	Ankrd35	0.107582096	0.537360393	0.01420769
ENSMUSG00000030168	Adipor2	0.24549984	0.458009464	0.01420769
ENSMUSG00000021702	Thbs4	0.032212081	0.854937018	0.01420769
ENSMUSG00000036880	Acaa2	0.186704974	0.466924299	0.014589073
ENSMUSG00000024830	Rps6kb2	0.094447072	0.560466433	0.014806506
ENSMUSG00000090071	Cdk5r2	0.26176225	0.434953178	0.014925461
ENSMUSG00000062729	Ppox	0.083188481	0.578391799	0.015048326
ENSMUSG00000038803	Ost4	0.197963565	0.458444561	0.015048326
ENSMUSG00000074676	Foxs1	0.005316557	2.360046211	0.015064354
ENSMUSG00000019831	Wasf1	0.868162492	0.386258688	0.015064354
ENSMUSG00000038936	Sccpdh	0.397178085	-0.399600796	0.015177206
ENSMUSG00000074457	S100a16	0.445652576	-0.389029143	0.015204127
ENSMUSG00000039740	Alg2	0.293974331	-0.426883406	0.015204127
ENSMUSG00000019984	Med23	0.128222846	0.508543361	0.015204127
ENSMUSG00000030757	Zkscan2	0.045972582	0.72150267	0.015266352
ENSMUSG00000066705	Fxyd6	0.622037175	-0.392809939	0.015266352
ENSMUSG00000071637	Cebpd	0.160122189	0.478690707	0.015266352
ENSMUSG00000109394	A230057D06Rik	0.038154115	0.782138468	0.015325132
ENSMUSG00000086859	Snhg20	0.444401622	0.405496486	0.015325132
ENSMUSG00000033880	Lgals3bp	0.079122878	0.587844655	0.015325132
ENSMUSG00000050856	Atp5k	5.16831893	0.357090001	0.015476647

ENSMUSG00000032590	Apeh	0.1019528	0.543268035	0.015476647
ENSMUSG00000006456	Rbm14	0.134477619	0.498721772	0.01560091
ENSMUSG000000109006	B230209E15Rik	0.015324194	-0.899376942	0.015772195
ENSMUSG000000033886	Frrs1	0.012509546	1.41016969	0.016084216
ENSMUSG000000057729	Prtn3	0.009694898	-1.072913197	0.016084216
ENSMUSG000000053964	Lgals4	0.013135023	1.353351558	0.016102281
ENSMUSG000000030792	Dkkl1	0.059420343	-0.575857785	0.016153113
ENSMUSG000000024665	Fads2	0.311174957	-0.409062724	0.016292566
ENSMUSG000000092341	Malat1	2.338972363	0.365456807	0.016307175
ENSMUSG000000029154	Cwh43	0.014385978	1.259283234	0.016357236
ENSMUSG000000046242	Nme9	0.015324194	1.249014898	0.016357236
ENSMUSG000000069919	Hba-a1	2.042808862	0.499297573	0.016633884
ENSMUSG000000020697	Lig3	0.080686572	0.586343086	0.016633884
ENSMUSG000000004328	Hif3a	0.02314266	0.985980492	0.016813296
ENSMUSG000000028962	Slc4a2	0.190770576	0.614793032	0.016954178
ENSMUSG000000006651	Aplp1	3.695632627	-0.361198536	0.017171863
ENSMUSG000000045996	Polr2k	0.669260711	0.38382557	0.017383245
ENSMUSG000000041957	Pkp2	0.089443254	0.558015158	0.01746401
ENSMUSG000000063320	1190007107Rik	0.069115242	0.606025452	0.017471463
ENSMUSG000000039323	Igfbp2	0.39154879	0.421677052	0.017703867
ENSMUSG000000018395	Kif3a	0.079435617	-0.529770872	0.017707306
ENSMUSG000000034390	Cmip	0.023455399	-1.662087949	0.018139958
ENSMUSG000000034486	Gbx2	0.067551548	0.907278322	0.018146116
ENSMUSG000000024660	Incenp	0.055354741	0.656865857	0.018196054
ENSMUSG0000000112454	Gm48619	0.010007637	1.556443423	0.01834398
ENSMUSG000000062997	Rpl35	4.461529581	0.351717692	0.018438638
ENSMUSG000000014294	Ndufa2	3.121444465	0.35357138	0.018438638
ENSMUSG000000030701	Plekhhb1	1.12585914	-0.372907437	0.018573672
ENSMUSG000000002831	Plin4	0.071929889	0.595614021	0.018573672
ENSMUSG000000003778	Brd8	0.167627916	0.464483621	0.018944915
ENSMUSG0000000049755	Zfp672	0.113836869	0.512049304	0.01942926
ENSMUSG000000024610	Cd74	0.033463036	0.807505188	0.01969607
ENSMUSG000000020810	Cygb	0.217353362	-0.423302056	0.01970471
ENSMUSG000000021099	Six6	0.003752864	-1.487950696	0.01970471
ENSMUSG000000032128	Robo3	0.049725445	0.68423028	0.020015662
ENSMUSG000000028463	Car9	0.00469108	2.512049304	0.020086813
ENSMUSG000000020776	Fbf1	0.146674427	0.475676914	0.020107538
ENSMUSG000000092074	Dynlt1a	0.055980218	0.646350396	0.020107538
ENSMUSG000000031441	Atp11a	0.15762028	0.467049319	0.020115024
ENSMUSG000000055200	Sertad3	0.008756682	-1.089401319	0.020325956
ENSMUSG000000044986	Tst	0.143859779	-0.453108947	0.020487093
ENSMUSG000000037706	Cd81	2.84467076	0.392491117	0.020644725
ENSMUSG000000097383	1500026H17Rik	0.045659843	0.700494394	0.020680502
ENSMUSG000000056155	Nanos3	0.022829921	0.966615168	0.020708069
ENSMUSG000000027429	Sec23b	0.341510606	0.446255653	0.020809577
ENSMUSG000000024268	Cellf4	0.819375263	-0.37284039	0.020809577
ENSMUSG000000022974	Paxbp1	0.131662972	0.488314655	0.020811009
ENSMUSG000000052296	Ppp6r1	0.143859779	0.478029195	0.020831961
ENSMUSG000000095845	Gm5741	0.127284631	0.716869096	0.020871573
ENSMUSG000000033526	Ppip5k1	0.118527948	0.500704331	0.020988901
ENSMUSG000000093989	Rnasek	1.514906021	-0.360550774	0.021269738
ENSMUSG000000103034	Gm8797	0.013447762	1.271041205	0.021329043
ENSMUSG000000028843	Sh3bgrl3	1.387934129	-0.361326202	0.021329043
ENSMUSG000000017165	Gast	0.001876432	-1.850520775	0.021329043
ENSMUSG000000008658	Rbfox1	0.08569039	-0.506196405	0.02178793
ENSMUSG000000073627	C130036L24Rik	0.056605696	0.636139652	0.02192364
ENSMUSG000000087336	Gm15860	0.040030547	0.741916846	0.021960441
ENSMUSG000000016346	Kcnq2	0.652060085	0.371781996	0.02234933
ENSMUSG000000037221	Mospd3	0.03252482	-0.674571986	0.022670369
ENSMUSG000000039108	Lsm14b	0.246125318	0.421574123	0.022815723
ENSMUSG000000046999	1110032F04Rik	0.094759811	0.531158127	0.023163756
ENSMUSG000000020027	Socs2	0.035026729	-0.65645642	0.023202106
ENSMUSG000000030125	Lrrc23	0.015949671	1.168094903	0.023376142

ENSMUSG00000060636	Rpl35a	7.147954584	0.34140213	0.023504128
ENSMUSG00000086040	Wipf3	0.524462716	0.392477459	0.023517568
ENSMUSG00000026841	Fibcd1	0.076308231	0.566044194	0.023842504
ENSMUSG00000048234	Rnf149	0.009694898	-1.042539548	0.023882392
ENSMUSG00000029797	Sspo	0.008443944	1.859972608	0.023981905
ENSMUSG00000036241	Ube2r2	0.404683813	-0.386424274	0.024153337
ENSMUSG00000032854	Ugt8a	0.137292267	-0.474775307	0.024260072
ENSMUSG0000001248	Gramd1a	0.481304782	0.382231064	0.024260072
ENSMUSG00000034587	8430429K09Rik	0.03940507	0.732549666	0.024290387
ENSMUSG00000071604	Fam189a2	0.114775085	0.563936046	0.024370997
ENSMUSG00000049892	Rasd1	0.113211391	0.504122388	0.024601007
ENSMUSG00000073125	Xlr3b	0.009382159	1.765805896	0.024693864
ENSMUSG0000001014	Icam4	0.021578967	0.968906979	0.024743735
ENSMUSG00000030761	Myo7a	0.046910797	0.684364853	0.024801872
ENSMUSG00000090002	Gm16006	0.013135023	1.294457869	0.024857321
ENSMUSG00000034064	Poglut1	0.332128446	0.45875811	0.025168192
ENSMUSG00000006333	Rps9	3.143336171	-0.346624395	0.025224262
ENSMUSG00000003934	Efnb3	0.249878181	-0.40442734	0.025224262
ENSMUSG00000001103	Sebox	0.01845158	1.061387895	0.025224262
ENSMUSG00000015377	Dennd6b	0.167002439	0.451323074	0.025224262
ENSMUSG00000040225	Prrc2c	0.08350122	-0.501346289	0.0253572
ENSMUSG00000045608	Dbx2	0.102891016	-0.476979578	0.025507516
ENSMUSG00000017376	Nlk	0.298665411	0.411507918	0.025536069
ENSMUSG00000078193	Gm2000	0.090068731	0.532156878	0.025537444
ENSMUSG00000006476	Nsmf	1.617484298	0.356230476	0.026193667
ENSMUSG00000026751	Nr5a1	0.003440125	-1.487950696	0.026461101
ENSMUSG00000085084	4930570G19Rik	0.055980218	0.628862969	0.026675213
ENSMUSG00000020919	Stat5b	0.118527948	0.485715156	0.027488115
ENSMUSG00000039883	Lrrc17	0.075682753	0.560344861	0.028160592
ENSMUSG00000029104	Htt	0.214538714	0.422487997	0.028166665
ENSMUSG00000021186	Fbln5	0.039092331	0.721144903	0.028198589
ENSMUSG00000000732	Icosl	0.02783374	1.303462682	0.028251607
ENSMUSG00000095789	Nupr1l	0.021266228	0.976717571	0.028498279
ENSMUSG00000035133	Arhgap5	0.283966694	-0.387734666	0.028510796
ENSMUSG00000041577	Prelp	0.111334959	0.909680527	0.028511361
ENSMUSG00000041444	Arhgap32	0.101014584	-0.47228124	0.028511361
ENSMUSG00000039648	Kyat1	0.060984037	0.603197192	0.028799167
ENSMUSG00000026727	Rsu1	0.070678935	-0.516270592	0.028849951
ENSMUSG00000008958	Vps72	0.094759811	-0.478427922	0.028981283
ENSMUSG00000041264	Uspl1	0.103516493	0.503384443	0.028997434
ENSMUSG00000027860	Vang1	0.029397433	0.815118372	0.029573969
ENSMUSG00000048029	Eno4	0.020328012	0.971480923	0.030080894
ENSMUSG00000028441	1110017D15Rik	0.072868105	0.562235061	0.030154009
ENSMUSG00000037664	Cdkn1c	0.071304412	0.67882775	0.030154009
ENSMUSG00000004626	Stxbp2	0.056918434	0.618358206	0.030154009
ENSMUSG00000023952	Gtpbp2	0.08099931	0.54006368	0.030154009
ENSMUSG00000002210	Smg9	0.156369325	0.447293096	0.030331671
ENSMUSG00000027327	1700037H04Rik	0.359962186	-0.38613217	0.03070747
ENSMUSG00000117172	A230051N06Rik	0.026895524	1.048102204	0.031177944
ENSMUSG00000074466	Gm15417	0.106331141	0.52053577	0.03139407
ENSMUSG00000089669	Tnfsf13	0.028771956	0.822389425	0.03139407
ENSMUSG00000076439	Mog	0.658627597	-0.37697416	0.03139407
ENSMUSG00000078202	Nrarp	0.042532456	-0.594489757	0.031551801
ENSMUSG00000035674	Ndufa3	2.838103249	0.334865888	0.031578057
ENSMUSG00000049932	H2afx	0.117276994	-0.451031232	0.031585432
ENSMUSG00000031309	Rps6ka3	0.104767448	0.499225264	0.03160933
ENSMUSG00000034156	Tspoap1	0.281777524	0.401254965	0.03165467
ENSMUSG00000073418	C4b	0.091319686	0.5169816	0.031863777
ENSMUSG00000026072	Il1r1	0.020640751	0.96342865	0.032032882
ENSMUSG000000055723	Rras2	0.080686572	0.540172905	0.0320985
ENSMUSG000000050732	Vamp8	0.207971202	0.438157037	0.03210183
ENSMUSG00000005268	Prlr	0.036903161	0.734441725	0.032170661
ENSMUSG00000039904	Gpr37	0.18764319	-0.414076451	0.032309085

ENSMUSG00000019232	Etnppl	0.21078585	0.451361377	0.032371595
ENSMUSG00000037029	Zfp146	0.00688025	-1.134313741	0.032371595
ENSMUSG00000074748	Atxn7i3b	0.417193359	-0.37211321	0.032789
ENSMUSG00000006676	Usp19	0.29428707	0.394453073	0.032792038
ENSMUSG00000117979	Gm50341	0.002501909	3.681974306	0.03290133
ENSMUSG00000027087	ltgav	0.284592171	0.389160238	0.034186143
ENSMUSG00000008136	Fhl2	0.249565443	0.400884248	0.034228983
ENSMUSG00000034271	Jdp2	0.080061094	0.534680279	0.034277741
ENSMUSG00000085241	Snhg3	0.179511985	0.426802018	0.034548346
ENSMUSG00000042258	Isl1	0.019389796	-0.777457313	0.034548346
ENSMUSG00000032621	Srek1	0.197963565	0.419508898	0.034807112
ENSMUSG00000034312	lqsec1	0.487872294	0.360415943	0.03485044
ENSMUSG00000047671	Tctex1d4	0.014385978	1.15974756	0.035003874
ENSMUSG00000089997	1810020005Rik	0.009382159	1.466245615	0.035082594
ENSMUSG00000041559	Fmod	0.053478309	0.616385964	0.035166392
ENSMUSG00000021700	Rab3c	0.411876802	0.369380521	0.03529573
ENSMUSG00000041084	Ostc	0.281152046	-0.383253317	0.035384421
ENSMUSG00000064210	Ano6	0.012822285	-0.890049139	0.035384421
ENSMUSG00000060429	Sntb1	0.03002291	0.864034633	0.035571461
ENSMUSG00000024018	Ccdc167	0.18295211	0.423717806	0.035641927
ENSMUSG00000035781	R3hdm4	0.536659523	0.362905865	0.035864608
ENSMUSG00000052248	Zeb2os	0.015949671	1.083206005	0.035932586
ENSMUSG00000020888	Dvl2	0.062860469	0.57780375	0.035932586
ENSMUSG00000050335	Lgals3	0.015949671	1.083206005	0.035932586
ENSMUSG00000020752	Recql5	0.071304412	0.556837226	0.03608344
ENSMUSG00000024038	Ndufv3	2.306134805	0.331534595	0.03608344
ENSMUSG00000071424	Grid2	0.023455399	-0.715756613	0.036336435
ENSMUSG00000056537	Rlim	0.200465475	0.414312502	0.036353552
ENSMUSG00000036353	P2ry12	0.06942798	-0.504034419	0.036372135
ENSMUSG00000097573	G730003C15Rik	0.010007637	1.386518422	0.036802055
ENSMUSG00000027900	Dram2	0.087879561	-0.480256304	0.037030652
ENSMUSG00000052087	Rgs14	0.106956618	0.482902958	0.037030652
ENSMUSG00000036606	Plxnb2	0.180137462	0.424733549	0.037030652
ENSMUSG00000037683	Armc3	0.010945853	1.360046211	0.037184616
ENSMUSG00000039720	Got1l1	0.010945853	1.360046211	0.037184616
ENSMUSG00000035725	Prkx	0.001250955	-1.973377523	0.037184616
ENSMUSG00000029189	Sel1l3	0.122280812	0.46498105	0.037188886
ENSMUSG00000055912	Tmem150a	0.048474491	0.637580186	0.037188886
ENSMUSG00000054509	Parp4	0.016887887	1.045481504	0.037370091
ENSMUSG00000022415	Syng1	0.918826154	0.344034543	0.037370091
ENSMUSG00000073678	Pgap1	0.140419654	0.449313549	0.037473354
ENSMUSG00000113902	Ndufb1-ps	1.50114552	0.334432042	0.037719128
ENSMUSG00000024907	Gal	0.163875053	0.60277908	0.037841477
ENSMUSG00000026632	Tatdn3	0.061296775	0.579512272	0.038615763
ENSMUSG00000018909	Arrb1	0.343074299	0.373113114	0.038615763
ENSMUSG00000027434	Nkx2-2	0.02095349	-0.740337857	0.039622788
ENSMUSG00000003974	Grm3	0.024080876	-0.702394364	0.040350034
ENSMUSG00000045282	Tmem86b	0.013760501	1.145921405	0.040350034
ENSMUSG00000086775	Snhg7os	0.006567512	1.801555921	0.040439658
ENSMUSG00000079659	Tmem243	0.037215899	-0.603427913	0.04045687
ENSMUSG00000064370	mt-Cytb	49.06619227	-0.324250754	0.041031722
ENSMUSG00000028245	Nsmaf	0.079748356	0.523364617	0.041049776
ENSMUSG00000052605	Isoc2b	0.054103786	0.624075922	0.041113799
ENSMUSG00000061576	Dpp6	0.404996552	-0.364846551	0.041192215
ENSMUSG00000039682	Lap3	0.165751484	-0.408362431	0.041358652
ENSMUSG00000053877	Srcap	0.010945853	-0.932735539	0.041506583
ENSMUSG00000086943	4732414G09Rik	0.025644569	0.887088735	0.041667248
ENSMUSG00000027858	Tspan2	0.402494643	-0.365268176	0.041667754
ENSMUSG00000079427	Mthfsl	0.068177026	0.803020586	0.041714759
ENSMUSG00000021902	Phf7	0.026270047	0.833977399	0.042130259
ENSMUSG00000024339	Tap2	0.021578967	0.913411867	0.042132071
ENSMUSG00000000787	Ddx3x	0.622975391	0.347361828	0.042132071
ENSMUSG00000020695	Mrc2	0.025331831	0.847233496	0.042270004

ENSMUSG00000020961	Ston2	0.044408888	0.753057404	0.042612765
ENSMUSG00000050074	Spink8	0.156994802	0.428472171	0.042653705
ENSMUSG00000007872	Id3	0.425637303	-0.352564113	0.04296661
ENSMUSG00000021032	Ngb	0.142296086	-0.470443978	0.043471741
ENSMUSG00000022623	Shank3	0.00469108	-1.269310409	0.044045858
ENSMUSG00000064363	mt-Nd4	30.14300204	-0.322018503	0.044045858
ENSMUSG00000033735	Spr	0.306483877	0.369341103	0.044398269
ENSMUSG00000084883	Ccdc85c	0.091006947	0.536966936	0.044653526
ENSMUSG00000031808	Slc27a1	0.325248196	0.36462686	0.045209475
ENSMUSG00000020658	Efr3b	0.324935457	0.37454578	0.045427486
ENSMUSG00000024165	Jpt2	0.011258591	-0.90785395	0.045427486
ENSMUSG00000024824	Rad9a	0.029710172	-0.644455182	0.045427486
ENSMUSG00000043461	Sptssb	0.011884069	-0.902988195	0.045697929
ENSMUSG00000030098	Grip2	0.054729264	0.596441491	0.046205117
ENSMUSG00000000318	Clec10a	0.005942034	1.833977399	0.046205117
ENSMUSG00000021520	Uqcrb	2.186981379	0.322863495	0.046377692
ENSMUSG00000097617	Gm10687	0.000312739	-2.657875697	0.04668102
ENSMUSG00000092009	Myh15	0.000312739	-2.657875697	0.04668102
ENSMUSG00000027284	Cdan1	0.065675116	0.553668393	0.047842698
ENSMUSG00000078485	Plekhn1	0.139481438	0.436597076	0.047842698
ENSMUSG00000057278	Snrpg	0.888490505	0.335483966	0.047842698
ENSMUSG00000007783	Cpt1c	0.426575519	0.358778465	0.047859947
ENSMUSG00000035578	Iqcg	0.020015274	0.919707273	0.047859947
ENSMUSG00000025758	Plk4	0.02095349	0.899072427	0.04811178
ENSMUSG00000033029	1700088E04Rik	0.082875742	0.506635808	0.04811178
ENSMUSG00000030321	Efcab12	0.021891705	0.88043671	0.048114851
ENSMUSG00000025481	Urah	0.022829921	0.863521675	0.048114851
ENSMUSG00000057614	Gnai1	0.235492203	-0.378678628	0.048397047
ENSMUSG00000038011	Dnah10	0.011258591	1.262071051	0.048918078
ENSMUSG00000032855	Pkd1	0.244874363	0.385292162	0.048918078
ENSMUSG00000005204	Senp3	0.134790358	0.437214071	0.049306353
ENSMUSG00000010592	Dazl	0.015949671	1.042564021	0.049592223
ENSMUSG00000030309	Caprin2	0.01845158	0.959508281	0.049677114
ENSMUSG00000009292	Trpm2	0.075057276	0.697018186	0.049677114

Table S2C. DEGs at ZT4 in female and male white matter tracts (WMT). The average number of counts per spot in the RHY condition, the log2 fold change in gene expression (RHY relative to saline), and the adjusted p-value (FDR) are shown.

ZT4 FEMALES - WMT					ZT4 MALES - WMT				
FeatureID	FeatureName	ZT4RF count average	ZT4RF Log2FoldChange	ZT4RF FDR	FeatureID	FeatureName	ZT4RM count average	ZT4RM Log2FoldChange	ZT4RM FDR
ENSMUSG00000019970	Sgk1	12.22844387	4.341656905	4.39497E-48	ENSMUSG00000023067	Cdkn1a	1.406913391	4.326396111	1.57205E-21
ENSMUSG00000023067	Cdkn1a	1.511577619	5.115798269	3.29374E-31	ENSMUSG00000019970	Sgk1	13.10120628	2.427985905	4.10734E-15
ENSMUSG00000090137	Uba52	0.709784273	-2.723652859	1.34045E-22	ENSMUSG00000025591	Tma16	1.162232801	3.341042887	2.57966E-13
ENSMUSG00000030880	Polr3e	2.313370964	3.027854235	6.25148E-22	ENSMUSG00000034936	Arl4d	1.867488619	2.669923743	3.22343E-13
ENSMUSG00000002910	Arrdc2	1.673688842	2.802939004	9.95692E-18	ENSMUSG00000027525	Phactr3	3.382349329	2.178804079	4.22436E-11
ENSMUSG00000020108	Ddit4	1.551010078	2.830917161	1.05911E-17	ENSMUSG00000090137	Uba52	1.147839825	-1.835628947	1.61915E-10
ENSMUSG00000034936	Arl4d	1.419568546	2.989842039	1.1297E-17	ENSMUSG00000030880	Polr3e	2.392832238	2.058643156	1.68261E-09
ENSMUSG00000027525	Phactr3	3.325470761	2.443670727	1.1793E-17	ENSMUSG00000002910	Arrdc2	1.525655442	2.201997198	2.54621E-09
ENSMUSG00000021025	Nfkbia	1.235550401	2.562793878	5.4901E-14	ENSMUSG00000021025	Nfkbia	1.352939731	2.174949747	4.71984E-09
ENSMUSG000000060143	Gm10076	2.874188168	-1.848432251	1.02926E-12	ENSMUSG00000024222	Fkbp5	0.345431421	2.963675806	2.86293E-06
ENSMUSG00000005057	Sh2b2	0.381180443	3.877567254	8.17257E-12	ENSMUSG00000005057	Sh2b2	0.291457761	3.52866989	6.86038E-06
ENSMUSG00000113902	Ndufb1-ps	0.963904568	-1.82921913	8.92748E-11	ENSMUSG00000020108	Ddit4	1.464485294	1.653718669	9.27128E-06
ENSMUSG00000002831	Plin4	0.530147513	3.233395755	1.13858E-10	ENSMUSG00000032788	Pdkx	1.122652118	1.679777019	7.19249E-05
ENSMUSG00000025591	Tma16	0.617775201	2.830917161	1.31266E-10	ENSMUSG00000025915	Sgk3	0.744836501	1.784094762	9.42119E-05
ENSMUSG00000067288	Rps28	3.106401541	-1.657726379	3.46855E-10	ENSMUSG00000031167	Rbm3	1.30616256	1.393510307	0.000808791
ENSMUSG00000064360	mt-Nd3	3.750465048	-1.618979319	7.68493E-10	ENSMUSG00000074170	Plekhn1	0.87077504	1.452074199	0.002009625
ENSMUSG00000026822	Lcn2	0.240976142	5.810453058	1.22152E-09	ENSMUSG00000048572	Tmem252	0.219492882	3.540351695	0.003093199
ENSMUSG00000074170	Plekhn1	0.687877351	2.448897889	1.2759E-09	ENSMUSG00000025509	Pnpla2	0.913953968	1.384111609	0.004632009
ENSMUSG000000071637	Cebpd	0.499477822	2.600660673	6.24814E-09	ENSMUSG00000027301	Oxt	0.014392976	-2.899271442	0.007142704
ENSMUSG00000057322	Rpl38	8.066128684	-1.489137818	6.88532E-09	ENSMUSG00000109517	Gm44763	0.003598244	-3.7357721	0.012880888
ENSMUSG00000079641	Rpl39	3.575209672	-1.505724597	1.01234E-08	ENSMUSG00000019947	Arid5b	0.604504986	1.442714305	0.012880888
ENSMUSG000000041841	Rpl37	8.092416991	-1.464824944	1.3282E-08	ENSMUSG00000002831	Plin4	0.597308498	1.467359337	0.013950836
ENSMUSG00000028998	Tom7	0.788649192	-1.651874086	1.35926E-08	ENSMUSG00000029780	Nt5c3	0.831194356	1.301178426	0.014280348

ENSMUSG00000032788	Pdxk	0.858751343	2.040187455	1.43373E-08	ENSMUSG00000028967	Errfi1	0.784417185	1.302048755	0.014433618
ENSMUSG00000070369	Itgad	0.521384744	2.450557113	1.83137E-08	ENSMUSG00000031431	Tsc22d3	2.274090187	1.11962757	0.014433618
ENSMUSG00000025059	Pnpla2	1.152304098	1.897745136	2.08864E-08	ENSMUSG00000037855	Zfp365	1.108259142	1.1946534	0.018431726
ENSMUSG00000021290	Atp5mpl	1.586061154	-1.560510487	2.59163E-08	ENSMUSG00000024096	Ralbp1	0.636889182	1.361449098	0.019388471
ENSMUSG00000046516	Cox17	0.832463036	-1.591900545	3.28424E-08	ENSMUSG00000034579	Pla2g3	0.136733271	2.871557604	0.021469178
ENSMUSG00000090733	Rps27	3.824948583	-1.444580915	4.67892E-08	ENSMUSG00000020713	Gh	0	-4.916344956	0.02164322
ENSMUSG00000017778	Cox7c	4.096594416	-1.418858777	5.86828E-08	ENSMUSG00000060143	Gm10076	3.112481031	-0.911436823	0.02164322
ENSMUSG00000016427	Ndufa1	0.62653797	-1.627876762	7.82712E-08	ENSMUSG00000070369	Itgad	0.406601568	1.544576281	0.023462441
ENSMUSG00000035674	Ndufa3	2.046106516	-1.430317893	1.15425E-07	ENSMUSG00000017697	Ada	0.212296394	2.078008481	0.026821531
ENSMUSG00000024222	Fkbp5	0.372417674	2.622007969	1.39384E-07	ENSMUSG00000030268	Bcat1	0.694461086	1.279177631	0.026821531
ENSMUSG00000034892	Rps29	9.757343064	-1.356158548	1.9106E-07	ENSMUSG00000054277	Arfgap3	0.568522547	1.354717824	0.027317196
ENSMUSG00000071528	Atp5md	3.010011084	-1.397185597	2.43899E-07	ENSMUSG00000031608	Galnt7	0.147528003	2.563435308	0.027547377
ENSMUSG00000039001	Rps21	10.78258701	-1.323977433	3.18576E-07	ENSMUSG00000034858	Fam214a	0.38141386	1.520267449	0.034530271
ENSMUSG00000062997	Rpl35	3.299182455	-1.360322088	3.68464E-07	ENSMUSG00000059325	Hopx	0.22668937	-1.27182561	0.039112207
ENSMUSG00000050856	Atp5k	2.352803424	-1.371488980	4.24416E-07	ENSMUSG00000023019	Gpd1	0.90675748	1.15411146	0.039112207
ENSMUSG00000006205	Htra1	2.790941864	1.45014603	6.72739E-07	ENSMUSG00000052296	Ppp6r1	0.057571903	-1.828882114	0.040786959
ENSMUSG00000104960	Snhg8	0.363654905	-1.692047282	1.02527E-06	ENSMUSG00000037235	Mxd4	0.939141675	1.138451697	0.040794241
ENSMUSG00000031431	Tsc22d3	2.076776207	1.485490903	1.16123E-06	ENSMUSG00000038267	Slc22a23	0.136733271	-1.497676206	0.049979817
ENSMUSG00000065947	mt-Nd4l	0.933234878	-1.437829231	1.16123E-06					
ENSMUSG00000021453	Gadd45g	0.902565187	1.863695079	1.32737E-06					
ENSMUSG00000048572	Tmem252	0.254120295	5.885741185	1.32737E-06					
ENSMUSG00000074754	Smim26	0.214687836	-1.745363097	1.87517E-06					
ENSMUSG00000014313	Cox6c	5.616934804	-1.255619349	1.97326E-06					
ENSMUSG00000078974	Sec61g	1.266220092	-1.338593214	2.40458E-06					
ENSMUSG00000023019	Gpd1	1.055913641	1.636559154	2.7334E-06					
ENSMUSG00000025739	Gng13	0.460045362	-1.608831412	4.11047E-06					
ENSMUSG00000037458	Azin1	0.76674227	1.655174833	4.11088E-06					
ENSMUSG00000098234	Snhg6	0.052576613	-2.446209265	4.30478E-06					
ENSMUSG00000015112	Slc25a13	0.245357527	2.666063149	6.8017E-06					
ENSMUSG00000093674	Rpl41	7.25557257	-1.193947973	6.86236E-06					
ENSMUSG00000025915	Sgk3	0.692258736	1.672124902	8.12701E-06					
ENSMUSG00000016252	Atp5e	3.023155237	-1.217204937	9.53806E-06					
ENSMUSG00000028967	Errfi1	0.62653797	1.780705715	9.53806E-06					
ENSMUSG00000079523	Tmsb10	2.243268814	-1.274857619	1.36974E-05					
ENSMUSG00000087687	Pet100	0.433757056	-1.424508037	1.37257E-05					
ENSMUSG00000064356	mt-Atp8	0.639682123	-1.426586139	1.51735E-05					
ENSMUSG00000038489	Poir2l	0.192780914	-1.714502133	1.77089E-05					
ENSMUSG00000041378	Cldn5	0.135822916	-1.879544913	1.95124E-05					
ENSMUSG00000073616	Cops9	1.958478828	-1.202171481	2.37348E-05					
ENSMUSG00000019947	Arid5b	0.4775709	1.926476854	2.40989E-05					
ENSMUSG00000036372	Tmem258	0.98581149	-1.295663974	2.79951E-05					
ENSMUSG00000030711	Sult1a1	0.236594758	2.614532848	3.03101E-05					
ENSMUSG0000007659	Bcl2l1	1.415187162	1.331720883	3.15693E-05					
ENSMUSG00000057863	Rpl36	4.679318541	-1.119731069	3.82418E-05					
ENSMUSG00000021285	Ppp1r13b	0.302315524	2.132381153	4.492E-05					
ENSMUSG00000037152	Ndufc1	1.616730844	-1.174604216	6.51201E-05					
ENSMUSG00000028407	Smim27	0.131441532	-1.756951071	7.02204E-05					
ENSMUSG00000031760	Mt3	7.676185473	-1.105462102	7.15215E-05					
ENSMUSG00000089665	Fcor	0.096390457	-1.981134548	8.22504E-05					
ENSMUSG00000021342	Pri	0.083246304	-4.847401278	8.22504E-05					
ENSMUSG00000046330	Rpl37a	5.49425604	-1.088753391	8.33272E-05					
ENSMUSG00000038690	Atp5j2	3.110782926	-1.110035902	8.33272E-05					
ENSMUSG00000038803	Ost4	0.240976142	-1.529396945	8.63053E-05					
ENSMUSG00000020163	Uqcrr11	2.843518477	-1.101754601	9.38887E-05					
ENSMUSG00000046768	Rhoj	0.254120295	2.300778685	9.38887E-05					
ENSMUSG00000060636	Rpl35a	6.563313834	-1.048423722	0.000172196					
ENSMUSG00000017697	Ada	0.227831989	2.271586972	0.000182913					
ENSMUSG00000057963	Itpk1	1.629874998	1.215213078	0.000184656					
ENSMUSG00000067847	Romo1	0.73607258	-1.203352741	0.000187801					
ENSMUSG00000021750	Fam107a	0.933234878	1.387013118	0.000218167					
ENSMUSG00000000791	Il12rb1	0.092009072	4.462529755	0.000226816					
ENSMUSG00000054312	Mrps21	0.801793346	-1.159840435	0.000243807					
ENSMUSG00000042737	Dpm3	0.468808131	-1.247638911	0.000308753					

ENSMUSG00000041020	Map7d2	0.552054435	1.499929726	0.000348178
ENSMUSG00000084786	Ubl5	1.634256382	-1.084818454	0.000362143
ENSMUSG00000079435	Rpl36a	2.317752349	-1.043768469	0.000398385
ENSMUSG00000028298	Cga	0	-4.697341582	0.000448602
ENSMUSG0000001025	S100a6	0.757979502	-1.205010059	0.000454702
ENSMUSG00000020018	Snrpf	0.205925067	-1.48875496	0.000464375
ENSMUSG00000021986	Amer2	0.490715053	1.501349004	0.000547678
ENSMUSG00000059534	Uqcr10	2.352803424	-1.020836524	0.000562737
ENSMUSG00000070394	Tmem256	0.828081652	-1.275669196	0.000580622
ENSMUSG00000053907	Mat2a	2.041725131	1.082474316	0.000658375
ENSMUSG00000029313	Aff1	0.166492607	2.481145433	0.000676437
ENSMUSG00000031483	Erlin2	0.503859206	1.468761708	0.000676437
ENSMUSG00000033863	Klf9	0.823700268	1.317413047	0.000699194
ENSMUSG00000062006	Rpl34	5.75275772	-0.969748361	0.000741944
ENSMUSG00000047721	Bola2	0.854369958	-1.092998454	0.000794055
ENSMUSG00000057278	Snrpg	0.661589045	-1.132678643	0.000795953
ENSMUSG00000044734	Serp1b1a	0.788649192	-1.119107796	0.000806958
ENSMUSG00000047617	Paxx	1.331940858	1.116212216	0.001033532
ENSMUSG00000021981	Cab39l	0.324222446	1.70835487	0.001033532
ENSMUSG00000023089	Ndufa5	1.822655911	-0.996901864	0.001202916
ENSMUSG00000030168	Adipor2	1.038388103	1.183670382	0.001223374
ENSMUSG00000025362	Rps26	4.609216391	-0.953791624	0.001229531
ENSMUSG00000054277	Arfgap3	0.521384744	1.386426776	0.001350648
ENSMUSG00000034317	Trim59	0.188399529	-1.514750169	0.001820467
ENSMUSG00000035342	Lzts2	1.020862566	1.145542401	0.00186583
ENSMUSG00000022820	Ndufb4	1.629874998	-0.987199776	0.001917707
ENSMUSG00000028645	Slc2a1	1.634256382	1.132140081	0.001989417
ENSMUSG00000014846	Tppp3	4.433961015	0.976289339	0.001989417
ENSMUSG00000029780	Nt5c3	0.749216733	1.239538332	0.002128345
ENSMUSG00000014294	Ndufa2	2.16002251	-0.955425228	0.002128345
ENSMUSG00000037855	Zfp365	0.920090724	1.139234824	0.00248826
ENSMUSG00000025508	Rplp2	3.259749995	-0.912159664	0.003160292
ENSMUSG00000053332	Gas5	4.223654564	-0.901897523	0.003511849
ENSMUSG00000034579	Pla2g3	0.118297379	2.810453058	0.003768934
ENSMUSG00000055148	Klf2	0.21906922	1.97508376	0.003838673
ENSMUSG00000037419	Endod1	4.942201606	0.927182049	0.003903619
ENSMUSG00000020713	Gh	0.096390457	-4.550155505	0.003903619
ENSMUSG00000042541	Sem1	0.718547042	-1.027184431	0.004311289
ENSMUSG00000098120	Gm5914	0.026288306	-2.318829959	0.005145062
ENSMUSG00000035048	Anapc13	0.65720766	-1.039267895	0.005252416
ENSMUSG00000029465	Arpc3	0.968285953	1.097074284	0.006027555
ENSMUSG00000086841	2410006H16Rik	0.512621975	-1.062626046	0.006730073
ENSMUSG00000018143	Mafk	0.254120295	1.637813672	0.006907777
ENSMUSG00000037302	Rpl31	2.479863572	-0.881742666	0.007053162
ENSMUSG00000019689	Fmc1	0.495096437	-1.034376569	0.008386571
ENSMUSG00000019558	Slc6a8	0.705402889	1.133494773	0.008503054
ENSMUSG00000002416	Ndufb2	1.489670697	-0.907454482	0.008917102
ENSMUSG00000078784	Rbis	0.503859206	-1.021563918	0.00914761
ENSMUSG00000021040	Slirp	0.354892137	-1.090560971	0.01040907
ENSMUSG00000010406	Mrp152	0.823700268	-0.954295693	0.01098157
ENSMUSG00000037235	Mxd4	0.722928426	1.092735348	0.012008421
ENSMUSG00000038717	Atp5l	2.900476474	-0.843205324	0.012008421
ENSMUSG00000033326	Kdm4a	0.280408602	1.501903993	0.012032127
ENSMUSG00000036781	Rps27l	0.460045362	-1.023868912	0.012872243
ENSMUSG00000098188	Sowahc	0.013144153	-2.640758054	0.014078021
ENSMUSG00000051495	Irf2bp2	0.80617473	1.075047978	0.014184404
ENSMUSG00000039601	Rcan2	2.790941864	0.873427524	0.014184404
ENSMUSG00000028936	Rpl22	2.725221098	-0.840517984	0.014406366
ENSMUSG00000047369	Dnah14	0.17963676	1.810453058	0.016046823
ENSMUSG00000042312	S100a13	1.090964716	-0.892204485	0.017066517
ENSMUSG00000027200	Sema6d	0.188399529	-1.237909964	0.017623323
ENSMUSG00000045503	Sys1	2.698932792	0.858596886	0.017623323
ENSMUSG00000097451	Rian	0.346129368	1.325026231	0.017656671

ENSMUSG00000066687	Zbtb16	0.056957997	3.810453058	0.018604346
ENSMUSG00000032766	Gng11	2.234506045	-0.832612397	0.020028156
ENSMUSG00000068523	Gng5	1.310033936	-0.889616691	0.020359508
ENSMUSG00000031770	Herpu1	0.58710551	1.125717423	0.021371414
ENSMUSG0000007656	Arpp19	1.121634407	-0.861642034	0.023330043
ENSMUSG00000038332	Sesn1	0.407468749	1.235758893	0.02392477
ENSMUSG00000024018	Ccdc167	0.096390457	-1.450619831	0.024268268
ENSMUSG00000043587	Pxylp1	0.105153226	2.325026231	0.024726799
ENSMUSG00000042213	Zfand4	0.105153226	2.325026231	0.024777212
ENSMUSG00000090247	Bloc1s1	0.21906922	-1.144655484	0.025650293
ENSMUSG00000028982	Slc25a33	0.69664012	1.021245483	0.025895916
ENSMUSG00000058600	Rpl30	7.347581642	-0.758587801	0.028371748
ENSMUSG00000021702	Thbs4	0.315459677	1.549066505	0.028423356
ENSMUSG00000039958	Etfbkmt	0.074483535	3.173023137	0.030565811
ENSMUSG00000106918	Mrp133	0.530147513	-0.936529246	0.031065199
ENSMUSG00000030494	Rhpn2	0.197162298	1.71930517	0.031065199
ENSMUSG00000022321	Cdh10	0.021906922	-2.318829959	0.032800179
ENSMUSG00000025511	Tspan4	0.271645833	1.395415559	0.033819812
ENSMUSG00000022340	Sybu	0.065720766	-1.640758054	0.034920174
ENSMUSG00000024535	Snx24	0.306696908	1.29486426	0.035376339
ENSMUSG00000045975	C2cd2	0.184018145	1.622007969	0.036200029
ENSMUSG00000031681	Smad1	0.240976142	1.488524963	0.036218642
ENSMUSG00000027434	Nkx2-2	0.061339382	-1.613573224	0.037046344
ENSMUSG00000039221	Rpl22l1	1.450238237	-0.831315798	0.037046344
ENSMUSG00000039911	Spsb1	0.451282593	1.118575353	0.037046344
ENSMUSG00000078572	Ndufaf8	0.350510752	-1.049369284	0.037607137
ENSMUSG00000030087	Klf15	0.569579972	1.036521138	0.039271913
ENSMUSG00000021520	Uqcrb	1.54224731	-0.800164031	0.039304576
ENSMUSG00000043300	B3galnt1	0.271645833	1.33652187	0.040729041
ENSMUSG00000034858	Fam214a	0.271645833	1.33652187	0.040729041
ENSMUSG00000079480	Pin4	0.424994287	-0.952047628	0.042306858
ENSMUSG00000055839	Elob	3.562065519	-0.747977058	0.044309259
ENSMUSG00000024176	Sox8	0.670351814	1.021957163	0.044556246
ENSMUSG00000034855	Cxcl10	0.004381384	-4.041295983	0.044585512
ENSMUSG00000045996	Polr2k	0.499477822	-0.906299315	0.044585512
ENSMUSG00000041926	Rnpep	0.297934139	1.304267671	0.044945226
ENSMUSG00000066129	Kndc1	0.87627688	0.953710109	0.045155614
ENSMUSG00000050423	Ppp1r3g	0.127060148	1.909988732	0.045155614
ENSMUSG0000001827	Folr1	0.105153226	2.325026231	0.04581761
ENSMUSG00000056501	Cebpb	0.254120295	1.426309567	0.047308218
ENSMUSG00000008683	Rps15a	4.929057452	-0.726416964	0.049963412

Table S2D. DEGs at ZT14 in female and male white matter tracts (WMT). The average number of counts per spot in the RHY condition, the log2 fold change in gene expression (RHY relative to saline), and the adjusted p-value (FDR) are shown.

#### ZT14 FEMALES - WMT

FeatureID	FeatureName	ZT14RF count average	ZT14RF Log2FoldChange	ZT14RF FDR
ENSMUSG00000019970	Sgk1	15.33411555	3.103763158	2.33957E-32
ENSMUSG00000023067	Cdkn1a	1.657876779	3.882743633	8.05058E-28
ENSMUSG00000021025	Nfkbia	2.135823238	2.852953251	1.10911E-20
ENSMUSG00000034936	Ar14d	1.807235047	2.726726061	4.1166E-17
ENSMUSG00000020108	Ddit4	2.235395416	2.442103549	2.77813E-16
ENSMUSG00000027525	Phactr3	5.486427058	2.113487614	6.90934E-16
ENSMUSG0000002910	Arrdc2	2.260288461	2.172642874	8.64123E-14
ENSMUSG00000048572	Tmem252	0.333566799	5.130822698	1.97842E-08
ENSMUSG00000025591	Tma16	0.677090817	2.334037018	8.09277E-08
ENSMUSG00000028967	Erff1	0.9459357	1.746319567	1.25206E-06
ENSMUSG00000017697	Ada	0.492882286	2.272178547	1.30959E-06
ENSMUSG00000021453	Gadd45g	0.911085437	1.742493377	5.41865E-06
ENSMUSG00000074170	Plekhh1	0.935978482	1.63597593	7.33623E-06
ENSMUSG00000031765	Mt1	63.35279883	1.244744334	1.01557E-05
ENSMUSG00000018143	Mafk	0.602411682	1.858619977	2.68255E-05
ENSMUSG00000031762	Mt2	5.2872827	1.300705288	3.37333E-05

#### ZT14 MALES - WMT

FeatureID	FeatureName	ZT14RM count average	ZT14RM Log2FoldChange	ZT14RM FDR
ENSMUSG00000098178	Gm42418	1.963501908	-2.102590143	9.74786E-21
ENSMUSG00000022949	Clic6	0.303350014	4.115248792	1.05426E-13
ENSMUSG00000062591	Tubb4a	2.029687366	-1.57402006	1.37227E-12
ENSMUSG00000035202	Lars2	0.270257285	-1.906230936	4.03595E-10
ENSMUSG00000061808	Ttr	33.09824424	2.449730537	4.08047E-10
ENSMUSG00000061718	Ppp1r1b	0.639792757	1.930331076	2.89429E-09
ENSMUSG00000011884	Gltp	0.435720929	-1.543438749	5.69047E-08
ENSMUSG00000090137	Uba52	2.178604645	1.232194144	7.57462E-08
ENSMUSG00000050063	Klk6	0.170979099	-1.933692117	1.17322E-07
ENSMUSG00000033208	S100b	1.180307327	-1.311692027	2.39415E-07
ENSMUSG00000019970	Sgk1	3.232056511	1.127177058	2.62209E-07
ENSMUSG00000015090	Ptgds	39.63957363	0.994931811	1.53213E-06
ENSMUSG0000001827	Folr1	0.193040918	3.062781372	3.30714E-06
ENSMUSG00000032246	Calml4	0.204071828	2.818855789	3.30714E-06
ENSMUSG00000018217	Pmp22	0.209587282	-1.622641311	8.71003E-06
ENSMUSG00000024516	Sec11c	1.285100968	-1.100965055	1.1544E-05



ENSMUSG0000000507	Sh2b2	0.32858819	2.170849592	3.53707E-05	ENSMUSG00000115625	2900040C04Rik	0.159948189	3.214784465	1.30988E-05
ENSMUSG00000002831	Plin4	0.821470476	1.593970853	4.52786E-05	ENSMUSG00000026051	Ecrq4	0.204071828	2.555821383	2.38502E-05
ENSMUSG00000002509	Pnpla2	1.433839376	1.376983285	6.24583E-05	ENSMUSG00000068696	Gpr88	0.182010008	2.658391117	4.09486E-05
ENSMUSG000000090137	Uba52	6.327811969	1.143543787	0.000128374	ENSMUSG00000092341	Malat1	1.582935527	-1.156387149	7.09617E-05
ENSMUSG00000060143	Gm10076	13.35262919	1.113319075	0.000164886	ENSMUSG00000027400	Pdyn	0.154432734	2.750837366	0.000163777
ENSMUSG000000034579	Pla2g3	0.174251313	2.798247359	0.000341716	ENSMUSG00000002910	Arrdc2	0.512937296	1.425077409	0.000203533
ENSMUSG000000036390	Gadd45a	0.298716537	2.035497739	0.000360506	ENSMUSG00000032766	Gng11	0.667370031	-1.110096947	0.000247004
ENSMUSG000000033585	Ndn	0.37837428	-1.488595394	0.000644606	ENSMUSG00000015341	Golga7	0.54051457	-1.143122927	0.000247004
ENSMUSG00000015090	Ptgds	97.48116315	1.044514612	0.001718155	ENSMUSG00000045573	Penk	0.606700028	1.959351782	0.000346754
ENSMUSG000000025915	Sgk3	0.811513258	1.327662879	0.002194032	ENSMUSG00000013523	Bcas1	1.378863699	-0.962148563	0.000378069
ENSMUSG00000079484	Phyh1	0.687048034	1.337872494	0.00272086	ENSMUSG00000039323	Igf1p2	0.281288195	1.785941166	0.000456881
ENSMUSG00000019947	Arid5b	0.672112208	1.375935196	0.002934949	ENSMUSG00000025739	Gng13	0.904534587	1.140237512	0.000469143
ENSMUSG000000030880	Polr3e	1.692727041	1.076166002	0.004824638	ENSMUSG00000020163	Uqcr11	3.469221068	0.843336235	0.000611732
ENSMUSG000000027845	Dclre1b	0.258887665	1.771280311	0.006566404	ENSMUSG00000061762	Tac1	0.375050926	1.509527731	0.000699013
ENSMUSG00000071637	Cebpd	0.582497247	1.466571287	0.007114369	ENSMUSG00000026830	Ernm	1.152730053	-0.943644897	0.00077584
ENSMUSG000000045664	Cdc42ep2	0.592454464	-1.133672031	0.010264593	ENSMUSG00000079523	Tmsb10	2.619841029	0.905031084	0.000786511
ENSMUSG000000021750	Fam107a	1.41392494	1.075781334	0.011093968	ENSMUSG00000021750	Fam107a	0.904534587	1.05950624	0.000929967
ENSMUSG00000026822	Lcn2	0.80155604	6.38320986	0.011506063	ENSMUSG00000027570	Col9a3	0.231649102	1.859689506	0.001166228
ENSMUSG000000034317	Trim59	0.333566799	-1.209027305	0.011800922	ENSMUSG00000020681	Ace	0.170979099	2.192416652	0.001511259
ENSMUSG000000032788	Pdxk	1.070400923	1.107085454	0.011800922	ENSMUSG00000031760	Mt3	9.530705891	0.759835275	0.001900172
ENSMUSG000000050370	Ch25h	0.074679134	4.628322357	0.011982577	ENSMUSG00000043164	Tmem212	0.066185458	4.593296089	0.001906343
ENSMUSG000000030711	Sult1a1	0.388331498	1.505838351	0.012459407	ENSMUSG00000048583	Igf2	0.115824551	2.767325488	0.001908205
ENSMUSG000000027301	Oxt	0	-3.956640143	0.012924531	ENSMUSG00000008682	Rpl10	2.277882831	-0.827284601	0.001975214
ENSMUSG00000029780	Nt5c3	1.100272577	1.065186219	0.012924531	ENSMUSG00000072235	Tuba1a	4.153137463	-0.797243521	0.00216524
ENSMUSG000000027875	Hmgcs2	0.119486615	2.464823625	0.016454046	ENSMUSG00000027199	Gatm	1.869739176	-0.834743806	0.002389341
ENSMUSG000000059824	Dbp	0.433138978	-1.145865701	0.016454046	ENSMUSG00000027562	Car2	3.187932873	-0.796230304	0.002389341
ENSMUSG000000031681	Smad1	0.363438453	1.4454583	0.020250815	ENSMUSG00000034936	Arl4d	0.408143655	1.340315347	0.002389341
ENSMUSG000000074466	Gm15417	0.771684387	1.106369654	0.025726804	ENSMUSG00000030605	Mfge8	0.766648217	1.056355103	0.002514509
ENSMUSG000000037235	Mxd4	1.110229795	1.043359857	0.02742538	ENSMUSG00000025597	Klhl4	0.099278186	-1.614103618	0.002529692
ENSMUSG000000036564	Ndrq4	0.721898297	-1.088743679	0.029851459	ENSMUSG00000032060	Cryab	5.454784795	-0.767344858	0.002793927
ENSMUSG000000021259	Cyp46a1	0.129443833	-1.411206007	0.034073755	ENSMUSG00000034858	Fam214a	0.242680011	1.684269749	0.003025315
ENSMUSG000000050105	Grrp1	0.149358268	2.997556167	0.034449183	ENSMUSG00000025889	Snca	0.507421841	1.203196491	0.00308563
ENSMUSG000000032523	Hhatl	0.358459844	1.391882162	0.034449183	ENSMUSG00000004207	Psap	5.565093891	0.747582478	0.00308563
ENSMUSG000000049907	Rasi11b	0.542668375	1.14289553	0.040105802	ENSMUSG00000089661	Mia	0.14891728	2.240779674	0.004015601
ENSMUSG000000058297	Spock2	0.243951838	-1.243521291	0.041089504	ENSMUSG00000092274	Neat1	0.843864584	0.98971791	0.004108782
ENSMUSG000000022548	Apod	46.84373157	0.834301573	0.041089504	ENSMUSG00000090247	Bloc1s1	0.352989107	1.360635332	0.004653044
ENSMUSG000000113902	Ndufb1-ps	4.211903168	0.840812921	0.043211036	ENSMUSG00000032014	Oaf	0.215102737	1.755352847	0.004904564
ENSMUSG000000038332	Sesn1	0.532711157	1.135282346	0.044142416	ENSMUSG00000003863	Pp1a3	0.198556373	1.780381641	0.006252628
ENSMUSG000000058672	Tubb2a	0.99074318	-0.980486885	0.046102722	ENSMUSG00000028495	Rps6	1.946955544	-0.784196322	0.006541904
					ENSMUSG000000041577	Pre1p	0.132370915	2.214784465	0.006936334
					ENSMUSG00000030711	Sult1a1	0.209587282	1.718826971	0.006936334
					ENSMUSG000000024176	Sox8	0.12685546	-1.416998892	0.006936334
					ENSMUSG00000039530	Tusc3	0.474329113	1.165874865	0.007201947
					ENSMUSG00000018411	Mapt	0.463298203	-1.001533442	0.007217052
					ENSMUSG00000014313	Cox6c	6.215917557	0.683679569	0.008110117
					ENSMUSG00000039901	Armh3	0.066185458	3.593296089	0.009744557
					ENSMUSG00000025221	Kcnp2	0.170979099	1.89285637	0.009801111
					ENSMUSG000000034317	Trim59	0.154432734	-1.30444507	0.010324173
					ENSMUSG00000073616	Cops9	2.294429196	0.735673038	0.010377688
					ENSMUSG00000025006	Sorbs1	0.005515455	-3.151537749	0.011149644
					ENSMUSG000000031425	Plp1	33.99726337	-0.685617178	0.011162901
					ENSMUSG00000005089	Slc1a2	3.320303788	0.715242633	0.014387197
					ENSMUSG00000098234	Snhg6	0.088247277	2.658391117	0.016368532
					ENSMUSG00000016024	Lbp	0.071700912	3.115248792	0.016368532
					ENSMUSG00000004626	Stxbp2	0.071700912	3.115248792	0.016368532
					ENSMUSG000000031833	Mast3	0.832833674	0.89285637	0.016368532
					ENSMUSG00000000184	Ccnd2	0.220618192	1.606552185	0.017892589
					ENSMUSG00000073702	Rpl31	2.956283772	0.680863878	0.018688173
					ENSMUSG000000044734	Serpinb1a	0.325411833	-1.014034225	0.019137933
					ENSMUSG00000027525	Phactr3	1.202369146	0.79727871	0.019202402
					ENSMUSG00000089810	Gm16536	0.093762732	2.477818871	0.019330015
					ENSMUSG00000064360	mt-Nd3	4.313085652	0.650856484	0.019330015
					ENSMUSG00000035772	Mrps2	0.005515455	-3.014034225	0.021606706

ENSMUSG00000063446	Plppr1	0.077216367	2.799746966	0.022973206
ENSMUSG00000034675	Dbn1	0.198556373	1.57874778	0.024853923
ENSMUSG00000060126	Tpt1	8.493800389	-0.642905954	0.027517938
ENSMUSG00000026959	Grin1	0.364020017	1.151590639	0.027855242
ENSMUSG00000032118	Fez1	1.185822782	-0.74457355	0.028194312
ENSMUSG00000035133	Arhgap5	0.159948189	-1.211480289	0.028335846
ENSMUSG00000083282	Ctsf	0.386081836	1.111866152	0.028335846
ENSMUSG00000006333	Rps9	3.408551065	-0.661484515	0.028625451
ENSMUSG00000038393	Txnip	0.170979099	1.644928857	0.029471822
ENSMUSG00000020431	Adcy1	0.281288195	1.271367994	0.031814539
ENSMUSG00000034312	Iqsec1	0.424690019	1.048975572	0.033350768
ENSMUSG00000032554	Trf	6.12767028	-0.639254248	0.033550336
ENSMUSG00000034574	Daam1	0.286803649	1.26322482	0.036927745
ENSMUSG00000010064	Slc38a3	0.253710921	1.318162205	0.037045319
ENSMUSG00000026500	Cox20	0.457782748	1.018387252	0.039154114
ENSMUSG00000041736	Tspo	0.13788637	1.785941166	0.040391676
ENSMUSG00000037843	Vstm2l	0.193040918	1.477818871	0.040561208
ENSMUSG00000037625	Cldn11	6.364834837	0.608126893	0.040561208
ENSMUSG00000003411	Rab3b	0.226133647	1.378283198	0.040561208
ENSMUSG00000030701	Plekhh1	4.097982915	-0.641456972	0.040561208
ENSMUSG00000066129	Kndc1	0.694947305	0.870313802	0.040561208
ENSMUSG00000031980	Agt	0.452267293	-0.984769631	0.040561208
ENSMUSG00000035383	Pmch	0.077216367	-2.634881262	0.040561208
ENSMUSG00000049154	Fam183b	0.071700912	2.700211292	0.040561208
ENSMUSG00000020640	Itsn2	0.204071828	1.440344166	0.040561208
ENSMUSG00000028971	Cort	0.297834559	3.214784465	0.040696967
ENSMUSG00000024740	Ddb1	0.700462759	0.859433369	0.043285987
ENSMUSG00000015806	Qdpr	5.796742992	-0.618971426	0.045274106
ENSMUSG00000026289	Atg16l1	0.143401825	1.740853277	0.04751763

Table S2E . DEGs at ZT4 in female and male cerebral cortex. The average number of counts per spot in the RHY condition, the log2 fold change in gene expression (RHY relative to saline), and the adjusted p-value (FDR) are shown.

#### ZT4 FEMALES - Cerebral cortex

FeatureID	FeatureName	ZT4RF count average	ZT4RF Log2FoldChange	ZT4RF FDR
ENSMUSG00000021342	Prl	0.003002926	-7.02545104	1.68909E-34
ENSMUSG00000020713	Gh	0.003002926	-6.111424263	1.55108E-22
ENSMUSG00000090137	Uba52	1.414377981	-2.344029123	1.63692E-19
ENSMUSG00000113902	Ndufb1-ps	3.288203586	-1.923062154	4.15684E-14
ENSMUSG00000038489	Polr2l	0.51049736	-2.057796864	6.59881E-13
ENSMUSG00000060143	Gm10076	5.047918017	-1.796835481	1.02109E-12
ENSMUSG00000028998	Tom7	2.084030401	-1.752396128	1.28277E-11
ENSMUSG00000016427	Ndufa1	2.032980665	-1.72773316	4.25484E-11
ENSMUSG00000067288	Rps28	4.717596195	-1.614465245	3.41311E-10
ENSMUSG00000046516	Cox17	2.135080137	-1.6222146	5.49444E-10
ENSMUSG00000064360	mt-Nd3	9.861607833	-1.563790999	9.9814E-10
ENSMUSG00000098234	Snhg6	0.129125803	-2.167757635	1.93963E-09
ENSMUSG00000071637	Cebpd	0.489476881	2.410103476	2.60781E-09
ENSMUSG00000103034	Gm8797	0.264257457	3.475817483	2.69729E-09
ENSMUSG00000019970	Sgk1	2.147091839	1.848311255	2.69729E-09
ENSMUSG00000048572	Tmem252	0.306298416	3.908977	2.82903E-09
ENSMUSG00000071528	Atp5md	13.58823856	-1.491613199	3.96338E-09
ENSMUSG00000057322	Rpl38	16.24582776	-1.452325602	1.13707E-08
ENSMUSG00000021290	Atp5mpl	5.576432931	-1.463596803	1.21767E-08
ENSMUSG00000025739	Gng13	2.495431215	-1.474401913	1.73006E-08
ENSMUSG00000074170	Plekhh1	0.156152134	4.535359428	2.38487E-08
ENSMUSG000000104960	Snhg8	0.645629015	-1.610101033	3.2633E-08
ENSMUSG00000017778	Cox7c	11.73843636	-1.407449028	3.67381E-08
ENSMUSG00000078974	Sec61g	2.699630159	-1.430668491	4.9453E-08
ENSMUSG00000050856	Atp5k	7.843641796	-1.397815143	5.50533E-08
ENSMUSG00000079641	Rpl39	5.954801563	-1.394763861	6.29281E-08
ENSMUSG00000041841	Rpl37	14.41404312	-1.372965336	8.65117E-08
ENSMUSG00000097383	1500026H17Rik	0.06906729	-2.294099053	1.8319E-07

#### ZT4 MALES - Cerebral cortex

FeatureID	FeatureName	ZT4RM count average	ZT4RM Log2FoldChange	ZT4RM FDR
ENSMUSG00000090137	Uba52	1.763018452	-1.713776154	3.56536E-09
ENSMUSG0000002831	Plin4	0.18060189	4.071153169	0.000201854
ENSMUSG00000071637	Cebpd	0.39560414	2.184047225	0.000581514
ENSMUSG00000035383	Pmch	0.210702205	-1.618145992	0.00442071
ENSMUSG00000038059	Smim3	0.348303645	2.095549823	0.00466838
ENSMUSG00000019970	Sgk1	2.287623943	1.243448518	0.010090375
ENSMUSG00000025509	Pnpla2	0.442904635	1.701471942	0.011487033
ENSMUSG00000096768	Gm47283	1.659817372	-1.076334444	0.012421973
ENSMUSG00000045471	Hcrt	0.055900585	-2.07131862	0.013987563
ENSMUSG00000023067	Cdkn1a	0.481605041	1.510871066	0.022296484
ENSMUSG00000045903	Npas4	0.012900135	-3.055551304	0.022296484
ENSMUSG00000025217	Btrc	0.584806121	1.457518278	0.023362874
ENSMUSG00000041378	Cldn5	0.28380297	-1.468931486	0.025869487
ENSMUSG00000048572	Tmem252	0.193502025	2.361095448	0.02616895
ENSMUSG00000061808	Ttr	21.78402799	1.017376487	0.033118309
ENSMUSG00000002910	Arrdc2	0.39560414	1.599084724	0.033197769
ENSMUSG00000025591	Tma16	0.374103915	1.580758076	0.039228942

ENSMUSG00000042737	Dpm3	0.675658271	-1.493915581	2.50514E-07
ENSMUSG00000062997	Rpl35	6.056901035	-1.321394599	4.29448E-07
ENSMUSG00000039001	Rps21	18.1466797	-1.303698423	4.88767E-07
ENSMUSG00000035674	Ndufa3	4.690569864	-1.321817671	4.94299E-07
ENSMUSG00000074754	Smim26	0.48347103	-1.503762714	7.14016E-07
ENSMUSG00000079523	Tmsb10	10.96067862	-1.288298257	1.6591E-06
ENSMUSG00000016252	Atp5e	8.113905105	-1.243426341	2.64334E-06
ENSMUSG00000047721	Bola2	1.501462825	-1.303379017	3.96385E-06
ENSMUSG00000034892	Rps29	13.54019175	-1.22122426	4.8033E-06
ENSMUSG00000090733	Rps27	5.831681611	-1.225229986	5.0446E-06
ENSMUSG00000021025	Nfkbia	0.630614386	1.828098444	5.0446E-06
ENSMUSG00000014313	Cox6c	18.93344622	-1.208713737	5.0446E-06
ENSMUSG00000065947	mt-Nd4l	2.216159129	-1.260251901	6.27153E-06
ENSMUSG00000042541	Sem1	1.510471602	-1.259675222	7.50238E-06
ENSMUSG00000024222	Fkbp5	0.429418368	1.889901134	7.50238E-06
ENSMUSG00000038803	Ost4	0.387377409	-1.455595432	7.62221E-06
ENSMUSG00000078747	Gm20878	0.072070216	-2.087863647	8.46808E-06
ENSMUSG00000073616	Cops9	5.03890924	-1.192990591	9.16904E-06
ENSMUSG00000031760	Mt3	16.55813203	-1.182190852	9.16904E-06
ENSMUSG00000070394	Tmem256	2.12607136	-1.210759243	1.38181E-05
ENSMUSG00000036372	Tmem258	1.099070788	-1.257887274	1.38974E-05
ENSMUSG00000037152	Ndufc1	4.816692742	-1.180828065	1.50838E-05
ENSMUSG00000021040	Slirp	0.543529543	-1.357191728	1.56548E-05
ENSMUSG00000020018	Snrpf	0.60058513	-1.326144181	1.96305E-05
ENSMUSG00000035048	Anapc13	1.054026903	-1.242904412	2.04801E-05
ENSMUSG00000031431	Tsc22d3	2.306246899	1.280536596	2.78422E-05
ENSMUSG00000020163	Uqcr11	7.837635945	-1.131040358	3.29858E-05
ENSMUSG00000091050	9330020H09Rik	0.024023405	-2.695061367	3.80865E-05
ENSMUSG00000060636	Rpl35a	10.55528366	-1.110895155	4.77746E-05
ENSMUSG00000093674	Rpl41	15.80740062	-1.09917758	5.79467E-05
ENSMUSG00000057278	Snrpg	1.516477453	-1.163763762	6.017E-05
ENSMUSG00000033685	Ucp2	0.318310119	2.025344004	6.15997E-05
ENSMUSG00000023089	Ndufa5	5.831681611	-1.097024051	8.0566E-05
ENSMUSG00000038690	Atp5j2	8.64842587	-1.075518078	0.000107812
ENSMUSG00000038570	Saxo2	0.132128729	-1.65490424	0.00011235
ENSMUSG00000057863	Rpl36	7.264077146	-1.075567785	0.00011235
ENSMUSG00000087687	Pet100	0.951927431	-1.18573976	0.000119776
ENSMUSG00000064356	mt-Atp8	1.423386758	-1.132084567	0.000133914
ENSMUSG00000002910	Arrdc2	0.378368632	1.751729541	0.000223294
ENSMUSG00000084786	Ubl5	4.924798065	-1.037232848	0.000300913
ENSMUSG00000059534	Uqcr10	7.543349231	-1.026004883	0.000329332
ENSMUSG00000038059	Smim3	0.399389111	1.551600069	0.000428535
ENSMUSG00000067847	Romo1	1.909860713	-1.0510886	0.00044978
ENSMUSG00000034634	Ly6d	0.201196019	2.435470196	0.0004791
ENSMUSG00000030677	Kif2d	0.129125803	-1.55330837	0.00049786
ENSMUSG00000019689	Fmc1	1.093064936	-1.085949836	0.000520631
ENSMUSG00000020108	Ddit4	0.519506137	1.443027548	0.000553122
ENSMUSG00000030087	Klf15	0.471459327	1.496509878	0.000604595
ENSMUSG00000090247	Bloc1s1	0.195190167	-1.405554749	0.000705559
ENSMUSG00000079435	Rpl36a	4.156049099	-0.988711944	0.000900315
ENSMUSG000000114018	Gm36495	0.003002926	-3.777523527	0.001150749
ENSMUSG00000026822	Lcn2	0.477465178	7.129367069	0.001202189
ENSMUSG000000106918	Mrp133	1.243211219	-1.028923232	0.001202189
ENSMUSG00000079017	Ifi2712a	0.018017554	-2.555131106	0.001238144
ENSMUSG00000078784	Rbis	1.444407237	-1.016073621	0.001244523
ENSMUSG00000024038	Ndufv3	3.765668764	-0.97323084	0.001323479
ENSMUSG00000002416	Ndufb2	4.804681039	-0.954539916	0.001656034
ENSMUSG00000061808	Ttr	13.16782897	-1.22829725	0.001864424
ENSMUSG00000062006	Rpl34	9.57332697	-0.930883174	0.0020991
ENSMUSG00000089665	Fcor	0.192187242	-1.29947623	0.002150436
ENSMUSG00000086841	2410006H16Rik	0.97294791	-1.020692627	0.002268015
ENSMUSG00000025508	Rplp2	5.798649429	-0.928630258	0.002501366
ENSMUSG00000046330	Rpl37a	8.537317621	-0.9179141	0.002775929

ENSMUSG00000038717	Atp5l	8.624402465	-0.913367459	0.002911552
ENSMUSG00000050074	Spink8	0.32431597	1.621426988	0.002911552
ENSMUSG00000023067	Cdkn1a	0.450438847	1.401987523	0.003162964
ENSMUSG00000054312	Mrps21	2.582516059	-0.92952662	0.003200791
ENSMUSG00000053332	Gas5	4.651531831	-0.914180647	0.003346799
ENSMUSG00000070369	Itgad	0.093090695	2.807438974	0.003346799
ENSMUSG00000014294	Ndufa2	5.110979455	-0.905781533	0.003766082
ENSMUSG00000026500	Cox20	0.810789925	-1.005229748	0.003838844
ENSMUSG00000028298	Cga	0	-4.280023867	0.005188058
ENSMUSG00000039634	Zfp189	0.108105323	2.431929839	0.005529261
ENSMUSG00000085241	Snhg3	0.309301342	-1.135977498	0.005533673
ENSMUSG00000037095	Lrg1	0.096093621	2.529904998	0.005985448
ENSMUSG00000052296	Ppp6r1	0.213207721	-1.212460584	0.006725315
ENSMUSG00000045996	Polr2k	1.453416014	-0.92177178	0.007250412
ENSMUSG00000025362	Rps26	6.696524198	-0.869177216	0.007289026
ENSMUSG00000095366	Gm21860	0	-4.192561026	0.00753414
ENSMUSG00000084883	Ccdc85c	0.04804681	-1.805537903	0.008975534
ENSMUSG00000085255	Taco1os	0.012011703	-2.5710772649	0.00950672
ENSMUSG00000010156	Gm42067	0.150146282	-1.327490606	0.009813861
ENSMUSG00000029062	Cdk11b	0.465453476	-1.015683264	0.010521618
ENSMUSG00000024066	Xdh	0.144140431	2.100220723	0.010521618
ENSMUSG00000098120	Gm5914	0.111108249	-1.387577009	0.010603885
ENSMUSG00000068240	Gm11808	0.351342301	-1.078102302	0.01191302
ENSMUSG00000046707	Csnk2a2	0.297289639	-1.087863647	0.012097919
ENSMUSG00000059991	Nptx2	0.267260383	-1.184523707	0.012364583
ENSMUSG0000002831	Plin4	0.111108249	2.248011565	0.01243912
ENSMUSG00000010406	Mrp152	1.432395535	-0.878534006	0.012692312
ENSMUSG00000025509	Pnp1a2	0.468456401	1.195169127	0.015894641
ENSMUSG00000018585	Atox1	2.465401958	-0.842721793	0.016680786
ENSMUSG00000045471	Hert	0.033032182	-1.999915948	0.018335053
ENSMUSG00000070858	Gm1673	2.828755962	-0.828132015	0.018522808
ENSMUSG00000039202	Abhd2	0.084081918	-1.443104488	0.021284535
ENSMUSG00000044894	Uqcrcq	10.36009349	-0.797314272	0.022282675
ENSMUSG00000073702	Rpl31	5.888737199	-0.798933222	0.024023701
ENSMUSG00000024778	Fas	0.087084844	2.392401475	0.025274243
ENSMUSG00000037926	Ssh2	0.168163836	1.640328988	0.025350438
ENSMUSG00000022820	Ndufb4	5.753605544	-0.792248853	0.025350438
ENSMUSG00000024018	Ccdc167	0.237231126	-1.109037671	0.025504214
ENSMUSG00000037820	Tgm2	0.135131654	2.009072835	0.030804723
ENSMUSG00000028936	Rpl22	3.549458118	-0.79168159	0.030804723
ENSMUSG00000078572	Ndufaf8	0.879857215	-0.857074826	0.031348968
ENSMUSG00000030905	Crym	1.183152706	0.957414386	0.031448866
ENSMUSG00000021903	Galnt15	0.066064364	2.746038429	0.036169197
ENSMUSG00000090101	Snhg9	0.072070216	-1.431347886	0.03714152
ENSMUSG00000019232	Etnppl	0.234228201	1.410780004	0.03739686
ENSMUSG00000028656	Cap1	0.918895249	0.940250802	0.039347962
ENSMUSG00000034390	Cmp1	0.129125803	1.807438974	0.039347962
ENSMUSG00000023034	Nr4a1	0.222216498	-1.072266792	0.039525825
ENSMUSG00000056071	S100a9	0.042040959	3.714329569	0.03978326
ENSMUSG00000030711	Sult1a1	0.249242829	1.392401475	0.03991156
ENSMUSG00000038418	Egr1	0.852830884	-0.857921879	0.040910434
ENSMUSG00000032330	Cox7a2	11.98767919	-0.753110628	0.042375928

Table S2F. DEGs at ZT14 in female and male cerebral cortex. The average number of counts per spot in the RHY condition, the log2 fold change in gene expression (RHY relative to saline), and the adjusted p-value (FDR) are shown.

ZT14 FEMALES - Cerebral cortex					ZT14 MALES - Cerebral cortex				
FeatureID	FeatureName	ZT14RF count average	ZT14RF Log2FoldChange	ZT14RF FDR	FeatureID	FeatureName	ZT14RM count average	ZT14RM Log2FoldChange	ZT14RM FDR
ENSMUSG00000048572	Tmem252	0.196267198	5.057580732	8.26296E-11	ENSMUSG00000098178	Gm42418	5.176275493	-1.565230904	1.93103E-08
ENSMUSG00000026822	Lcn2	0.282384438	7.162933732	1.7136E-09	ENSMUSG00000071753	Cdr1os	0.317028334	-1.583771128	8.43705E-06
ENSMUSG00000019970	Sgk1	2.050791946	1.630890515	2.57911E-08					
ENSMUSG00000071637	Cebpd	0.402548029	1.864043174	2.61222E-06					
ENSMUSG00000020108	Ddit4	0.646880663	1.545681694	7.02411E-06					

ENSMUSG00000030711	Sult1a1	0.450613465	1.51143748	4.67368E-05
ENSMUSG00000031765	Mt1	54.15172211	1.042833921	0.00028467
ENSMUSG00000061808	Ttr	5.781871435	1.764207802	0.00028467
ENSMUSG00000048001	Hes5	0.278378985	-1.321054743	0.000418649
ENSMUSG00000090137	Uba52	9.536983641	1.017129648	0.000528063
ENSMUSG00000033585	Ndn	1.748380243	-0.981852826	0.003350996
ENSMUSG00000095366	Gm21860	0.042057257	4.472618232	0.003350996
ENSMUSG00000031762	Mt2	4.335902894	0.945527558	0.004519423
ENSMUSG00000021025	Nfkbia	0.604823406	1.158328513	0.007085098
ENSMUSG00000060143	Gm10076	20.80232026	0.871497488	0.009964843
ENSMUSG00000090247	Bloc1s1	0.867180579	0.999950786	0.011402831
ENSMUSG00000052397	Ezr	0.767044253	0.998236271	0.01976613
ENSMUSG00000103034	Gm8797	0.118160864	-1.209205808	0.025812148
ENSMUSG00000023067	Cdkn1a	0.25835172	1.280666924	0.025812148
ENSMUSG00000115783	Bc1	0.446608012	-0.917550725	0.046984042

Table S2G. DEGs at ZT4 in female and male basolateral amygdala (BLA). The average number of counts per spot in the RHY condition, the log2 fold change in gene expression (RHY relative to saline), and the adjusted p-value (FDR) are shown.

ZT4 FEMALES - BLA					ZT4 MALES - BLA				
FeatureID	FeatureName	ZT4RF count average	ZT4RF Log2FoldChange	ZT4RF FDR	FeatureID	FeatureName	ZT4RM count average	ZT4RM Log2FoldChange	ZT4RM FDR
ENSMUSG00000090137	Uba52	1.852354195	-2.333993921	1.48E-10	ENSMUSG00000061808	Ttr	0.930888315	-2.390990387	0.000108547
ENSMUSG00000113902	Ndufb1-ps	4.106051799	-2.085446327	2.95E-10	ENSMUSG00000090137	Uba52	3.016078142	-1.537809812	0.002900805
ENSMUSG00000025739	Gng13	3.087256992	-2.084253057	2.95E-10	ENSMUSG00000035383	Pmch	0.539915223	-2.147963119	0.002900805
ENSMUSG00000060143	Gm10076	7.13156365	-1.955787675	5.52E-10					
ENSMUSG00000061808	Ttr	5.665116579	3.430250654	3.84E-09					
ENSMUSG00000064360	mt-Nd3	13.3369502	-1.779163451	5.18E-09					
ENSMUSG00000071528	Atp5md	16.6248789	-1.750598369	5.99E-09					
ENSMUSG00000028998	Tomm7	2.716786153	-1.893096563	8.33E-09					
ENSMUSG00000021290	Atp5mpl	6.313440548	-1.722904903	1.89E-08					
ENSMUSG00000038489	Polr2l	0.555706258	-2.445361465	0.00000002					
ENSMUSG00000067288	Rps28	7.594652199	-1.677486933	2.66E-08					
ENSMUSG00000050856	Atp5k	9.200025835	-1.658994857	4.65E-08					
ENSMUSG00000035674	Ndufa3	5.32551831	-1.664488696	4.65E-08					
ENSMUSG00000046516	Cox17	2.284570174	-1.844758975	6.22E-08					
ENSMUSG00000016427	Ndufa1	2.300066459	-1.820189385	6.22E-08					
ENSMUSG00000073616	Cops9	5.495317445	-1.626560987	7.89E-08					
ENSMUSG00000079523	Tmsn10	15.79131951	-1.636966829	8.57E-08					
ENSMUSG00000021342	Pr1	0.015436285	-5.972005006	0.00000151					
ENSMUSG00000017778	Cox7c	14.52554415	-1.528073743	0.00000158					
ENSMUSG00000057322	Rpl38	19.58864561	-1.50798231	0.00000159					
ENSMUSG00000034892	Rps29	18.55441452	-1.541958721	0.00000164					
ENSMUSG00000020018	Snrpf	0.432215979	-2.223648502	0.00000023					
ENSMUSG00000062997	Rpl35	7.841632759	-1.489667814	0.000000435					
ENSMUSG00000031760	Mt3	17.96783569	-1.465741215	0.000000435					
ENSMUSG00000014313	Cox6c	18.58528709	-1.435191542	0.000000496					
ENSMUSG00000079641	Rpl39	7.795323904	-1.491511772	0.000000562					
ENSMUSG00000047721	Bola2	2.161079894	-1.664899557	0.000000611					
ENSMUSG00000078974	Sec61g	3.164438416	-1.604899307	0.000000611					
ENSMUSG00000039001	Rps21	20.66918556	-1.423523049	0.00000087					
ENSMUSG00000016252	Atp5e	8.953045275	-1.430426388	0.000000904					
ENSMUSG00000090733	Rps27	8.165794743	-1.453401098	0.00000135					
ENSMUSG00000041841	Rpl37	18.80139508	-1.363366010	0.00000179					
ENSMUSG00000093674	Rpl41	20.96247497	-1.342732193	0.00000233					
ENSMUSG00000059534	Uqcr10	7.826196474	-1.387640266	0.00000274					
ENSMUSG00000020163	Uqcr11	9.24633469	-1.377901852	0.00000362					
ENSMUSG00000035383	Pmch	0.077181425	-3.282072946	0.0000099					
ENSMUSG00000104960	Snhg8	0.926177097	-1.643005882	0.0000151					
ENSMUSG00000037152	Ndufc1	6.544984822	-1.299579664	0.0000261					
ENSMUSG00000057278	Snrpg	1.96040819	-1.415239397	0.0000273					
ENSMUSG00000023067	Cdkn1a	0.617451398	3.218437013	0.0000457					
ENSMUSG00000057863	Rpl36	8.860427566	-1.205316523	0.0000626					
ENSMUSG00000098234	Snhg6	0.138926565	-2.724077493	0.000065					

ENSMUSG00000038690	Atp5j2	10.86714461	-1.20217726	0.0000683
ENSMUSG00000087687	Pet100	1.250339082	-1.446898905	0.0000733
ENSMUSG00000084786	Ubl5	6.081896273	-1.213845867	0.0000753
ENSMUSG00000078784	Rbis	1.821481625	-1.378723549	0.0000985
ENSMUSG00000014294	Ndufa2	5.726861719	-1.194280785	0.000113408
ENSMUSG00000074754	Smim26	0.879868243	-1.575754746	0.0001276
ENSMUSG00000021040	Slirp	0.679196538	-1.745293979	0.00013659
ENSMUSG00000061718	Ppp1r1b	1.559064781	1.948347849	0.000148098
ENSMUSG00000046330	Rpl37a	12.56513596	-1.123989466	0.000229821
ENSMUSG00000035048	Anapc13	0.895304528	-1.485290633	0.000243845
ENSMUSG00000060636	Rpl35a	14.18594588	-1.104196576	0.000243845
ENSMUSG00000025508	Rplp2	7.841632759	-1.1191367	0.000270929
ENSMUSG00000032330	Cox7a2	13.84634761	-1.096727682	0.000285646
ENSMUSG00000090247	Bloc1s1	0.108053995	-2.598546611	0.000314002
ENSMUSG00000036372	Tmem258	1.559064781	-1.318438691	0.000390128
ENSMUSG00000027133	Nop10	2.516114448	-1.281408874	0.000402898
ENSMUSG00000031431	Tsc22d3	2.269133889	1.578485277	0.000402898
ENSMUSG00000024038	Ndufv3	4.399341213	-1.144150582	0.000462901
ENSMUSG00000023089	Ndufa5	6.051023703	-1.075318341	0.0004946
ENSMUSG00000042541	Sem1	2.191952464	-1.273864404	0.000495083
ENSMUSG00000020713	Gh	0.03087257	-5.387042505	0.000563178
ENSMUSG00000067847	Romo1	2.855712717	-1.146850641	0.000569283
ENSMUSG00000038717	Atp5l	10.85170833	-1.039432934	0.000707645
ENSMUSG00000035215	Lsm7	2.269133889	-1.196448167	0.000927156
ENSMUSG00000070394	Tmem256	2.886585287	-1.150580178	0.001230609
ENSMUSG00000067786	Nnat	12.42620939	1.286702346	0.001391618
ENSMUSG00000019970	Sgk1	1.92953562	1.75070209	0.001391618
ENSMUSG000000103034	Gm8797	0.355034554	4.445847509	0.001556516
ENSMUSG00000044442	Ngamt1	0.586578828	2.561324726	0.001802378
ENSMUSG00000090223	Pcp4	15.31279468	-1.091857705	0.002062422
ENSMUSG000000106918	Mrpl33	1.68255506	-1.203245329	0.002090551
ENSMUSG00000025362	Rps26	10.69734548	-0.997239346	0.002090551
ENSMUSG00000002416	Ndufb2	5.695989149	-1.03189982	0.002138803
ENSMUSG00000054312	Mrps21	2.454369308	-1.165915051	0.002158799
ENSMUSG00000079435	Rpl36a	6.267131693	-0.983957604	0.002846168
ENSMUSG00000041431	Ccnb1	0	-4.387042505	0.003152361
ENSMUSG00000048572	Tmem252	0.370470839	3.504741198	0.003152361
ENSMUSG00000022820	Ndufb4	7.40941678	-0.974055746	0.003855154
ENSMUSG00000062006	Rpl34	12.61144481	-0.922589578	0.004008837
ENSMUSG00000044894	Uqcrc	11.14499774	-0.934734804	0.004008837
ENSMUSG00000024208	Uqcc2	5.57249887	-0.979119108	0.004520007
ENSMUSG00000031231	Cox7b	10.69734548	-0.95180555	0.004850455
ENSMUSG00000021025	Nfkbia	0.771814248	2.073878731	0.005099429
ENSMUSG00000073412	Lst1	0.216107989	-1.932664115	0.005099429
ENSMUSG00000064356	mt-Atp8	2.253697604	-1.08410089	0.005266929
ENSMUSG00000035885	Cox8a	23.67926113	-0.880959632	0.005668951
ENSMUSG00000053332	Gas5	7.054382226	-0.934722254	0.006094416
ENSMUSG00000010834	Gm39469	0.185235419	-1.898106892	0.006099485
ENSMUSG00000055839	Elob	13.18258735	-0.879114646	0.006233565
ENSMUSG00000056023	Gm9989	0.108053995	-2.226577833	0.006468478
ENSMUSG00000042737	Dpm3	0.987922237	-1.182836369	0.008478432
ENSMUSG00000021520	Uqcrb	5.804043144	-0.918316181	0.008662715
ENSMUSG00000058351	Smim4	0.355034554	-1.531432415	0.010683698
ENSMUSG00000038803	Ost4	0.663760253	-1.294393217	0.010992173
ENSMUSG00000053093	Myh7	1.65168249	1.406319145	0.012061155
ENSMUSG00000040055	Gjb6	0.895304528	1.656065216	0.012557795
ENSMUSG00000010406	Mrpl52	2.068462184	-1.039579318	0.012572698
ENSMUSG00000061787	Rps17	5.942969709	-0.875332882	0.014800974
ENSMUSG00000073702	Rpl31	7.795323904	-0.856561135	0.016859279
ENSMUSG00000026344	Lypd1	13.21345992	1.144604784	0.017598406
ENSMUSG00000039221	Rpl22l1	8.536265582	-0.834337001	0.018939642
ENSMUSG00000059278	Naa38	3.272492411	-0.92010521	0.020462198
ENSMUSG00000028936	Rpl22	3.905380094	-0.898623155	0.021053948

ENSMUSG00000097451	Rian	3.82819867	1.065999438	0.024223762
ENSMUSG00000036751	Cox6b1	11.09868888	-0.802080005	0.028070135
ENSMUSG00000068523	Gng5	1.265775367	-1.040199966	0.033966122
ENSMUSG00000052837	Junb	0.740941678	1.66823993	0.040027598
ENSMUSG00000021377	Dek	2.083898469	1.166988136	0.040092184
ENSMUSG00000054428	Atpf1	13.66111219	-0.768964959	0.042542539
ENSMUSG00000026411	Tmem9	2.670477298	1.037041963	0.043891971
ENSMUSG00000087269	D330023K18Rik	0.12349028	-1.969189991	0.046653223
ENSMUSG00000008683	Rps15a	10.74365433	-0.768241609	0.046653223
ENSMUSG00000050668	Micos10	5.171155461	-0.823613166	0.047679553

Table S2H. DEGs at ZT14 in female and male basolateral amygdala (BLA). The average number of counts per spot in the RHY condition, the log<sub>2</sub> fold change in gene expression (RHY relative to saline), and the adjusted p-value (FDR) are shown.

ZT14 FEMALES - BLA

FeatureID	FeatureName	ZT14RF count average	ZT14RF Log2FoldChange	ZT14RF FDR
ENSMUSG00000061808	Ttr	1.328497359	2.112642623	0.033319254

ZT14 MALES - BLA

FeatureID	FeatureName	ZT14RM count average	ZT14RM Log2FoldChange	ZT14RM FDR
ENSMUSG00000092341	Malat1	6.912736451	1.685515117	0.002017662
ENSMUSG00000098178	Gm42418	5.069340064	-1.373612314	0.0055336
ENSMUSG00000061808	Ttr	2.801962508	1.741951062	0.007760099
ENSMUSG00000028656	Cap1	0.294943422	-1.926427446	0.010236631

Table S2I. DEGs at ZT4 in female and male hippocampus. The average number of counts per spot in the RHY condition, the log<sub>2</sub> fold change in gene expression (RHY relative to saline), and the adjusted p-value (FDR) are shown.

ZT4 FEMALES - Hippocampus

FeatureID	FeatureName	ZT4RF count average	ZT4RF Log2FoldChange	ZT4RF FDR
ENSMUSG00000021342	Pr1	0.006490427	-6.452346191	2.27939E-33
ENSMUSG00000020713	Gh	0.003245213	-6.058682343	2.36301E-22
ENSMUSG00000090137	Uba52	1.515514643	-2.333275709	5.99736E-19
ENSMUSG00000026822	Lcn2	1.52200507	8.905297445	1.03031E-17
ENSMUSG000000113902	Ndufb1-ps	3.186799528	-1.873307806	3.46221E-13
ENSMUSG00000038489	Polr2l	0.483536792	-2.043897006	1.1523E-12
ENSMUSG00000060143	Gm10076	5.354602058	-1.674144136	1.07882E-10
ENSMUSG00000016427	Ndufa1	2.015277502	-1.723871733	1.10319E-10
ENSMUSG000000104960	Snhg8	0.749644288	-1.716864852	2.02351E-09
ENSMUSG00000067288	Rps28	6.055568145	-1.575372163	2.02351E-09
ENSMUSG00000098234	Snhg6	0.155770242	-2.124693982	2.32329E-09
ENSMUSG00000079523	Tmsb10	6.003644731	-1.562662541	5.1304E-09
ENSMUSG00000028998	Tom7	2.096407836	-1.553950455	6.8718E-09
ENSMUSG00000048572	Tmem252	0.415387311	3.339568036	9.58994E-09
ENSMUSG00000074754	Smim26	0.580893193	-1.656785943	1.07172E-08
ENSMUSG00000042737	Dpm3	0.743153861	-1.593335001	3.27726E-08
ENSMUSG00000035674	Ndufa3	4.910007826	-1.437737148	4.8815E-08
ENSMUSG00000079641	Rpl39	6.139943693	-1.43348896	6.29577E-08
ENSMUSG00000017778	Cox7c	11.50103618	-1.403048004	7.37716E-08
ENSMUSG00000103034	Gm8797	0.201203229	3.1987055	9.84175E-08
ENSMUSG00000078974	Sec61g	3.079707487	-1.435337437	9.84175E-08
ENSMUSG00000038803	Ost4	0.444594231	-1.624246277	1.08775E-07
ENSMUSG00000057322	Rpl38	16.29097111	-1.373884733	1.51878E-07
ENSMUSG00000050856	Atp5k	7.282258799	-1.373752087	1.73174E-07
ENSMUSG00000021290	Atp5mpl	5.718065955	-1.379078889	1.76957E-07
ENSMUSG00000046516	Cox17	2.096407836	-1.406736806	1.76957E-07
ENSMUSG00000071528	Atp5md	13.95117227	-1.363473016	1.76957E-07
ENSMUSG00000097383	1500026H17Rik	0.051923414	-2.438345512	2.34158E-07
ENSMUSG00000041841	Rpl37	15.22329591	-1.339024311	3.07549E-07
ENSMUSG00000020018	Snrpf	0.639307034	-1.481414234	5.15731E-07
ENSMUSG00000016252	Atp5e	7.820964218	-1.282721519	1.36916E-06

ZT4 MALES - Hippocampus

FeatureID	FeatureName	ZT4RM count average	ZT4RM Log2FoldChange	ZT4RM FDR
ENSMUSG00000090137	Uba52	1.600379074	-1.610239306	3.8161E-08
ENSMUSG00000023067	Cdkn1a	0.37544438	2.711688789	4.11612E-06
ENSMUSG00000048572	Tmem252	0.326143603	4.247741689	4.11612E-06
ENSMUSG00000031431	Tsc22d3	1.661056954	1.567924982	6.92184E-05
ENSMUSG00000027301	Oxt	0	-5.417594228	0.000128445
ENSMUSG00000028645	Slc2a1	1.460061478	1.6071783	0.000145559
ENSMUSG00000026822	Lcn2	0.682626145	5.304644081	0.00101572
ENSMUSG0000002910	Arrdc2	0.269258091	2.237757601	0.003373802
ENSMUSG00000024066	Xdh	0.170656536	3.32836015	0.005156005
ENSMUSG00000021025	Nfkbia	0.652287206	1.398124167	0.023762108

ENSMUSG00000042541	Sem1	1.509024216	-1.339454284	1.36916E-06
ENSMUSG00000057278	Snrpg	1.762150859	-1.327736203	1.8155E-06
ENSMUSG00000025739	Gng13	1.479817296	-1.339740291	2.61979E-06
ENSMUSG000000031760	Mt3	21.61636625	-1.246312453	2.63115E-06
ENSMUSG00000023067	Cdkn1a	0.334256977	2.269788598	3.35547E-06
ENSMUSG00000019970	Sgk1	1.853016833	1.537600144	4.17588E-06
ENSMUSG000000031431	Tsc2d3	1.872488114	1.422346467	5.41124E-06
ENSMUSG00000090247	Bloc1s1	0.246636216	-1.611323557	5.97719E-06
ENSMUSG00000095845	Gm5741	0.032452134	-3.369768878	6.00137E-06
ENSMUSG00000064360	mt-Nd3	12.44863848	-1.24240872	6.64286E-06
ENSMUSG00000036372	Tmem258	1.294840134	-1.265472638	9.02664E-06
ENSMUSG00000039001	Rps21	19.47777064	-1.192066123	1.02698E-05
ENSMUSG00000089665	Fcor	0.188222375	-1.66600528	1.08575E-05
ENSMUSG00000038690	Atp5j2	8.028657873	-1.186851038	1.17232E-05
ENSMUSG00000070394	Tmem256	2.018522715	-1.229227764	1.20657E-05
ENSMUSG00000062997	Rpl35	6.853890634	-1.178807882	1.40528E-05
ENSMUSG00000061808	Ttr	19.59459832	3.884970883	1.87036E-05
ENSMUSG00000038570	Saxo2	0.136298961	-1.684506099	2.7619E-05
ENSMUSG00000057863	Rpl36	7.655458336	-1.147920913	2.80128E-05
ENSMUSG00000014313	Cox6c	17.97199163	-1.12581186	3.78953E-05
ENSMUSG00000023153	Tmem52	0.175241522	2.64021521	4.06128E-05
ENSMUSG00000090733	Rps27	7.412067333	-1.14163549	4.25324E-05
ENSMUSG00000067847	Romo1	1.953618448	-1.166702914	4.58069E-05
ENSMUSG00000050315	Synpo2	0.094111188	-1.84568862	4.95057E-05
ENSMUSG00000033685	Ucp2	0.444594231	1.77975295	5.21308E-05
ENSMUSG00000029516	Cit	0.090865974	-1.907654373	6.91185E-05
ENSMUSG00000034892	Rps29	16.79397918	-1.108570984	8.73119E-05
ENSMUSG00000037152	Ndufc1	5.25075523	-1.100680728	9.1634E-05
ENSMUSG00000078784	Rbis	1.379215682	-1.149399218	9.94601E-05
ENSMUSG00000087687	Pet100	1.093636905	-1.157179853	0.000101229
ENSMUSG00000019689	Fmc1	1.142315106	-1.165906611	0.000104513
ENSMUSG00000023089	Ndufa5	6.376844269	-1.05496528	0.000225229
ENSMUSG00000020163	Uqcr11	8.405102624	-1.044231406	0.000248782
ENSMUSG00000002910	Arrdc2	0.285578776	1.919551429	0.000287375
ENSMUSG00000059534	Uqcr10	7.476971601	-1.035186552	0.000303926
ENSMUSG00000030785	Cox6a2	0.431613378	-1.314521247	0.000316859
ENSMUSG00000084786	Ubl5	4.549789142	-1.019752012	0.00054524
ENSMUSG00000058351	Smim4	0.31803091	-1.266675385	0.000625366
ENSMUSG00000093674	Rpl41	15.92750721	-0.99225746	0.000641463
ENSMUSG00000025508	Rplp2	6.568311858	-0.983633672	0.000902378
ENSMUSG00000021040	Slirp	0.681494807	-1.117399053	0.000902378
ENSMUSG00000029062	Cdk11b	0.340747404	-1.220578971	0.00093606
ENSMUSG00000110156	Gm42067	0.253126643	-1.267351596	0.001191486
ENSMUSG00000065947	mt-Nd4l	3.245213368	-1.006808258	0.001397974
ENSMUSG00000030711	Sult1a1	0.30829527	1.56934888	0.001631043
ENSMUSG00000021025	Nfkbia	0.61659054	1.358281813	0.001631043
ENSMUSG00000048483	Zdhhc22	0.188222375	-1.410504547	0.001631043
ENSMUSG000000034936	Ar14d	0.421877738	1.507614648	0.001987894
ENSMUSG00000106918	Mrp133	1.262388	-0.995066244	0.00212992
ENSMUSG00000002831	Plin4	0.094111188	2.936571094	0.002151113
ENSMUSG00000063594	Gng8	0.055168627	-2.210685436	0.00234901
ENSMUSG00000060636	Rpl35a	12.72448162	-0.926388498	0.002416879
ENSMUSG00000047721	Bola2	1.927656741	-0.968792764	0.00266627
ENSMUSG00000073616	Cops9	7.415312547	-0.936407905	0.002682761
ENSMUSG00000022820	Ndufb4	5.247510017	-0.922709552	0.002917477
ENSMUSG00000021948	Prkcd	0.538705419	-1.114992215	0.003265356
ENSMUSG00000074170	Plekhf1	0.175241522	2.109700494	0.003426424
ENSMUSG00000024985	Tcf7l2	0.197958015	-1.356873194	0.003518387
ENSMUSG00000035048	Anapc13	1.109862972	-1.008586354	0.003826771
ENSMUSG00000062006	Rpl34	10.62482857	-0.893155805	0.004484613
ENSMUSG00000079435	Rpl36a	4.98140252	-0.889088805	0.005837457
ENSMUSG00000046707	Csnk2a2	0.253126643	-1.15929185	0.006416007
ENSMUSG00000025362	Rps26	7.859906778	-0.878387932	0.006416007



ENSMUSG00000055839	Elob	10.01472845	-0.869328489	0.006890533
ENSMUSG00000014294	Ndufa2	4.809406212	-0.875188675	0.007209803
ENSMUSG00000038059	Smim3	0.571157553	1.174457954	0.007365981
ENSMUSG000000444894	Uqcrc	10.03419974	-0.857723288	0.008090527
ENSMUSG00000054312	Mrps21	2.609151548	-0.880616953	0.008942773
ENSMUSG00000070858	Gm1673	2.219725944	-0.878811968	0.008942773
ENSMUSG00000024066	Xdh	0.133053748	2.25117292	0.008942773
ENSMUSG00000042312	S100a13	0.746399075	-0.995987407	0.00915835
ENSMUSG00000024038	Ndufv3	3.731995374	-0.868636574	0.00915835
ENSMUSG00000002416	Ndufb2	5.000873801	-0.856365883	0.009782948
ENSMUSG00000026500	Cox20	0.88594325	-0.92575547	0.010934257
ENSMUSG00000098120	Gm5914	0.246636216	-1.139061189	0.01184317
ENSMUSG00000037095	Lrg1	0.074639907	4.613742999	0.012499731
ENSMUSG00000090101	Snhg9	0.107092041	-1.391551301	0.013035723
ENSMUSG00000084883	Ccdc85c	0.035697347	-1.878110097	0.013177563
ENSMUSG00000068240	Gm11808	0.382935177	-1.018916244	0.013565945
ENSMUSG00000089809	Rasgef1b	0.051923414	-1.665116374	0.014008476
ENSMUSG00000046330	Rpl37a	9.813525226	-0.823977782	0.015275847
ENSMUSG00000028407	Smim27	0.165505882	-1.201517121	0.015818236
ENSMUSG00000032338	Hcn4	0.012980853	-2.456646329	0.016341364
ENSMUSG00000087336	Gm15860	0.035697347	-1.84568862	0.016403722
ENSMUSG00000027133	Nop10	2.161312103	-0.839974968	0.018493662
ENSMUSG00000032766	Gng11	0.421877738	-1.025259341	0.018493662
ENSMUSG00000006360	Crip1	0.210938869	-1.394430932	0.019501369
ENSMUSG00000025572	Tmc6	0.081130334	2.407292122	0.020479896
ENSMUSG00000038530	Rgs4	0.707456514	-0.934524702	0.020593516
ENSMUSG00000061086	Myl4	0.084375548	-1.406165558	0.020710856
ENSMUSG00000010406	Mrp52	1.833545553	-0.840581729	0.020710856
ENSMUSG00000053332	Gas5	6.159414973	-0.804709165	0.021473776
ENSMUSG00000032368	Zic1	0.165505882	-1.270779784	0.021498035
ENSMUSG00000028298	Cga	0	-3.971219502	0.021620364
ENSMUSG00000063320	119007107Rik	0.155770242	-1.189399672	0.022292943
ENSMUSG00000031231	Cox7b	7.908584979	-0.796552688	0.022292943
ENSMUSG00000045996	Poir2k	1.632342324	-0.829989933	0.023272487
ENSMUSG00000027985	Lef1	0.045432987	-1.708185096	0.023533696
ENSMUSG00000072844	G530011006Rik	0.123318108	2.144257716	0.024363618
ENSMUSG00000056608	Chd9	0.220674509	-1.091513735	0.024528512
ENSMUSG00000024903	Lao1	0.042187774	3.83613542	0.02557891
ENSMUSG00000078747	Gm20878	0.016226067	-2.244237996	0.027147526
ENSMUSG00000052384	Nrros	0.142789388	1.820193877	0.029240642
ENSMUSG00000055148	Klf2	0.331011764	1.255849407	0.030148458
ENSMUSG000000110834	Gm39469	0.139544175	-1.19828841	0.030197716
ENSMUSG00000041881	Ndufa7	3.852068268	-0.779961631	0.03334443
ENSMUSG00000044145	1810024B03Rik	0.02920692	-1.858744772	0.036984958
ENSMUSG00000019828	Grm1	0.107092041	-1.276074083	0.036984958
ENSMUSG00000024018	Ccdc167	0.438103805	-0.955219023	0.036984958
ENSMUSG00000028645	Slc2a1	1.165031599	0.950777986	0.039009523
ENSMUSG00000045625	Pigz	0.103846828	-1.319142805	0.042379045
ENSMUSG00000054364	Rhob	4.491375302	0.77620045	0.042956137
ENSMUSG00000095687	Rnaset2a	0.058413841	2.691745511	0.042956137
ENSMUSG00000032330	Cox7a2	10.5112461	-0.745111665	0.0450318
ENSMUSG00000025422	Agap2	0.730173008	0.966316411	0.0450318
ENSMUSG00000020774	Aspa	0.123318108	-1.270779784	0.0450318
ENSMUSG00000030677	Klf22	0.155770242	-1.124693982	0.046432463
ENSMUSG00000053113	Socs3	0.071394694	2.967379954	0.046628785

Table S2J. DEGs at ZT14 in female and male hippocampus. The average number of counts per spot in the RHY condition, the log2 fold change in gene expression (RHY relative to saline), and the adjusted p-value (FDR) are shown.

ZT14 FEMALES - Hippocampus					ZT14 MALES - Hippocampus				
FeatureID	FeatureName	ZT14RF count average	ZT14RF Log2FoldChange	ZT14RF FDR	FeatureID	FeatureName	ZT14RM count average	ZT14RM Log2FoldChange	ZT14RM FDR
ENSMUSG00000026822	Lcn2	0.505808848	7.648477359	3.03434E-16	ENSMUSG00000098178	Gm42418	3.826001176	-1.772203119	3.19309E-11
ENSMUSG00000064179	Tnnt1	0.072258407	-2.560976006	1.43436E-10	ENSMUSG00000035202	Lars2	0.474697026	-1.326498787	0.001322907

ENSMUSG00000048572	Tmem252	0.258065739	3.879596585	1.0493E-09	ENSMUSG00000092274	Neat1	0.201817298	2.168099686	0.001322907
ENSMUSG00000090137	Uba52	9.438324284	1.055344888	5.73367E-07	ENSMUSG00000044349	Snhg11	1.938583063	1.028485416	0.004689054
ENSMUSG00000019970	Sgk1	1.686029493	1.384249771	5.73367E-07					
ENSMUSG00000023067	Cdkn1a	0.185807332	2.760952089	9.60092E-07					
ENSMUSG00000031765	Mt1	64.117293	1.049684728	1.28934E-06					
ENSMUSG00000060143	Gm10076	18.71492737	0.949435725	8.20126E-06					
ENSMUSG00000021025	Nfkbia	0.598712514	1.414501675	1.33409E-05					
ENSMUSG00000048001	Hes5	0.127312431	-1.560976006	0.000134514					
ENSMUSG00000090247	Bloc1s1	0.812046858	1.147858153	0.000168402					
ENSMUSG00000029394	Cdk2ap1	0.082581036	-1.724474738	0.0003238					
ENSMUSG00000038489	Polr2l	1.89592296	0.921839608	0.00052978					
ENSMUSG00000060803	Gstp1	2.532485116	0.887729206	0.000689449					
ENSMUSG00000076498	Trbc2	0.22709785	1.750225682	0.001226888					
ENSMUSG00000061808	Ttr	7.301539967	1.520806759	0.001327999					
ENSMUSG00000028967	Errfi1	0.443873071	1.232573116	0.001624137					
ENSMUSG00000041378	Cldn5	0.175484702	-1.336269719	0.001624137					
ENSMUSG00000074896	Ifit3	0.027527012	-2.321788342	0.001624137					
ENSMUSG00000113902	Ndufb1-ps	11.87446486	0.76126557	0.001935362					
ENSMUSG00000033585	Ndn	1.286887817	-0.824010412	0.005352643					
ENSMUSG00000003541	Ier3	0.30623801	1.573325086	0.005687186					
ENSMUSG00000031762	Mt2	5.484757167	0.782595768	0.007242177					
ENSMUSG00000045471	Hcrt	0.030967889	-2.020407625	0.00920427					
ENSMUSG00000076617	Ighm	0.529894983	1.014708681	0.013635941					
ENSMUSG00000095845	Gm5741	0.082581036	2.760952089	0.015140115					
ENSMUSG00000030711	Sult1a1	0.37505554	1.132920866	0.01594955					
ENSMUSG00000037279	Ovol2	0.06881753	2.831341417	0.017808339					
ENSMUSG00000061086	Myl4	0.289033627	1.263452429	0.018466199					
ENSMUSG00000089762	Ier5l	0.103226295	-1.33470015	0.02013557					
ENSMUSG00000037095	Lrg1	0.072258407	3.313493112	0.02027057					
ENSMUSG00000095366	Gm21860	0.041290518	4.139463712	0.023950468					
ENSMUSG00000026701	Prdx6	2.398290932	-0.731360245	0.024320571					
ENSMUSG00000113919	Gm34466	0.116989802	-1.251871952	0.024445993					
ENSMUSG00000074170	Plekhf1	0.116989802	1.867867293	0.026720514					
ENSMUSG00000085007	Gm11549	0.175484702	1.495607522	0.028709249					
ENSMUSG00000034936	Arl4d	0.323442393	1.175989588	0.028709249					
ENSMUSG00000079242	C730034F03Rik	0.072258407	2.576527518	0.034555723					
ENSMUSG00000017697	Ada	0.058494901	3.023986495	0.03672282					
ENSMUSG00000002910	Arrdc2	0.258065739	1.227519889	0.03672282					
ENSMUSG00000019960	Dusp6	0.14795769	-1.123912201	0.041050137					
ENSMUSG00000027525	Phactr3	1.321296582	0.765643784	0.042676578					
ENSMUSG00000060063	Alox5ap	0.230538727	1.278559322	0.047421181					
ENSMUSG00000014846	Tppp3	0.705379686	0.89670583	0.047421181					
ENSMUSG00000021948	Prkcd	0.340646775	-0.950542818	0.047421181					

**Table S2K. DEGs at ZT4 in female and male thalamus. The average number of counts per spot in the RHY condition, the log<sub>2</sub> fold change in gene expression (RHY relative to saline), and the adjusted p-value (FDR) are shown.**

ZT4 FEMALES - Thalamus					ZT4 MALES - Thalamus				
FeatureID	FeatureName	ZT4RF count average	ZT4RF Log2FoldChange	ZT4RF FDR	FeatureID	FeatureName	ZT4RM count average	ZT4RM Log2FoldChange	ZT4RM FDR
ENSMUSG00000021342	Prl	0.050593522	-5.564013646	5.71824E-47	ENSMUSG00000023067	Cdkn1a	0.919225887	3.239040362	3.43701E-16
ENSMUSG00000020713	Gh	0.02069735	-5.740301312	7.1886E-39	ENSMUSG00000061808	Ttr	1.143089088	-2.014638228	9.91958E-14
ENSMUSG00000023067	Cdkn1a	0.862389579	4.03488668	1.25456E-27	ENSMUSG00000027301	Oxt	0	-6.676494328	9.266E-13
ENSMUSG00000090137	Uba52	1.016469851	-2.423540564	1.32588E-20	ENSMUSG00000048572	Tmem252	0.342728618	4.52133667	3.26176E-11
ENSMUSG00000026822	Lcn2	0.450742287	7.625911603	3.00306E-17	ENSMUSG00000019970	Sgk1	3.96614273	1.693193055	5.95993E-07
ENSMUSG00000048572	Tmem252	0.482938164	4.024519255	4.20017E-17	ENSMUSG00000037727	Avp	0.033678535	-2.817771015	1.57545E-06
ENSMUSG00000019970	Sgk1	3.233385995	2.078562105	8.87524E-14	ENSMUSG00000025591	Tma16	0.570553999	2.165856016	1.93987E-06
ENSMUSG00000060143	Gm10076	3.631235054	-1.852483002	2.55283E-13	ENSMUSG00000034936	Arl4d	0.570553999	1.895766852	2.54335E-05
ENSMUSG00000002910	Arrdc2	0.554229036	2.674795508	3.71918E-13	ENSMUSG00000090137	Uba52	1.046015665	-1.302843086	3.18161E-05
ENSMUSG00000028298	Cga	0.006899117	-4.471873647	4.8879E-13	ENSMUSG00000002910	Arrdc2	0.471499485	1.58694256	0.00214153
ENSMUSG000000113902	Ndufb1-ps	3.525448599	-1.793789061	1.50466E-12	ENSMUSG00000024222	Fkbp5	0.556686367	1.463057025	0.002763405
ENSMUSG00000038489	Polr2l	0.595623736	-1.917752317	1.91225E-12	ENSMUSG00000071637	Cebpd	0.303106812	1.821617759	0.002993239
ENSMUSG00000034209	Rasi10a	0.597923442	2.359340439	5.03652E-12	ENSMUSG00000030880	Polr3e	0.653759791	1.449080581	0.0034392
ENSMUSG00000103034	Gm8797	0.246068493	3.588822285	5.84812E-12	ENSMUSG0000002114	Spry2	0.06933816	-1.817771015	0.0034392

ENSMUSG00000064360	mt-Nd3	10.75572283	-1.732889914	5.84812E-12	ENSMUSG00000070369	ltgad	0.116884326	2.663355675	0.005083074
ENSMUSG00000046516	Cox17	1.45571361	-1.730144566	3.44387E-11	ENSMUSG00000045471	Hcrt	0.174335944	-1.479296396	0.005083074
ENSMUSG00000070369	ltgad	0.167878505	4.21331315	5.08692E-11	ENSMUSG00000021025	Nfkb1a	0.946961151	1.268029502	0.005083074
ENSMUSG00000067288	Rps28	4.994960442	-1.665763967	5.08692E-11	ENSMUSG0000002831	Plin4	0.237730833	1.82733141	0.005083074
ENSMUSG00000028998	Tom7	1.777672386	-1.68477456	7.89655E-11	ENSMUSG00000038059	Smim3	0.293201361	1.712599194	0.005083074
ENSMUSG00000034936	Ar14d	0.42314582	2.535241245	9.51641E-11	ENSMUSG00000019960	Dusp6	0.267447187	-1.243534921	0.005651003
ENSMUSG00000098234	Snhg6	0.121884394	-2.142119522	3.32559E-10	ENSMUSG0000002146	Osmr	0.101035604	2.778832892	0.00632507
ENSMUSG00000002831	Plin4	0.183976444	3.758747286	3.87424E-10	ENSMUSG00000041378	Cldn5	0.402161326	-1.214965768	0.008411763
ENSMUSG000000104960	Snhg8	0.551929331	-1.737886908	4.64682E-10	ENSMUSG00000034579	Pla2g3	0.108959965	2.563820002	0.009940146
ENSMUSG00000024222	Fkbp5	0.457641403	2.124154018	3.07524E-09	ENSMUSG00000025509	Pnpla2	0.709230318	1.26245246	0.010295107
ENSMUSG00000079641	Rpl39	5.284723341	-1.513002063	3.46023E-09	ENSMUSG00000096768	Gm47283	1.032148033	-1.004836499	0.01316389
ENSMUSG00000016427	Ndufa1	2.081233518	-1.524816402	4.43716E-09	ENSMUSG00000035615	Frrmpd1	0.459612944	1.327869475	0.015994508
ENSMUSG00000090733	Rps27	5.029456025	-1.498795693	5.62238E-09	ENSMUSG00000034640	Tiparp	0.410085687	1.352568138	0.018404754
ENSMUSG00000071528	Atp5md	11.30075304	-1.486799134	5.62238E-09	ENSMUSG00000021215	Net1	0.570553999	1.299122546	0.02128259
ENSMUSG00000021290	Atp5mpl	5.201933941	-1.498227988	5.82341E-09	ENSMUSG00000047712	Ust	0.035659625	-1.959081531	0.02243376
ENSMUSG00000034892	Rps29	12.80935988	-1.481678024	6.50088E-09	ENSMUSG00000021250	Fos	0.07330034	-1.60441665	0.022869049
ENSMUSG00000025591	Tma16	0.418546409	2.234157403	1.92781E-08	ENSMUSG00000063445	Nmral1	0.364520611	1.400321269	0.025565819
ENSMUSG00000074754	Smim26	0.450742287	-1.590834255	3.48647E-08	ENSMUSG00000030157	Clec2d	0.118865416	2.20177559	0.034344683
ENSMUSG00000035674	Ndufa3	4.594811677	-1.431156362	3.48647E-08	ENSMUSG00000031431	Tsc22d3	3.833409681	0.969350415	0.038497342
ENSMUSG00000021025	Nfkb1a	0.777300474	1.750789764	3.91716E-08	ENSMUSG00000023153	Tmem52	0.063394889	3.122787294	0.049220572
ENSMUSG00000030711	Sult1a1	0.287463193	2.337283518	7.38328E-08	ENSMUSG00000015112	Slc25a13	0.112922146	2.129019247	0.049220572
ENSMUSG00000057322	Rpl38	14.66752196	-1.380693386	8.2583E-08					
ENSMUSG00000038059	Smim3	0.390949943	2.13631008	8.2583E-08					
ENSMUSG00000041841	Rpl37	10.87990693	-1.382696976	8.54028E-08					
ENSMUSG00000039001	Rps21	14.5571361	-1.360329851	1.50993E-07					
ENSMUSG00000062997	Rpl35	4.859277815	-1.360036668	1.8198E-07					
ENSMUSG00000038803	Ost4	0.386350531	-1.540704616	2.09976E-07					
ENSMUSG00000020018	Snrpf	0.44384317	-1.499515182	2.81041E-07					
ENSMUSG00000017778	Cox7c	12.57478992	-1.336781387	2.81995E-07					
ENSMUSG00000050856	Atp5k	7.112989248	-1.303823058	7.23647E-07					
ENSMUSG000000071637	Cebpd	0.416246704	2.052222806	7.3527E-07					
ENSMUSG00000021215	Net1	0.538131097	1.751093714	7.9809E-07					
ENSMUSG00000078974	Sec61g	2.412391116	-1.3153177	8.89696E-07					
ENSMUSG000000005057	Sh2b2	0.126483805	3.226252205	1.39872E-06					
ENSMUSG00000035283	Adrb1	0.112685572	-1.786912254	4.10973E-06					
ENSMUSG00000025730	Rab40c	1.050965434	1.408435344	6.33735E-06					
ENSMUSG00000046330	Rpl37a	7.30846422	-1.196846407	1.06112E-05					
ENSMUSG00000042737	Dpm3	0.577226092	-1.308879139	1.18793E-05					
ENSMUSG00000064356	mt-Atp8	1.81676738	-1.235885071	1.26732E-05					
ENSMUSG00000014313	Cox6c	16.41299847	-1.179966403	1.34477E-05					
ENSMUSG00000034579	Pla2g3	0.119584688	2.924425317	1.39477E-05					
ENSMUSG00000060981	Hist1h4h	0.032195878	-2.337177134	1.59367E-05					
ENSMUSG00000016252	Atp5e	7.554532713	-1.166748011	1.93685E-05					
ENSMUSG00000070394	Tmem256	1.50170772	-1.208095469	2.02019E-05					
ENSMUSG00000027525	Phactr3	1.938651774	1.269631752	2.15186E-05					
ENSMUSG00000028407	Smim27	0.096587633	-1.709426814	2.17339E-05					
ENSMUSG00000057278	Snrpg	1.044066317	-1.225761942	2.17339E-05					
ENSMUSG00000025509	Pnpla2	0.708309308	1.417341817	2.70547E-05					
ENSMUSG00000057863	Rpl36	6.266697608	-1.143664327	3.14698E-05					
ENSMUSG00000017697	Ada	0.080489694	3.588822285	3.65702E-05					
ENSMUSG00000031760	Mt3	17.5467533	-1.129150941	3.65702E-05					
ENSMUSG00000030880	Polr3e	0.579525797	1.479058719	4.45642E-05					
ENSMUSG00000025915	Sgk3	0.271365254	1.854283428	4.54498E-05					
ENSMUSG00000093674	Rpl41	11.41573832	-1.118374173	4.77508E-05					
ENSMUSG00000030827	Fgf21	0.06209205	4.811214706	4.77875E-05					
ENSMUSG00000073616	Cops9	5.420405968	-1.120906108	5.28498E-05					
ENSMUSG00000087687	Pet100	0.97047574	-1.183018351	5.82054E-05					
ENSMUSG00000079523	Tmsb10	12.21833556	-1.106512765	6.35288E-05					
ENSMUSG00000074170	Plekfh1	0.269065549	1.757219816	8.82349E-05					
ENSMUSG00000047721	Bola2	1.517805659	-1.127479642	0.00010775					
ENSMUSG00000031431	Tsc22d3	3.599039177	1.122872832	0.00011436					
ENSMUSG00000067847	Romo1	1.77537268	-1.096173499	0.00018447					
ENSMUSG00000079435	Rpl36a	3.454157727	-1.043817448	0.000342707					

ENSMUSG00000053332	Gas5	4.771889004	-1.030475369	0.000395903
ENSMUSG00000035048	Anapc13	1.096959545	-1.079691867	0.000395903
ENSMUSG00000060636	Rpl35a	8.971151328	-1.022155231	0.000397235
ENSMUSG00000028655	Mfsd2a	0.600223147	1.309362331	0.000494523
ENSMUSG00000054364	Rhob	6.770333122	1.022100149	0.000534347
ENSMUSG00000030790	Adm	0.285163487	1.543379314	0.000577421
ENSMUSG00000000739	Sult5a1	0.045994111	-1.907603541	0.000582835
ENSMUSG00000025739	Gng13	1.299333633	-1.059716331	0.000582835
ENSMUSG00000073412	Lst1	0.027596467	-2.153681493	0.000582835
ENSMUSG00000064220	Hist2h2aa1	0.011498528	-2.73310581	0.000584104
ENSMUSG00000028645	Slc2a1	1.766173858	1.13948846	0.000584104
ENSMUSG00000037152	Ndufc1	4.992660737	-1.008376327	0.000589121
ENSMUSG000000114639	Gm31946	0.050593522	-1.794506355	0.000589121
ENSMUSG00000036372	Tmem258	1.0785619	-1.053313924	0.000598766
ENSMUSG00000042541	Sem1	1.460313021	-1.039709231	0.000614784
ENSMUSG00000023089	Ndufa5	5.183536297	-1.000930575	0.000643635
ENSMUSG00000020163	Uqcr11	7.30846422	-0.996593965	0.000654836
ENSMUSG00000036545	Adamts2	0.305860837	1.45523913	0.000817948
ENSMUSG00000065947	mt-Nd4l	2.994216619	-1.006070852	0.000840612
ENSMUSG00000038690	Atp5j2	8.207649087	-0.975586628	0.00098459
ENSMUSG00000012123	Crybg2	0.156379977	1.864456727	0.000993474
ENSMUSG00000037095	Lrg1	0.045994111	4.396177207	0.001018217
ENSMUSG00000097383	1500026H17Rik	0.043694405	-1.823959241	0.001027951
ENSMUSG00000021040	Slirp	0.666914608	-1.052056205	0.001128039
ENSMUSG00000025362	Rps26	5.772260916	-0.967415927	0.001194227
ENSMUSG00000052384	Nrros	0.14948086	1.960791062	0.001264819
ENSMUSG00000024175	Tekt4	0.075890283	2.76939453	0.001303184
ENSMUSG00000025508	Rplp2	4.804084882	-0.962973352	0.001314683
ENSMUSG00000020108	Ddit4	0.609421969	1.1887775	0.001887163
ENSMUSG00000058351	Smim4	0.282863782	-1.150468362	0.00205367
ENSMUSG000000097162	2310010J17Rik	0.059792344	-1.633570137	0.002270527
ENSMUSG000000106918	Mrpl33	0.864689285	-1.003773541	0.002280845
ENSMUSG00000010406	Mrpl52	1.409719499	-0.966466298	0.002392987
ENSMUSG00000059534	Uqcr10	6.841623994	-0.925350892	0.002648568
ENSMUSG000000110156	Gm42067	0.12878351	-1.312997321	0.002648568
ENSMUSG00000027364	Usp50	0.059792344	-1.616292145	0.002764971
ENSMUSG00000074794	Arrdc3	0.303561132	1.386716878	0.002764971
ENSMUSG00000020424	Castor1	0.114985277	2.091322625	0.003018725
ENSMUSG00000026525	Opn3	0.17017821	-1.251137303	0.003148715
ENSMUSG00000021250	Fos	0.0413947	-1.770580516	0.003196101
ENSMUSG00000035615	Frmpd1	0.351854948	1.293366401	0.003278232
ENSMUSG00000027985	Lef1	0.397849059	-1.076758676	0.003340506
ENSMUSG00000014846	Tppp3	1.050965434	1.055161013	0.003771968
ENSMUSG00000019689	Fmc1	1.138354244	-0.94431902	0.004403397
ENSMUSG000000063714	Sp3os	0.147181155	-1.249896808	0.004435594
ENSMUSG00000022856	Tmem41a	1.671885931	0.972495613	0.004435594
ENSMUSG00000002416	Ndufb2	4.406235823	-0.898860519	0.004460829
ENSMUSG00000078784	Rbis	1.320030982	-0.929384409	0.004546392
ENSMUSG00000086765	Gm11827	0.036795289	4.091322625	0.004546392
ENSMUSG00000050211	Pla2g4e	0.052893228	3.003859784	0.004648781
ENSMUSG00000024778	Fas	0.078189989	2.325787879	0.00485383
ENSMUSG00000038570	Saxo2	0.0827894	-1.41604347	0.004902562

Table S2L. DEGs at ZT14 in female and male thalamus. The average number of counts per spot in the RHY condition, the log<sub>2</sub> fold change in gene expression (RHY relative to saline), and the adjusted p-value (FDR) are shown.

ZT14 FEMALES - Thalamus					ZT14 MALES - Thalamus				
FeatureID	FeatureName	ZT14RF count average	ZT14RF Log2FoldChange	ZT14RF FDR	FeatureID	FeatureName	ZT14RM count average	ZT14RM Log2FoldChange	ZT14RM FDR
ENSMUSG00000061808	Ttr	3.232929116	3.394445966	1.57E-25	ENSMUSG00000061808	Ttr	3.440108055	2.612381186	9.84948E-49
ENSMUSG00000023067	Cdkn1a	0.487621285	2.96010256	2.56E-14	ENSMUSG00000022421	Nptxr	1.213466784	2.126876067	1.16796E-36
ENSMUSG00000019970	Sgk1	2.986680368	2.059132849	7.15E-13	ENSMUSG00000098178	Gm42418	2.537035767	-1.576775804	1.34457E-29
ENSMUSG00000045471	Hcrt	0.19748662	-3.321006529	2E-12	ENSMUSG00000035202	Lars2	0.424010594	-1.643996378	3.57087E-25
ENSMUSG00000026822	Lcn2	0.226743897	5.897010257	5.31E-10	ENSMUSG00000071753	Cdr1os	0.086676199	-2.283313121	5.2083E-25

ENSMUSG00000035383	Pmch	0.47055454	-2.760704141	1.25E-09	ENSMUSG00000021268	Meg3	3.452992355	1.409865203	5.61753E-22
ENSMUSG00000002910	Arrdc2	0.416916198	2.18372366	1.65E-08	ENSMUSG00000090223	Pcp4	7.100420507	-1.281130499	1.15287E-20
ENSMUSG000000031765	Mt1	65.5582436	1.350383794	0.00000103	ENSMUSG00000003657	Calb2	2.118881672	1.391583784	4.49771E-16
ENSMUSG000000048572	Tmem252	0.17066745	3.492168525	0.00000134	ENSMUSG00000046093	Hpcal4	0.401755895	1.771008001	2.09575E-15
ENSMUSG000000034936	Arl4d	0.331582473	2.082901484	0.00000245	ENSMUSG00000044349	Snhg11	1.930302375	1.245522568	1.99067E-14
ENSMUSG000000071637	Cebpδ	0.380344602	1.936602436	0.00000441	ENSMUSG00000006522	Itih3	0.643043692	1.448031055	2.18193E-14
ENSMUSG000000020108	Ddit4	0.70217465	1.586609751	0.00000579	ENSMUSG00000064354	mt-Co2	16.32675049	-0.968509547	5.66833E-12
ENSMUSG000000031762	Mt2	5.536939686	1.239503093	0.0000338	ENSMUSG00000095041	AC149090.1	0.640701092	1.319918582	5.66833E-12
ENSMUSG000000021025	Nfkbia	0.607088499	1.475315676	0.0000455	ENSMUSG00000009394	Syn2	1.643333879	1.092251218	1.03665E-11
ENSMUSG000000090137	Uba52	6.553630064	1.188380986	0.0000613	ENSMUSG00000006930	Hap1	0.286968496	1.713021658	1.20973E-11
ENSMUSG00000002831	Plin4	0.182857982	2.1309173	0.000163152	ENSMUSG00000064370	mt-Cytb	17.95954267	-0.896148087	2.75949E-10
ENSMUSG000000048001	Hes5	0.117029108	-1.612724359	0.000541281	ENSMUSG00000039059	Hrh3	0.865590689	1.115312371	5.73533E-10
ENSMUSG000000030711	Sult1a1	0.338896793	1.564813827	0.000637091	ENSMUSG000000064363	mt-Nd4	12.47668744	-0.886243081	7.0226E-10
ENSMUSG000000060143	Gm10076	13.63389112	1.031108073	0.001558424	ENSMUSG00000043388	Tmem130	0.549339693	1.237379858	7.30306E-10
ENSMUSG000000027525	Phactr3	1.860275201	1.10286661	0.002153135	ENSMUSG00000096768	Gm47283	0.237773897	1.676131671	7.76362E-10
ENSMUSG000000069806	Cacng7	0.097524257	-1.52884528	0.002306344	ENSMUSG00000097767	Miat	0.214347897	1.716302109	2.21724E-09
ENSMUSG000000090247	Bloc1s1	0.73630814	1.193277966	0.002306344	ENSMUSG00000025889	Snca	0.645386292	1.150704933	2.42518E-09
ENSMUSG000000017697	Ada	0.085333725	2.512346407	0.003541877	ENSMUSG00000019986	Ahi1	0.267056397	1.546517114	2.79605E-09
ENSMUSG000000034579	Pla2g3	0.09508615	2.342421406	0.004912788	ENSMUSG00000070802	Pnmal2	0.624302892	1.155825288	2.8281E-09
ENSMUSG000000017144	Rnd3	0.046324022	-1.727967922	0.008696063	ENSMUSG00000018451	6330403K07Rik	0.73323379	1.106550163	3.04479E-09
ENSMUSG000000034209	Rasl10a	0.285258451	1.294327117	0.025654769	ENSMUSG00000064345	mt-Nd2	11.10275255	-0.845180263	4.6604E-09
ENSMUSG000000049649	Gpr3	0.009752426	-2.505575501	0.035049565	ENSMUSG00000034892	Rps29	2.520637567	-1.28157E-08	1.42815E-08
ENSMUSG000000021453	Gadd45g	0.70217465	1.033531311	0.041140168	ENSMUSG00000032060	Cryab	0.427524494	-1.007453379	2.03324E-08
ENSMUSG000000038393	Txnip	0.180419875	1.526845977	0.041300337	ENSMUSG00000021708	Rasgrf2	0.156954198	1.86901782	3.7689E-08
ENSMUSG000000025509	Pnpla2	0.597336074	1.06576739	0.042431145	ENSMUSG00000064367	mt-Nd5	1.54260208	-0.85387332	3.89594E-08
ENSMUSG00000002289	Angptl4	0.078019406	2.06488743	0.048701561	ENSMUSG00000064357	mt-Atp6	26.13404526	-0.794789346	4.33592E-08
					ENSMUSG00000024736	Tmem132a	0.432209694	1.188068713	5.31248E-08
					ENSMUSG000000050071	Bex1	0.814053489	0.998769068	6.37808E-08
					ENSMUSG00000040147	Maob	0.370130795	1.202420868	2.03419E-07
					ENSMUSG00000064356	mt-Atp8	0.245972997	-1.064356288	1.21174E-07
					ENSMUSG00000027562	Car2	0.343190896	-0.988870875	2.39957E-07
					ENSMUSG00000031425	Plp1	2.620198066	-0.820861804	3.1335E-07
					ENSMUSG00000031980	Agt	1.168957385	0.888047874	4.14404E-07
					ENSMUSG000000034111	Rab3b	0.105416999	2.09646347	6.14815E-07
					ENSMUSG00000036699	Zcchc12	0.544654493	1.01428196	9.06008E-07
					ENSMUSG00000092274	Neat1	0.200292297	1.534940643	9.32843E-07
					ENSMUSG00000006373	Pgrmc1	1.082281186	0.872922275	1.06084E-06
					ENSMUSG00000064351	mt-Co1	44.83502081	-0.71811359	1.64958E-06
					ENSMUSG00000021913	Ogdhl	0.199120997	1.669486357	2.06109E-06
					ENSMUSG00000033585	Ndn	0.672326191	1.085151251	3.22015E-06
					ENSMUSG00000039307	Hexdc	0.098389199	1.998059765	3.52957E-06
					ENSMUSG00000015806	Qdpr	0.688724391	-0.849976207	4.52919E-06
					ENSMUSG00000058897	Col25a1	0.447436594	1.086880047	4.67562E-06
					ENSMUSG00000064358	mt-Co3	40.61951217	-0.686198519	6.02465E-06
					ENSMUSG00000025266	Gnl3l	0.477890394	0.973394565	8.57961E-06
					ENSMUSG00000016346	Kcnq2	0.664127091	0.904194421	9.37813E-06
					ENSMUSG00000038112	AW551984	0.052708499	3.038230204	9.37813E-06
					ENSMUSG00000039801	Cplane1	0.094875299	1.946220834	9.60386E-06
					ENSMUSG00000034796	Cpne7	0.632501992	0.899272839	9.90571E-06
					ENSMUSG00000032936	Camkv	0.78242839	0.856136529	1.04445E-05
					ENSMUSG00000008682	Rpl10	0.77891449	-0.771289302	1.11127E-05
					ENSMUSG00000090733	Rps27	1.020202287	-0.747262758	1.1198E-05
					ENSMUSG00000066357	Wdr6	0.692238291	0.866140618	1.38095E-05
					ENSMUSG00000022212	Cpne6	0.274084196	1.143257681	1.38095E-05
					ENSMUSG0000002625	Akap8l	0.316250996	1.19082493	1.42662E-05
					ENSMUSG00000041120	Nbl1	0.258857297	1.155278778	1.80112E-05
					ENSMUSG00000039218	Srrm2	0.340848296	1.072224591	1.80112E-05
					ENSMUSG00000023861	Mpc1	0.679353991	-0.770542949	1.88426E-05
					ENSMUSG00000019874	Fabp7	0.0363103	-1.639137088	2.03395E-05
					ENSMUSG00000024261	Syt4	0.74260419	0.838870094	2.0441E-05
					ENSMUSG00000023942	Slc29a1	0.373644695	0.998653101	2.3433E-05
					ENSMUSG00000049281	Scn3b	0.256514697	1.142222625	2.48193E-05
					ENSMUSG000000117465	Gm49980	0.101903099	1.772466005	2.64917E-05

ENSMUSG00000046314	Stxbp6	0.377158595	0.992077607	2.80804E-05
ENSMUSG00000026575	Nme7	0.446265294	1.391657358	3.89423E-05
ENSMUSG00000047507	Baiap3	0.060907599	2.394591796	3.99738E-05
ENSMUSG00000046447	Camk2n1	4.494278041	0.683390878	4.1795E-05
ENSMUSG00000064373	Selenop	0.569251793	-0.765056249	4.54373E-05
ENSMUSG00000031508	Ankrd10	0.117129998	1.58791723	4.62877E-05
ENSMUSG00000025579	Gaa	0.979206787	0.767603026	4.79556E-05
ENSMUSG00000063511	Snrnp70	0.236602597	1.144380255	4.88443E-05
ENSMUSG00000018909	Arrb1	0.298681496	1.042180476	4.88443E-05
ENSMUSG00000020230	Prmt2	0.354903895	0.975999399	5.49229E-05
ENSMUSG00000018339	Gpx3	0.115958698	1.622471537	5.49229E-05
ENSMUSG00000021273	Fdft1	0.421667994	0.923060433	5.70073E-05
ENSMUSG00000064341	mt-Nd1	14.32499881	-0.630652636	5.70073E-05
ENSMUSG00000060126	Tpt1	2.30628967	-0.659254627	7.11475E-05
ENSMUSG00000025555	Farp1	0.220204397	1.150911254	8.06518E-05
ENSMUSG00000021957	Tkt	0.231917397	1.151292868	0.000103477
ENSMUSG00000034486	Gbx2	0.368959495	1.270012371	0.000103479
ENSMUSG00000046844	Vat1l	0.105416999	1.589503481	0.000113091
ENSMUSG00000004187	Kifc2	0.658270591	0.813716118	0.000113091
ENSMUSG00000002012	Pnck	0.267056397	1.031943941	0.00014077
ENSMUSG00000062328	Rpl17	1.882279075	-0.640346287	0.00019829
ENSMUSG00000053963	Stum	0.79882659	0.801126999	0.000222503
ENSMUSG00000052296	Ppp6r1	0.171009798	1.203378673	0.000247709
ENSMUSG00000034220	Gpc1	0.315079696	1.018594176	0.000252851
ENSMUSG00000064179	Tnnt1	0.409954995	-0.752470556	0.000252851
ENSMUSG00000030729	Pgm2l1	0.666469691	0.767412778	0.000252851
ENSMUSG00000043384	Gprasp1	1.56368548	0.663794581	0.000280937
ENSMUSG00000042750	Bex2	3.422538555	0.628731268	0.000280937
ENSMUSG00000019230	Lhx9	0.154611598	1.248022588	0.000290952
ENSMUSG00000028004	Npy2r	0.042166799	2.724121613	0.000290952
ENSMUSG00000037072	Selenof	0.325621396	-0.784116183	0.00029739
ENSMUSG00000040690	Col16a1	0.071449299	1.883902058	0.000299048
ENSMUSG00000028137	Celf3	0.161639398	1.227616961	0.000302078
ENSMUSG000000115783	Bc1	0.428695794	0.840532757	0.000346925
ENSMUSG00000031654	Cbln1	0.114787399	1.421558843	0.000358756
ENSMUSG00000021130	Galnt16	0.327963996	0.915740227	0.000395572
ENSMUSG00000024423	Impact	0.873789789	0.709135434	0.000395572
ENSMUSG00000004207	Psap	4.918288636	0.596063935	0.000397538
ENSMUSG00000029516	Cit	0.857391589	0.706807304	0.000456177
ENSMUSG00000024603	Dctn4	0.298681496	0.953953293	0.000468868
ENSMUSG00000069919	Hba-a1	0.277598096	-1.560907527	0.000561286
ENSMUSG00000021508	Cxcl14	0.222546997	-0.833902343	0.000564941
ENSMUSG00000075486	Commd6	0.094875299	-1.063239495	0.000564941
ENSMUSG00000016194	Hsd11b1	0.046851999	-1.345010464	0.000592005
ENSMUSG00000050708	Ftl1	0.917127888	-0.637482052	0.000597196
ENSMUSG00000027495	Fam210b	0.180380198	1.112720748	0.000601273
ENSMUSG00000026688	Mgst3	0.607904692	-0.672417305	0.000624267
ENSMUSG00000032621	Srek1	0.142898598	1.224521996	0.000656116
ENSMUSG00000026163	Sphkap	0.253000797	0.968790955	0.000696576
ENSMUSG00000029723	Tsc22d4	0.415811495	-0.790958035	0.000728408
ENSMUSG00000062296	Trank1	0.089018799	1.579820927	0.000728408
ENSMUSG00000022982	Sod1	1.029572687	0.717089248	0.00074965
ENSMUSG00000053286	Trmt1l	0.078477099	1.676131671	0.000789863
ENSMUSG00000000088	Cox5a	1.481694481	-0.598808954	0.000792926
ENSMUSG00000035847	Ids	0.453293094	0.792652995	0.000792926
ENSMUSG00000072966	Gprasp2	0.472033894	0.780562308	0.000804991
ENSMUSG00000002957	Ap2a2	1.129133185	1.019662444	0.000820628
ENSMUSG00000028677	Rnf220	0.858562889	0.680275563	0.000827339
ENSMUSG00000023147	Wrb	0.363102995	0.841242708	0.000832218
ENSMUSG00000070304	Scn2b	0.76485889	0.693888141	0.000854797
ENSMUSG00000030541	Idh2	0.204977497	1.029241421	0.000857719
ENSMUSG00000017677	Wsb1	0.131185598	1.264457882	0.000874152
ENSMUSG00000058756	Thra	0.913613988	0.670988021	0.000893538

ENSMUSG00000030711	Sult1a1	0.127671698	1.260404052	0.000908713
ENSMUSG00000026568	Mpc2	0.672326191	-0.657763609	0.000910025
ENSMUSG00000039735	Fnbp1l	0.110102199	1.362057832	0.000910025
ENSMUSG00000020297	Nsg2	1.645676479	0.61625758	0.000910025
ENSMUSG00000037266	Rsrp1	0.678182691	0.708166403	0.000920267
ENSMUSG00000007783	Cpt1c	0.354903895	0.836596343	0.000920267
ENSMUSG00000020483	Dynll2	1.827227976	0.602508021	0.000940508
ENSMUSG00000005973	Rcn1	0.096046599	1.456748272	0.000951093
ENSMUSG00000032788	Pdxk	0.349047395	0.841429496	0.000955255
ENSMUSG00000022048	Dpysl2	1.779204677	0.60717033	0.000980385
ENSMUSG00000020894	Vamp2	3.593548353	0.573091927	0.001005855
ENSMUSG00000051853	Arf3	1.224008484	0.633643802	0.001039209
ENSMUSG00000046500	Tafa4	0.0327964	-1.455169782	0.001047196
ENSMUSG00000023473	Celsr3	0.081990999	1.594026039	0.001047196
ENSMUSG00000024897	Apba1	0.215519197	0.992938372	0.001047196
ENSMUSG00000041773	Enc1	0.570423093	0.728414691	0.001075044
ENSMUSG00000032314	Etfa	0.052708499	-1.239754543	0.001120091
ENSMUSG00000021700	Rab3c	0.667640991	0.699322529	0.001120091
ENSMUSG00000049517	Rps23	1.339967182	-0.59846153	0.001152714
ENSMUSG00000023484	Prph	0.078477099	1.602131089	0.001250333
ENSMUSG00000039706	Ldb2	0.092532699	1.458084719	0.001278831
ENSMUSG00000030062	Rpn1	0.435723594	0.772297849	0.001319982
ENSMUSG00000019124	Scrn1	0.439237494	0.981794258	0.001330157
ENSMUSG00000027895	Kcnc4	0.101903099	1.389137366	0.001347162
ENSMUSG00000058672	Tubb2a	2.111853872	0.595588243	0.001348125
ENSMUSG00000046287	Pnma3	0.065592799	1.762595761	0.001349825
ENSMUSG00000029405	G3bp2	0.860905489	0.656254725	0.001372823
ENSMUSG00000052305	Hbb-bs	0.907757488	-1.386061646	0.001372823
ENSMUSG00000047842	Diras2	0.541140593	0.725680441	0.001372823
ENSMUSG00000007872	Id3	0.173352398	-0.8390529	0.001381172
ENSMUSG00000044986	Tst	0.094875299	-1.005523997	0.001411509
ENSMUSG00000067274	Rplp0	0.687553091	-0.620156176	0.001682484
ENSMUSG00000048756	Foxo3	0.160468098	1.087139804	0.001682484
ENSMUSG00000016918	Sulf1	0.039824199	2.380916859	0.001701476
ENSMUSG00000025905	Oprk1	0.0257686	3.360158299	0.001723681
ENSMUSG00000031239	Itm2a	0.108930899	-0.95754296	0.001755609
ENSMUSG00000029878	Dbpht2	0.330306596	0.821383249	0.001781471
ENSMUSG00000002910	Arrdc2	0.086676199	1.480452533	0.001852495
ENSMUSG00000047215	Rpl9	2.169247572	-0.555684005	0.001856537
ENSMUSG00000015222	Map2	0.73206249	0.663090816	0.001979855
ENSMUSG000000112117	Rmst	0.043338099	2.277168934	0.002036851
ENSMUSG00000063229	Ldha	0.633673292	0.689926694	0.002061324
ENSMUSG00000022132	Cldn10	0.192093197	-0.797081443	0.002082363
ENSMUSG00000053550	Shisa7	0.098389199	1.339096683	0.002128031
ENSMUSG00000041141	Pnmal1	0.446265294	0.741599829	0.002128031
ENSMUSG00000022577	Ly6h	1.035429186	0.617701366	0.002170425
ENSMUSG00000024985	Tcf7l2	1.875251276	0.608810663	0.00218457
ENSMUSG00000026185	Igfbp5	0.331477896	0.806434372	0.00219798
ENSMUSG00000006369	Fbln1	0.105416999	1.299996864	0.00219798
ENSMUSG00000030499	Kctd15	0.071449299	1.620867652	0.002399594
ENSMUSG00000030231	Plekha5	0.134699498	1.139988486	0.00244209
ENSMUSG00000032580	Rbm5	0.277598096	0.873433111	0.00244209
ENSMUSG00000058740	Kcnt1	0.161639398	1.04864682	0.002456796
ENSMUSG00000061689	Dlgap4	0.881988888	0.626832731	0.002520846
ENSMUSG00000030726	Poid3	0.060907599	1.757161875	0.002525802
ENSMUSG00000060301	2610008E11Rik	0.055051099	1.836596343	0.002525802
ENSMUSG00000024186	Rgs11	0.058564999	1.808581967	0.002570124
ENSMUSG00000020886	Dlg4	0.638358492	0.667258638	0.002696619
ENSMUSG00000029869	Ephb6	0.094875299	1.336167352	0.002854479
ENSMUSG00000025575	Cant1	0.156954198	1.055430945	0.002854479
ENSMUSG00000075590	Nrbp2	0.425181894	0.836596343	0.002983152
ENSMUSG00000041697	Cox6a1	2.154020672	-0.532232727	0.003006917
ENSMUSG00000022836	Mylk	0.083162299	1.421558843	0.003006917

ENSMUSG00000022974	Paxbp1	0.083162299	1.421558843	0.003006917
ENSMUSG00000083282	Ctsf	0.296338896	0.814053774	0.003188529
ENSMUSG00000052105	Mtdc1	0.099560499	1.308664787	0.003241347
ENSMUSG00000031066	Usp11	0.180380198	0.983437731	0.003411547
ENSMUSG00000033208	S100b	0.435723594	-0.675654272	0.003446905
ENSMUSG00000021314	Amph	0.498973793	0.692045553	0.003562599
ENSMUSG00000024566	Atp9b	0.115958698	1.195050314	0.003568618
ENSMUSG00000073755	5730409E04Rik	0.270570296	0.836596343	0.003644247
ENSMUSG00000017466	Timp2	0.979206787	0.669163209	0.003761335
ENSMUSG00000003778	Brd8	0.119472598	1.165544865	0.00377789
ENSMUSG00000027221	Chst1	0.579793492	0.661509636	0.00389604
ENSMUSG00000001525	Tubb5	2.685790865	0.556266476	0.0039125
ENSMUSG00000024270	Slc39a6	0.122986498	1.138252043	0.004000849
ENSMUSG00000056222	Spock1	1.009660587	0.598291246	0.004036719
ENSMUSG00000042524	Sun2	0.113616099	1.241852821	0.004136352
ENSMUSG00000012848	Rps5	1.001461487	-0.581808008	0.00421804
ENSMUSG00000024767	Otub1	0.74494679	0.639993251	0.004260771
ENSMUSG00000033735	Spr	0.183894098	0.950552532	0.004391216
ENSMUSG00000024516	Sec11c	0.427524494	-0.630697394	0.004443768
ENSMUSG00000032532	Cck	2.517123667	-0.517449002	0.00445929
ENSMUSG00000058420	Syt17	0.165153298	1.342487272	0.004591707
ENSMUSG00000008668	Rps18	0.702779991	-0.579640903	0.004595777
ENSMUSG00000018707	Dync1h1	1.065882986	0.59108799	0.004837147
ENSMUSG00000022415	Syngn1	0.715664291	0.622308971	0.004886982
ENSMUSG00000026822	Lcn2	0.0187408	3.924051984	0.004945197
ENSMUSG00000029068	Ccnl2	0.181551498	1.055909371	0.004956936
ENSMUSG00000022018	Rgcc	0.048023299	-1.180477171	0.004958967
ENSMUSG00000069917	Hba-a2	0.229574797	-1.399323833	0.004987139
ENSMUSG00000061028	Clasrp	0.096046599	1.257439464	0.005039893
ENSMUSG00000025151	Maged1	1.789746377	0.561659479	0.005218961
ENSMUSG00000004933	Matk	0.315079696	0.76366482	0.005516616
ENSMUSG00000040584	Abcb1a	0.0199121	-1.578441157	0.005653543
ENSMUSG00000032594	Ip6k1	0.364274295	0.729681139	0.005653543
ENSMUSG00000009216	Fam163b	0.076134499	1.421558843	0.005707147
ENSMUSG00000005045	Chd5	0.199120997	0.896896853	0.005708095
ENSMUSG00000001248	Gramd1a	0.373644695	0.72389621	0.005802396
ENSMUSG00000033434	Gtpbp6	0.141727298	1.039413226	0.005895536
ENSMUSG00000031442	Mcf2l	0.120643898	1.110771306	0.005917938
ENSMUSG00000003378	Grik5	0.366616895	0.721826156	0.006089711
ENSMUSG00000003469	Phyhip	0.160468098	1.014383462	0.006089711
ENSMUSG0000005912	Tmem150a	0.059736299	1.630145465	0.006119832
ENSMUSG00000031808	Slc27a1	0.238945197	0.829575915	0.006190681
ENSMUSG00000036427	Gpi1	1.769834277	0.534652622	0.006202377
ENSMUSG00000009079	Ewsr1	0.326792696	0.746710839	0.006202377
ENSMUSG00000061032	Rrp1	0.614932492	0.627587819	0.00625301
ENSMUSG00000034949	Zfr2	0.094875299	1.239952037	0.00625301
ENSMUSG00000021750	Fam107a	0.76485889	0.608542586	0.00625301
ENSMUSG00000073940	Hbb-bt	0.083162299	-1.452910274	0.00636549
ENSMUSG00000022715	Tmem114	0.0269399	2.836596343	0.006660958
ENSMUSG00000019831	Wasf1	0.356075195	0.722939561	0.006900518
ENSMUSG00000042804	Gpr153	0.400584595	0.696418685	0.007026243
ENSMUSG00000022621	Rabl2	0.080819699	1.380916859	0.007223338
ENSMUSG00000014602	Kif1a	1.619907879	0.531443961	0.007299015
ENSMUSG00000064329	Scn1a	0.0374816	-1.248292555	0.007299015
ENSMUSG00000078861	Zfp931	0.0245973	-1.458859541	0.007299015
ENSMUSG00000109336	Samd4b	0.045680699	-1.163403657	0.007299015
ENSMUSG00000004937	Sgta	0.589163892	0.629000923	0.007299015
ENSMUSG00000040867	Begain	0.255343397	0.80402848	0.007299015
ENSMUSG00000090101	Snhg9	0.063250199	1.711065461	0.007299015
ENSMUSG00000039579	Grin3a	0.155782898	0.971948196	0.007405342
ENSMUSG00000027405	Nop56	0.208491397	0.860980501	0.00744215
ENSMUSG00000074923	Pak6	0.035139	2.205830152	0.007497526
ENSMUSG000000040759	Cmtm5	0.138213398	-0.807744705	0.007497526



ENSMUSG00000023067	Cdkn1a	0.060907599	1.564516797	0.007625932
ENSMUSG00000054387	Mdm4	0.100731799	1.192076997	0.007635863
ENSMUSG00000013787	Ehmt2	0.385357695	0.695123917	0.00817316
ENSMUSG00000016541	Atxn10	1.125619285	0.551732572	0.00825078
ENSMUSG00000003352	Cacnb3	0.274084196	0.770598784	0.008301854
ENSMUSG00000032554	Trf	0.500145093	-0.596862353	0.008372109
ENSMUSG00000019302	Atp6v0a1	0.74846069	0.588668829	0.00841391
ENSMUSG00000090071	Cdk5r2	0.182722798	1.001934075	0.008505697
ENSMUSG00000021340	Gpld1	0.151097698	0.976321106	0.008676146
ENSMUSG00000034312	lqsec1	0.494288594	0.642246959	0.00879622
ENSMUSG00000024735	Prpf19	0.486089494	0.648292812	0.00879622
ENSMUSG00000024608	Rps14	2.210243071	-0.502951746	0.008915466
ENSMUSG00000092627	D130058E05Rik	0.089018799	1.245401888	0.008964427
ENSMUSG00000026117	Zap70	0.064421499	1.474026263	0.009109656
ENSMUSG00000006676	Usp19	0.174523698	0.915667914	0.009155646
ENSMUSG00000031775	Plip	0.174523698	-0.741939889	0.009178182
ENSMUSG00000055065	Ddx17	0.428695794	0.662745638	0.009461148
ENSMUSG00000036006	Ripor2	0.110102199	1.121049732	0.009774808
ENSMUSG00000015377	Dennd6b	0.138213398	1.003493651	0.009774808
ENSMUSG00000087651	1500009L16Rik	0.081990999	-0.932519775	0.009882989
ENSMUSG00000060314	Zfp941	0.071449299	1.39847523	0.009920993
ENSMUSG00000051022	Hs3st1	0.0363103	-1.229492848	0.010122716
ENSMUSG00000067786	Nnat	0.514200693	0.62927137	0.010206745
ENSMUSG00000029602	Rasa1	0.077305799	1.317723032	0.010213014
ENSMUSG00000024843	Chka	0.219033097	0.821329586	0.010213014
ENSMUSG00000022707	Gbe1	0.038652899	-1.205223833	0.010450115
ENSMUSG00000052373	Mpp3	0.057393699	1.573561937	0.010712543
ENSMUSG00000024581	Napg	0.521228493	0.626268987	0.010712543
ENSMUSG00000061436	Hipk2	0.0046852	-2.365037518	0.010767365
ENSMUSG00000043461	Sptssb	0.0292825	-1.320944934	0.011066906
ENSMUSG00000024101	Washc1	0.101903099	1.166744944	0.011100225
ENSMUSG00000026199	Ankzf1	0.055051099	1.614203921	0.011339626
ENSMUSG00000006476	Nsmf	2.752554964	0.493590624	0.011637432
ENSMUSG00000034156	Tspoap1	0.217861797	0.813635194	0.011666204
ENSMUSG00000022296	Baalc	0.242459097	-0.667535083	0.011666204
ENSMUSG00000031617	Tmem184c	0.057393699	-1.043109424	0.011671627
ENSMUSG00000032297	Cellf6	0.063250199	1.448031055	0.011879397
ENSMUSG00000036667	Tcaf1	0.412297595	0.656264526	0.011978869
ENSMUSG00000038886	Man2a2	0.288139796	0.729681139	0.011978869
ENSMUSG00000020882	Cacnb1	0.126500398	1.019818167	0.011978869
ENSMUSG00000028653	Trit1	0.046851999	1.734716729	0.012016708
ENSMUSG00000029817	Tra2a	0.167495898	0.897996887	0.012016708
ENSMUSG00000028081	Rps3a1	1.611708779	-0.492647136	0.012087149
ENSMUSG00000033161	Atp1a1	0.669983591	0.581135157	0.012176476
ENSMUSG00000028139	Rriad1	0.042166799	1.876124707	0.012323131
ENSMUSG00000022957	Its1n1	0.293996296	0.726413425	0.012352872
ENSMUSG00000037103	Dcaf15	0.070277999	1.375016258	0.012633398
ENSMUSG00000038332	Sesn1	0.183894098	0.854974872	0.012804536
ENSMUSG00000006435	Neurl1a	0.110102199	1.084523856	0.013132632
ENSMUSG00000039904	Gpr37	0.081990999	-0.908474301	0.013645031
ENSMUSG00000028034	Fubp1	0.185065398	0.84569855	0.013845276
ENSMUSG00000026525	Opn3	0.045680699	-1.108262103	0.013898279
ENSMUSG00000010097	Nxf1	0.127671698	1.158524438	0.014035775
ENSMUSG00000078517	Emc1	0.289311096	0.724703463	0.0140764
ENSMUSG00000054850	Smim10l2a	0.056222399	1.544415591	0.014143919
ENSMUSG00000015944	Castor2	0.206148797	0.812348797	0.01419254
ENSMUSG00000035596	Mboat7	0.285797196	0.717951846	0.014819883
ENSMUSG00000027533	Fabp5	0.814053489	-0.51649977	0.014870083
ENSMUSG00000030744	Rps3	1.361050582	-0.508222387	0.014974886
ENSMUSG00000027674	Pex5l	0.142898598	-0.760047963	0.014978645
ENSMUSG00000001120	Pcbp3	0.212005297	0.805232172	0.014978645
ENSMUSG00000078771	Evi2a	0.053879799	-1.068246424	0.014978645
ENSMUSG00000000805	Car4	0.065592799	-0.974369833	0.014978645

ENSMUSG00000032855	Pkd1	0.167495898	0.877238327	0.014978645
ENSMUSG00000050121	Opalin	0.103074399	-0.837417346	0.0152566
ENSMUSG00000079523	Tmsb10	4.692227739	0.467838798	0.015400386
ENSMUSG00000076439	Mog	0.285797196	-0.661393946	0.015514149
ENSMUSG00000027712	Anxa5	0.159296798	-0.730707491	0.01555272
ENSMUSG00000062981	Mrpl42	0.267056397	-0.632538899	0.01555272
ENSMUSG00000007476	Lrrc8a	0.188579298	0.836596343	0.015616304
ENSMUSG00000027248	Pdia3	0.353732595	0.67037939	0.015704259
ENSMUSG00000076609	Igkc	0.048023299	1.643951265	0.015704259
ENSMUSG00000020386	Sar1b	0.135870798	-0.760644488	0.015763895
ENSMUSG00000008206	Cers4	0.112444799	1.044191762	0.015916163
ENSMUSG00000031278	Acs14	0.323278796	0.683551968	0.015916163
ENSMUSG00000027067	Ssrp1	0.242459097	0.755676347	0.015924871
ENSMUSG00000028809	Srrm1	0.115958698	1.021020914	0.016137232
ENSMUSG00000016940	Kctd2	0.416982795	0.636896507	0.016137232
ENSMUSG00000070814	Zswim9	0.0292825	2.537036061	0.0162026
ENSMUSG00000068523	Gng5	0.230746097	-0.65298811	0.016320881
ENSMUSG00000040430	Pitpnc1	0.272912896	-0.628429292	0.016320881
ENSMUSG00000067288	Rps28	1.127961885	-0.501996732	0.016320881
ENSMUSG00000026830	Ernm	0.113616099	-0.806081656	0.016476835
ENSMUSG00000022054	Nefm	0.305709296	-0.629826543	0.016476835
ENSMUSG00000024019	Cmtr1	0.202634897	0.803806408	0.016869398
ENSMUSG00000029168	Dpysl5	0.106588299	1.07475608	0.016983481
ENSMUSG00000022103	Gfra2	0.038652899	1.924059184	0.017049353
ENSMUSG00000027439	Gzf1	0.072620599	1.29031431	0.017134085
ENSMUSG00000003429	Rps11	1.694871078	-0.488516511	0.017134085
ENSMUSG00000034936	Arl4d	0.072620599	1.29031431	0.017134085
ENSMUSG000000031778	Cx3cl1	1.029572687	0.519923973	0.017284541
ENSMUSG000000096210	H1fo	0.283454596	0.706126411	0.017406079
ENSMUSG00000049775	Tmsb4x	3.705993152	-0.451293252	0.017430562
ENSMUSG00000057176	Ccdc189	0.0269399	2.421558843	0.017759738
ENSMUSG00000021134	Srsf5	0.315079696	0.684593249	0.017772611
ENSMUSG00000025200	Cwf19l1	0.043338099	1.762595761	0.017772611
ENSMUSG00000016349	Eef1a2	2.053288873	0.485035054	0.017874469
ENSMUSG00000061524	Zic2	0.0023426	-2.748366158	0.017874469
ENSMUSG00000019878	Hsf2	0.055051099	1.514668248	0.017911939
ENSMUSG00000011884	Gltp	0.053879799	-1.018297742	0.018129773
ENSMUSG00000008036	Ap2s1	1.270860483	0.522661039	0.018247546
ENSMUSG00000030088	Aldh1l1	0.281111996	0.70509156	0.018295001
ENSMUSG00000026034	Clk1	0.188579298	0.818894341	0.018318802
ENSMUSG00000020176	Grb10	0.107759599	1.053827059	0.018433598
ENSMUSG00000021194	Chga	0.633673292	0.71417424	0.018536699
ENSMUSG00000015396	Cd83	0.185065398	0.827551203	0.018564073
ENSMUSG00000034799	Unc13a	0.234259997	0.746181048	0.018627172
ENSMUSG00000059070	Rpl18	1.038943086	-0.494401261	0.01894278
ENSMUSG00000026895	Ndufa8	0.550510993	-0.531747921	0.019034361
ENSMUSG00000026765	Lypd6b	0.052708499	1.552803377	0.019034361
ENSMUSG00000046330	Rpl37a	1.834255776	-0.466986272	0.019178228
ENSMUSG00000036636	Clcn7	0.090190099	1.121998562	0.019706169
ENSMUSG00000030102	Itpr1	0.528256293	0.585312943	0.019878139
ENSMUSG00000022194	Pabpn1	0.045680699	-1.070294253	0.020087315
ENSMUSG00000032332	Col12a1	0.046851999	1.609185847	0.020508823
ENSMUSG00000059439	Bcas3	0.127671698	1.003246212	0.020604004
ENSMUSG00000024271	Elp2	0.201463597	0.795491139	0.020604004
ENSMUSG00000023328	Ache	0.316250996	0.670817871	0.020761419
ENSMUSG00000041629	Fam104a	0.119472598	-0.771523879	0.020850819
ENSMUSG00000071659	Hnrrnpul2	0.343190896	0.652564395	0.020850819
ENSMUSG00000000538	Tom1l2	0.489603394	0.593206466	0.020912192
ENSMUSG00000053411	Cbx7	0.098389199	1.076062277	0.020939679
ENSMUSG00000006333	Rps9	1.267346583	-0.473829719	0.021503479
ENSMUSG00000063882	Uqcrh	1.731181377	-0.459545807	0.021655128
ENSMUSG00000032579	Hemk1	0.065592799	1.347558262	0.021700725
ENSMUSG00000039623	Ap5z1	0.056222399	1.451306187	0.02177641

ENSMUSG00000027858	Tspan2	0.229574797	-0.634108979	0.021786227
ENSMUSG00000074457	S100a16	0.213176597	-0.647703819	0.021941515
ENSMUSG00000047844	Bex4	0.188579298	0.801406914	0.021941515
ENSMUSG00000048218	Amigo2	0.110102199	1.014134528	0.022238182
ENSMUSG00000039087	Rreb1	0.081990999	1.17898854	0.022308139
ENSMUSG00000048814	Lonrf2	0.387700295	0.626673273	0.022506783
ENSMUSG00000000296	Tpd52l1	0.112444799	-0.782659336	0.022506783
ENSMUSG00000031343	Gabra3	0.227232197	0.743486938	0.022506783
ENSMUSG00000027188	Pamr1	0.125329098	0.947627655	0.022750676
ENSMUSG00000032766	Gng11	0.130014298	-0.933477563	0.022750676
ENSMUSG00000039108	Lsm14b	0.145241198	0.895490032	0.022771949
ENSMUSG00000032238	Rora	0.674668791	-0.508645537	0.022771949
ENSMUSG00000015476	Prrt1	0.374815995	0.631644369	0.022771949
ENSMUSG00000096188	Cmtm4	0.189750598	0.793007074	0.022985233
ENSMUSG00000020022	Ndufa12	1.055341286	-0.478276995	0.02319016
ENSMUSG00000040952	Rps19	1.51097698	-0.463941422	0.02349639
ENSMUSG00000033278	Ptprm	0.224889597	0.756628038	0.02349639
ENSMUSG00000040479	Dgkz	0.317422296	0.657272643	0.023974067
ENSMUSG00000056413	Adap1	0.577450892	0.5609619	0.023974067
ENSMUSG00000020634	Ubxn2a	0.0222547	-1.365037518	0.023974844
ENSMUSG00000041351	Rap1gap	0.887845388	0.555929478	0.024908359
ENSMUSG00000045608	Dbx2	0.038652899	-1.120334935	0.024908359
ENSMUSG00000030002	Dusp11	0.066764099	1.302259915	0.025075414
ENSMUSG00000030400	Ercc2	0.066764099	1.302259915	0.025075414
ENSMUSG00000005338	Cadm3	0.457978294	0.587120042	0.025472551
ENSMUSG00000022354	Ndufb9	1.755778677	-0.452647942	0.025472551
ENSMUSG00000004626	Stxbp2	0.048023299	1.528474047	0.025623784
ENSMUSG00000024098	Twsg1	0.048023299	1.528474047	0.025623784
ENSMUSG00000084883	Ccdc85c	0.086676199	1.258060111	0.0258226
ENSMUSG00000022425	Enpp2	0.482575594	0.578227083	0.025917114
ENSMUSG00000031837	Necab2	0.664127091	0.539260236	0.026008444
ENSMUSG00000022973	Synj1	0.880817588	0.510459348	0.026008444
ENSMUSG00000039630	Hnrnpu	0.611418592	0.545335384	0.026245225
ENSMUSG00000024067	Dpy30	0.072620599	-0.886563452	0.026357437
ENSMUSG00000029060	Mib2	0.144069898	0.883902058	0.026367051
ENSMUSG00000022763	Aifm3	0.267056397	0.687115444	0.026367051
ENSMUSG00000039782	Cpeb2	0.120643898	0.95207356	0.026689866
ENSMUSG00000048154	Kmt2d	0.045680699	1.573561937	0.026689866
ENSMUSG00000041607	Mbp	5.103354033	-0.433428225	0.026770757
ENSMUSG00000035754	Wdr18	0.241287797	0.709904338	0.026887239
ENSMUSG00000022890	Atp5j	1.467638881	-0.456044525	0.026887239
ENSMUSG00000005986	Ankrd13d	0.206148797	0.749613041	0.026887239
ENSMUSG00000056812	St8sia3	0.260028597	0.694981737	0.027489328
ENSMUSG00000011877	Git1	0.520057193	0.562795506	0.027784106
ENSMUSG00000029578	Wipi2	0.224889597	0.728613662	0.027800876
ENSMUSG00000021186	Fbin5	0.084333599	1.119530306	0.027964132
ENSMUSG00000017639	Rab11fip4	0.384186395	0.606083079	0.028554228
ENSMUSG00000038685	Rtel1	0.0281112	2.480452533	0.028750645
ENSMUSG00000004961	Syt5	0.216690497	0.731898964	0.028750645
ENSMUSG00000046688	Tifa	0.0163982	-1.504440575	0.028888144
ENSMUSG00000022489	Pde1b	0.604390792	0.542277783	0.028888144
ENSMUSG00000071054	Safb	0.213176597	0.737586337	0.029356678
ENSMUSG00000031153	Gripap1	0.146412498	0.859679956	0.030274662
ENSMUSG00000012405	Rpl15	1.205267684	-0.462175844	0.030328783
ENSMUSG00000020658	Efr3b	0.373644695	0.611629978	0.030436638
ENSMUSG00000021573	Tppp	0.401755895	0.611809406	0.030489655
ENSMUSG00000003808	Farsa	0.107759599	0.983437731	0.031471021
ENSMUSG00000021288	Klc1	1.801459376	0.477467585	0.031471021
ENSMUSG00000041354	Rgl2	0.122986498	0.920660608	0.031471021
ENSMUSG00000032244	Fem1b	0.296338896	0.655356028	0.031552065
ENSMUSG00000055862	Izumo4	0.085504899	1.091853398	0.031552065
ENSMUSG00000049422	Chchd10	1.652704278	-0.440503328	0.032035284
ENSMUSG00000031285	Dcx	0.0210834	2.499561355	0.032035284

ENSMUSG00000022044	Stmn4	1.834255776	0.515220758	0.032169119
ENSMUSG00000035545	Leng8	0.089018799	1.058988764	0.032353263
ENSMUSG00000027624	Epb4111	0.144069898	0.860055316	0.032859464
ENSMUSG00000039661	Dusp26	0.349047395	0.617654521	0.033045893
ENSMUSG00000029064	Gnb1	1.964270074	0.452408189	0.033349556
ENSMUSG00000108348	Gm42372	0.199120997	0.746654217	0.033350213
ENSMUSG00000006576	Slc4a3	0.265885097	0.669486357	0.033377537
ENSMUSG0000001666	Ddt	0.255343397	-0.593187742	0.033377537
ENSMUSG00000038141	Tmem181a	0.046851999	1.493708629	0.033601925
ENSMUSG00000050069	Grem2	0.062078899	1.26955575	0.033692887
ENSMUSG00000045294	Insig1	0.221375697	0.748240468	0.03385957
ENSMUSG0000007207	Stx1a	0.226060897	0.70858873	0.03385957
ENSMUSG00000020044	Timp3	0.479061694	0.561880132	0.03385957
ENSMUSG00000037541	Shank2	0.120643898	0.922326217	0.03394193
ENSMUSG00000042066	Tmcc2	0.267056397	0.664572875	0.034447816
ENSMUSG00000065947	mt-Nd4l	0.474376494	-0.514876028	0.034447816
ENSMUSG00000021136	Smoc1	0.072620599	1.170020076	0.034599681
ENSMUSG00000116165	Pdpx	0.922984388	0.500475901	0.034599681
ENSMUSG00000026175	Vil1	0.0175695	2.836596343	0.035078617
ENSMUSG00000028161	Ppp3ca	0.826937789	-0.469326722	0.035078617
ENSMUSG00000048905	4930539E08Rik	0.0175695	2.836596343	0.035078617
ENSMUSG00000034579	Pla2g3	0.0210834	2.499561355	0.035403526
ENSMUSG00000022111	Uchl3	0.066764099	-0.890385163	0.035403526
ENSMUSG00000053907	Mat2a	0.359589095	0.627649452	0.035491083
ENSMUSG00000004113	Cacna1b	0.133528198	0.874731472	0.035540635
ENSMUSG00000001227	Sema6b	0.365445595	0.831994441	0.035540635
ENSMUSG00000042699	Dhx9	0.128842998	0.876124707	0.035697388
ENSMUSG00000030852	Tacc2	0.179208898	0.763532881	0.035878191
ENSMUSG00000028691	Prdx1	0.570423093	-0.49945286	0.035943914
ENSMUSG00000097451	Rian	0.461492194	0.687518126	0.03629676
ENSMUSG00000027438	Napb	0.815224789	0.496976343	0.036331708
ENSMUSG00000006517	Mvd	0.110102199	0.947020332	0.036625924
ENSMUSG00000038762	Abcf1	0.344362196	0.606539259	0.036652207
ENSMUSG00000039953	Clstn1	2.487841168	0.436572835	0.037233347
ENSMUSG00000036966	Spry3	0.284625896	0.648392608	0.037308855
ENSMUSG00000037400	Atp11b	0.070277999	1.18237118	0.037462153
ENSMUSG00000043670	Diras1	0.251829497	0.797067979	0.037462153
ENSMUSG00000001082	Mfsd10	0.069106699	1.28405532	0.037483641
ENSMUSG00000100252	Mir124-2hg	0.189750598	0.742381001	0.038237704
ENSMUSG00000018012	Rac3	0.221375697	0.706012233	0.038237704
ENSMUSG00000047181	Samd14	0.176866298	0.762595761	0.038514656
ENSMUSG00000079018	Ly6c1	0.270570296	-0.572209203	0.038627203
ENSMUSG00000057894	Zfp329	0.057393699	1.310527531	0.038874046
ENSMUSG00000078515	Ddi2	0.073791899	1.136156625	0.038911007
ENSMUSG00000022515	Anks3	0.073791899	1.136156625	0.038911007
ENSMUSG00000030647	Ndufc2	0.689895691	-0.476501901	0.039082226
ENSMUSG00000034751	Mast4	0.160468098	0.79537368	0.039082226
ENSMUSG00000024130	Abca3	0.319764896	0.62174547	0.039082226
ENSMUSG00000027977	Ndst3	0.0269399	2.099630749	0.039144179
ENSMUSG00000033295	Ptprf	0.099560499	0.977458879	0.039342276
ENSMUSG00000017167	Cntnap1	0.213176597	0.708439991	0.039342276
ENSMUSG00000025085	Ablim1	0.222546997	0.699779653	0.039462954
ENSMUSG00000033615	Cplx1	1.459439781	-0.435663962	0.039673012
ENSMUSG00000034472	Rasd2	0.169838498	0.778493388	0.039885344
ENSMUSG00000060261	Gtf2i	0.709807791	0.504720221	0.039945098
ENSMUSG00000029152	Ociad1	1.038943086	0.471140872	0.040233431
ENSMUSG00000062683	Atp5g2	0.469691294	-0.537491528	0.040430594
ENSMUSG00000044080	S100a1	0.466177394	-0.506152296	0.040533359
ENSMUSG00000033068	Entpd6	0.161639398	0.785612414	0.041208704
ENSMUSG00000038615	Nfe2l1	0.477890394	0.546769091	0.041764013
ENSMUSG00000086968	4933431E20Rik	0.171009798	0.769482147	0.042195998
ENSMUSG00000085438	Oip5os1	0.603219492	0.51690672	0.042317946
ENSMUSG00000061702	Tmem91	0.179208898	0.745830879	0.042400963

ENSMUSG00000030846	Tial1	0.213176597	0.708439991	0.042425798
ENSMUSG00000019188	H13	0.188579298	0.73350285	0.04255296
ENSMUSG00000003526	Prodh	0.112444799	0.912947229	0.04255296
ENSMUSG000000031393	Mecp2	0.153440298	0.793527621	0.04255296
ENSMUSG00000037095	Lrg1	0.0163982	3.743486938	0.042736583
ENSMUSG00000050821	Fam131a	0.097217899	0.980986252	0.042776365
ENSMUSG00000038602	Slc35f1	0.100731799	0.957611744	0.04280376
ENSMUSG00000053819	Camk2d	0.440408794	0.555813268	0.042821178
ENSMUSG00000032850	Rnft2	0.190921898	0.734716729	0.042848891
ENSMUSG00000031781	Ciapin1	0.174523698	0.875590474	0.042861879
ENSMUSG00000034403	Pja1	0.407612395	0.597179042	0.043067723
ENSMUSG00000037224	Zfyve28	0.074963199	1.104076654	0.043329168
ENSMUSG00000030811	Fbxl19	0.085504899	1.046049708	0.043337848
ENSMUSG00000093930	Hmgcs1	0.620788992	0.522842179	0.043373773
ENSMUSG00000025375	Aatk	0.541140593	0.526557799	0.04351797
ENSMUSG00000050875	Minar2	0.130014298	0.862591551	0.044059922
ENSMUSG00000062248	Cks2	0.0140556	-1.507358058	0.044824946
ENSMUSG00000059213	Ddn	0.168667198	0.768577919	0.045047663
ENSMUSG00000031546	Gins4	0.023426	-1.262939331	0.045376398
ENSMUSG00000044783	Hjurp	0.086676199	1.021020914	0.04578739
ENSMUSG00000026554	Dcaf8	0.284625896	0.648392608	0.04578739
ENSMUSG00000028582	Cc2d1b	0.069106699	1.158524438	0.04578739
ENSMUSG00000051515	Fam181b	0.046851999	-0.975776654	0.04578739
ENSMUSG00000035762	Tmem161b	0.0199121	2.421558843	0.04578739
ENSMUSG00000017713	Tha1	0.0304538	2.006521344	0.046259935
ENSMUSG00000028656	Cap1	0.063250199	-0.889838584	0.046277221
ENSMUSG00000024940	Ltbp3	0.099560499	1.092936096	0.046277221
ENSMUSG00000024953	Prdx5	0.833965589	-0.46364746	0.047069917
ENSMUSG00000027447	Cst3	8.093682894	-0.396344205	0.047147292
ENSMUSG00000022843	Clcn2	0.048023299	1.421558843	0.047147292
ENSMUSG00000041380	Htr2c	0.178037598	0.736432181	0.047163899
ENSMUSG00000013076	Amotl1	0.525913693	0.536635368	0.047289062
ENSMUSG00000032178	Ilf3	0.187407998	0.724569725	0.047289062
ENSMUSG00000031622	Sin3b	0.265885097	0.636063355	0.047364452
ENSMUSG00000028876	Epha10	0.062078899	1.199166422	0.047434679
ENSMUSG00000027332	Ivd	0.165153298	0.757524772	0.047454283
ENSMUSG00000022353	Mtss1	0.165153298	0.757524772	0.047454283
ENSMUSG00000033287	Kctd17	1.226351084	0.47555665	0.047454283
ENSMUSG00000049630	C1ql3	0.040995499	1.547089726	0.047790869
ENSMUSG00000050022	Amz1	0.040995499	1.547089726	0.047790869
ENSMUSG00000024136	Dnase1l2	0.0128843	3.421558843	0.048028948
ENSMUSG00000073678	Pgap1	0.115958698	0.895490032	0.049554377
ENSMUSG00000021669	Col4a3bp	0.132356898	0.836596343	0.049837251
ENSMUSG00000039686	Zer1	0.343190896	0.60164046	0.049985936
ENSMUSG00000020189	Ospb18	0.221375697	0.678531497	0.049985936

Table S2M. DEGs at ZT4 in female and male hypothalamus (LH + DMVH). The average number of counts per spot in the RHY condition, the log2 fold change in gene expression (RHY relative to saline), and the adjusted p-value (FDR) are shown.

ZT4 FEMALES - Hypothalamus					ZT4 MALES - Hypothalamus				
FeatureID	FeatureName	ZT4RF count average	ZT4RF Log2FoldChange	ZT4RF FDR	FeatureID	FeatureName	ZT4RM count average	ZT4RM Log2FoldChange	ZT4RM FDR
ENSMUSG00000021342	Prl	1.978699864	-5.654865506	5.62742E-18	ENSMUSG00000061808	Ttr	0.759038645	-2.340355734	3.77522E-14
ENSMUSG00000028298	Cga	0.160435124	-6.190119041	4.53065E-16	ENSMUSG00000024907	Gal	0.504741434	-3.741804169	5.73868E-13
ENSMUSG000000090137	Uba52	2.044062322	-2.301182933	1.10646E-14	ENSMUSG00000027301	Oxt	0.115589641	-7.678059154	2.64473E-08
ENSMUSG00000019970	Sgk1	2.329280321	2.944841987	3.11128E-13	ENSMUSG00000023067	Cdkn1a	0.766744621	2.581034431	2.64473E-08
ENSMUSG00000020713	Gh	0.825943787	-5.99547161	4.10665E-12	ENSMUSG00000019970	Sgk1	3.298157767	1.907740132	8.7814E-07
ENSMUSG00000023067	Cdkn1a	0.754639288	3.380904269	1.01509E-11	ENSMUSG0000005705	Agp	0	-7.904124013	1.45867E-06
ENSMUSG000000113902	Ndufb1-ps	4.824937808	-1.872222513	8.93262E-11	ENSMUSG00000090137	Uba52	2.138408365	-1.416007377	2.37671E-06
ENSMUSG00000060143	Gm10076	9.465672325	-1.843654735	1.46504E-10	ENSMUSG00000040856	Dlk1	1.051865737	-1.5925262	6.63177E-06
ENSMUSG00000067288	Rps28	9.584513157	-1.780392506	4.75265E-10	ENSMUSG00000048572	Tmem252	0.323650996	3.516494179	0.000120894
ENSMUSG00000103034	Gm8797	0.475363331	3.836231489	1.4611E-09	ENSMUSG00000045005	Fzd5	0.015411952	-4.094530618	0.000344534
ENSMUSG00000028998	Tom7	2.810585693	-1.783129513	1.4611E-09	ENSMUSG00000027400	Pdyn	0.601066135	-1.727559025	0.000377447
ENSMUSG00000048572	Tmem252	0.297102082	5.753769329	7.50199E-09	ENSMUSG00000021453	Gadd45g	1.229103187	1.546388288	0.000406886

ENSMUSG00000034892	Rps29	20.65453672	-1.633671901	1.07021E-08	ENSMUSG00000056380	Gpr50	0.023117928	-3.892896757	0.001292256
ENSMUSG00000064360	mt-Nd3	11.70582202	-1.633047916	1.24045E-08	ENSMUSG00000025591	Tma16	0.685831872	1.890479302	0.001638317
ENSMUSG00000090733	Rps27	12.30596823	-1.629130055	1.2884E-08	ENSMUSG00000031431	Tsc22d3	3.949312747	1.258169217	0.001827015
ENSMUSG00000046516	Cox17	3.291891066	-1.673447236	1.2884E-08	ENSMUSG00000035202	Lars2	1.194426294	-1.204583024	0.002288506
ENSMUSG00000079641	Rpl39	9.590455199	-1.619714044	1.2884E-08	ENSMUSG00000020713	Gh	0.003852988	-5.140824271	0.002529156
ENSMUSG00000016427	Ndufa1	2.656092611	-1.683053735	1.2884E-08	ENSMUSG00000021680	Crihbp	0.381445817	2.165996932	0.005665505
ENSMUSG00000002910	Arrdc2	0.635798455	2.666306488	2.56179E-08	ENSMUSG00000002831	Plin4	0.308239044	2.125025151	0.006694902
ENSMUSG00000027857	Tshb	0	-7.137824534	3.45454E-08	ENSMUSG00000002910	Arrdc2	0.504741434	1.692065744	0.006719216
ENSMUSG000000104960	Snhg8	0.921016453	-1.780458719	3.45772E-08	ENSMUSG00000023964	Calcr	0.100177689	-1.86592971	0.006836577
ENSMUSG00000064356	mt-Atp8	1.408263867	-1.731197382	5.2367E-08	ENSMUSG00000037727	Avp	0.65115498	-5.008537166	0.007989381
ENSMUSG00000071528	Atp5md	16.75061537	-1.511950443	1.19775E-07	ENSMUSG00000018604	Tbx3	0.011558964	-3.214824852	0.008873304
ENSMUSG00000021290	Atp5mpl	6.173781259	-1.53200632	1.23405E-07	ENSMUSG00000078640	Gm11627	0.385298805	1.85842413	0.008873304
ENSMUSG00000089661	Mia	0.041594291	-4.068403133	1.73006E-07	ENSMUSG00000092035	Peg10	0.277415139	-1.471256523	0.011007318
ENSMUSG00000038489	Polr2l	0.814059704	-1.674317701	5.2724E-07	ENSMUSG00000047502	Mroh7	0.034676892	-2.570968662	0.011998874
ENSMUSG00000026822	Lcn2	0.320870248	4.8627037	5.60506E-07	ENSMUSG00000054360	Bsx	0.023117928	-2.729398025	0.015002692
ENSMUSG00000046330	Rpl37a	15.00959717	-1.443185713	5.7433E-07	ENSMUSG00000021025	Nfkbia	0.770597609	1.365837511	0.016667502
ENSMUSG00000074754	Smin26	0.921016453	-1.619095731	7.12561E-07	ENSMUSG00000027210	Meis2	0.566389243	1.85712499	0.019329747
ENSMUSG00000098234	Snhg6	0.118840833	-2.39670331	7.86557E-07	ENSMUSG00000027525	Phactr3	2.015112748	1.118158431	0.022616389
ENSMUSG00000062997	Rpl35	11.20669052	-1.42533281	8.32876E-07	ENSMUSG00000063564	Col23a1	0.03852988	-3.291446134	0.023726566
ENSMUSG00000057322	Rpl38	28.59904639	-1.382928986	1.70659E-06	ENSMUSG00000060143	Gm10076	7.043262148	-0.892896757	0.02537904
ENSMUSG00000035674	Ndufa3	6.310448216	-1.397573043	1.85751E-06	ENSMUSG00000029819	Npy	0.489329482	-2.14556219	0.027979162
ENSMUSG00000071637	Cebpδ	0.570435997	2.359328734	3.70704E-06	ENSMUSG00000034936	Arl4d	0.612625099	1.474835027	0.029150868
ENSMUSG00000070369	Itgad	0.184203291	5.081343987	4.99999E-06	ENSMUSG00000022096	Hr	0.423828685	1.579591014	0.029150868
ENSMUSG00000050856	Atp5k	9.70335399	-1.339860768	5.245E-06	ENSMUSG00000054160	Nkx2-4	0.050088845	-2.085541835	0.0300094
ENSMUSG00000017778	Cox7c	14.64119059	-1.330764181	5.37963E-06	ENSMUSG00000031880	Rrad	0.123295617	-1.706483633	0.030019959
ENSMUSG00000078974	Sec61g	5.205228472	-1.366827662	7.32859E-06	ENSMUSG00000090247	Bloc1s1	0.346768924	-1.192457039	0.030019959
ENSMUSG00000047721	Bola2	2.299570113	-1.387521449	7.63596E-06	ENSMUSG00000091705	H2-Q2	0.19650239	-1.684310135	0.030645124
ENSMUSG00000020018	Snrpf	0.938842578	-1.506639866	9.34481E-06	ENSMUSG00000019817	Plagl1	0.29668008	-1.375678863	0.03257112
ENSMUSG00000042737	Dpm3	1.265654868	-1.480969775	9.62087E-06	ENSMUSG00000020660	Pomc	0.547124303	-2.630870876	0.041865115
ENSMUSG00000096956	Snhg18	0.059420416	-2.781152489	9.65024E-06	ENSMUSG00000042607	Asb4	0.154119522	-1.643869209	0.045051143
ENSMUSG00000034936	Arl4d	0.445653123	2.521916578	1.05238E-05	ENSMUSG00000025509	Pnpla2	0.839951394	1.20946496	0.045051143
ENSMUSG00000002831	Plin4	0.243623707	3.888698909	1.05238E-05					
ENSMUSG00000041841	Rpl37	28.33165452	-1.286962462	1.18188E-05					
ENSMUSG00000038803	Ost4	0.713044996	-1.538951587	1.24349E-05					
ENSMUSG00000039001	Rps21	33.14470824	-1.274472503	1.58087E-05					
ENSMUSG00000025739	Gng13	1.533046742	-1.397702752	2.17103E-05					
ENSMUSG00000016252	Atp5e	9.99451403	-1.245547415	3.16019E-05					
ENSMUSG00000057278	Snrpg	2.151019072	-1.31720539	5.96406E-05					
ENSMUSG00000097383	1500026H17Rik	0.0713045	-2.347499312	6.50101E-05					
ENSMUSG00000087687	Pet100	1.206234452	-1.309625752	9.98101E-05					
ENSMUSG00000057863	Rpl36	13.66075372	-1.181429038	0.000109509					
ENSMUSG00000042541	Sem1	2.537251778	-1.249991561	0.000122574					
ENSMUSG00000027525	Phactr3	1.996525989	1.379916685	0.000122993					
ENSMUSG00000014313	Cox6c	19.24627286	-1.173690413	0.000122993					
ENSMUSG00000079523	Tmsb10	24.94469078	-1.159386579	0.000160804					
ENSMUSG00000058351	Smin4	0.386232706	-1.518118084	0.000185675					
ENSMUSG00000052296	Ppp6r1	0.160435124	-1.825546609	0.000196251					
ENSMUSG00000078784	Rbis	2.335222363	-1.224382156	0.000198751					
ENSMUSG00000073616	Cops9	6.262911883	-1.154078188	0.000260913					
ENSMUSG00000093655	Rab26os	0.101014708	-2.015517552	0.000260913					
ENSMUSG00000064179	Tnnt1	0.350580456	2.666306488	0.000310029					
ENSMUSG00000100916	Lhb	0	-4.726010935	0.000310029					
ENSMUSG00000093674	Rpl41	25.44976432	-1.124500589	0.000310029					
ENSMUSG00000031431	Tsc22d3	3.648413564	1.253029446	0.000371284					
ENSMUSG00000030711	Sult1a1	0.404058831	2.102405602	0.000391551					
ENSMUSG00000031760	Mt3	20.27424606	-1.10534451	0.000402243					
ENSMUSG00000065947	mt-Nd4l	3.131455942	-1.173469912	0.000504658					
ENSMUSG00000090101	Snhg9	0.089130625	-2.02718047	0.00107887					
ENSMUSG00000020163	Uqcrr11	8.651612621	-1.04921156	0.001388064					
ENSMUSG00000021948	Prkcd	0.90913237	1.733420683	0.001388064					
ENSMUSG00000067847	Romo1	3.612761314	-1.071369619	0.00151982					
ENSMUSG00000070570	Slc17a7	0.457537206	1.84318425	0.00151982					
ENSMUSG00000021453	Gadd45g	1.473626325	1.259986205	0.00151982					

ENSMUSG00000036372	Tmem258	1.711307991	-1.112236792	0.002001772
ENSMUSG00000060636	Rpl35a	23.10859992	-1.015122543	0.002146088
ENSMUSG00000079435	Rpl36a	8.520887705	-1.013962973	0.002380416
ENSMUSG000000106918	Mrp133	1.5984092	-1.099228259	0.00272204
ENSMUSG00000068240	Gm11808	0.499131497	-1.243974697	0.002754748
ENSMUSG00000038690	Atp5j2	13.12596997	-1.000809872	0.002754788
ENSMUSG00000025362	Rps26	15.99003404	-0.999166703	0.002812796
ENSMUSG00000019689	Fmc1	1.81826474	-1.078625934	0.003091672
ENSMUSG00000070394	Tmem256	2.477831362	-1.045767931	0.003152552
ENSMUSG00000022018	Rgcc	0.831885829	1.362914344	0.003542383
ENSMUSG00000084786	Ubl5	6.785811547	-0.988865015	0.003835236
ENSMUSG00000090247	Bloc1s1	0.356522498	-1.371622968	0.004337865
ENSMUSG00000050288	Fzd2	0.380290665	1.781783705	0.004448522
ENSMUSG00000038717	Atp5l	11.99698206	-0.965731321	0.004931629
ENSMUSG00000096215	Smim22	0	-4.240584108	0.005049629
ENSMUSG00000035048	Anapc13	1.396379784	-1.0666801	0.005667956
ENSMUSG00000037152	Ndufc1	8.348568497	-0.957130161	0.006226643
ENSMUSG00000062006	Rpl34	17.16655828	-0.948301475	0.006226643
ENSMUSG00000039960	Rhou	0.742755204	1.358184192	0.006934866
ENSMUSG00000059534	Uqcr10	8.79422162	-0.944720801	0.007875137
ENSMUSG00000021040	Slirp	1.467684284	-1.019742138	0.008130211
ENSMUSG00000045996	Polr2k	2.026236198	-0.994658948	0.009085592
ENSMUSG00000053332	Gas5	10.58871819	-0.93434857	0.009287802
ENSMUSG00000024222	Fkbp5	0.665508663	1.409669853	0.009350504
ENSMUSG00000060981	Hist1h4h	0.03565225	-2.281226093	0.00974932
ENSMUSG00000025508	Rplp2	10.3332104	-0.913672606	0.012308663
ENSMUSG00000064220	Hist2h2aa1	0.017826125	-2.673543515	0.012841243
ENSMUSG00000010406	Mrp152	2.935368568	-0.947510876	0.012869087
ENSMUSG00000045394	Epcam	0.005942042	-3.619095731	0.013363983
ENSMUSG00000073702	Rpl31	9.043787368	-0.908198211	0.013807877
ENSMUSG00000028407	Smim27	0.202029416	-1.461798338	0.015748189
ENSMUSG00000033715	Akr1c14	0	-4.088581015	0.015901553
ENSMUSG00000051159	Cited1	1.78261249	1.206439207	0.015987177
ENSMUSG00000046768	Rhoj	0.154493083	2.514303394	0.017640506
ENSMUSG00000014294	Ndufa2	7.344363461	-0.886221282	0.019034875
ENSMUSG00000023089	Ndufa5	8.574366079	-0.882744835	0.020141701
ENSMUSG00000022820	Ndufb4	7.504798585	-0.878731285	0.020797722
ENSMUSG00000087590	Epb414aos	0.392174748	-1.183483701	0.022262226
ENSMUSG00000032330	Cox7a2	12.92394056	-0.865648267	0.023615558
ENSMUSG00000079480	Pin4	1.651887575	-0.936641759	0.027860133
ENSMUSG00000032532	Cck	3.28006983	1.175671369	0.031481806
ENSMUSG00000021025	Nfkbia	0.641740497	1.234818468	0.031481806
ENSMUSG00000024038	Ndufv3	5.621171387	-0.860365225	0.031481806
ENSMUSG00000029054	Gabrd	0.243623707	1.888698909	0.031528134
ENSMUSG00000087336	Gm15860	0.041594291	-2.088581015	0.031528134
ENSMUSG00000046215	Rprml	0.695218871	1.263547318	0.031528134
ENSMUSG00000048603	Gm9828	0.011884083	-2.793125131	0.031528134
ENSMUSG00000028583	Pdpn	0.041594291	-2.166583527	0.031961723
ENSMUSG00000052384	Nrros	0.136666958	2.666306488	0.031961723
ENSMUSG00000089665	Fcor	0.21985554	-1.343153842	0.035059894
ENSMUSG00000098332	2310009A05Rik	0.487247414	-1.082775393	0.035320562
ENSMUSG00000041046	Ramp3	0.87348012	1.383906757	0.0374818
ENSMUSG00000085241	Snhg3	0.511015581	-1.053141345	0.040340308
ENSMUSG00000063935	Zar1	0.279275957	1.759415892	0.041322093
ENSMUSG00000017734	Dbndd2	3.470152315	0.929340893	0.042579832
ENSMUSG00000024018	Ccdc167	0.380290665	-1.153676043	0.042897511
ENSMUSG00000091050	9330020H09Rik	0.101014708	-1.581621026	0.044051321
ENSMUSG00000038570	Saxo2	0.225797582	-1.262610414	0.046119486
ENSMUSG00000074170	Plekfh1	0.332754332	1.666306488	0.046961213
ENSMUSG00000028645	Slc2a1	1.895511282	0.977007327	0.048067423
ENSMUSG00000030677	Kif22	0.202029416	-1.297167636	0.049947565

Table S2N. DEGs at ZT14 in female and male hypothalamus (LH+DMVH). The average number of counts per spot in the RHY condition, the log2 fold change in gene expression (RHY relative to saline), and the adjusted p-value (FDR) are shown.

ZT14 FEMALES - Hypothalamus					ZT14 MALES - Hypothalamus				
FeatureID	FeatureName	ZT14RF count average	ZT14RF Log2FoldChange	ZT14RF FDR	FeatureID	FeatureName	ZT14RM count average	ZT14RM Log2FoldChange	ZT14RM FDR
ENSMUSG00000037727	Avp	0.116561404	-9.112164234	4.65898E-12	ENSMUSG00000024907	Gal	5.945300548	2.536753074	1.4494E-127
ENSMUSG00000019970	Sgk1	1.9491657	2.271902072	8.60226E-09	ENSMUSG00000035383	Pmch	30.62436446	-1.97345778	2.04563E-49
ENSMUSG00000027301	Oxt	0	-12.62259643	2.77485E-08	ENSMUSG00000061808	Ttr	2.875584143	2.007105212	4.08821E-46
ENSMUSG00000048572	Tmem252	0.531001951	5.163424266	3.60707E-06	ENSMUSG0000006522	Itih3	3.457980931	1.54415204	8.69837E-41
ENSMUSG00000071637	Cebpd	0.589282653	3.196469573	4.00702E-06	ENSMUSG00000031425	Plp1	4.295176315	-1.391146053	8.66446E-39
ENSMUSG00000035383	Pmch	363.3024693	2.01899502	8.22172E-06	ENSMUSG00000064354	mt-Co2	45.4633493	-0.962654012	6.80502E-36
ENSMUSG00000023067	Cdkn1a	0.407964914	2.788384835	8.22172E-06	ENSMUSG00000098178	Gm42418	3.257782035	-1.932232959	2.2589E-35
ENSMUSG00000021342	Pr1	0.012951267	-4.887180215	8.19715E-05	ENSMUSG00000064357	mt-Atp6	61.15166278	-0.945894129	2.2589E-35
ENSMUSG00000020713	Gh	0.032378168	-4.064057977	0.000424301	ENSMUSG00000064345	mt-Nd2	27.90651278	-0.95255922	2.76426E-33
ENSMUSG00000026822	Lcn2	1.560627687	6.292210573	0.00049881	ENSMUSG00000037852	Cpe	21.56081444	0.886159442	2.91809E-33
ENSMUSG00000027360	Hdc	0.18131774	4.231328331	0.000723699	ENSMUSG00000064363	mt-Nd4	35.08333987	-0.848470399	1.89294E-28
ENSMUSG00000025400	Tac2	2.596729055	1.834574468	0.001024751	ENSMUSG00000041607	Mbp	8.887617657	-0.91621057	6.57152E-23
ENSMUSG00000043102	Qrfp	0	-6.241362509	0.004258072	ENSMUSG00000041841	Rpl37	29.86603531	0.718664513	1.53292E-22
ENSMUSG00000033585	Ndn	6.13890061	-1.063379562	0.00600644	ENSMUSG00000008682	Rpl10	5.132371698	-0.897267608	4.9648E-22
ENSMUSG00000051851	Rtl8c	0.187793373	2.958309836	0.020282481	ENSMUSG00000064351	mt-Co1	101.1611088	-0.729535052	1.34415E-21
ENSMUSG00000024647	Cbln2	0.388538013	1.660228483	0.031013223	ENSMUSG00000092341	Malat1	1.644057601	-1.141090271	6.95E-21
ENSMUSG00000021025	Nfkbia	0.602233921	1.404374231	0.032969559	ENSMUSG00000064341	mt-Nd1	32.21988899	-0.693464577	3.91917E-19
ENSMUSG00000021453	Gadd45g	0.822405461	1.264822879	0.032969559	ENSMUSG00000090137	Uba52	3.937244955	0.937429674	6.87149E-18
ENSMUSG00000031765	Mt1	56.30563376	0.898673092	0.037259892	ENSMUSG00000031760	Mt3	22.30094369	0.663204359	2.43274E-17
					ENSMUSG00000045573	Penk	2.038388759	1.150526755	2.52641E-16
					ENSMUSG00000079523	Tmsb10	22.47687605	0.60394459	1.21395E-14
					ENSMUSG00000078974	Sec61g	4.956439335	0.779479971	2.80945E-14
					ENSMUSG00000062328	Rpl17	11.06553898	-0.660971788	2.85071E-14
					ENSMUSG00000073702	Rpl31	8.990750421	0.668171691	2.93804E-14
					ENSMUSG00000021647	Cartpt	4.556041543	-1.140825439	2.99558E-14
					ENSMUSG00000064370	mt-Cytb	70.4518115	-0.59009197	5.12731E-14
					ENSMUSG00000062591	Tubb4a	1.6986573	-0.92718056	2.42574E-13
					ENSMUSG00000000214	Th	1.213326643	1.302162859	3.89732E-13
					ENSMUSG00000004366	Sst	2.056588659	-0.872111056	4.11358E-13
					ENSMUSG00000022982	Sod1	3.815912291	0.79659962	8.91932E-13
					ENSMUSG00000031765	Mt1	20.0016897	0.564501686	1.16419E-12
					ENSMUSG00000057322	Rpl38	28.22804434	0.567490062	5.42047E-12
					ENSMUSG00000038274	Fau	26.15325578	0.531564314	9.79877E-12
					ENSMUSG00000093674	Rpl41	22.41014309	0.538702134	1.52076E-11
					ENSMUSG00000004558	Ndrp2	10.33147636	0.583928557	1.98278E-11
					ENSMUSG00000029819	Npy	0.709796086	-1.161391201	4.4825E-11
					ENSMUSG00000031980	Agt	5.011039034	0.68350999	4.53189E-11
					ENSMUSG00000014313	Cox6c	16.22217721	0.537643167	8.98663E-11
					ENSMUSG00000064356	mt-Atp8	0.545996989	-1.227218999	9.97746E-11
					ENSMUSG00000028234	Rps20	17.37483752	0.525870727	1.08716E-10
					ENSMUSG00000038690	Atp5j2	11.22327144	0.555690118	2.24373E-10
					ENSMUSG00000020660	Pomc	0.946394781	-1.088215415	2.46296E-10
					ENSMUSG00000023089	Ndufa5	7.650024481	0.592265384	2.75389E-10
					ENSMUSG00000025579	Gaa	9.015016954	0.571633434	7.39175E-10
					ENSMUSG00000032554	Trf	0.934261515	-0.978127553	8.69668E-10
					ENSMUSG00000030088	Aldh11	0.818995484	1.346620123	9.14013E-10
					ENSMUSG00000064367	mt-Nd5	4.756240439	-0.621823832	1.02202E-09
					ENSMUSG00000021268	Meg3	5.648035521	0.623240443	1.05587E-09
					ENSMUSG00000041453	Rpl21	35.70213646	0.466130093	2.82709E-09
					ENSMUSG00000037152	Ndufc1	7.000894728	0.571647433	3.87112E-09
					ENSMUSG00000018593	Sparc	13.91078996	0.558021729	3.87112E-09
					ENSMUSG00000093989	Rnasek	2.49338625	-0.702844746	3.93447E-09
					ENSMUSG00000030711	Sult1a1	0.424664325	1.903669093	4.1088E-09
					ENSMUSG00000073616	Cops9	7.164693824	0.780122976	4.91511E-09
					ENSMUSG00000046516	Cox17	2.86951751	0.731409434	5.23593E-09
					ENSMUSG00000025290	Rps24	30.70323069	0.456293245	7.81797E-09
					ENSMUSG00000056201	Cfl1	6.157632711	-0.572748781	8.43581E-09
					ENSMUSG00000032060	Cryab	1.443858705	-0.905370328	9.26111E-09
					ENSMUSG00000006333	Rps9	5.690501954	-0.690974034	1.70523E-08



ENSMUSG00000027375	Mal	1.249726442	-0.83294006	1.80584E-08
ENSMUSG00000028495	Rps6	4.841173304	-0.576614562	2.41628E-08
ENSMUSG00000054428	Atpif1	10.12521083	0.508534628	2.41628E-08
ENSMUSG00000020163	Uqcr11	7.55295835	0.529215686	2.53227E-08
ENSMUSG00000032399	Rpl4	12.82486261	0.703768547	2.95007E-08
ENSMUSG00000035215	Lsm7	3.227448869	0.664015001	4.4911E-08
ENSMUSG00000102252	Snrpn	5.902834116	-0.558007071	5.41356E-08
ENSMUSG00000042750	Bex2	19.17056095	0.45042539	8.09689E-08
ENSMUSG00000034892	Rps29	11.68433557	-0.492661599	9.07978E-08
ENSMUSG00000044349	Snhg11	4.907906269	0.564518908	1.73979E-07
ENSMUSG00000095041	AC149090.1	1.437792071	0.874551679	2.16908E-07
ENSMUSG00000024517	Grp	0.242665329	2.400980595	2.51427E-07
ENSMUSG00000061762	Tac1	0.861461916	-0.919096704	2.5301E-07
ENSMUSG00000032532	Cck	0.867528549	-0.881164007	3.03502E-07
ENSMUSG00000022194	Pabpn1	0.16986573	-1.579717104	4.70209E-07
ENSMUSG00000040856	Dlk1	1.504525037	0.833505521	5.02039E-07
ENSMUSG00000028656	Cap1	0.090999498	-1.956571409	5.25391E-07
ENSMUSG00000086841	2410006H16Rik	1.941322628	0.735652058	9.05542E-07
ENSMUSG00000018707	Dync1h1	2.711785046	0.647843454	9.51771E-07
ENSMUSG00000020922	Lsm12	0.0181999	-3.072048627	2.1647E-06
ENSMUSG00000024608	Rps14	8.881551023	-0.466870901	2.44585E-06
ENSMUSG00000015806	Qdpr	2.481252984	-0.586946572	4.59692E-06
ENSMUSG00000024038	Ndufv3	4.822973404	0.51124183	5.06034E-06
ENSMUSG00000064358	mt-Co3	144.5314697	-0.3895819	5.06034E-06
ENSMUSG00000020460	Rps27a	25.97732342	0.386165691	5.46913E-06
ENSMUSG00000015812	Gnrh1	0.157732464	3.160886172	5.46913E-06
ENSMUSG00000013523	Bcas1	0.394331159	-1.082102291	5.73204E-06
ENSMUSG00000090841	Myl6	8.420486899	0.437651476	6.66809E-06
ENSMUSG00000037499	Nenf	7.522625184	0.461353765	6.82843E-06
ENSMUSG00000022090	Pdlim2	0.18806563	-1.416003028	7.91135E-06
ENSMUSG00000026385	Dbi	9.785479372	0.423729049	8.69047E-06
ENSMUSG00000036699	Zcchc12	5.047438833	0.493461511	9.02664E-06
ENSMUSG00000033615	Cplx1	1.298259508	-0.696665041	9.31539E-06
ENSMUSG00000090223	Pcp4	6.521630704	-0.469236413	1.0422E-05
ENSMUSG00000025739	Gng13	1.795723431	0.696353682	1.04433E-05
ENSMUSG00000039001	Rps21	27.66991408	0.385632561	1.12224E-05
ENSMUSG00000021910	Nisch	4.428642245	0.504286285	1.26165E-05
ENSMUSG00000043384	Gprasp1	5.769368185	0.476084943	1.26165E-05
ENSMUSG00000002957	Ap2a2	1.613724435	0.7118071	1.80722E-05
ENSMUSG00000072966	Gprasp2	4.21024345	0.503206221	2.00395E-05
ENSMUSG00000024740	Ddb1	1.595524535	0.714715891	2.12783E-05
ENSMUSG00000022048	Dpysl2	4.283043048	0.499010907	2.14767E-05
ENSMUSG00000035202	Lars2	0.32153156	-1.535584644	2.17791E-05
ENSMUSG00000028998	Tomm7	2.153654791	0.625691942	2.61142E-05
ENSMUSG00000047126	Cltc	3.397314599	0.531429361	2.64733E-05
ENSMUSG00000057863	Rpl36	12.32739869	0.39619847	2.93366E-05
ENSMUSG00000054360	Bsx	0.127399297	3.08782271	3.11032E-05
ENSMUSG00000019970	Sgk1	0.903928349	0.903013471	3.32953E-05
ENSMUSG00000004207	Psap	12.33346532	0.390879112	3.79686E-05
ENSMUSG00000060636	Rpl35a	17.15037209	0.377138035	3.79686E-05
ENSMUSG00000044258	Ctla2a	0.303331661	1.637851421	4.00753E-05
ENSMUSG00000028452	Vcp	3.524713897	0.512532562	4.74203E-05
ENSMUSG00000005716	Pvalb	0.461064124	-0.995593298	4.86719E-05
ENSMUSG00000026575	Nme7	0.928194882	1.194737914	6.96338E-05
ENSMUSG00000021750	Fam107a	1.225459909	0.754568197	7.7419E-05
ENSMUSG00000030541	Idh2	0.867528549	0.891425497	7.81674E-05
ENSMUSG00000008668	Rps18	3.312381734	-0.488910911	8.66691E-05
ENSMUSG00000054452	Tle5	4.744107172	-0.44757351	9.97878E-05
ENSMUSG00000071528	Atp5md	13.47399237	0.374257548	0.000104227
ENSMUSG00000002477	Snrpd1	2.918050575	0.526330086	0.000114862
ENSMUSG00000018339	Gpx3	2.317453887	-0.529626373	0.000126249
ENSMUSG00000020777	Acox1	1.468125237	0.682838875	0.000130175
ENSMUSG00000050071	Bex1	6.285032008	0.425809899	0.000134039

ENSMUSG00000014294	Ndufa2	6.418497939	0.418704555	0.000140107
ENSMUSG00000017390	Aldoc	13.98965619	0.359324212	0.000154088
ENSMUSG00000037706	Cdb1	6.55196387	0.40886135	0.000161801
ENSMUSG00000027574	Nkain4	1.595524535	0.650417398	0.000166212
ENSMUSG00000027133	Nop10	2.554052583	0.539990086	0.000169927
ENSMUSG00000011884	Gltpr	0.133465931	-1.442993542	0.000172127
ENSMUSG00000027422	Rrbp1	0.467130757	1.176827716	0.000174058
ENSMUSG00000020658	Efr3b	0.788662318	0.898048439	0.000193602
ENSMUSG00000016346	Kcnq2	1.079860712	0.754654864	0.000247637
ENSMUSG00000021290	Atp5mpl	5.496369691	0.426365391	0.000295894
ENSMUSG00000049422	Chchd10	5.866434317	-0.415641677	0.000308185
ENSMUSG00000027562	Car2	1.085927345	-0.645732493	0.000308251
ENSMUSG00000062997	Rpl35	10.20407706	0.398304278	0.000310797
ENSMUSG00000027301	Oxt	16.33744324	1.14230139	0.000322769
ENSMUSG00000029831	Npvf	0.309398294	1.454361692	0.000322769
ENSMUSG00000084786	Ubl5	5.490303058	0.415584719	0.000322769
ENSMUSG00000039686	Zer1	1.219393276	0.716746966	0.000323502
ENSMUSG00000027643	Ghrh	0.897861715	1.803165492	0.000327263
ENSMUSG00000076439	Mog	0.576330155	-0.809014221	0.000358691
ENSMUSG00000067274	Rplp0	2.984783541	-0.470559192	0.000367186
ENSMUSG00000020018	Snrpf	0.782595684	0.860681974	0.00037179
ENSMUSG00000028936	Rpl22	3.500447364	0.463466771	0.000434794
ENSMUSG00000020483	Dynll2	4.731973906	0.422720371	0.000473133
ENSMUSG0000002625	Akap8l	0.879661816	0.81821565	0.000488082
ENSMUSG00000059534	Uqcr10	7.279959855	0.384029567	0.000491203
ENSMUSG00000059291	Rpl11	19.68622478	0.329219758	0.000495644
ENSMUSG00000020496	Rnf187	4.725907273	0.41980447	0.000541491
ENSMUSG00000090101	Snhg9	0.236598695	1.677300692	0.000541491
ENSMUSG00000037771	Slc32a1	2.159721424	0.548475613	0.000541888
ENSMUSG00000035674	Ndufa3	5.68443532	0.406438181	0.000541888
ENSMUSG00000063457	Rps15	13.5710585	0.340643644	0.000571357
ENSMUSG00000060126	Tpt1	8.984683788	-0.460941144	0.000578096
ENSMUSG00000032855	Pkd1	0.52779709	1.028929021	0.000604199
ENSMUSG00000016252	Atp5e	8.735951826	0.4400073	0.000605776
ENSMUSG00000046711	Hmga1	0.175932363	-1.237307817	0.000610138
ENSMUSG00000027245	Hypk	1.073794079	0.717543469	0.000615157
ENSMUSG00000006651	Aplp1	5.120238432	-0.402575259	0.000669064
ENSMUSG00000023147	Wrb	1.18906011	0.685658292	0.000669064
ENSMUSG00000032294	Pkm	10.91387315	0.381026142	0.000689855
ENSMUSG00000028756	Pink1	3.639979928	0.443166578	0.000741343
ENSMUSG00000043388	Tmem130	4.398309079	0.415683135	0.000937049
ENSMUSG00000092274	Neat1	0.394331159	1.17028487	0.000937049
ENSMUSG00000005360	Slc1a3	2.329587154	0.509746595	0.000938171
ENSMUSG00000035805	Mlc1	2.196121223	0.517506985	0.001046811
ENSMUSG00000025151	Maged1	7.753157246	0.383772172	0.001094625
ENSMUSG00000074656	Eif2s2	0.922128248	-0.637783022	0.001285399
ENSMUSG00000012848	Rps5	8.117155239	-0.364768919	0.001289768
ENSMUSG000000115718	Gm49179	0.145599197	2.156770064	0.001289768
ENSMUSG00000034156	Tspoap1	0.570263522	0.950319186	0.00131889
ENSMUSG00000040907	Atp1a3	1.674390767	-0.519961588	0.00136709
ENSMUSG00000058135	Gstm1	1.807856697	-0.586399087	0.001397357
ENSMUSG00000042541	Sem1	1.577324635	0.579481491	0.001415367
ENSMUSG00000021186	Fbln5	0.194132263	1.734185755	0.001429529
ENSMUSG00000044894	Uqcrq	8.996817054	0.344019571	0.001473138
ENSMUSG00000030701	Plekhhb1	1.813923331	-0.503271554	0.001555475
ENSMUSG00000079484	Phyhd1	0.388264526	1.148258564	0.00176979
ENSMUSG00000054312	Mrps21	2.34172042	0.489871227	0.00176979
ENSMUSG00000022884	Eif4a2	3.548980429	-0.415256794	0.001796776
ENSMUSG00000029455	Aldh2	0.994927847	0.70315886	0.001836626
ENSMUSG00000038545	Cu17	0.327598193	1.239825803	0.002036476
ENSMUSG00000029064	Gnb1	3.85231209	0.54609697	0.002105335
ENSMUSG00000007850	Hnrnp1	1.6622575	0.55176981	0.002109309
ENSMUSG00000023072	Cep89	0.181998996	1.77523248	0.002139448

ENSMUSG00000020267	Hint1	13.32839317	0.317091441	0.002169538
ENSMUSG00000013236	Ptprs	1.407458905	0.593723959	0.002183937
ENSMUSG00000055839	Elob	10.65300792	0.325140526	0.002222286
ENSMUSG00000024735	Prpf19	1.51059167	0.575511532	0.002222286
ENSMUSG00000027858	Tspan2	0.515663823	-0.765523116	0.002247436
ENSMUSG0000002012	Pncc	3.02118334	0.441539977	0.002247436
ENSMUSG00000033208	S100b	1.504525037	-0.520131433	0.002383875
ENSMUSG00000022425	Enpp2	0.649129754	-0.70064389	0.002383875
ENSMUSG00000024208	Uqcc2	5.575235923	0.368845672	0.002383875
ENSMUSG00000073982	Rhog	0.157732464	-1.211667996	0.002386903
ENSMUSG00000039463	Slc9a8	0.370064626	1.145182089	0.002390417
ENSMUSG00000018909	Arrb1	0.788662318	0.771043163	0.002390417
ENSMUSG00000029516	Cit	0.448930858	1.015907528	0.002575421
ENSMUSG00000040759	Cmtm5	0.479264024	-0.782130927	0.002604097
ENSMUSG00000039661	Dusp26	1.716857199	0.536552224	0.002606636
ENSMUSG00000050708	Ftl1	4.792640238	-0.378281044	0.002653271
ENSMUSG00000053192	Mllt11	2.426653285	-0.446388791	0.002669472
ENSMUSG00000032788	Pdkk	1.176926843	0.630859347	0.002678241
ENSMUSG00000022037	Clu	10.05847787	0.388833082	0.002680902
ENSMUSG00000025508	Rplp2	7.607558049	0.428007291	0.00269237
ENSMUSG00000006782	Cnp	2.050522026	-0.500446018	0.003183032
ENSMUSG00000001415	Smg5	0.430730958	1.025726589	0.003265613
ENSMUSG00000037166	Ppp1r14a	0.333664827	-0.886182082	0.003268578
ENSMUSG00000005892	Trh	1.15266031	1.251623609	0.003294077
ENSMUSG00000004110	Cacna1e	0.461064124	0.988287036	0.00340367
ENSMUSG00000048721	Fndc9	0.248731962	1.396217649	0.003710085
ENSMUSG00000070858	Gm1673	4.440775512	0.377876155	0.003856649
ENSMUSG00000022415	Syng1	1.6622575	0.528738841	0.003856649
ENSMUSG00000029311	Hsd17b11	0.260865228	1.350857116	0.003914666
ENSMUSG00000038570	Saxo2	0.260865228	1.350857116	0.003914666
ENSMUSG00000017778	Cox7c	9.324415248	0.323441716	0.003914666
ENSMUSG00000034994	Eef2	6.642963368	0.336971085	0.003984312
ENSMUSG00000039126	Prune2	0.734062619	0.760386637	0.004157421
ENSMUSG00000020230	Prmt2	1.856389763	0.503904883	0.004305585
ENSMUSG00000051483	Cbr1	1.486325137	0.548537784	0.004305585
ENSMUSG00000097156	Gm3764	0.485330657	0.938493751	0.004522539
ENSMUSG00000039801	Cplane1	0.394331159	1.149223255	0.004522539
ENSMUSG00000026830	Ernm	0.181998996	-1.099236638	0.004527716
ENSMUSG00000032244	Fem1b	0.958528048	0.668255552	0.004552111
ENSMUSG00000074657	Kif5a	3.075783039	0.417403433	0.004552111
ENSMUSG00000017740	Slc12a5	1.917056095	0.493786626	0.004735723
ENSMUSG00000027706	Sec62	0.812928851	-0.616721407	0.004784791
ENSMUSG00000026688	Mgst3	0.922128248	-0.587250288	0.004884901
ENSMUSG00000005089	Slc1a2	4.331576114	0.373224929	0.004921413
ENSMUSG00000031026	Trim66	0.230532062	1.41129297	0.005037454
ENSMUSG00000015149	Sirt2	0.806862217	-0.618402674	0.005161102
ENSMUSG00000028618	Tmem59	1.474191871	-0.49976526	0.005185774
ENSMUSG00000006435	Neur1a	0.667329653	0.788609938	0.005239864
ENSMUSG00000020607	Lratd1	0.315464927	1.186386544	0.005257484
ENSMUSG00000040591	1110051M20Rik	1.395325639	0.55334998	0.00551426
ENSMUSG00000018293	Pfn1	1.116260511	-0.545283794	0.00551426
ENSMUSG00000036752	Tubb4b	4.052510986	0.377628871	0.005599417
ENSMUSG00000022389	Tef	1.213326643	0.588280878	0.005628663
ENSMUSG00000053046	Brsk2	0.570263522	0.840694695	0.005629298
ENSMUSG00000030683	Sez6l2	3.160715904	0.406788539	0.005650135
ENSMUSG00000053310	Nrgn	1.929189362	-0.453652253	0.005751499
ENSMUSG00000015837	Sqstm1	4.446842145	0.366667631	0.005751499
ENSMUSG00000058756	Thra	4.319442847	0.369183764	0.005751499
ENSMUSG00000057880	Abat	2.19005459	0.460534047	0.005931687
ENSMUSG00000018451	6330403K07Rik	18.27876587	0.28574273	0.006058167
ENSMUSG00000029104	Htt	0.412531058	0.999949954	0.006199186
ENSMUSG00000032594	Ip6k1	1.413525539	0.544559501	0.006244013
ENSMUSG00000054226	Tprkb	0.206265529	-1.032402822	0.006249616

ENSMUSG00000028298	Cga	0.0181999	-2.996099774	0.006315679
ENSMUSG00000059208	Hnrnpm	0.818995484	0.69348612	0.00645024
ENSMUSG00000021497	Txndc15	1.401392272	0.543857581	0.00667553
ENSMUSG00000020577	Tspan13	0.861461916	-0.589671077	0.006714586
ENSMUSG00000044550	Tceal3	3.087916305	0.403576008	0.006747161
ENSMUSG00000053646	Plxnb1	0.521730456	0.874937374	0.006938583
ENSMUSG00000041697	Cox6a1	5.277970895	-0.34598508	0.006993497
ENSMUSG00000034161	Scx	0.127399297	1.972345493	0.006993497
ENSMUSG00000024176	Sox8	0.012133266	-2.59400133	0.006993497
ENSMUSG00000045763	Basp1	2.857384243	-0.398858943	0.007178761
ENSMUSG00000045996	Polr2k	1.486325137	0.526511477	0.0076356
ENSMUSG00000087336	Gm15860	0.139532564	1.891425497	0.007653844
ENSMUSG00000060036	Rpl3	10.52560862	-0.320577149	0.007701886
ENSMUSG00000030310	Slc6a1	1.716857199	0.495821972	0.007976853
ENSMUSG00000070394	Tmem256	1.874589663	0.475457527	0.007976853
ENSMUSG00000022055	Nefl	1.35892584	-0.496427173	0.007976853
ENSMUSG00000026614	Slc30a10	0.230532062	1.369472794	0.00830351
ENSMUSG00000032333	Stoml1	0.715862719	0.733131924	0.00830351
ENSMUSG00000066357	Wdr6	3.427647765	0.383597245	0.00834646
ENSMUSG00000024287	Thoc1	0.303331661	1.157858479	0.008827276
ENSMUSG00000025374	Nabp2	0.539930356	-0.687110734	0.008872901
ENSMUSG00000042453	Reln	0.254798595	1.282066342	0.008889327
ENSMUSG00000020282	Rhbdf1	0.097066131	2.300816433	0.009019268
ENSMUSG00000040952	Rps19	8.141421771	-0.43088927	0.009084193
ENSMUSG000000112639	A730063M14Rik	0.084932865	2.535281687	0.009084193
ENSMUSG00000021957	Tkt	0.655196387	0.862596844	0.009084193
ENSMUSG00000063236	1110038F14Rik	0.454997491	0.906692254	0.009198362
ENSMUSG00000015759	Cnih1	0.673396287	-0.633927514	0.009439808
ENSMUSG00000024736	Tmem132a	0.746195885	0.708118284	0.00983618
ENSMUSG00000010406	Mrpl52	2.444853185	0.422416429	0.009921851
ENSMUSG00000061046	Haghl	1.777523531	0.476387998	0.010027521
ENSMUSG00000027894	Slc6a17	0.879661816	0.648290649	0.010272113
ENSMUSG00000000826	Dnajc5	1.553058102	0.501301718	0.010294881
ENSMUSG00000036241	Ubezr2	0.673396287	-0.626749912	0.010294881
ENSMUSG00000050121	Opalin	0.35793136	-0.79861905	0.010352452
ENSMUSG00000057278	Snrpg	1.722923832	0.482475328	0.010719082
ENSMUSG00000020570	Sypl	0.224465429	-0.964983649	0.010906331
ENSMUSG00000039218	Srrm2	0.685529553	0.948211523	0.0113453
ENSMUSG00000004980	Hnrnpa2b1	2.820984444	0.459154234	0.01171382
ENSMUSG00000028572	Hook1	0.32153156	1.61068909	0.012453139
ENSMUSG00000035183	Slc24a5	0.260865228	1.213353592	0.012506322
ENSMUSG00000029499	Pxmp2	0.260865228	1.213353592	0.012506322
ENSMUSG00000063253	Scoc	1.953455895	-0.427104021	0.012506322
ENSMUSG00000000881	Dlg3	0.552063622	0.806178211	0.012506322
ENSMUSG00000020368	Canx	3.615713395	0.366162435	0.012523367
ENSMUSG00000005804	Bloc1s6	0.485330657	0.852763877	0.012667919
ENSMUSG00000077450	Rab11b	1.225459909	-0.496349922	0.012929535
ENSMUSG00000038068	Rnf144b	0.15166583	1.665865797	0.01310998
ENSMUSG00000024423	Impact	4.276976415	0.345961087	0.013297173
ENSMUSG00000026181	Ppm1f	0.370064626	0.997624901	0.013313113
ENSMUSG00000025203	Scd2	9.470014445	0.287256954	0.013455422
ENSMUSG00000059412	Fxyd2	0.327598193	1.040516995	0.014651252
ENSMUSG00000056222	Spock1	1.273992975	0.533573344	0.014859672
ENSMUSG00000038668	Lpar1	0.066732965	-1.487086126	0.014863484
ENSMUSG00000034059	Ypel4	0.351864726	1.029907451	0.014918801
ENSMUSG00000027199	Gatm	0.50959719	-0.67646349	0.014918801
ENSMUSG00000017009	Sdc4	0.740129252	0.680134666	0.014918801
ENSMUSG00000004897	Hdgf	0.552063622	-0.659689233	0.014918801
ENSMUSG00000042712	Tceal9	1.613724435	-0.447049665	0.014918801
ENSMUSG00000032009	Sesn3	0.879661816	0.628391091	0.015329503
ENSMUSG00000049775	Tmsb4x	16.22217721	-0.278990806	0.015329503
ENSMUSG00000027674	Pex5l	0.181998996	-1.022274656	0.01538034
ENSMUSG00000079435	Rpl36a	6.321431808	0.348093331	0.01538034

ENSMUSG00000050856	Atp5k	8.89368429	0.292175864	0.01584459
ENSMUSG00000031708	Tecr	3.931178322	-0.346192898	0.01584459
ENSMUSG00000028843	Sh3bgrl3	1.613724435	-0.445339297	0.015961663
ENSMUSG00000019986	Ahi1	4.440775512	0.336560286	0.015961663
ENSMUSG00000062825	Actg1	13.78339066	0.289928714	0.016099424
ENSMUSG00000001289	Pfdn5	9.918945303	0.285220764	0.016391304
ENSMUSG000000038520	Tbc1d17	0.570263522	0.771981945	0.016694466
ENSMUSG00000024099	Ndufv2	3.506513997	-0.354060707	0.016852175
ENSMUSG00000015341	Golga7	0.32153156	-0.806545965	0.016912608
ENSMUSG00000018585	Atox1	2.329587154	0.409750805	0.016928088
ENSMUSG00000033152	Podxl2	4.355842647	0.49985355	0.017165646
ENSMUSG00000057069	Ero1lb	0.242665329	1.213353592	0.017165646
ENSMUSG00000051335	Gfod1	0.230532062	1.250828297	0.017165646
ENSMUSG00000028803	Nipal3	0.643063121	0.716415839	0.017605978
ENSMUSG00000005986	Ankrd13d	0.606663321	0.732013722	0.01804529
ENSMUSG00000057649	Brd9	0.412531058	0.912487113	0.018106904
ENSMUSG00000062044	Lmtk3	0.442864225	0.868218106	0.018434337
ENSMUSG00000044709	Gemin7	0.448930858	-0.69737907	0.018563158
ENSMUSG00000006930	Hap1	3.882645256	0.345241324	0.018775231
ENSMUSG00000039016	Timm8b	5.569169289	0.315807657	0.019149666
ENSMUSG00000047675	Rps8	25.32212703	0.250100995	0.019313615
ENSMUSG00000035048	Anap13	1.383192373	0.497968528	0.019313615
ENSMUSG00000015222	Map2	2.214321123	0.413903868	0.019337681
ENSMUSG00000020926	Adam11	0.479264024	0.834841969	0.019375316
ENSMUSG00000021087	Rtn1	9.89467877	-0.291329108	0.019375316
ENSMUSG00000022211	Carmil3	0.285131761	1.097876375	0.019375316
ENSMUSG00000049191	Rtl5	0.351864726	0.966713624	0.019375316
ENSMUSG00000019738	Polr2i	1.031327646	0.565116916	0.019655733
ENSMUSG00000008206	Cers4	0.479264024	0.821036169	0.020117635
ENSMUSG00000038664	Herc1	0.928194882	0.591396884	0.020117635
ENSMUSG00000070304	Scn2b	0.994927847	0.574051257	0.020475253
ENSMUSG00000061751	Kalrn	0.260865228	1.149223255	0.020475253
ENSMUSG00000071658	Gng3	5.617702355	-0.320389836	0.020684983
ENSMUSG00000033161	Atp1a1	2.766384745	0.442073633	0.020757256
ENSMUSG00000022216	Psm1	1.419592172	0.486244194	0.0208661
ENSMUSG00000032854	Ugt8a	0.115266031	-1.178963831	0.021022467
ENSMUSG00000060743	H3f3a	2.469119718	-0.379836112	0.021026254
ENSMUSG00000060803	Gstp1	2.153654791	-0.394392304	0.021149674
ENSMUSG00000049517	Rps23	7.279959855	-0.297671549	0.021576161
ENSMUSG00000014602	Kif1a	2.250720922	0.403784249	0.022258804
ENSMUSG00000067889	Sptbn2	0.67946292	0.67598055	0.022441747
ENSMUSG00000053226	Dand5	0.18806563	1.355372597	0.022569773
ENSMUSG00000022548	Apod	1.261859708	-1.070809122	0.022569773
ENSMUSG00000042751	Nmnat2	0.946394781	0.583161837	0.022877574
ENSMUSG00000048756	Foxo3	0.260865228	1.118196359	0.022877574
ENSMUSG00000047844	Bex4	1.607657801	0.461281105	0.022877574
ENSMUSG00000079657	Rab26	0.503530557	0.785492052	0.023131229
ENSMUSG00000040860	Crocc	0.200198896	1.300816433	0.023304583
ENSMUSG00000049154	Fam183b	0.612729954	0.715853933	0.023426418
ENSMUSG00000005417	Mpp1	1.013127747	0.561276895	0.023426418
ENSMUSG00000019362	D8ErtD738e	2.990850174	0.364059298	0.023573911
ENSMUSG00000002930	Ppp1r17	0.224465429	1.213353592	0.023815726
ENSMUSG00000026667	Uhmk1	1.401392272	0.482619952	0.024237759
ENSMUSG00000058239	Usf2	0.594530055	0.713427195	0.024790811
ENSMUSG00000018669	Cdk5rap3	0.442864225	0.837844457	0.024920038
ENSMUSG00000021400	Wrnip1	0.691596186	0.66652622	0.024920038
ENSMUSG00000020198	Ap3d1	0.976727947	0.564518908	0.024958729
ENSMUSG00000044627	Swi5	5.217304563	0.373571873	0.025101343
ENSMUSG00000027474	Ccm2l	0.048533066	3.383278593	0.025601807
ENSMUSG00000066129	Kndc1	0.855395283	0.601549479	0.025644208
ENSMUSG00000024403	Atp6v1g2	2.268920822	-0.383104548	0.025644208
ENSMUSG00000002763	Pex6	0.479264024	0.807361232	0.025644208
ENSMUSG00000037103	Dcaf15	0.230532062	1.213353592	0.025828926

ENSMUSG0000003469	Phyhip	0.412531058	0.86244643	0.02596094
ENSMUSG00000033735	Spr	0.776529051	0.624668005	0.026587158
ENSMUSG00000031775	Plip	0.461064124	-0.669606987	0.026587158
ENSMUSG00000027244	Atg13	0.479264024	0.793814701	0.026660584
ENSMUSG00000022992	Kansl2	0.497463923	0.781038101	0.026726274
ENSMUSG00000010803	Gabra1	1.134460411	-0.47523154	0.027068996
ENSMUSG00000029817	Tra2a	0.588463422	0.719538979	0.027184501
ENSMUSG00000042699	Dhx9	0.33973146	0.958780765	0.027275372
ENSMUSG00000041351	Rap1gap	1.195126743	0.511793334	0.027911923
ENSMUSG00000061032	Rrp1	2.456986451	0.380837672	0.028454113
ENSMUSG00000032046	Abhd12	1.383192373	-0.441298069	0.028456707
ENSMUSG00000027523	Gnas	22.85300731	0.276153162	0.028456707
ENSMUSG00000031683	Lsm6	1.577324635	0.4500967	0.028456707
ENSMUSG000000110156	Gm42067	0.418597692	0.850783513	0.028456707
ENSMUSG00000006476	Nsmf	1.219393276	0.500877668	0.028634644
ENSMUSG00000057897	Camk2b	1.965589161	0.415542443	0.028835047
ENSMUSG00000014606	Slc25a11	1.735057099	0.435746013	0.028835047
ENSMUSG00000030854	Ptpn5	1.134460411	0.52001493	0.029255761
ENSMUSG00000026238	Ptma	3.366981433	-0.338361584	0.029384128
ENSMUSG00000056972	Magel2	0.454997491	0.817424916	0.029529223
ENSMUSG00000033475	Tommm6	3.142516004	-0.344484508	0.029671357
ENSMUSG00000032249	Anp32a	0.333664827	-0.754078546	0.029775323
ENSMUSG00000031310	Zmym3	0.770462418	0.620896555	0.029775323
ENSMUSG00000046160	Olig1	0.909994982	-0.525521592	0.031167435
ENSMUSG00000062006	Rpl34	10.95633958	0.264550058	0.031221576
ENSMUSG00000005034	Prkacb	3.925111689	0.324384904	0.031298375
ENSMUSG00000057751	Megf6	0.121332664	1.698780419	0.031521721
ENSMUSG00000074884	Serf2	5.071705366	0.303134449	0.03153985
ENSMUSG00000036634	Mag	1.037394279	-0.484502965	0.031695474
ENSMUSG00000030137	Tube8	0.084932865	2.120244188	0.031866423
ENSMUSG00000019505	Ubb	35.45947113	0.229359575	0.032389572
ENSMUSG00000042439	Zfp532	0.285131761	1.016956379	0.03249908
ENSMUSG00000013787	Ehmt2	0.946394781	0.553778031	0.032509682
ENSMUSG00000009621	Vav2	0.097066131	1.978888338	0.032798841
ENSMUSG00000027797	Dclk1	1.201193376	0.519061334	0.032993977
ENSMUSG00000019232	Etnppl	0.703729453	0.640774816	0.034216426
ENSMUSG000000116165	Pdpx	2.632918814	0.365356685	0.034315312
ENSMUSG00000031066	Usp11	1.346792573	0.471221672	0.034315312
ENSMUSG000000117465	Gm49980	0.224465429	1.175878887	0.034843212
ENSMUSG00000038503	Mesd	1.182993476	0.497146558	0.034843981
ENSMUSG00000036357	Gpr101	0.394331159	0.848356775	0.034843981
ENSMUSG00000037400	Atp11b	0.200198896	1.256422314	0.035014782
ENSMUSG00000023092	Fhl1	1.055594179	0.525013351	0.037044433
ENSMUSG00000017631	Abr	1.898856196	0.409942258	0.037257381
ENSMUSG00000030757	Zkscan2	0.163799097	1.376852324	0.037964657
ENSMUSG00000025786	Zdhhc3	0.181998996	-0.940974554	0.038342672
ENSMUSG00000024076	Vit	0.115266031	1.727926765	0.038342672
ENSMUSG00000044252	Osbpl1a	0.315464927	-0.752212911	0.038361467
ENSMUSG00000040687	Madd	1.00099448	0.628391091	0.038515486
ENSMUSG00000026173	Plcd4	0.224465429	1.139353011	0.039616513
ENSMUSG00000029415	Sdad1	0.175932363	1.312889266	0.039616513
ENSMUSG000000104960	Snhg8	0.818995484	0.579717245	0.039669568
ENSMUSG00000032890	Rims3	1.401392272	0.46030979	0.039669568
ENSMUSG00000024858	Grk2	0.994927847	0.529827257	0.039669568
ENSMUSG00000031227	Magee1	1.553058102	0.437618428	0.04015754
ENSMUSG00000025266	Gnl3l	1.067727445	0.516052215	0.04015754
ENSMUSG00000033685	Ucp2	0.333664827	-0.734178988	0.040321563
ENSMUSG00000024985	Tcf7l2	0.564196889	0.701853253	0.040561658
ENSMUSG00000026404	Ddx59	0.115266031	2.365356685	0.040971476
ENSMUSG00000058740	Kcnt1	0.473197391	0.762246838	0.040971476
ENSMUSG00000070802	Pnmal2	3.154649271	0.337626346	0.040971476
ENSMUSG00000034818	Cellf5	0.436797591	0.788468307	0.040971476
ENSMUSG00000000325	Arvcf	0.242665329	1.111473978	0.040971476

ENSMUSG00000006676	Usp19	0.643063121	0.65103983	0.041962897
ENSMUSG00000068240	Gm11808	0.50959719	0.727926765	0.042118482
ENSMUSG00000010277	2610507B11Rik	0.424664325	0.80851186	0.042170815
ENSMUSG00000029697	Fezf1	0.200198896	-0.898855912	0.042669083
ENSMUSG00000030846	Tial1	0.685529553	0.628391091	0.042669083
ENSMUSG00000032480	Dhx30	0.545996989	0.698780419	0.042669083
ENSMUSG00000060002	Chpt1	0.224465429	-0.85160185	0.042669083
ENSMUSG00000022054	Nefm	0.442864225	-0.806011733	0.042669083
ENSMUSG00000059920	4930453N24Rik	0.084932865	-1.237307817	0.042669083
ENSMUSG00000024127	Prepl	0.084932865	-1.237307817	0.042669083
ENSMUSG00000000787	Ddx3x	1.104127245	0.505051756	0.042669083
ENSMUSG00000025982	Sf3b1	0.897861715	0.549879063	0.043163672
ENSMUSG00000008036	Ap2s1	3.803779024	0.315681526	0.043509767
ENSMUSG00000019817	Plagl1	0.479264024	0.753921973	0.043509767
ENSMUSG00000021951	Eef1akmt1	0.770462418	0.591301773	0.043509767
ENSMUSG00000022897	Dyrk1a	0.376131259	0.850783513	0.043509767
ENSMUSG00000030706	Mprl48	1.425658805	0.448538215	0.043647071
ENSMUSG00000003934	Efnb3	0.35793136	-0.699934775	0.043647071
ENSMUSG00000021913	Ogdhl	0.242665329	1.0790525	0.043647071
ENSMUSG00000006740	Kif5b	0.67946292	-0.547668027	0.043647071
ENSMUSG00000026473	Glul	2.990850174	0.339946842	0.04390829
ENSMUSG00000075700	Selenot	1.553058102	0.431075582	0.04390829
ENSMUSG00000036606	Plxnb2	0.394331159	0.831482957	0.04390829
ENSMUSG00000041261	Car8	0.127399297	1.585322369	0.045224056
ENSMUSG00000020262	Adarb1	0.952461414	0.534140766	0.045224056
ENSMUSG00000048731	Ggnbp1	0.127399297	1.585322369	0.045224056
ENSMUSG00000017639	Rab11fip4	0.673396287	0.628391091	0.045565914
ENSMUSG00000039067	Psmc7	0.533863723	-0.596315196	0.045869774
ENSMUSG00000042532	Golga7b	0.734062619	0.59719647	0.046140835
ENSMUSG00000020919	Stat5b	0.448930858	0.769746941	0.046968234
ENSMUSG00000023169	Slc38a1	0.740129252	0.601279246	0.047210131
ENSMUSG00000097767	Miat	0.503530557	0.723027965	0.047816003
ENSMUSG00000062661	Ncs1	1.346792573	0.455832779	0.048337464
ENSMUSG00000050608	Micos10	4.695574107	0.36742655	0.048384015
ENSMUSG000000109006	B230209E15Rik	0.024266533	-1.857035736	0.048658054
ENSMUSG00000020990	Cdkl1	0	-3.178963831	0.048705171
ENSMUSG00000021071	Trim9	0.964594681	0.524054432	0.049414861
ENSMUSG00000022390	Zc3h7b	0.291198394	0.970082441	0.049414861
ENSMUSG00000024773	Atg2a	0.291198394	0.970082441	0.049414861
ENSMUSG00000029578	Wipi2	0.643063121	0.641937623	0.04946882
ENSMUSG00000026333	Gin1	0.024266533	-1.890983068	0.049661827
ENSMUSG00000006390	Elov1	0.090999498	-1.178963831	0.049694097
ENSMUSG00000038602	Slc35f1	0.303331661	0.931582624	0.049694097
ENSMUSG00000006058	Snf8	0.740129252	-0.520088936	0.049694097

Table S20. DEGs at ZT4 in female and male lateral hypothalamus (LH). The average number of counts per spot in the RHY condition, the log2 fold change in gene expression (RHY relative to saline), and the adjusted p-value (FDR) are shown.

ZT4 FEMALES - LH

FeatureID	FeatureName	ZT4RF count average	ZT4RF Log2FoldChange	ZT4RF FDR
ENSMUSG000000021342	Prl	1.375169903	-6.786365676	1.22011E-16
ENSMUSG00000028298	Cga	0.173340744	-6.71023795	5.47115E-12
ENSMUSG000000090137	Uba52	1.837411888	-2.417527753	1.07506E-11
ENSMUSG00000019970	Sgk1	3.050797097	3.24025382	4.12921E-10
ENSMUSG00000020713	Gh	0.739587175	-7.520932748	4.12921E-10
ENSMUSG000000060143	Gm10076	8.528364611	-1.965107557	3.35918E-09
ENSMUSG00000034892	Rps29	18.95192136	-1.817291199	4.21161E-08

ZT4 MALES - LH

FeatureID	FeatureName	ZT4RM count average	ZT4RM Log2FoldChange	ZT4RM FDR
ENSMUSG000000061808	Ttr	0.571219563	-2.2803153	4.20083E-07
ENSMUSG00000019970	Sgk1	4.74112237	2.356302045	1.0211E-05
ENSMUSG00000023067	Cdkn1a	0.780666736	3.383155315	0.000965066
ENSMUSG000000090137	Uba52	1.837422927	-1.458060465	0.001047777
ENSMUSG00000024907	Gal	0.552178911	-2.217765524	0.001424408
ENSMUSG00000025591	Tma16	0.904430974	2.423153383	0.007674619

ENSMUSG00000067288	Rps28	9.048386843	-1.837137189	4.45871E-08
ENSMUSG00000064360	mt-Nd3	10.65467774	-1.796977427	8.88087E-08
ENSMUSG000000113902	Ndufb1-ps	4.564639595	-1.812290855	9.38102E-08
ENSMUSG00000028998	Tom7	2.415214368	-1.789610352	7.19538E-07
ENSMUSG00000090733	Rps27	11.30181652	-1.660638793	8.69631E-07
ENSMUSG00000027857	Tshb	0.01155605	-6.601601687	1.9162E-06
ENSMUSG00000064356	mt-Atp8	1.386725953	-1.90071558	2.03345E-06
ENSMUSG00000104960	Snhg8	0.832035572	-1.920165104	2.6602E-06
ENSMUSG00000079641	Rpl39	9.187059439	-1.575429542	2.95563E-06
ENSMUSG00000046330	Rpl37a	13.1854526	-1.516204593	7.57475E-06
ENSMUSG00000023067	Cdkn1a	0.681806927	3.044828447	1.89871E-05
ENSMUSG00000046516	Cox17	3.131689444	-1.469081571	5.71333E-05
ENSMUSG00000062997	Rpl35	10.23865995	-1.386684469	6.22085E-05
ENSMUSG00000035383	Pmch	414.7235083	2.069694876	9.4124E-05
ENSMUSG00000071528	Atp5md	15.87801216	-1.339867295	0.00012338
ENSMUSG00000057322	Rpl38	27.06426818	-1.318716236	0.000130809
ENSMUSG00000005705	Agrp	0.520022232	3.883892228	0.000136388
ENSMUSG00000017778	Cox7c	13.56680224	-1.325395205	0.000137962
ENSMUSG00000041841	Rpl37	25.76999063	-1.310881547	0.00013874
ENSMUSG00000065947	mt-Nd4l	2.842788204	-1.466089556	0.0001565
ENSMUSG00000039001	Rps21	30.26529392	-1.298804112	0.00016258
ENSMUSG00000089661	Mia	0.034668149	-4.624562835	0.000207816
ENSMUSG00000016427	Ndufa1	2.611667212	-1.36258506	0.000289872
ENSMUSG00000035674	Ndufa3	6.19404259	-1.293129758	0.000331583
ENSMUSG00000002910	Arrdc2	0.681806927	2.682258367	0.000331583
ENSMUSG00000042737	Dpm3	1.132492862	-1.575097726	0.000352322
ENSMUSG00000103034	Gm8797	0.439129885	3.645732491	0.000390158
ENSMUSG00000096956	Snhg18	0.046224198	-3.192210751	0.000398798
ENSMUSG00000021290	Atp5mpl	6.332715185	-1.224340214	0.000966939
ENSMUSG00000050856	Atp5k	9.244839687	-1.19858244	0.001108275
ENSMUSG00000025400	Tac2	2.184093376	2.871292192	0.001326848
ENSMUSG00000078974	Sec61g	5.038437629	-1.233044468	0.001326848
ENSMUSG00000093674	Rpl41	23.16987946	-1.153043752	0.001522974
ENSMUSG00000042541	Sem1	2.126313128	-1.311228326	0.001819579
ENSMUSG00000034936	Ar14d	0.462241984	2.980916683	0.001917705
ENSMUSG00000029819	Npy	1.201829159	2.135976335	0.002015659
ENSMUSG00000021948	Prkcd	0.924483969	2.285142776	0.002259617
ENSMUSG00000074754	Smim26	0.843591621	-1.445166704	0.002740503
ENSMUSG00000016252	Atp5e	10.06531921	-1.124938978	0.002740503
ENSMUSG00000058351	Smim4	0.30045729	-1.823381681	0.002740503
ENSMUSG00000087687	Pet100	1.109380762	-1.306543426	0.002862031
ENSMUSG00000060981	Hist1h4h	0.023112099	-3.277099648	0.00293295
ENSMUSG00000038803	Ost4	0.704919026	-1.449239071	0.003602502
ENSMUSG00000057863	Rpl36	13.67080669	-1.076475042	0.005107021
ENSMUSG00000078784	Rbis	2.06853288	-1.20671032	0.005845884
ENSMUSG00000070394	Tmem256	2.06853288	-1.231739115	0.006302443
ENSMUSG00000100916	Lhb	0	-4.514138846	0.007489616
ENSMUSG00000057278	Snrpg	1.906748185	-1.222699616	0.007925194
ENSMUSG00000038489	Polr2l	0.855147671	-1.285320155	0.007925194
ENSMUSG00000020018	Snrpf	0.843591621	-1.345099748	0.009286494
ENSMUSG00000079435	Rpl36a	7.811889535	-1.04186416	0.009286494
ENSMUSG00000067847	Romo1	3.154801543	-1.093666256	0.010126745
ENSMUSG00000031760	Mt3	18.94036531	-1.025381341	0.010126745
ENSMUSG00000060636	Rpl35a	21.28624338	-1.023050553	0.010126745
ENSMUSG00000085241	Snhg3	0.392905687	-1.464583021	0.012996313
ENSMUSG00000032532	Cck	3.027684997	1.414356154	0.012996313
ENSMUSG00000098178	Gm42418	5.153998125	-1.15295132	0.015029545
ENSMUSG00000025362	Rps26	14.56062251	-0.978356341	0.018344421
ENSMUSG00000001029	Icam2	0.01155605	-3.30263474	0.027022777
ENSMUSG00000014313	Cox6c	19.34482704	-0.950241365	0.027022777
ENSMUSG00000045394	Epcam	0	-4.30263474	0.03000204
ENSMUSG00000048572	Tmem252	0.265789141	4.530255274	0.030241254
ENSMUSG00000047721	Bola2	2.484550666	-1.024333578	0.034543761



ENSMUSG0000009079	Ewsr1	0.87825977	-1.180238109	0.034543761
ENSMUSG00000097383	1500026H17Rik	0.069336298	-2.201548615	0.035984768
ENSMUSG00000027525	Phactr3	1.860523987	1.219053585	0.037223367
ENSMUSG00000045471	Hcrt	124.1928651	1.53374946	0.037388548
ENSMUSG00000058420	Syt17	0.450685935	1.945292773	0.03805242
ENSMUSG00000098234	Snhg6	0.115560496	-1.952827613	0.042058026
ENSMUSG00000019539	Rcn3	0.034668149	-3.054707227	0.044021407
ENSMUSG00000020163	Uqcr11	8.539920661	-0.917788461	0.044598924
ENSMUSG00000053332	Gas5	9.776417969	-0.922813672	0.045596224
ENSMUSG00000020473	Aebp1	0.080892347	-2.340109446	0.048729861
ENSMUSG00000062006	Rpl34	16.02824081	-0.897845401	0.049137587
ENSMUSG00000073616	Cops9	6.448275682	-0.925182235	0.049946804
ENSMUSG00000066637	Ttc32	0.28890124	2.645732491	0.049946804

Table S2P. DEGs at ZT14 in female and male lateral hypothalamus (LH). The average number of counts per spot in the RHY condition, the log2 fold change in gene expression (RHY relative to saline), and the adjusted p-value (FDR) are shown.

#### ZT14 FEMALES - LH

FeatureID	FeatureName	ZT14RF count average	ZT14RF Log2FoldChange	ZT14RF FDR
ENSMUSG00000037727	Avp	0.026226657	-9.226531502	2.3256E-13
ENSMUSG00000035383	Pmch	502.9092534	3.027155608	4.69757E-09
ENSMUSG00000027301	Oxt	0	-12.12594974	0.002027866
ENSMUSG00000019970	Sgk1	1.901432603	1.808402901	0.006389625
ENSMUSG00000035413	Tmem98	0.065566641	-2.546480904	0.026958944

#### ZT14 MALES - LH

FeatureID	FeatureName	ZT14RM count average	ZT14RM Log2FoldChange	ZT14RM FDR
ENSMUSG00000052305	Hbb-bs	37.32690729	5.390754979	1.37552E-34
ENSMUSG00000069917	Hba-a2	10.21721915	5.326481166	6.97737E-25
ENSMUSG00000069919	Hba-a1	12.43094996	5.00992389	4.3607E-24
ENSMUSG00000027301	Oxt	80.10299812	5.687720491	2.76025E-22
ENSMUSG00000037727	Avp	63.5511031	4.343816881	2.06896E-20
ENSMUSG00000073940	Hbb-bt	3.23545273	4.807107007	1.04956E-18
ENSMUSG00000098178	Gm42418	4.120945056	-1.645589957	6.69664E-14
ENSMUSG00000064354	mt-Co2	40.97104878	-1.132599104	1.32362E-08
ENSMUSG00000064357	mt-Atp6	57.79540298	-0.988089402	1.07325E-06
ENSMUSG00000020932	Gfap	1.873156844	2.57006781	2.99781E-06
ENSMUSG00000061808	Ttr	1.941271638	1.670734565	4.8471E-06
ENSMUSG00000015090	Ptgds	25.71333486	1.04967731	5.18416E-06
ENSMUSG00000064345	mt-Nd2	27.21186033	-0.959156858	5.41726E-06
ENSMUSG00000045471	Hcrt	14.16787722	-2.009301163	1.20522E-05
ENSMUSG00000026697	Myoc	0.47680356	4.129035102	1.32654E-05
ENSMUSG00000037852	Cpe	15.35988612	0.815911276	2.37809E-05
ENSMUSG00000064363	mt-Nd4	34.22768415	-0.85855384	6.59217E-05
ENSMUSG00000031760	Mt3	21.5583324	0.719911902	9.14437E-05
ENSMUSG00000019970	Sgk1	1.702869858	1.70474529	0.000294996
ENSMUSG00000064351	mt-Co1	94.7136215	-0.765617054	0.00084692
ENSMUSG00000062328	Rpl17	8.548406687	-0.849743442	0.001183737
ENSMUSG00000027643	Ghrh	0.885492326	4.169677087	0.001380958
ENSMUSG00000006333	Rps9	3.780371085	-0.963438908	0.001446574
ENSMUSG00000030711	Sult1a1	0.47680356	2.959110101	0.001516386
ENSMUSG00000017344	Vtn	1.157951503	1.650987805	0.001627684
ENSMUSG00000008682	Rpl10	4.325289439	-0.928872032	0.001631068
ENSMUSG00000078974	Sec61g	4.665863411	0.896040736	0.001861285
ENSMUSG000000102252	Snrpn	4.325289439	-0.917406846	0.001891456
ENSMUSG00000041841	Rpl37	24.28292417	0.630462408	0.003513643
ENSMUSG00000064341	mt-Nd1	31.29874799	-0.696822406	0.004699813
ENSMUSG00000000214	Th	0.817377532	1.866000696	0.00561609
ENSMUSG00000069516	Lyz2	0.340573972	3.35964803	0.006884644
ENSMUSG00000090137	Uba52	3.780371085	0.869628092	0.007370812
ENSMUSG00000056201	Cfl1	4.733978205	-0.8506963	0.009401936
ENSMUSG00000038274	Fau	22.47788213	0.561363741	0.010195362
ENSMUSG00000092341	Malat1	1.805042049	-1.034195247	0.011854983
ENSMUSG00000090223	Pcp4	4.972379985	-0.808203584	0.012126081
ENSMUSG00000079484	Phyh1	0.47680356	2.428595384	0.013346405
ENSMUSG00000028495	Rps6	3.678198893	-0.85516122	0.013346405
ENSMUSG00000031765	Mt1	19.03808501	0.562709191	0.0150342
ENSMUSG00000006522	Itih3	2.077501227	1.0470578	0.015946773
ENSMUSG00000037706	Cd81	7.765086552	0.753009264	0.016827013
ENSMUSG00000073418	C4b	0.374631369	2.807107007	0.017049361
ENSMUSG00000047261	Gap43	3.576026702	-0.860506674	0.01903113

ENSMUSG00000052387	Trpm3	0.613033149	1.946510064	0.022447144
ENSMUSG00000028234	Rps20	15.6323453	0.549965169	0.025094366
ENSMUSG00000050711	Scg2	3.099223142	-0.861623851	0.026343221
ENSMUSG00000024403	Atp6v1g2	1.294181092	-1.073653857	0.026343221
ENSMUSG00000092274	Neat1	0.544918355	2.061679834	0.026343221
ENSMUSG00000030541	idh2	0.919549723	1.505937472	0.032293599
ENSMUSG00000032399	Rpl4	14.47439379	1.094216769	0.032860839
ENSMUSG00000084786	Ubi5	5.449183546	0.679617272	0.032942304
ENSMUSG00000034892	Rps29	9.570128602	-0.67722313	0.032942304
ENSMUSG00000068240	Gm11808	0.749262738	1.658243621	0.040583204
ENSMUSG00000026676	Ccdc3	0.170286986	4.807107007	0.043367352
ENSMUSG00000042485	Mustn1	0.170286986	4.807107007	0.043367352
ENSMUSG00000057322	Rpl38	23.05685788	0.496072065	0.046101016

Table S2Q. DEGs at ZT4 in female and male dorso-medial-ventral hypothalamus (DMVH). The average number of counts per spot in the RHY condition, the log2 fold change in gene expression (RHY relative to saline), and the adjusted p-value (FDR) are shown.

#### ZT4 FEMALES - DMVH

FeatureID	FeatureName	ZT4RF count average	ZT4RF Log2FoldChange	ZT4RF FDR
ENSMUSG00000090137	Uba52	1.96882357	-2.223594237	2.23848E-11
ENSMUSG00000019970	Sgk1	2.437019419	2.994200473	2.23848E-11
ENSMUSG00000060143	Gm10076	7.67120891	-2.111184277	1.5028E-10
ENSMUSG00000032532	Cck	5.09012923	2.304632929	6.62678E-10
ENSMUSG00000023067	Cdkn1a	0.900376633	3.513119116	1.70164E-09
ENSMUSG000000113902	Ndufb1-ps	4.309802815	-1.838284518	8.62741E-09
ENSMUSG00000090733	Rps27	10.0361982	-1.778040896	1.17313E-08
ENSMUSG00000067288	Rps28	8.811685978	-1.745189167	2.03219E-08
ENSMUSG00000048572	Tmem252	0.360150653	5.919827631	3.75316E-08
ENSMUSG00000079641	Rpl39	8.41552026	-1.70864647	3.75316E-08
ENSMUSG00000046516	Cox17	2.857195181	-1.774650469	4.534E-08
ENSMUSG000000104960	Snhg8	0.756316371	-1.968059334	1.21939E-07
ENSMUSG00000028998	Tomm7	2.761155007	-1.686445376	1.2616E-07
ENSMUSG00000002910	Arrdc2	0.648271176	2.746991034	3.00353E-07
ENSMUSG000000103034	Gm8797	0.396165718	4.053094162	4.29623E-07
ENSMUSG00000062997	Rpl35	9.712062611	-1.54564304	5.93495E-07
ENSMUSG00000057322	Rpl38	24.77836493	-1.505124543	6.54865E-07
ENSMUSG00000034892	Rps29	19.55618046	-1.523899007	6.54865E-07
ENSMUSG00000016427	Ndufa1	2.593084702	-1.620438816	6.54865E-07
ENSMUSG00000038489	Polr2l	0.600251088	-1.924185762	7.03223E-07
ENSMUSG00000078974	Sec61g	4.189752597	-1.607604692	7.38982E-07
ENSMUSG00000046330	Rpl37a	13.43361936	-1.493097516	8.22909E-07
ENSMUSG00000021647	Cartpt	1.644687982	-2.879313185	1.11251E-06
ENSMUSG00000031431	Tsc22d3	3.997672249	1.548435713	2.13677E-06
ENSMUSG00000074754	Smim26	0.768321393	-1.733100055	2.97588E-06
ENSMUSG00000021290	Atp5mpl	5.882460667	-1.487106888	2.97588E-06
ENSMUSG00000041841	Rpl37	23.86598328	-1.405075808	4.12428E-06
ENSMUSG00000071528	Atp5md	15.89464882	-1.399416734	5.42018E-06
ENSMUSG00000064360	mt-Nd3	11.84895649	-1.409056208	7.44724E-06
ENSMUSG00000039001	Rps21	28.37987146	-1.371346476	7.48762E-06
ENSMUSG00000035383	Pmch	18.53575361	-2.842457102	1.0694E-05
ENSMUSG00000079523	Tmsb10	19.17201976	-1.360083614	1.13032E-05
ENSMUSG00000027525	Phactr3	1.96882357	1.659528193	1.27602E-05
ENSMUSG00000035674	Ndufa3	5.642360231	-1.389602861	1.65715E-05
ENSMUSG00000057863	Rpl36	11.63286609	-1.321981108	2.03481E-05
ENSMUSG00000093674	Rpl41	21.09282325	-1.350540788	2.33115E-05
ENSMUSG00000021342	Pri	2.749149985	-6.712593716	5.32092E-05
ENSMUSG00000057278	Snrpg	1.896793439	-1.416714016	7.29222E-05
ENSMUSG00000020018	Snrpf	0.852356546	-1.557930636	7.29222E-05
ENSMUSG00000038803	Ost4	0.61225611	-1.642267992	8.19196E-05
ENSMUSG00000047721	Bola2	2.112883831	-1.364424655	8.19196E-05
ENSMUSG00000050856	Atp5k	9.135821566	-1.255543465	0.000112159
ENSMUSG00000071637	Cebpd	0.61225611	2.344142944	0.000120635
ENSMUSG00000020713	Gh	1.800753265	-5.895640495	0.000219948

#### ZT4 MALES - DMVH

FeatureID	FeatureName	ZT4RM count average	ZT4RM Log2FoldChange	ZT4RM FDR
ENSMUSG00000024907	Gal	0.411714734	-4.162043042	3.27962E-09
ENSMUSG00000061808	Ttr	0.797288849	-2.087004451	7.87488E-09
ENSMUSG00000027400	Pdyn	0.33329288	-2.461603324	1.45532E-05
ENSMUSG00000040856	Dlk1	0.810359158	-1.734427047	7.64395E-05
ENSMUSG0000005705	Agrp	0	-7.375638515	0.000104185
ENSMUSG00000023067	Cdkn1a	0.660050605	2.364531433	0.000104185
ENSMUSG00000090137	Uba52	2.038968204	-1.378131275	0.000107851
ENSMUSG00000078640	Gm11627	0.372503807	2.92859871	0.000481398
ENSMUSG00000019970	Sgk1	3.019241379	1.755561097	0.000541481
ENSMUSG00000048572	Tmem252	0.26140618	3.750097814	0.000887925
ENSMUSG00000021453	Gadd45g	1.169792656	1.67494554	0.001824611
ENSMUSG00000027301	Oxt	0.058816391	-8.285526096	0.005484349
ENSMUSG00000056380	Gpr50	0.006535155	-4.736737207	0.006653239
ENSMUSG00000045005	Fzd5	0.013070309	-3.270419203	0.013544148
ENSMUSG00000031431	Tsc22d3	3.646616211	1.206367327	0.015719899
ENSMUSG00000020660	Pomc	0.287546798	-3.726625891	0.017298432
ENSMUSG00000070369	Itgad	0.156843708	4.036401999	0.019843932
ENSMUSG00000027210	Meis2	0.758077922	1.940982434	0.022101418
ENSMUSG00000042607	Asb4	0.13070309	-2.048026782	0.027579895
ENSMUSG00000035202	Lars2	1.026019257	-1.161654437	0.031051324
ENSMUSG00000023964	Calcr	0.084957009	-2.085501487	0.044979456
ENSMUSG00000019817	Plagl1	0.222195253	-1.60745419	0.046212612
ENSMUSG00000038760	Trhr	0.045746082	-2.362341693	0.046212612
ENSMUSG00000034936	Arl4d	0.65351545	1.65843987	0.047225161

ENSMUSG0000016252	Atp5e	9.483967197	-1.180798163	0.000341356
ENSMUSG00000098234	Snhg6	0.132055239	-2.204293681	0.000408241
ENSMUSG00000060636	Rpl35a	19.23204487	-1.146865909	0.000441032
ENSMUSG00000073616	Cops9	5.63035521	-1.189208329	0.00055217
ENSMUSG0000017778	Cox7c	14.62211651	-1.1354815	0.00055217
ENSMUSG00000070369	Itgad	0.264110479	4.489193277	0.000557791
ENSMUSG00000025362	Rps26	13.19351892	-1.136568691	0.000557791
ENSMUSG00000053332	Gas5	8.787675935	-1.160555481	0.000558739
ENSMUSG00000036372	Tmem258	1.584662872	-1.303266791	0.000566134
ENSMUSG00000028298	Cga	0.240100435	-6.591513236	0.000580949
ENSMUSG00000078784	Rbis	1.896793439	-1.277991779	0.000594279
ENSMUSG00000068240	Gm11808	0.396165718	-1.583530459	0.000594279
ENSMUSG00000079435	Rpl36a	7.26303817	-1.148196788	0.000631311
ENSMUSG00000093565	Rab26os	0.060025109	-2.599153298	0.000710069
ENSMUSG00000070570	Sic17a7	0.780326415	2.36616925	0.000815705
ENSMUSG00000041046	Ramp3	1.15248209	1.758189241	0.00082466
ENSMUSG00000021948	Prkcd	1.42859759	2.287559415	0.000989993
ENSMUSG00000089661	Mia	0.024010044	-4.884034406	0.000988599
ENSMUSG00000042737	Dpm3	1.332557416	-1.309162799	0.001094566
ENSMUSG00000064356	mt-Atp8	1.620677939	-1.317593245	0.001123905
ENSMUSG00000067847	Romo1	3.037270507	-1.162027954	0.001203437
ENSMUSG00000017734	Dbndd2	4.249777706	1.339274452	0.001348015
ENSMUSG00000019689	Fmc1	1.476617678	-1.224830612	0.001603984
ENSMUSG00000090247	Bloc1s1	0.20408537	-2.024315015	0.001695827
ENSMUSG00000064179	Tnnt1	0.684286241	3.501684221	0.001707864
ENSMUSG00000019539	Rcn3	0.012005022	-4.078762799	0.002006961
ENSMUSG00000014313	Cox6c	18.87189422	-1.053954106	0.002015175
ENSMUSG00000062006	Rpl34	15.35442284	-1.039993229	0.002124412
ENSMUSG00000045471	Hcrt	14.82620188	-2.426130172	0.002124412
ENSMUSG00000022194	Pabpn1	1.392582525	1.312434084	0.002167558
ENSMUSG00000087687	Pet100	1.080451959	-1.271407877	0.002228075
ENSMUSG00000042541	Sem1	2.413009376	-1.137708429	0.002305896
ENSMUSG00000034936	Arl4d	0.40817074	2.094914337	0.002775493
ENSMUSG00000028645	Sic2a1	1.980828592	1.351986065	0.002963942
ENSMUSG00000010406	Mrp152	2.388999332	-1.121831521	0.002963942
ENSMUSG00000020163	Uqcr11	7.839279215	-1.034920063	0.003448891
ENSMUSG00000021040	Slrp	1.15248209	-1.202640162	0.003487606
ENSMUSG00000096956	Snhg18	0.072030131	-3.072503808	0.003487606
ENSMUSG00000025739	Gng13	1.512632743	-1.218111501	0.003904045
ENSMUSG00000028936	Rpl22	3.745566792	-1.089755079	0.004470734
ENSMUSG00000054364	Rhob	4.741983599	1.017559113	0.005030639
ENSMUSG00000026822	Lcn2	0.264110479	3.489193277	0.005819557
ENSMUSG00000061718	Ppp1r1b	0.588246067	1.751506515	0.005831754
ENSMUSG00000106918	Mrpl33	1.488622699	-1.104758007	0.008097034
ENSMUSG00000058351	Smin4	0.372155675	-1.391920684	0.008107385
ENSMUSG00000073702	Rpl31	7.935319389	-0.971451305	0.008247898
ENSMUSG00000008683	Rps15a	12.82136325	-0.962781107	0.008247898
ENSMUSG00000025508	Rplp2	9.051786414	-0.966890465	0.009378429
ENSMUSG00000031760	Mt3	19.97635622	-0.951218265	0.00943239
ENSMUSG00000030711	Sult1a1	0.40817074	1.846986824	0.009649036
ENSMUSG00000035048	Anapc13	1.380577503	-1.095250922	0.010217727
ENSMUSG00000002831	Pliin4	0.168070305	3.872521916	0.010397566
ENSMUSG00000098332	2310009A05Rik	0.420175762	-1.340177109	0.010819553
ENSMUSG00000050288	Fzd2	0.348145631	1.96563132	0.011606092
ENSMUSG00000054312	Mrps21	2.473034484	-1.01507399	0.012078269
ENSMUSG00000084786	Ubl5	6.182586211	-0.949437419	0.012265919
ENSMUSG00000022096	Hr	0.432180784	2.005159685	0.012734338
ENSMUSG00000022018	Rgcc	0.900376633	1.38066882	0.01322385
ENSMUSG00000015090	Ptgds	20.97277303	0.978064851	0.013299252
ENSMUSG00000030790	Adm	0.144060261	4.666071039	0.013967404
ENSMUSG00000038690	Atp5j2	12.22111216	-0.913335581	0.014866361
ENSMUSG00000020660	Pomc	0.672281219	-2.215499136	0.015596128
ENSMUSG00000033174	Mgll	0.732306328	1.460396012	0.01614652

ENSMUSG00000038717	Atp5l	10.87654972	-0.907246297	0.01614652
ENSMUSG00000019890	Nts	0.684286241	-2.184816306	0.016188412
ENSMUSG000000039114	Nrn1	0.900376633	1.458671332	0.016188412
ENSMUSG000000029641	Rasl11a	0.396165718	2.146203566	0.0169259
ENSMUSG00000079480	Pin4	1.35656746	-1.046968716	0.017513845
ENSMUSG000000063935	Zar1	0.264110479	2.319268275	0.019693633
ENSMUSG000000026500	Cox20	1.080451959	-1.06573285	0.02140617
ENSMUSG00000070348	Ccnd1	0.072030131	-2.059903772	0.022890178
ENSMUSG00000006205	Htra1	2.98925042	0.983048374	0.023042588
ENSMUSG000000036781	Rps27l	1.104462003	-1.072638696	0.023533606
ENSMUSG000000033715	Akr1c14	0	-4.356296774	0.024363321
ENSMUSG000000037568	Vash2	0.192080348	2.468131661	0.024885812
ENSMUSG000000070394	Tmem256	2.413009376	-0.949804384	0.024987075
ENSMUSG000000026278	Bok	1.22451222	1.128569892	0.026552935
ENSMUSG000000070637	Srarp	0.216090392	2.628596333	0.028160412
ENSMUSG000000028583	Pdpn	0.012005022	-2.98856499	0.029467631
ENSMUSG000000020108	Ddit4	0.636266154	1.550593821	0.030089379
ENSMUSG000000052296	PPP6r1	0.156065283	-1.61933118	0.031074995
ENSMUSG000000020427	Igfbp3	0.060025109	-2.149845897	0.033416145
ENSMUSG000000049154	Fam183b	0.432180784	-1.394770922	0.036491533
ENSMUSG00000079018	Ly6c1	2.725139941	1.147469643	0.038595648
ENSMUSG000000024038	Ndufv3	5.150154339	-0.87207728	0.039045599
ENSMUSG000000046215	Rprml	0.444185805	1.513119116	0.040164772
ENSMUSG000000039960	Rhou	0.648271176	1.354673611	0.042390492
ENSMUSG000000087590	Epb41laos	0.360150653	-1.269996928	0.043003241
ENSMUSG000000052384	Nrros	0.132055239	2.96563132	0.045593175
ENSMUSG000000021453	Gadd45g	1.368572482	1.042937047	0.045996425
ENSMUSG000000026335	Pam	0.492205893	-1.24938157	0.046276353
ENSMUSG000000071451	Psmg4	0.432180784	-1.191237528	0.046380195
ENSMUSG000000040856	Dlk1	1.536642786	-1.203050514	0.048003757
ENSMUSG000000027364	Usp50	0	-4.078762799	0.04928374

Table S2R. DEGs at ZT14 in female and male dorso-medial-ventral hypothalamus (DMVH). The average number of counts per spot in the RHY condition, the log2 fold change in gene expression (RHY relative to saline), and the adjusted p-value (FDR) are shown.

#### ZT14 FEMALES - DMVH

FeatureID	FeatureName	ZT14RF count average	ZT14RF Log2FoldChange	ZT14RF FDR
ENSMUSG000000019970	Sgk1	2.230997998	2.535042475	6.45981E-08
ENSMUSG000000037727	Avp	0.00851526	-11.23355207	2.52328E-06
ENSMUSG000000027301	Oxt	0.00851526	-10.02895523	6.90888E-06
ENSMUSG000000071637	Cebpd	0.817464915	3.880307637	6.90888E-06
ENSMUSG000000048572	Tmem252	0.766373358	5.958114436	1.14063E-05
ENSMUSG000000026822	Lcn2	2.443879487	7.620244797	5.20717E-05
ENSMUSG000000023067	Cdkn1a	0.459824015	2.909751415	0.000159024
ENSMUSG000000031762	Mt2	5.075094683	1.447905243	0.000401332
ENSMUSG000000025400	Tac2	2.57160838	1.938606277	0.001676427
ENSMUSG000000045471	Hcrt	15.97462689	-2.150694047	0.003589792
ENSMUSG000000031765	Mt1	58.58498561	1.124915477	0.003684561
ENSMUSG000000021025	Nfkbia	0.723797061	1.92238824	0.004979644
ENSMUSG000000051851	Rtl8c	0.17882045	3.909751415	0.007493165
ENSMUSG000000033585	Ndn	5.160247279	-1.105835857	0.018370209
ENSMUSG000000090137	Uba52	8.336439086	0.99249504	0.029054179
ENSMUSG000000027360	Hdc	0.153274672	3.698247309	0.032528142
ENSMUSG000000027875	Hmgcs2	0.170305191	3.257674718	0.036603739

#### ZT14 MALES - DMVH

FeatureID	FeatureName	ZT14RM count average	ZT14RM Log2FoldChange	ZT14RM FDR
ENSMUSG000000061808	Ttr	2.789054253	2.021688075	8.26556E-18
ENSMUSG000000024907	Gal	4.767496679	2.550448482	8.26556E-18
ENSMUSG00000006522	Itih3	3.792014649	1.650090451	1.08413E-11
ENSMUSG00000004154	Ccdc153	0.838090194	4.342987407	3.62616E-11
ENSMUSG000000049154	Fam183b	1.099134681	1.769283084	3.58646E-07
ENSMUSG000000031760	Mt3	26.06323112	0.950629767	4.02563E-07
ENSMUSG000000098178	Gm42418	3.09131629	-1.465025991	4.02563E-07
ENSMUSG000000064357	mt-Atp6	52.2501149	-1.039459716	5.58888E-07
ENSMUSG00000032246	Calml4	0.329740404	3.617609787	7.61999E-07
ENSMUSG000000024033	mt-Nd2	24.12600625	-1.032527905	7.61999E-07
ENSMUSG000000064354	mt-Co2	38.23614771	-1.036316261	7.61999E-07
ENSMUSG000000045471	Hcrt	78.97282683	1.839577055	8.36245E-07
ENSMUSG000000024033	Rsph1	5.0834979	2.484715517	1.61064E-06
ENSMUSG000000040856	Dlk1	1.56626692	1.392978894	2.29809E-06
ENSMUSG00000017754	Pltp	1.346439984	1.648913907	2.52772E-06
ENSMUSG000000035383	Pmch	36.05161754	-1.943832735	4.64909E-06
ENSMUSG00000008682	Rpl10	4.369060357	-1.050908457	7.36993E-06
ENSMUSG000000043164	Tmem212	0.343479588	3.451800894	7.75249E-06
ENSMUSG000000062328	Rpl17	8.779338264	-0.95895329	1.07815E-05
ENSMUSG000000034467	Dynlrb2	0.343479588	3.259155816	1.13653E-05
ENSMUSG00000009281	Rarres2	1.071656314	1.73321383	1.1972E-05
ENSMUSG000000026385	Dbi	12.9148325	1.00318157	1.25927E-05
ENSMUSG000000026879	Gsn	0.686959176	1.873589436	1.25927E-05
ENSMUSG000000034227	Foxj1	0.288522854	3.210792795	2.26598E-05
ENSMUSG000000022982	Sod1	4.259146889	0.947703165	2.26598E-05
ENSMUSG000000064363	mt-Nd4	31.16046821	-0.902621746	2.26598E-05

ENSMUSG00000031765	Mt1	21.35069118	0.824350625	5.79787E-05
ENSMUSG00000015090	Ptgds	21.70790995	1.352447737	6.85274E-05
ENSMUSG00000047021	Cfap65	0.206087753	3.973753598	7.59208E-05
ENSMUSG00000026679	Enkur	0.302262037	2.76034996	0.000146793
ENSMUSG00000073616	Cops9	7.116897059	0.843597206	0.000260544
ENSMUSG00000045573	Penk	1.689919572	1.353041072	0.000260544
ENSMUSG00000032399	Rpl4	14.35744677	0.884614995	0.000278044
ENSMUSG00000064351	mt-Co1	88.4116459	-0.806796195	0.000278044
ENSMUSG000000118506	1700094D03Rik	0.453393056	2.186747321	0.000321669
ENSMUSG00000052861	Dnah6	0.206087753	3.558716098	0.000321669
ENSMUSG00000032532	Cck	0.54956734	-1.387512645	0.000395562
ENSMUSG000000110332	Gm19935	0.384697138	2.16876958	0.00043915
ENSMUSG00000090137	Uba52	3.668361998	0.97016926	0.000534508
ENSMUSG00000027744	Stoml3	0.178609386	3.78110852	0.000580786
ENSMUSG00000078974	Sec61g	4.932366881	0.800270777	0.000580786
ENSMUSG00000074555	Gm10714	0.192348569	3.465606694	0.000729911
ENSMUSG00000041841	Rpl37	28.05541273	0.676372302	0.000780581
ENSMUSG00000047139	Cd24a	0.632002442	1.589742994	0.000806343
ENSMUSG00000026649	Cfap126	0.23356612	2.921286178	0.000813785
ENSMUSG00000035805	Mlc1	2.775315069	0.96195717	0.001175074
ENSMUSG00000102252	Snrpn	4.946106064	-0.808066232	0.001207706
ENSMUSG00000064341	mt-Nd1	28.67367599	-0.744854727	0.001384885
ENSMUSG00000091345	Col6a5	0.164870202	3.674193316	0.001538911
ENSMUSG00000044772	Sntn	0.164870202	3.674193316	0.001538911
ENSMUSG00000028139	Rriad1	0.563306524	1.593481516	0.001694295
ENSMUSG00000028656	Cap1	0.041217551	-2.611208903	0.00187796
ENSMUSG00000060962	Dmkn	0.206087753	2.973753598	0.001976593
ENSMUSG00000020473	Aebp1	0.577045708	3.815055852	0.002718925
ENSMUSG00000066129	Kndc1	1.126613048	1.100865516	0.0035915
ENSMUSG00000089661	Mia	0.522088973	1.558716098	0.00429902
ENSMUSG00000044475	Ascc1	0.714437543	1.332440243	0.00429902
ENSMUSG00000028234	Rps20	17.62737245	0.631889006	0.004823785
ENSMUSG00000024661	Fth1	65.10999066	0.680599203	0.005364967
ENSMUSG00000020163	Uqcr11	7.872552153	0.65888026	0.005807557
ENSMUSG00000073702	Rpl31	8.600728879	0.645244482	0.006719623
ENSMUSG00000086841	2410006H16Rik	1.937224875	0.875573204	0.006719623
ENSMUSG0000001025	S100a6	0.74191591	1.273986621	0.007681645
ENSMUSG00000056201	Cfl1	5.385759937	-0.719230803	0.008082349
ENSMUSG00000038274	Fau	26.72271193	0.582636979	0.00916536
ENSMUSG00000010044	Zmynd10	0.206087753	2.558716098	0.009656604
ENSMUSG000000115718	Gm49179	0.206087753	2.558716098	0.009656604
ENSMUSG00000073418	C4b	0.329740404	1.880644193	0.010698426
ENSMUSG00000071658	Gng3	4.410277907	-0.720469087	0.010837128
ENSMUSG00000042707	Dnali1	0.178609386	2.78110852	0.011097479
ENSMUSG00000029182	1700001C02Rik	0.178609386	2.78110852	0.011097479
ENSMUSG00000057816	Cfap299	0.137391835	3.433185216	0.011097479
ENSMUSG00000025784	Clec3b	0.137391835	3.433185216	0.011097479
ENSMUSG00000031137	Fgf13	0.178609386	-1.576443485	0.011097479
ENSMUSG00000045763	Basp1	2.102095077	-0.881856493	0.011451038
ENSMUSG00000046242	Nme9	0.151131019	3.143678599	0.011592795
ENSMUSG00000026688	Mgst3	0.673219992	-1.035832451	0.012461207
ENSMUSG00000033615	Cplx1	1.126613048	-0.905448258	0.013268367
ENSMUSG00000031980	Agt	4.520191376	0.691418636	0.01341726
ENSMUSG00000023084	Lrrc71	0.096174285	4.558716098	0.014178829
ENSMUSG00000021950	Anxa8	0.096174285	4.558716098	0.014178829
ENSMUSG00000069833	Ahnak	0.261044487	2.073289271	0.014178829
ENSMUSG00000034892	Rps29	9.521254174	-0.663824802	0.016351724
ENSMUSG00000067786	Nnat	12.4202219	0.628109434	0.019199533
ENSMUSG00000023150	lvns1abp	1.195308966	0.94133212	0.019244549
ENSMUSG00000048794	Cfap100	0.192348569	2.465606694	0.01939357
ENSMUSG00000018593	Sparc	13.78040106	0.614380273	0.021363873
ENSMUSG00000020799	Tekt1	0.178609386	2.558716098	0.022287136
ENSMUSG00000041577	Prelp	0.261044487	1.973753598	0.022502162

ENSMUSG00000027712	Anxa5	1.030438763	0.99928869	0.022502162
ENSMUSG00000062591	Tubb4a	1.511310186	-0.811774962	0.022502162
ENSMUSG00000049641	Vgll2	0.109913468	3.7286411	0.022537496
ENSMUSG00000033731	3300002A11Rik	0.109913468	3.7286411	0.022537496
ENSMUSG00000064370	mt-Cytb	65.60460127	-0.603266084	0.024263499
ENSMUSG00000006333	Rps9	5.715500341	-0.65400625	0.024295408
ENSMUSG00000027360	Hdc	0.123652652	3.295681693	0.02504895
ENSMUSG00000048416	Mlf1	0.123652652	3.295681693	0.02504895
ENSMUSG00000012126	Ubxn11	0.329740404	1.743140669	0.02504895
ENSMUSG00000057101	Zfp180	0.27478367	1.951033521	0.02504895
ENSMUSG00000052397	Ezr	0.27478367	1.951033521	0.02504895
ENSMUSG00000024403	Atp6v1g2	1.717397939	-0.77915354	0.02504895
ENSMUSG00000044646	Zbtb7c	0.151131019	2.821750504	0.02504895
ENSMUSG00000033161	Atp1a1	3.32488241	0.718657011	0.025766584
ENSMUSG00000004558	Ndrp2	10.05708233	0.581529902	0.026163689
ENSMUSG00000092274	Neat1	0.370957955	1.611183518	0.027287135
ENSMUSG00000064356	mt-Atp8	0.439653872	-1.11111353	0.028199658
ENSMUSG00000059991	Nptx2	0.632002442	1.182567612	0.028797953
ENSMUSG00000027800	Tm4sf1	0.343479588	1.615299627	0.030344844
ENSMUSG00000029455	Aldh2	1.195308966	0.995779904	0.033564769
ENSMUSG00000040952	Rps19	6.910809307	-0.619454709	0.036433608
ENSMUSG00000018451	6330403K07Rik	21.90025852	0.586109865	0.036433608
ENSMUSG00000026173	Plcd4	0.261044487	1.973753598	0.037906068
ENSMUSG00000074656	Eif2s2	0.755655093	-0.923947827	0.037906068
ENSMUSG00000038570	Saxo2	0.329740404	1.617609787	0.037906068
ENSMUSG00000070436	Serpinh1	0.316001221	1.68424698	0.037906068
ENSMUSG00000035539	Ccdc180	0.082435101	4.36607102	0.03822583
ENSMUSG00000050335	Lgals3	0.082435101	4.36607102	0.03822583
ENSMUSG00000004207	Psap	13.60179168	0.534177422	0.038282804
ENSMUSG00000042613	Pbxip1	0.357218771	1.558716098	0.039817307
ENSMUSG00000041037	Irgq	0.480871423	1.302376345	0.040671778
ENSMUSG00000024076	Vit	0.164870202	2.451800894	0.042323041
ENSMUSG00000004110	Cacna1e	0.535828157	1.236788003	0.042912982
ENSMUSG00000031513	Leprpt1	0.206087753	-1.360147139	0.042912982
ENSMUSG00000019817	Plagl1	0.535828157	1.236788003	0.042912982
ENSMUSG00000074748	Atxn7l3b	0.357218771	-1.137607511	0.043859397
ENSMUSG00000030711	Sult1a1	0.439653872	1.603110218	0.044906018
ENSMUSG00000020932	Gfap	0.590784891	1.185257703	0.044906018
ENSMUSG00000020018	Snrpf	0.824351011	1.013720005	0.045436595
ENSMUSG00000063428	Ddo	0.151131019	2.558716098	0.046847112
ENSMUSG00000057322	Rpl38	26.37923234	0.505270012	0.046847112
ENSMUSG00000029311	Hsd17b11	0.247305303	1.899753016	0.048739351
ENSMUSG00000031927	1700012B09Rik	0.247305303	1.899753016	0.048739351

**Table S3. Gene Ontology analysis performed with DAVID for the DEG sets for bulk, white matter tracts (WMT), cerebral cortex, hippocampus, thalamus, and hypothalamus (LH+DMVH).**

The tables show the results for the FunctAnn\_ChartD - Functional Annotation Chart (obtained checking the options BP\_DIRECT + CC\_DIRECT + MF\_DIRECT + KEGG terms).

**Table S3A. Bulk analysis**

ZT4F (556 DEGs used; 19 not found in DAVID)							
Sublist	Category	Term	Count	Genes	%	P-Value	Benjamini
Ribosome	KEGG_PATHWAY	Ribosome	31	Mrpl33,Mrps21,Rp	5.6	3.10E-19	3.30E-17
	GOTERM_MF_DIRECT	structural constituent of ribosome	35	Ndufa7,Mrpl33,Mr	6.3	1.90E-17	9.60E-15
	GOTERM_CC_DIRECT	ribosome	30	Mt3,Mrpl33,Mrpl5	5.4	1.10E-16	3.70E-14
	GOTERM_CC_DIRECT	cytosolic large ribosomal subunit	17	Rpl2211,Rpl22,Rpl2	3.1	1.20E-10	1.40E-08
	GOTERM_CC_DIRECT	intracellular ribonucleoprotein complex	29	Dhx9,Lsm5,Nop10,	5.2	5.60E-10	3.60E-08
	GOTERM_BP_DIRECT	translation	32	Mrpl33,Mrpl52,Mr	5.8	5.70E-10	1.10E-06
	GOTERM_CC_DIRECT	cytosolic small ribosomal subunit	11	Rps15a,Rps17,Rps2	2	1.90E-07	7.90E-06
	GOTERM_BP_DIRECT	ribosomal small subunit assembly	6	Rps17,Rps25,Rps21	1.1	6.40E-05	4.20E-02
	GOTERM_CC_DIRECT	small ribosomal subunit	6	Rps21,Rps23,Rps21	1.1	3.80E-04	1.00E-02
	Mitochondria	KEGG_PATHWAY	Oxidative phosphorylation	31	Atp8,Atp5j2,Atp5l,	5.6	8.70E-20
GOTERM_CC_DIRECT		mitochondrial inner membrane	35	Atp5j2,Atp5l,Atp5e	6.3	6.70E-12	1.10E-09
GOTERM_CC_DIRECT		respiratory chain	14	Ndufa1,Ndufa2,Nd	2.5	2.90E-10	2.40E-08
GOTERM_CC_DIRECT		mitochondrion	75	Atp8,Atp5j2,Atp5l,	13.5	1.30E-08	7.30E-07
GOTERM_CC_DIRECT		mitochondrial respiratory chain complex I	11	Ndufa1,Ndufa2,Nd	2	5.80E-08	2.70E-06
GOTERM_MF_DIRECT		cytochrome-c oxidase activity	9	Cox8a,Cox8b,Cox7c	1.6	7.60E-08	2.00E-05
GOTERM_CC_DIRECT		mitochondrial proton-transporting ATP synthase complex	7	Atp8,Atp5j2,Atp5l,	1.3	1.60E-06	5.80E-05
GOTERM_BP_DIRECT		ATP biosynthetic process	6	Atp8,Atp5j2,Atp5l,	1.1	1.00E-04	5.00E-02
GOTERM_MF_DIRECT		ubiquinol-cytochrome-c reductase activity	4	Uqcrc,Uqcrc,Uqcrc1	0.7	3.00E-04	3.90E-02
GOTERM_CC_DIRECT		proton-transporting ATP synthase complex, coupling factor F(o)	4	Atp8,Atp5j2,Atp5l,	0.7	2.00E-03	4.00E-02
Disease	GOTERM_CC_DIRECT	mitochondrial proton-transporting ATP synthase complex, coupling factor F(o)	4	Atp8,Atp5j2,Atp5l,	0.7	2.00E-03	4.00E-02
	KEGG_PATHWAY	Parkinson's disease	26	Atp8,Atp5e,Ndufa1	4.7	6.70E-14	4.70E-12
	KEGG_PATHWAY	Huntington's disease	29	Atp8,Atp5e,Ndufa1	5.2	1.60E-13	8.70E-12
	KEGG_PATHWAY	Non-alcoholic fatty liver disease (NAFLD)	25	Fas,Ndufa1,Ndufa2	4.5	1.80E-12	7.70E-11
	KEGG_PATHWAY	Alzheimer's disease	26	Atp8,Atp5e,Fas,Nd	4.7	3.70E-12	1.30E-10
Membrane	GOTERM_CC_DIRECT	membrane	190	Akap12,Arl4d,Atp8,	34.2	2.10E-04	6.30E-03
	GOTERM_CC_DIRECT	focal adhesion	20	Akap12,Tek,Fzd2,Ki	3.6	1.10E-03	2.80E-02
	GOTERM_CC_DIRECT	extracellular space	52	Cd14,Cmtm3,Fas,2l	9.4	1.20E-03	2.90E-02
Others	KEGG_PATHWAY	Cardiac muscle contraction	15	Fxyd2,Cacng1,Cox8	2.7	9.30E-09	2.80E-07
	GOTERM_BP_DIRECT	hydrogen ion transmembrane transport	6	Atp6v0e,Cox8a,Cox	1.1	3.80E-05	3.70E-02
	GOTERM_MF_DIRECT	intracellular	59	Akap12,Arl4d,Depd	10.6	1.00E-04	3.30E-03
GOTERM_MF_DIRECT	growth factor binding	7	Htra1,Tek,Ghrhr,Kd	1.3	2.30E-04	3.90E-02	

ZT4M (453 DEGs used; 5 not found in DAVID)							
Sublist	Category	Term	Count	Genes	%	P-Value	Benjamini
Transcription	GOTERM_MF_DIRECT	transcriptional activator activity, RNA polymerase II core promoter	24	Cebpd,Fos,Pou4f1,	5.3	3.30E-09	1.00E-06
	GOTERM_BP_DIRECT	positive regulation of transcription from RNA polymerase II promot	49	Bcl3,Cebpd,Fos,Klf1	10.8	7.60E-09	1.80E-05
	GOTERM_MF_DIRECT	sequence-specific DNA binding	33	Cebpd,Fos,Irf5,Lhx1	7.3	8.30E-07	1.30E-04
	GOTERM_BP_DIRECT	positive regulation of transcription, DNA-templated	31	Bcl3,Fos,Klf15,Sox1	6.8	1.30E-06	1.50E-03
	GOTERM_MF_DIRECT	RNA polymerase II core promoter proximal region sequence-specifi	23	Cebpd,Fos,Sox10,Sc	5.1	2.30E-06	2.80E-04
	GOTERM_MF_DIRECT	transcription factor activity, sequence-specific DNA binding	37	Bcl3,Cebpd,Fos,Klf1	8.2	2.20E-05	2.00E-03
	GOTERM_MF_DIRECT	transcription regulatory region sequence-specific DNA binding	8	Pou2f1,Sox2,Sox9,E	1.8	7.00E-05	5.40E-03
	GOTERM_CC_DIRECT	transcription factor complex	17	Fos,Pou2f1,Sox2,Sc	3.8	8.00E-05	5.10E-03
	GOTERM_CC_DIRECT	nuclear transcription factor complex	5	Sox14,Sox18,Sox2,	1.1	1.70E-04	8.40E-03
	GOTERM_MF_DIRECT	DNA binding	59	Bcl3,Cebpd,Dhx9,Fr	13	1.60E-04	1.10E-02
	Membrane	GOTERM_CC_DIRECT	extracellular region	73	Bpifa1,Fas,Lao1,Lyf	16.1	1.10E-09
GOTERM_CC_DIRECT		extracellular space	56	Bpifa1,Cmtm3,Fas,	12.4	5.20E-06	8.30E-04
GOTERM_CC_DIRECT		cell surface	30	Cd74,Cd93,Fas,Ada	6.6	2.00E-05	2.10E-03
KEGG_PATHWAY		Cell adhesion molecules (CAMs)	15	Cdh15,Cdh5,Cldn14	3.3	2.70E-05	5.90E-03
GOTERM_CC_DIRECT		bicellular tight junction	12	Cdh5,Cgnl1,Cldn14	2.6	5.50E-05	4.40E-03
GOTERM_CC_DIRECT		external side of plasma membrane	18	Clec14a,Cd74,Fas,	4	1.80E-04	8.40E-03
GOTERM_CC_DIRECT		integral component of plasma membrane	40	Cd74,Fas,Gpr50,Ac	8.8	4.00E-04	1.60E-02
GOTERM_CC_DIRECT		cell junction	29	Shank1,Stard8,Ada,	6.4	4.50E-04	1.60E-02
Protein binding	GOTERM_CC_DIRECT	apicolateral plasma membrane	5	Cldn3,Cldn5,Cldn7,	1.1	6.70E-04	2.10E-02
	GOTERM_MF_DIRECT	protein binding	137	Bcl3,Cebpd,Cd74,C	30.2	4.20E-12	2.60E-09
	GOTERM_MF_DIRECT	protein heterodimerization activity	24	Cebpd,Fos,Sox14,Sc	5.3	1.90E-04	1.20E-02
Hormone	GOTERM_MF_DIRECT	neuropeptide hormone activity	9	Agrip,Avp,Gal,Nppa	2	5.60E-08	1.20E-05
	GOTERM_MF_DIRECT	hormone activity	12	Avp,Gal,Cga,Gnrh1,	2.6	1.20E-05	1.20E-03
Apoptosis	GOTERM_BP_DIRECT	negative regulation of apoptotic process	28	Bcl3,Cd74,Fas,Pou4	6.2	2.10E-05	1.70E-02
Tissue development	GOTERM_BP_DIRECT	angiogenesis	16	Sox18,Acrv11,Anxa2	3.5	8.00E-05	3.80E-02
	GOTERM_BP_DIRECT	cell fate commitment	9	Sox2,Sox8,Sox9,Fgf	2	8.20E-05	3.80E-02
Disease	KEGG_PATHWAY	Pathways in cancer	23	Fos,Fas,Traf1,Adcyf	5.1	1.50E-04	1.60E-02
	KEGG_PATHWAY	HTLV-I infection	18	Fos,Adcy8,Cdkn1a,I	4	2.70E-04	2.00E-02
Immune	GOTERM_CC_DIRECT	mast cell granule	5	Anxa1,Chga,Nppa,	1.1	8.00E-04	2.30E-02
	GOTERM_CC_DIRECT	MHC class II protein complex	4	Cd74,H2-Aa,H2-Ab	0.9	1.40E-03	3.80E-02

ZT14F (114 DEGs used; 3 not found in DAVID)							
Sublist	Category	Term	Count	Genes	%	P-Value	Benjamini
Membrane	GOTERM_CC_DIRECT	extracellular space	25	Aebp1,Fas,S100a8,	21.7	3.70E-07	4.60E-05
	GOTERM_CC_DIRECT	extracellular region	25	Aebp1,Fas,S100a8,	21.7	5.50E-06	2.30E-04
	GOTERM_CC_DIRECT	secretory granule	8	Fas,Avp,Gh,Hcrt,Ox	7	1.70E-06	1.00E-04
Hormone	GOTERM_MF_DIRECT	neuropeptide hormone activity	5	Avp,Hcrt,Oxt,Qrfp,	4.3	1.50E-05	2.90E-03
	GOTERM_MF_DIRECT	hormone activity	7	Avp,Gh,Oxt,Pmch,F	6.1	2.60E-05	2.90E-03

**ZT14M (627 DEGs used; 14 not found in DAVID)**

Sublist	Category	Term	Count	Genes	%	P-Value	Benjamini	
Mitochondria	GOTERM_CC_DIRECT	mitochondrion	93	Hmgcs2Mthfslmt-A	14.8	2.20E-09	1.10E-06	
	KEGG_PATHWAY	Oxidative phosphorylation	21	mt-Atp6mt-Atp8Atf	3.3	3.90E-09	5.50E-07	
	GOTERM_CC_DIRECT	respiratory chain	14	mt-Nd2mt-Nd3mt-I	2.2	5.60E-09	1.40E-06	
	KEGG_PATHWAY	Thermogenesis	27	mt-Atp6mt-Atp8Atf	4.3	7.20E-09	6.80E-07	
	GOTERM_BP_DIRECT	mitochondrial ATP synthesis coupled proton transport	14	mt-Atp6mt-Atp8Atf	2.2	9.50E-09	2.60E-05	
	GOTERM_CC_DIRECT	mitochondrial inner membrane	39	Hmgcs2mt-Atp6Atf	6.2	1.20E-08	2.10E-06	
	GOTERM_BP_DIRECT	aerobic respiration	12	mt-Nd2mt-Nd3mt-I	1.9	3.00E-06	2.70E-03	
	KEGG_PATHWAY	Chemical carcinogenesis - reactive oxygen species	22	mt-Atp6mt-Atp8mt	3.5	3.80E-06	1.50E-04	
	GOTERM_CC_DIRECT	mitochondrial respiratory chain complex I	10	mt-Nd2mt-Nd3mt-I	1.6	5.90E-06	3.30E-04	
	GOTERM_CC_DIRECT	mitochondrial proton-transporting ATP synthase complex	6	mt-Atp6mt-Atp8Atf	1	7.60E-05	3.50E-03	
	Disease	KEGG_PATHWAY	Huntington disease	32	mt-Atp6mt-Atp8mt	5.1	2.30E-09	5.50E-07
		KEGG_PATHWAY	Parkinson disease	28	mt-Atp6mt-Atp8Gp	4.5	2.90E-08	2.00E-06
		KEGG_PATHWAY	Pathways of neurodegeneration - multiple diseases	35	mt-Atp6mt-Atp8Gp	5.6	2.20E-06	1.20E-04
		KEGG_PATHWAY	Amyotrophic lateral sclerosis	30	mt-Atp6mt-Atp8mt	4.8	2.50E-06	1.20E-04
KEGG_PATHWAY		Prion disease	23	mt-Atp6mt-Atp8mt	3.7	2.10E-05	7.70E-04	
KEGG_PATHWAY		Diabetic cardiomyopathy	19	mt-Atp6mt-Atp8mt	3	7.50E-05	2.40E-03	
KEGG_PATHWAY		Alzheimer disease	27	mt-Atp6mt-Atp8mt	4.3	1.00E-04	3.00E-03	
KEGG_PATHWAY		Non-alcoholic fatty liver disease	15	Ndufv3Ndufa1Ndu	2.4	2.80E-04	6.20E-03	
KEGG_PATHWAY		Coronavirus disease - COVID-19	20	VwfAceC4bChuklkb	3.2	1.90E-04	4.40E-03	
Ribosome		GOTERM_CC_DIRECT	cytosolic ribosome	14	Rpl10Rpl17Rpl22Rl	2.2	1.60E-07	1.70E-05
		GOTERM_CC_DIRECT	cytosolic large ribosomal subunit	13	Rpl10Rpl17Rpl22Rl	2.1	1.60E-07	1.70E-05
	GOTERM_CC_DIRECT	ribosome	19	Mt3Mrps21Gm118	3	3.40E-06	2.20E-04	
	GOTERM_MF_DIRECT	structural constituent of ribosome	20	Mrps21Gm11808G	3.2	6.20E-07	5.20E-04	
	GOTERM_BP_DIRECT	cytoplasmic translation	13	Rpl17Rpl22Rpl31Rl	2.1	2.80E-06	2.70E-03	
	KEGG_PATHWAY	Ribosome	16	Mrps21Rpl10Rpl17	2.6	3.60E-04	7.40E-03	
	GOTERM_CC_DIRECT	cytosolic small ribosomal subunit	8	Ddx3xHba-a1Hba-z	1.3	2.60E-04	1.00E-02	
Membrane	GOTERM_CC_DIRECT	extracellular region	82	Adamts14Cap1Cartj	13.1	2.80E-06	2.00E-04	
	GOTERM_CC_DIRECT	membrane	221	Arl4dmt-Atp8Atp5n	35.2	3.40E-05	1.70E-03	
	GOTERM_CC_DIRECT	extracellular space	77	CartptCd74Cmtrm5l	12.3	3.10E-04	1.10E-02	
	GOTERM_CC_DIRECT	extracellular matrix	18	Adamts14SspoVwfA	2.9	1.50E-03	4.40E-02	
Cytosol	GOTERM_CC_DIRECT	cytoplasm	246	MthfslAkap8Arl4d	39.2	1.10E-06	9.30E-05	
	GOTERM_CC_DIRECT	cytosol	139	MthfslAhnakAtp8b	22.2	1.30E-03	4.40E-02	
Others	GOTERM_MF_DIRECT	protein binding	187	AhnakAtpif1Atp8b2	29.8	1.30E-05	5.40E-03	
	GOTERM_BP_DIRECT	neuropeptide signaling pathway	11	CartptEcrg4Gpr37E	1.8	1.10E-04	7.70E-02	
	GOTERM_CC_DIRECT	myelin sheath	16	Car2Cldn11Cntnap	2.6	1.60E-04	6.70E-03	
	KEGG_PATHWAY	Retrograde endocannabinoid signaling	15	mt-Nd2mt-Nd3mt-I	2.4	1.60E-04	4.20E-03	
	KEGG_PATHWAY	Cardiac muscle contraction	10	Fxyd2Cacng2mt-Cy	1.6	1.30E-03	2.40E-02	
	GOTERM_CC_DIRECT	postsynaptic density	21	mt-Nd2NsmfArhga	3.3	1.40E-03	4.40E-02	

**ZT4 F&M COMMON DEGs < 0.05 (105 used : 3 not found in DAVID)**

Category	Term	Count	Genes	%	P-Value	Benjamini
GOTERM_MF_DIRECT	transcriptional activator activity, RNA polymerase II core promoter	9	Cebpd,Sox2,Sox9,Ej	8.6	3.00E-05	6.30E-03
KEGG_PATHWAY	PI3K-Akt signaling pathway	9	Ddit4,Tek,Fgf21,Gh	8.6	4.40E-04	4.10E-02

**ZT14 F&M COMMON DEGs < 0.05 (28 used : 1 not found in DAVID)**

Category	Term	Count	Genes	%	P-Value	Benjamini
GOTERM_CC_DIRECT	extracellular space	8	S100a8,Bloc1s1,F3	29.6	1.20E-03	5.50E-02
GOTERM_BP_DIRECT	steroid metabolic process	3	Hmgcs2,Ch25h,Sult	11.1	4.20E-03	8.00E-01



Table S3B. DAVID GO analysis for white matter tracts (WMT).

ZT4F WMT					
Category	Term	Count	%	P-Value	Benjamini
GOTERM_MF_ALL	structural constituent of ribosome	28	15.1	1E-21	5E-19
KEGG_PATHWAY	Ribosome	25	13.5	1.3E-20	1.8E-18
GOTERM_CC_ALL	ribosome	28	15.1	2.5E-20	9.6E-18
GOTERM_CC_ALL	ribosomal subunit	25	13.5	8E-20	1.5E-17
GOTERM_CC_ALL	cytosolic ribosome	22	11.9	2.2E-19	2.8E-17
GOTERM_CC_ALL	inner mitochondrial membrane protein complex	18	9.7	6.8E-16	6.5E-14
GOTERM_CC_ALL	cytosolic part	23	12.4	2.8E-15	2.1E-13
GOTERM_CC_ALL	mitochondrial inner membrane	27	14.6	3.3E-15	2.1E-13
GOTERM_CC_ALL	mitochondrial protein complex	19	10.3	3.8E-15	2.1E-13
GOTERM_CC_ALL	organelle inner membrane	28	15.1	6.7E-15	3.2E-13
KEGG_PATHWAY	Oxidative phosphorylation	20	10.8	8.5E-15	5.7E-13
GOTERM_CC_ALL	mitochondrial membrane part	20	10.8	1.2E-14	5.1E-13
GOTERM_CC_ALL	large ribosomal subunit	17	9.2	4.8E-14	1.9E-12
GOTERM_CC_ALL	cytosolic large ribosomal subunit	15	8.1	5.4E-14	1.9E-12
GOTERM_CC_ALL	mitochondrial envelope	31	16.8	7.7E-14	2.4E-12
GOTERM_CC_ALL	cytoplasmic part	112	60.5	8.2E-14	2.4E-12
GOTERM_CC_ALL	mitochondrion	50	27	2.3E-13	6.2E-12
GOTERM_MF_ALL	structural molecule activity	31	16.8	3.7E-13	9.2E-11
GOTERM_CC_ALL	mitochondrial membrane	29	15.7	5.4E-13	1.4E-11
GOTERM_CC_ALL	mitochondrial part	34	18.4	8.2E-13	2E-11
GOTERM_CC_ALL	cytoplasm	136	73.5	3.3E-12	7.4E-11
GOTERM_CC_ALL	intracellular part	156	84.3	1.5E-11	3.2E-10
GOTERM_CC_ALL	respiratory chain	13	7	1.6E-11	3.2E-10
GOTERM_CC_ALL	organelle	151	81.6	2.8E-11	5.3E-10
GOTERM_BP_ALL	organonitrogen compound metabolic process	49	26.5	3.8E-11	0.00000011
GOTERM_CC_ALL	intracellular organelle	143	77.3	7.9E-11	1.4E-09
GOTERM_BP_ALL	translation	28	15.1	8.8E-11	0.00000013
GOTERM_CC_ALL	respiratory chain complex	12	6.5	9E-11	1.6E-09
GOTERM_CC_ALL	mitochondrial respiratory chain	12	6.5	1E-10	1.7E-09
GOTERM_CC_ALL	intracellular organelle part	108	58.4	1.1E-10	1.7E-09
GOTERM_CC_ALL	intracellular	158	85.4	1.3E-10	1.9E-09
GOTERM_BP_ALL	peptide biosynthetic process	28	15.1	1.7E-10	0.00000016
GOTERM_CC_ALL	cytosol	48	25.9	2E-10	2.9E-09
GOTERM_CC_ALL	organelle part	108	58.4	5.5E-10	7.9E-09
GOTERM_CC_ALL	intracellular ribonucleoprotein complex	31	16.8	5.9E-10	0.00000008
GOTERM_CC_ALL	ribonucleoprotein complex	31	16.8	6.1E-10	0.00000008
KEGG_PATHWAY	Parkinson's disease	16	8.6	6.2E-10	0.00000028
GOTERM_CC_ALL	organelle envelope	33	17.8	8.4E-10	0.00000011
GOTERM_CC_ALL	envelope	33	17.8	9.4E-10	0.00000012
GOTERM_BP_ALL	amide biosynthetic process	28	15.1	1.3E-09	0.00000089
GOTERM_CC_ALL	oxidoreductase complex	12	6.5	1.3E-09	0.00000016
GOTERM_BP_ALL	peptide metabolic process	29	15.7	1.5E-09	0.00000089
GOTERM_CC_ALL	macromolecular complex	82	44.3	1.7E-09	0.00000019
GOTERM_BP_ALL	organonitrogen compound biosynthetic process	36	19.5	2.4E-09	0.0000012
GOTERM_CC_ALL	NADH dehydrogenase complex	9	4.9	6.8E-09	0.00000073
GOTERM_CC_ALL	respiratory chain complex I	9	4.9	6.8E-09	0.00000073
GOTERM_CC_ALL	mitochondrial respiratory chain complex I	9	4.9	6.8E-09	0.00000073
GOTERM_BP_ALL	cellular amide metabolic process	30	16.2	0.00000016	0.0000065
KEGG_PATHWAY	Huntington's disease	16	8.6	0.00000032	0.0000011
GOTERM_BP_ALL	purine nucleoside triphosphate metabolic process	14	7.6	0.00000013	0.0000041
GOTERM_BP_ALL	purine ribonucleoside monophosphate metabolic process	14	7.6	0.00000014	0.0000041
GOTERM_CC_ALL	membrane-bounded organelle	136	73.5	0.00000014	0.0000015
GOTERM_BP_ALL	purine nucleoside monophosphate metabolic process	14	7.6	0.00000014	0.0000041
GOTERM_BP_ALL	purine ribonucleoside metabolic process	15	8.1	0.00000022	0.0000053
GOTERM_BP_ALL	ribonucleoside monophosphate metabolic process	14	7.6	0.00000024	0.0000053
GOTERM_BP_ALL	purine nucleoside metabolic process	15	8.1	0.00000026	0.0000053
GOTERM_BP_ALL	ATP metabolic process	13	7	0.00000026	0.0000053
GOTERM_BP_ALL	nucleoside monophosphate metabolic process	14	7.6	0.00000035	0.0000067
GOTERM_BP_ALL	nucleoside triphosphate metabolic process	14	7.6	0.0000004	0.0000072
KEGG_PATHWAY	Alzheimer's disease	14	7.6	0.00000041	0.0000011
GOTERM_BP_ALL	ribonucleoside metabolic process	15	8.1	0.00000057	0.0000096
GOTERM_BP_ALL	purine ribonucleoside triphosphate metabolic process	13	7	0.00000063	0.0001
KEGG_PATHWAY	Non-alcoholic fatty liver disease (NAFLD)	13	7	0.00000077	0.0000017
GOTERM_BP_ALL	ribonucleoside triphosphate metabolic process	13	7	0.00000087	0.00013
GOTERM_CC_ALL	mitochondrial proton-transporting ATP synthase complex	6	3.2	0.0000011	0.0000011
GOTERM_BP_ALL	nucleoside metabolic process	15	8.1	0.0000012	0.00017
GOTERM_CC_ALL	proton-transporting ATP synthase complex	6	3.2	0.0000014	0.0000014
GOTERM_MF_ALL	hydrogen ion transmembrane transporter activity	9	4.9	0.0000021	0.00035
GOTERM_BP_ALL	glycosyl compound metabolic process	15	8.1	0.0000024	0.00032
GOTERM_CC_ALL	cytosolic small ribosomal subunit	7	3.8	0.0000067	0.000064
GOTERM_CC_ALL	small ribosomal subunit	8	4.3	0.0000089	0.000084
GOTERM_CC_ALL	membrane protein complex	25	13.5	0.00001	0.000093
GOTERM_CC_ALL	intracellular membrane-bounded organelle	121	65.4	0.000017	0.00015
GOTERM_CC_ALL	cell part	167	90.3	0.000022	0.00019
GOTERM_CC_ALL	cell	167	90.3	0.000029	0.00025
GOTERM_BP_ALL	respiratory electron transport chain	7	3.8	0.000034	0.0004
GOTERM_BP_ALL	mitochondrial respiratory chain complex assembly	6	3.2	0.000037	0.0004
GOTERM_BP_ALL	purine-containing compound metabolic process	16	8.6	0.000039	0.0004
GOTERM_BP_ALL	purine ribonucleoside monophosphate biosynthetic process	7	3.8	0.00004	0.0004
GOTERM_BP_ALL	purine nucleoside monophosphate biosynthetic process	7	3.8	0.00004	0.0004
GOTERM_BP_ALL	electron transport chain	7	3.8	0.000054	0.00057
GOTERM_CC_ALL	catalytic complex	24	13	0.000058	0.00048

GOTERM_BP_ALL	purine nucleotide metabolic process	15	8.1	0.000062	0.0064
GOTERM_CC_ALL	proton-transporting two-sector ATPase complex	6	3.2	0.000067	0.00055
GOTERM_BP_ALL	ATP biosynthetic process	6	3.2	0.000069	0.0069
GOTERM_BP_ALL	ribonucleoside monophosphate biosynthetic process	7	3.8	0.000093	0.0089
GOTERM_BP_ALL	nucleoside monophosphate biosynthetic process	7	3.8	0.00013	0.012
GOTERM_BP_ALL	purine ribonucleotide metabolic process	14	7.6	0.00014	0.012
GOTERM_BP_ALL	cytochrome complex assembly	5	2.7	0.00014	0.012
GOTERM_BP_ALL	nitrogen compound metabolic process	80	43.2	0.00014	0.012
GOTERM_BP_ALL	oxidation-reduction process	21	11.4	0.00015	0.012
GOTERM_BP_ALL	purine ribonucleoside biosynthetic process	7	3.8	0.00015	0.012
GOTERM_BP_ALL	purine nucleoside biosynthetic process	7	3.8	0.00015	0.012
GOTERM_BP_ALL	generation of precursor metabolites and energy	12	6.5	0.00016	0.012
GOTERM_BP_ALL	proton transport	7	3.8	0.00017	0.012
GOTERM_CC_ALL	mitochondrial proton-transporting ATP synthase complex, coupling factor F(o)	4	2.2	0.00018	0.0014
GOTERM_BP_ALL	purine ribonucleoside triphosphate biosynthetic process	6	3.2	0.00018	0.012
GOTERM_BP_ALL	hydrogen transport	7	3.8	0.00018	0.012
GOTERM_BP_ALL	ribonucleotide metabolic process	14	7.6	0.00019	0.012
GOTERM_BP_ALL	hydrogen ion transmembrane transport	6	3.2	0.0002	0.012
GOTERM_BP_ALL	cytoplasmic translation	6	3.2	0.0002	0.012
GOTERM_BP_ALL	purine nucleoside triphosphate biosynthetic process	6	3.2	0.0002	0.012
GOTERM_BP_ALL	nucleotide metabolic process	16	8.6	0.00021	0.013
GOTERM_MF_ALL	NADH dehydrogenase (quinone) activity	5	2.7	0.00021	0.02
GOTERM_MF_ALL	NADH dehydrogenase (ubiquinone) activity	5	2.7	0.00021	0.02
GOTERM_CC_ALL	vesicle	52	28.1	0.00022	0.0018
GOTERM_BP_ALL	energy derivation by oxidation of organic compounds	10	5.4	0.00024	0.014
GOTERM_MF_ALL	NADH dehydrogenase activity	5	2.7	0.00024	0.02
GOTERM_BP_ALL	ribose phosphate metabolic process	14	7.6	0.00024	0.014
GOTERM_BP_ALL	cellular nitrogen compound metabolic process	76	41.1	0.00024	0.014
GOTERM_BP_ALL	nucleoside phosphate metabolic process	16	8.6	0.00025	0.014
GOTERM_BP_ALL	response to endogenous stimulus	29	15.7	0.00025	0.014
GOTERM_CC_ALL	proton-transporting ATP synthase complex, coupling factor F(o)	4	2.2	0.00028	0.0021
GOTERM_BP_ALL	ribonucleoside triphosphate biosynthetic process	6	3.2	0.00028	0.016
GOTERM_BP_ALL	cellular biosynthetic process	71	38.4	0.00037	0.02
GOTERM_BP_ALL	cellular respiration	8	4.3	0.00038	0.02
GOTERM_BP_ALL	ribonucleoside biosynthetic process	7	3.8	0.00042	0.022
GOTERM_BP_ALL	nucleoside biosynthetic process	7	3.8	0.00042	0.022
GOTERM_CC_ALL	organelle membrane	37	20	0.00044	0.0033
GOTERM_BP_ALL	cellular nitrogen compound biosynthetic process	61	33	0.00045	0.023
GOTERM_BP_ALL	glycosyl compound biosynthetic process	7	3.8	0.00046	0.023
GOTERM_BP_ALL	metabolic process	115	62.2	0.00049	0.024
GOTERM_BP_ALL	cellular metabolic process	106	57.3	0.00054	0.026
GOTERM_MF_ALL	oxidoreductase activity, acting on NAD(P)H, quinone or similar compound as acceptor	5	2.7	0.00057	0.04
GOTERM_BP_ALL	cellular response to endogenous stimulus	23	12.4	0.00057	0.027
GOTERM_BP_ALL	nucleobase-containing small molecule metabolic process	16	8.6	0.00057	0.027
GOTERM_BP_ALL	biosynthetic process	72	38.9	0.00058	0.027
GOTERM_BP_ALL	nucleoside triphosphate biosynthetic process	6	3.2	0.0006	0.027
GOTERM_BP_ALL	organic substance biosynthetic process	71	38.4	0.00063	0.028

#### ZT14M WMT

Category	Term	Count	%	P-Value	Benjamini
GOTERM_BP_ALL	response to abiotic stimulus	11	27.5	0.000025	0.041
GOTERM_BP_ALL	response to nitrogen compound	10	25	0.000056	0.047

#### ZT14F WMT

Category	Term	Count	%	P-Value	Benjamini
GOTERM_BP_ALL	negative regulation of biological process	30	51.7	0.0000022	0.0043
GOTERM_CC_ALL	organelle	50	86.2	0.0000033	0.00023
GOTERM_CC_ALL	intracellular organelle	48	82.8	0.0000034	0.00023
GOTERM_CC_ALL	intracellular	52	89.7	0.0000043	0.00023
GOTERM_CC_ALL	intracellular part	51	87.9	0.0000051	0.00023
GOTERM_BP_ALL	response to glucocorticoid	7	12.1	0.0000058	0.0051
GOTERM_BP_ALL	intracellular signal transduction	20	34.5	0.0000089	0.0051
GOTERM_CC_ALL	intracellular membrane-bounded organelle	45	77.6	0.0000089	0.00032
GOTERM_BP_ALL	response to corticosteroid	7	12.1	0.00001	0.0051
GOTERM_CC_ALL	membrane-bounded organelle	47	81	0.000017	0.00053
GOTERM_BP_ALL	response to stimulus	40	69	0.000032	0.011
GOTERM_BP_ALL	signal transduction	31	53.4	0.000038	0.011
GOTERM_BP_ALL	single organism signaling	32	55.2	0.000045	0.011
GOTERM_BP_ALL	response to toxic substance	6	10.3	0.000051	0.011
GOTERM_BP_ALL	signaling	32	55.2	0.000051	0.011
GOTERM_BP_ALL	cellular response to stimulus	35	60.3	0.000061	0.011
GOTERM_BP_ALL	cell communication	32	55.2	0.000063	0.011
GOTERM_BP_ALL	negative regulation of cellular process	26	44.8	0.00008	0.013
GOTERM_BP_ALL	negative regulation of signal transduction	12	20.7	0.000089	0.014
GOTERM_BP_ALL	growth	12	20.7	0.000097	0.014
GOTERM_CC_ALL	cytoplasm	42	72.4	0.00022	0.0058
GOTERM_BP_ALL	negative regulation of cell communication	12	20.7	0.00027	0.032
GOTERM_BP_ALL	negative regulation of signaling	12	20.7	0.00027	0.032
GOTERM_BP_ALL	cell surface receptor signaling pathway	17	29.3	0.00028	0.032
GOTERM_BP_ALL	response to endogenous stimulus	14	24.1	0.00032	0.035
GOTERM_BP_ALL	enzyme linked receptor protein signaling pathway	10	17.2	0.00038	0.04
GOTERM_BP_ALL	transmembrane receptor protein tyrosine kinase signaling pathway	8	13.8	0.00044	0.044
GOTERM_BP_ALL	response to steroid hormone	7	12.1	0.00052	0.05
GOTERM_CC_ALL	cytosol	15	25.9	0.00067	0.015
GOTERM_CC_ALL	cytoplasmic part	32	55.2	0.00096	0.019

## ZT14M WMT

Category	Term	Count	%	P-Value	Benjamini
GOTERM_CC_ALL	extracellular region	51	49	1.1E-09	0.0000028
GOTERM_BP_ALL	behavior	20	19.2	2.1E-09	0.0000058
GOTERM_CC_ALL	extracellular vesicle	38	36.5	2.2E-09	0.0000028
GOTERM_CC_ALL	extracellular organelle	38	36.5	2.3E-09	0.0000028
GOTERM_CC_ALL	extracellular exosome	37	35.6	7.2E-09	0.0000064
GOTERM_CC_ALL	membrane-bounded vesicle	42	40.4	0.00000016	0.0000096
GOTERM_CC_ALL	extracellular region part	45	43.3	0.00000018	0.0000096
GOTERM_CC_ALL	vesicle	43	41.3	0.00000019	0.0000096
GOTERM_CC_ALL	neuron part	27	26	0.00000006	0.0000026
GOTERM_BP_ALL	single-organism behavior	15	14.4	0.00000021	0.00028
GOTERM_CC_ALL	axon	15	14.4	0.00000088	0.000033
GOTERM_CC_ALL	cell projection	29	27.9	0.00000094	0.000033
GOTERM_CC_ALL	extracellular space	24	23.1	0.0000024	0.000077
GOTERM_CC_ALL	neuron projection	21	20.2	0.000003	0.000089
GOTERM_BP_ALL	response to metal ion	11	10.6	0.000008	0.0055
GOTERM_BP_ALL	modulation of synaptic transmission	11	10.6	0.000008	0.0055
GOTERM_MF_ALL	G-protein coupled receptor binding	10	9.6	0.0000088	0.0038
GOTERM_CC_ALL	myelin sheath	9	8.7	0.000012	0.0003
GOTERM_CC_ALL	somatodendritic compartment	17	16.3	0.000012	0.0003
GOTERM_BP_ALL	regulation of neuronal synaptic plasticity	6	5.8	0.000019	0.008
GOTERM_CC_ALL	axon part	10	9.6	0.000023	0.00054
GOTERM_BP_ALL	cognition	10	9.6	0.000024	0.008
GOTERM_BP_ALL	long-term memory	5	4.8	0.000027	0.008
GOTERM_BP_ALL	response to inorganic substance	13	12.5	0.000028	0.008
GOTERM_BP_ALL	anterograde trans-synaptic signaling	13	12.5	0.000035	0.008
GOTERM_BP_ALL	synaptic signaling	13	12.5	0.000035	0.008
GOTERM_BP_ALL	chemical synaptic transmission	13	12.5	0.000035	0.008
GOTERM_BP_ALL	trans-synaptic signaling	13	12.5	0.000035	0.008
GOTERM_MF_ALL	hormone activity	7	6.7	0.000038	0.0083
GOTERM_BP_ALL	memory	7	6.7	0.000045	0.0096
GOTERM_BP_ALL	response to endogenous stimulus	22	21.2	0.000053	0.01
GOTERM_BP_ALL	response to abiotic stimulus	18	17.3	0.000069	0.012
GOTERM_BP_ALL	neurogenesis	22	21.2	0.000069	0.012
GOTERM_BP_ALL	response to hormone	15	14.4	0.000076	0.012
GOTERM_BP_ALL	learning or memory	9	8.7	0.000078	0.012
GOTERM_BP_ALL	response to oxygen-containing compound	22	21.2	0.000092	0.013
GOTERM_BP_ALL	regulation of synapse structure or activity	9	8.7	0.000098	0.013
GOTERM_BP_ALL	positive regulation of synaptic transmission	7	6.7	0.00011	0.015
GOTERM_BP_ALL	regulation of cellular component organization	27	26	0.00013	0.016
GOTERM_BP_ALL	nervous system development	26	25	0.00014	0.016
GOTERM_BP_ALL	aging	9	8.7	0.00015	0.017
GOTERM_CC_ALL	cytoplasm	71	68.3	0.00015	0.0033
GOTERM_BP_ALL	response to organonitrogen compound	15	14.4	0.00015	0.017
GOTERM_BP_ALL	cellular response to stimulus	56	53.8	0.00016	0.017
GOTERM_BP_ALL	response to nitrogen compound	16	15.4	0.00018	0.018
GOTERM_BP_ALL	response to organic cyclic compound	16	15.4	0.00018	0.018
GOTERM_BP_ALL	cellular component organization	48	46.2	0.00022	0.021
GOTERM_CC_ALL	cell body	13	12.5	0.00025	0.0053
GOTERM_BP_ALL	regulation of synaptic plasticity	7	6.7	0.00026	0.024
GOTERM_BP_ALL	regulation of neurogenesis	14	13.5	0.0003	0.026
GOTERM_CC_ALL	cell projection part	16	15.4	0.00031	0.0061
GOTERM_CC_ALL	dendrite	12	11.5	0.00033	0.0061
GOTERM_CC_ALL	membrane-bounded organelle	76	73.1	0.00036	0.0063
GOTERM_BP_ALL	cellular component organization or biogenesis	48	46.2	0.00046	0.039
GOTERM_BP_ALL	neuron-neuron synaptic transmission	6	5.8	0.00048	0.04
GOTERM_BP_ALL	astrocyte differentiation	5	4.8	0.00052	0.041
GOTERM_BP_ALL	response to lipid	15	14.4	0.00052	0.041
GOTERM_CC_ALL	ribosome	8	7.7	0.00057	0.0096
GOTERM_BP_ALL	regulation of biological quality	32	30.8	0.00059	0.045
GOTERM_BP_ALL	response to transition metal nanoparticle	6	5.8	0.00062	0.046
GOTERM_BP_ALL	neuropeptide signaling pathway	5	4.8	0.00063	0.046
GOTERM_BP_ALL	gliogenesis	8	7.7	0.00068	0.047
GOTERM_BP_ALL	generation of neurons	19	18.3	0.00069	0.047
GOTERM_BP_ALL	regulation of long-term neuronal synaptic plasticity	4	3.8	0.0007	0.047
GOTERM_BP_ALL	response to organic substance	29	27.9	0.00073	0.048

Table S3C. DAVID GO analysis for the cerebral cortex.

ZT4F Cortex		Count	%	P-Value	Benjamini
Category	Term				
GOTERM_MF_ALL	structural constituent of ribosome	23	17.4	1.3E-20	4.3E-18
KEGG_PATHWAY	Ribosome	21	15.9	3.1E-19	3.3E-17
GOTERM_CC_ALL	ribosome	23	17.4	7.2E-19	1.3E-16
GOTERM_CC_ALL	ribosomal subunit	21	15.9	8.3E-19	1.3E-16
GOTERM_CC_ALL	cytosolic ribosome	18	13.6	1.8E-17	1.8E-15
KEGG_PATHWAY	Oxidative phosphorylation	19	14.4	7.8E-17	4.2E-15
GOTERM_CC_ALL	mitochondrial envelope	28	21.2	3.5E-16	2.6E-14
GOTERM_CC_ALL	mitochondrion	43	32.6	4.3E-16	2.6E-14
GOTERM_CC_ALL	mitochondrial membrane part	18	13.6	1.7E-15	8.4E-14
GOTERM_CC_ALL	mitochondrial inner membrane	23	17.4	1.9E-15	8.4E-14
GOTERM_CC_ALL	mitochondrial membrane	26	19.7	6.5E-15	2.5E-13
GOTERM_CC_ALL	mitochondrial part	30	22.7	7.4E-15	2.5E-13
GOTERM_CC_ALL	inner mitochondrial membrane protein complex	15	11.4	1.2E-14	3.6E-13
GOTERM_CC_ALL	cytosolic part	19	14.4	2E-14	5.4E-13
GOTERM_CC_ALL	organelle inner membrane	23	17.4	2.3E-14	5.4E-13
GOTERM_CC_ALL	mitochondrial protein complex	16	12.1	2.3E-14	5.4E-13
GOTERM_CC_ALL	large ribosomal subunit	15	11.4	3.6E-14	7.8E-13
GOTERM_CC_ALL	respiratory chain	13	9.8	1E-13	2.1E-12
GOTERM_CC_ALL	cytoplasmic part	81	61.4	1.4E-13	2.7E-12
GOTERM_CC_ALL	cytosolic large ribosomal subunit	13	9.8	1.5E-13	2.7E-12
GOTERM_CC_ALL	mitochondrial respiratory chain	12	9.1	1E-12	1.7E-11
GOTERM_CC_ALL	organelle envelope	29	22	8.3E-12	1.3E-10
KEGG_PATHWAY	Huntington's disease	17	12.9	9.2E-12	3.3E-10
GOTERM_CC_ALL	envelope	29	22	9.3E-12	1.4E-10
GOTERM_MF_ALL	structural molecule activity	23	17.4	1.7E-11	2.8E-09
KEGG_PATHWAY	Alzheimer's disease	16	12.1	2.3E-11	6E-10
GOTERM_CC_ALL	respiratory chain complex	11	8.3	2.7E-11	3.9E-10
KEGG_PATHWAY	Parkinson's disease	15	11.4	2.8E-11	6E-10
GOTERM_BP_ALL	translation	23	17.4	4.8E-11	0.000000084
KEGG_PATHWAY	Non-alcoholic fatty liver disease (NAFLD)	15	11.4	5.8E-11	0.000000001
GOTERM_BP_ALL	peptide biosynthetic process	23	17.4	8.3E-11	0.000000084
GOTERM_CC_ALL	intracellular ribonucleoprotein complex	26	19.7	8.6E-11	1.2E-09
GOTERM_CC_ALL	ribonucleoprotein complex	26	19.7	8.8E-11	1.2E-09
GOTERM_CC_ALL	cytoplasm	93	70.5	2.5E-10	3.2E-09
GOTERM_BP_ALL	organonitrogen compound metabolic process	36	27.3	4.7E-10	0.00000024
GOTERM_BP_ALL	amide biosynthetic process	23	17.4	4.8E-10	0.00000024
GOTERM_BP_ALL	peptide metabolic process	23	17.4	2.1E-09	0.00000084
GOTERM_BP_ALL	organonitrogen compound biosynthetic process	28	21.2	2.9E-09	0.00000098
GOTERM_CC_ALL	cytosol	35	26.5	4.2E-09	0.000000051
GOTERM_CC_ALL	oxidoreductase complex	10	7.6	6.7E-09	0.000000078
GOTERM_CC_ALL	mitochondrial respiratory chain complex I	8	6.1	8.9E-09	0.000000093
GOTERM_CC_ALL	NADH dehydrogenase complex	8	6.1	8.9E-09	0.000000093
GOTERM_CC_ALL	respiratory chain complex I	8	6.1	8.9E-09	0.000000093
GOTERM_BP_ALL	cellular amide metabolic process	24	18.2	9.1E-09	0.0000027
GOTERM_MF_ALL	hydrogen ion transmembrane transporter activity	9	6.8	0.000000055	0.0000061
GOTERM_CC_ALL	macromolecular complex	57	43.2	0.000000059	0.00000059
GOTERM_CC_ALL	intracellular organelle	94	71.2	0.0000002	0.0000019
GOTERM_CC_ALL	organelle	98	74.2	0.0000005	0.0000047
GOTERM_CC_ALL	intracellular organelle part	70	53	0.000000058	0.0000053
UP_SEQ_FEATURE	zinc finger region:C4-type	8	6.1	0.0000011	0.00032
GOTERM_BP_ALL	metabolic process	84	63.6	0.0000016	0.00041
GOTERM_CC_ALL	organelle part	70	53	0.0000016	0.000015
GOTERM_CC_ALL	intracellular part	100	75.8	0.000002	0.000017
GOTERM_BP_ALL	cellular protein metabolic process	47	35.6	0.0000096	0.0022
GOTERM_CC_ALL	intracellular	101	76.5	0.000011	0.000093
GOTERM_CC_ALL	membrane protein complex	19	14.4	0.000021	0.00017
GOTERM_BP_ALL	mitochondrion organization	15	11.4	0.000023	0.0047
GOTERM_CC_ALL	organelle membrane	30	22.7	0.000038	0.0003
GOTERM_BP_ALL	cellular nitrogen compound metabolic process	55	41.7	0.000056	0.0094
GOTERM_BP_ALL	nitrogen compound metabolic process	57	43.2	0.000057	0.0094
GOTERM_BP_ALL	cellular metabolic process	75	56.8	0.00006	0.0094
GOTERM_BP_ALL	mitochondrial respiratory chain complex assembly	5	3.8	0.0001	0.015
GOTERM_CC_ALL	small ribosomal subunit	6	4.5	0.00012	0.00096
GOTERM_BP_ALL	ATP metabolic process	8	6.1	0.00017	0.023
GOTERM_CC_ALL	membrane-bounded organelle	87	65.9	0.00019	0.0014
GOTERM_BP_ALL	oxidation-reduction process	16	12.1	0.0002	0.025
GOTERM_BP_ALL	protein metabolic process	47	35.6	0.00023	0.027
GOTERM_CC_ALL	cytosolic small ribosomal subunit	5	3.8	0.00024	0.0018
GOTERM_CC_ALL	mitochondrial proton-transporting ATP synthase complex	4	3	0.00026	0.0019
GOTERM_BP_ALL	purine ribonucleoside triphosphate metabolic process	8	6.1	0.00028	0.031
GOTERM_CC_ALL	proton-transporting ATP synthase complex	4	3	0.0003	0.0021
GOTERM_BP_ALL	ribonucleoside triphosphate metabolic process	8	6.1	0.00033	0.034
GOTERM_BP_ALL	purine nucleoside triphosphate metabolic process	8	6.1	0.00035	0.034
KEGG_PATHWAY	Metabolic pathways	24	18.2	0.00035	0.0053
GOTERM_BP_ALL	purine ribonucleoside monophosphate metabolic process	8	6.1	0.00036	0.034
GOTERM_MF_ALL	monovalent inorganic cation transmembrane transporter activity	9	6.8	0.00037	0.031
GOTERM_BP_ALL	purine nucleoside monophosphate metabolic process	8	6.1	0.00037	0.034
GOTERM_BP_ALL	cytoplasmic translation	5	3.8	0.0004	0.035
GOTERM_CC_ALL	focal adhesion	10	7.6	0.00043	0.003
GOTERM_CC_ALL	cell-substrate adherens junction	10	7.6	0.00047	0.0032
GOTERM_BP_ALL	ribonucleoside monophosphate metabolic process	8	6.1	0.00048	0.041
GOTERM_CC_ALL	cell-substrate junction	10	7.6	0.00051	0.0034

KEGG_PATHWAY	Cardiac muscle contraction	6	4.5	0.00056	0.0075
GOTERM_MF_ALL	ubiquinol-cytochrome-c reductase activity	3	2.3	0.00057	0.032
GOTERM_MF_ALL	oxidoreductase activity, acting on diphenols and related substances as donors, cytochrome as accepto	3	2.3	0.00057	0.032
GOTERM_BP_ALL	gene expression	46	34.8	0.00057	0.046
GOTERM_BP_ALL	nucleoside monophosphate metabolic process	8	6.1	0.00058	0.046
GOTERM_BP_ALL	nucleoside triphosphate metabolic process	8	6.1	0.00062	0.047
GOTERM_BP_ALL	cytochrome complex assembly	4	3	0.00068	0.048
GOTERM_BP_ALL	positive regulation of cell death	12	9.1	0.00068	0.048
GOTERM_MF_ALL	electron carrier activity	5	3.8	0.00073	0.032
GOTERM_MF_ALL	oxidoreductase activity, acting on diphenols and related substances as donors	3	2.3	0.00075	0.032

#### ZT14M Cortex

Category	Term	Count	%	P-Value	Benjamini
GOTERM_MF_ALL	hormone activity	3	18.8	0.0022	0.25
GOTERM_BP_ALL	positive regulation of biological process	9	56.2	0.0037	0.75
GOTERM_BP_ALL	response to glucocorticoid	3	18.8	0.0043	0.75
GOTERM_MF_ALL	protein binding	10	62.5	0.0051	0.29
GOTERM_BP_ALL	response to corticosteroid	3	18.8	0.0052	7.5E

#### ZT14F Cortex

Term	RT	Count	%	P-Value	Benjamini
GOTERM_BP_ALL	response to toxic substance	4	28.6	0.000081	0.047
GOTERM_CC_ALL	cytosol	7	50	0.00061	0.047
GOTERM_BP_ALL	cellular transition metal ion homeostasis	3	21.4	0.0012	0.21
GOTERM_BP_ALL	homeostatic process	6	42.9	0.0021	0.21
GOTERM_BP_ALL	transition metal ion homeostasis	3	21.4	0.0024	0.21

#### ZT14M Cortex

Only two DEGs, GO analysis not possible

Table S3D. DAVID GO analysis for the hippocampus.

ZT4F ZT14M Hippocampus					
Category	Term	Count	%	P-Value	Benjamini
GOTERM_CC_ALL	mitochondrial membrane part	22	26.8	5.6E-25	1.5E-22
GOTERM_CC_ALL	inner mitochondrial membrane protein complex	19	23.2	4.8E-24	6.2E-22
GOTERM_CC_ALL	mitochondrial envelope	30	36.6	7.9E-24	6.8E-22
GOTERM_CC_ALL	mitochondrial protein complex	20	24.4	1.4E-23	9.3E-22
GOTERM_CC_ALL	mitochondrial inner membrane	25	30.5	2.9E-22	1.5E-20
KEGG_PATHWAY	Oxidative phosphorylation	21	25.6	6.4E-22	5.5E-20
GOTERM_CC_ALL	organelle inner membrane	25	30.5	4.6E-21	2E-19
GOTERM_CC_ALL	mitochondrial membrane	27	32.9	7.3E-21	2.7E-19
GOTERM_CC_ALL	mitochondrial part	30	36.6	2.3E-20	7.5E-19
GOTERM_CC_ALL	respiratory chain	15	18.3	1.9E-19	5.6E-18
GOTERM_CC_ALL	respiratory chain complex	14	17.1	2.6E-18	6.7E-17
KEGG_PATHWAY	Parkinson's disease	19	23.2	2.7E-18	1.2E-16
GOTERM_CC_ALL	mitochondrial respiratory chain	14	17.1	3.1E-18	7.2E-17
GOTERM_CC_ALL	organelle envelope	30	36.6	6.1E-18	1.3E-16
GOTERM_CC_ALL	envelope	30	36.6	6.9E-18	1.4E-16
GOTERM_CC_ALL	mitochondrion	36	43.9	2E-17	3.7E-16
GOTERM_CC_ALL	cytoplasmic part	63	76.8	2.6E-16	4.5E-15
GOTERM_CC_ALL	cytosolic ribosome	15	18.3	5.9E-16	9.5E-15
GOTERM_CC_ALL	macromolecular complex	54	65.9	6.2E-16	9.5E-15
GOTERM_MF_ALL	structural constituent of ribosome	16	19.5	7.4E-15	1.6E-12
GOTERM_CC_ALL	ribosome	17	20.7	1.1E-14	1.5E-13
GOTERM_CC_ALL	membrane protein complex	26	31.7	2.7E-14	3.7E-13
KEGG_PATHWAY	Ribosome	16	19.5	3E-14	8.6E-13
GOTERM_CC_ALL	ribosomal subunit	15	18.3	7.6E-14	9.8E-13
GOTERM_CC_ALL	cytosolic part	16	19.5	9.6E-14	1.2E-12
KEGG_PATHWAY	Huntington's disease	17	20.7	1.8E-13	3.9E-12
KEGG_PATHWAY	Alzheimer's disease	16	19.5	5.9E-13	1E-11
GOTERM_CC_ALL	oxidoreductase complex	11	13.4	5.1E-12	6E-11
GOTERM_CC_ALL	respiratory chain complex I	9	11	8.5E-12	8.8E-11
GOTERM_CC_ALL	NADH dehydrogenase complex	9	11	8.5E-12	8.8E-11
GOTERM_CC_ALL	mitochondrial respiratory chain complex I	9	11	8.5E-12	8.8E-11
GOTERM_CC_ALL	cytoplasm	68	82.9	1.5E-11	1.5E-10
KEGG_PATHWAY	Non-alcoholic fatty liver disease (NAFLD)	14	17.1	3.5E-11	5E-10
GOTERM_MF_ALL	hydrogen ion transmembrane transporter activity	10	12.2	4.6E-11	4.8E-09
GOTERM_CC_ALL	cytosolic large ribosomal subunit	10	12.2	6.4E-11	6.1E-10
GOTERM_CC_ALL	intracellular organelle part	57	69.5	1.2E-10	1.1E-09
GOTERM_CC_ALL	intracellular part	74	90.2	3E-10	2.6E-09
GOTERM_CC_ALL	organelle part	57	69.5	3.5E-10	0.000000003
GOTERM_CC_ALL	large ribosomal subunit	10	12.2	2.1E-09	0.000000017
GOTERM_BP_ALL	organonitrogen compound metabolic process	28	34.1	2.1E-09	0.000000032
GOTERM_CC_ALL	intracellular	74	90.2	0.000000005	0.000000041
GOTERM_CC_ALL	intracellular ribonucleoprotein complex	19	23.2	9.5E-09	0.000000074
GOTERM_CC_ALL	ribonucleoprotein complex	19	23.2	9.7E-09	0.000000074
GOTERM_CC_ALL	cytosol	27	32.9	0.000000011	0.000000078
GOTERM_MF_ALL	structural molecule activity	16	19.5	0.000000012	0.000000081
GOTERM_CC_ALL	catalytic complex	20	24.4	0.000000012	0.000000086
GOTERM_BP_ALL	organonitrogen compound biosynthetic process	22	26.8	0.000000013	0.00001
GOTERM_CC_ALL	mitochondrial proton-transporting ATP synthase complex	6	7.3	0.000000018	0.000000012
GOTERM_CC_ALL	proton-transporting ATP synthase complex	6	7.3	0.000000022	0.000000015
GOTERM_CC_ALL	organelle membrane	28	34.1	0.000000049	0.000000032
GOTERM_BP_ALL	translation	16	19.5	0.00000006	0.00003
GOTERM_BP_ALL	peptide biosynthetic process	16	19.5	0.000000087	0.000033
GOTERM_CC_ALL	protein complex	37	45.1	0.00000025	0.0000016
GOTERM_BP_ALL	amide biosynthetic process	16	19.5	0.00000029	0.000086
GOTERM_BP_ALL	electron transport chain	7	8.5	0.00000047	0.00012
GOTERM_BP_ALL	peptide metabolic process	16	19.5	0.00000078	0.00017
GOTERM_CC_ALL	proton-transporting two-sector ATPase complex	6	7.3	0.0000012	0.0000075
GOTERM_BP_ALL	ATP metabolic process	9	11	0.0000012	0.00023
GOTERM_CC_ALL	intracellular organelle	65	79.3	0.0000013	0.0000077
GOTERM_CC_ALL	organelle	68	82.9	0.0000013	0.0000077
GOTERM_MF_ALL	monovalent inorganic cation transmembrane transporter activity	10	12.2	0.0000016	0.000084
GOTERM_BP_ALL	oxidation-reduction process	16	19.5	0.0000017	0.00029
GOTERM_BP_ALL	purine ribonucleoside triphosphate metabolic process	9	11	0.0000023	0.00034
GOTERM_BP_ALL	ribonucleoside triphosphate metabolic process	9	11	0.0000029	0.00035
GOTERM_BP_ALL	purine nucleoside triphosphate metabolic process	9	11	0.0000031	0.00035
GOTERM_BP_ALL	purine ribonucleoside monophosphate metabolic process	9	11	0.0000032	0.00035
GOTERM_BP_ALL	purine nucleoside monophosphate metabolic process	9	11	0.0000033	0.00035
GOTERM_BP_ALL	ribonucleoside monophosphate metabolic process	9	11	0.0000045	0.00044
GOTERM_BP_ALL	nucleoside metabolic process	10	12.2	0.0000047	0.00044
GOTERM_BP_ALL	nucleoside monophosphate metabolic process	9	11	0.0000057	0.0005
GOTERM_BP_ALL	nucleoside triphosphate metabolic process	9	11	0.0000063	0.0005
GOTERM_BP_ALL	cellular amide metabolic process	16	19.5	0.0000064	0.0005
GOTERM_CC_ALL	cytochrome complex	5	6.1	0.0000065	0.000038
GOTERM_BP_ALL	respiratory electron transport chain	6	7.3	0.0000075	0.00054
GOTERM_BP_ALL	glycosyl compound metabolic process	10	12.2	0.0000075	0.00054
GOTERM_BP_ALL	purine nucleotide metabolic process	11	13.4	0.000012	0.00079
GOTERM_BP_ALL	purine ribonucleoside metabolic process	9	11	0.000014	0.00091
KEGG_PATHWAY	Cardiac muscle contraction	7	8.5	0.000015	0.00018
GOTERM_BP_ALL	purine nucleoside metabolic process	9	11	0.000015	0.00096
KEGG_PATHWAY	Metabolic pathways	23	28	0.000019	0.0002
GOTERM_BP_ALL	purine-containing compound metabolic process	11	13.4	0.000023	0.0014
GOTERM_BP_ALL	ribonucleoside metabolic process	9	11	0.000025	0.0014

GOTERM_BP_ALL	cellular respiration	7	8.5	0.000027	0.0015
GOTERM_BP_ALL	proton transport	6	7.3	0.000031	0.0017
GOTERM_BP_ALL	hydrogen transport	6	7.3	0.000033	0.0017
GOTERM_BP_ALL	energy derivation by oxidation of organic compounds	8	9.8	0.000035	0.0017
GOTERM_MF_ALL	inorganic cation transmembrane transporter activity	10	12.2	0.000036	0.0015
GOTERM_BP_ALL	generation of precursor metabolites and energy	9	11	0.000039	0.0019
GOTERM_BP_ALL	ATP synthesis coupled electron transport	5	6.1	0.000046	0.0021
GOTERM_BP_ALL	purine ribonucleotide metabolic process	10	12.2	0.000048	0.0022
GOTERM_CC_ALL	cytosolic small ribosomal subunit	5	6.1	0.00005	0.00029
GOTERM_BP_ALL	ribonucleotide metabolic process	10	12.2	0.000064	0.0028
GOTERM_BP_ALL	ribose phosphate metabolic process	10	12.2	0.000076	0.0033
GOTERM_MF_ALL	oxidoreductase activity	12	14.6	0.000083	0.0023
GOTERM_BP_ALL	nucleotide metabolic process	11	13.4	0.000083	0.0035
GOTERM_BP_ALL	hydrogen ion transmembrane transport	5	6.1	0.000092	0.0037
GOTERM_BP_ALL	nucleoside phosphate metabolic process	11	13.4	0.000095	0.0038
GOTERM_MF_ALL	heme-copper terminal oxidase activity	4	4.9	0.00011	0.0023
GOTERM_MF_ALL	oxidoreductase activity, acting on a heme group of donors, oxygen as acceptor	4	4.9	0.00011	0.0023
GOTERM_MF_ALL	cytochrome-c oxidase activity	4	4.9	0.00011	0.0023
GOTERM_MF_ALL	cation transmembrane transporter activity	10	12.2	0.00012	0.0023
GOTERM_MF_ALL	oxidoreductase activity, acting on a heme group of donors	4	4.9	0.00013	0.0023
GOTERM_MF_ALL	electron carrier activity	5	6.1	0.00013	0.0023
GOTERM_BP_ALL	oxidative phosphorylation	5	6.1	0.00014	0.0054
GOTERM_BP_ALL	metabolic process	57	69.5	0.00016	0.0059
GOTERM_BP_ALL	ribonucleoprotein complex biogenesis	9	11	0.00018	0.0066
GOTERM_MF_ALL	substrate-specific transmembrane transporter activity	12	14.6	0.00018	0.0028
GOTERM_BP_ALL	nucleobase-containing small molecule metabolic process	11	13.4	0.00018	0.0066
GOTERM_BP_ALL	establishment of localization	32	39	0.00019	0.0067
GOTERM_BP_ALL	single-organism metabolic process	28	34.1	0.00022	0.0075
GOTERM_MF_ALL	NADH dehydrogenase (quinone) activity	4	4.9	0.00022	0.0028
GOTERM_MF_ALL	NADH dehydrogenase (ubiquinone) activity	4	4.9	0.00022	0.0028
GOTERM_MF_ALL	ubiquinol-cytochrome-c reductase activity	3	3.7	0.00023	0.0028
GOTERM_MF_ALL	oxidoreductase activity, acting on diphenols and related substances as donors, cytochrome as ac	3	3.7	0.00023	0.0028
GOTERM_MF_ALL	NADH dehydrogenase activity	4	4.9	0.00024	0.0028
GOTERM_BP_ALL	organophosphate metabolic process	13	15.9	0.00024	0.0081
GOTERM_BP_ALL	transport	31	37.8	0.00027	0.0088
GOTERM_CC_ALL	small ribosomal subunit	5	6.1	0.0003	0.0017
GOTERM_MF_ALL	oxidoreductase activity, acting on diphenols and related substances as donors	3	3.7	0.00031	0.0034
GOTERM_CC_ALL	heterotrimeric G-protein complex	4	4.9	0.00041	0.0023
GOTERM_MF_ALL	transmembrane transporter activity	12	14.6	0.00042	0.0044
GOTERM_CC_ALL	membrane-bounded organelle	60	73.2	0.00042	0.0023
GOTERM_MF_ALL	oxidoreductase activity, acting on NAD(P)H, quinone or similar compound as acceptor	4	4.9	0.00047	0.0047
GOTERM_BP_ALL	ribosome biogenesis	7	8.5	0.00067	0.021
GOTERM_BP_ALL	carbohydrate derivative metabolic process	13	15.9	0.00072	0.022
GOTERM_BP_ALL	mitochondrial ATP synthesis coupled electron transport	4	4.9	0.00076	0.023
GOTERM_MF_ALL	substrate-specific transporter activity	12	14.6	0.00081	0.0077
GOTERM_BP_ALL	ATP biosynthetic process	4	4.9	0.00092	0.028
GOTERM_MF_ALL	transporter activity	13	15.9	0.00096	0.0087
GOTERM_MF_ALL	ion transmembrane transporter activity	10	12.2	0.00099	0.0087
GOTERM_CC_ALL	mitochondrial proton-transporting ATP synthase complex, coupling factor F(o)	3	3.7	0.0011	0.0058
GOTERM_CC_ALL	proton-transporting ATP synthase complex, coupling factor F(o)	3	3.7	0.0015	0.0076
GOTERM_BP_ALL	purine ribonucleoside triphosphate biosynthetic process	4	4.9	0.0016	0.048
GOTERM_BP_ALL	cellular nitrogen compound metabolic process	37	45.1	0.0016	0.048
GOTERM_BP_ALL	purine nucleoside triphosphate biosynthetic process	4	4.9	0.0017	0.048
GOTERM_BP_ALL	protein targeting	9	11	0.002	0.055
GOTERM_CC_ALL	respiratory chain complex IV	3	3.7	0.0021	0.011
GOTERM_BP_ALL	ribonucleoside triphosphate biosynthetic process	4	4.9	0.0021	0.058
GOTERM_BP_ALL	nitrogen compound metabolic process	38	46.3	0.0022	0.06
GOTERM_CC_ALL	cell part	74	90.2	0.0024	0.012
GOTERM_CC_ALL	intracellular membrane-bounded organelle	54	65.9	0.0024	0.012
GOTERM_CC_ALL	cell	74	90.2	0.0027	0.013
GOTERM_BP_ALL	purine nucleoside monophosphate biosynthetic process	4	4.9	0.0027	0.071
GOTERM_BP_ALL	purine ribonucleoside monophosphate biosynthetic process	4	4.9	0.0027	0.071
GOTERM_MF_ALL	oxidoreductase activity, acting on NAD(P)H	4	4.9	0.0028	0.023
GOTERM_BP_ALL	ribosomal small subunit biogenesis	4	4.9	0.0028	0.072
GOTERM_BP_ALL	nucleoside triphosphate biosynthetic process	4	4.9	0.0034	0.085
GOTERM_BP_ALL	ribosomal small subunit assembly	3	3.7	0.0034	0.085
GOTERM_MF_ALL	RNA binding	14	17.1	0.004	0.032

#### ZT4M ZT14M Hippocampus

Category	Term	Count	%	P-Value	Benjamini
GOTERM_BP_ALL	response to abiotic stimulus	3	50	0.022	1
GOTERM_BP_ALL	circadian rhythm	2	33.3	0.045	1
GOTERM_BP_ALL	response to stimulus	5	83.3	0.06	1
GOTERM_BP_ALL	rhythmic process	2	33.3	0.08	1

**ZT14F ZT14M Hippocampus**

Term	RT	Count	%	P-Value	Benjamini
GOTERM_BP_ALL	response to toxic substance	6	25	0.00000034	0.00047
GOTERM_BP_ALL	cellular response to chemical stimulus	13	54.2	0.0000015	0.001
GOTERM_BP_ALL	response to organic substance	13	54.2	0.0000061	0.0028
GOTERM_BP_ALL	cellular response to organic substance	11	45.8	0.000015	0.0052
GOTERM_BP_ALL	response to glucocorticoid	5	20.8	0.000023	0.0062
GOTERM_CC_ALL	cytosol	11	45.8	0.000025	0.0035
GOTERM_BP_ALL	response to chemical	14	58.3	0.000027	0.0062
GOTERM_BP_ALL	response to corticosteroid	5	20.8	0.000033	0.0065
GOTERM_BP_ALL	cellular response to stimulus	17	70.8	0.0001	0.018
GOTERM_BP_ALL	response to endogenous stimulus	9	37.5	0.00012	0.018
GOTERM_BP_ALL	regulation of cell proliferation	9	37.5	0.00014	0.019
GOTERM_BP_ALL	response to stimulus	18	75	0.00031	0.035
GOTERM_BP_ALL	cellular response to growth factor stimulus	6	25	0.00031	0.035
GOTERM_BP_ALL	response to growth factor	6	25	0.00037	0.038
GOTERM_BP_ALL	response to lipid	7	29.2	0.00039	0.038
GOTERM_BP_ALL	response to organic cyclic compound	7	29.2	0.00042	0.038
GOTERM_BP_ALL	response to steroid hormone	5	20.8	0.00052	0.045

**ZT14M Hippocampus**

Only two DEGs, GO analysis not possible



Table S3E. DAVID GO analysis for the thalamus.

ZT4F Thalamus		Gene count	%	P-Value	Benjamini
GOTERM_CC_ALL	ribosome	20	15	3.9E-15	1.3E-12
GOTERM_MF_ALL	structural constituent of ribosome	18	13.5	2.9E-14	1E-11
KEGG_PATHWAY	Ribosome	17	12.8	3.2E-14	4.5E-12
GOTERM_CC_ALL	ribosomal subunit	17	12.8	1.3E-13	2.2E-11
GOTERM_CC_ALL	cytosolic ribosome	15	11.3	2.6E-13	2.8E-11
KEGG_PATHWAY	Oxidative phosphorylation	16	12	3.2E-13	2.2E-11
GOTERM_CC_ALL	inner mitochondrial membrane protein complex	14	10.5	3.3E-13	2.8E-11
GOTERM_CC_ALL	mitochondrial protein complex	15	11.3	5.3E-13	3.4E-11
GOTERM_CC_ALL	mitochondrial membrane part	16	12	6.1E-13	3.4E-11
GOTERM_CC_ALL	cytoplasmic part	79	59.4	4.8E-12	2.3E-10
GOTERM_CC_ALL	mitochondrial inner membrane	19	14.3	3E-11	1.3E-09
GOTERM_CC_ALL	mitochondrial envelope	22	16.5	1.5E-10	5.6E-09
GOTERM_CC_ALL	organelle inner membrane	19	14.3	2.1E-10	6.9E-09
GOTERM_CC_ALL	mitochondrial membrane	21	15.8	2.9E-10	8.9E-09
GOTERM_CC_ALL	large ribosomal subunit	12	9	3.4E-10	9.7E-09
GOTERM_CC_ALL	cytosolic part	15	11.3	6.1E-10	0.000000015
GOTERM_CC_ALL	cytoplasm	93	69.9	6.2E-10	0.000000015
GOTERM_CC_ALL	mitochondrial part	24	18	8.5E-10	0.000000019
GOTERM_CC_ALL	mitochondrion	34	25.6	1.2E-09	0.000000024
GOTERM_CC_ALL	respiratory chain	10	7.5	2.1E-09	0.000000041
GOTERM_CC_ALL	cytosolic large ribosomal subunit	10	7.5	2.8E-09	0.000000053
KEGG_PATHWAY	Parkinson's disease	13	9.8	0.000000003	0.00000014
GOTERM_CC_ALL	intracellular organelle part	75	56.4	5.4E-09	0.000000095
GOTERM_CC_ALL	intracellular ribonucleoprotein complex	23	17.3	0.000000017	0.000000027
GOTERM_CC_ALL	ribonucleoprotein complex	23	17.3	0.000000017	0.000000027
GOTERM_CC_ALL	organelle part	75	56.4	0.000000018	0.000000027
GOTERM_CC_ALL	respiratory chain complex	9	6.8	0.000000018	0.000000027
GOTERM_CC_ALL	mitochondrial respiratory chain	9	6.8	0.00000002	0.000000029
GOTERM_MF_ALL	structural molecule activity	19	14.3	0.000000029	0.0000005
GOTERM_CC_ALL	intracellular part	103	77.4	0.000000012	0.00000016
GOTERM_BP_ALL	organonitrogen compound biosynthetic process	25	18.8	0.000000013	0.00021
GOTERM_CC_ALL	intracellular organelle	95	71.4	0.000000014	0.0000018
GOTERM_BP_ALL	organonitrogen compound metabolic process	31	23.3	0.000000019	0.00021
KEGG_PATHWAY	Alzheimer's disease	12	9	0.000000021	0.00000075
GOTERM_CC_ALL	macromolecular complex	56	42.1	0.000000024	0.000003
GOTERM_CC_ALL	cytosol	32	24.1	0.000000026	0.00000031
GOTERM_BP_ALL	translation	18	13.5	0.000000026	0.00021
GOTERM_CC_ALL	respiratory chain complex I	7	5.3	0.000000029	0.00000032
GOTERM_CC_ALL	NADH dehydrogenase complex	7	5.3	0.000000029	0.00000032
GOTERM_CC_ALL	mitochondrial respiratory chain complex I	7	5.3	0.000000029	0.00000032
GOTERM_CC_ALL	organelle	99	74.4	0.000000037	0.00000039
GOTERM_BP_ALL	peptide biosynthetic process	18	13.5	0.000000039	0.00024
KEGG_PATHWAY	Huntington's disease	12	9	0.000000066	0.0000019
GOTERM_CC_ALL	organelle envelope	22	16.5	0.000000078	0.00000079
GOTERM_CC_ALL	envelope	22	16.5	0.000000084	0.00000083
GOTERM_BP_ALL	amide biosynthetic process	18	13.5	0.000000014	0.00068
GOTERM_CC_ALL	oxidoreductase complex	8	6	0.000000002	0.00000019
GOTERM_CC_ALL	intracellular	103	77.4	0.000000027	0.00000025
GOTERM_BP_ALL	peptide metabolic process	18	13.5	0.000000041	0.00016
KEGG_PATHWAY	Non-alcoholic fatty liver disease (NAFLD)	10	7.5	0.000000059	0.00014
GOTERM_CC_ALL	mitochondrial proton-transporting ATP synthase complex	5	3.8	0.000000072	0.0000066
GOTERM_CC_ALL	proton-transporting ATP synthase complex	5	3.8	0.000000087	0.0000077
GOTERM_BP_ALL	response to abiotic stimulus	20	15	0.000000011	0.0038
GOTERM_MF_ALL	hydrogen ion transmembrane transporter activity	7	5.3	0.000000014	0.00016
GOTERM_BP_ALL	response to glucocorticoid	8	6	0.000000031	0.00088
GOTERM_BP_ALL	cellular amide metabolic process	18	13.5	0.000000037	0.00088
GOTERM_BP_ALL	purine nucleoside triphosphate metabolic process	9	6.8	0.000000042	0.00088
GOTERM_BP_ALL	purine ribonucleoside monophosphate metabolic process	9	6.8	0.000000043	0.00088
GOTERM_BP_ALL	purine nucleoside monophosphate metabolic process	9	6.8	0.000000044	0.00088
GOTERM_BP_ALL	response to corticosteroid	8	6	0.000000058	0.01
GOTERM_BP_ALL	ribonucleoside monophosphate metabolic process	9	6.8	0.000000061	0.01
GOTERM_BP_ALL	nucleoside monophosphate metabolic process	9	6.8	0.000000076	0.012
GOTERM_BP_ALL	nucleoside triphosphate metabolic process	9	6.8	0.000000082	0.012
GOTERM_CC_ALL	membrane protein complex	18	13.5	0.000000084	0.00072
GOTERM_BP_ALL	ATP metabolic process	8	6	0.000000014	0.00019
GOTERM_BP_ALL	purine ribonucleoside metabolic process	9	6.8	0.000000018	0.00023
GOTERM_CC_ALL	proton-transporting two-sector ATPase complex	5	3.8	0.000000019	0.00016
GOTERM_BP_ALL	purine nucleoside metabolic process	9	6.8	0.000000019	0.00024
GOTERM_BP_ALL	response to extracellular stimulus	11	8.3	0.00000002	0.00024
GOTERM_BP_ALL	purine ribonucleoside triphosphate metabolic process	8	6	0.000000023	0.00026
GOTERM_BP_ALL	purine nucleotide metabolic process	11	8.3	0.000000024	0.00027
GOTERM_CC_ALL	cytosolic small ribosomal subunit	5	3.8	0.000000025	0.00021
GOTERM_BP_ALL	ribonucleoside triphosphate metabolic process	8	6	0.000000028	0.00029
GOTERM_BP_ALL	ribonucleoside metabolic process	9	6.8	0.000000003	0.0003
GOTERM_CC_ALL	membrane-bounded organelle	87	65.4	0.000000032	0.00026
GOTERM_BP_ALL	nucleoside metabolic process	9	6.8	0.000000045	0.00043
GOTERM_BP_ALL	purine-containing compound metabolic process	11	8.3	0.000000046	0.00043
GOTERM_BP_ALL	response to hormone	14	10.5	0.000000049	0.00043
GOTERM_BP_ALL	response to nutrient levels	10	7.5	0.000000054	0.00047

**ZT14M Thalamus**

Category	Term	Gene count	%	P_Value	Benjamini
GOTERM_BP_ALL	neuropeptide hormone activity	3	8.8	0.00084	0.35
GOTERM_BP_ALL	neurohypophyseal hormone activity	2	5.9	0.0029	0.14
GOTERM_BP_ALL	maternal aggressive behavior	2	5.9	0.0054	0.85
GOTERM_BP_ALL	negative regulation of transmission of nerve impulse	2	5.9	0.0067	0.85

**ZT14F Thalamus**

Category	Term	Gene count	%	P-Value	Benjamini
GOTERM_CC_DIRE	cytosol	12	38.7	0.000025	0.0013
GOTERM_BP_DIRE	detoxification of copper ion	2	6.5	0.0057	0.91
GOTERM_BP_DIRE	regulation of cell cycle	3	9.7	0.011	0.91
GOTERM_BP_DIRE	response to drug	4	12.9	0.012	0.91
GOTERM_BP_DIRE	negative regulation of growth	2	6.5	0.017	0.91

**ZT14M Thalamus**

Category	Term	Gene count	%	P-Value	Benjamini
GOTERM_CC_DIRE	myelin sheath	28	5.3	3.4E-13	1.5E-10
GOTERM_CC_DIRE	neuron projection	37	7	1.2E-10	0.00000027
GOTERM_CC_DIRE	neuronal cell body	42	8	1.9E-10	0.00000027
GOTERM_CC_DIRE	cytoplasm	232	44.1	3.5E-10	0.00000036
GOTERM_CC_DIRE	cytosolic small ribosomal subunit	14	2.7	4.1E-10	0.00000036
GOTERM_CC_DIRE	ribosome	22	4.2	0.00000001	0.00000075
GOTERM_CC_DIRE	membrane	234	44.5	0.00000025	0.0000015
GOTERM_CC_DIRE	intracellular ribonucleoprotein complex	28	5.3	0.00000038	0.0000021
GOTERM_CC_DIRE	extracellular exosome	111	21.1	0.00000047	0.0000022
KEGG_PATHWAY	Ribosome	19	3.6	0.00000063	0.000014
GOTERM_CC_DIRE	synapse	35	6.7	0.00000017	0.0000075
GOTERM_MF_DIRE	poly(A) RNA binding	58	11	0.00000046	0.00033
GOTERM_CC_DIRE	dendrite	33	6.3	0.00000079	0.000031
GOTERM_BP_DIRE	cellular oxidant detoxification	5	1	0.0000021	0.0044
GOTERM_CC_DIRE	terminal bouton	14	2.7	0.0000048	0.00018
GOTERM_CC_DIRE	synaptic vesicle	14	2.7	0.000016	0.00054
GOTERM_CC_DIRE	cytosol	72	13.7	0.000054	0.0017
GOTERM_MF_DIRE	haptoglobin binding	4	0.8	0.000066	0.02
GOTERM_CC_DIRE	small ribosomal subunit	7	1.3	0.000068	0.002
GOTERM_MF_DIRE	protein homodimerization activity	40	7.6	0.000092	0.02
GOTERM_MF_DIRE	peroxidase activity	7	1.3	0.00012	0.02
GOTERM_CC_DIRE	haptoglobin-hemoglobin complex	4	0.8	0.00015	0.004
GOTERM_MF_DIRE	protein complex binding	23	4.4	0.00015	0.02
GOTERM_MF_DIRE	structural constituent of ribosome	19	3.6	0.00017	0.02
KEGG_PATHWAY	Huntington's disease	16	3	0.00031	0.034
GOTERM_CC_DIRE	postsynapse	6	1.1	0.0004	0.01
GOTERM_CC_DIRE	axon	22	4.2	0.00043	0.01
GOTERM_CC_DIRE	extracellular matrix	19	3.6	0.00045	0.01
GOTERM_CC_DIRE	postsynaptic density	16	3	0.001	0.022
GOTERM_CC_DIRE	neurofilament	4	0.8	0.0012	0.024
GOTERM_CC_DIRE	nucleolus	37	7	0.0012	0.024
GOTERM_CC_DIRE	synaptic membrane	6	1.1	0.0013	0.024

Table S3F. DAVID GO analysis for the hypothalamus (LH+DMVH).

ZT4F Hypothalamus					
Category	Term	Count	%	P-Value	Benjamini
KEGG_PATHWAY	Oxidative phosphorylation	20	15.3	1.3E-18	1.4E-16
GOTERM_CC_ALL	mitochondrial membrane part	20	15.3	2.2E-18	7.5E-16
GOTERM_CC_ALL	inner mitochondrial membrane protein complex	17	13	9.5E-18	1.6E-15
GOTERM_CC_ALL	mitochondrial protein complex	18	13.7	2.7E-17	3.1E-15
KEGG_PATHWAY	Ribosome	19	14.5	7E-17	3.7E-15
GOTERM_MF_ALL	structural constituent of ribosome	20	15.3	1.1E-16	3.6E-14
GOTERM_CC_ALL	ribosome	21	16	1.2E-16	1E-14
GOTERM_CC_ALL	ribosomal subunit	19	14.5	2.1E-16	1.4E-14
GOTERM_CC_ALL	cytosolic ribosome	17	13	2.9E-16	1.7E-14
GOTERM_CC_ALL	mitochondrial inner membrane	23	17.6	1.1E-15	5.5E-14
GOTERM_CC_ALL	mitochondrial envelope	27	20.6	1.9E-15	8E-14
GOTERM_CC_ALL	organelle inner membrane	23	17.6	1.2E-14	4.8E-13
GOTERM_CC_ALL	mitochondrion	40	30.5	2.6E-14	8.6E-13
GOTERM_CC_ALL	mitochondrial part	29	22.1	2.7E-14	8.6E-13
GOTERM_CC_ALL	mitochondrial membrane	25	19.1	3.2E-14	9.1E-13
GOTERM_CC_ALL	respiratory chain	13	9.9	7.3E-14	1.9E-12
GOTERM_CC_ALL	cytosolic part	18	13.7	1.8E-13	4.6E-12
GOTERM_CC_ALL	large ribosomal subunit	14	10.7	5.7E-13	1.3E-11
GOTERM_CC_ALL	mitochondrial respiratory chain	12	9.2	7.7E-13	1.7E-11
KEGG_PATHWAY	Parkinson's disease	16	12.2	9E-13	3.2E-11
GOTERM_CC_ALL	cytosolic large ribosomal subunit	12	9.2	3.3E-12	6.7E-11
GOTERM_CC_ALL	respiratory chain complex	11	8.4	2.1E-11	4E-10
GOTERM_CC_ALL	cytoplasmic part	75	57.3	6E-11	1.1E-09
GOTERM_CC_ALL	organelle envelope	27	20.6	1.4E-10	2.5E-09
GOTERM_CC_ALL	envelope	27	20.6	1.6E-10	2.6E-09
GOTERM_CC_ALL	respiratory chain complex I	9	6.9	1.9E-10	2.8E-09
GOTERM_CC_ALL	mitochondrial respiratory chain complex I	9	6.9	1.9E-10	2.8E-09
GOTERM_CC_ALL	NADH dehydrogenase complex	9	6.9	1.9E-10	2.8E-09
KEGG_PATHWAY	Huntington's disease	15	11.5	6.8E-10	0.00000018
GOTERM_CC_ALL	cytoplasm	90	68.7	9.2E-10	0.00000013
GOTERM_CC_ALL	intracellular ribonucleoprotein complex	24	18.3	1.6E-09	0.00000021
GOTERM_CC_ALL	ribonucleoprotein complex	24	18.3	1.6E-09	0.00000021
GOTERM_CC_ALL	macromolecular complex	59	45	1.8E-09	0.00000022
KEGG_PATHWAY	Alzheimer's disease	14	10.7	1.9E-09	0.00000004
GOTERM_CC_ALL	intracellular organelle part	73	55.7	5.1E-09	0.00000006
GOTERM_CC_ALL	oxidoreductase complex	10	7.6	5.2E-09	0.00000006
GOTERM_BP_ALL	translation	20	15.3	5.5E-09	0.00000046
GOTERM_MF_ALL	structural molecule activity	20	15.3	5.7E-09	0.00000093
GOTERM_BP_ALL	amide biosynthetic process	21	16	6.7E-09	0.00000046
GOTERM_BP_ALL	organonitrogen compound metabolic process	33	25.2	7.7E-09	0.00000046
GOTERM_BP_ALL	peptide biosynthetic process	20	15.3	8.8E-09	0.00000046
GOTERM_CC_ALL	organelle part	73	55.7	0.00000017	0.00000019
GOTERM_BP_ALL	organonitrogen compound biosynthetic process	26	19.8	0.00000002	0.00000082
GOTERM_MF_ALL	hydrogen ion transmembrane transporter activity	9	6.9	0.000000055	0.0000006
KEGG_PATHWAY	Non-alcoholic fatty liver disease (NAFLD)	12	9.2	0.000000063	0.00000011
GOTERM_CC_ALL	mitochondrial proton-transporting ATP synthase complex	6	4.6	0.00000012	0.00000013
GOTERM_BP_ALL	peptide metabolic process	20	15.3	0.00000013	0.00000046
GOTERM_CC_ALL	proton-transporting ATP synthase complex	6	4.6	0.00000016	0.00000016
GOTERM_BP_ALL	cellular amide metabolic process	21	16	0.00000004	0.000012
GOTERM_CC_ALL	membrane protein complex	21	16	0.00000009	0.00000092
UP_SEQ_FEATURE	zinc finger region:C4-type	8	6.1	0.00000094	0.00027
GOTERM_CC_ALL	cytosol	30	22.9	0.00000013	0.000012
GOTERM_CC_ALL	intracellular part	98	74.8	0.00000013	0.000012
GOTERM_CC_ALL	intracellular	99	75.6	0.00000068	0.000064
GOTERM_CC_ALL	proton-transporting two-sector ATPase complex	6	4.6	0.00000078	0.000071
GOTERM_CC_ALL	organelle	93	71	0.00001	0.000093
GOTERM_CC_ALL	intracellular organelle	88	67.2	0.000012	0.0001
GOTERM_MF_ALL	NADH dehydrogenase (ubiquinone) activity	5	3.8	0.000033	0.002
GOTERM_MF_ALL	NADH dehydrogenase (quinone) activity	5	3.8	0.000033	0.002
GOTERM_MF_ALL	NADH dehydrogenase activity	5	3.8	0.000037	0.002
GOTERM_CC_ALL	mitochondrial proton-transporting ATP synthase complex, coupling factor F(o)	4	3.1	0.000047	0.00039
GOTERM_MF_ALL	monovalent inorganic cation transmembrane transporter activity	10	7.6	0.000064	0.003
GOTERM_CC_ALL	proton-transporting ATP synthase complex, coupling factor F(o)	4	3.1	0.000074	0.00061
GOTERM_MF_ALL	oxidoreductase activity, acting on NAD(P)H, quinone or similar compound as acceptor	5	3.8	0.000091	0.0037
GOTERM_BP_ALL	ATP metabolic process	8	6.1	0.00012	0.028
GOTERM_BP_ALL	ATP biosynthetic process	5	3.8	0.00014	0.028
GOTERM_BP_ALL	metabolic process	76	58	0.00014	0.028
GOTERM_BP_ALL	proton transport	6	4.6	0.00015	0.028
GOTERM_CC_ALL	organelle membrane	28	21.4	0.00016	0.0013
GOTERM_BP_ALL	hydrogen transport	6	4.6	0.00016	0.028
GOTERM_BP_ALL	purine ribonucleoside triphosphate metabolic process	8	6.1	0.0002	0.032
GOTERM_CC_ALL	cytosolic small ribosomal subunit	5	3.8	0.00022	0.0017
GOTERM_BP_ALL	ribonucleoside triphosphate metabolic process	8	6.1	0.00024	0.032
GOTERM_MF_ALL	substrate-specific transmembrane transporter activity	15	11.5	0.00024	0.0089
GOTERM_BP_ALL	purine nucleoside triphosphate metabolic process	8	6.1	0.00026	0.032
GOTERM_BP_ALL	purine ribonucleoside monophosphate metabolic process	8	6.1	0.00027	0.032
GOTERM_BP_ALL	purine nucleoside monophosphate metabolic process	8	6.1	0.00027	0.032
GOTERM_BP_ALL	purine ribonucleoside triphosphate biosynthetic process	5	3.8	0.00031	0.032
GOTERM_BP_ALL	hydrogen ion transmembrane transport	5	3.8	0.00033	0.032
GOTERM_BP_ALL	purine nucleoside triphosphate biosynthetic process	5	3.8	0.00033	0.032
GOTERM_BP_ALL	ATP synthesis coupled proton transport	4	3.1	0.00035	0.032
GOTERM_BP_ALL	energy coupled proton transport, down electrochemical gradient	4	3.1	0.00035	0.032

GOTERM_BP_ALL	ribonucleoside monophosphate metabolic process	8	6.1	0.00035	0.032
GOTERM_CC_ALL	proton-transporting two-sector ATPase complex, proton-transporting domain	4	3.1	0.00036	0.0028
GOTERM_BP_ALL	establishment of localization	40	30.5	0.00042	0.034
GOTERM_BP_ALL	nucleoside monophosphate metabolic process	8	6.1	0.00043	0.034
GOTERM_BP_ALL	ribonucleoside triphosphate biosynthetic process	5	3.8	0.00044	0.034
GOTERM_MF_ALL	substrate-specific transporter activity	16	12.2	0.00045	0.015
GOTERM_BP_ALL	transport	39	29.8	0.00046	0.034
GOTERM_BP_ALL	nucleoside triphosphate metabolic process	8	6.1	0.00046	0.034
GOTERM_BP_ALL	nitrogen compound metabolic process	68	50.4	0.0000019	0.0000075
GOTERM_MF_ALL	hormone activity	6	4.6	0.0005	0.015
GOTERM_BP_ALL	cellular nitrogen compound metabolic process	50	38.2	0.00052	0.036
GOTERM_BP_ALL	purine nucleoside monophosphate biosynthetic process	5	3.8	0.00061	0.04
GOTERM_BP_ALL	purine ribonucleoside monophosphate biosynthetic process	5	3.8	0.00061	0.04
GOTERM_BP_ALL	cellular nitrogen compound biosynthetic process	41	31.3	0.00063	0.04
GOTERM_MF_ALL	transmembrane transporter activity	15	11.5	0.00064	0.018
GOTERM_BP_ALL	nucleoside triphosphate biosynthetic process	5	3.8		

#### ZT14M Hypothalamus

Category	Term	Count	%	P-Value	Benjamini
GOTERM_MF_ALL	neuropeptide hormone activity	7	16.3	1.9E-11	4.1E-09
GOTERM_MF_ALL	hormone activity	9	20.9	1E-10	0.00000011
GOTERM_BP_ALL	single-multicellular organism process	26	60.5	0.0000071	0.012
GOTERM_BP_ALL	neuropeptide signaling pathway	5	11.6	0.000014	0.012
GOTERM_MF_ALL	G-protein coupled receptor binding	7	16.3	0.000014	0.001
GOTERM_BP_ALL	maternal aggressive behavior	3	7	0.000022	0.013
GOTERM_MF_ALL	protein binding	29	67.4	0.000034	0.0015
GOTERM_MF_ALL	neuropeptide receptor binding	4	9.3	0.000035	0.0015
GOTERM_BP_ALL	behavior	9	20.9	0.000044	0.019
GOTERM_CC_ALL	extracellular space	13	30.2	0.000048	0.0054
GOTERM_CC_ALL	secretory granule	7	16.3	0.000066	0.0054
GOTERM_BP_ALL	feeding behavior	5	11.6	0.000082	0.026
GOTERM_BP_ALL	single organism signaling	24	55.8	0.00012	0.026
GOTERM_BP_ALL	signaling	24	55.8	0.00013	0.026
GOTERM_BP_ALL	response to peptide	7	16.3	0.00014	0.026
GOTERM_BP_ALL	single-organism process	36	83.7	0.00014	0.026
GOTERM_BP_ALL	cell communication	24	55.8	0.00016	0.027
GOTERM_BP_ALL	endocrine hormone secretion	4	9.3	0.00017	0.027
GOTERM_BP_ALL	aggressive behavior	3	7	0.0002	0.029
GOTERM_BP_ALL	response to organonitrogen compound	10	23.3	0.00011	0.031
GOTERM_BP_ALL	single-organism behavior	7	16.3	0.00032	0.04
GOTERM_BP_ALL	multicellular organismal process	27	62.8	0.00037	0.043
GOTERM_BP_ALL	negative regulation of biological process	20	46.5	0.0004	0.043
GOTERM_CC_ALL	secretory vesicle	7	16.3	0.00042	0.023
KEGG_PATHWAY	Adipocytokine signaling pathway	4	9.3	0.00058	0.041
GOTERM_MF_ALL	receptor binding	11	25.6	0.00073	0.026

#### ZT14F Hypothalamus

Category	Term	Count	%	P-Value	Benjamini
GOTERM_MF_ALL	hormone activity	6	31.6	0.000000047	0.0000065
GOTERM_BP_ALL	regulation of biological quality	13	68.4	0.0000016	0.002
GOTERM_BP_ALL	positive regulation of blood pressure	4	21.1	0.000012	0.0072
GOTERM_BP_ALL	regulation of blood pressure	5	26.3	0.000018	0.0075
GOTERM_BP_ALL	response to oxygen-containing compound	9	47.4	0.000034	0.011
GOTERM_BP_ALL	cellular metal ion homeostasis	6	31.6	0.000064	0.014
GOTERM_BP_ALL	grooming behavior	3	15.8	0.000077	0.014
GOTERM_BP_ALL	maternal behavior	3	15.8	0.00011	0.014
GOTERM_BP_ALL	cellular cation homeostasis	6	31.6	0.00011	0.014
GOTERM_BP_ALL	metal ion homeostasis	6	31.6	0.00012	0.014
GOTERM_BP_ALL	parental behavior	3	15.8	0.00012	0.014
GOTERM_BP_ALL	cellular ion homeostasis	6	31.6	0.00013	0.014
GOTERM_BP_ALL	response to lipid	7	36.8	0.00013	0.014
GOTERM_BP_ALL	single organism signaling	14	73.7	0.00014	0.014
GOTERM_BP_ALL	signaling	14	73.7	0.00015	0.014
GOTERM_BP_ALL	cell communication	14	73.7	0.00017	0.014
GOTERM_BP_ALL	positive regulation of biological process	13	68.4	0.00021	0.016
GOTERM_BP_ALL	cation homeostasis	6	31.6	0.00021	0.016
GOTERM_BP_ALL	inorganic ion homeostasis	6	31.6	0.00024	0.016
GOTERM_BP_ALL	regulation of growth	6	31.6	0.00024	0.016
GOTERM_BP_ALL	behavior	6	31.6	0.00026	0.016
GOTERM_MF_ALL	neuropeptide hormone activity	3	15.8	0.00028	0.019
GOTERM_BP_ALL	response to abiotic stimulus	7	36.8	0.0003	0.017
GOTERM_BP_ALL	ion homeostasis	6	31.6	0.0003	0.017
GOTERM_BP_ALL	cellular chemical homeostasis	6	31.6	0.00039	0.021
GOTERM_BP_ALL	response to nutrient levels	5	26.3	0.00046	0.024
GOTERM_BP_ALL	signal transduction	13	68.4	0.0005	0.024
GOTERM_BP_ALL	positive regulation of cellular process	12	63.2	0.00051	0.024
GOTERM_BP_ALL	blood circulation	5	26.3	0.00053	0.024
GOTERM_BP_ALL	circulatory system process	5	26.3	0.00054	0.024
GOTERM_BP_ALL	response to extracellular stimulus	5	26.3	0.0006	0.026
GOTERM_BP_ALL	cellular homeostasis	6	31.6	0.0007	0.029
GOTERM_BP_ALL	response to organonitrogen compound	6	31.6	0.00074	0.03
GOTERM_BP_ALL	single-organism behavior	5	26.3	0.00075	0.03
GOTERM_BP_ALL	reproductive behavior	3	15.8	0.00084	0.032
GOTERM_BP_ALL	response to stress	10	52.6	0.0012	0.044
GOTERM_MF_ALL	protein binding	14	73.7	0.0013	0.047
GOTERM_BP_ALL	regulation of multicellular organismal process	9	47.4	0.0013	0.047

GOTERM_BP_ALL	response to nitrogen compound	6	31.6	0.0014	0.047
GOTERM_BP_ALL	response to organic cyclic compound	6	31.6	0.0014	0.047
GOTERM_MF_ALL	G-protein coupled receptor binding	4	21.1	0.0015	0.047
GOTERM_MF_ALL	neurohypophyseal hormone activity	2	10.5	0.0017	0.047

#### ZT14M Hypothalamus

Category	Term	Count	%	P-Value	Benjamini
GOTERM_CC_ALL	cytoplasm	343	72.8	6.1E-27	3.3E-24
GOTERM_CC_ALL	cytoplasmic part	272	57.7	1E-26	3.3E-24
GOTERM_CC_ALL	neuron part	109	23.1	1.2E-25	2.5E-23
GOTERM_CC_ALL	cytosolic ribosome	35	7.4	2.5E-24	4.2E-22
GOTERM_BP_ALL	organonitrogen compound metabolic process	129	27.1	1E-23	2.9E-20
GOTERM_CC_ALL	intracellular organelle	359	76.2	1.7E-22	2.3E-20
GOTERM_CC_ALL	ribosome	43	9.1	2.3E-22	2.5E-20
KEGG_PATHWAY	Ribosome	35	7.4	4.4E-22	9E-20
GOTERM_CC_ALL	intracellular part	389	82.6	7.9E-22	7.4E-20
GOTERM_CC_ALL	intracellular organelle part	267	56.7	9.4E-22	7.7E-20
GOTERM_CC_ALL	organelle	376	79.8	1.6E-21	1.2E-19
GOTERM_CC_ALL	neuron projection	87	18.5	4.3E-21	2.8E-19
GOTERM_CC_ALL	ribosomal subunit	36	7.6	3.1E-20	1.9E-18
GOTERM_CC_ALL	organelle part	267	56.7	4.5E-20	2.5E-18
GOTERM_CC_ALL	membrane-bounded organelle	354	75.2	5E-20	2.5E-18
GOTERM_MF_ALL	structural constituent of ribosome	38	8.1	1.2E-18	1.2E-15
GOTERM_CC_ALL	cytosol	109	23.1	2E-18	9.5E-17
GOTERM_CC_ALL	somatodendritic compartment	69	14.6	2.4E-18	1.1E-16
GOTERM_CC_ALL	macromolecular complex	198	42	4.8E-18	1.9E-16
GOTERM_CC_ALL	intracellular	391	83	5.5E-18	2.1E-16
GOTERM_CC_ALL	cytosolic part	37	7.9	8.1E-18	2.9E-16
GOTERM_BP_ALL	localization	216	45.9	8.8E-18	2.6E-14
GOTERM_CC_ALL	myelin sheath	33	7	1.5E-17	5.3E-16
GOTERM_CC_ALL	intracellular membrane-bounded organelle	325	69	1.8E-17	5.8E-16
GOTERM_CC_ALL	intracellular ribonucleoprotein complex	68	14.4	1.9E-17	6E-16
GOTERM_CC_ALL	ribonucleoprotein complex	68	14.4	2E-17	6E-16
GOTERM_CC_ALL	axon	52	11	2.6E-17	7.5E-16
GOTERM_BP_ALL	establishment of localization	181	38.4	4.7E-16	7.7E-13
GOTERM_BP_ALL	transport	175	37.2	2.3E-15	2.9E-12
GOTERM_CC_ALL	membrane-bounded vesicle	146	31	3.4E-15	9.4E-14
GOTERM_CC_ALL	vesicle	150	31.8	6.8E-15	1.8E-13
GOTERM_BP_ALL	organonitrogen compound biosynthetic process	80	17	1.5E-14	1.5E-11
GOTERM_CC_ALL	cell projection	104	22.1	2E-14	5E-13
GOTERM_CC_ALL	cell body	54	11.5	3.5E-14	8.4E-13
GOTERM_CC_ALL	extracellular vesicle	119	25.3	1.9E-13	4.5E-12
GOTERM_CC_ALL	extracellular organelle	119	25.3	2.3E-13	5.3E-12
GOTERM_CC_ALL	neuronal cell body	49	10.4	2.4E-13	5.3E-12
GOTERM_CC_ALL	extracellular exosome	118	25.1	3.1E-13	6.6E-12
GOTERM_CC_ALL	cytosolic small ribosomal subunit	16	3.4	4.3E-13	8.8E-12
KEGG_PATHWAY	Oxidative phosphorylation	25	5.3	1.1E-12	1.2E-10
GOTERM_CC_ALL	synapse part	50	10.6	1.5E-12	3.1E-11
GOTERM_MF_ALL	structural molecule activity	52	11	1.6E-12	7.7E-10
GOTERM_CC_ALL	mitochondrial protein complex	24	5.1	1.7E-12	3.3E-11
GOTERM_CC_ALL	mitochondrial envelope	48	10.2	1.9E-12	3.6E-11
GOTERM_BP_ALL	regulation of biological quality	140	29.7	2.6E-12	1.9E-09
GOTERM_BP_ALL	cellular amide metabolic process	64	13.6	2.7E-12	1.9E-09
GOTERM_CC_ALL	dendrite	47	10	3.1E-12	5.7E-11
GOTERM_CC_ALL	extracellular region part	150	31.8	4.6E-12	8.1E-11
GOTERM_CC_ALL	inner mitochondrial membrane protein complex	21	4.5	5E-12	8.6E-11
GOTERM_BP_ALL	nervous system development	105	22.3	5.3E-12	3.3E-09
KEGG_PATHWAY	Parkinson's disease	25	5.3	5.4E-12	3.7E-10
GOTERM_BP_ALL	peptide metabolic process	57	12.1	6.7E-12	3.7E-09
GOTERM_CC_ALL	mitochondrion	87	18.5	9.4E-12	1.6E-10
GOTERM_CC_ALL	respiratory chain	18	3.8	1E-11	1.6E-10
GOTERM_BP_ALL	translation	50	10.6	1.5E-11	7.7E-09
GOTERM_CC_ALL	cytosolic large ribosomal subunit	18	3.8	1.8E-11	2.8E-10
GOTERM_CC_ALL	mitochondrial inner membrane	36	7.6	2.1E-11	3.3E-10
GOTERM_CC_ALL	mitochondrial membrane part	25	5.3	2.3E-11	3.4E-10
GOTERM_BP_ALL	amide biosynthetic process	53	11.3	3.5E-11	0.000000016
GOTERM_CC_ALL	mitochondrial part	54	11.5	4.3E-11	6.3E-10
GOTERM_BP_ALL	peptide biosynthetic process	50	10.6	4.3E-11	0.000000018
GOTERM_CC_ALL	small ribosomal subunit	17	3.6	5.1E-11	7.4E-10
GOTERM_CC_ALL	synapse	54	11.5	5.4E-11	7.7E-10
GOTERM_CC_ALL	extracellular region	161	34.2	9.6E-11	1.3E-09
GOTERM_BP_ALL	single-organism localization	133	28.2	1E-10	0.000000004
GOTERM_CC_ALL	mitochondrial membrane	43	9.1	1.1E-10	1.5E-09
GOTERM_CC_ALL	respiratory chain complex	16	3.4	2.2E-10	2.9E-09
GOTERM_BP_ALL	cellular localization	102	21.7	2.2E-10	0.000000079
GOTERM_BP_ALL	central nervous system development	57	12.1	3.8E-10	0.00000013
GOTERM_CC_ALL	axon part	29	6.2	3.8E-10	0.000000005
GOTERM_CC_ALL	organelle inner membrane	36	7.6	5.3E-10	6.8E-09
GOTERM_MF_ALL	protein binding	248	52.7	5.8E-10	0.00000019
GOTERM_CC_ALL	cell projection part	59	12.5	8.7E-10	0.000000011
GOTERM_CC_ALL	large ribosomal subunit	19	4	1.3E-09	0.000000016
GOTERM_CC_ALL	mitochondrial respiratory chain	15	3.2	2.7E-09	0.000000032
GOTERM_CC_ALL	intracellular non-membrane-bounded organelle	145	30.8	3.8E-09	0.000000044
GOTERM_CC_ALL	non-membrane-bounded organelle	145	30.8	3.8E-09	0.000000044
GOTERM_BP_ALL	cell-cell signaling	66	14	0.000000004	0.0000012
GOTERM_BP_ALL	regulation of hormone levels	37	7.9	4.1E-09	0.0000012

GOTERM_BP_ALL	single-organism transport	122	25.9	4.7E-09	0.0000013
GOTERM_BP_ALL	generation of precursor metabolites and energy	29	6.2	6.3E-09	0.0000015
GOTERM_BP_ALL	oxidative phosphorylation	14	3	6.3E-09	0.0000015
GOTERM_BP_ALL	secretion	58	12.3	6.4E-09	0.0000015
GOTERM_CC_ALL	perikaryon	19	4	0.00000008	0.00000092
KEGG_PATHWAY	Huntington's disease	24	5.1	0.00000012	0.00000061
GOTERM_MF_ALL	poly(A) RNA binding	61	13	0.00000015	0.0000035
GOTERM_BP_ALL	brain development	45	9.6	0.00000018	0.0000041
GOTERM_MF_ALL	RNA binding	77	16.3	0.00000023	0.0000045
GOTERM_BP_ALL	neurogenesis	75	15.9	0.00000027	0.0000059
GOTERM_CC_ALL	membrane protein complex	53	11.3	0.00000034	0.0000038
GOTERM_BP_ALL	head development	46	9.8	0.00000038	0.0000079
GOTERM_MF_ALL	inorganic cation transmembrane transporter activity	34	7.2	0.00000052	0.0000084
GOTERM_BP_ALL	energy derivation by oxidation of organic compounds	23	4.9	0.00000053	0.00001
GOTERM_BP_ALL	ribonucleoprotein complex biogenesis	31	6.6	0.00000056	0.000011
GOTERM_MF_ALL	monovalent inorganic cation transmembrane transporter activity	27	5.7	0.00000077	0.000011
GOTERM_BP_ALL	respiratory electron transport chain	13	2.8	0.00000087	0.000016
GOTERM_BP_ALL	purine ribonucleoside triphosphate metabolic process	22	4.7	0.00000009	0.000016
GOTERM_CC_ALL	cell	420	89.2	0.00000098	0.0000011
GOTERM_BP_ALL	ATP metabolic process	21	4.5	0.0000001	0.000018
GOTERM_BP_ALL	secretion by cell	50	10.6	0.00000012	0.000019
GOTERM_BP_ALL	cellular respiration	18	3.8	0.00000013	0.000021
GOTERM_CC_ALL	cell part	419	89	0.00000014	0.0000016
GOTERM_CC_ALL	organelle membrane	91	19.3	0.00000015	0.0000016
GOTERM_BP_ALL	ribonucleoside triphosphate metabolic process	22	4.7	0.00000015	0.000024
GOTERM_BP_ALL	neuron development	55	11.7	0.00000016	0.000025
GOTERM_BP_ALL	purine nucleoside triphosphate metabolic process	22	4.7	0.00000017	0.000025
GOTERM_BP_ALL	generation of neurons	69	14.6	0.00000018	0.000025
GOTERM_BP_ALL	ribosome biogenesis	24	5.1	0.00000018	0.000025
GOTERM_MF_ALL	hormone activity	16	3.4	0.0000002	0.000024
GOTERM_BP_ALL	electron transport chain	13	2.8	0.00000022	0.000027
GOTERM_BP_ALL	anterograde trans-synaptic signaling	36	7.6	0.00000022	0.000027
GOTERM_BP_ALL	synaptic signaling	36	7.6	0.00000022	0.000027
GOTERM_BP_ALL	trans-synaptic signaling	36	7.6	0.00000022	0.000027
GOTERM_BP_ALL	chemical synaptic transmission	36	7.6	0.00000022	0.000027
GOTERM_MF_ALL	neuropeptide hormone activity	9	1.9	0.00000023	0.000025
GOTERM_BP_ALL	ATP synthesis coupled electron transport	11	2.3	0.0000003	0.000035
GOTERM_BP_ALL	gliogenesis	24	5.1	0.00000031	0.000035
GOTERM_BP_ALL	modulation of synaptic transmission	26	5.5	0.00000033	0.000037
GOTERM_CC_ALL	organelle envelope	52	11	0.00000033	0.0000035
GOTERM_BP_ALL	hormone transport	27	5.7	0.00000034	0.000038
GOTERM_BP_ALL	nitrogen compound metabolic process	204	43.3	0.00000037	0.000039
GOTERM_BP_ALL	positive regulation of synaptic transmission	17	3.6	0.00000037	0.000039
GOTERM_CC_ALL	envelope	52	11	0.00000038	0.0000039
GOTERM_CC_ALL	presynapse	25	5.3	0.00000051	0.0000052
GOTERM_BP_ALL	neuron differentiation	63	13.4	0.00000052	0.000054
GOTERM_BP_ALL	nitrogen compound transport	40	8.5	0.00000055	0.000056
GOTERM_BP_ALL	cellular metabolic process	280	59.4	0.00000056	0.000056
GOTERM_MF_ALL	hydrogen ion transmembrane transporter activity	14	3	0.00000057	0.000055
GOTERM_BP_ALL	single-organism behavior	32	6.8	0.00000063	0.000062
GOTERM_BP_ALL	system development	154	32.7	0.00000067	0.000064
GOTERM_MF_ALL	cation transmembrane transporter activity	35	7.4	0.00000067	0.000059
GOTERM_BP_ALL	hormone secretion	26	5.5	0.00000079	0.000074
GOTERM_BP_ALL	purine ribonucleoside monophosphate metabolic process	21	4.5	0.0000008	0.000074
GOTERM_BP_ALL	purine nucleoside monophosphate metabolic process	21	4.5	0.00000086	0.000078
GOTERM_BP_ALL	nucleoside triphosphate metabolic process	22	4.7	0.00000088	0.000078
GOTERM_CC_ALL	focal adhesion	27	5.7	0.00000094	0.0000095
GOTERM_CC_ALL	cell-substrate adherens junction	27	5.7	0.0000012	0.000012
GOTERM_BP_ALL	cellular component organization or biogenesis	189	40.1	0.0000014	0.000012
GOTERM_BP_ALL	macromolecule localization	101	21.4	0.0000015	0.000012
GOTERM_CC_ALL	cell-substrate junction	27	5.7	0.0000015	0.000015
GOTERM_BP_ALL	ribonucleoside monophosphate metabolic process	21	4.5	0.0000017	0.000015
GOTERM_MF_ALL	rRNA binding	12	2.5	0.0000019	0.000015
GOTERM_BP_ALL	signal release	29	6.2	0.0000022	0.000018
GOTERM_BP_ALL	homeostatic process	71	15.1	0.0000025	0.00002
GOTERM_BP_ALL	neuron projection development	46	9.8	0.0000026	0.000021
GOTERM_CC_ALL	oxidoreductase complex	13	2.8	0.0000028	0.000027
GOTERM_BP_ALL	nucleoside monophosphate metabolic process	21	4.5	0.0000028	0.000022
GOTERM_BP_ALL	oxidation-reduction process	46	9.8	0.0000034	0.000026
GOTERM_BP_ALL	behavior	38	8.1	0.0000034	0.000026
GOTERM_CC_ALL	inclusion body	11	2.3	0.0000035	0.000034
GOTERM_BP_ALL	regulation of secretion by cell	38	8.1	0.0000036	0.000027
GOTERM_BP_ALL	glial cell differentiation	19	4	0.0000039	0.000029
GOTERM_CC_ALL	protein complex	135	28.7	0.0000046	0.000043
GOTERM_BP_ALL	regulation of localization	94	20	0.0000049	0.000036
GOTERM_BP_ALL	purine ribonucleoside metabolic process	22	4.7	0.000005	0.000036
GOTERM_BP_ALL	cellular nitrogen compound metabolic process	190	40.3	0.0000056	0.0004
GOTERM_BP_ALL	chemical homeostasis	51	10.8	0.0000057	0.0004
GOTERM_CC_ALL	axon terminus	17	3.6	0.0000057	0.000053
GOTERM_BP_ALL	purine nucleoside metabolic process	22	4.7	0.0000062	0.000043
GOTERM_BP_ALL	establishment of localization in cell	70	14.9	0.0000066	0.000045
GOTERM_BP_ALL	regulation of secretion	39	8.3	0.0000074	0.00005
GOTERM_BP_ALL	purine nucleotide metabolic process	29	6.2	0.0000076	0.00005
GOTERM_BP_ALL	purine ribonucleotide metabolic process	28	5.9	0.0000076	0.00005
GOTERM_BP_ALL	ribose phosphate metabolic process	29	6.2	0.0000078	0.00005
GOTERM_BP_ALL	response to toxic substance	15	3.2	0.0000089	0.000057

GOTERM_CC_ALL	mitochondrial respiratory chain complex I	9	1.9	0.000089	0.000079
GOTERM_CC_ALL	NADH dehydrogenase complex	9	1.9	0.000089	0.000079
GOTERM_CC_ALL	respiratory chain complex I	9	1.9	0.000089	0.000079
GOTERM_BP_ALL	protein localization	88	18.7	0.00011	0.00067
GOTERM_BP_ALL	glycosyl compound metabolic process	24	5.1	0.00011	0.00068
GOTERM_BP_ALL	positive regulation of amine transport	8	1.7	0.00012	0.00071
GOTERM_BP_ALL	mitochondrial ATP synthesis coupled electron transport	9	1.9	0.00012	0.00073
KEGG_PATHWAY	Cardiac muscle contraction	12	2.5	0.00012	0.00051
GOTERM_BP_ALL	nucleotide metabolic process	33	7	0.00012	0.00075
GOTERM_BP_ALL	cell projection organization	59	12.5	0.00013	0.00076
GOTERM_BP_ALL	nucleoside metabolic process	23	4.9	0.00014	0.0008
GOTERM_CC_ALL	neuron projection terminus	17	3.6	0.00014	0.00012
GOTERM_BP_ALL	ribonucleotide metabolic process	28	5.9	0.00014	0.00083
GOTERM_BP_ALL	cellular protein localization	62	13.2	0.00016	0.0009
GOTERM_CC_ALL	nucleus	194	41.2	0.00017	0.00014
GOTERM_BP_ALL	ribonucleoside metabolic process	22	4.7	0.00017	0.00096
GOTERM_BP_ALL	nucleoside phosphate metabolic process	33	7	0.00018	0.00099
GOTERM_BP_ALL	ribonucleoprotein complex subunit organization	18	3.8	0.00018	0.001
GOTERM_BP_ALL	ribosome assembly	10	2.1	0.0002	0.0011
GOTERM_BP_ALL	cellular macromolecule localization	62	13.2	0.0002	0.0011
GOTERM_BP_ALL	multicellular organism development	162	34.4	0.00021	0.0011
GOTERM_BP_ALL	cellular component organization	179	38	0.00021	0.0011
GOTERM_BP_ALL	response to organonitrogen compound	42	8.9	0.00022	0.0011
GOTERM_BP_ALL	single-multicellular organism process	186	39.5	0.00022	0.0012
GOTERM_BP_ALL	ion transport	57	12.1	0.00023	0.0012
GOTERM_BP_ALL	aging	21	4.5	0.00026	0.0013
GOTERM_BP_ALL	RNA processing	38	8.1	0.00027	0.0013
GOTERM_BP_ALL	single-organism metabolic process	121	25.7	0.00029	0.0014
GOTERM_BP_ALL	metabolic process	296	62.8	0.0003	0.0015
GOTERM_CC_ALL	perinuclear region of cytoplasm	35	7.4	0.0003	0.00025
GOTERM_CC_ALL	postsynaptic density	18	3.8	0.00031	0.00026
GOTERM_CC_ALL	postsynaptic specialization	18	3.8	0.00031	0.00026
GOTERM_BP_ALL	intracellular transport	55	11.7	0.00032	0.0015
GOTERM_BP_ALL	purine-containing compound metabolic process	29	6.2	0.00033	0.0016
GOTERM_CC_ALL	postsynapse	26	5.5	0.00033	0.00027
GOTERM_BP_ALL	cellular homeostasis	41	8.7	0.00036	0.0017
GOTERM_BP_ALL	response to abiotic stimulus	50	10.6	0.00036	0.0017
GOTERM_BP_ALL	ribonucleoprotein complex assembly	17	3.6	0.00036	0.0017
GOTERM_BP_ALL	response to extracellular stimulus	27	5.7	0.00038	0.0018
GOTERM_BP_ALL	regulation of homeostatic process	28	5.9	0.00039	0.0018
GOTERM_CC_ALL	adherens junction	34	7.2	0.00042	0.00034
GOTERM_BP_ALL	cation transport	42	8.9	0.00049	0.0022
GOTERM_MF_ALL	ion transmembrane transporter activity	37	7.9	0.00052	0.0039
GOTERM_BP_ALL	cytoskeleton-dependent intracellular transport	11	2.3	0.00053	0.0024
KEGG_PATHWAY	Alzheimer's disease	17	3.6	0.00054	0.0019
GOTERM_CC_ALL	cell projection cytoplasm	9	1.9	0.00056	0.00045
GOTERM_BP_ALL	ribosomal small subunit biogenesis	10	2.1	0.00057	0.0025
GOTERM_CC_ALL	synaptic vesicle	14	3	0.00057	0.00045
GOTERM_BP_ALL	regulation of neurogenesis	39	8.3	0.00057	0.0025
GOTERM_CC_ALL	terminal bouton	12	2.5	0.00057	0.00045
GOTERM_BP_ALL	small molecule metabolic process	68	14.4	0.00057	0.0025
GOTERM_BP_ALL	regulation of hormone secretion	20	4.2	0.00059	0.0026
GOTERM_BP_ALL	organelle disassembly	16	3.4	0.00063	0.0027
GOTERM_CC_ALL	catalytic step 2 spliceosome	11	2.3	0.00065	0.0005
GOTERM_BP_ALL	regulation of nervous system development	42	8.9	0.00066	0.0028
GOTERM_BP_ALL	mitochondrion disassembly	15	3.2	0.00068	0.0029
GOTERM_BP_ALL	mitophagy	15	3.2	0.00068	0.0029
GOTERM_CC_ALL	anchoring junction	34	7.2	0.00068	0.00052
GOTERM_CC_ALL	cytochrome complex	7	1.5	0.00069	0.00052
GOTERM_CC_ALL	membrane-enclosed lumen	115	24.4	0.0007	0.00052
GOTERM_MF_ALL	oxidoreductase activity, acting on NAD(P)H, quinone or similar compound as acceptor	8	1.7	0.00075	0.0052
GOTERM_BP_ALL	anatomical structure development	174	36.9	0.0008	0.0033
GOTERM_BP_ALL	nucleobase-containing small molecule metabolic process	33	7	0.00083	0.0034
GOTERM_BP_ALL	regulation of transport	69	14.6	0.00083	0.0034
GOTERM_MF_ALL	neuropeptide receptor binding	7	1.5	0.00084	0.0054
GOTERM_BP_ALL	oligodendrocyte differentiation	11	2.3	0.00085	0.0034
GOTERM_BP_ALL	response to nutrient levels	25	5.3	0.00085	0.0034
GOTERM_BP_ALL	phosphate-containing compound metabolic process	98	20.8	0.00085	0.0034
GOTERM_BP_ALL	amine transport	10	2.1	0.00086	0.0034
GOTERM_CC_ALL	excitatory synapse	18	3.8	0.00089	0.00065
GOTERM_BP_ALL	myelination	12	2.5	0.00089	0.0035
GOTERM_CC_ALL	transport vesicle	20	4.2	0.0009	0.00066
GOTERM_BP_ALL	phosphorus metabolic process	98	20.8	0.00092	0.0036
GOTERM_MF_ALL	substrate-specific transporter activity	46	9.8	0.00093	0.0056
GOTERM_BP_ALL	peptide hormone secretion	19	4	0.00093	0.0036
GOTERM_BP_ALL	organic substance transport	87	18.5	0.00095	0.0037
GOTERM_BP_ALL	regulation of mitochondrial membrane potential	9	1.9	0.00096	0.0037
GOTERM_BP_ALL	peptide transport	20	4.2	0.001	0.0038
GOTERM_MF_ALL	oxidoreductase activity	38	8.1	0.001	0.0059
GOTERM_BP_ALL	response to nitrogen compound	44	9.3	0.001	0.0039
GOTERM_BP_ALL	axon ensheathment	12	2.5	0.001	0.0039
GOTERM_BP_ALL	ensheathment of neurons	12	2.5	0.001	0.0039
GOTERM_CC_ALL	mitochondrial proton-transporting ATP synthase complex	6	1.3	0.0011	0.00078
GOTERM_CC_ALL	secretory vesicle	26	5.5	0.0012	0.00085
GOTERM_BP_ALL	cellular chemical homeostasis	36	7.6	0.0012	0.0045
GOTERM_CC_ALL	extracellular matrix	27	5.7	0.0014	0.00094

GOTERM_CC_ALL	proton-transporting ATP synthase complex	6	1.3	0.00014	0.00094
GOTERM_MF_ALL	substrate-specific transmembrane transporter activity	40	8.5	0.00014	0.0068
GOTERM_MF_ALL	NADH dehydrogenase (ubiquinone) activity	7	1.5	0.00014	0.0068
GOTERM_MF_ALL	NADH dehydrogenase (quinone) activity	7	1.5	0.00014	0.0068
GOTERM_CC_ALL	exocytic vesicle	14	3	0.00014	0.00099
GOTERM_BP_ALL	peptide secretion	19	4	0.00015	0.0053
GOTERM_MF_ALL	receptor binding	60	12.7	0.00015	0.0068
GOTERM_BP_ALL	single-organism cellular localization	42	8.9	0.00016	0.0057
GOTERM_BP_ALL	regulation of neuron differentiation	33	7	0.00016	0.0058
GOTERM_MF_ALL	NADH dehydrogenase activity	7	1.5	0.00017	0.0074
GOTERM_CC_ALL	nuclear part	113	24	0.00017	0.0011
GOTERM_BP_ALL	regulation of synaptic transmission, GABAergic	7	1.5	0.00017	0.0062
GOTERM_BP_ALL	single-organism developmental process	174	36.9	0.00018	0.0062
GOTERM_BP_ALL	cellular protein metabolic process	142	30.1	0.00018	0.0064
KEGG_PATHWAY	Non-alcoholic fatty liver disease (NAFLD)	15	3.2	0.00018	0.0052
GOTERM_MF_ALL	transporter activity	51	10.8	0.00019	0.0079
KEGG_PATHWAY	GABAergic synapse	11	2.3	0.0002	0.0052
GOTERM_BP_ALL	autophagy	25	5.3	0.0002	0.0071
GOTERM_BP_ALL	phosphorylation	74	15.7	0.00021	0.0072
GOTERM_BP_ALL	cell development	80	17	0.00021	0.0072
GOTERM_BP_ALL	regulation of cell projection organization	32	6.8	0.00021	0.0073
GOTERM_BP_ALL	amide transport	20	4.2	0.00021	0.0073
GOTERM_MF_ALL	G-protein coupled receptor binding	18	3.8	0.00021	0.0087
GOTERM_BP_ALL	ion homeostasis	34	7.2	0.00021	0.0073
GOTERM_BP_ALL	developmental process	176	37.4	0.00022	0.0073
GOTERM_BP_ALL	cellular component biogenesis	90	19.1	0.00024	0.0081
GOTERM_BP_ALL	regulation of cellular component organization	83	17.6	0.00025	0.0082
GOTERM_BP_ALL	catecholamine secretion	8	1.7	0.00025	0.0084
GOTERM_BP_ALL	RNA splicing, via transesterification reactions with bulged adenosine as nucleophile	16	3.4	0.00026	0.0086
GOTERM_BP_ALL	mRNA splicing, via spliceosome	16	3.4	0.00026	0.0086
GOTERM_BP_ALL	RNA splicing, via transesterification reactions	16	3.4	0.00027	0.0089
GOTERM_CC_ALL	main axon	9	1.9	0.00028	0.0019
GOTERM_BP_ALL	programmed cell death	68	14.4	0.00028	0.009
GOTERM_BP_ALL	glial cell development	10	2.1	0.00028	0.009
GOTERM_BP_ALL	organophosphate metabolic process	41	8.7	0.0003	0.0094
GOTERM_BP_ALL	cerebellum development	11	2.3	0.0003	0.0096
GOTERM_BP_ALL	axo-dendritic transport	7	1.5	0.00031	0.0098
GOTERM_BP_ALL	response to inorganic substance	28	5.9	0.00033	0.01
GOTERM_BP_ALL	response to oxygen-containing compound	62	13.2	0.00033	0.01
GOTERM_BP_ALL	regulation of amine transport	9	1.9	0.00033	0.01
GOTERM_BP_ALL	cell morphogenesis involved in neuron differentiation	27	5.7	0.00034	0.01
GOTERM_CC_ALL	nuclear lumen	99	21	0.00034	0.0023
GOTERM_BP_ALL	apoptotic process	65	13.8	0.00035	0.011
GOTERM_BP_ALL	mitophagy in response to mitochondrial depolarization	12	2.5	0.00037	0.011
GOTERM_BP_ALL	response to mitochondrial depolarization	12	2.5	0.00037	0.011
GOTERM_BP_ALL	organic substance metabolic process	280	59.4	0.00037	0.011
GOTERM_BP_ALL	regulation of multicellular organismal process	93	19.7	0.00039	0.012
GOTERM_BP_ALL	neuropeptide signaling pathway	9	1.9	0.0004	0.012
GOTERM_BP_ALL	positive regulation of transport	42	8.9	0.0004	0.012
GOTERM_MF_ALL	oxidoreductase activity, acting on diphenols and related substances as donors, cytochrome as acceptor	4	0.8	0.00041	0.015
GOTERM_MF_ALL	ubiquinol-cytochrome-c reductase activity	4	0.8	0.00041	0.015
GOTERM_BP_ALL	cell death	71	15.1	0.00041	0.012
GOTERM_BP_ALL	regulation of cell development	42	8.9	0.00042	0.012
GOTERM_MF_ALL	electron carrier activity	9	1.9	0.00042	0.015
GOTERM_MF_ALL	pyrophosphatase activity	35	7.4	0.00043	0.015
GOTERM_BP_ALL	monovalent inorganic cation transport	23	4.9	0.00043	0.012
GOTERM_BP_ALL	mRNA processing	23	4.9	0.00043	0.012
GOTERM_BP_ALL	neuron projection morphogenesis	28	5.9	0.00045	0.013
GOTERM_MF_ALL	hydrolase activity, acting on acid anhydrides, in phosphorus-containing anhydrides	35	7.4	0.00045	0.015
GOTERM_BP_ALL	metal ion transport	35	7.4	0.00046	0.013
GOTERM_CC_ALL	organelle lumen	109	23.1	0.00046	0.0031
GOTERM_BP_ALL	macromitophagy	12	2.5	0.00047	0.013
GOTERM_BP_ALL	regulation of neuron projection development	26	5.5	0.00048	0.014
GOTERM_MF_ALL	hydrolase activity, acting on acid anhydrides	35	7.4	0.00049	0.016
GOTERM_BP_ALL	regulation of peptide transport	16	3.4	0.00052	0.014
GOTERM_BP_ALL	response to ethanol	12	2.5	0.00053	0.015
GOTERM_BP_ALL	vesicle localization	14	3	0.00054	0.015
GOTERM_BP_ALL	purine ribonucleoside triphosphate biosynthetic process	8	1.7	0.00054	0.015
GOTERM_CC_ALL	endomembrane system	111	23.6	0.00058	0.0038
GOTERM_CC_ALL	cytoplasmic vesicle	46	9.8	0.00058	0.0038
GOTERM_BP_ALL	animal organ development	111	23.6	0.0006	0.016
GOTERM_BP_ALL	purine nucleoside triphosphate biosynthetic process	8	1.7	0.0006	0.016
GOTERM_BP_ALL	cytoplasmic translation	8	1.7	0.0006	0.016
GOTERM_CC_ALL	intracellular organelle lumen	108	22.9	0.00061	0.0039
GOTERM_BP_ALL	cellular component disassembly	22	4.7	0.00062	0.017
GOTERM_CC_ALL	intracellular vesicle	46	9.8	0.00062	0.004
GOTERM_BP_ALL	primary metabolic process	265	56.3	0.00064	0.017
GOTERM_MF_ALL	nucleoside-triphosphatase activity	33	7	0.00064	0.02
GOTERM_MF_ALL	oxidoreductase activity, acting on diphenols and related substances as donors	4	0.8	0.00065	0.02
GOTERM_BP_ALL	hormone metabolic process	13	2.8	0.00066	0.017
GOTERM_BP_ALL	negative regulation of protein kinase activity by regulation of protein phosphorylation	4	0.8	0.00066	0.017
GOTERM_BP_ALL	metencephalon development	11	2.3	0.00068	0.018
GOTERM_CC_ALL	aggresome	6	1.3	0.00068	0.0043
KEGG_PATHWAY	Endocrine and other factor-regulated calcium reabsorption	8	1.7	0.00071	0.016
GOTERM_BP_ALL	regulation of neuronal synaptic plasticity	8	1.7	0.00073	0.019
GOTERM_BP_ALL	positive regulation of cell death	29	6.2	0.00076	0.02



GOTERM_BP_ALL	regulation of synaptic plasticity	13	2.8	0.00077	0.02
GOTERM_BP_ALL	response to organic cyclic compound	41	8.7	0.00077	0.02
GOTERM_CC_ALL	proton-transporting two-sector ATPase complex	7	1.5	0.00077	0.0048
GOTERM_BP_ALL	neuron-neuron synaptic transmission	11	2.3	0.00078	0.02
GOTERM_CC_ALL	nucleoplasm	76	16.1	0.00079	0.0049
GOTERM_BP_ALL	regulation of membrane potential	21	4.5	0.00081	0.021
KEGG_PATHWAY	Mineral absorption	7	1.5	0.00083	0.017
GOTERM_CC_ALL	cytoplasmic, membrane-bounded vesicle	42	8.9	0.00085	0.0052
GOTERM_BP_ALL	sodium ion homeostasis	7	1.5	0.00086	0.022
GOTERM_CC_ALL	cell junction	51	10.8	0.00087	0.0053
GOTERM_BP_ALL	positive regulation of catecholamine secretion	5	1.1	0.00087	0.022
GOTERM_MF_ALL	sodium ion transmembrane transporter activity	11	2.3	0.00089	0.025
GOTERM_MF_ALL	protein kinase binding	28	5.9	0.0009	0.025
GOTERM_BP_ALL	locomotory behavior	16	3.4	0.0009	0.023
GOTERM_CC_ALL	ribonucleoprotein granule	12	2.5	0.00091	0.0055
GOTERM_BP_ALL	establishment of localization by movement along microtubule	10	2.1	0.00093	0.023
GOTERM_BP_ALL	adult behavior	13	2.8	0.00094	0.023
GOTERM_BP_ALL	establishment of vesicle localization	13	2.8	0.00094	0.023
GOTERM_MF_ALL	kinase binding	30	6.4	0.00094	0.025
GOTERM_MF_ALL	transmembrane transporter activity	40	8.5	0.00094	0.025
GOTERM_BP_ALL	ribonucleoside triphosphate biosynthetic process	8	1.7	0.00096	0.024
GOTERM_BP_ALL	cellular process	397	84.3	0.001	0.025
GOTERM_BP_ALL	regulation of ion homeostasis	14	3	0.001	0.025
GOTERM_BP_ALL	catecholamine transport	8	1.7	0.001	0.025
GOTERM_BP_ALL	ATP biosynthetic process	7	1.5	0.0011	0.026
GOTERM_BP_ALL	response to endogenous stimulus	58	12.3	0.0011	0.026
GOTERM_CC_ALL	prespliceosome	5	1.1	0.0011	0.0066
GOTERM_BP_ALL	organelle organization	112	23.8	0.0011	0.027
GOTERM_MF_ALL	ATPase activity	22	4.7	0.0011	0.03
GOTERM_BP_ALL	response to alcohol	13	2.8	0.0011	0.027
GOTERM_BP_ALL	regulation of peptide hormone secretion	15	3.2	0.0012	0.027
GOTERM_BP_ALL	response to transition metal nanoparticle	11	2.3	0.0012	0.027
GOTERM_BP_ALL	regulation of catecholamine secretion	7	1.5	0.0012	0.027
GOTERM_BP_ALL	macroautophagy	18	3.8	0.0012	0.027
GOTERM_BP_ALL	regulation of cellular protein catabolic process	13	2.8	0.0012	0.027
GOTERM_BP_ALL	rRNA processing	13	2.8	0.0012	0.027
GOTERM_BP_ALL	positive regulation of secretion	22	4.7	0.0012	0.027
GOTERM_CC_ALL	U4 snRNP	4	0.8	0.0012	0.0071
GOTERM_BP_ALL	positive regulation of secretion by cell	21	4.5	0.0012	0.028
GOTERM_BP_ALL	response to chemical	124	26.3	0.0012	0.028
GOTERM_BP_ALL	RNA splicing	19	4	0.0013	0.029
GOTERM_BP_ALL	regulation of response to food	5	1.1	0.0013	0.029
GOTERM_BP_ALL	positive regulation of neurogenesis	24	5.1	0.0013	0.03
GOTERM_MF_ALL	metal ion transmembrane transporter activity	21	4.5	0.0014	0.035
GOTERM_BP_ALL	organic substance biosynthetic process	167	35.5	0.0014	0.032
GOTERM_BP_ALL	regulation of peptide secretion	15	3.2	0.0014	0.032
GOTERM_BP_ALL	astrocyte differentiation	8	1.7	0.0015	0.033
GOTERM_BP_ALL	regulation of blood pressure	13	2.8	0.0015	0.033
GOTERM_BP_ALL	cellular cation homeostasis	27	5.7	0.0015	0.033
GOTERM_BP_ALL	maintenance of protein location	9	1.9	0.0015	0.033
GOTERM_BP_ALL	rRNA metabolic process	13	2.8	0.0016	0.034
GOTERM_BP_ALL	synaptic transmission, GABAergic	6	1.3	0.0016	0.035
GOTERM_BP_ALL	regulation of dendrite morphogenesis	9	1.9	0.0016	0.035
GOTERM_BP_ALL	regulation of programmed cell death	54	11.5	0.0017	0.037
GOTERM_CC_ALL	spliceosomal snRNP complex	7	1.5	0.0017	0.01
GOTERM_BP_ALL	establishment of protein localization	65	13.8	0.0017	0.037
GOTERM_BP_ALL	single-organism organelle organization	60	12.7	0.0018	0.037
GOTERM_BP_ALL	proton transport	9	1.9	0.0018	0.037
GOTERM_BP_ALL	establishment of organelle localization	19	4	0.0018	0.038
GOTERM_BP_ALL	regulation of developmental process	76	16.1	0.0018	0.038
GOTERM_BP_ALL	substantia nigra development	6	1.3	0.0018	0.038
GOTERM_BP_ALL	positive regulation of cell development	27	5.7	0.0018	0.038
GOTERM_BP_ALL	ribosomal small subunit assembly	5	1.1	0.0019	0.038
GOTERM_BP_ALL	hydrogen transport	9	1.9	0.0019	0.039
GOTERM_BP_ALL	forebrain development	21	4.5	0.0019	0.039
GOTERM_BP_ALL	learning or memory	16	3.4	0.0019	0.039
GOTERM_BP_ALL	endocrine hormone secretion	7	1.5	0.0019	0.039
GOTERM_BP_ALL	insulin secretion	13	2.8	0.002	0.04
GOTERM_CC_ALL	mitochondrial intermembrane space	8	1.7	0.002	0.012
GOTERM_BP_ALL	cognition	17	3.6	0.002	0.041
GOTERM_BP_ALL	positive regulation of hormone secretion	11	2.3	0.002	0.041
GOTERM_BP_ALL	feeding behavior	10	2.1	0.0021	0.042
GOTERM_BP_ALL	regulation of cell death	57	12.1	0.0021	0.042
GOTERM_BP_ALL	response to drug	22	4.7	0.0021	0.042
GOTERM_BP_ALL	organelle transport along microtubule	7	1.5	0.0021	0.042
GOTERM_CC_ALL	cytoplasmic ribonucleoprotein granule	11	2.3	0.0021	0.012
GOTERM_BP_ALL	cellular ion homeostasis	27	5.7	0.0022	0.043
GOTERM_BP_ALL	biosynthetic process	168	35.7	0.0022	0.043
GOTERM_BP_ALL	regulation of appetite	5	1.1	0.0022	0.043
GOTERM_BP_ALL	anterograde axonal transport	5	1.1	0.0022	0.043
GOTERM_BP_ALL	negative regulation of protein complex assembly	10	2.1	0.0022	0.043
GOTERM_BP_ALL	regulation of apoptotic process	53	11.3	0.0022	0.043
GOTERM_BP_ALL	protein transport	60	12.7	0.0022	0.043
GOTERM_BP_ALL	cell projection morphogenesis	34	7.2	0.0022	0.043
GOTERM_BP_ALL	response to metal ion	18	3.8	0.0023	0.044
GOTERM_BP_ALL	transition metal ion transport	9	1.9	0.0023	0.044

GOTERM_BP_ALL	cellular response to external stimulus	16	3.4	0.0023	0.044
GOTERM_BP_ALL	response to food	6	1.3	0.0023	0.044
GOTERM_BP_ALL	positive regulation of homeostatic process	14	3	0.0023	0.044
GOTERM_BP_ALL	ribosomal large subunit biogenesis	8	1.7	0.0023	0.044
GOTERM_MF_ALL	angiotensin receptor binding	4	0.8	0.0024	0.059
GOTERM_BP_ALL	exocytosis	17	3.6	0.0024	0.045
GOTERM_BP_ALL	growth	40	8.5	0.0024	0.045
GOTERM_BP_ALL	positive regulation of ion transport	15	3.2	0.0024	0.045
GOTERM_BP_ALL	positive regulation of apoptotic process	26	5.5	0.0025	0.046
GOTERM_BP_ALL	nucleoside triphosphate biosynthetic process	8	1.7	0.0025	0.046
GOTERM_CC_ALL	dendritic spine	11	2.3	0.0026	0.015
GOTERM_BP_ALL	axon development	22	4.7	0.0026	0.048
GOTERM_BP_ALL	hindbrain development	12	2.5	0.0026	0.048
GOTERM_BP_ALL	carbohydrate homeostasis	15	3.2	0.0027	0.049
GOTERM_BP_ALL	glucose homeostasis	15	3.2	0.0027	0.049
GOTERM_CC_ALL	melanosome	9	1.9	0.0027	0.015
GOTERM_CC_ALL	pigment granule	9	1.9	0.0027	0.015
GOTERM_BP_ALL	cellular metal ion homeostasis	24	5.1	0.0027	0.049
GOTERM_BP_ALL	regulation of cell morphogenesis	26	5.5	0.0027	0.05
GOTERM_BP_ALL	regulation of ion transport	26	5.5	0.0028	0.05
GOTERM_BP_ALL	positive regulation of programmed cell death	26	5.5	0.0028	0.05
GOTERM_CC_ALL	neuron spine	11	2.3	0.0028	0.016
GOTERM_CC_ALL	small nuclear ribonucleoprotein complex	7	1.5	0.0029	0.016
GOTERM_CC_ALL	small nucleolar ribonucleoprotein complex	5	1.1	0.0029	0.016
GOTERM_CC_ALL	U12-type spliceosomal complex	5	1.1	0.0029	0.016
GOTERM_CC_ALL	internode region of axon	3	0.6	0.0029	0.016
GOTERM_CC_ALL	spliceosomal complex	12	2.5	0.0031	0.016